Acta Neurochirurgica Supplement 116

Mikhail F. Chernov · Motohiro Hayashi
Jeremy C. Ganz · Kintomo Takakura
Editors

Gamma Knife Neurosurgery in the Management of Intracranial Disorders

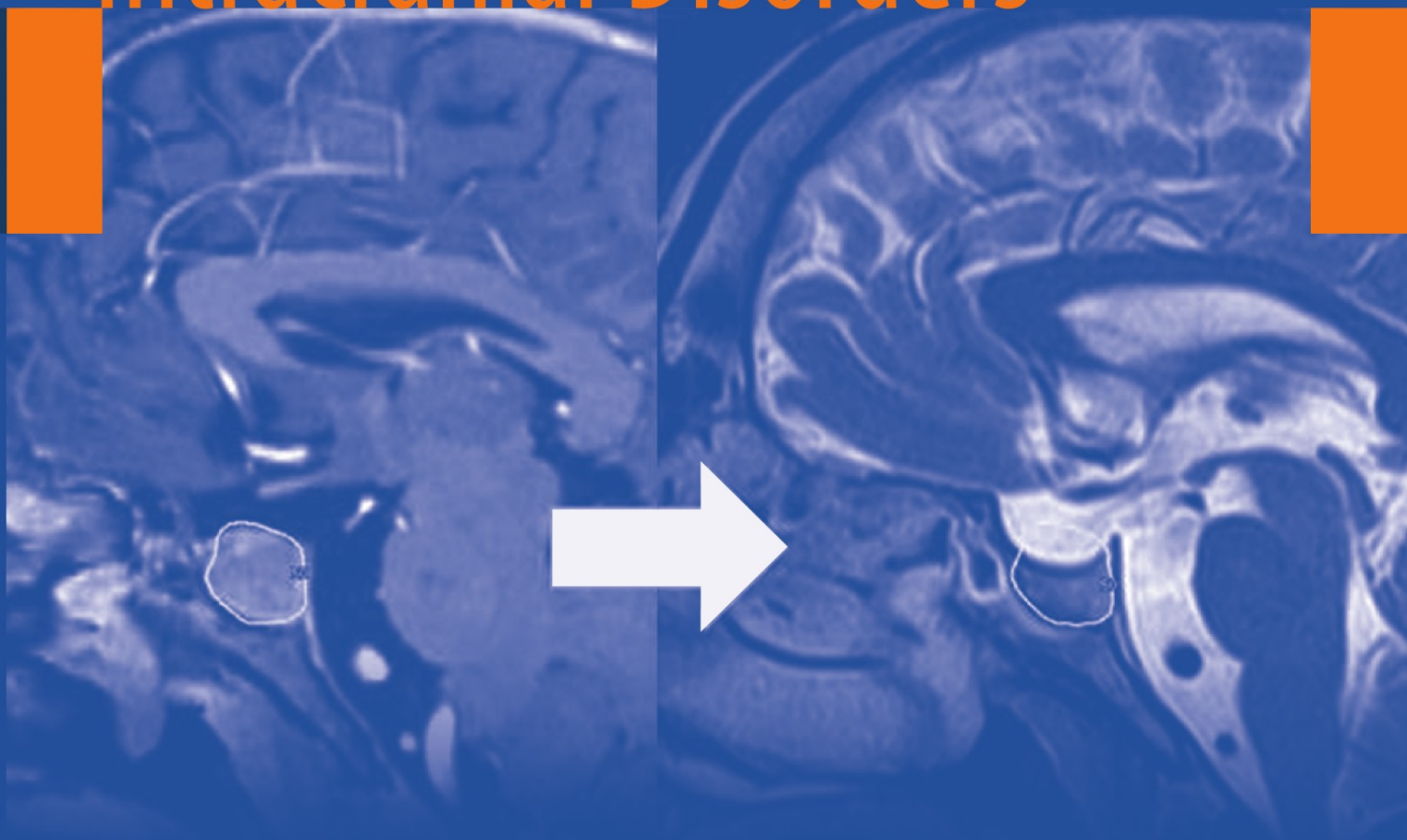

Springer

Acta Neurochirurgica
Supplements

Editor: H.-J. Steiger

Gamma Knife Neurosurgery in the Management of Intracranial Disorders

Edited by
Mikhail F. Chernov, Motohiro Hayashi,
Jeremy C. Ganz, Kintomo Takakura

Acta Neurochirurgica
Supplement 116

Springer

Mikhail F. Chernov
Faculty of Advanced Techno-Surgery and Department of Neurosurgery
Tokyo Women's Medical University
Tokyo, Japan

Motohiro Hayashi
Department of Neurosurgery and Faculty of Advanced Techno-Surgery
Tokyo Women's Medical University
Tokyo, Japan

Jeremy C. Ganz
Department of Neurosurgery
Haukeland University Hospital
Bergen, Norway

Kintomo Takakura
Institute of Advanced Biomedical Engineering and Science
Tokyo Women's Medical University
Tokyo, Japan

Typesetting: SPI, Pondichery, India
Printed on acid-free and chlorine-free bleached paper

Library of Congress Control Number: 2012954885

With 77 (partly coloured) Figures

ISSN 0065-1419
ISBN 978-3-7091-1375-2 ISBN 978-3-7091-1376-9 (eBook)
DOI 10.1007/978-3-7091-1376-9
SpringerWienNewYork

Sponsors of the Fifth Annual Meeting of the Asian Gamma Knife Academy (September 29–October 1, 2011; Saint Petersburg, Russia) and Publication of Its Proceedings

ELEKTA

DTC IIBS
Diagnostic and Treatment Center
International Institute of Biological
Systems named after Dr. S.M.Berezin

JAPAN BRAIN FOUNDATION
公益財団法人
日本脳神経財団

FATS
Faculty of Advanced Techno-Surgery
TWMU

BRACCO
LIFE FROM INSIDE

A Product of Bracco
ProHance
gadoteridol

To my parents.

M.F. Chernov

To colleagues in the field of the Gamma Knife who manage various diseases while caring deeply about the lives of their patients.

M. Hayashi

To all those colleagues around the world whose ceaseless efforts continue to improve and refine the use of the Gamma Knife.

J.C. Ganz

To my patients.

K. Takakura

Preface

The present volume of *Acta Neurochirurgica Supplement* contains the Proceedings of the Fifth Annual Meeting of the Asian Gamma Knife Academy held on September 29 to October 1, 2011 in Saint Petersburg, Russia. This event was organized by the International Institute of the Biological Systems (St. Petersburg, Russia) and was supported by Elekta Instruments AB (Stockholm, Sweden). It was joined by 70 participants from 19 countries on five continents. The scientific program covered various options for optimal management of brain tumors, vascular lesions, and functional disorders.

There are at least three factors that make this meeting unique. First, it is unusual that a conference of an Asian professional society was organized in a European country. This issue raised multiple questions, but the reason for the decision was, in fact, rather simple. At the time of preparation for the meeting, there was no functioning Gamma Knife facility in the Asian part of the Russian Federation. Thus, it was decided to organize the conference in St. Petersburg, where a young, but already well-established radiosurgical program was in place at the Diagnostic and Treatment Center of the International Institute of the Biological Systems.

Second, the meeting was definitely multidisciplinary, involving not only Gamma Knife users but microneurosurgeons and neuroradiologists, which maintained a good balance between microneurosurgery and radiosurgery, in keeping with the intended design of the conference. The presentation and discussion of information from multiple treatment methods will help provide better service to patients. These objectives were realized through the scientific sessions with the presentation of alternative surgical and radiosurgical treatment options, with open discussions on their advantages and disadvantages. Moreover, an overview of current radiological modalities and their possible application for Gamma Knife treatment planning and subsequent follow-up was offered during the special symposium dedicated to advanced neuroimaging for radiosurgery.

Third, following the traditions of the Asian Gamma Knife Academy meetings, a special workshop was organized on the last day of the conference at the Radiosurgical Center of the International Institute of the Biological Systems. Leading professionals demonstrated real-time dose planning for various brain diseases and shared their opinions on possible solutions to specific practical problems.

The materials included in this volume reflect the scientific program of the meeting. Some articles, specifically highlighting alternative treatment options, are accompanied by editorials prepared by recognized experts in the field. We hope that all of our colleagues worldwide, who are looking for the best possible treatment for their patients, find the presented material scientifically interesting and practically useful.

The Editors

Contents

Advanced Neuroimaging for Gamma Knife Neurosugery

Asian Gamma Knife Academy: Its Goals and Activities

Motohiro Hayashi

Keywords Asian Gamma Knife Academy • Asian Leksell Gamma Knife Society • Asian radiosurgery • Gamma Knife radiosurgery

Lars Leksell initially described the concept of stereotactic radiosurgery in 1951 and initiated use of the first Gamma Knife in Stockholm, Sweden in 1968. During the next 14 years, 762 patients with various brain disorders underwent radiosurgical treatment [3]. Highly promising results led to steady worldwide dissemination of the technique. In 1987, the first Gamma Knife facility in North America became operational at the University of Pittsburgh [3].

Development of Gamma Knife radiosurgery (GKS) in Asia started in 1990, when units at the University of Tokyo Hospital (Tokyo, Japan) and ASAN Medical Center (Seoul, Korea) were opened [2, 5]. Since then, the number of new centers gradually increased, reflecting the clinical need [1, 2, 7, 8]. By the end of 2010, a total of 120 Gamma Knife centers were operating in 14 Australasian countries [6]. Several national radiosurgical societies were established, and their regular scientific meetings were organized. Asian doctors actively participated in the worldwide congresses of the Leksell Gamma Knife Society and International Stereotactic Radiosurgery Society. However, no international professional organization dedicated to GKS had existed in the South-East Asia until 2007, which limited collaboration of the practicing radiosurgeons.

M. Hayashi
Department of Neurosurgery, Neurological Institute,
Tokyo Women's Medical University,
8-1 Kawada-cho, Shinjuku-ku, Tokyo 162-8666, Japan

Faculty of Advanced Techno-Surgery,
Institute of Advanced Biomedical Engineering and Science,
Tokyo Women's Medical University, Tokyo, Japan

Saitama Gamma Knife Center, Sanai Hospital,
Saitama, Japan
e-mail: gkrmoto@aol.com

There was also another reason to initiate international Gamma Knife activities here. Whereas the doctors from well-developed countries could be trained abroad in the leading European and North American radiosurgical centers, their colleagues, particularly the younger ones, from countries with low income rarely had such an opportunity. Even the short-term visits for participation in practical workshops organized by Elekta Instruments AB (Stockholm, Sweden) at designated training centers were difficult as none of these centers was located in Asia.

These problems were highlighted during my talks with Dr. Maheep Singh Gaur from India, whom I met during the international conference in 2005. We both had advanced GKS training under the supervision of leading specialists: I had spent 2.5 years in Marseille working with professor Jean Régis, and Dr. Gaur had a year of training in Japan with Dr. Tatsuo Hirai. It was evident to us that the knowledge and experience we obtained during these fellowships should be spread more widely to our colleagues to improve the quality of Asian radiosurgery.

Therefore, along with some colleagues we founded the Asian Gamma Knife Training Program (AGKTP) in 2007. The initial group of faculty members was joined by Professor Jung Kyo Lee from ASAN Medical Center (Seoul, Korea), Dr. Chung Ping Yu from Canossa Hospital (Hong Kong, China), Professor David Hung-Chi Pan from Taipei Veterans General Hospital (Taipei, Taiwan), Dr. Mikhail Chernov from Russia, who at the time was a Clinical and Research Fellow in the Department of Neurosurgery of the Tokyo Women's Medical University, and three Japanese colleagues: Drs. Hiroyuki Kenai, Toru Serizawa, and Takashi Shuto. The objectives of the new organization were to exchange ideas and skills among Asian radiosurgeons and disseminate knowledge regarding the Gamma Knife technique in Asian countries, particularly among those colleagues who were not familiar with it. Special emphasis was placed on educating young neurosurgeons and training them in GKS.

The first meeting of the AGKTP was organized the same year (2007) at Saitama Gamma Knife Center of the Sanai

M.F. Chernov et al. (eds.), *Gamma Knife Neurosurgery in the Management of Intracranial Disorders*,
Acta Neurochirurgica Supplement, Vol. 116, DOI 10.1007/978-3-7091-1376-9_1, © Springer-Verlag Wien 2013

Hospital (Saitama, Japan). At that time, the organizers did not have any official sponsor of their activities. The donations, which were generously provided by the president of Sanai Hospital Mr. Teruhisa Watayou and former presidents of the Japan Gamma Knife Society Professors Kintomo Takakura and Tomokatsu Hori, were mainly spent to support several young participants of the meeting who came from India, Korea, Russia, and Japan. All faculty members covered their own expenses for travel and accommodation. They received no honorarium for presentations. Despite these possible obstacles, the 3-day event was rather successful. The activities included multiple educational lectures, which covered in depth nearly all of the main topics regarding GKS. We allowed generous time for discussion after each talk, with the goal of clarifying all possible nuances and to make the presented material suitable for clinical application. Practical training was performed during the meeting as well. It focused on the technique of stereotactic frame fixation on the patient's head and on real-time treatment planning with the use of the GammaPlan (Elekta Instruments AB) for various brain disorders. The latter was accompanied by critical evaluations and comparisons of the different radiosurgical strategies and concepts. Special efforts were made to involve younger colleagues in simulating the clinical decision-making, which was considered an important educational part of the program. In fact, such practical training and detailed discussions organized in the free and friendly atmosphere became the typical features of subsequent AGKTP activities (Fig. 1).

Fig. 1 Typical features of AGKA meetings: wide and open panel discussions on the various aspects of GKS (*upper*) and practical hands-on sessions with the real-time treatment planning using the Leksell GammaPlan (*lower*)

Subsequently, the annual AGKTP meetings were organized first by me in Tokyo, Japan (2008), Professor Jung Kyo Lee in Busan, Korea (2009), and Professor David Hung-Chi Pan in Taipei, Taiwan (2010). These meetings obtained partial financial support from Bracco Co. (Italy) and Elekta K.K. The number of participants steadily increased, and the quality of the scientific program gradually improved. Several leading professionals from outside Asia were invited to participate in these activities (Fig. 2). In 2009, AGKTP was renamed the Asian Gamma Knife Academy (AGKA) to reflect its educational and scientific objectives, which were now directed not only at radiosurgical practitioners but neurosurgeons from other subspecialties and colleagues from different medical fields (e.g., neurology, oncology). Nevertheless, the original unique concept of the meetings, which made it somewhat different from typical professional conferences, was generally preserved: that is, in-depth coverage of up-to-date knowledge of the all main aspects of contemporary GKS by educational lectures instead of usual scientific reports, clinical practice-oriented presentations, wide discussions, and hands-on workshops with real-time radiosurgical treatment planning (although because of technical reasons the latter were not organized at the 2009 and 2010 meetings).

In 2011, for the first time AGKA went outside Asia for its fifth annual meeting, which was organized by Dr. Mikhail Chernov in St. Petersburg, Russia. The decision to do so was based on wanting to bring knowledge about the clinical possibilities of GKS in the management of various brain disorders to the wide Russian medical community as the use of radiosurgery had rapidly increased there. The event was welcomed by European Gamma Knife users [4], many of whom took an active part in this program. The list of invited speakers included not only representatives of Eurasia but also North America (Professor Ian E. McCutcheon from The University of Texas M. D. Anderson Cancer Center, Houston, Texas, USA), South America (Professor Julio C. Antico from FLENI, Buenos Aires, Argentina), and Africa (Professor Abdeslam El Khamlichi from Mohammed V University, Rabat, Morocco). It reflected the growth of international interest in our activities.

All AGKA faculty members are eager to disseminate knowledge about contemporary GKS, particularly among those who are not yet familiar with it. Continuing education of radiosurgical practitioners is another goal. Initiating the

Saitama, Japan (2007) Busan, Korea (2009)

Taipei, Taiwan (2010) Saint Petersburg, Russia (2011)

Fig. 2 Faculty members and participants of AGKA meetings

development and realization of multicenter scientific research projects in the field of GKS with involvement of Gamma Knife users from different countries is also important. Wide collaboration with colleagues from outside Asia and close cooperation with other national and international professional organizations, particularly the Asian Leksell Gamma Knife Society (organized in 2009), are planned. Our main objective is still the same: improving the quality of radiosurgery in Asia (and beyond) for the greatest benefit of the patients.

Conflict of Interest The author declares that he has no conflict of interest.

References

1. Abdullah J, Ridzuan MY (1997) Incidence of tumours suitable for radiosurgery in a developing country like Malaysia: retrospective study done before the decision to start a radiosurgery programme. Stereotact Funct Neurosurg 69:152–155
2. Hwang SN (2005) History of Korean stereotactic and functional neurosurgery. Neurosurgery 56:406–409
3. Lasak JM, Gorecki JP (2009) The history of stereotactic radiosurgery and radiotherapy. Otolaryngol Clin North Am 42:593–599
4. Leeds Gamma Knife Centre Welcomes Asian Gamma Knife Academy to Europe (2011) Web-site of the Leeds Gamma Knife Centre. http://www.leedsgammaknife.com/leeds-gamam-knife-centre-welcomes-asian-gamma-knife-academy-to-europe.html. Accessed 15 Oct 2011
5. Otto S (2009) History and present status of Gamma Knife radiosurgery in Japan. Prog Neurol Surg 22:1–10
6. ELEKTA (2010) Leksell Gamma Knife® Sites per country in Asia Pacific. In: Program and Abstracts of the 2nd Meeting of the Asian Leksell Gamma Knife Society and the 14th Meeting of the Japanese Leksell Gamma Knife Society, November 11-13, 2010, Nagoya, Japan, pp 5–9
7. Teshima T, Numasaki H, Shibuya H, Nishio M, Ikeda H, Sekiguchi K, Kamikonya N, Koizumi M, Tago M, Ando Y, Tsukamoto N, Terahara A, Nakamura K, Mitsumori M, Nishimura T, Hareyama M, Japanese Society of Therapeutic Radiology and Oncology Database Committee (2010) Japanese structure survey of radiation oncology in 2007 based on institutional stratification of patterns of care study. Int J Radiat Oncol Biol Phys 78:1483–1493
8. Yin W, Chen B, Tian F, Yu Y, Kong FM (2008) The growth of radiation oncology in mainland China during the last 10 years. Int J Radiat Oncol Biol Phys 70:795–798

Concept of Robotic Gamma Knife Microradiosurgery and Results of Its Clinical Application in Benign Skull Base Tumors

Motohiro Hayashi, Mikhail F. Chernov, Noriko Tamura, Masahiro Izawa, Yoshihiro Muragaki, Hiroshi Iseki, Yoshikazu Okada, Pavel Ivanov, Jean Régis, and Kintomo Takakura

Abstract The availability of advanced computer-aided robotized devices for the Gamma Knife (i.e., an automatic positioning system and PerfeXion) resulted in significant changes in radiosurgical treatment strategy. The possibility of applying irradiation precisely and the significantly improved software for treatment planning led to the development of the original concept of robotic Gamma Knife microradiosurgery, which is comprised of the following: (1) precise irradiation of the lesion with regard to conformity and selectivity; (2) intentional avoidance of excessive irradiation of functionally important anatomical structures, particularly cranial nerves, located both within the target and in its vicinity; (3) delivery of sufficient radiation energy to the tumor with a goal of shrinking it while keeping the dose at the margins low enough to prevent complications. Realization of such treatment principles requires detailed evaluation of the microanatomy of the target area, which is achieved with an advanced neuroimaging protocol. From 2003, we applied the described microradiosurgical concept in our clinic for patients with benign skull base tumors. Overall, 75 % of neoplasms demonstrated shrinkage, and 47 % showed 50 % and more volume reduction. Treatment-related complications were encountered in only 6 % of patients and were mainly related to transient cranial nerve palsy. Just 2 % of neoplasms showed regrowth after irradiation. In conclusion, applying the microradiosurgical principles based on advanced neuroimaging and highly precise treatment planning is beneficial for patients, providing a high rate of tumor shrinkage and a low morbidity rate.

Keywords Automatic positioning system • Gamma Knife PerfeXion • Gamma Knife radiosurgery • Microradiosurgery • Robotics • Skull base tumor

M. Hayashi (✉)
Department of Neurosurgery, Neurological Institute,
Tokyo Women's Medical University,
8-1 Kawada-cho, Shinjuku-ku, Tokyo 162-8666, Japan

Faculty of Advanced Techno-Surgery,
Institute of Advanced Biomedical Engineering and Science,
Tokyo Women's Medical University, Tokyo, Japan

Saitama Gamma Knife Center, Sanai Hospital,
Saitama, Japan
e-mail: gkrmoto@aol.com

M.F. Chernov, Y. Muragaki, H. Iseki, and K. Takakura
Department of Neurosurgery, Neurological Institute,
Tokyo Women's Medical University, Tokyo, Japan

Faculty of Advanced Techno-Surgery,
Institute of Advanced Biomedical Engineering and Science,
Tokyo Women's Medical University, Tokyo, Japan

N. Tamura, M. Izawa, and Y. Okada
Department of Neurosurgery, Neurological Institute,
Tokyo Women's Medical University, Tokyo, Japan

P. Ivanov
Radiosurgical Center, International Institute of the Biological Systems,
Saint Petersburg, Russia

J. Régis
Department of Functional and Stereotactic Neurosurgery,
Timone University Hospital, Marseille, France

Faculty of Advanced Techno-Surgery,
Institute of Advanced Biomedical Engineering and Science,
Tokyo Women's Medical University, Tokyo, Japan

Introduction

The concept of stereotactic radiosurgery as precise delivery of a single-fraction high-dose radiation to an imaging-defined target was originally developed by Professor Lars Leksell from Karolinska University in Stockholm, Sweden. In 1951, he performed the first radiosurgical procedure to treat a patient with trigeminal neuralgia. The technique involved focusing multiple beams of ionizing radiation in such a way that they collided at the same point in the three-dimensional (3D) space. Each beam contained a dose low enough to avoid altering normal brain, but at the point of intersection of all of

M.F. Chernov et al. (eds.), *Gamma Knife Neurosurgery in the Management of Intracranial Disorders*,
Acta Neurochirurgica Supplement, Vol. 116, DOI 10.1007/978-3-7091-1376-9_2, © Springer-Verlag Wien 2013

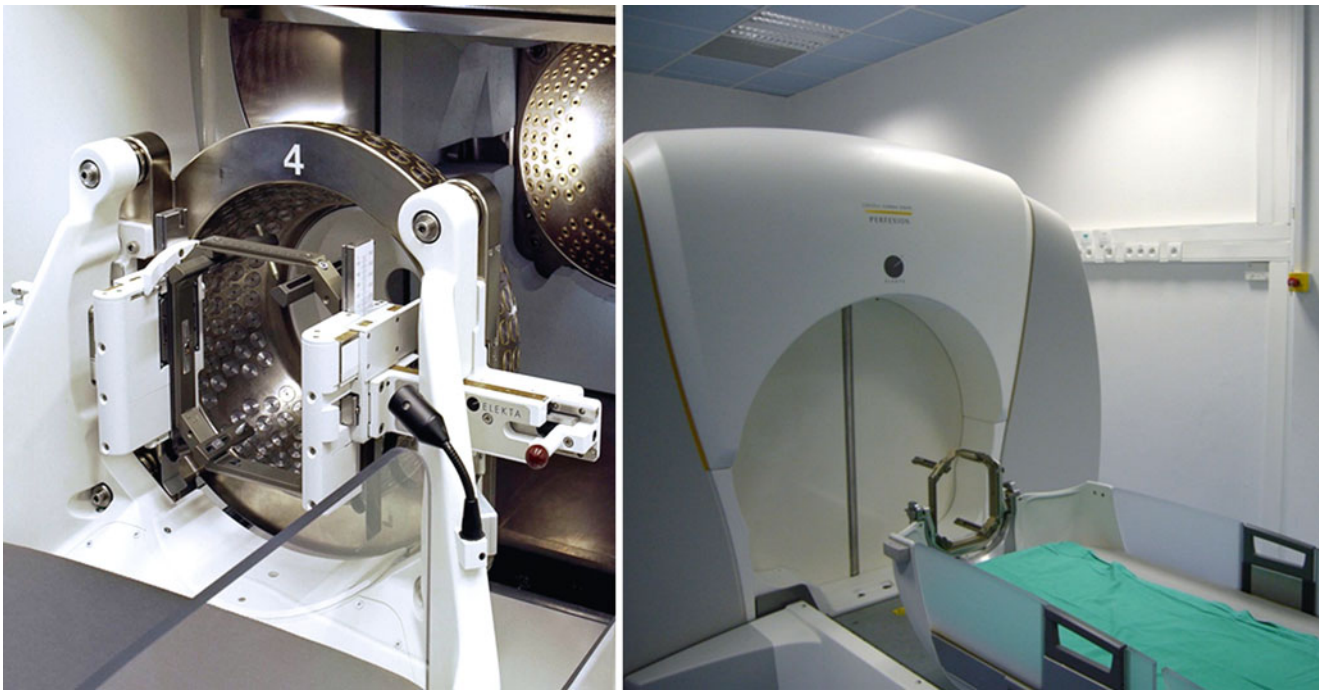

Fig. 1 Modern computer-aided robotized devices for Gamma Knife radiosurgery: automatic positioning system (*left*) and Leksell Gamma Knife PerfeXion (*right*)

the beams a destructive dose of radiation was delivered. Initially X-rays were used, but later they were replaced by radioactive cobalt emitting a form of high-energy radiation called gamma rays. Therefore, the new technique was designated Gamma Knife stereotactic radiosurgery (GKS).

At present, GKS is an approved and widely accepted management option for a variety of intracranial tumors, vascular malformations, and functional brain disorders. Around 50,000 patients undergo treatment each year worldwide, and the number is growing. Contemporary technological achievements have resulted in profoundly improved safety and clinical applicability of radiosurgery and currently permit administration of treatment with microsurgical precision and even better. Moreover, at the beginning of the new millennium, advanced computer-aided robotized devices were introduced into clinical practice, including an automatic positioning system (APS) and later the newest model of the Gamma Knife designated PerfeXion (Elekta Instruments AB, Stockholm, Sweden) (Fig. 1).

Advantages of the Modern Computer-Aided Robotized Devices for Gamma Knife Radiosurgery

The APS is a robotized computer-controlled device for automatic positional changes of the patient's head fixed in a Leksell G stereotactic frame during radiosurgery using Gamma Knife model C or 4C (Elekta Instruments AB). The device provides extremely high mechanical precision, within 0.1 mm in any coordinate direction. The initial evaluation of the system after its introduction into clinical practice showed beneficial effects regarding the treatment time and significantly improved options for multi-isocenter radiosurgery with application of small collimators, which resulted in a prominent increase in the precision of GKS [20, 21, 26, 27, 36, 42]. Particularly, in cases of vestibular schwannomas, application of APS resulted in increased conformity and selectivity indices from 95 to 97 % and from 78 to 84 %, respectively [36], whereas in a cohort of cavernous sinus tumors utilization of the device led to a significant reduction of the radiation dose delivered to the optic chiasm [27]. It became possible to create radiosurgical treatment plans with more homogeneous high-dose distribution and avoid underdosed areas within the lesion [21]. Finally, there was a significant decrease of extracranial irradiation, which is important in patients with benign lesions and long life expectancy [26]. Among the limitations of APS is that technically it cannot be used in some cases, particularly for peripherally located intracranial lesions [26, 36, 42].

All of the above-mentioned treatment advantages associated with application of APS are augmented with the use of PerfeXion [29, 37, 46]. This fully robotized model of the Leksell Gamma Knife has several unique features that make it fundamentally different from its predecessors. First, it has an integrated permanent collimator system that incorporates openings for collimators of three diameters (4, 8, and 16 mm),

which are separated into eight independently movable sectors around the circumference of the device. During treatment, the collimator size of each sector can be individually chosen or blocked off. The device allows generation of a single isocenter composed of different beam diameters (called a composite or hybrid shot) with optimized shape. This feature significantly increases conformity and selectivity of radiation delivery and is especially effective for complex targets located in the vicinity of critical anatomical structures [29, 46]. The improved dose homogeneity and greater precision of GKS permits its application to intracranial lesions of larger volume than traditionally considered suitable for such treatment. Additionally, modification of dose distribution is possible with "dynamic shaping." It requires only delineation of the critical structure or area and its definition as a "risk volume" with resultant automatic blocking of the beams that pass through it [29, 46]. Second, improved dosimetry usually permits the treatment to be done as a single run [37]. This advantage, along with the ability to block all the beams during fast transition of coordinates from one isocenter to another, eliminates the need to remove the patient from the machine during GKS, which in turn results in relatively increased effective (beam on) treatment time, shortens the total treatment time, and reduces the extralesional (particularly extracranial) irradiation doses [29, 37]. Third, the coach itself represents the positioning system, which provides not only <0.05 mm mechanical accuracy but also greater comfort for the patient because no movements of the head are necessary during irradiation [37]. Fourth, the significantly increased volume of the radiation cavity and the change of its shape from hemispheric to cylindrical practically eliminates the possibility of collisions. It also has an important implication on the management of multiple brain metastases and avoids staged treatment with reapplication of the stereotactic frame even for patients with lesions located in the opposite intracranial areas [29, 37]. Moreover, at least theoretically, PerfeXion provides an opportunity to apply GKS to previously nonaccessible lesions of the external skull base, maxillofacial region, and cervical spine [29, 37]. Finally, full automatization and robotization of the device greatly alleviates the workload of the staff because establishing the gamma angle (70º, 90º, or 110º) remains the only manipulation that is set up manually [29]. It also results in significantly increased safety of the treatment because it eliminates the risk of human error during adjustment of the isocenter position [37]. The operator does not have a choice of switching to manual mode or blocking of the individual beams to protect distant structures (e.g., the lens) and these points represent potential disadvantages of the device. However, they are of limited if any clinical significance [29, 37]. It should be emphasized that despite technological complexity the technical failures during use of PerfeXion are exceptionally rare [29, 37, 46].

Availability of the described computer-aided robotized devices for GKS led to significant changes in the radiosurgical treatment strategy. The possibility of applying highly conformal and selective irradiation and the significantly improved software for treatment planning and dosimetry (Leksell GammaPlan; Elekta Instruments AB) permitted for us to create the concept of robotic Gamma Knife microradiosurgery [7, 40]. It was originally developed and then applied in practice after installation of the Leksell Gamma Knife model 4C with APS in our clinic (December 2002).

Concept of Robotic Gamma Knife Microradiosurgery

The concept of microradiosurgical treatment is based on three main principles: (1) precise irradiation of the lesion with regard to conformity and selectivity; (2) intentional avoidance of excessive irradiation of functionally important anatomical structures, particularly cranial nerves, located both within the target and in its vicinity; (3) delivery of sufficient radiation energy to the tumor with the goal of shrinking it while keeping the dose at the margins low enough to prevent complications. Realization of such treatment principles requires detailed evaluation of the microanatomy of the target area, which is performed using the advanced neuroimaging protocol.

Advanced Neuroimaging Protocol

The original neuroimaging protocol for robotic Gamma Knife microradiosurgery requires access to high-resolution thin-sliced plain constructive interference in steady state (CISS) images, gadolinium-enhanced CISS images, and gadolinium-enhanced axial modified time-of-flight (TOF) images obtained with a 1.5 T clinical magnetic resonance imaging (MRI) scanner [11, 13, 19]. Usually for MRI examinations of benign skull base tumors, a single dose (0.1 mmol/kg) of the gadolinium-based contrast medium gadoteridol (ProHance®; Eisai, Tokyo, Japan) is administered intravenously. Additionally, thin-sliced plain, "bone window," and contrast-enhanced axial computed tomography (CT) scans are obtained. The recognizable advantages of the CT scans include a low risk of image distortion artifacts and clear visualization of the osseous structures, which can be important during radiosurgery of skull base lesions [24, 35]. In some cases, metabolic information obtained with positron emission tomography (PET) or multivoxel proton magnetic resonance spectroscopy (^{1}H-MRS) is used for radiosurgical treatment planning and can be particularly helpful during repeat GKS of recurrent tumors [24, 28].

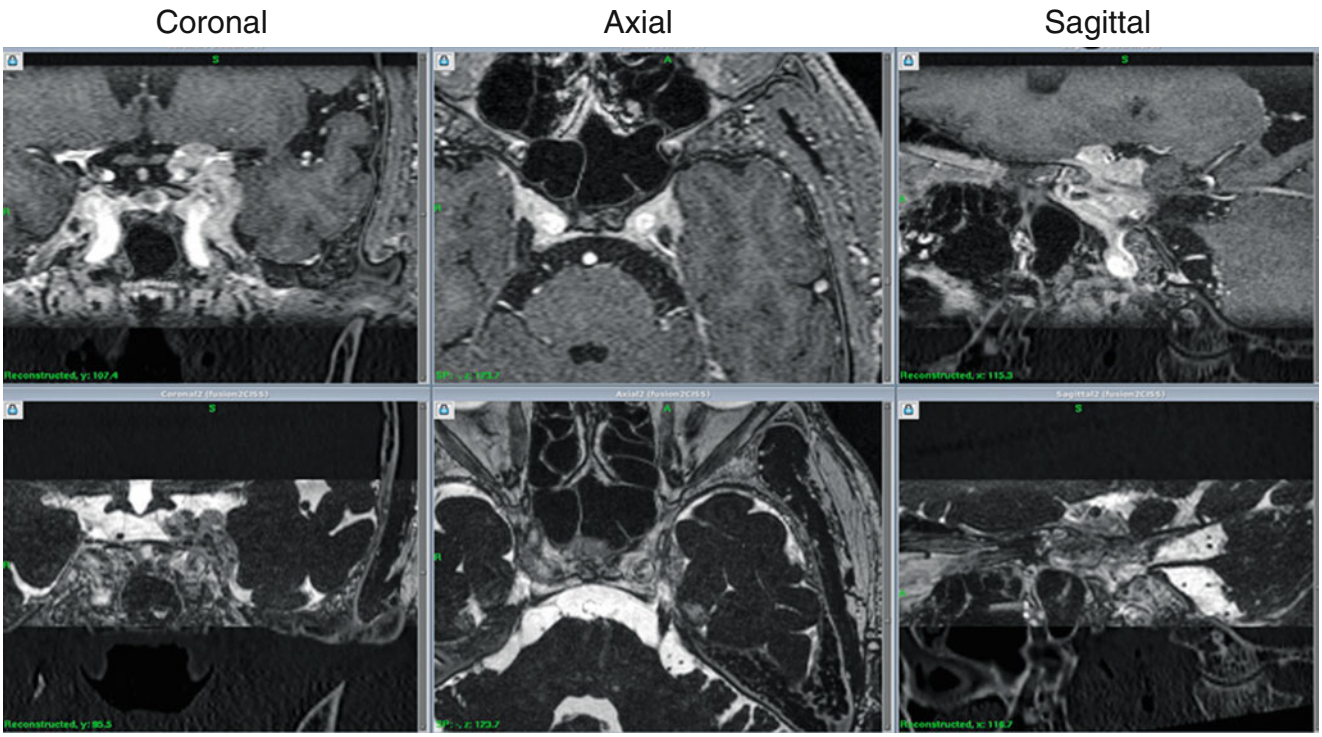

Fig. 2 Gadolinium-enhanced multiplanar reconstructed (*MPR*) magnetic resonance (*MR*) images (*upper row*) and constructive interference in steady state (*CISS*) MR images (*lower row*) of a left cavernous sinus meningioma. Note the greater resolution of the CISS images, which permits detailed evaluation of the local neuranatomy

Detailed Evaluation of the Target Neuroanatomy

All neuroimaging data are exported via the Intranet to Leksell GammaPlan (current version 8.3). This advanced software dedicated to planning the GKS and dosimetry provides an opportunity for highly accurate and precise co-registration and fusion of the various images obtained with different modalities and their magnification and reconstruction. It also allows for the surgeon to delineate various intracranial structures and to perform their evaluation from different angles and directions using 3D visualization [24].

After constructing the original workspace, the local neuroanatomy is assessed in detail. Identification of the cranial nerves either in the vicinity of the lesion or within its mass is especially emphasized. Plain CISS images permit clear visualization of the anatomical structures located intradurally or within the subarachnoid cisterns. Moreover, separate components of some cranial nerves can be differentiated from each other even with 1.5 T MR scanners. In the same time gadolinium-enhanced CISS images make the tumor "lucid" or half-tone but do not affect signal intensity of the adjacent cranial nerves. Therefore, the cranial nerves can be clearly delineated in the vicinity of the lesion (Figs. 2 and 3). Gadolinium-enhanced TOF proved helpful for 3D evaluation of the interrelations between the neoplasm and adjacent vessels. Fused "bone window" CT and MRI permit simultaneous visualization of soft tissue and bone structures [24, 35].

Even with the advanced neuroimaging protocol and evaluation of images within the Leksell GammaPlan, delineation of the cranial nerves in the vicinity of large neoplasms is sometimes impossible. In such cases, identifying the tumor's origin may allow the surgeon to presume the direction of its growth and the corresponding shift of adjacent anatomical structures. Therefore, their expected location can be predicted rather precisely and taken into consideration during radiosurgical treatment planning.

Principles of Microradiosurgical Treatment Planning

Microradiosurgical treatment planning is performed by referring to simultaneous onscreen displays of all obtained images in the 3D workspace of the Leksell GammaPlan. The dose plan is created with the use of multiple small isocenters, which are carefully positioned within the border of the mass with the goal of attaining its conformal and selective coverage with the prescribed isodose (Fig. 4). For GKS of benign skull base tumors, we usually try to attain a conformity index (CI) > 0.95 and a selectivity index (SI) > 0.90 [3, 46]. Although it requires a significant number of shots, it should

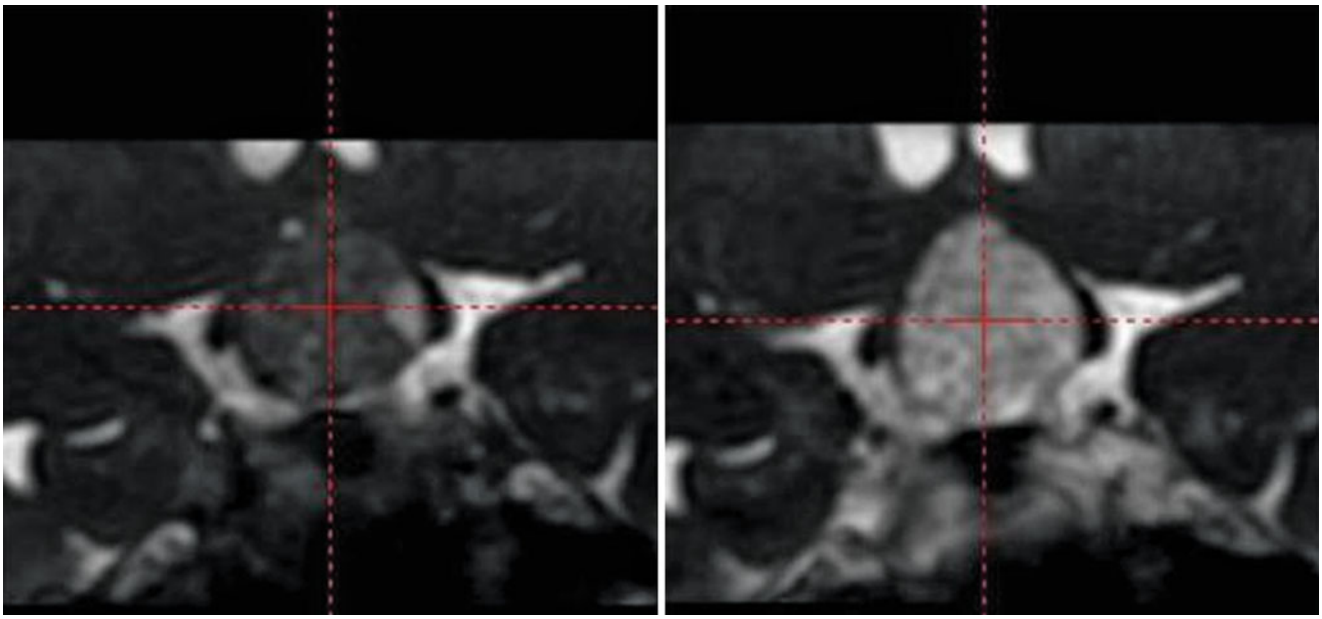

Fig. 3 CISS images of a craniopharyngioma. Plain image (*left*) provides clear differentiation of the tumor border and subarachnoid cisterns, whereas administration of gadolinium (*right*) makes the tumor half-tone and facilitates determination of its border along adjacent cerebral structures, including visual pathways (from Yomo et al. [45])

not be an obstacle for treatment using robotized computer-aided devices such as APS or PerfeXion. Special emphasis is placed on avoiding projection of any isocenter on functionally important anatomical structures located nearby, particularly the cranial nerves. If the cranial nerves cannot be visualized, excessive irradiation of areas where they would presumably be located are intentionally avoided. It is easily done as Leksell GammaPlan allows adjustment of the isocenters' coordinates with 0.1 mm precision.

Usually, a 50 % prescription isodose is applied to the border of the neoplasm. For benign skull base lesions, the dose at the margins varies from 10 to 14 Gy, depending on the lesion volume and location. In the vast majority of cases it constitutes 11–12 Gy. An exception to this guideline is hormone-secreting pituitary adenomas, which require larger irradiation doses to inhibit excessive hormone production. In such cases, a dose at the margins of, at least, ≥20 Gy seems necessary.

Specific Technique Directed at Tumor Shrinkage

The traditional goal of radiosurgery for intracranial tumors is growth control. However, reduction of the mass volume seems important for restoring the affected neuronal functions, particularly those related to direct compression of the cranial nerves. In fact, in one-third to two-thirds of cases, GKS results in shrinkage of benign skull base neoplasms (meningiomas, schwannomas, pituitary adenomas). Our experience demonstrated that reduction of the lesion volume after radiosurgery is directly associated with the amount of delivered radiation energy. Its variations may correspond to differences in the treatment effects despite the use of similar doses at the tumor margins [10, 16, 18]. This is in concordance with the experimental results of Massager et al. [30], which clearly showed that the presence of a "hot spot" within the target volume is likely to lead to the desired radiobiological result of GKS. It seemingly does not increase the risk of complications unless the radiosurgical treatment planning was insufficiently selective and the high-dose radiation extended to the adjacent normal tissue [2]. Therefore, in each case we try to attain a homogeneous dose distribution with creation of a wide 80 % prescription isodose area within the tumor while keeping a sufficiently low dose at the margins, which usually corresponds to a 50 % isodose. For skull base meningiomas, the suspected area of tumor origin on the dura mater is included in the high-dose irradiation area for possible obliteration of the feeding vessels [16].

To evaluate the high-dose area within the target, the homogeneity index (HI) is calculated as:

$$HI = TV_{piv80\%} / TV_{piv50\%}$$

where $TV_{piv80\%}$ and $TV_{piv50\%}$ correspond to target volumes covered by 80 % and 50 % prescription isodoses, respectively. During GKS of benign skull base tumors, we try to keep the HI at least at the level of 0.5. If the volume or distribution of the high-dose irradiation area in the target is considered insufficient, it can be optimized by adding additional small, low-weight isocenter(s). An original parameter, designated the unit energy (UE), reflects the

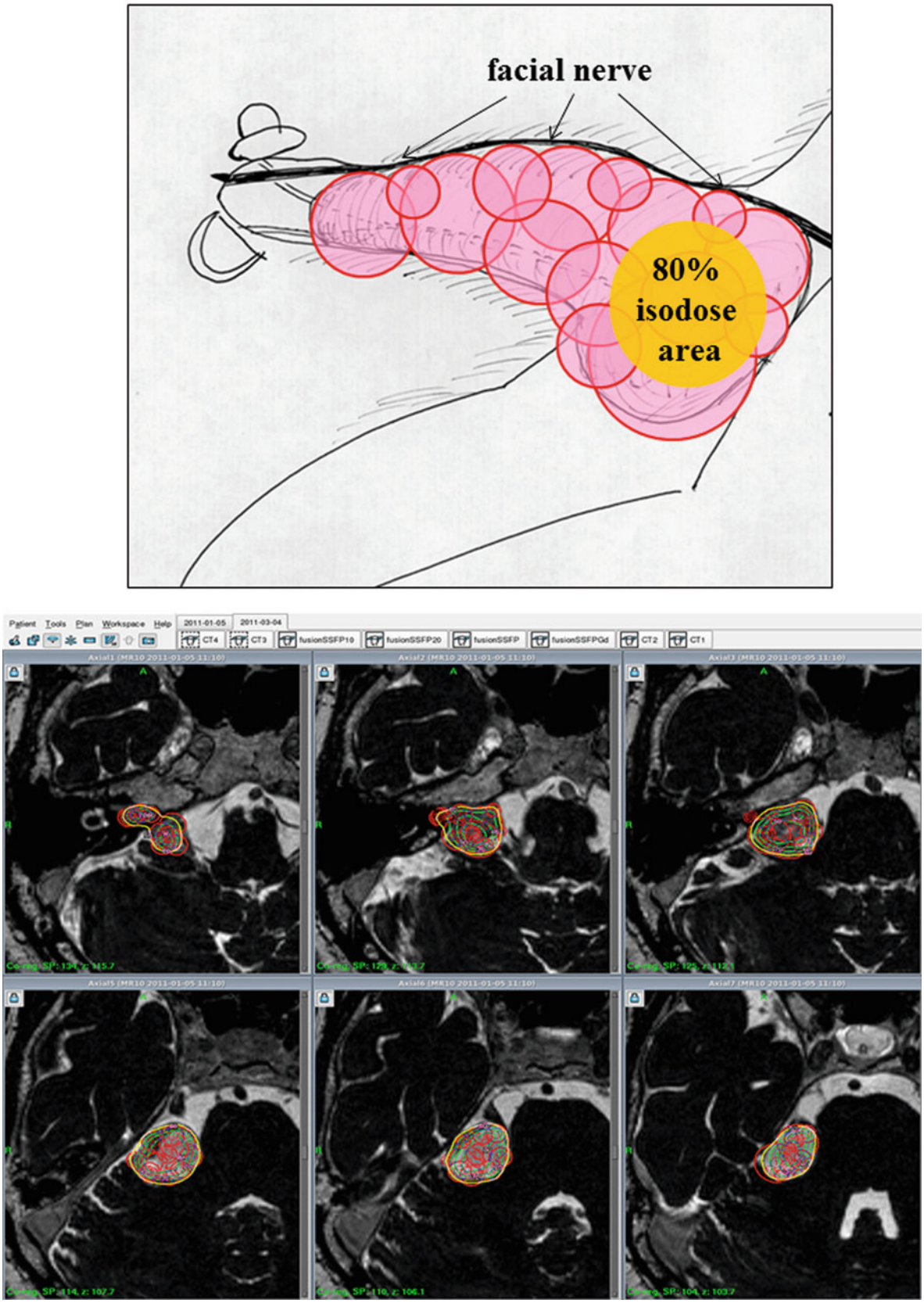

Fig. 4 Schematic (*upper*) and actual (*lower*) treatment planning for a Koos grade III right-sided vestibular schwannoma according to the concept of robotic Gamma Knife microradiosurgery. Note the use of multiple small isocenters, providing conformal and selective coverage of the lesion with a 50 % prescription isodose line, limited irradiation of the anterior border of the tumor for preventing facial nerve injury, and avoidance of extending the 80 % isodose area to the intracanalicular part of the neoplasm

average amount of radiation energy delivered to a unit of the tumor volume (mJ/cm^3). The radiosurgical plan corresponding to current treatment standards and safety requirements, but providing the greatest possible UE, seems preferable because it provides greater probability of tumor shrinkage [10, 16, 18].

Safety Considerations

Low-dose GKS for skull base tumors provides optimal balance between good growth control and low risk of treatment-related morbidity, even for neoplasms of prominent size [4, 5, 23]. Additionally, use of multi-isocenter treatment with application of small isocenters provides a steep dose falloff outside the treated volume [21, 26, 29]. Even in relatively large skull base neoplasms, the described technique allows a gradient index far below 3, which is usually recommended for safe radiosurgical practice [3, 32].

To avoid complications, the maximum doses to specific functionally important structures should be kept within the safety range (Table 1). Particularly, excessive irradiation of the cranial nerves should be avoided. Although it is widely accepted that oculomotor, trochlear, and abducent nerves may safely tolerate doses up to 40 Gy [41], we prefer to keep their irradiation as low as possible. Therefore, if they are located within the target, which is not uncommon with cavernous sinus tumors, the treatment plan is preferably created in such a way that cranial nerves remain not covered by the high-dose irradiation area within a mass. A similar technique is used to protect the trigeminal nerve in the case of petroclival and Meckel's cave neoplasms.

Additionally, the intratumoral 80 % prescription isodose area should not extend to the parts of the lesion located in strictly confined areas (e.g., internal acoustic canal, superior orbital fissure) to avoid possible compression of the adjacent cranial nerves during the period of temporary enlargement of the neoplasm after irradiation. The latter is a well-described phenomenon after GKS of vestibular schwannomas. It has also been demonstrated with nonvestibular schwannomas [15] and pituitary adenomas [33]. It usually appears 6–9 months after irradiation and does not require treatment unless symptomatic.

In more than half of the patients with cranial nerve dysfunction after GKS, the neuropathy is caused not by irradiation of the nerves themselves but by its effects on the the brain stem, which is usually associated with edema [1, 5]. This point strongly supports the need for precise dose planning and prevention of the inadvertent excessive irradiation of the functionally important brain structures. Higher selectivity of GKS with more rapid falloff of the dose outside the target is associated with less risk of adverse reactions in adjacent tissues [20, 23, 31].

Table 1 Maximum safe irradiation doses for functionally important intracranial structures during GKS for benign skull base tumors

Anatomical structures	Maximum safe irradiation dose (Gy)
Brain stem	14
Cranial nerves III, IV, VI	20
Cranial nerves V, VII, VIII	12
Optic pathways	10
Unaffected venous sinuses	8
Cochlea	4

Evaluation and Correction of Distortion Artifacts on MR Images

Targeting accuracy has a significant effect on the outcome of GKS. Although in general MRI allows detailed characterization of the intracranial lesion and allows creation of a precise radiosurgical treatment plan, mislocalization errors caused by distortion of the images during their acquisition and/or stereotactic transformation are possible [20]. Fusion with "bone window" CT allows 3D evaluation and correction of distortion artifacts on MRI scans, which is particularly important for GKS in the vicinity of functionally important anatomical structures [16, 35–37]. For this purpose, after completing the treatment planning and calculating the radiosurgical parameters (CI, SI, HI, UE), several anatomical landmarks in the vicinity of the target are defined and their position on MRI compared to that on CT is checked in the axial, sagittal, and coronal planes. If a difference is identified, it is considered the result of MRI distortion artifacts. Therefore, coordinates of all isocenters are shifted in a measured distance along the *X*, *Y*, or *Z* axes to compensate for mislocalization error.

Clinical Results

During the last decade the described microradiosurgical treatment strategy was consistently applied in our clinic for GKS of benign skull base tumors. Among cases with at least 2 years of follow-up after treatment, 75 % of neoplasms demonstrated shrinkage, and in 47 % of lesions ≥50 % volume reduction was noted. Occasionally, it was accompanied by definite improvement of the affected neurological functions. Treatment-related complications were encountered in only 6 % of patients, and they were mainly related to transient cranial nerve palsy. Just 2 % of neoplasms showed regrowth after GKS.

Benign Meningioma

The results of GKS for 66 benign skull base meningiomas, which were followed 26–80 months after treatment, were reported recently [16]. At the time of radiosurgery, the volume of the lesion varied from 0.3 to 50.6 cm^3 (mean 6.6 cm^3). Tumor growth control was attained in 99 % of cases. Shrinkage of the neoplasm was marked in 82 % of patients. Tumor volume reduction of 50 % and more was noted in 23 % of cases. Treatment-related morbidity was limited to transient abducent nerve palsy in one patient with a cavernous sinus tumor.

Vestibular Schwannoma

From December 2002, a total of 260 consecutive patients with a vestibular schwannoma underwent GKS in our clinic [10, 12, 18]. At the time of treatment, the tumor volume varied from 0.1 to 9.0 cm^3 (mean 1.6 cm^3). More than 3 years of follow-up data after irradiation were available for 182 patients. Tumor growth control was attained in 98 % of cases. Shrinkage of the neoplasm was marked in 76 % of patients. Tumor volume reduction of 50 % and more was noted in 55 % of cases. Postoperative complications included deterioration of hearing in 8 % of patients and occasional mild vertigo during the period of temporary enlargement of the neoplasm after irradiation.

Nonvestibular Schwannoma

Four patients with abducent nerve schwannoma were followed 7–43 months after GKS [15]. At the time of radiosurgery, the volume of the neoplasm varied from 1.7 to 4.9 cm^3 (mean 3.0 cm^3). Tumor growth control was attained in all cases. Shrinkage of the neoplasm was marked in three patients, who were followed at least 12 months after irradiation. Treatment-related morbidity included deterioration of vision with transient amaurosis (one case), transient (two cases) and permanent (one case) abducent nerve palsy, and formation of the intratumoral cyst (one case), which demonstrated spontaneous regression during long-term follow-up.

Recently, we analyzed results of GKS in six patients with a facial nerve schwannoma who were followed for 6–72 months after treatment. Tumor shrinkage was noted in three cases. None of the neoplasms regrew after irradiation. Transient facial nerve palsy after irradiation was marked in two patients.

Sellar Tumors

The results of GKS on 89 pituitary adenomas invading the cavernous sinus that were followed for 24–76 months after treatment were reported [14]. There were 43 nonfunctional and 46 hormone-producing tumors. Growth control was attained in 97 % of cases. Shrinkage of the lesion was marked in 64 % of cases. In 80 % of patients with secreting pituitary adenomas, radiosurgery resulted in normalization or improvement of endocrinological function. Treatment-related morbidity included transitory deterioration of the extraocular movements in two patients.

The results of GKS on 18 craniopharyngiomas followed for 12–52 months after treatment were analyzed as well [45]. Tumor growth control was attained in 94 % of cases. Shrinkage of the lesion was marked in 72 % of patients. There were no cases of treatment-related morbidity.

It should be specifically emphasized that none of the patients with a sellar tumor experienced diabetes insipidus, new pituitary hormone deficit, or deterioration of visual function after GKS.

Cavernous Sinus Hemangiomas

Cavernous sinus hemangiomas are rare benign skull base neoplasms for which surgical treatment is extremely difficult owing to abundant vascularization. It was demonstrated, however, that radiosurgery can be effective in these cases [22, 43, 44]. From December 2002, six patients with cavernous sinus hemangioma underwent GKS in our clinic and were followed for 30–78 months thereafter. Shrinkage of the neoplasm was marked in all of them. Reduced tumor volume of >50 % was noted in five cases (83 %). No treatment-related morbidity was noted.

Other Applications of Robotic Gamma Knife Microradiosurgery

With some modification, the described principles of robotic Gamma Knife microradiosurgery can be applied to parenchymal brain tumors [17, 39]. It has also been used to manage trigeminal neuralgia [9] and other intractable pain syndromes [6, 8].

Future Perspectives

The advent of modern technology and introduction of the described microradiosurgical treatment principles may change the paradigm of GKS for benign skull base

neoplasms from attaining just tumor growth control to clinically meaningful reduction of lesion volume. The latter may lead to reversal of the neurological deficit, particularly that related to dysfunction of the cranial nerves. Further research should clarify optimal radiosurgical parameters for attaining such treatment goals with minimal risk of side effects and complications. Particularly, possible application of staged GKS for larger neoplasms requires thorough clinical evaluation.

Future advances of robotic Gamma Knife microradiosurgery will be definitely influenced by the development of new neuroimaging modalities and their application for treatment planning. Radiosurgical experience with functional MRI, diffusion-tensor imaging (DTI), and tractography has already demonstrated the high effectiveness of these methods in visualizing eloquent cortical areas and fiber tracts [24, 25, 34]. DTI is also helpful for identifying cranial nerves in cases of their being severely compressed by the tumor [38]. It may lead to prevention of excessive irradiation of functionally important anatomical structures and significantly increased treatment safety. Certainly, advanced MRI techniques can be effectively used with utilization of high-magnetic-field clinical scanners, which is usually considered unacceptable for GKS because of the high risk of distortion artifacts. Currently developing neuroimaging protocols directed at acquisition of geometrically accurate images may allow us to overcome this problem and pave the way for effective use of 3 T MRI for radiosurgical treatment planning [47].

The improved dose homogeneity and greater precision of GKS attained with available robotic devices may permit effective application of low-dose treatment to large-volume intracranial lesions [4, 5]. Nevertheless, the size of the neoplasm still represents the major limitation for radiosurgery [1, 2]. It should be noted, however, that large benign skull base tumors are frequently not suitable for total surgical resection because of the high risk of postoperative complications, particularly those related to injury of the cranial nerves. The best functional outcome in such cases can be attained with combined application of microneurosurgery and radiosurgery. Detailed 3D evaluation of the local neuroanatomy and treatment simulation within the Leksell GammaPlan may permit precise planning of combined management, with clear delineation of the part of the tumor amenable to safe resection and identification of the portion of the mass that is to be left in situ for subsequent irradiation.

Conclusion

The availability of robotic computer-aided devices for GKS led to significant changes in radiosurgical treatment strategy, particularly for benign skull base tumors. Application of the principles of Gamma Knife robotic microradiosurgery based on advanced neuroimaging and highly conformal and selective treatment planning is beneficial for patients, providing a high rate of tumor shrinkage and a low morbidity rate.

Conflict of Interest The authors declare that they have no conflict of interest.

References

1. Davidson L, Zada G, Yu C, Petrovich Z, Pagnini PG, Zee CS, Giannotta SL, Zelman V, Apuzzo MLJ (2009) Delayed toxicity from gamma knife radiosurgery to lesions in or adjacent to the brainstem. J Clin Neurosci 16:1139–1147
2. Flickinger JC (2002) Radiobiological and dosimetric considerations in stereotactic radiosurgery. In: Pollock BE (ed) Contemporary radiosurgery: technique and evaluation. Futura, Armonk, pp 37–52
3. Ganz JC (2011) Gamma Knife neurosurgery. Springer, Wien, pp 101–102
4. Ganz JC, Reda WA, Abdelkarim K (2009) Gamma Knife surgery of large meningiomas: early response to treatment. Acta Neurochir (Wien) 151:1–8
5. Ganz JC, Reda WA, Abdelkarim K (2009) Adverse radiation effects after Gamma Knife surgery in relation to dose and volume. Acta Neurochir (Wien) 151:9–19
6. Hayashi M, Taira T, Chernov M, Fukuoka S, Liscak R, Yu CP, Ho RTK, Regis J, Katayama Y, Kawakami Y, Hori T (2002) Gamma knife surgery for cancer pain – pituitary gland – stalk ablation: a multicenter prospective protocol since 2002. J Neurosurg 97(Suppl):433–437
7. Hayashi M, Chernov M, Izawa M, Iseki H, Hori T, Takakura K (2003) Robotized micro Gamma Knife surgery for 21st century. In: The 12th annual meeting of the Japanese Society of Stereotactic Radiosurgery: program and abstracts, Kyoto, Jun 21–22, 2003, p 35 (in Japanese)
8. Hayashi M, Taira T, Ochiai T, Chernov M, Takasu Y, Izawa M, Kouyama N, Tomida M, Tokumaru O, Katayama Y, Kawakami Y, Hori T, Takakura K (2005) Gamma knife surgery of the pituitary: new treatment for thalamic pain syndrome. J Neurosurg 102(Suppl):38–41
9. Hayashi M, Ochiai T, Murata N, Nakaya K, Izawa M, Chernov M, Hori T, Regis J, Takakura K (2006) Gamma knife surgery for essential trigeminal neuralgia: advantages in new treatment strategy with robotized micro-radiosurgery. In: Kondziolka D (ed) Radiosurgery, vol 6. Karger, Basel, pp 260–267
10. Hayashi M, Ochiai T, Nakaya K, Chernov M, Tamura N, Maruyama T, Yomo S, Izawa M, Hori T, Takakura K, Regis J (2006) Current treatment strategy for vestibular schwannoma: image-guided robotic microradiosurgery. J Neurosurg 105(Suppl):5–11
11. Hayashi M, Ochiai T, Nakaya K, Chernov M, Tamura N, Yomo S, Izawa M, Hori T, Takakura K, Regis J (2006) Image-guided microradiosurgery for skull base tumors: advantages of using gadolinium-enhanced constructive interference in steady-state imaging. J Neurosurg 105(Suppl):12–17
12. Hayashi M, Tamura N, Maruyama T, Nakaya K, Ochiai T, Chernov M, Yomo S, Anami H, Izawa M, Ono Y, Okada Y, Hori T, Takakura K (2010) Current treatment strategy of Gamma Knife surgery for vestibular schwannoma: image-guided and robotized microradiosurgery. In: McDermott MW (ed) Radiosurgery, vol 7. Karger, Basel, pp 175–188
13. Hayashi M, Tamura N, Nakaya K, Ochiai T, Chernov M, Yomo S, Anami H, Izawa M, Okada Y, Ono Y, Hori T, Takakura K (2010) Image-guided micro Gamma Knife surgery for skull-base tumors

to avoid underlying dysfunction of the surrounding vital structures using CISS with gadolinium enhancement. In: McDermott MW (ed) Radiosurgery, vol 7. Karger, Basel, pp 227–236
14. Hayashi M, Chernov M, Tamura N, Nagai M, Yomo S, Ochiai T, Amano K, Izawa M, Hori T, Muragaki Y, Iseki H, Okada Y, Takakura K (2010) Gamma Knife robotic microradiosurgery of pituitary adenomas invading the cavernous sinus: treatment concept and results in 89 cases. J Neurooncol 98:185–194
15. Hayashi M, Chernov M, Tamura N, Yomo S, Ochiai T, Nagai M, Tamura M, Izawa M, Muragaki Y, Iseki H, Okada Y, Takakura K (2010) Gamma Knife surgery for abducent nerve schwannoma: report of 4 cases. J Neurosurg 113(Suppl):136–143
16. Hayashi M, Chernov M, Tamura N, Izawa M, Muragaki Y, Iseki H, Okada Y, Takakura K (2011) Gamma Knife robotic microradiosurgery for benign skull base meningiomas: tumor shrinkage may depend on the amount of radiation energy delivered per lesion volume (unit energy). Stereotact Funct Neurosurg 89:6–16
17. Hayashi M, Chernov M, Tamura N, Tamura M, Izawa M, Muragaki Y, Iseki H, Okada Y (2011) "Donut's shape" radiosurgical treatment planning for large cystic metastatic brain tumors. Minim Invasive Neurosurg 54:286–289
18. Hayashi M, Chernov MF, Lipski SM, Tamura N, Yomo S, Horiba A, Tsuzuki S, Izawa M, Okada Y, Muragaki Y, Iseki H, Ivanov P, Regis J, Takakura K (2013) Do we really still need an open surgery for treatment of patients with vestibular schwannomas? Acta Neurochir Suppl 116:25–36 (present volume)
19. Hayashi M, Chernov MF, Tamura N, Yomo S, Tamura M, Horiba A, Izawa M, Muragaki Y, Iseki H, Okada Y, Ivanov P, Regis J, Takakura K (2013) Usefulness of the advanced neuroimaging protocol based on plain and gadolinium-enhanced constructive interference in steady state images for Gamma Knife radiosurgery and planning microsurgical procedures for skull base tumors. Acta Neurochir Suppl 116:167–178 (present volume)
20. Herman MG, McCullough EC (2002) Physical aspects of cranial stereotactic radiosurgery. In: Pollock BE (ed) Contemporary radiosurgery: technique and evaluation. Futura, Armonk, pp 17–36
21. Horstmann GA, Van Eck AT (2002) Gamma Knife model C with automatic positioning system and its impact on the treatment of vestibular schwannomas. J Neurosurg 97(5 Suppl):450–455
22. Ivanov P, Chernov M, Hayashi M, Nakaya K, Izawa M, Murata N, Kubo O, Ujiie H, Muragaki Y, Nakamura R, Iseki H, Hori T, Takakura K (2008) Low-dose gamma knife radiosurgery for cavernous sinus hemangioma: report of 3 cases and literature review. Minim Invasive Neurosurg 51:140–146
23. Karlsson B (2002) Dose selection and prediction of stereotactic radiosurgery outcomes. In: Pollock BE (ed) Contemporary radiosurgery: technique and evaluation. Futura, Armonk, pp 53–73
24. Koga T, Maruyama K, Igaki H, Tago M, Saito N (2009) The value of image coregistration during stereotactic radiosurgery. Acta Neurochir (Wien) 151:465–471
25. Koga T, Maruyama K, Kamada K, Ota T, Shin M, Itoh D, Kunii N, Ino K, Terahara A, Aoki S, Masutani Y, Saito N (2012) Outcomes of diffusion tensor tractography-integrated stereotactic radiosurgery. Int J Radiat Oncol Biol Phys 82:799–802
26. Kondziolka D, Maitz AH, Niranjan A, Flickinger JC, Lunsford LD (2002) An evaluation of the model C Gamma Knife with automatic patient positioning. Neurosurgery 50:429–432
27. Kuo JS, Yu C, Giannotta SL, Petrovich Z, Apuzzo MLJ (2004) The Leksell gamma knife model U versus model C: a quantitative comparison of radiosurgical treatment parameters. Neurosurgery 55:168–173
28. Levivier M, Massager N, Wikler D, Goldman S (2004) Modern multimodal neuroimaging for radiosurgery: the example of PET scan integration. Acta Neurochir Suppl 91:1–7
29. Lindquist C, Paddick I (2007) The Leksell Gamma Knife Perfexion and comparison with its Predecessors. Neurosurgery 61(3 Suppl):130–141
30. Massager N, Maris C, Nissim O, Devriendt D, Salmon I, Levivier M (2009) Experimental analysis of radiation dose distribution in radiosurgery: I. Dose hot spot inside target volume. Stereotact Funct Neurosurg 87:82–87
31. Massager N, Maris C, Nissim O, Devriendt D, Salmon I, Levivier M (2009) Experimental analysis of radiation dose distribution in radiosurgery: II. Dose fall-off outside the target volume. Stereotact Funct Neurosurg 87:137–142
32. Paddick I, Lippitz B (2006) A simple dose gradient measurement tool to complement the conformity index. J Neurosurg 105(Suppl): 194–201
33. Pamir MN, Kilic T, Belirgen M, Abacioglu U, Karabekiroglu N (2007) Pituitary adenomas treated with Gamma Knife radiosurgery: volumetric analysis of 100 cases with minimum 3 year follow-up. Neurosurgery 61:270–280
34. Pantelis E, Papadakis N, Verigos K, Stathochristopoulou I, Antypas C, Lekas L, Tzouras A, Georgiou E, Salvaras N (2010) Integration of functional MRI and white matter tractography in stereotactic radiosurgery clinical practice. Int J Radiat Oncol Biol Phys 82:257–267
35. Regis J, David P, Wikler D, Porcheron D, Levrier O (2004) Stereotactic mapping for radiosurgical treatment of vestibular schwannomas. Neurochirurgie 50:270–281 (in French)
36. Regis J, Hayashi M, Porcheron D, Delsanti C, Muracciole X, Peragut JC (2002) Impact of the model C and automatic positioning system on Gamma Knife radiosurgery: an evaluation in vestibular schwannomas. J Neurosurg 97(5 Suppl):588–591
37. Regis J, Tamura M, Guillot C, Yomo S, Muraciolle X, Nagaje M, Arka Y, Porcheron D (2009) Radiosurgery with the world's first fully robotized Leksell Gamma Knife PerfeXion in clinical use: a 200-patient prospective, randomized, controlled comparison with the Gamma Knife 4C. Neurosurgery 64:346–356
38. Roundy N, Delashaw JB, Cetas JS (2012) Preoperative identification of the facial nerve in patients with large cerebellopontine angle tumors using high-density diffusion tensor imaging. J Neurosurg 116:697–702
39. Takakura K, Hayashi M, Chernov MF, Tamura N, Izawa M, Okada Y, Tamura M, Muragaki Y, Iseki H (2013) Gamma Knife treatment strategy for metastatic brain tumors. Acta Neurochir Suppl 116:63–69 (present volume)
40. Takakura K, Iseki H, Chernov M, Hayashi M (2010) Development of a concept of Gamma Knife robotic microradiosurgery and its application in management of various intracranial diseases. In: IREIIMS achievement report 2005–2010. IREIIMS, Tokyo Women's Medical University, Tokyo, p 50
41. Tishler RB, Loeffler JS, Lunsford LD, Duma C, Alexander E III, Kooy HM, Flickinger JC (1993) Tolerance of cranial nerves of the cavernous sinus to radiosurgery. Int J Radiat Oncol Biol Phys 27:215–221
42. Tlachacova D, Schmitt M, Novotny J Jr, Novotny J, Majali M, Liscak R (2005) A comparison of the Gamma Knife model C and the automatic positioning system with Leksell model B. J Neurosurg 102(Suppl):25–28
43. Wang X, Mei G, Liu X, Dai J, Pan L, Wang E (2012) The role of stereotactic radiosurgery in cavernous sinus hemangiomas: a systematic review and meta-analysis. J Neurooncol 107:239–245
44. Yamamoto M, Kida Y, Fukuoka S, Iwai Y, Jokura H, Akabane A, Serizawa T (2010) Gamma Knife radiosurgery for hemangiomas of the cavernous sinus: a seven-institute study in Japan. J Neurosurg 112:772–779
45. Yomo S, Hayashi M, Chernov M, Tamura N, Izawa M, Okada Y, Hori T, Iseki H (2009) Stereotactic radiosurgery of residual and recurrent craniopharyngioma: new treatment concept using Leksell

Gamma Knife model C with automatic positioning system. Stereotact Funct Neurosurg 87:360–367

46. Yomo S, Tamura M, Carron R, Porcheron D, Regis J (2010) A quantitative comparison of radiosurgical treatment parameters in vestibular schwannomas: the Leksell Gamma Knife Perfexion versus model 4C. Acta Neurochir (Wien) 152:47–55
47. Zhang B, MacFadden D, Damyanovich AZ, Rieker M, Stainsby J, Bernstein M, Jaffray DA, Mikulis D, Menard C (2010) Development of a geometrically accurate imaging protocol at 3 Tesla MRI for stereotactic radiosurgery treatment planning. Phys Med Biol 55:6601–6615

Contemporary Role of Microsurgery, Radiosurgery, and Stereotactic Radiotherapy in the Management of Vestibular Schwannomas

Chung Ping Yu

Keywords Management • Radiosurgery • Stereotactic radiotherapy • Surgery • Vestibular schwannoma

Management of vestibular schwannomas (VSs) had been the neurosurgeons' responsibility since Cushing's time. This practice, however, has been changing during the last 10–15 years. With the blossoming of microsurgery, skull base approaches, radiosurgery, and stereotactic radiotherapy, neurosurgeons, otologists, and radiation oncologists are claiming a role as stakeholders, as individuals or as part of a multidisciplinary team. The good news is that expertise in each of the specialties pushes the standard of care to unprecedented heights with near-zero operative mortality. Facial nerve injury is a rare occurrence, and hearing preservation is a realistic goal. However, such high standards may not be achievable in communities where the case load, surgical expertise, and/or state-of-the-art technology are lacking.

Many treatment algorithms exist, with consensus in some areas but controversy in others. For example, most agree that small intracanalicular VSs in elderly patients can be actively observed. VSs with a diameter of <3 cm can be treated by microsurgery or radiosurgery, depending on the availability of expertise or by patient choice. In this volume of *Acta Neurochirurgica Supplement*, Hori and Maruyama [2] highlight the excellent microsurgical outcome, and Hayashi et al. [1] illustrate the class leading results of Gamma Knife surgery (GKS). Also, Polovnikov et al. [5], discussing multifraction stereotactic radiotherapy, provide an additional choice for patients who are not suitable candidates for open surgery or radiosurgery.

There is no consensus, however, on the management of large VSs with diameters equal or larger than 3 cm. Treatment options range from gross total resection (GTR), subtotal resection, combined microsurgery and GKS, and stereotactic radiotherapy alone. The proponents of GTR claimed excellent results, but facial nerve damage still occurred in 25 % even in the best hands [9]. To minimize this devastating complication, some authors recommend subtotal debulking and use radiosurgery as salvage. Recently, one center reported planned microsurgery and GKS for large VSs with excellent results: 92 % tumor control rate and only 6 % facial nerve injury [10]. We use a similarly planned microsurgery plus GKS approach for large VSs in a prospective study that has been ongoing since 1998. Additionally, it is the same neurosurgeon who performs the case selection, informed consent, microsurgery, and subsequent radiosurgery. In this era of super subspecialization, this same team approach is rather unique but has obvious advantages. Professor Lars Leksell, inventor of the Gamma Knife, already had this vision in 1983, stating that "the same individual can be a competent microsurgeon and also a stereotactic radiosurgeon" [3]. We presented our preliminary results of 63 cases of large VSs previously, reporting a mean 90 % volume reduction in all cases and zero mortality plus near-zero facial nerve injury [11].

Further controversy exists when radiation is used to treat VSs [4, 7]. We believe in healthy competition rather than monopoly by a single technology, be it GKS, LINAC, proton beam, or stereotactic radiotherapy. Nevertheless, based on having a larger volume of published data, particularly studies with long-term follow-up [6], GKS seems to lead the field.

Vestibular schwannoma is an uncommon disease. Its prevalence is around 1:100,000 per year. The mean number of neurosurgeons in developed countries, such as the European Union, is approximately 1:100,000 population [8]. In a closed community, this equates to one new case per neurosurgeon per year. Inevitably, some patients are managed by otologists or radiation oncologists, further diluting the case load per neurosurgeon. Without concentrated experience, young neurosurgeons may never achieve the level of surgical skills of the giants in the field, such as House, Samii, or Malis.

Vestibular schwannoma used to be a disease managed primarily by neurosurgeons. It remains a fact that no

C.P. Yu
Canossa Hospital,
1, Old Peak Road, Hong Kong, China
e-mail: chungpingyu@gmail.com

M.F. Chernov et al. (eds.), *Gamma Knife Neurosurgery in the Management of Intracranial Disorders*,
Acta Neurochirurgica Supplement, Vol. 116, DOI 10.1007/978-3-7091-1376-9_3, © Springer-Verlag Wien 2013

other specialist has the same depth of knowledge in clinical presentation, neuroimaging, neuroanatomy, surgical anatomy, operative approaches, stereotactic techniques, and treatment-related complications and how to deal with them. We propose that neurosurgeons take the leadership by setting up Centers of Excellence with an open and accountable database in their community. All neurosurgeons with interests in VS must have thorough training in the skull base approach, microsurgical technique, and intraoperative neuromonitoring as well as training in stereotactic radiosurgery, such as with the Gamma Knife. For complex cases such as large VSs in patients with serious co-morbid diseases, VS affecting the only hearing ear, and VS in patients with neurofibromatosis type 2, among others, engaging in dialogue with otologists, radiation oncologists, and patients themselves is crucial for selecting the best treatment options. With the team approach led by neurosurgeons, the 21st century can witness near-zero mortality and morbidity when managing VS of whatever size and medical complexity.

Conflict of Interest The author declares that he has no conflict of interest.

References

1. Hayashi M, Chernov MF, Lipski SM, Tamura N, Yomo S, Horiba A, Tsuzuki S, Izawa M, Okada Y, Muragaki Y, Iseki H, Ivanov P, Regis J, Takakura K (2013) Do we really still need an open surgery for treatment of patients with vestibular schwannomas? Acta Neurochir Suppl 116:25–36 (present volume)
2. Hori T, Maruyama T (2013) Whether gamma knife radiosurgery is really necessary for treatment of patients with vestibular schwannomas. Acta Neurochir Suppl 116:19–23 (present volume)
3. Leksell L (1983) Stereotactic radiosurgery. J Neurol Neurosurg Psychiatry 46:797–803
4. Murphy ES, Suh JH (2011) Radiotherapy for vestibular schwannomas: a critical review. Int J Radiat Oncol Biol Phys 79:985–997
5. Polovnikov ES, Anikeeva OY, Filatov PV, Krivoshapkin AL, Melidi EG, Gavronina OA, Gaitan AS, Bedny IV (2013) Stereotactic radiosurgery and hypofractionated stereotactic radiotherapy for management of vestibular schwannomas: initial experience with 17 cases. Acta Neurochir Suppl 116:37–44 (present volume)
6. Prasad D, Steiner M, Steiner L (2000) Gamma surgery for vestibular schwannoma. J Neurosurg 92:745–759
7. Radiosurgery Practice Guideline Initiative (2006) Stereotactic radiosurgery for patients with vestibular schwannomas: radiosurgery practice guideline report #4-06. http://www.irsa.org/AN%20Guideline.pdf. Accessed 30 Dec 2011
8. Reulen HJ, Hide RA, Bettag M, Bodosi M, Cunha E, Sa M (2009) A report on neurosurgical workforce in the countries of the EU and associated states. Task Force "Workforce Planning", UEMS Section of Neurosurgery. Acta Neurochir (Wien) 151:715–721
9. Samii M, Gerganov VM, Samii A (2010) Functional outcome after complete surgical removal of giant vestibular schwannomas. J Neurosurg 112:860–867
10. van de Langenberg R, Hanssens PE, van Overbeeke JJ, Verheul JB, Nelemans PJ, de Bondt BJ, Stokroos RJ (2011) Management of large vestibular schwannoma. Part I. Planned subtotal resection followed by Gamma Knife surgery: radiological and clinical aspects. J Neurosurg 115:875–884
11. Yu CP, Leung S, Poon C, Fan YW, Ng B, Chan J, Ho R (2010) Combined microsurgery plus Gamma Knife by the same team for large skull base tumors: towards zero mortality and near zero morbidity in 381 cases. In: Scientific program and schedule of events of the 15th international meeting of the Leksell Gamma Knife® Society, Athens, 16–20 May 2010, p 99

Whether Gamma Knife Radiosurgery Is Really Necessary for Treatment of Patients with Vestibular Schwannomas

Tomokatsu Hori and Takashi Maruyama

Abstract The present study was directed at establishing the role of Gamma Knife radiosurgery (GKS) in the management of vestibular schwannomas (VSs), particularly those that are large. We analyzed a consecutive series of 222 tumors operated on by a single neurosurgeon (T. Hori) at Tottori University (1981–1998) and Tokyo Women's Medical University (1998–2011). The surgical strategy for sporadic unilateral VSs was typically total or nearly total tumor removal with facial nerve preservation, whereas in some cases of neurofibromatosis type 2 intentional subtotal resection was performed. In all, 15 patients (8.6 %) in the series underwent GKS before (4 cases), after (9 cases), or before and after (2 cases) tumor removal. Overall, 211 patients (95 %) were cured by microsurgery alone. Of note, six patients underwent primary radiosurgery but were operated later on for regrowth of the neoplasm, and in four of them near-total resection led to good long-term tumor control. GKS was required in only 5 % of cases for management of residual VS or, more frequently, its regrowth. Radiosurgery resulted in volume reduction in one-third of these tumors. In other cases it stabilized the lesion, preventing further progression. Thus, GKS is considered a reasonable management option for residual or regrowing small VSs to obtain maximum tumor growth control after initially attempting complete surgical removal.

T. Hori (✉)
Department of Neurosurgery, Neurological Institute, Tokyo Women's Medical University, Tokyo, Japan

Moriyama Memorial Hospital, 7-12-7, Nishikasai, Edogawa-ku, Tokyo 134-0088, Japan
e-mail: thori@moriyamaikai.or.jp

T. Maruyama
Department of Neurosurgery, Neurological Institute, Tokyo Women's Medical University, Tokyo, Japan

Keywords Endoscopy • Gamma Knife • Koos stage • Retrosigmoid transmeatal approach • Vestibular schwannoma

Introduction

Many medical practitioners, including neurosurgeons, consider radiosurgery an option for treating patients with a vestibular schwannoma (VS). It is an effective alternative to open surgery. The technique might be helpful for improving tumor growth control after incomplete removal of large neoplasms and for small residual lesions [9, 10]. At present irradiation is frequently used for primary management of VSs of various sizes. Although its usefulness is advocated widely [4], the efficacy of stereotactic irradiation in such cases raises serious concerns. The present study focused on establishing the role of Gamma Knife radiosurgery (GKS) in the management of VS, particularly large ones by analyzing a consecutive series of such tumors operated on by a single surgeon (T. Hori).

Materials and Methods

The series included 222 patients with a VS. The initial 48 patients were treated surgically at Tottori University (1981–1998). None of these patients underwent GKS before or after tumor removal. The VS recurred in two of the patients in this group, and both underwent reoperation, which led to excellent long-term tumor control. Hence, the efficacy of radiosurgery in this cohort could not be analyzed. Among the subsequent 174 patients with a VS surgically treated at Tokyo Women's Medical University (1998–2011), 15 (8.6 %) underwent GKS before (4 cases), after (9 cases), or before and after (2 cases) tumor removal. Their clinical course was evaluated in the present study.

M.F. Chernov et al. (eds.), *Gamma Knife Neurosurgery in the Management of Intracranial Disorders*,
Acta Neurochirurgica Supplement, Vol. 116, DOI 10.1007/978-3-7091-1376-9_4, © Springer-Verlag Wien 2013

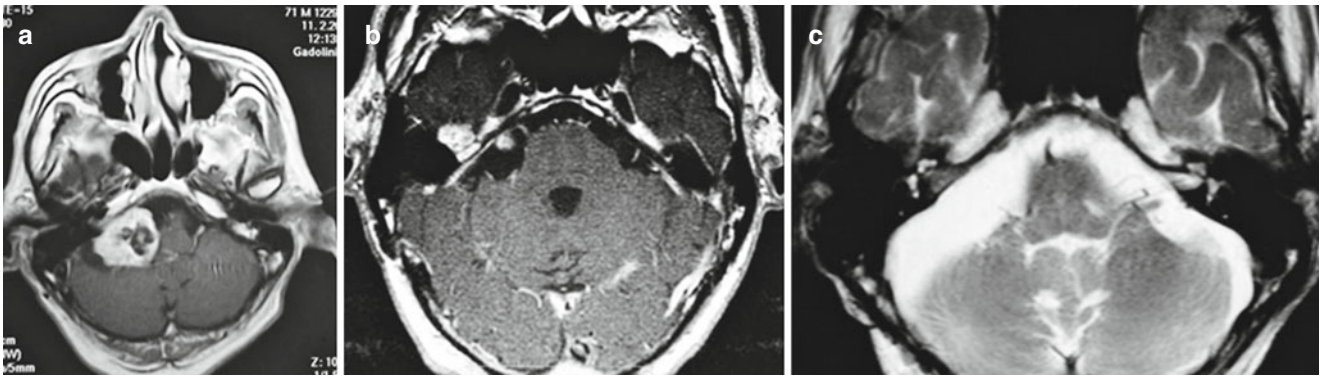

Fig. 1 Right-sided Koos stage IV tumor in a 71-year-old man (**a**). Initial near-total surgical resection was followed 5 years later by Gamma Knife surgery (GKS) when regrowth (**b**) was discovered. GKS resulted in reduction of the lesion volume (**c**)

There were six men and nine women (mean age 47.4 years). In all, 14 VSs were classified as Koos stage IV, and 1 VS was a Koos stage III tumor [6, 7]. The latter patient initially underwent GKS abroad, but there was subsequent tumor regrowth. In all cases, the lesion was removed via a retrosigmoid transmeatal approach with or without endoscopic assistance [5, 8]. The surgical strategy in 11 cases of sporadic unilateral VS was typically directed at total or near-total tumor removal with facial nerve preservation. The strategy differed slightly in four patients with neurofibromatosis type 2 (NF2), who underwent intentional subtotal resection. Nevertheless, the latter cases were included in the analyzed group because the efficacy of radiosurgery is considered similar in cases of sporadic VS and NF2 [4].

All of the patients were categorized into three groups according to time of GKS application with regard to surgery and the effectiveness of the irradiation.

1. GKS was performed after surgery for management of a residual or regrowing tumor, and it resulted in shrinkage of the tumor (three cases).
2. GKS was performed after surgery for management of a residual or regrowing tumor, and it resulted in stabilization of the tumor (six cases).
3. GKS was performed as the initial treatment, but the patient was later operated on because the tumor had increased in size (six cases).

All 15 patients were followed with regular clinical evaluations and yearly magnetic resonance imaging (MRI) to check the size and characteristics of the residual tumor.

Results

Group 1

If GKS of the residual or regrowing VS after the initial surgical resection resulted in shrinkage of the neoplasm, none of the lesions exhibited regrowth during subsequent follow-up.

Illustrative Case

A 71-year-old man presented with right-sided deafness. MRI disclosed a VS of Koos stage IV (Fig. 1). The retrosigmoid transmeatal approach was used to remove the tumor. Despite the large size of the neoplasm, the facial nerve was functionally preserved, and postoperative House-Brackmann grade 2 was noted. There was a small residual intrameatal lesion, which was followed by yearly MRI. At 5 years after surgery, it exhibited mild regrowth into the posterior and middle cranial fossae. After detailed discussion with the patient and his family, it was decided to perform GKS. Four years later the tumor showed definite size reduction, and there was no facial nerve dysfunction.

Group 2

If GKS of the residual or regrowing VS after initial surgical resection resulted in stabilization of the VS, none of these patients experienced regrowth of the lesion during subsequent follow-up (Fig. 2).

Group 3

At the time of primary radiosurgery, the group 3 patients typically had large tumors. One of the patients with regrowth of the neoplasm 2 years after GKS was initially operated on elsewhere, but there was progression of the lesion 1 year later. Reoperation was undertaken at our clinic. We performed the initial tumor removal in the other five patients.

In four cases near-total removal of the lesion was attained. None of the four, including one who had been operated on twice after the primary GKS, had further progression of the tumor (Fig. 3). In the other two patients, postoperative observation revealed regrowth of the residual neoplasm. It led to a

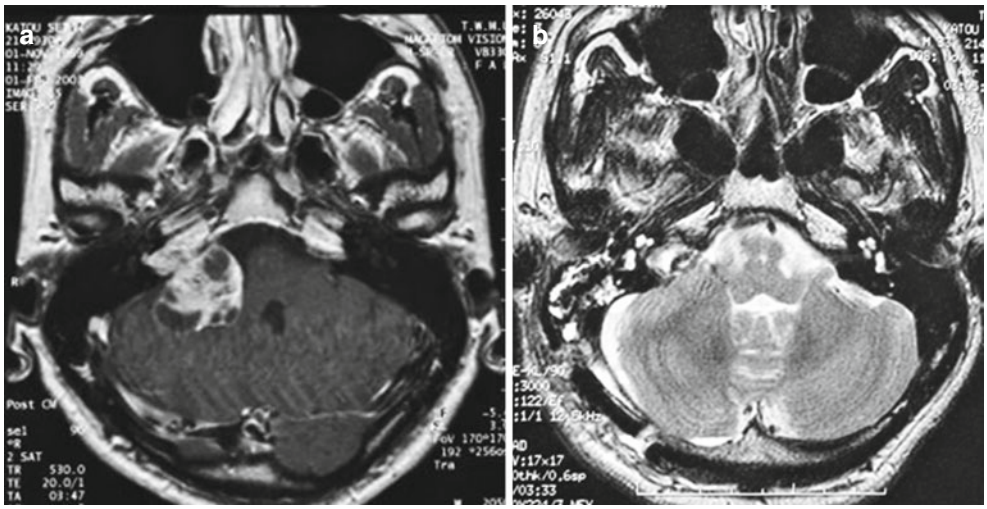

Fig. 2 Right-sided Koos stage IV tumor in a 33-year-old man (**a**). Initial near-total surgical resection was followed by GKS 2 years later after a neoplastic remnant was found to have infiltrated the pyramidal bone. GKS resulted in stabilization of the lesion (**b**)

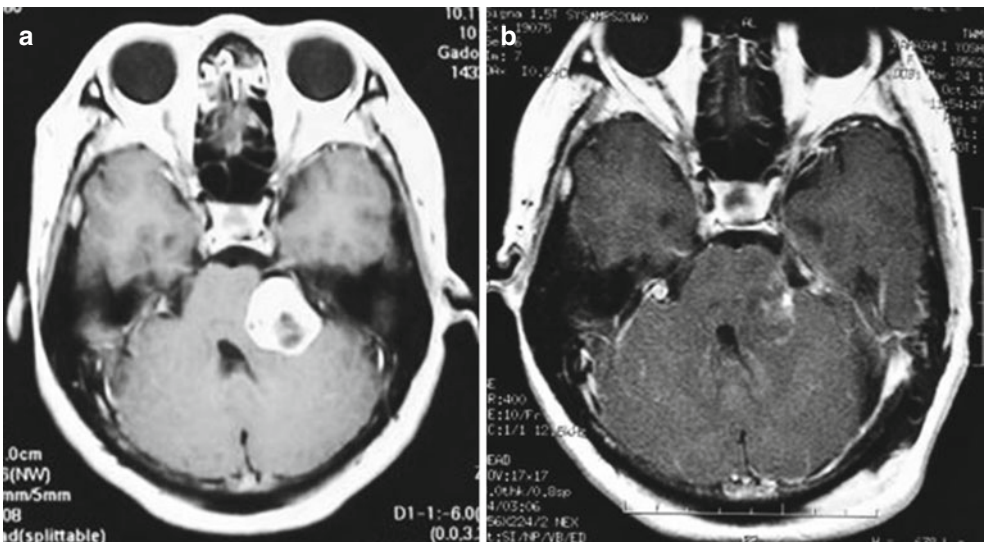

Fig. 3 Left-sided VS in a 42-year-old woman. Primary GKS was undertaken. Five years later the tumor had enlarged, reaching Koos stage IV (**a**). Near-total surgical resection was performed. No further regrowth was noted during the postoperative follow-up (**b**)

second GKS, which resulted in stabilization of the lesion in both cases.

Discussion

Hasegawa et al. [4] reported long-term outcomes in patients with VS after GKS and 10-year subsequent follow-up. It was found that if there was good tumor control during the initial 5 years after radiosurgery there is a minimal risk of further recurrence or the need for additional treatment. Hence, this interval may be the minimal limit of close clinical and radiological observation after stereotactic irradiation. In that series, there were no cases of delayed malignant transformation of the neoplasm. Because GKS was effective in the majority of patients over a prolonged period of time, it was suggested that such treatment is an acceptable alternative to microsurgical resection.

It should be mentioned, however, that in the same study the outcome depended on tumor size. Actuarial 10-year progression-free survival after GKS of a VS with volume of <10 cm^3 was 93 %, whereas in neoplasms with volume of 10 cm^3 and more it was 64%; this difference was statistically significant in both univariate ($P=0.0013$) and multivariate ($P=0.0054$) analyses [4]. It is evident that the large size of the tumor may preclude use of a sufficient radiation dose, which may lead to treatment failure. Of note, in the present series, tumors progressing after primary GKS (group 3) and requiring subsequent surgical resection usually were large at

the time of irradiation. Radiosurgery of large VSs is sometimes associated with a high risk of neurological deterioration, particularly impairment of cranial nerve function, during the period of temporary tumor enlargement. This is a well-recognized phenomenon, typically observed within 3–4 months after treatment. Hence, for patients with a Koos stage III or IV VS, microsurgery is a better option. In particular, indications for radiosurgical management of tumors compressing the brain stem are limited. Our strategy in such cases is total or near-total removal of the neoplasm, which corresponds well with the opinions of others [9, 12, 14].

The true efficacy of GKS regarding tumor growth control has not been definitively established for small VSs (Koos stage I or II). Several recent studies on conservative management of such neoplasms reported prolonged stability of their growth, particularly in cases of small intra-canalicular lesions. For example, Bakkouri et al. [1] reported results in 386 cases of unilateral VS, analyzing their progression and consequences of observational policy. The annual tumor growth rate was <1 mm/year in 58.6 % of patients, 1–3 mm/year in 29.2 %, and 3 mm/year or greater in 12.2 %. The growth rates of intrameatal (1.02 ± 1.8 mm/year) and extrameatal (1.40 ± 3.1 mm/year) neoplasms did not differ significantly, and no associations were found with sex, age, initial hearing status, or tumor grade. Taking these results into consideration, it seems that the true effectiveness of GKS for tumor control of small asymptomatic VSs can be established only in a randomized controlled study (RCT). Because an RCT has not yet been done, observation may be the method of choice for patients with a Koos stage I or II tumor if the neoplasm does not cause cranial nerve dysfunction.

In the presence of even a mild neurological deficit associated with a small lesion, however, initiation of treatment with radiosurgery or microsurgery is definitely reasonable to prevent further functional deterioration. Modern methodology and technical achievements have allowed application of GKS without risk of severe cranial nerve injury. The treatment usually results in stabilizing tumor growth or even a small reduction of its volume. However, there are also real disadvantages of stereotactic irradiation compared to microsurgery. Contemporary surgical equipment and meticulous technique frequently allow total or near-total removal of the VS, even its most peripheral intrameatal part [5, 8, 9, 12, 14]. Removing the bulk of the neoplasm makes adjuvant postoperative treatment unnecessary and in fact leads to cure. There are also several reports on malignant transformation of VSs after GKS or the occurrence of another tumor in the irradiated field [3, 13].

There is no doubt that, compared to microsurgery, GKS provides a better chance of preserving hearing and facial nerve function [8]. In 2005, Betchen et al. [2] reported long-term results of hearing preservation after VS removal. Of 142 patients deemed eligible, 38 (26.8 %) retained their hearing immediately postoperatively. Repeated testing at a mean follow-up of 7 years revealed functional hearing in 30 of 35 cases (85.7 %). In fact, the rate of postoperative hearing preservation in cases of VS depends on the size of the tumor, the level of preoperative hearing, and the skills of the surgeon [6, 7]. For small tumors it varies from 20 % to 70 %. However, even with large neoplasms some patients still have useful hearing, and in some of them it is preserved after tumor removal [5, 6, 8, 9, 12, 14]. In our series of 222 VS, the hearing preservation rate in eligible patients was 62.5 %, and the facial nerve was preserved in 90 %.

In the present study, all but one patient who underwent operation before or after GKS had a Koos stage IV tumor. If surgery was chosen as the primary treatment modality and for some reason the lesion was not totally removed, a "wait and see" policy with regular MRI examinations was the preferred follow-up. Radiosurgery was then applied immediately after detecting tumor regrowth, which frequently was found only after many years. Despite the typically small size of the lesion at the time of irradiation (usually <1.5 cm), its volume reduction after GKS was marked only in one-third of cases. Application of a second GKS was effective in two patients who had been operated on after failed primary radiosurgery and exhibited tumor progression after microsurgical removal.

Even if surgery was performed after failed primary radiosurgery, we tried to achieve complete resection. This goal is sometimes difficult to meet because of the presence of radiation-induced adhesions between the tumor and adjacent anatomical structures. In such cases, intentional subtotal removal of the lesion has been recommended [11]. In our opinion, however, total elimination of the neoplasm has a significant impact on its long-term control, which was achieved in four of six of our patients operated on after failed primary GKS.

The question, then, is whether GKS is really necessary for management of VS. In our opinion, it should be considered a reasonable management option for residual or regrowing small tumors to obtain the best possible growth control after the initial attempt at complete surgical resection. In fact, these cases are not uncommon—even when the operation is performed by experienced surgeons [9, 12, 14]. Nevertheless, in the present series, adjuvant or salvage radiosurgery was required in only 5 % of patients. The other 95 % were cured by microsurgery alone. Tumor removal should be considered a mainstream treatment option for VSs, particularly for large neoplasms. Our results support this statement.

Conclusion

In the presented consecutive series of 222 VSs surgically treated by a single neurosurgeon, 211 patients (95 %) were cured by microsurgery alone. Six patients underwent primary GKS but were later operated on for regrowth of the

neoplasm. In four of the six, near-total resection led to good long-term tumor control. Radiosurgery was required just in 5 % of our cases for management of residual or, more frequently, regrowing VS. GKS consistently resulted in good control of lesion progression, including two cases in which primary irradiation performed before tumor resection had failed.

Conflict of Interest The authors declare that they have no conflict of interest.

References

1. Bakkouri WE, Kania RE, Guichard JP, Lot G, Herman P, Huy PT (2009) Conservative management of 386 cases of unilateral vestibular schwannoma: tumor growth and consequences for treatment. J Neurosurg 110:662–669
2. Betchen SA, Walsh J, Post KD (2005) Long-term hearing preservation after surgery for vestibular schwannoma. J Neurosurg 102:6–9
3. Demetriades AK, Saunders N, Rose P, Fisher C, Rowe J, Tranter R, Hardwidge C (2010) Malignant transformation of acoustic neuroma/vestibular schwannoma 10 years after gamma knife stereotactic radiosurgery. Skull Base 20:381–387
4. Hasegawa T, Kida Y, Kobayashi T, Yoshimoto M, Mori Y, Yoshida J (2005) Long-term outcomes in patients with vestibular schwannomas treated using gamma knife surgery: 10-year follow up. J Neurosurg 102:10–16
5. Hori T, Okada Y, Maruyama T, Chernov M, Attia W (2006) Endoscope-controlled removal of intrameatal vestibular schwannomas. Minim Invasive Neurosurg 49:25–29
6. Koos WT (1988) Criteria for preservation of vestibulocochlear nerve function during microsurgical removal of acoustic neurinomas. Acta Neurochir (Wien) 92:55–66
7. Koos WT, Day JD, Matula C, Levy DI (1998) Neurotopographic considerations in the microsurgical treatment of small acoustic neurinomas. J Neurosurg 88:506–512
8. Maruyama T, Muragaki Y, Hori T (2006) Surgical technique for vestibular schwannoma. No Shinkei Geka 34:681–693 (in Japanese)
9. Park CK, Jung HW, Kim JE, Son YJ, Paek SH, Kim DG (2006) Therapeutic strategy for large vestibular schwannomas. J Neurooncol 77:167–171
10. Pollock BE, Lunsford LD, Flickinger JC, Clyde BL, Kondziolka D (1998) Vestibular schwannoma management. Part I: failed microsurgery and the role of delayed stereotactic radiosurgery. J Neurosurg 89:944–948
11. Pollock BE, Lunsford LD, Kondziolka D, Sekula R, Subach BR, Foote RL, Flickinger JC (1998) Vestibular schwannoma management. Part II: failed radiosurgery and the role of delayed microsurgery. J Neurosurg 89:949–955
12. Samii M, Gerganov VM, Samii A (2010) Functional outcome after complete surgical removal of giant vestibular schwannomas. J Neurosurg 112:860–867
13. Schmitt WR, Carlson ML, Giannini C, Driscoll CL, Link MJ (2011) Radiation-induced sarcoma in a large vestibular schwannoma following stereotactic radiosurgery: case report. Neurosurgery 68:E840–E846
14. Wanibuchi M, Fukushima T, McElveen JT Jr, Friedman AH (2009) Hearing preservation in surgery for large vestibular schwannomas. J Neurosurg 111:845–854

Do We Really Still Need an Open Surgery for Treatment of Patients with Vestibular Schwannomas?

Motohiro Hayashi, Mikhail F. Chernov, Samuel M. Lipski, Noriko Tamura, Shoji Yomo, Ayako Horiba, Shyunsuke Tsuzuki, Masahiro Izawa, Yoshikazu Okada, Yoshihiro Muragaki, Hiroshi Iseki, Pavel Ivanov, Jean Régis, and Kintomo Takakura

Abstract *Background*: Gamma Knife surgery (GKS) should be considered a standard treatment option for small and medium-sized vestibular schwannomas (VSs). It results in a tumor control rate similar to that seen with microsurgery and provides better preservation of facial nerve function and hearing.

Methods: From December 2002 to April 2011, a total of 260 patients with VS underwent GKS using Leksell Gamma Knife model 4C with an automatic positioning system. There were 30 Koos stage I tumors, 112 stage II, 100 stage III, and 18 stage IV. All patients were treated with the use of high-resolution magnetic resonance imaging; creation of the highly precise conformal and selective multi-isocenter dose planning with small collimators, carefully sparing adjacent cranial nerves of any excessive irradiation; and creation of a wide 80 % isodose area within the tumor while applying a low marginal dose (mean 11.9 Gy) at the 50 % isodose line.

Results: Among 182 patients who were followed for more than 3 years after treatment, the tumor control and shrinkage rates were 98.4 % and 76.4 %, respectively. Volume reduction of >50 % was marked in 54.9 % of VSs. Preservation of facial nerve function and hearing at the pretreatment level was noted in 97.8 % and 87.9 %, respectively. There was marked improvement of facial nerve function and hearing after GKS in 2.2 % and 3.8 %, respectively. There was no major morbidity.

Conclusion: Due to contemporary technological and methodological achievements GKS can be focused not only on growth control but on shrinking the VS, with possible reversal of the neurological deficit.

Keywords Gamma Knife surgery • Outcome • Treatment • Vestibular schwannoma

M. Hayashi (✉)
Department of Neurosurgery, Neurological Institute,
Tokyo Women's Medical University,
8-1 Kawada-cho, Shinjuku-ku, Tokyo162-8666, Japan

Faculty of Advanced Techno-Surgery,
Institute of Advanced Biomedical Engineering and Science,
Tokyo Women's Medical University, Tokyo, Japan

Saitama Gamma Knife Center, Sanai Hospital, Saitama, Japan
e-mail: gkrmoto@aol.com

M.F. Chernov, Y. Muragaki, H. Iseki, and K. Takakura
Department of Neurosurgery, Neurological Institute,
Tokyo Women's Medical University, Tokyo, Japan

Faculty of Advanced Techno-Surgery,
Institute of Advanced Biomedical Engineering and Science,
Tokyo Women's Medical University, Tokyo, Japan

S.M. Lipski
Department of Ear, Nose, and Throat, Tivoli University Hospital,
La Louviere, Belgium

N. Tamura, A. Horiba, S. Tsuzuki, M. Izawa, and Y. Okada
Department of Neurosurgery, Neurological Institute,
Tokyo Women's Medical University, Tokyo, Japan

S. Yomo
Saitama Gamma Knife Center, Sanai Hospital, Saitama, Japan

P. Ivanov
Radiosurgical Center, International Institute of the Biological Systems,
Saint Petersburg, Russia

J. Régis
Department of Functional and Stereotactic Neurosurgery,
Timone University Hospital, Marseille, France

Faculty of Advanced Techno-Surgery,
Institute of Advanced Biomedical Engineering and Science,
Tokyo Women's Medical University, Tokyo, Japan

Introduction

There are two main options for management of vestibular schwannomas (VSs): microsurgery and radiosurgery. In general, surgical resection is recommended first. However, during the last decade there is a gradual increase in the number of patients who are undergoing radiosurgery, particularly using Gamma Knife surgery (GKS) as the primary treatment

M.F. Chernov et al. (eds.), *Gamma Knife Neurosurgery in the Management of Intracranial Disorders*,
Acta Neurochirurgica Supplement, Vol. 116, DOI 10.1007/978-3-7091-1376-9_5, © Springer-Verlag Wien 2013

modality. If previously the main indication for stereotactic irradiation in cases of VS was advanced age or inability to perform craniotomy for any reason, nowadays many other factors influence the decisions of both the neurosurgeon and the patient.

The traditional objective of GKS in cases of VS is to control its growth while preserving neurological functions, particularly those related to adjacent cranial nerves. Multiple published reports have demonstrated >95 % tumor control rate. Although transient enlargement of the neoplasm is frequently observed at 6–12 months after irradiation, the lesions usually not only return to their pretreatment size but demonstrate some volume reduction during subsequent years. Compared to surgical resection, GKS definitely provides higher rates of preserving facial nerve function and hearing [14]. Moreover, with recent achievements in technology and neuroimaging, the main goal of contemporary radiosurgery is to achieve not only growth control but shrinkage of the intracranial neoplasm, which in turn may reverse the neurological deficit. Herein we report the details of our current GKS strategy in cases of VS and discuss the treatment results.

Materials and Methods

Leksell Gamma Knife model 4C with an automatic positioning system (APS) (Elekta Instruments AB, Stockholm, Sweden) was installed at the Tokyo Women's Medical University in December 2002, and until April 2011 a total of 260 patients with VS underwent radiosurgical treatment.

According to the Koos topographical classification (stages I through IV [11, 12]) 30 tumors (11.5 %) were stage I ("intracanalicular"), 112 (43.1 %) were stage II, 100 (38.5 %) were stage III, and 18 (6.9 %) were stage IV. At the time of GKS the mean maximum diameter of VS was 18.3 mm (range 8.2–33.7 mm), and its mean volume was 1.6 cm^3 (range 0.1–9.0 cm^3).

According to the House-Brackmann scale (grades 1–6 [10]), before GKS 214 patients (82.3 %) had grade 1 facial nerve function ("normal"), 22 (8.5 %) had grade 2, 14 (5.4 %) had grade 3, and 10 (3.8 %) had grade 4 or 5. According to the Gardner-Robertson classification (classes I–V [4]), before GKS 46 patients (17.7 %) had class I hearing ("good to excellent"), 54 (20.8 %) had class II, 64 (24.6 %) had class III, 28 (10.8 %) had class IV, and 68 (26.1 %) had class V.

From the whole cohort, 182 patients (70 %) were followed clinically and radiologically for more than 3 years after GKS.

Radiosurgical Technique

All patients were treated according to our concept of robotic Gamma Knife microradiosurgery [7, 8]. Of note: pretreatment simulation of GKS has recently been performed routinely in our practice using new functions ("Image merge" and "Preplan") available in the latest versions of Leksell GammaPlan (Elekta Instruments AB).

On the day of treatment, a Leksell G stereotactic frame (Elekta Instruments AB) was attached to the patient's head under local anesthesia. Computed tomography (CT) and magnetic resonance imaging (MRI) were performed routinely. Thin-sliced (slice thickness 1.0 mm) axial CT was used not only to evaluate the tumor but always included "bone window" images. In all cases, our original MRI protocol was used. Axial plain and gadolinium-enhanced constructive interference in steady state (CISS) images (slice thickness 0.5 mm), and axial modified time-of-flight (TOF) images (slice thickness 1.0 mm) were obtained. All neuroimaging data were exported to the Leksell GammaPlan. The CT and MR images were fused.

An original workspace was constructed in the GammaPlan for detailed 3D understanding of the interrelations between the VS and functionally important anatomical structures. The main emphasis during treatment planning was clear identification of the borders of the neoplasm and adjacent VII and VIII cranial nerves. They can be clearly distinguished with plain CISS images, which provide excellent visualization of the structures in the pontocerebellar cistern. Although it is difficult to define the anatomy within the internal acoustic canal (IAC) with those images, the problem can be resolved with the use of gadolinium-enhanced CISS images, on which the neoplasm becomes "lucid." Its distinction from the adjacent cranial nerves is thus possible. The fundus of the IAC can be effectively evaluated with fused "bone window" CT and CISS images. The modified TOF provides 3D understanding of the interrelations between the neoplasm and adjacent vessels.

Even with such advanced MRI protocol, delineation of the facial and vestibulocochlear nerves is often impossible for large tumors (Koos stages III and IV). Therefore, during treatment planning we tried to identify the origin of the neoplasm and differentiate three types of VS: those arising from the cochlear, superior vestibular, and inferior vestibular nerves. It is our opinion that this differentiation helps the surgeon predict the direction the adjacent cranial nerves shift during growth of the neoplasm. Therefore, even if they cannot be visualized directly, their location, particularly in the IAC, can be presumed and taken into consideration.

The treatment planning was carefully performed with a goal of attaining both conformal and selective coverage of the tumor with a 50 % isodose. The radiosurgical parameters in the present series of VSs are presented in Table 1.

Table 1 Treatment parameters during Gamma Knife surgery for vestibular schwannomas

Treatment parameters	Mean (range)
Target volume (cm^3)	1.96 (0.14–12.9)
Marginal dose (Gy)	11.9 (11–12)
No. of isocenters	18.5 (2–50)
Conformity index	0.94 (0.33–1.00)
Selectivity index	0.83 (0.26–1.00)
Energy delivered to tumor (mJ)	25.1 (1.8–126.4)
Unit energy delivered to tumor (mJ/cm^3)	16.8 (14.0–19.6)

All patients were treated with the Leksell Gamma Knife model 4C with automatic positioning system version 1.1 and 1.2 (Elekta Instruments AB, Stockholm, Sweden)

In cases of Koos stage III and IV neoplasms we intentionally avoided excessive irradiation of the anterior border of the tumor, where the facial and vestibulocochlear nerves were presumably located. After treatment planning was completed, the positions of the isocenters were visualized simultaneously and carefully checked once again. If some of them projected on the adjacent cranial nerve in its visualized or presumed position, the coordinates of this isocenter were corrected with 0.1 mm precision to avoid any coverage of the nerve. In this way we tried to put all isocenters only within the border of the neoplasm without involving other anatomical structures located nearby, particularly the anterior and inferior walls of the IAC.

Finally, the location of the 80 % isodose area was evaluated. If its volume or distribution within the tumor was considered insufficient, another low-weight isocenter was added to make the high-dose irradiation reach as much of the neoplasm as possible. However, in cases with preserved hearing we usually avoided extension of the 80% isodose area on the intracanalicular part of the lesion.

Results

Of 260 tumors, 246 (94.6 %) showed loss of central contrast enhancement on T1-weighted MRI scans within a median period of 6 months after GKS. Significant transient enlargement of the lesion (>2 mm in any dimension) was noted in 67 cases (25.8 %), although almost all of these neoplasms shrank to pretreatment size by 12 months after radiosurgery.

Among 182 patients who were followed for >3 years after treatment, tumor control and shrinkage rates were 98.4 % (179 cases) and 76.4 % (139 cases), respectively. Volume reduction of >50 % was marked in 54.9 % of the VSs (100 cases). In 178 patients (97.8 %), facial nerve function rate was preserved at the pretreatment level, and in 4 (2.2 %) patients it had improved. In 160 patients (87.9 %) hearing was preserved at the pretreatment level, and in 7 (3.8 %) patients it had improved.

Although some patients complained on mild vertigo during the period when the VS was temporarily enlarged after GKS, major posttreatment morbidity was not noted in the present series. No cases of hydrocephalus or trigeminal neuropathy were identified. Also there were no cases in which suggestive malignant transformation of the tumor was marked, although the length of follow-up was too short for reliable evaluation of this particular complication.

Illustrative Cases

Case 1

A 58-year-old woman developed a sudden episode of deafness. MRI disclosed right-sided VS (Koos stage I). Her hearing on the ipsilateral side corresponded to Gardner-Robertson class II. Facial nerve function was normal (House-Brackmann grade 1). The patient decided to undergo GKS. On the day of treatment, thin-sliced CT and MRI were performed under stereotactic conditions and a total of 280 images were transported to the Leksell GammaPlan. The dose planning is shown in Fig. 1. On the coronal view, it was clearly seen that the neoplasm was localized to the groove right under the horizontal bar (inferior vestibular groove). Therefore, it was thought to be an inferior vestibular schwannoma. On the axial view, facial and cochlear nerves were directly visualized in front of the lesion and were not included in the 50 % isodose area, which covered the neoplasm both conformally and selectively. At 6 years after GKS the tumor demonstrated approximately 30 % volume reduction, and there were no neurological deficits.

Case 2

A 70-year-old woman complained on progressive hearing disturbance. MRI demonstrated left-sided VS (Koos stage II). Her hearing on the ipsilateral side corresponded to Gardner-Robertson class IV, and facial nerve function was normal (House-Brackmann grade 1). We performed a simulation of the radiosurgical treatment using "Preplan" based on 360 thin-sliced MRI and "bone window" CT (Fig. 2, *upper*). Detailed analysis of images revealed that the tumor extended to the fundus and was destroying the inferior wall of the IAC. Therefore, the inferior vestibular groove was wider than usual. It was suspected that the neoplasm originated from the inferior vestibular nerve, so the facial nerve should be, presumably, shifted to the anterosuperior direction, whereas the cochlear nerve would be shifted anteriorly. Because the elderly patient had progressive hearing loss, it was decided to perform GKS despite the small size of the neoplasm. On the day of treatment, only CT was undertaken

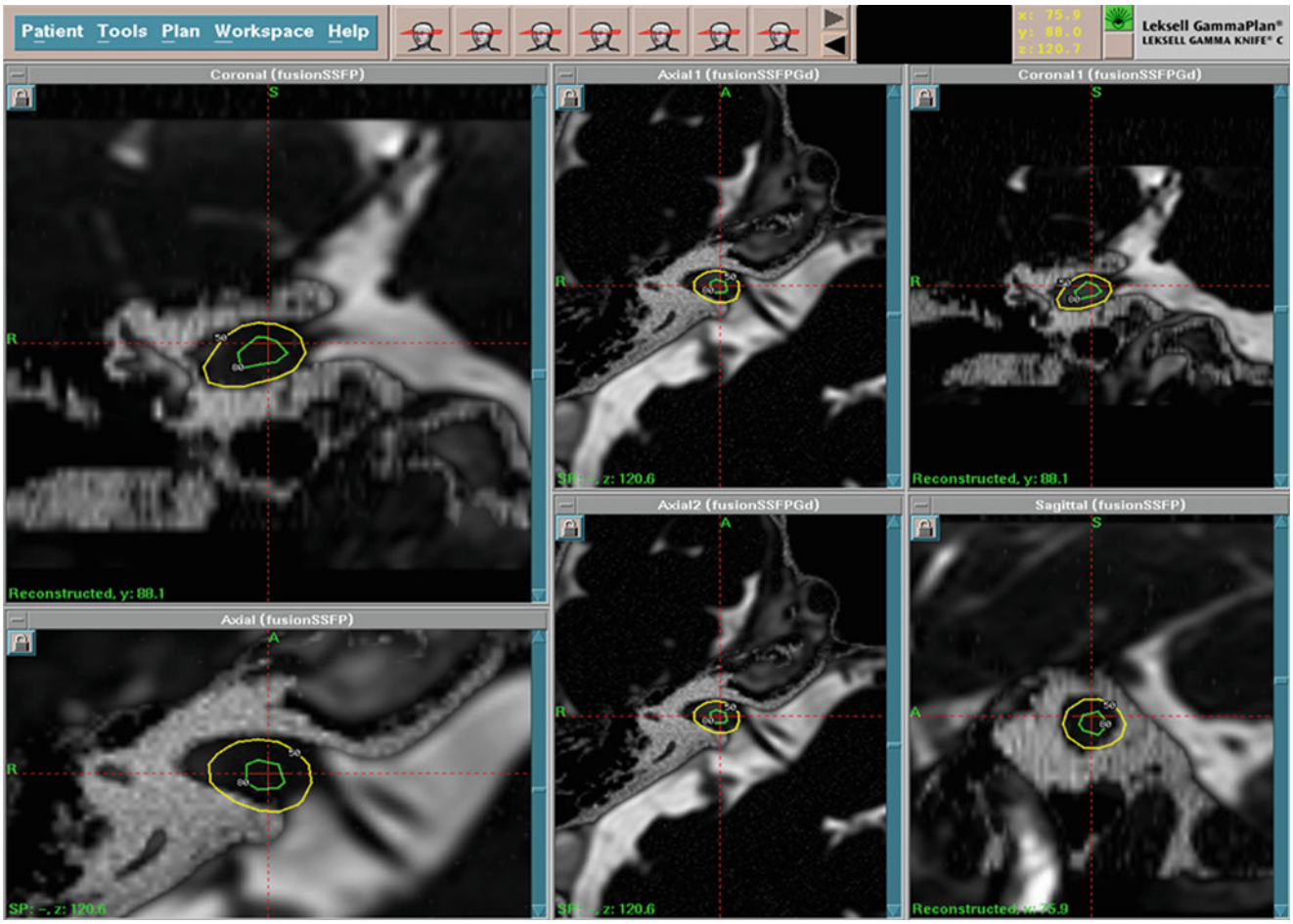

Fig. 1 Dose planning for a Koos stage I vestibular schwannoma based on fused plain constructive interference in steady state (CISS) and "bone window" computed tomography (CT) images. The facial and vestibulocochlear nerves could be clearly detected. *Yellow* and *green circles* correspond to 50 and 80 % isodose lines, respectively

(320 images) and was fused with the preplan MRI. Treatment planning was carefully done with a special emphasis on avoiding excessive irradiation of the anterosuperior portion of the tumor and excluding the anterosuperior wall of the IAC from projection of any isocenter. The lesion was conformally and selectively covered with a 50 % isodose (Fig. 2, *lower*), and an 80 % isodose area widely covered the bulk of the mass to increase the intratumoral irradiation dose.

Case 3

A 65-year-old woman had gradual hearing disturbance and balance problems. MRI revealed right-sided VS (Koos stage IV). Her hearing on the ipsilateral side corresponded to Gardner-Robertson class IV, and facial nerve function was normal (House-Brackmann grade 1). Because of a documented history of myocardial infarction, the patient decided to be treated with GKS instead of microsurgery. The treatment planning is shown in Fig. 3. The large size of the tumor prevented the facial and vestibulocochlear nerves to be visualized on axial plain CISS images, but use of gadolinium-enhanced CISS images made the lesion "lucid." The VII nerve could then be seen adhering to its anterior part, and the VIII nerve was visualized under it. The full extents of these nerves were excluded from the 50 % isodose area, which covered the tumor conformally and selectively (Fig. 4). The 80 % isodose area widely covered the bulk of the mass to increase the intratumoral irradiation dose.

Case 4

A 56-year-old woman had gradual hearing disturbance and balance problems. MRI revealed right-sided VS (Koos stage III). Her hearing on the ipsilateral side corresponded to Gardner-Robertson class III, and facial nerve function was normal (House-Brackmann grade 1). It was decided to perform GKS. On the day of treatment, thin-sliced CT and MRI were performed under stereotactic conditions and a total of 360 images were transported to the Leksell GammaPlan. The dose planning is shown in Fig. 5 (*upper*). Visualizing the facial

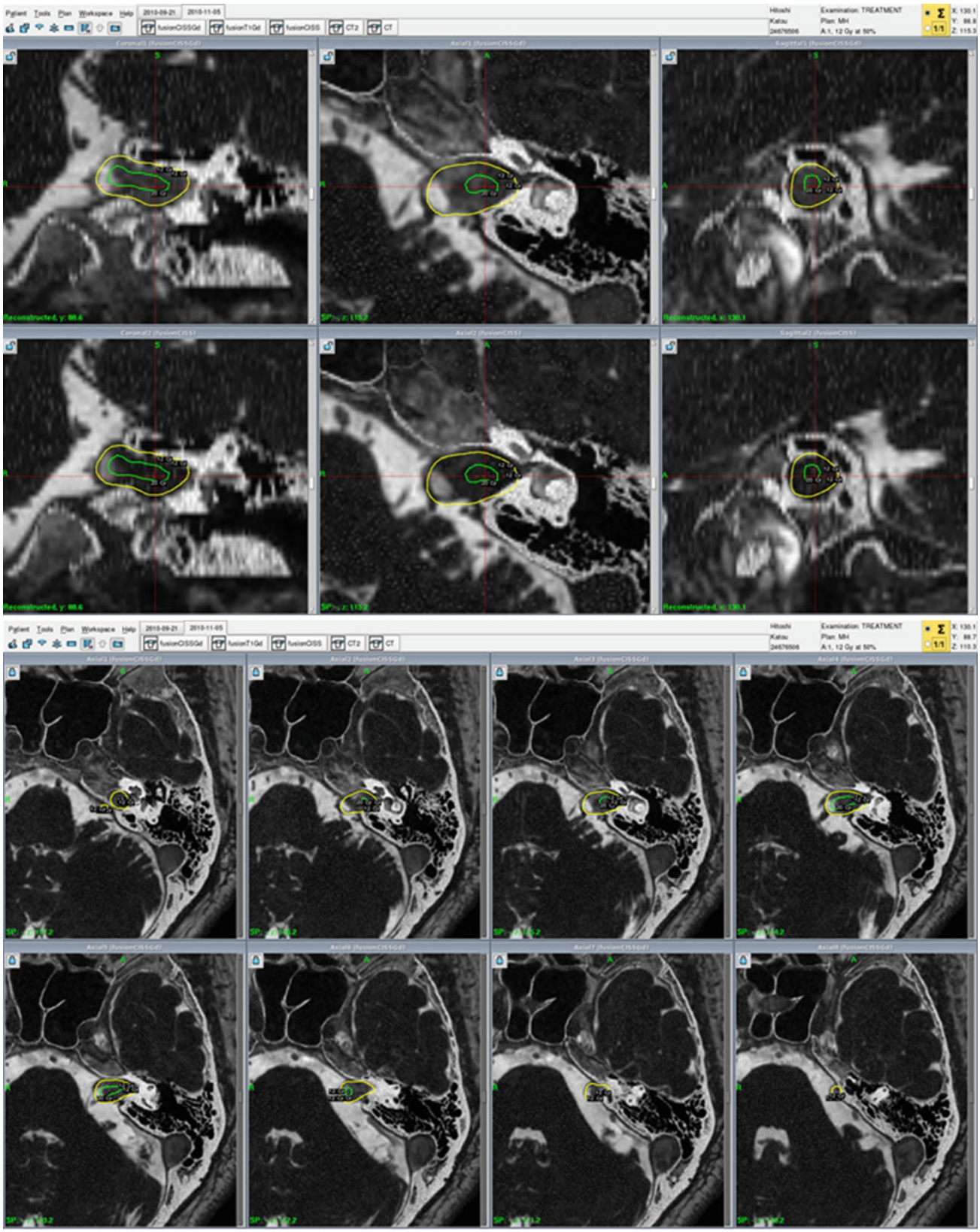

Fig. 2 Preplan simulation (*upper*) and Gamma Knife surgery (GKS) dose planning (*lower*) for a Koos stage II vestibular schwannoma based on fused gadolinium-enhanced CISS and "bone window" CT images. The inferior vestibular groove was enlarged by the tumor, which presumably corresponded to its origin. During treatment planning special emphasis was placed on excluding the facial nerve from the 50 % isodose area. *Yellow* and *green circles* correspond to 50 and 80 % isodose lines, respectively

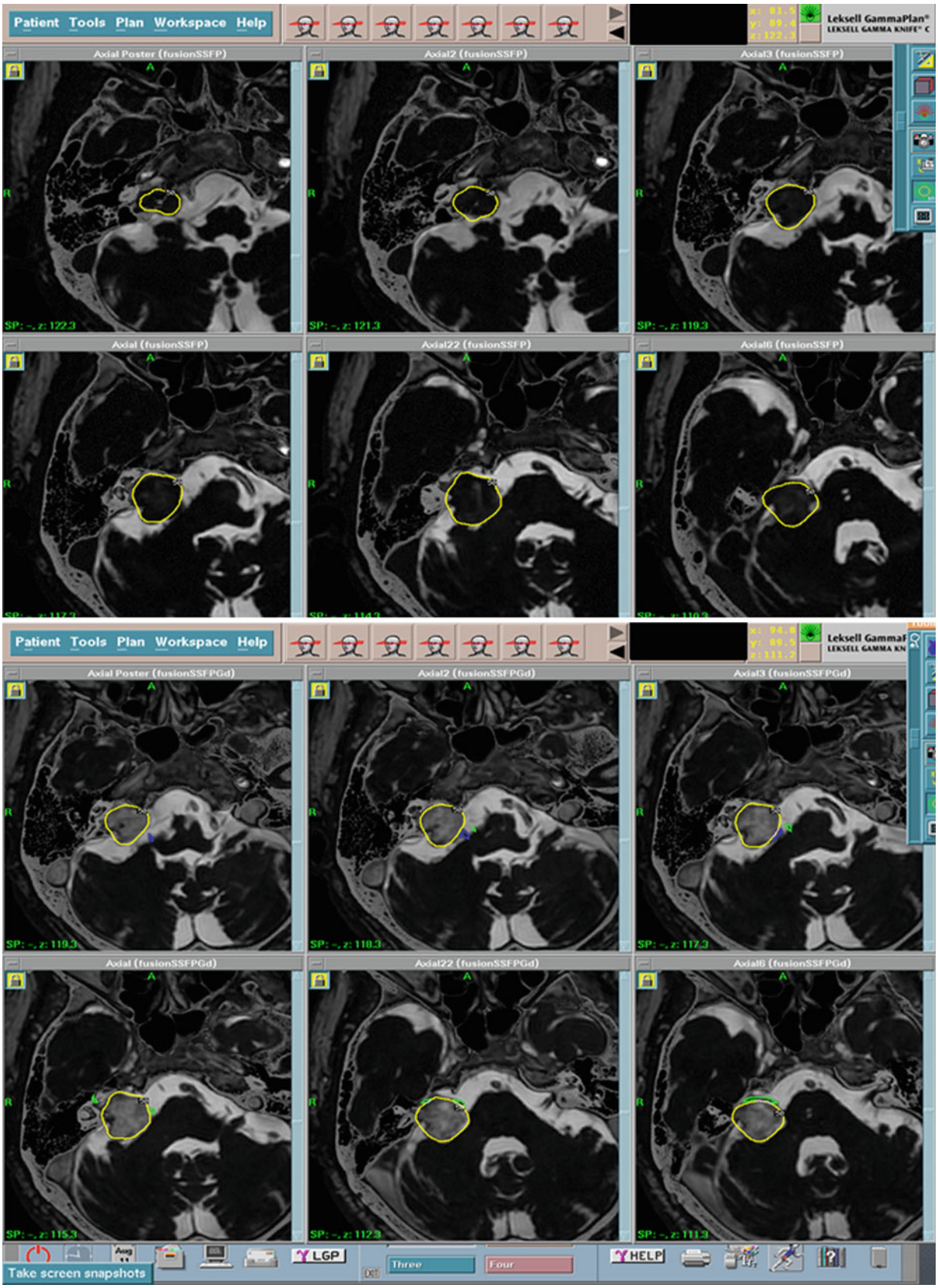

Fig. 3 GKS dose planning for a Koos stage IV vestibular schwannoma. Adjacent cranial nerves are not identifiable on plain CISS images (*upper*) but can be visualized on gadolinium-enhanced CISS images (*lower*), which made the tumor "lucid." *Yellow circles* correspond to the 50 % isodose line, whereas the delineated VII and VIII cranial nerves are marked *green and blue*, respectively

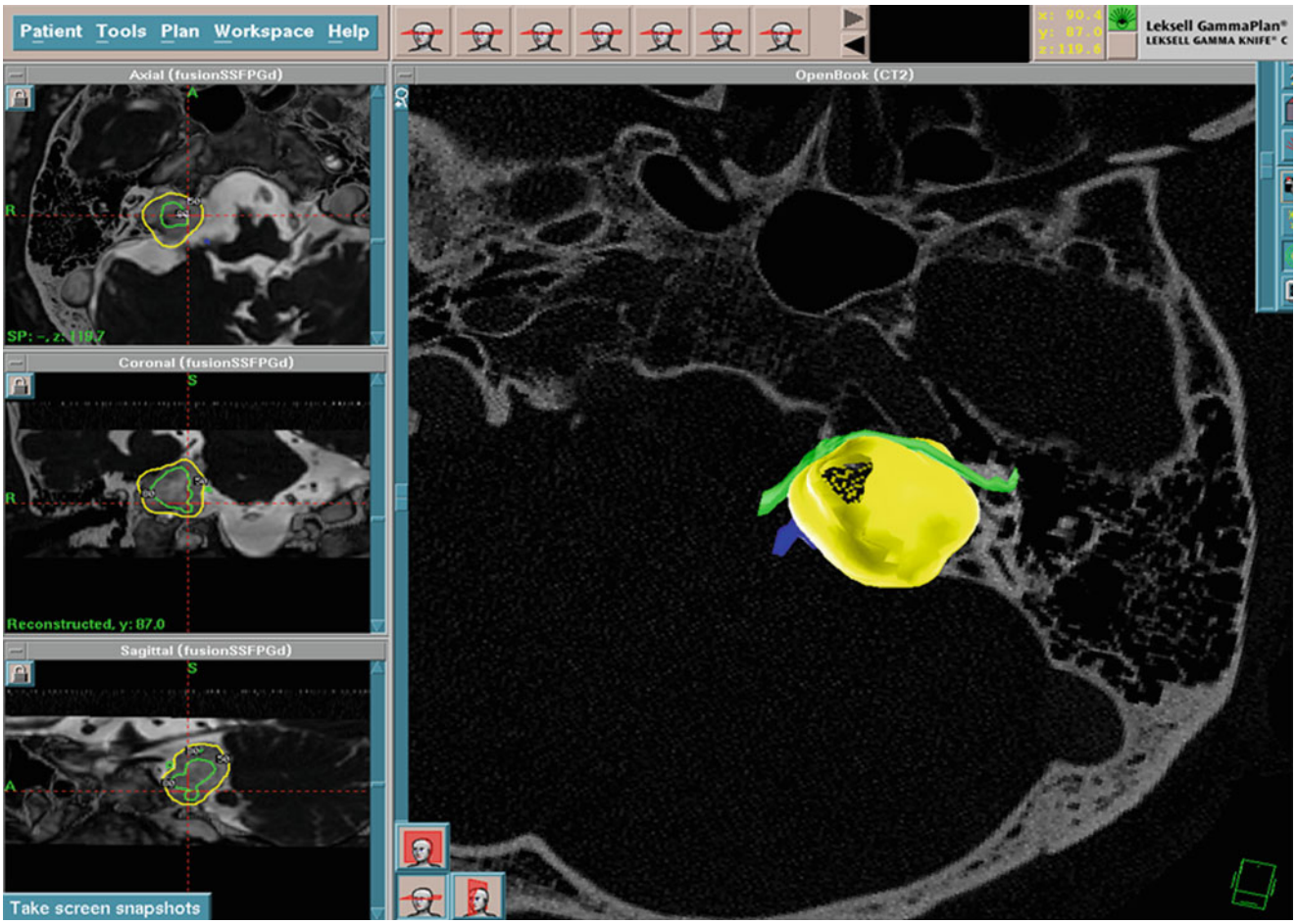

Fig. 4 Three-dimensional view of radiosurgical treatment planning for a Koos stage IV vestibular schwannoma. The entire extent of the facial (*green*) and vestibulocochlear (*blue*) nerves adjacent to the tumor are excluded from the 50 % isodose area (*yellow circles*)

and vestibulocochlear nerves on the axial view was difficult. Therefore, during treatment planning, emphasis was placed on avoiding excessive irradiation to the anteroinferior part of the tumor and eliminating projection of any isocenter on the anterior wall of the IAC. With this plan, the lesion was conformally and selectively covered with a 50 % isodose. The 80 % isodose area widely covered the bulk of the mass to increase the intratumoral irradiation dose. At 2 years after GKS there was a >50 % volume reduction of the VS (Fig. 5, *lower*), and it remains the same size at 8 years after treatment.

Discussion

The Koos topographical classification [11, 12] is useful during the decision-making process regarding optimal management of VS and evaluation of its risks and advantages. A tumor is characterized as stage I if it is located purely within the IAC, as stage II if it protrudes into the posterior cranial fossa from the internal acoustic meatus (IAM) but does not touch the brain stem, stage III if it reaches the brain stem but does not compress it, and stage IV if it compress the brain stem. Usually VSs of Koos stages II and III are considered the most suitable for radiosurgery. However, such treatment is now applied also to Koos stage I tumors, with the goal of having a better chance to preserve hearing than is attained with observation or microsurgery. Despite recent technical and methodological advances in GKS, the majority of patients with Koos stage IV neoplasms should be treated with surgical resection. Nevertheless, the present series included 18 such tumors, and their management was not accompanied by any major morbidity.

Volumetric Changes After Gamma Knife Radiosurgery for Vestibular Schwannoma

It is well established that low-dose radiosurgery for VS (marginal dose of 12–13 Gy at the 50 % isodose line) provides optimal results with regard to tumor growth control and

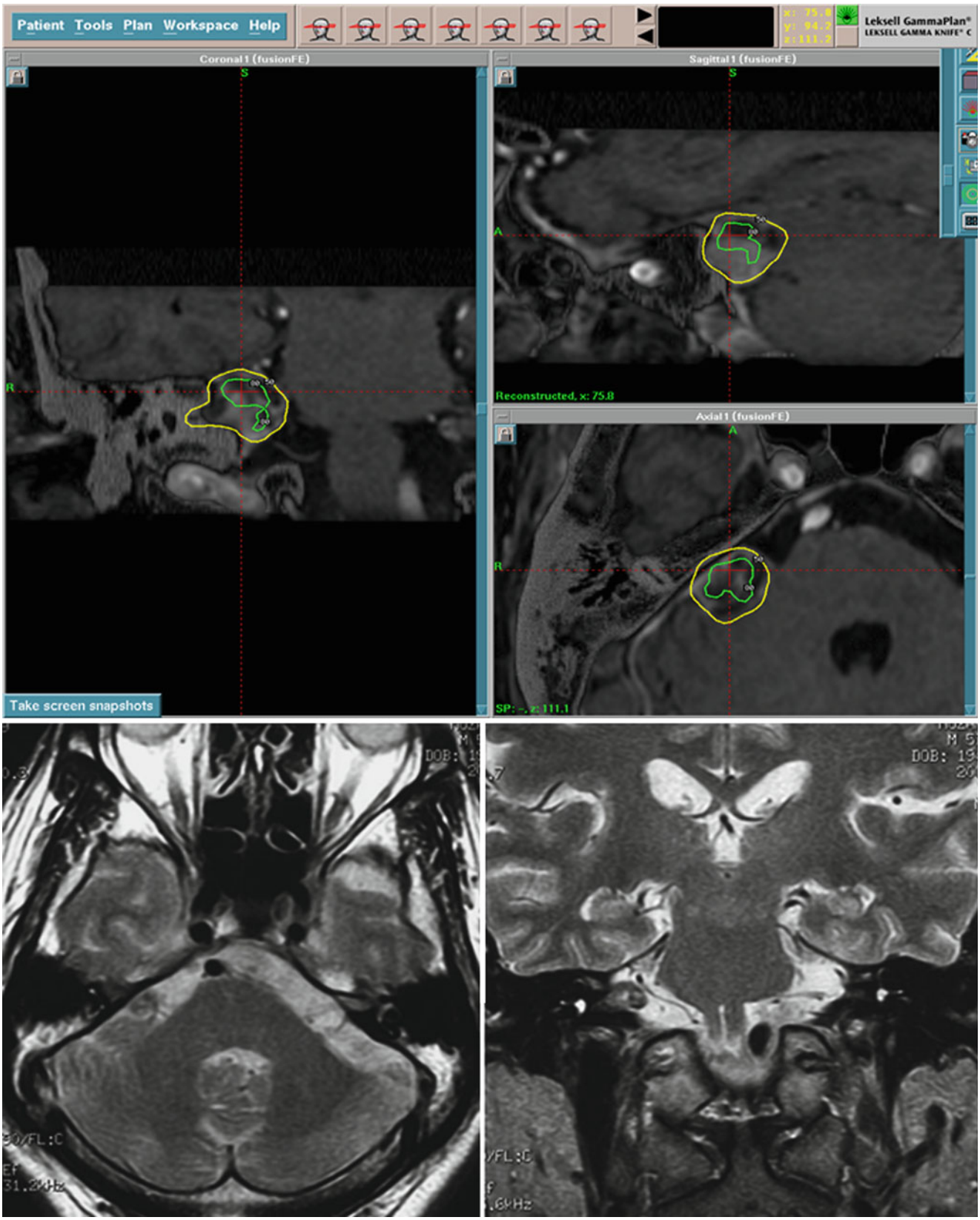

Fig. 5 GKS dose planning for a Koos stage III vestibular schwannoma (*upper*) and follow-up magnetic resonance imaging 2 years thereafter (*lower*). The treatment was based on fused gadolinium-enhanced T1-weighted and "bone window" CT images. The tumor was conformally and selectively covered with the 50 % isodose (*yellow circles*), whereas the 80 % isodose area widely occupied the bulk of the mass (*green circles*). After treatment the tumor demonstrated volume reduction of >50 %

preservation of facial nerve function and hearing. Multiple reports had been published to date highlighting the outcomes of such treatment. With few inconsistencies, the tumor control rate has varied in recent studies from 87 % to 97 % (average 93 %) [1–3, 5–7, 13, 18–20, 23, 27]. In our patients with short- to medium-term follow-up it was 98.4 %. Of note, even in series reporting posttreatment observation of >10 years, tumor control rates were 91–97 % [5, 13]. It was suggested that if no regrowth of VS is evident during the first 3 years after GKS the probability of its long-term growth control is high [6, 18].

Nevertheless, it should be clearly recognized that 14.4–41.0 % of VSs show transient enlargement after radiosurgery [7, 18, 20, 27]. This phenomenon was observed in 25.8 % of our patients. It usually appears 6–9 months after treatment and is typically accompanied by loss of central contrast enhancement, which is encountered in 70–84 % of tumors [1, 7, 18]. Pollock [20] investigated transiently enlarged VSs after GKS and found loss of central enhancement in 93 % of the cases. These changes are caused by subacute inflammation induced by irradiation, and in most cases both contrast enhancement of the lesion and its size return to the pretreatment level within a few subsequent months [18, 27].

Three patterns of volumetric changes of VS after radiosurgery are usually mentioned [20]: transient enlargement (57 % of cases), stabilization of size (29 %), and continuous growth (14 %). Less attention is devoted to possible shrinkage of the neoplasm, although its rate was 60 % at 5 years in one study [14] and 70 % at 10 years in another [5]. In the present series, it was seemingly even greater as 76.4 % of our patients demonstrated shrinkage of VS during short- to medium-term follow-up after GKS. Also, in more than half of the tumors volume reduction of >50 % was noted, which is considered clinically significant.

Cranial Nerves Function After Gamma Knife Radiosurgery for Vestibular Schwannoma

When GKS is compared with microsurgery, the postoperative complication rate—e.g., facial nerve dysfunction and hearing disturbances—should always be taken into consideration.

If currently recommended marginal irradiation doses of 12–13 Gy are used, temporary or permanent treatment-related dysfunction of the VII cranial nerve after GKS for VS can be avoided in 99 % of cases. This figure corresponds to the results obtained in the present series: There was no deterioration of facial nerve function after treatment in any of the patients. Tamura et al. [25] reported better preservation of lacrimal function with radiosurgery than with microsurgery. These results are reflected in a comparative evaluation of the patients' quality of life after treatment of VS, which also demonstrated the superiority of GKS [16].

Results on hearing preservation after radiosurgery for VS are controversial. Combs et al. [2] preserved hearing in 55 % of 27 VS patients at 9 years after LINAC-based treatment, whereas the rate after GKS varies from 63 % to 84 % (average 75 %) [3, 5, 7, 13, 15, 19, 23, 27]. It was demonstrated that hearing preservation rate can be improved from 70 % to 84 % if the maximum dose to the tumor is lowered from 26 to 20 Gy [27]. Based on detailed evaluation of the treatment planning, Massager et al. [15] reported that a large lesion volume in the IAC and high integrated dose to the neoplasm have negative associations with hearing preservation. In concordance, Paek et al. [19] identified hearing deterioration more frequently in patients with high irradiation dose to the cochlea and emphasized that an excessive dose to the intracanalicular part of the VS could have a negative impact on hearing preservation. Excellent radiosurgical results in cases of intracanalicular VS (Koos stage I) have been reported, particularly among patients who presented with tinnitus and serviceable hearing, with a hearing preservation rate of >90 % [3, 6, 13]. In the present series of tumors of various sizes, the hearing preservation rate was 87.9 %. It seems that low-dose GKS is sufficiently safe and provides a high probability of hearing preservation in patients with a VS. Hence, this treatment can be recommended even in patients with neurofibromatosis type 2 and an unfavorable prognosis for hearing preservation after observation or surgery.

Analysis of the series of patients with VS treated at Tokyo Women's Medical University by Maruyama et al. [14] revealed a higher preservation rate for facial nerve function and hearing after GKS than after microsurgery. However, restoration of the preexisting neurological deficit was not investigated and its possible resolution remained unclear. In the present study, improvement of the function of cranial nerves VII and VIII was demonstrated in 2.2 % and 3.8 % of patients, respectively, during short- to medium-term follow-up after GKS.

Radiosurgery for large VSs (Koos stages III and IV) is associated with a higher rate of posttreatment neurological deterioration, particularly, trigeminal neuropathy. The latter is sometimes considered a consequence of the temporary tumor enlargement after irradiation, but the 2–5 % incidence of this complication seems low when seen in relation to the rate of volumetric changes [5, 13, 19, 20, 23]. There were no disturbances of the V cranial nerve in the present series despite a significant proportion of large tumors and rather frequent observation of temporary enlargement of the lesion after treatment. Therefore, inadvertent inclusion of the trigeminal nerve in the irradiation field seems a more likely cause of that complication.

Recent Advances in Gamma Knife Equipment and Neuroimaging Modalities

During recent years GKS equipment has undergone significant technological upgrading. Conventional manual procedures were replaced by fully automatic robotic devices, such as the APS and PerfeXion (Elekta Instruments AB), which provide 0.1 mm preciseness of radiation delivery. Additionally, computer-aided manipulations significantly reduced the risk of human error and, correspondingly, increased treatment safety [8, 21, 26].

These technical changes were accompanied by the development of advanced methods in diagnostic radiology. Previously, GKS for VS was usually depended on conventional gadolinium-enhanced T1-weighted images. Those ones provide sufficient information regarding the anatomical interrelations between tumor, brain stem, and cerebellum but do not permit visualization of the VII and VIII cranial nerves. Hence, these nerves were at risk of being inadvertently included in the irradiation field. In fact, the desire to preserve the cranial nerves and avoid posttreatment neuropathy was one of the main reason for wide introduction of low-dose radiosurgery for VS. High precision treatment planning requires detailed understanding of neuroanatomy, which can be attained at present with advanced neuroimaging protocols.

Currently available thin-sliced CISS images provide clear visualization of the facial and vestibulocochlear nerves, which allows their preservation by avoiding excessive irradiation during radiosurgical treatment [9, 17, 22]. In cases of small VSs (Koos stages I and II), cerebrospinal fluid separates the neoplasm and brain stem, which permits for the surgeon to visualize clearly the intracisternal part of the nerves [9, 17, 22]. Even with 1.5 T MR scanners, the components of the VIII cranial nerve (cochlear, superior vestibular, inferior vestibular) can be differentiated. GammaPlan provides 3D visualization, so the course of the nerve can be followed from the brain stem to the internal auditory meatus (IAM). When visualization of the intracanalicular part of the cranial nerves is limited by the IAC being occupied by tumor, the problem can be effectively resolved with the use of gadolinium-enhanced CISS images, which make the neoplasm "lucid" and in many cases permit tracking the nerves to the most peripheral part [24]. Additionally, fusion of MRI and "bone window" CT images within the GammaPlan allows identification of such landmarks as the facial notch, which runs from the IAM to geniculate ganglia. As result, the whole length of the intracanalicular cranial nerves can be clearly delineated even if the tumor reaches the fundus, which is not uncommon. Being experienced with such neuroimaging technique, we strongly advocate it for detailed visualization of the anatomical structures adjacent to the VS. In contrast, gadolinium-enhanced T1-weighted imaging may cause partial enhancement of the IAC content and preclude its detailed differentiation. Therefore we do not recommend its use for radiosurgical treatment planning.

Concept of Robotic Gamma Knife Microradiosurgery

The concept of robotic Gamma Knife microradiosurgery was developed by us when the Leksell Gamma Knife model 4C with APS became available to our practice (December 2002). It is based on high-resolution neuroimaging protocol that permits detailed understanding of the neuroanatomy in the vicinity to the target, and use of computer-aided device (APS) that provides 0.1 mm treatment preciseness and significantly facilitates multi-isocenter radiosurgery [7, 8]. According to our treatment strategy, the dose planning is conformal and selective, preserving all adjacent functionally important anatomical structures, particularly the cranial nerves, by protecting them from excessive irradiation. Such treatment goals are not new in radiosurgery, but only the availability of the upgraded equipment and advanced neuroimaging modalities made possible reliable incorporation of these principles into routine everyday clinical practice.

We apply the marginal dose at the 50 % isodose line and consistently place special emphasis on wider distribution of the 80 % isodose area within the tumor. Sometimes a small low-weighted isocenter is added to increase the area of higher irradiation inside the mass, consequently maximizing the integrated dose delivered to the lesion. A new parameter, the unit energy (mJ/cm^3), has been established to allow comparison of the treatment plans. It is linearly associated with the mean intratumoral dose and reflects the average amount of radiation energy delivered to a unit of tumor volume. In our current practice, unit energy is calculated routinely and recorded in a prospectively maintained database. Retrospective analysis of the conventional GKS technique for VSs revealed an average value of approximately 15 mJ/cm^3, whereas in the present series with application of the described treatment strategy it was greater (mean 16.8 mJ/cm^3). We believe that it is a possible reason for the rather high tumor shrinkage rate and significant prominence of volume reduction attained in our patients after treatment. In fact, variations of the unit energy may make a difference in effectiveness of radiosurgery in patients treated with similar doses at the tumor margins.

It should be noted that in some of our patients the tumor volume reduction after GKS was accompanied by improved facial nerve function and even hearing. These changes might have been caused by elimination of nerve compression due to the tumor pressing against the walls of the IAM or IAC. It can be hypothesized that such functional recovery is more likely in cases with shorter duration and lesser severity of symptoms, lower Koos stage of the VS, and less filling of the IAC by the tumor. This important issue should be evaluated in further studies.

New Goals and Challenges of Gamma Knife Radiosurgery for Vestibular Schwannoma

The results of the present study strongly suggest that meticulous treatment planning—optimal dose selection, conformal and selective tumor coverage, prevention of the excessive irradiation of adjacent anatomical structures, homogeneous intratumoral dose distribution—is directly related to improved radiosurgical outcomes. Based on the above-mentioned treatment considerations, we suggest that the goals of GKS for VSs be expanded, and should not be limited to controlling the growth of the neoplasm and preserving neurological functions but also be focused on reducing lesion volume (preferably early), restoring the neurological functions (particularly that related to cranial nerves), and eliminating the risk of further tumor progression.

To attain such objectives, GKS should be considered not just a radiation treatment but a microsurgical procedure. Neurosurgeons dealing with radiosurgical methods should use their best efforts to create precise treatment planning using the same microsurgical principles that are applied during tumor resection under an operating microscope. Thus, all functionally important anatomical structures should be spared and the lesion treated as aggressively as possible to achieve the maximum treatment effect with minimal risk of postoperative complications. Of course, detailed knowledge of neuroanatomy, neurophysiology, and neurosurgery (!) is absolutely necessary. Currently available GKS equipment and neuroimaging modalities allow us to attain such treatment standards, but their importance still requires understanding and acceptance by radiosurgical practitioners.

A number of reports have advocated fractionated stereotactic radiotherapy as the safest method for preserving neurological functions during management of VSs. In contrast, we think that contemporary radiosurgery provides optimal treatment conformity and selectivity as well as sufficient homogeneity of irradiation dose distribution within the lesion, which better corresponds to microsurgical principles of the management of benign tumors.

Conclusions

Recent technological and methodological achievements in radiosurgery and neuroimaging may result in changing the main goals of GKS for VSs. Whereas previously the treatment was directed at controlling tumor growth and preserving neurological functions, it is now possible to reduce the volume of the neoplasm and restore the neurological functions, particularly related to cranial nerves. In the present series, 54.9 % of patients demonstrated tumor shrinkage of >50 % during short- to medium-term follow-up. Nevertheless, radiosurgery of large VSs compressing the brain stem is still a significant challenge because of the risk of neurological deterioration, mainly during the period of temporary enlargement of the neoplasm at 6–12 months after treatment. These patients should preferably undergo microsurgical tumor resection.

Acknowledgment Drs. Pavel Ivanov and Samuel M. Lipski had training fellowships in the Gamma Knife Unit of the Tokyo Women's Medical University from May to September 2007 and from October to November 2009, respectively.

Conflict of Interest The authors declare that they have no conflict of interest.

References

1. Chung WY, Liu KD, Shiau CY, Wu HM, Wang LW, Guo WY, Ho DM, Pan DH (2005) Gamma knife surgery for vestibular schwannoma: 10-year experience of 195 cases. J Neurosurg 102(Suppl): 87–96
2. Combs SE, Thilmann C, Debus J, Schulz-Ertner D (2006) Long-term outcome of stereotactic radiosurgery (SRS) in patients with acoustic neuromas. Int J Radiat Oncol Biol Phys 64:1341–1347
3. Gabert K, Regis J, Delsanti C, Roche PH, Facon F, Tamura M, Pellet W, Thomassin JM (2004) Preserving hearing function after Gamma Knife radiosurgery for unilateral vestibular schwannoma. Neurochirurgie 50:350–357 (in French)
4. Gardner G, Robertson JH (1988) Hearing preservation in unilateral acoustic neuroma surgery. Ann Otol Rhinol Laryngol 97:55–66
5. Hasegawa T, Fujitani S, Katsumata S, Kida Y, Yoshimoto M, Koike J (2005) Stereotactic radiosurgery for vestibular schwannomas: analysis of 317 patients followed more than 5 years. Neurosurgery 57:257–265
6. Hasegawa T, Kida Y, Kobayashi T, Yoshimoto M, Mori Y, Yoshida J (2005) Long-term outcomes in patients with vestibular schwannomas treated using gamma knife surgery: 10-year follow up. J Neurosurg 102:10–16
7. Hayashi M, Ochiai T, Nakaya K, Chernov M, Tamura N, Maruyama T, Yomo S, Izawa M, Hori T, Takakura K, Regis J (2006) Current treatment strategy for vestibular schwannoma: image-guided robotic microradiosurgery. J Neurosurg 105(Suppl):5–11
8. Hayashi M, Tamura N, Maruyama T, Nakaya K, Ochiai T, Chernov M, Yomo S, Anami H, Izawa M, Ono Y, Okada Y, Hori T, Takakura K (2010) Current treatment strategy of Gamma Knife

surgery for vestibular schwannoma: image-guided and robotized microradiosurgery. In: McDermott MW (ed) Radiosurgery, vol 7. Karger, Basel, pp 175–188
9. Held P, Fellner C, Seitz J, Graf S, Fellner F, Strutz J (1999) The value of T2(*)-weighted MR images for the diagnosis of acoustic neuromas. Eur J Radiol 30:237–244
10. House WF, Brackmann DE (1985) Facial nerve grading system. Otolaryngol Head Neck Surg 93:184–193
11. Koos WT (1988) Criteria for preservation of vestibulocochlear nerve function during microsurgical removal of acoustic neurinomas. Acta Neurochir (Wien) 92:55–66
12. Koos WT, Day JD, Matula C, Levy DI (1998) Neurotopographic considerations in the microsurgical treatment of small acoustic neurinomas. J Neurosurg 88:506–512
13. Lunsford LD, Niranjan A, Flickinger JC, Maitz A, Kondziolka D (2005) Radiosurgery of vestibular schwannomas: summary of experience in 829 cases. J Neurosurg 102(Suppl):195–199
14. Maruyama T, Muragaki Y, Hori T (2006) Surgical technique for vestibular schwannoma. No Shinkei Geka 34:681–693 (in Japanese)
15. Massager N, Nissim O, Delbrouck C, Devriendt D, David P, Desmedt F, Wikler D, Hassid S, Brotchi J, Levivier M (2006) Role of intracanalicular volumetric and dosimetric parameters on hearing preservation after vestibular schwannoma radiosurgery. Int J Radiat Oncol Biol Phys 64:1331–1340
16. Myrseth E, Moller P, Pedersen PH, Vassbotn FS, Wentzel-Larsen T, Lund-Johansen M (2005) Vestibular schwannomas: clinical results and quality of life after microsurgery or gamma knife radiosurgery. Neurosurgery 56:927–935
17. Naganawa S, Koshikawa T, Fukatsu H, Ishigaki T, Fukuta T (2001) MR cisternography of the cerebellopontine angle: comparison of three-dimensional fast asymmetrical spin-echo and three-dimensional constructive interference in the steady-state sequences. AJNR Am J Neuroradiol 22:1179–1185
18. Nakamura H, Jokura H, Takahashi K, Boku N, Akabane A, Yoshimoto T (2000) Serial follow-up MR imaging after gamma knife radiosurgery for vestibular schwannoma. AJNR Am J Neuroradiol 21:1540–1546
19. Paek SH, Chung HT, Jeong SS, Park CK, Kim CY, Kim JE, Kim DG, Jung HW (2005) Hearing preservation after gamma knife stereotactic radiosurgery of vestibular schwannoma. Cancer 104:580–590
20. Pollock BE (2006) Management of vestibular schwannomas that enlarge after stereotactic radiosurgery: treatment recommendations based on a 15 year experience. Neurosurgery 58:241–248
21. Regis J, Hayashi M, Porcheron D, Delsanti C, Muracciole X, Peragut JC (2002) Impact of the model C and Automatic Positioning System on gamma knife radiosurgery: an evaluation in vestibular schwannomas. J Neurosurg 97(5 Suppl):588–591
22. Regis J, David P, Wikler D, Porcheron D, Levrier O (2004) Stereotactic mapping for radiosurgical treatment of vestibular schwannomas. Neurochirurgie 50:270–281 (in French)
23. Rowe JG, Radatz MW, Walton L, Hampshire A, Seaman S, Kemeny AA (2003) Gamma knife stereotactic radiosurgery for unilateral acoustic neuromas. J Neurol Neurosurg Psychiatry 74:1536–1542
24. Shigematsu Y, Korogi Y, Hirai T, Okuda T, Ikushima I, Sugahara T, Liang L, Takahashi M (1999) Contrast-enhanced CISS MRI of vestibular schwannomas: phantom and clinical studies. J Comput Assist Tomogr 23:224–231
25. Tamura M, Murata N, Hayashi M, Regis J (2004) Injury of the lacrimal component of the nervus intermedius function after radiosurgery versus microsurgery. Neurochirurgie 50:338–344
26. Tlachacova D, Schmitt M, Novotny J Jr, Novotny J, Majali M, Liscak R (2005) A comparison of the gamma knife model C and the automatic positioning system with Leksell model B. J Neurosurg 102(Suppl):25–28
27. van Eck AT, Horstmann GA (2005) Increased preservation of functional hearing after gamma knife surgery for vestibular schwannoma. J Neurosurg 102(Suppl):204–206

Stereotactic Radiosurgery and Hypofractionated Stereotactic Radiotherapy for Management of Vestibular Schwannomas: Initial Experience with 17 Cases

Evgeniy S. Polovnikov, Olga Y. Anikeeva, Petr V. Filatov, Aleksey L. Krivoshapkin, Evstafiy G. Melidi, Oksana A. Gavronina, Aleksey S. Gaitan, and Igor V. Bedny

Abstract *Background*: Nowadays radiation treatment of patients with vestibular schwannomas (VSs) applied either as stereotactic radiosurgery (SRS) or stereotactic radiotherapy (SRT) represents a real alternative to surgical tumor resection.

Methods: During 2010–2011, 17 consecutive patients (19–75 years old) with a VS underwent treatment with SRS or SRT in our center. Microsurgery was initially offered in all cases but was declined for various reasons. Five lesions recurred after the initial partial resection. Two other patients with neurofibromatosis type 2 underwent initial surgery for a large tumor on the contralateral side and had the only hearing ear on the side of the remaining neoplasm. Three elderly persons had somatic problems that were too severe for them to undergo craniotomy. Five small tumors without brain stem compression underwent single-fraction SRS (12.0–12.5 Gy at the 80 % isodose line). Other patients, mainly with large neoplasms that caused brain stem compression, were treated with hypofractionated SRT (five or six daily fractions at a dose of 4.5–5.0 Gy each). Treatment was performed with a dedicated linear accelerator (Elekta Axesse). Various stereotactic fixation devices were used: Leksell G frame, noninvasive HeadFIX frame, reinforced thermoplastic masks.

Results: No adverse reactions or complications were seen in any case. Within 3 months after treatment three tumors demonstrated shrinkage accompanied by improvement of the neurological functions.

Conclusion: Radiation treatment, particularly hypofractionated SRT, can be safely applied even for large VSs that cause brain stem compression and are accompanied by prominent neurological symptoms.

Keywords Radiosurgery • Stereotactic radiotherapy • Vestibular schwannoma

Introduction

Vestibular schwannoma (VS) is a benign neoplasm originating from the Schwann cells covering vestibular portions of the VIII cranial nerve. It accounts for 5–10 % of all primary intracranial tumors and holds third place among such lesions [7, 11]. The majority of VSs are sporadic, although it is common in patients with neurofibromatosis (NF) types 1 and 2. In NF2 patients, bilateral lesions are typical. Usually schwannomas do not infiltrate the surrounding tissue but cause more or less severe compression. Malignant VSs are rare.

The growth rate of VS is on average 1–2 mm per year but may be as much as 20 mm per year. The clinical symptoms and signs mainly correspond to the size of the lesion and stage of the disease. The tumor usually manifests clinically with ipsilateral hearing loss or tinnitus, which are typical for intracanalicular VS. As the size of the neoplasm increases, it extends into the cerebellopontine cistern, which usually is accompanied by the appearance of ataxia and dysfunction of the facial and trigeminal nerves. Further growth may result in brain stem compression with corresponding symptoms and in the development of occlusive hydrocephalus.

For a long time surgery was the only option for management of VSs. Even now it is still advocated by many neurosurgeons, particularly when confronted with a large neoplasm. Despite the development of microsurgical techniques and advanced intraoperative neurophysiological methods, surgery for a VS represents a significant challenge [3, 6]. Even removal of small tumors carries the risk of hearing and facial nerve function loss. On the other hand, the current

E.S. Polovnikov, P.V. Filatov, and I.V. Bedny
Center of Radiosurgery and Radiotherapy,
Meshalkin Research Institute of Circulation Pathology,
Novosibirsk, Russian Federation

O.Y. Anikeeva (✉)
Center of Radiosurgery and Radiotherapy,
Meshalkin Research Institute of Circulation Pathology,
Rechkunovskaya str.15, Novosibirsk, Russian Federation
e-mail: sibradiolog@list.ru

A.L. Krivoshapkin, E.G. Melidi, O.A. Gavronina, and A.S. Gaitan
Center of Neurosurgery,
Meshalkin Research Institute of Circulation Pathology,
Novosibirsk, Russian Federation

M.F. Chernov et al. (eds.), *Gamma Knife Neurosurgery in the Management of Intracranial Disorders*,
Acta Neurochirurgica Supplement, Vol. 116, DOI 10.1007/978-3-7091-1376-9_6, © Springer-Verlag Wien 2013

availability of advanced imaging systems and image-guided devices for stereotactic radiosurgery (SRS) and radiotherapy (SRT) provides an opportunity for effective and safe irradiation of VSs. Particularly, dedicated linear accelerators (LINACs) allow us to treat tumors of any size, including the large ones that cause brain stem compression and are accompanied by prominent dysfunction of the cranial nerves. In the present study, we review our initial experience with SRS and hypofractionated SRT of patients with a VS.

Patients and Methods

During 2010–2011, a total of 17 consecutive patients with VS underwent treatment with SRS or SRT at the Center of Radiosurgery and Radiotherapy of the Meshalkin Research Institute of Circulation Pathology (Novosibirsk, Russia). The main clinical characteristics and treatment details for these cases are presented in Table 1.

There were nine women and eight men whose ages varied from 19 to 75 years (mean 47.8 years). NF2 was diagnosed in two patients. Each of these two patients had undergone previous surgery for a contralateral tumor and had the only hearing ear on the side of the remaining neoplasm. Five lesions were recurrent after previous partial resection. Recent subtotal microsurgical removal of the tumor preceded radiation treatment in four patients. A ventriculoperitoneal shunt was implanted in two cases.

There was a marked decrease or total loss of hearing on the side of the lesion in all of the patients. Eight were also deaf on the contralateral ear, mainly as a consequence of the prior surgery in those with bilateral tumors. Dysfunction of the VII and V cranial nerves on the side of the lesion was seen in 12 (71 %) and 4 (24 %) patients, respectively.

The maximum diameter of the tumor, measured on gadolinium-enhanced T1-weighted thin-slice (thickness 1.0–1.5 mm) magnetic resonance imaging (MRI) scans at the level of the internal auditory canal, varied from 11 to 38 mm (median 18 mm). The volume of the neoplasm ranged from 0.6 to 25.9 cm^3 (median 6.6 cm^3).

Indications for Radiation Treatment

Indications for SRS or SRT were determined by the radiation oncologist and the neurosurgeon. The patient was considered eligible for radiation treatment if there were typical neuroimaging features of VS, documented tumor progression or hearing deterioration on the side of the lesion during 12 previous months, and preservation of hearing on the side of the lesion according to objective (Gardner-Robertson class I–III) or subjective criteria. Irradiation was usually recommended for relatively small tumors without brain stem compression and occlusive hydrocephalus or if there were contraindications for craniotomy, particularly somatic disease(s), which was marked in three elderly patients of the present series. Clinical manifestations of VS and the patient's preference were also taken into consideration. Microsurgery was consistently offered as an alternative option. If radiation treatment was indicated but hydrocephalus was presented, ventriculoperitoneal shunting was performed initially. In such cases irradiation was administered after stabilization of the patient's condition.

Radiation Treatment

In all cases, radiation treatment was performed with a stereotactic LINAC (Elekta Axesse; Elekta Instruments AB, Stockholm, Sweden). The choice between SRS and SRT depended mainly on tumor size and the presence of brainstem compression. Small VSs without brain stem compression underwent single-fraction SRS. To reduce the risk of complications in patients with large neoplasms that caused brain stem compression, hypofractionated SRT was used. In a few patients eligible for SRS, SRT was performed because of additional concerns regarding treatment safety.

Three fixation devices were used to immobilize the patient's head: Leksell G frame (Elekta Instruments AB), noninvasive HeadFIX frame (Elekta Instruments AB), IMRT thermoplastic masks (CIVCO, Orange City, IA, USA). The choice of the immobilization device was mainly determined by the type of radiation treatment (SRS or SRT).

With a patient's head fixed in the immobilization device, axial thin-sliced (maximum slice thickness 1.5 mm) contrast-enhanced T1-weighted MRI was performed with a 1.5 T scanner (Philips Achieva; Philips MRI Equipment, Eindhoven, The Netherlands). Thereafter, thin-sliced computed tomography (CT) (slice thickness 1 mm) was undertaken using a dedicated scanner (Aquilion LB; Toshiba Medical Systems, Tokyo, Japan) with a gantry angle of 0°. The fusion of images and delineation of the target and adjacent anatomical structures were performed using FocalPro station (Elekta Instruments AB). Dose planning was undertaken with the ERGO++ stereotactic treatment planning system (TPS) (Elekta Instruments AB). Planning target volumes (PTVs) were created with a margin of 0–1 mm if Leksell G or HeadFIX frames were used and with a margin of 2–3 mm if thermoplastic masks were applied. The target volume was covered with the 80 % isodose. All treatment plans were calculated for 6 MeV energy on the Elekta Axesse LINAC. Doses were calculated with 1 mm grid resolution. For SRS the marginal dose constituted 12.0–12.5 Gy at the 80 % isodose line.

Table 1 Clinical characteristics and treatment details of patients in the present series

Case no.	Sex	Age	Cranial nerve dysfunction			Tumor volume (cm^3)	No. of fractions	Marginal dose at the 80% isodose line (Gy)	Maximum dose to the brain stem (Gy/cm^3)	Immobilization device
			VIII	VII	V					
1	M	46	+	–	–	5.4	5	5	4.25	Thermoplastic mask
2	F	63	+	+	–	15.1	6	4.5	5.0	Thermoplastic mask
3	M	52	+	+	–	4.5	5	5	3.95	Thermoplastic mask
4	M	31	+	+	+	5.8	5	5	3.65	Thermoplastic mask
5	F	36	+	+	–	3.2	5	5	4.6	Thermoplastic mask
6	F	51	+	–	–	1.6	SRS	12.5	4.7	HeadFIX
7	F	24	+	+	–	2.1	5	5	3.3	Thermoplastic mask
8	M	52	+	+	+	15.1	5	5	4.9	Thermoplastic mask
9	F	58	+	+	+	1.2	SRS	12	11	Leksell G Frame
10	M	53	+	+	+	1.9	5	5	2.1	Thermoplastic mask
11	F	19	+	+	–	20.0	6	5	4.45	Thermoplastic mask
12	M	53	+	–	–	0.5	SRS	12.5	4.5	HeadFIX
13	M	50	+	+	–	1.3	5	5	4.9	Thermoplastic mask
14	F	67	+	–	–	1.7	SRS	12.5	4.2	HeadFIX
15	F	21	+	+	–	11.7	5	5	5.6	HeadFIX
16	M	75	+	+	–	25.9	5	5	5.9	Thermoplastic mask
17	F	62	+	–	–	0.6	SRS	12	8.9	HeadFIX

SRS stereotactic radiosurgery

For hypofractionated SRT the dose of 4.5–5.0 Gy was applied to the 80 % isodose line during each of five or six daily fractions.

All treatment plans for SRT included a volumetric modulated arc therapy (VMAT) technique, which is a commonly used contemporary method for small brain targets. It allows highly conformal distribution of the dose with a minimal load to normal tissue. All 12 SRT treatment plans had one noncoplanar arc added for optimal dose distribution, whereas SRS treatment plans included five to seven noncoplanar arcs, individually modified for protecting adjacent critical structures. The minimal field size provided by the beam modulator was 8 mm, which is suitable for most cases and similar to that of the Gamma Knife.

Quality Assurance and Treatment Plan Verification

For precise stereotactic delivery of irradiation, quality assurance (QA) procedures for LINAC and TPS were emphasized. Standard testing confirmed that the mechanical accuracy for gantry, collimator, and leaf movements was ~0.5 mm. For table movements it was <1 mm. Additional care was taken when testing the XVI imaging system and Hexapod system (Elekta Instruments AB). The correlation between KV and MV isocenters was better than 0.2 mm in every direction and better than 0.3 mm on the radius. The accuracy of the Hexapod system according to calibration procedures was about 0.2–0.3 mm (for small shifts <2 cm and 2°).

Another QA procedure was directed at treatment plan verification. It was performed to check the delivered dose and to avoid any risks that could lead to collisions or inadvertent injury of the patient during treatment. For this purpose, we used a cylindrical phantom containing an ionic chamber. This chamber was located precisely at the isocenter, and the dose was measured continuously throughout the procedure. The measured dose was then compared with the planned dose recalculated for the QA phantom. The verified deviation of the delivered and planned irradiation doses for all patients was <5 %.

Follow-Up

Regular MRI investigations were performed after treatment using the 1.5 T Philips Achieva scanner. Axial thin-sliced (thickness 1.0–1.5 mm) contrast-enhanced T1-weighted images were usually obtained, and maximum diameter of the tumor was measured at the level of the internal auditory canal and compared with pretreatment data. Changes in lesion size were considered significant if they exceeded 2–3 mm in any dimension. If the change was <2 mm, it was not taken into consideration because it might be a measurement error. Volumetric evaluations of the tumor were not performed during follow-up.

Results

Radiation treatment was performed on an outpatient basis in all cases. None of the patients required admission to the hospital. Medical sedation and general anesthesia were needed in three female patients.

High reproducibility and accuracy of patient positioning were achieved using the intensity guided radiation therapy (IGRT) technique supported by the XVI imaging system and Hexapod system for each treatment. The overall accuracy of dose delivery was estimated to be ~1 mm.

Stereotactic radiosurgery was performed in five patients. The invasive stereotactic Leksell G Frame was used in one case (at a time when alternative methods for immobilizing the patient's head were not available at our center). The noninvasive HeadFIX frame was used in the other four cases. The positional accuracy during SRS sessions was better than 0.3 mm. During SRS the brain stem received 9–25 % (average 14.6 %) of the total dose delivered to the target volume.

Hypofractionated SRT was performed in 12 patients. The reinforced thermoplastic mask was typically applied for immobilizing the patient's head during SRT. It provided accuracy of repositioning within 1–2 mm. However, in one case it lost the required elasticity, and with each subsequent fraction immobilization of the patient's head encountered some difficulty. It caused loss of time and the risk of mistakes with the repositioning. Therefore, it was finally decided to use HeadFIX frame in this patient. For all of the SRT patients, the brain stem received 15–75 % (average 35 %) of the total dose delivered to the entire target volume.

Clinical Results

No adverse reactions or complications occurred in any of the patients. None required surgical treatment of the tumor during the follow-up period.

Three tumors demonstrated some shrinkage within 3 months after treatment. In four patients with follow-up of >6 months, the tumor showed definite structural changes, with appearance of central lucency as a result of

irradiation. Such changes were observed after both SRS and SRT (Figs. 1 and 2).

Tumor shrinkage was accompanied by some resolution of the neurological symptoms. After SRT, two patients exhibited improvement of the facial nerve function. Objective evaluation of hearing did not reveal any changes from the pretreatment level in any of the patients.

Discussion

The number of patients with VS who are undergoing SRS or SRT as an alternative to microsurgical tumor resection is increasing. Among the most common reasons for choosing these minimally invasive treatments are the following: mild (if any) clinical manifestations of the disease, which

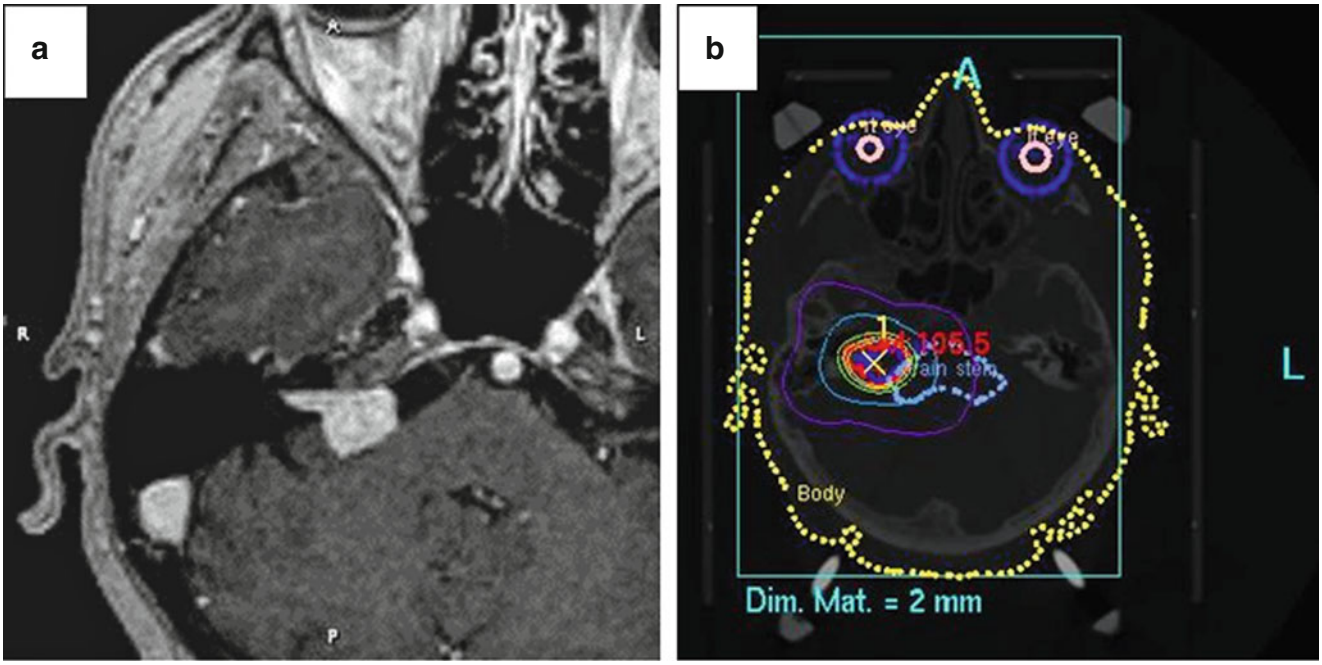

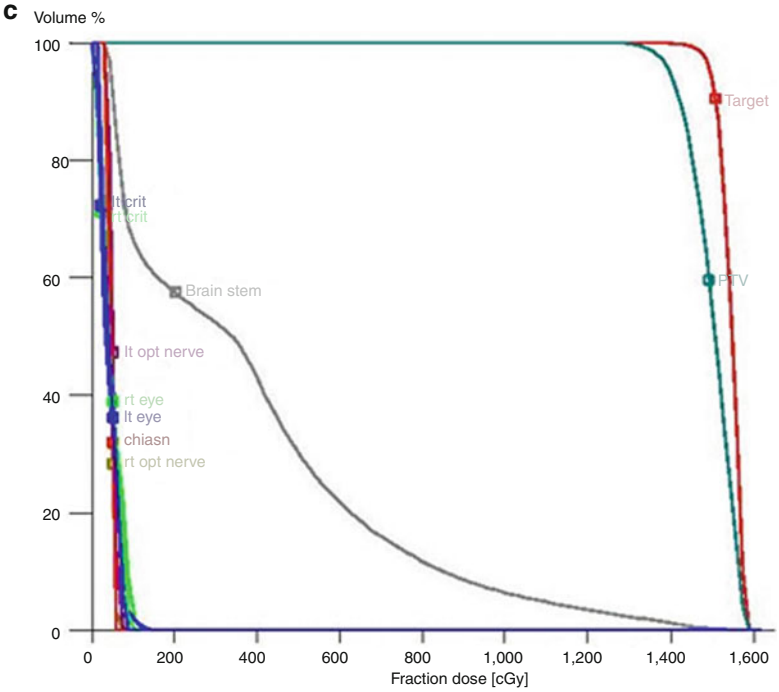

VOI	Vol. (cm^3)	Area	Fraction dose [cGy] Max	Min	Avg.
Target	1.2	103	1,575	1,365	1,544
rt crit	25.9	3	120	0	44
lt crit	26.1	3	135	0	41
rt opt ne	0.5	3	60	30	45
lt opt ne	0.3	3	75	30	51
PTV	3.1	100	1,575	1,230	1,499
Brain stem	21.1	25	1,530	30	177
Chiasn	0.4	3	45	30	46
rt eye	9.3	3	90	0	47
lt eye	9.5	3	75	15	44

Fig. 1 A 58-year-old woman (case 9) with a right-sided vestibular schwannoma: The tumor did not cause brain stem compression (**a**). Therefore, stereotactic radiosurgery was performed using the marginal dose of 12 Gy at the 80 % isodose line. The isodose lines (**b**) and dose-volume histogram (**c**) are shown. At 6 months after treatment, contrast-enhanced magnetic resonance imaging (MRI) demonstrated the appearance of central lucency (**d**) as an effect of the irradiation

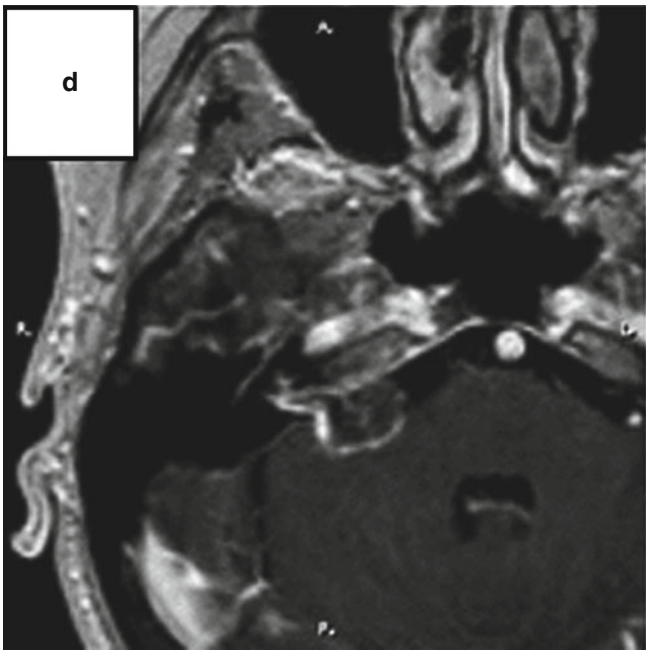

Fig. 1 (continued)

would be at risk of aggravation after surgical removal of the tumor; previous incomplete resection of the neoplasm; presence of contraindication(s) for craniotomy; patient's preference.

The choice between SRS and SRT in cases of VS is still not strictly determined, although tumor size is one of the most important factors. The goal of fractionated irradiation is to reduce the dose load to adjacent anatomical structures, particularly the brain stem. Therefore, it is usually recommended for patients with large tumors. The fractionated approach seems reasonable to minimize the possible risk of treatment-related morbidity [4, 5, 12, 15]. Correspondingly, in the present series, small VSs without brain stem compression usually underwent SRS, whereas SRT was offered to patients who had more prominent VSs. Nevertheless, additional concerns regarding treatment safety led to application of SRT in a few patients who were eligible for SRS [1, 2, 9, 16, 17].

One of the most significant risk factors for complications after radiation treatment of VS is dose excess to the brain stem. We tried to eliminate the risk by using low-dose SRS and applying no more than 5 Gy per fraction during hypofractionated SRT. In the majority of our cases the irradiation dose to the brain stem did not exceed 5 Gy/cm^3, although it

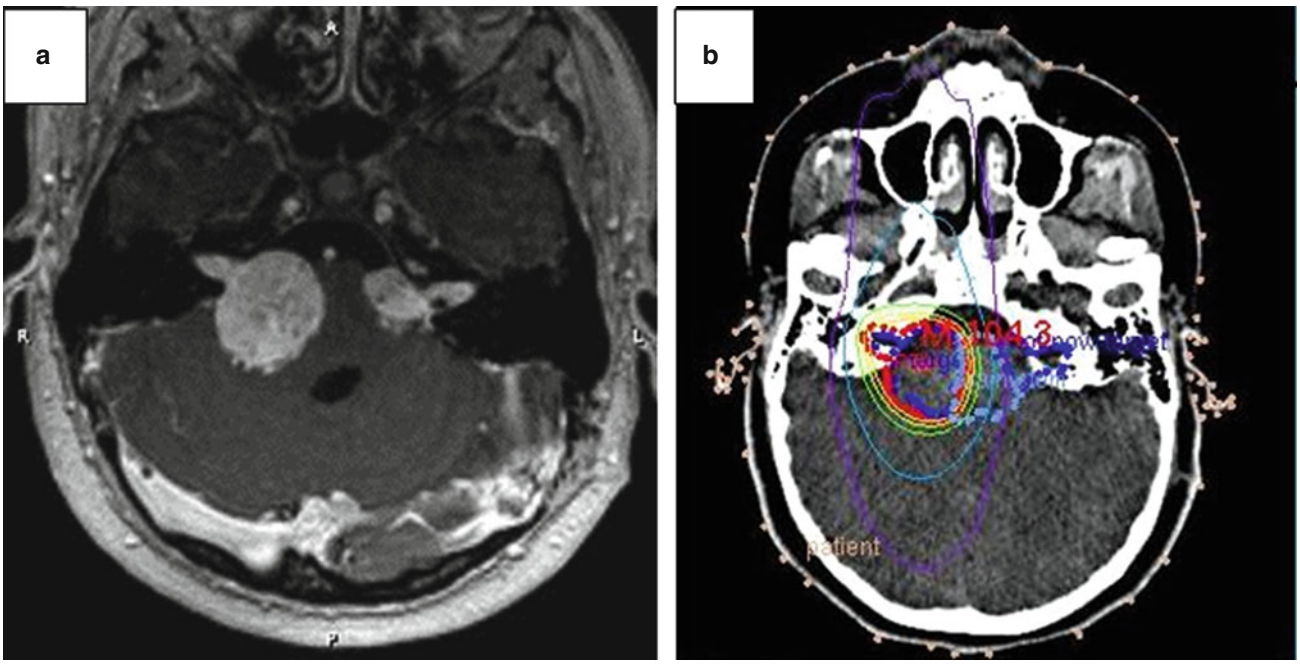

Fig. 2 A 21-year-old woman (case 15) with neurofibromatosis type 2 and bilateral vestibular schwannomas: The left-sided tumor was operated on. The right-sided tumor was causing prominent brain stem compression (**a**) so SRT was applied using five fractions with a dose of 5 Gy for each. The isodose lines (**b**) and dose-volume histogram (**c**) are shown. At 6 months after treatment contrast-enhanced MRI demonstrated the appearance of central lucency (**d**) as an effect of the irradiation

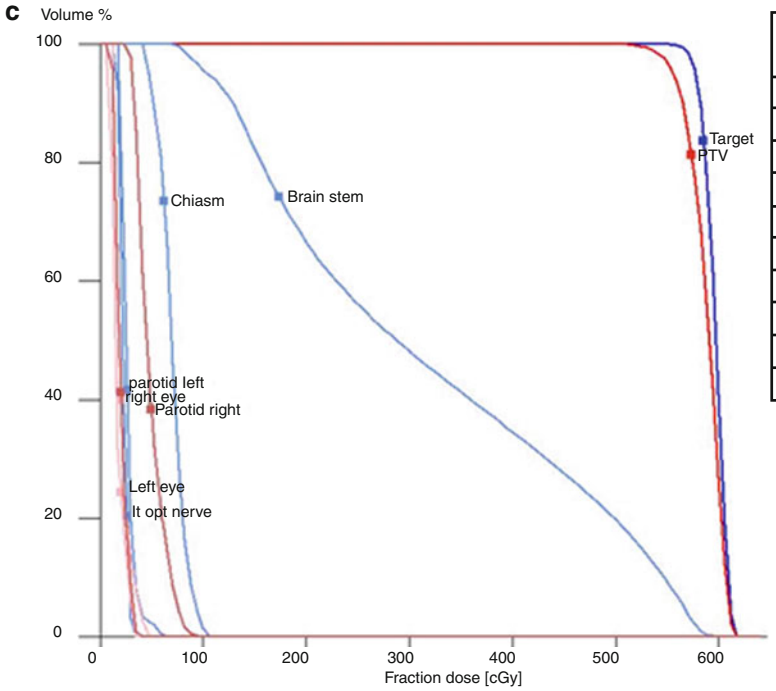

VOI	Vol. (cm^3)	Area	Fraction dose [cGy] Max	Min	Avg.
Target	11.6	101	611	535	596
PTV	18.7	100	611	476	587
Chiasm	0.7	12	106	35	69
Brain stem	19.8	54	594	64	315
rt opt ne	0.4	4	58	17	26
lt opt ne	0.4	4	29	11	22
Right eye	6.3	4	47	11	20
Left eye	4.7	3	29	5	16
Parotid r	13.4	8	94	17	48
Parotid l	12.4	3	35	6	19

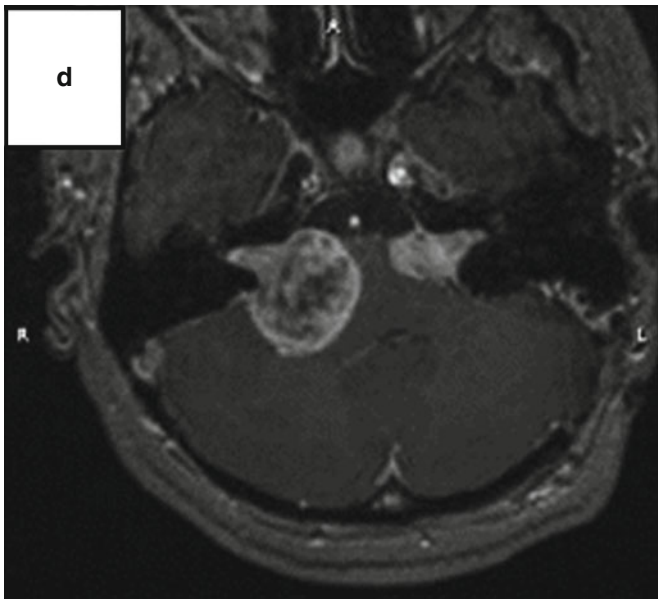

Fig. 2 (continued)

was relatively greater in four patients (cases 9, 15, 16, 17) in whom there was a relatively large target volume. No adverse effects were noted in these four patients during the post-treatment course. Of interest, there was marked improvement of facial nerve function in two of them.

Although of less significance than tumor size, the type of immobilization device influences the choice of the radiation treatment [8, 10, 13, 14, 18–20]. The Leksell G frame, which is frequently used for SRS, particularly with the use of Gamma Knife, provides precise positioning accuracy (<0.1 mm). However, this type of head immobilization has some limitations, such as the requirement of a special room for sterilization and fixation of the device, involvement of a neurosurgeon, the need to apply the radiation treatment within a relatively short period after fixation of the frame on the head, and the difficulty of using it with a fractionated regimen. Also some patients experience psychological discomfort during and after fixation of an invasive frame on the head. Therefore, we prefer to use an alternative immobilization device, the noninvasive HeadFIX frame. It was used during SRS in four patients of the present series and provided positional accuracy within 0.2–0.3 mm in each direction, which

seems sufficient for radiosurgical procedures. The main requirement for its application is an absence of the major defects of the upper jaw because it is necessary to create a mold of the upper teeth to produce accurate fixation. For SRT we prefer the reinforced thermoplastic mask, which provides positional accuracy of 1–2 mm.

Although minimally invasive radiation treatment is a real alternative to microsurgical tumor resection in patients with VS, it usually is not considered suitable for prominent tumors at a late stage of the disease. The typical requirements for SRT include the following: the largest diameter of the lesion <37 mm; its volume <18 cm^3; absence of severe symptoms of brain stem compression, hydrocephalus, or intracranial hypertension. Nevertheless, several patients in the present series underwent radiation treatment for large VSs that were accompanied by prominent neurological symptoms. The short duration of the follow-up in our series precludes to draw definitive conclusions regarding treatment efficacy. It should be noted, however, that no adverse reactions or treatment-related complications were seen in any of our patients, and none required additional surgical removal of the tumor.

Conclusion

Both SRS and SRT can be used effectively as an alternative to microsurgical resection in patients with a VS. The results of this study demonstrate that particularly hypofractionated SRT can be safely applied even for large tumors that cause brain stem compression and that are accompanied by prominent neurological symptoms. Additional studies with more patients and longer follow-up are needed to confirm these findings and prove the usefulness of radiation treatment in these cases.

Conflict of Interest The authors declare that they have no conflict of interest.

References

1. Arriaga MA, Luxford WM, Atkins JS Jr, Kwartler JA (1993) Predicting long-term facial nerve outcome after acoustic neuroma surgery. Otolaryngol Head Neck Surg 108:220–224
2. Chang SD, Poen J, Hancock SL, Martin DP, Adler JR Jr (1998) Acute hearing loss following fractionated stereotactic radiosurgery for acoustic neuroma: report of two cases. J Neurosurg 89:321–325
3. Chin LS, Regine WF (eds) (2008) Principles and practice of stereotactic radiosurgery. Springer, Wien/New York, 721 p
4. Cohen NL, Lewis WS, Ransohoff J (1993) Hearing preservation in cerebellopontine angle tumor surgery: the NYU experience 1974–1991. Am J Otol 14:423–433
5. Flickinger JC, Kondziolka D, Pollock BE, Lunsford LD (1996) Evolution in technique for vestibular schwannoma radiosurgery and effect on outcome. Int J Radiat Oncol Biol Phys 36: 275–280
6. Gormley WB, Sekhar LN, Wright DC, Kamerer D, Schessel D (1997) Acoustic neuromas: results of current surgical management. Neurosurgery 41:50–60
7. Halperin EC, Perez CA, Brady LW (eds) (2008) Perez and Brady's principles and practice of radiation oncology, 5th edn. Lippincott Williams & Wilkins, Philadelphia, 2106 p
8. Inoue HK (2005) Low-dose radiosurgery for large vestibular schwannomas: long-term results of functional preservation. J Neurosurg 102:111–113
9. Ito K, Shin M, Matsuzaki M, Sugasawa K, Sasaki T (2000) Risk factors for neurological complications after acoustic neurinoma radiosurgery: refinement from further experiences. Int J Radiat Oncol Biol Phys 48:75–80
10. Iwai Y, Yamanaka K, Shiotani M, Uyama T (2003) Radiosurgery for acoustic neuromas: results of low-dose treatment. Neurosurgery 53:282–287
11. Lu JJ, Brady LW, Heilmann HP, Molls M, Nieder C (eds) (2008) Radiation oncology: an evidence-based approach (medical radiology/radiation oncology). Springer, Wien/New York, 676 p
12. Mandl ES, Meijer OWM, Slotman BJ, Vandertop WP, Peerdeman SM (2010) Stereotactic radiation therapy for large vestibular schwannomas. Radiother Oncol 95:94–98
13. McClelland S 3rd, Gerbi BJ, Cho KH, Hall WA (2007) The treatment of a large acoustic tumor with fractionated stereotactic radiotherapy. J Robot Surg 1:227–230
14. Meijer OW, Vandertop WP, Baayen JC, Slotman BJ (2003) Single-fraction vs. fractionated linac-based stereotactic radiosurgery for vestibular schwannoma: a single-institution study. Int J Radiat Oncol Biol Phys 56:1390–1396
15. Mendenhall WM, Friedman WA, Buatti JM, Bova FJ (1996) Preliminary results of linear accelerator radiosurgery for acoustic schwannomas. J Neurosurg 85:1013–1019
16. Miller RC, Foote RL, Coffey RJ, Sargent DJ, Gorman DA, Schomberg PJ, Kline RW (1999) Decrease in cranial nerve complications after radiosurgery for acoustic neuromas: a prospective study of dose and volume. Int J Radiat Oncol Biol Phys 43: 305–311
17. Nissen AJ, Sikand A, Welsh JE, Curto FS, Gardi J (1997) A multifactorial analysis of facial nerve results in surgery for cerebellopontine angle tumors. Ear Nose Throat J 76:37–40
18. Park CK, Jung HW, Kim JE, Son YJ, Paek SH, Kim DG (2006) Therapeutic strategy for large vestibular schwannomas. J Neurooncol 77:167–171
19. Poen JC, Golby AJ, Forster KM, Martin DP, Chinn DM, Hancock SL, Adler JR Jr (1999) Fractionated stereotactic radiosurgery and preservation of hearing in patients with vestibular schwannoma: a preliminary report. Neurosurgery 45:1299–1307
20. Williams JA (2002) Fractionated stereotactic radiotherapy for acoustic neuromas. Int J Radiat Oncol Biol Phys 54:500–504

What Is the Role of Radiosurgery in the Management of Sellar Tumors?

Tomokatsu Hori

Keywords Craniopharyngioma • Management • Pituitary adenoma • Radiosurgery

Pituitary adenomas and craniopharyngiomas comprise, respectively, around 10–20 % and 2–5 % of all intracranial neoplasms. Their management therefore constitutes an important part of neurosurgical practice. In the following articles, El Khamlichi et al. [1] and Saleem et al. [13] present their experience with Gamma Knife radiosurgery (GKS) in such cases. Herein I discuss the role of stereotactic irradiation and share my own view on the optimal contemporary treatment of patients with sellar tumors based on the lifelong clinical experience.

Pituitary Adenoma

I strongly believe that, at present, the primary goal of neurosurgeons in cases of pituitary adenomas should be total removal of the lesion without postoperative morbidity. To attain cure, extracapsular resection of the tumor should be achieved irrespective of its histopathological subtype. Lee et al. [8] reported results of aggressive microsurgical management of 616 pituitary adenomas over a period of 14 years. A pseudocapsule was identified in 343 patients (55.7 %) that was considered distinct (180 cases) or incompletely developed (163 cases). It frequently contained infiltrating tumor clusters. In cases of extracapsular tumor removal, the remission rate after surgery was 86.2 %, whereas the recurrence rates after total and subtotal resection of the neoplasm were 0.8 and 42.1 %, respectively [8]. These data correspond well to earlier results of our group [6] and those of others [11], which demonstrated that aggressive resection of the pseudocapsule is essential for remission of the preexisting excessive hormone secretion. Also, this resection does not pose any additional risk of pituitary dysfunction. In fact, since adopting the mentioned technique, our surgical results in cases of pituitary adenoma have improved dramatically. For example, in cases of growth hormone-secreting tumors of Knosp grades 0/1 and 2/3 the respective postoperative cure rates, corresponding to the Cortina criteria, had risen from 76.7 and 40 % during 2002–2005 to 100 and 75 % during 2006–2008.

It should be emphasized that complete resection of pituitary adenomas is facilitated by the introduction of dedicated long-length surgical instruments [4] and application of the endoscopy-assistant technique, which is particularly useful for removing tumors invading the cavernous sinus or extending into the third ventricle. Taking into account these considerations, it is our current policy to treat all patients with pituitary adenomas (with the possible exception for prolactinomas) with initial microsurgical resection directed at the maximum possible removal of the lesion. If such a goal is not attained at the time of the initial surgery, a second-look procedure can be considered.

Even with such an aggressive surgical strategy, radiosurgery plays an important role in the management of pituitary adenomas [12, 14]. Irradiation has long been used in such cases as adjunctive treatment modality because the reported rates of recurrence following pure surgical removal of the tumor in historical series were 20 % after 5 years of follow-up and 40 % after 10 years [9]. It was reduced to 6 % after 10 years and 12 % after 20 years with application of fractionated radiotherapy [9]. This technique, however, is not selective and is associated with certain side effects, including optic neuropathy, deterioration of pituitary function, radiation-induced necrosis of the mesial temporal lobe, and development of secondary malignancies. In contrast, radiosurgery, particularly GKS, offers the advantage of reducing the undesirable damage to adjacent anatomical structures because it

T. Hori
Department of Neurosurgery, Neurological Institute,
Tokyo Women's Medical University, Tokyo, Japan

Moriyama Memorial Hospital,
7-12-7, Nishikasai, Edogawa-ku, Tokyo 134-0088, Japan
e-mail: thori@moriyamaikai.or.jp

M.F. Chernov et al. (eds.), *Gamma Knife Neurosurgery in the Management of Intracranial Disorders*,
Acta Neurochirurgica Supplement, Vol. 116, DOI 10.1007/978-3-7091-1376-9_7, © Springer-Verlag Wien 2013

provides highly conformal delivery of the irradiation and a steep dose falloff outside the target volume.

Gopalan et al. [2] investigated long-term outcomes after GKS in patients with a nonfunctioning pituitary adenoma and reported frequent durable treatment effects, particularly for lesions with a volume of <5 cm^3. Larger neoplasms had a significantly higher incidence of regrowth. In their series of 48 patients, overall tumor control was attained in 83 % of cases, 75 % of neoplasms shrank, in 8 % of tumors the growth was stabilized, and 17 % showed further progression. New hormonal deficiency occurred in 39 % of patients. Park et al. [12] studied results of GKS in 125 patients with nonfunctioning pituitary adenomas over 22 years of follow-up after treatment. Volume reduction of the tumor was marked in 53 % of cases, stabilization occurred in 37 %, and progression was seen in 10 %. Once again, large tumor volume (>4.5 cm^3) and two or more previous recurrences were associated with shorter progression-free survival. Based on these data it can be concluded that radiosurgery can effectively manage patients with pituitary adenomas. However, the large size of a tumor should be a matter of concern because cure rate decreases as the size of the neoplasm increases.

In my opinion, radiosurgery is useful for controlling tumor growth and improving or normalizing hormone secretion after incomplete surgical removal of a pituitary adenoma. If a small amount of residual neoplasm is left in an area difficult to access surgically (e.g., on the lateral side of the internal carotid artery, within the cavernous sinus, or attached to ventral part of the optic chiasm), the lesion can be effectively controlled by GKS. Additionally, in agreement with El Khamlichi et al. [1], in exceptional patients who are not suitable for surgery under general anesthesia because of advanced age or poor general medical condition, we do consider use of radiosurgery as a primary treatment option as an alternative to tumor removal.

In 2000, Izawa et al. [5] analyzed the results of GKS in 108 patients with pituitary adenoma who were treated at our center during a 7-year period. The authors reported the outcomes for 79 of them (73 %) who were followed for >6 months after radiosurgery. In their series, the mean marginal irradiation dose was 22.5 Gy: 19.5 Gy in 23 nonfunctioning neoplasms and 23.8 Gy in 56 hormone-secreting tumors. Overall, tumor growth control was attained in 93.6 % of cases. The rates were 95.6 and 92.8 % for nonfunctioning and hormone-secreting pituitary adenomas, respectively: 100 % for patients with acromegaly, 86.7 % for those with prolactinomas, and 83.3 % for patients with Cushing disease. Reduction of tumor volume was marked in 24.1 % of patients. The rates were 26.1 and 23.2 % for nonfunctioning and hormone-secreting pituitary adenomas, respectively: 44.8 % for patients with acromegaly, 20.0 % for those with prolactinomas, and 8.3 % for patients with Cushing disease. Thus, the rate of shrinkage was most prominent in patients with acromegaly. Endocrinological improvement was marked in 80.3 % of patients with hormone-secreting pituitary adenomas: a rate of 93.1 % for those with acromegaly, 73.3 % for those with prolactinomas, and 58.3 % for patients with Cushing disease. Moreover, normalization of excessive hormone secretion was noted in 30.3 % of these cases, being 16.7 % for patients with Cushing disease. The treatment-associated morbidity rate was 2.5 %, but none of the patients developed hypopituitarism after stereotactic irradiation [5].

During the last decade the results of GKS for pituitary adenomas in our Gamma Knife unit were further improved owing to installation of upgraded radiosurgical equipment, development of an advanced neuroimaging protocol for dose planning, and creation of a new treatment concept directed at maximally effective management of the tumor with minimum risk of associated complications [3].

Craniopharyngioma

Whereas craniopharyngioma is a histologically benign tumor, its well-known propensity for locally infiltrative growth may hamper radical surgical resection without visual, pituitary, and/or hypothalamic dysfunction [10]. Yamada et al. [15] analyzed the results of transsphenoidal surgery in 90 cases of such neoplasms. Total tumor removal, which was attained in 77.8 % of patients, was more frequently performed at the time of the initial surgery than at a secondary operation (90.3 % vs. 50.0 %). Subtotal resection of the lesion was done in 18.9 % of cases and partial resection in 3.3 %. Postoperative endocrinological deterioration was marked in 66.0 % of patients, who had normal anterior pituitary function or only partial hypopituitarism before surgery. New onset of the diabetes insipidus after tumor resection was noted in 52.2 % of cases. On the other hand, 90.2 % of patients with preoperative visual impairment noted prominent improvement after surgery. Postoperative cerebrospinal fluid leak occurred in 12.2 % of cases, necessitating reoperation in nearly half of them. The early mortality rate was 2.2 %. During a mean follow-up of 4.6 years, tumor recurrence was observed in 7.8 % of patients. In fact, these results are better than those of several previous reports. Hence, it may be concluded that use of the transsphenoidal approach for management of craniopharyngioma is associated with acceptable postoperative morbidity. The problem is that by the time of surgery the majority of these tumors have already reached a large size and/or have widespread extension, necessitating transcranial resection.

Table 1 Tokyo Women's Medical University grading system of craniopharyngioma based on scoring surgically relevant tumor-associated factors

	Score			
Tumor-associated factors	0	1	2	3
Maximum sagittal diameter	–	<2 cm	2–4 cm	>4 cm
Maximum coronal diameter	–	<2 cm	2–4 cm	>4 cm
Structure	Cystic (single cyst)	Cystic (multiple cysts)	Mixed	Solid
Extension relatively to clinoidal line	Extending above clinoidal line	Located under clinoidal line	–	–
Extension relatively to foramen of Monro	Not reaching foramen of Monro	Reaching foramen of Monro	–	–
Extension relatively to mammillary bodies	Not reaching mammillary bodies	Reaching mammillary bodies	–	–

The total score may vary from 2 to 12, and corresponds to the grade of the craniopharyngioma: grade I (score 2), grade II (score 3–5), grade III (score 6–8), grade IV (score 9–11), grade V (score 12)

Our group at Tokyo Women's Medical University developed a dedicated grading system to aid in reliable comparisons of outcomes according to different surgical appoaches and treatment strategies for craniopharyngiomas. The system, which is based on scoring surgically relevant tumor-associated factors (i.e., maximum diameter, structure, extension) (Table 1), provides support for neurosurgeons' decision making regarding the choice of the optimal management. In our analysis of the surgical outcomes of 99 consecutive patients with craniopharyngioma (unpublished data) there were no one grade I tumors, 38 grade II (38.4 %), 44 grade III (44.4 %), 16 grade IV (16.2 %), and 1 grade V (1 %). Overall, 28 patients underwent GKS before or after surgical removal of the neoplasm, and 71 were treated with surgery alone. Overall, total tumor removal was achieved in 67.7 % of cases: in 50.0 % of patients operated on via the pterional approach, 79.3 % operated on via the transsphenoidal approach, and 65.5 % operated on via the anterior interhemispheric approach [4]. No recurrences were noted after total surgical removal of the tumor. Two patients who underwent several resections of their neoplasms died at 7 and 24 months, respectively, after the last operation as result of pneumonia in one patient and endocrinological complications in the other. All of the other 97 patients have maintained a good quality of life, with a mean Karnofsky Performance Status (KPS) score of 86.0 (the mean KPS score before surgery in this series was 73.7). Thus, our current strategy for management of craniopharyngiomas focuses on total or near-total resection of the tumor with close postoperative clinical and radiological follow-up.

It should be emphasized that as soon as craniopharyngioma recurrence is identified on magnetic resonance imaging (MRI) radiosurgery can be effectively applied. In 2003, Kobayashi et al. [7] analyzed long-term results of GKS of these neoplasms. With the mean maximum and marginal irradiation doses of 21.8 and 11.5 Gy, respectively, a complete tumor response was noted in 19 % of cases, partial response in 44 %, no volumetric changes in 14 %, and progression in 23 %. The age of the patient and structure of the tumor (cystic, mixed, solid) were identified as prognostically important factors [7]. Such beneficial results were confirmed by our own experience [16] and by the data of Saleem et al. [13]. Therefore, it can be concluded that GKS should be considered a safe and effective management option for residual and/or recurrent craniopharyngiomas after the initial surgical resection, providing durable treatment effect and acceptable risk of complications. Special emphasis, however, should be put on cystic, particularly multicystic, neoplasms as those ones are sometimes resistant to irradiation and demonstrate clinically significant expansion after treatment [13, 16]. Also, one of our patients developed an intratumoral hemorrhage 3 years after GKS of residual craniopharyngioma that necessitated emergency surgery with total resection of the lesion. However, it remained unclear whether this complication was related to irradiation.

Conclusion

Total or near-total surgical resection is the optimal management option for pituitary adenomas and craniopharyngiomas. It frequently results in complete cure, facilitates detailed histopathological diagnosis, and increases the effectiveness of adjuvant therapy, if it is required. Incomplete (near-total) removal of the lesion should not be considered an indication for immediate administration of radiation treatment unless other factors (e.g., excessive hormone secretion) are present. The residual lesion can be followed with neuroimaging over a prolonged period of time. GKS can be applied later on, if tumor progression is definitely diagnosed. In any case, close cooperation among neurosurgeon, radiosurgeon,

endocrinologist, radiologist, and pathologist is mandatory to attain optimal treatment results in patients with sellar tumors.

Conflict of Interest The author declares that he has no conflict of interest.

References

1. El Khamlichi A, Melhaoui A, Arkha Y, Jiddane M, El Gueddari BK (2013) Role of gamma knife radiosurgery in the management of pituitary adenomas and craniopharyngiomas. Acta Neurochir Suppl 116:49–54 (present volume)
2. Gopalan R, Schlesinger D, Vance ML, Laws E, Sheehan J (2011) Long-term outcomes after gamma knife radiosurgery for patients with a nonfunctioning pituitary adenoma. Neurosurgery 69: 284–293
3. Hayashi M, Chernov M, Tamura N, Nagai M, Yomo S, Ochiai T, Amano K, Izawa M, Hori T, Muragaki Y, Iseki H, Okada Y, Takakura K (2010) Gamma knife robotic microradiosurgery of pituitary adenomas invading the cavernous sinus: treatment concept and results in 89 cases. J Neurooncol 98:185–194
4. Hori T, Kawamata T, Amano K, Aihara Y, Ono M, Miki N (2010) Anterior interhemispheric approach for 100 tumors in and around the anterior third ventricle. Neurosurgery 66(3 Suppl Operative): 65–74
5. Izawa M, Hayashi M, Nakaya K, Satoh H, Ochiai T, Hori T, Takakura K (2000) Gamma knife radiosurgery for pituitary adenomas. J Neurosurg 93(Suppl 3):19–22
6. Kawamata T, Kubo O, Hori T (2005) Surgical removal of growth hormone-secreting pituitary adenomas with intensive microsurgical pseudocapsule resection results in complete remission of acromegaly. Neurosurg Rev 28:201–208
7. Kobayashi T, Kida Y, Hasegawa T (2003) Long-term results of gamma knife surgery for craniopharyngioma. Neurosurg Focus 14(5):E13
8. Lee EJ, Ahn JY, Noh T, Kim SH, Kim TS, Kim SH (2009) Tumor tissue identification in the pseudocapsule of pituitary adenoma: should the pseudocapsule be removed for total resection of pituitary adenoma? Neurosurgery 64(3 Suppl):62–70
9. Marcou Y, Plowman PN (2000) Stereotactic radiosurgery for pituitary adenomas. Trends Endocrinol Metab 11:132–137
10. Mortini P, Losa M, Pozzobon G, Barzaghi R, Riva M, Acerno S, Angius D, Weber G, Chiumello G, Giovanelli M (2011) Neurosurgical treatment of craniopharyngioma in adults and children: early and long-term results in a large case series. J Neurosurg 114:1350–1359
11. Oldfield EH, Vortmeyer AO (2006) Development of a histological pseudocapsule and its use as a surgical capsule in the excision of pituitary tumors. J Neurosurg 104:7–19
12. Park KJ, Kano H, Parry PV, Niranjan A, Flickinger JC, Lunsford LD, Kondziolka D (2011) Long-term outcomes after gamma knife stereotactic radiosurgery for nonfunctional pituitary adenomas. Neurosurgery 69:1188–1199
13. Saleem MA, Hashim ASM, Rashid A, Ali M (2013) Role of gamma knife radiosurgery in multimodality management of craniopharyngioma. Acta Neurochir Suppl 116:55–60 (present volume)
14. Sheehan JP, Niranjan A, Sheehan JM, Jane JA Jr, Laws ER, Kondziolka D, Flickinger J, Landolt AM, Loeffler JS, Lunsford LD (2005) Stereotactic radiosurgery for pituitary adenomas: an intermediate review of its safety, efficacy, and role in the neurosurgical treatment armamentarium. J Neurosurg 102:678–691
15. Yamada S, Fukuhara N, Oyama K, Takeshita A, Takeuchi Y, Ito J, Inoshita N (2010) Surgical outcome in 90 patients with craniopharyngioma: an evaluation of transsphenoidal surgery. World Neurosurg 74:320–330
16. Yomo S, Hayashi M, Chernov M, Tamura N, Izawa M, Okada Y, Hori T, Iseki H (2009) Stereotactic radiosurgery of residual and recurrent craniopharyngioma: new treatment concept using Leksell gamma knife model C with automatic positioning system. Stereotact Funct Neurosurg 87:360–367

Role of Gamma Knife Radiosurgery in the Management of Pituitary Adenomas and Craniopharyngiomas

Abdeslam El Khamlichi, Adyl Melhaoui, Yasser Arkha, Mohamed Jiddane, and Brahim Khalil El Gueddari

Abstract *Introduction*: Radical microsurgical removal of pituitary adenomas (PAs) and craniopharyngiomas (CPHs) is often difficult. In such cases radiosurgery can be used as a second-line treatment option.

Materials and Methods: Our series included 436 PAs and 164 CPHs. The majority of patients had large or giant tumors and were treated with microsurgery. Additionally, between June 2008 and August 2011, a total of 29 PAs and 10 CPHs underwent radiosurgery using Leksell Gamma Knife PerfeXion. At the time of treatment the volume of the PAs varied from 0.6 to 26.0 cm^3 (mean 5.9 cm^3) and that of the CPHs from 0.19 to 17.0 cm^3 (mean 6.6 cm^3). The marginal doses ranged from 12 to 15 Gy (mean 14.5 Gy) for nonsecreting PAs, from 22 to 25 Gy (mean 24 Gy) for hormone-secreting PAs, and from 8 to 14 Gy (mean 11 Gy) for CPHs.

Results: The postoperative mortality rates after surgical removal of PAs via the transsphenoidal approach and craniotomy were 2.4 % and 8.0 %, respectively, whereas after surgery for CPH it was 5.9 %. No major complications were noted in our limited number of patients after radiosurgical treatment. Taking into consideration only cases with radiological follow-up of at least 12 months, shrinkage of the tumor was demonstrated in 5 of 11 patients with a PA and in 4 out of 6 patients with a CPH.

Conclusion: Radiosurgery is safe and effective second-line management option in cases of recurrent or residual PA or CPH. Occasionally, it can be applied even as a primary treatment in selected patients.

Keywords Craniopharyngioma • Pituitary adenoma • Radiosurgery • Sellar tumors

Introduction

Pituitary adenomas (PA) and craniopharyngiomas (CPH) are the most common neoplasms in the sellar region, representing 12–18 % of all intracranial tumors (15 % in our experience). Despite their benign nature and significant technical achievements in management, these lesions remain a challenge for neurosurgeons.

PAs and CPHs are not similar tumors, and they arise from different anatomical structures. The former originates from the anterior pituitary gland, whereas the latter has an embryonic origin and grows from epithelial cells of Rathke's pouch. Nevertheless, although PA and CPH are differ in their origin, epidemiology, histology, morphology, and imaging appearance, they share some common characteristics, including benign nature, slow growth, and similar effects on adjacent anatomical structures (optic nerve, pituitary stalk, hypothalamus, pituitary gland). The latter results in typical clinical manifestations, mainly the optochiasmatic syndrome, endocrine dysfunction, and intracranial hypertension. Generally, the main treatment options are similar in cases of PA and CPH.

Because of the delay in diagnosis, most of the sellar tumors seeing in our practice in Morocco are large or giant, thus frequently requiring multimodality treatment, including sterotactic radiosurgery. From June 2008 to August 2011, a total of 477 patients with various brain pathologies were treated at our University Hospital by means of the Leksell Gamma Knife PerfeXion (Elekta Instruments AB, Stockholm, Sweden). This series included 29 PAs (6 %) and 10 CPHs

A. El Khamlichi (✉), A. Melhaoui, and Y. Arkha
Department of Neurosurgery, Hopital des Specialites, Mohammed V University Souissi, Rabat, Morocco
e-mail: fh2nch@menara.ma

M. Jiddane
Department of Radiology, Hopital des Specialites, Mohammed V University Souissi, Rabat, Morocco

B.K. El Gueddari
Oncology Institute, Mohammed V University Souissi, Rabat, Morocco

M.F. Chernov et al. (eds.), *Gamma Knife Neurosurgery in the Management of Intracranial Disorders*,
Acta Neurochirurgica Supplement, Vol. 116, DOI 10.1007/978-3-7091-1376-9_8, © Springer-Verlag Wien 2013

(2 %). Analysis of these limited cases along with evaluation of the role of Gamma Knife radiosurgery (GKS) in the management of PAs and CPHs represent the main objective of the present report.

Materials and Methods

Pituitary Adenomas

Our series of 436 PAs included 239 women (55 %) and 197 men (45 %) whose mean age was 36.7 years. Children represented just 5 % of the whole cohort. There were 136 nonsecreting or nonfunctional tumors (31 %). Hormone-secreting neoplasms included 122 prolactinomas (28 %), 72 growth hormone (GH)-secreting adenomas (16.5 %), 59 adrenocorticotropic hormone (ACTH)-secreting adenomas (13.5 %), and 47 other mixed adenomas (11 %). Microadenomas and intrasellar macroadenomas were noted in 95 cases (22 %), whereas 341 macroadenomas (78 %) extended into the suprasellar and/or laterosellar areas. Large and giant PAs predominated in our practice.

Surgery was done in 390 patients. Tumor removal was attained via the transsphenoidal approach in 81 % of cases, by craniotomy in 11 %, and by a combined approach in 7 %.

Radiosurgery

A total of 29 patients (22 men, 7 women) with PA underwent radiosurgical treatment at our center. Their age varied from 31 to 74 years (mean 51 years). There were 14 nonsecreting and 15 hormone-secreting tumors. The latter included 3 prolactinomas, 10 GH-secreting tumors, and 2 gonadotropin-secreting neoplasms.

In two peculiar cases, GKS was used as a primary treatment modality. The first case was a 65-year-old patient with purely intrasellar nonsecreting PA and agenesis of the sphenoid sinus, which precluded transsphenoidal surgery. The second case was a 60-year-old patient with multiple metastases from malignant melanoma and associated GH-secreting PA with endocrine complications. GKS was applied for management of both the metastatic brain tumors and the PA during the same session. In the other 27 cases, radiosurgery was used as complementary treatment, either for recurrent PA after initial gross total removal (4 cases), or for management of the residual neoplasm after surgery (23 cases), which was particularly located in the cavernous sinus (16 cases).

At the time of GKS, the tumor volume varied from 0.6 to 26 cm^3 (mean 5.9 cm^3). The marginal dose for nonsecreting and hormone-secreting PAs varied from 12 to 15 Gy (mean 14.5 Gy) and from 22 to 25 Gy (mean 24 Gy), respectively. An average of 26 isocenters were used per treatment (range 10–48). The mean duration of the procedure was 147 min (range 49–300 min).

Craniopharyngiomas

Our series of 164 patients with CPH included 73 women (44.5 %) and 91 men (54.5 %). Their mean age was 21 years, and 51 % of patients were under 15 years of age, providing almost the same distribution between adults and children in the whole cohort. There were 149 adamantinomatous (91 %) and 6 papillary (4 %) CPHs; 9 tumors remained unclassified (5 %). Cystic neoplasms were noted in 26 cases (16 %), solid in 15 (9 %), and mixed in 123 (75 %).

Surgery was performed in 156 cases. The tumor was removed successfully via the transsphenoidal approach in 6 % of patients. Other patients were operated on by craniotomy using mainly the frontolateral approach.

Radiosurgery

Ten patients with CPH underwent radiosurgery at our center. It was used as a complementary treatment in all of them to address recurrent (6 cases) or residual (4 cases) tumors after the initial surgery. At the time of GKS the volume of the lesion varied from 0.19 to 17.0 cm^3 (mean 6.6 cm^3). The marginal dose varied from 8 to 14 Gy (mean 11 Gy). The mean duration of the procedure was 69 min (range 36–124 min).

Results

Pituitary Adenomas

Of the 390 patients with PA who underwent surgery the tumor was totally removed in 241 (62 %). Subtotal or partial removal was achieved in 149 (38 %). Postoperative complications after total removal of PA included diabetes insipidus (18 cases, 7 %), rhinorrhea (16 cases, 7 %), meningitis (8 cases, 3 %), and new hypopituitarism (9 cases, 4 %). The mortality rates after use of the transsphenoidal approach and craniotomy were 2.4 % and 8.0 %, respectively.

For this study, more than 12 months follow-up was available in 15 of the 29 patients with PA who underwent radiosurgical treatment. No major complications were observed in any case. One patient with a recurrent macroadenoma who refused tumor removal before GKS was operated on 3 months thereafter

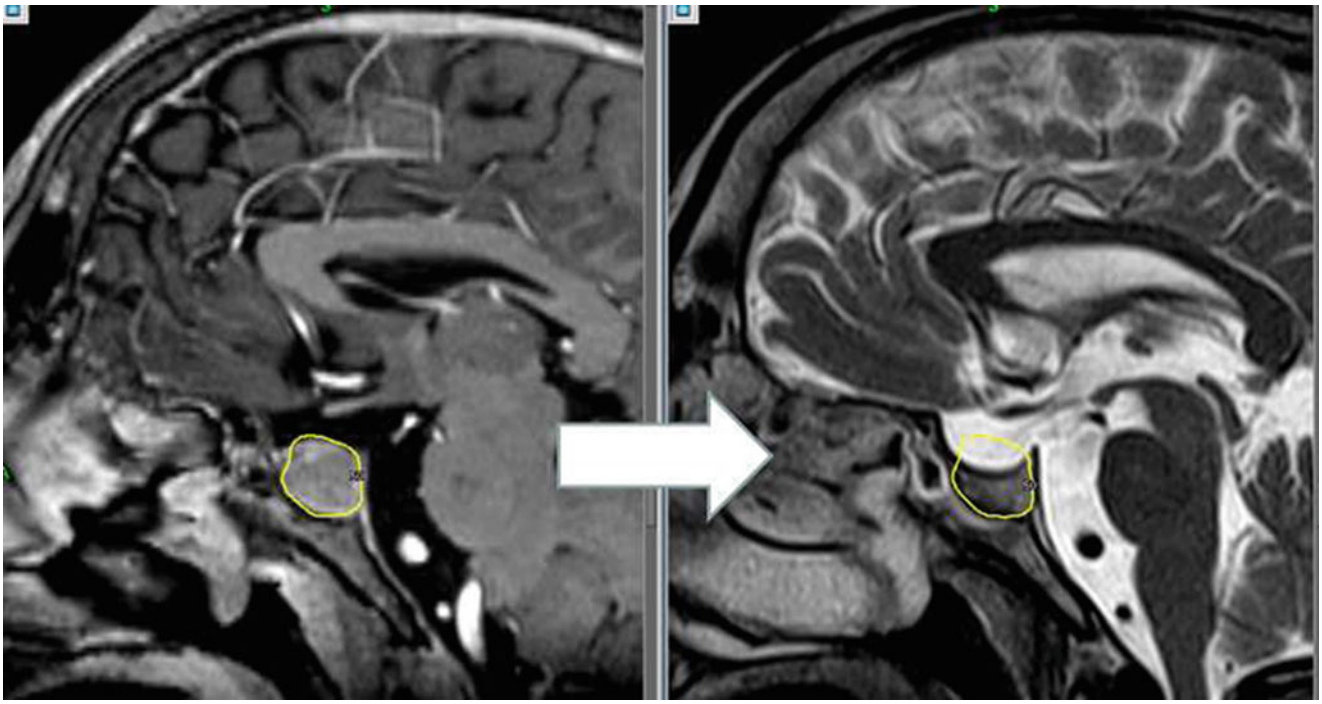

Fig. 1 A 42-year-old man with acromegaly initially underwent transsphenoidal removal of a growth hormone (GH)-secreting macroadenoma and had a good postoperative course. However, 2 years later the tumor recurred, which was accompanied by hormonal changes and arterial hypertension. The patient underwent Gamma Knife radiosurgery (*left*) with a marginal dose of 24 Gy applied to the 50 % isodose line (*yellow circle*). At the time of treatment, the tumor volume was 2.7 cm^3. Two years later there was significant clinical and endocrinological improvement along with markedly reduced tumor volume demonstrated by magnetic resonance imaging (MRI) (*right*) Prescription isodose line on the follow-up image is shown to facilitate comparison of the tumor size

because of deterioration of vision. In three patients with acromegaly, clinical improvement was observed. In two of them it was associated with an improved GH level. The other 11 patients remained clinically unchanged. Radiological follow-up with regular yearly magnetic resonance imaging (MRI) examinations was available for 11 patients. Tumor volume reduction was marked in five of them (Fig. 1), whereas there were no significant volumetric changes in the lesions of 6 other patients.

Craniopharyngiomas

Among 138 patients with CPH operated on via craniotomy, the tumor was totally removed in 73 (53 %), and subtotal or partial removal was achieved in 65 (47 %). Complications included diabetes insipidus in 25 % of cases, meningitis in 2 %, and cranial nerve palsy in 1.5 %. The postoperative mortality rate was 5.9 %.

During short- to mid-term follow-up after GKS, no complications or adverse effects were observed in any of 10 treated patients with CPH. Radiological follow-up longer than 12 months was available for six of these patients, and MRI demonstrated tumor shrinkage in four (Fig. 2).

Discussion

Current Treatment Modalities for Sellar Tumors

Microsurgery remains the gold standard for management of PA and CPH. The transsphenoidal approach is the most popular for PAs but also can be applied in some CPHs. Tumor removal is associated with various advantages, including histopathological confirmation of the diagnosis, immediate decompression of the optic apparatus, and rapid reduction of the excessive hormonal secretion. However, there are certain limitations for gross total resection of sellar neoplasms, which rate varies among series from 30 % to 90 %. Major morbidity after surgery (visual loss, ophthalmoplegia, stroke) is encountered in 3–4 % of cases, whereas less severe complications appear in 5–20 % [4]. Postoperative mortality, even in experienced hands, constitutes 1–3 %. The rate of postoperative complications is certainly higher, whereas surgical success is lower in cases of recurrent sellar tumors. Of note: the overall recurrence rate on the long-term follow-up after microsurgery for both PA and CPH varies between 8 % and 57 % [4].

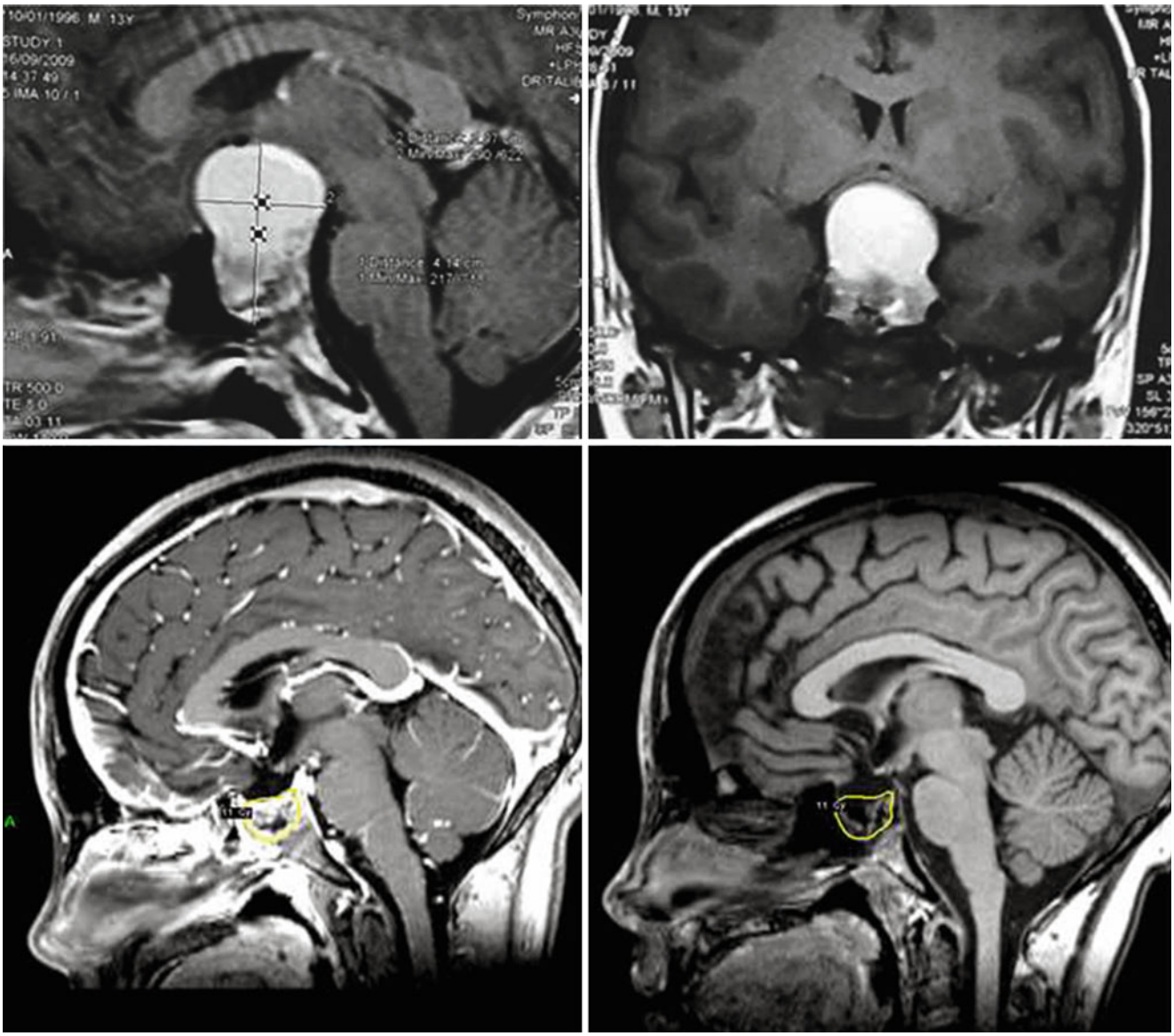

Fig. 2 A 4-year-old boy presented with optochiasmatic syndrome. He had significantly decreased visual acuity on the right eye, whereas the left eye was blind. MRI showed a giant suprasellar craniopharyngioma (*upper row*). The patient underwent subtotal tumor removal via the left frontolateral approach. His postoperative course was favorable. Control MRI scans at 3 months demonstrated an intrasellar tumor remnant, and Gamma Knife radiosurgery was performed (*lower left*). Tumor shrinkage was evident 12 months after treatment (*lower right*). *Yellow circle* designates prescription isodose line at the time of treatment

Recently Elliott et al. [1] performed a meta-analysis of 48 studies on CPHs (in total 2,995 cases), which included all main surgical series published between 1990 and 2010. The authors revealed that mortality varied from 0 % to 16 % and the gross total resection rate from 19 % to 100 %. Resection rates of the tumor were reported to be >90 % and >80 %, respectively, in only 3 and 9 of 48 series [1]. Recurrence after gross total resection varied from 3 % to 57 % and morbidity from 0 % to 20 %. The latter included diabetes insipidus (34–100 %), visual acuity worsening (5–41 %), and obesity and hyperphagia (6–70 %). Thus, although microsurgical tumor removal remains the best option for such tumors, there is a great need for other treatment modalities.

Medical treatment can be successfully applied to some hormone-secreting PAs. Particularly, dopamine agonists may be effective in prolactinomas, somatostatin analogs in acromegaly, and inhibitors of steroid synthesis in Cushing disease. Nevertheless, in a meta-analysis of 35 studies [4], the results of medical treatment of PA were considered limited, with hormonal normalization varying from 55 % to 90 % and the tumor volume reduction rate from 20 % to 80 %. Moreover, such therapeutic options have recognizable side

effects. Also, the drugs are not always available everywhere and are rather expensive, so some patients cannot afford such treatment for a lifelong duration.

Conventional fractionated radiotherapy (FRT) has long been recognized as an effective treatment option for both PAs and CPHs. In cases of hormone-secreting PAs, it results in endocrinological normalization in 10–83 % of patients [4]. Particulalrly, GH production can be controlled in 73–90 % of cases [4]. However, such effect is usually delayed, and the complication rate associated with the treatment is rather high. Optic neuropathy is encountered in 3–8 % of cases and long-term hormonal deficiency in 50–100 %. Radiation-induced neoplasms and stroke occur occasionally [4].

Finally, in addition to microsurgery and FRT, cystic CPH may be treated with intracavitary irradiation using isotopes of phosphorus or iridium or with intracavitary chemotherapy with bleomycin. The results of such treatment seem inconsistent, however.

All of the mentioned treatment modalities for sellar tumors are usually used in various combinations.

Stereotactic Radiosurgery for Sellar Tumors

During the last decades, stereotactic radiosurgery, particularly GKS, has become a widely recognizable option in multimodal treatment of patients with PA and CPH. It can be helpful in solving several problems associated with their management. Histopathological investigations have confirmed that the radiobiological effect of high-dose single-fraction irradiation has a more profound impact on the aberrant cells' behavior than do small radiation doses in a fractionated regimen.

Many studies have proved that radiosurgery is the best complementary treatment of PA if microsurgery and/or medical treatment does not control tumor growth or hormonal oversecretion, or if those modalities cannot be used for any reason. Good PA growth control after radiosurgery has been reported, whereas endocrinological cure rates in patients with hormone-secreting tumors vary widely. Overall, it seems that GH and ACTH oversecretion better controlled than excess of prolactin [4–6].

A meta-analysis of 1,621 cases from 35 published series on radiosurgery for PA evaluated the efficacy of this treatment [4]. In all, 22 series included 314 patients with Cushing disease. Tumor growth control was achieved in 68–100 % of cases, and in the series with at least 10 patients and a median follow-up period of 2 years the endocrinological cure rates varied from 17 % to 83 %. A total of 25 studies included 420 patients with acromegaly. Tumor growth control was achieved in 68–100 % of cases, and in the series with at least 10 patients and a median follow-up period of 2 years the endocrinological cure rates varied from 20 % to 96 %. Another 25 studies included 393 patients with prolactinomas. Tumor growth control was achieved in 68–100 % of cases, and endocrinological cure rates varied widely, from 0 % to 84 % [4]. It should be noted that in patients with hormone-secreting tumors radiosurgery appears to result in faster normalization of the hormonal levels than does FRT. Nevertheless, uniform endocrinological criteria for pre- and postradiosurgical evaluation of patients with sellar tumors still require clarification [3].

Although some morbidity accompanies radiosurgical treatment, according to the current data its risk in patients with sellar tumors is apparently lower than with FRT [3]. Reported complications of radiosurgery for PA were studied in the already mentioned meta-analysis of 1,621 cases in 35 series [4]. Visual worsening (i.e., radiation-related optic neuropathy) developed in 16 cases (1 %). The occurrence of new endocrine deficit may concern one-third of patients during the first 5 years after treatment. There were 13 cases of radiation injury to the brain parenchyma (mainly within the hypothalamus and/or temporal lobe), which clinical manifestations may appear as early as 5 h after treatment or as late as 1 year. Of note: 6 of the 13 patients with this complication had undergone previous FRT. Vascular complications were disclosed in two cases only. No cases of a secondary radiation-induced neoplasm was identified [4].

The results of radiosurgery continue to improve because of the technical advances that have resulted in the introduction of new devices (automatic positioning system, Leksell Gamma Knife PerfeXion), incorporation of the new imaging technologies into dose planning, and improved shielding techniques for better treatment conformity and steeper dose falloff outside the target volume. Moreover, whereas the role of radiosurgery as a second-line treatment for PAs and CPHs seems well established, its application as a primary option for management of such tumors is also possible in selected patients.

Nuances of the Radiosurgical Technique for Sellar Tumors

Radiosurgical treatment planning for sellar tumors has definite technical peculiarities, which are generally similar for PAs and CPHs. At present, treatment is usually recommended for small neoplasms that recur or are left in situ after attempted surgical resection. Good delineation of the lesion on MRI is the major issue.

Great care should be taken to avoid high-dose irradiation to the optic pathways. A dose of 8 Gy delivered to these anatomical structures seems sufficiently safe, whereas even 10 Gy, which is sometimes recommended, is associated with a low risk of complications. Also, for optimal treatment planning, the stereotactic frame should be fixed on the patient's head in an oblique position parallel to the optic pathways,

which optimizes their visualization on MRI and permits the surgeon to decrease irradiation to the optic tracts. Use of a 70° gamma angle for treatment is also helpful. Dosimetry should be fashioned in such a manner that the best gradient index is in the direction of the optic pathways. This is easier to achieve with the Gamma Knife PerfeXion and use of the "dynamic shaping" function, which allows the optic pathways to be defined as critical structures and ensuring that they are not exposed to excessive irradiation (>8 Gy). This tool permits delivery of 25 Gy dose to the target but decreases the dose to <3 Gy at 2–3 mm from its border. Using this technique, the automatically generated plugging pattern is displayed as shaded sectors.

The radiation dose delivered to the lesion must be sufficient to attain the desired outcome. When choosing the optimal dose, not only the volume of the neoplasm and distance to the optic pathways should be considered but also the nature and functional activity of the tumor, particularly for hormone-secreting PAs [4–6]. High-dose treatment is preferable in such cases as it can control hormone secretion (mean recommended dose is 25 Gy). In contrast, lower doses are effective for controlling the growth of nonsecreting PA (mean recommended dose is 15 Gy). Although CPHs are sometimes considered radioresistant, they usually demonstrate a good response to GKS even with low doses (9–12 Gy) [2].

Conclusion

Radiosurgery has been demonstrated to be a safe and effective second-line management option for PAs and CPHs. Occasionally, it is applied as primary treatment in patients who are deemed unfit for surgery or whose tumors are in inaccessible locations. The low tolerance of adjacent optic pathways to radiation represents the main limitation for the technique. To avoid possible complications, the dose delivered to these anatomical structures should not exceed 8 Gy.

Conflict of Interest The authors declare that they have no conflict of interest.

References

1. Elliott RE, Jane JA Jr, Wisoff JH (2011) Surgical management of craniopharyngiomas in children: meta-analysis and comparison of trancranial and transphenoidal approaches. Neurosurgery 48: 630–643
2. Gopalan R, Dassoulas K, Rainey J, Sherman JH, Sheehan JP (2008) Evaluation of the role of gamma knife surgery in the treatment of craniopharyngiomas. Neurosurg Focus 24(5):E5
3. Leenstra JL, Tanaka S, Kline RW, Brown PD, Link MJ, Nippoldt TB, Young WF Jr, Pollock BE (2010) Factors associated with endocrine deficits after stereotactic radiosurgery of pituitary adenomas. Neurosurgery 67:27–33
4. Sheehan JP, Niranjan A, Sheehan JM, Jane JA Jr, Laws ER, Kondziolka D, Flickinger J, Landolt AM, Loeffler JS, Lunsford LD (2005) Stereotactic radiosurgery for pituitary adenomas: an intermediate review of its safety, efficacy, and role in the neurosurgical treatment armamentarium. J Neurosurg 102:678–691
5. Stapleton CJ, Liu CY, Weiss MH (2010) The role of stereotactic radiosurgery in the multimodal management of growth hormone-secreting pituitary adenomas. Neurosurg Focus 29(4):E11
6. Tanaka S, Link MJ, Brown PD, Stafford SL, Young WF Jr, Pollock BE (2010) Gamma knife radiosurgery for patients with prolactin-secreting pituitary adenomas. World Neurosurg 74: 147–152

Role of Gamma Knife Radiosurgery in Multimodality Management of Craniopharyngioma

M. Abid Saleem, A. Sattar M. Hashim, Azher Rashid, and Muhammed Ali

Abstract *Objective*: This retrospective study evaluated the efficacy and safety of the use of Gamma Knife Radiosurgery (GKS) along with other surgical procedures in the management of craniopharyngioma.

Methods: Thirty-five patients (17 children and 18 adults) with craniopharyngioma were treated with GKS between May 2008 and August 2011. The age of the patients ranged from 2 to 53 years (mean 20 years). There were 26 males and 9 females. Craniopharyngiomas were solid in 7 patients, cystic in 4, and mixed in 24. Tumor size ranged from 1 to 33.3 cm^3 (mean 12 cm^3). The prescription dose ranged from 8 to 14 Gy (mean 11.5 Gy). Maximum dose ranged from 16 to 28 Gy (mean 23 Gy). Before GKS 11 patients underwent subtotal resection of the neoplasm, 2 – neuroendocopic fenestration of the large cystic component, and 10 – stereotactic aspiration of the neoplastic cyst content.

Results: The length of follow-up period varied from 6 to 36 months (mean 22 months). The tumor response rate and control rate were 77.1 % and 88.5 %, respectively. Clinical outcome was considered excellent in 10 cases, good in 17, fair in 4, and poor in 4. No one patient with normal pituitary function before GKS developed hypopituitarism thereafter. Deterioration of the visual function after treatment was noted in one patient.

Conclusion: After GKS tumor control can be achieved in significant proportion of patients with craniopharyngioma. Treatment-related neurological morbidity in such cases is rare. Therefore, radiosurgery may be considered useful for management of these tumors.

M.A. Saleem (✉) and A.S.M. Hashim
Department of Neurosurgery,
Pakistan Gamma Knife and Stereotactic Radiosurgery Center,
NeuroSpinal and Medical Institute,
100/1 Mansfield Street, M.A. Jinnah Road,
Sadder, Karachi 74400, Pakistan
e-mail: m_abidsaleem@hotmail.com

A. Rashid and M. Ali
Department of Radiation Oncology,
Pakistan Gamma Knife and Stereotactic Radiosurgery Center,
NeuroSpinal and Medical Institute,
Karachi, Pakistan

Keywords Craniopharyngioma • Gamma Knife radiosurgery • Neuroendoscopy • Stereotaxy

Introduction

Craniopharyngiomas are histologically benign tumors originating from embryonic epithelial cells deposited along the incompletely involuted hypophyseal-pharyngeal duct [24, 33]. Approximately 60 % of these lesions are primarily solitary cysts, 30 % have small neoplastic nodules with one or more cysts, and 10 % are solid [3]. Their management has been controversial. Attempted complete surgical resection can result in significant morbidity and mortality especially at facilities with a low case load. Alternatively, subtotal resection followed by conventional radiotherapy may lead to comparable outcomes while maintaining a good quality of life [25]. Particularly, the volume of cystic craniopharyngiomas can be easily reduced using various surgical techniques, including neuroendoscopic fenestration or stereotactic aspiration, with subsequent irradiation of the collapsed lesion [13, 22, 23, 26]. Nevertheless, still there are serious concerns considering possible posttreatment complications because of exposure of the peritumoral vital structures to irradiation.

Since the advent of radiosurgery, precise stereotactically guided radiation treatment has been applied to primary or residual intracranial tumors while sparing the surrounding tissues by a steep dose falloff outside the target volume [1–4, 31]. In the present study, we reviewed our experience with Gamma Knife radiosurgery (GKS) of craniopharyngiomas and analyzed the complementary role of this treatment modality along with other surgical methods in patients with these neoplasms.

Material and Methods

From May 2008 till August 2010, a total of 35 consecutive patients (17 children, 18 adults) with craniopharyngioma underwent GKS at the Pakistan Gamma Knife and Stereotactic

M.F. Chernov et al. (eds.), *Gamma Knife Neurosurgery in the Management of Intracranial Disorders*,
Acta Neurochirurgica Supplement, Vol. 116, DOI 10.1007/978-3-7091-1376-9_9, © Springer-Verlag Wien 2013

Table 1 Characteristics of patients with craniophharyngioma treated with GKS at the Pakistan Gamma Knife and Stereotactic Radiosurgery Center

No. of patients	35
Children/adults	17/18
Age (years)	2–53 (mean 20)
Sex (male/female)	26/9
Surgical procedures before GKS	
Microsurgical tumor resection	11
Neuroendoscopic cyst fenestration	2
Stereotactic aspiration of the cyst content	10
Ventriculoperitoneal shunting	17
Ommaya reservoir placement	5
Fractionated radiotherapy before GKS	2
Tumor volume (cm^3) at the time of GKS	1–33.3 (mean 12)
Type of tumor (solid/cystic/mixed)	7/4/24
Prescription radiation dose (Gy)	8–14 (mean 11.5)
Maximum irradiation dose (Gy)	16–28 (mean 23)
Length of follow-up (months)	3–36 (mean 22)
Tumor response to GKS	
Complete response	10 (28.6 %)
Partial response	17 (48.6 %)
No change	4 (11.4 %)
Progression	4 (11.4 %)
Additional surgical procedures after GKS	
Stereotactic aspiration of the cyst content	4
Ventriculoperitoneal shunting	2
Ommaya reservoir placement	2

GKS Gamma Knife radiosurgery

Radiosurgery Center. These cases were analyzed retrospectively. The main clinical, treatment, and outcome characteristics of the series are presented in Table 1.

The age of the patients varied from 2 to 53 years (mean 20 years). There were 26 males (74 %) and 9 females (26 %). Craniopharyngiomas were solid in 7 patients, cystic in 4, and mixed in 24. The tumor size ranged from 1.0 to 33.3 cm^3 (mean 12 cm^3). Before GKS, subtotal resection of the neoplasm was performed in 11 patients, neuroendocopic fenestration of the large cystic component was undertaken in 2 patients, stereotactic aspiration of the neoplastic cyst content was performed in 10 patients, a ventriculoperitoneal shunt was placed because of associated hydrocephalus in 17 patients, and an Ommaya reservoir was implanted in 5 patients to reduce the cyst size. Two patients underwent previous conventional fractionated radiotherapy.

Radiosurgical Technique

The Leksell G stereotactic head frame was attached to the patient's head after application of a local anesthetic. Children less than 12 years of age received general anesthesia. Gadolinium-enhanced axial T1-weighted and T2-weighted magnetic resonance imaging (MRI) and computed tomography (CT) scans were acquired in 1-mm slices and imported into the Leksell GammaPlan (Elekta Instruments AB, Stockholm, Sweden).

Radiosurgery was carried out using the Leksell Gamma Knife Model 4C (Elekta Instruments AB). Prescribed doses were calculated on the basis of the tumor volume, location, previous fractionated radiotherapy, and isodose line used. A progressively smaller dose was chosen for larger neoplasms and in cases with previous irradiation to reduce the possible risk of complications. The prescription and maximum radiation doses varied from 8 to 14 Gy (mean 11.5 Gy) and 16 to 28 Gy (mean 23 Gy), respectively. The maximum dose to the optic pathways was kept below 8–10 Gy in all patients who had not received prior radiotherapy. If it was deemed necessary, selected beam channels within each collimator were plugged to shift the peripheral isodose curves away from the optic nerve, chiasm, or optic tract.

Follow-Up

The follow-up period varied from 6 to 36 months (mean 22 months). After treatment, the patients were evaluated every 6 months with MRI or CT. Any changes in neuroendocrinological status and the presence of side effects were also assessed. Neuroimaging findings were classified into four groups to assess the tumor response, as described by Chung et al. [5]: complete response (CR)—residual tumor volume was <20 %; partial response (PR)—residual tumor volume was 20–50 %; no change (NC)—residual tumor volume was 50–80 %; progression (PG)—tumor volume increased or was >80 % of the initial volume. The clinical outcome was assessed by direct inquiry or clinical records and classified according to Kobayashi et al. [18] as excellent, good, fair, and poor.

Results

The tumor response rate and control rate after GKS were 77.1 % and 88.5 %, respectively. The overall responses of craniopharyngiomas evaluated on the latest postradiosurgery MRI scans were CR in 10 patients, PR in 17, NC in 4, and PG in 4. Solid and monocystic neoplasms after initial size reduction obtained with various surgical procedures had a

better control rate after radiosurgery than did the mixed-type craniopharyngiomas with multicystic components.

In the present series, five patients had long-standing complete visual loss before referral to our center. Among 14 other patients with visual impairment, visual acuity improved after GKS in 7 patients, whereas 6 others had maintained their original visual status at the latest follow-up. One patient with mixed-type multicystic craniopharyngioma complained of deteriorated vision after initial improvement despite a significantly reduced tumor volume. None of the patients in this series developed additional endocrinological impairment or neurological deterioration that could be attributed to radiosurgical treatment.

Increased neoplastic cyst volume at various time periods after GKS necessitated stereotactic aspiration of their contents in four patients and implantation of an Ommaya reservoir in two of them. Ventriculoperitoneal shunting was performed in two patients to relieve hydrocephalus.

Overall, the clinical outcome was considered excellent in 10 patients, good in 15, fair in 6, and poor in 4. Patients with mixed-type craniopharyngiomas harboring multicystic components had worse clinical outcomes than did those with single-component tumors.

Illustrative Cases

Case 1

A 7-year-old boy presented with headache and vomiting. A large cystic craniopharyngioma with associated obstructive hydrocephalus was diagnosed on neuroimaging. Neuroendoscopic fenestration of the cystic lesion was undertaken and a ventriculoperitoneal shunt was placed, which led to immediate relief of symptoms. GKS was performed subsequently. It was noted that prominent reduction of the cyst size permitted clear identification and delineation of the optic pathways and other adjacent anatomical structures, significantly facilitating treatment planning (Fig. 1a, b). The volume of the residual cystic lesion was 5.2 cm^3. A marginal dose of 12 Gy was applied to the 50 % isodose line with 98 % conformity. Multiple isocenters with 8- and 4-mm collimators were used in automatic positioning system (APS) mode. Follow-up CT scan after 1 year showed only a calcified spot (Fig. 1c). At 36 months after treatment, the child remains asymptomatic and is doing fine in school. The radiological findings are stable.

Case 2

A 32-year-old man was admitted after subtotal resection of a solid craniopharyngioma. He had reduced vision, which was more significant in the left eye, and experienced a single episode of generalized tonic-clonic seizure. The volume of the residual tumor was 7.2 cm^3. GKS was performed with a 12 Gy marginal dose applied to the 50 % isodose line with 98 % conformity (Fig. 2a). In all, 22 isocenters with 8- and 4-mm collimators were used in APS mode. At 6 months after treatment, the tumor size was reduced and central hypodensity had appeared, accompanied by markedly improved visual functions. At 12 months after GKS, the patient had no complaints and no neurological deficit. MRI demonstrated complete response of the tumor (Fig. 2b). At the 2-year follow-up, the patient had normal vision, and his clinical condition and MRI findings were stable (Fig. 2c).

Case 3

A 33-month-old child presented with headache and vomiting and was diagnosed with a craniopharyngioma. The tumor had a mixed structure and compressed the visual pathways. Parents refused the proposed surgical treatment but agreed to radiosurgery. At the time of GKS, the tumor volume was 3.0 cm^3. The marginal radiation dose of 10.5 Gy was applied to the 50 % isodose line with 89 % conformity (Fig. 3a). Three isocenters with an 8-mm collimator and 14 isocenters with a 4-mm collimator were used. At 3 months after treatment, 80 % reduction of the lesion volume was noted (Fig. 3b). Follow-up MRI at 1 year demonstrated a further reduction in the size of the neoplasm (Fig. 3c). At the last follow-up, the child is clinically asymptomatic.

Discussion

Craniopharyngiomas have haunted the most experienced investigators since the time of Cushing, who declared them to be neurosurgeons' most baffling problem [6]. Radical excision is the primary intervention [8, 21, 36] but is difficult to achieve without significant morbidity and mortality, despite the advances in microsurgery, neuroradiology, and neuroendocrinology [6, 7, 11, 12, 14, 15, 17, 23, 26, 28]. On the other hand, incomplete tumor resection has led to high rate of recurrences, which are even more difficult to treat [16, 17, 27, 29, 30, 32, 34].

During the 1960s, Kramer was seemingly the first to mention that craniopharyngiomas "are eminently suitable for radiation therapy and that combined treatment by surgery and irradiation offers these patients their best chance" [19]. This view was supported by various later studies [9–11, 14, 20, 27, 35]. As these tumors proved to be radiosensitive [5, 9, 18], stereotactic radiosurgery has been effective in their

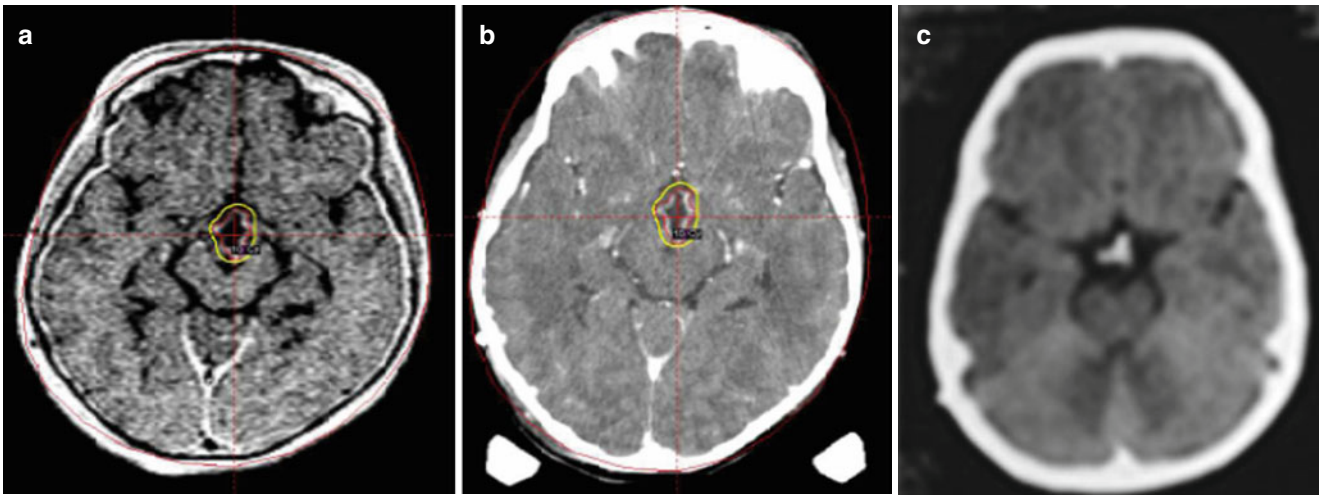

Fig. 1 Neuroimaging findings in a 7-year-old boy with a predominantly cystic craniopharyngioma treated with neurooendoscopic cyst fenestration, placement of a ventriculoperitoneal shunt, and GKS. Contrast-enhanced T1-weighted magnetic resonance imaging (MRI) (**a**) and computed tomography (CT) (**b**) performed at the time of radiosurgery demonstrated residual neoplastic cyst with a volume of 5.2 cm^3, and 12 Gy marginal dose was applied to the 50 % isodose line (*yellow circle*). CT at 12 months after treatment showed only a calcified spot (**c**)

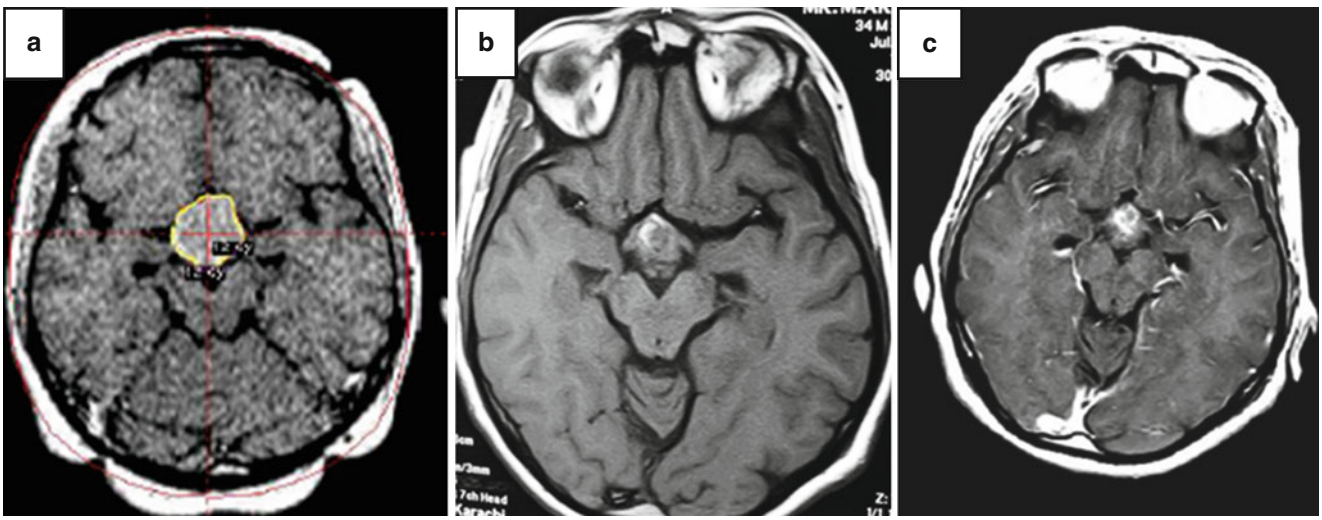

Fig. 2 Contrast-enhanced T1-weighted MRI of a 32-year-old man with a solid craniopharyngioma treated with subtotal resection and subsequent GKS. (**a**) At the time of radiosurgery, the volume of the residual tumor was 7.2 cm^3 and 12 Gy marginal dose was applied to the 50 % isodose line (*yellow circle*). (**b**) At 12 months after treatment, the tumor showed complete response, accompanied by significantly improved vision. (**c**) At 24 months after treatment, the tumor was stable, and visual functions of the patient were normal

management, particularly if combined with subtotal resection and/or other treatment modalities. The majority of lesions in our series were either purely cystic or had a significant cystic component. Their management was effective after initial application of subtotal microsurgical resection, neuroendoscopic cyst fenestration, stereotactic cyst aspiration, ventriculoperitoneal shunting, and/or Ommaya reservoir placement. Reduction of the lesion size, particularly of its cystic component, may significantly facilitate radiosurgical treatment planning. It not only reduces the target volume but permits clear identification and delineation of the adjacent anatomical structures. Nevertheless, our illustrative case 3 clearly demonstrates that GKS also can be used as a primary treatment modality in some patients with craniopharyngiomas. Thus, management can be individualized to the patient.

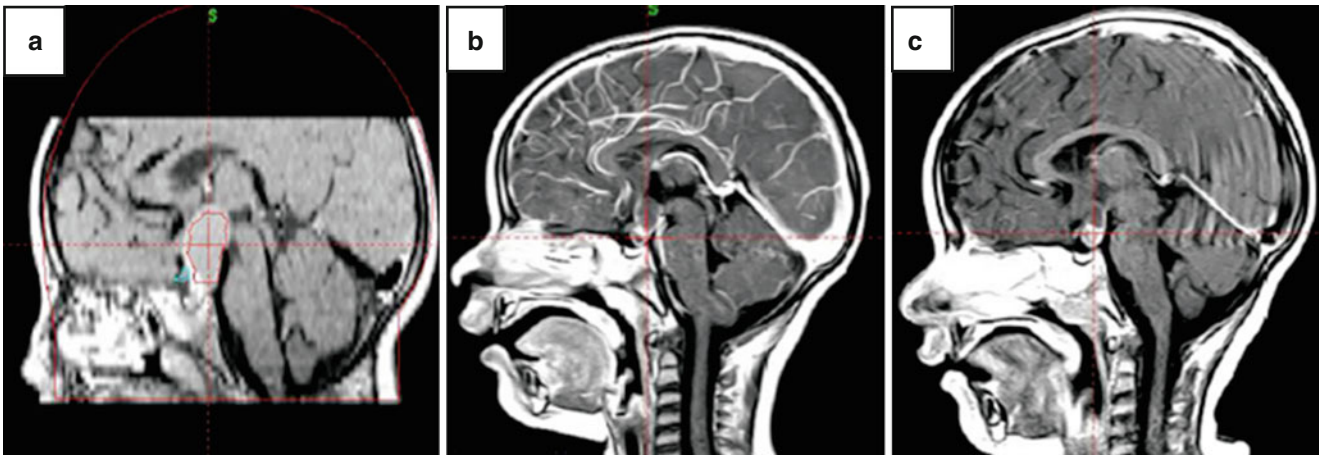

Fig. 3 Contrast-enhanced sagittal T1-weighted MRI in a 33-month-old child with a mixed-type craniopharyngioma treated solely with GKS. (**a**) At the time of radiosurgery, the volume of the tumor was 3.0 cm^3. At 3 months (**b**) and 1 year (**c**) after treatment, there was prominent reduction of the lesion size.

The optimal marginal doses usually recommended for GKS of craniopharyngioma vary from 6 to 12 Gy [5, 18, 31, 37]. In our series, marked regression of the tumor was frequently observed at doses of approximately 10 Gy. Such low doses allow preservation of the adjacent functionally important radiosensitive anatomical structures with or without use of the beam-plugging technique, even if the lesion is in direct contact with, for example, the visual pathways.

It was noted previously that cystic craniopharyngiomas may be resistant to radiosurgery [37]. In fact, in four our patients with mixed tumors, despite significant reduction of the solid component, prominent enlargement of the multicystic part of the neoplasm was observed after GKS. It necessitated stereotactic aspiration of the cyst content and implantation of an Ommaya reservoir in two of them. On the other hand, in many cases small monocystic craniopharyngiomas responded to radiosurgical treatment and showed excellent clinical outcomes within the limited follow-up period.

Conclusion

Gamma Knife radiosurgery may provide good tumor control and improve the quality of life of adult and pediatric patients with a craniopharyngioma. It may play a significant role in the management of such tumors as a single modality or in combination with other treatment options, such as microsurgery, neuroendoscopy, and stereotaxy.

Conflict of Interest The authors declare that they have no conflict of interests.

References

1. Backlund EO (1994) Treatment of craniopharyngiomas: the multimodality approach. Pediatr Neurosurg 21(Suppl):182–189
2. Barajas MA, Ramírez-Guzmán G, Rodríguez-Vázquez C, Toledo-Buenrostro V, Velásquez-Santana H, del Robles RV, Cuevas-Solorzano A, Rodriquez-Hernandez G (2002) Multimodal management of craniopharyngiomas: neuroendoscopy, microsurgery, and radiosurgery. J Neurosurg 97(5 Suppl):607–609
3. Chiou SM, Lunsford LD, Niranjan A, Kondziolka D, Flickinger JC (2001) Stereotactic radiosurgery of residual or recurrent craniopharyngioma, after surgery, with or without radiation therapy. Neuro Oncol 3:159–166
4. Chung WY, Pan HC, Guo WY, Shiau CY, Wang LW, Wu HM, Lee LS (1998) Protection of visual pathway in gamma knife radiosurgery for craniopharyngiomas. Stereotact Funct Neurosurg 70(Suppl 1):139–151
5. Chung WY, Pan DH, Shiau CY, Guo WY, Wang LW (2000) Gamma knife radiosurgery for craniopharyngiomas. J Neurosurg 93(3 Suppl):47–56
6. Cushing HW (1932) Intracranial tumors: notes upon a series of two thousand verified cases with surgical-mortality percentages pertaining thereto. Charles C Thomas, Springfield, p 97
7. De Vile CJ, Grant DB, Kendall BE, Neville BG, Stanhope R, Watkins KE, Hayward RD (1996) Management of childhood craniopharyngioma: can the morbidity of radical surgery be predicted? J Neurosurg 85:73–81
8. Fahlbusch R, Honegger J, Paulus W, Huk W, Buchfelder M (1999) Surgical treatment of craniopharyngiomas: experience with 168 patients. J Neurosurg 90:237–250
9. Fischer EG, Welch K, Shillito J Jr, Winston KR, Tarbell NJ (1990) Craniopharyngiomas in children. Long-term effects of conservative surgical procedures combined with radiation therapy. J Neurosurg 73:534–540
10. Flickinger JC, Lunsford LD, Singer J, Cano ER, Deutsch M (1990) Megavoltage external beam irradiation of craniopharyngiomas: analysis of tumor control and morbidity. Int J Radiat Oncol Biol Phys 19:117–122
11. Habrand JL, Ganry O, Couanet D, Rouxel V, Levy-Piedbois C, Pierre-Kahn A, Kalifa C (1999) The role of radiation therapy in the

management of craniopharyngioma: a 25-year experience and review of the literature. Int J Radiat Oncol Biol Phys 44:255–263
12. Hoffman HJ, De Silva M, Humphreys RP, Drake JM, Smith ML, Blaser SI (1992) Aggressive surgical management of craniopharyngiomas in children. J Neurosurg 76:47–52
13. Joki T, Oi S, Babapour B, Kaito N, Ohashi K, Ebara M, Kato M, Abe T (2002) Neuroendoscopic placement of Ommaya reservoir into a cystic craniopharyngioma. Childs Nerv Syst 18:629–633
14. Jose CC, Rajan B, Ashley S, Marsh H, Brada M (1992) Radiotherapy for the treatment of recurrent craniopharyngioma. Clin Oncol (R Coll Radiol) 4:287–289
15. Kalapurakal JA, Goldman S, Hsieh YC, Tomita T, Marymont MH (2003) Clinical outcome in children with craniopharyngioma treated with primary surgery and radiotherapy deferred until relapse. Med Pediatr Oncol 40:214–218
16. Katz EL (1975) Late results of radical excision of craniopharyngiomas in children. J Neurosurg 42:86–90
17. Kim SK, Wang KC, Shin SH, Choe G, Chi JG, Cho BK (2001) Radical excision of pediatric craniopharyngioma: recurrence pattern and prognostic factors. Childs Nerv Syst 17:531–537
18. Kobayashi T, Kida Y, Mori Y, Hasegawa T (2005) Long-term results of gamma knife surgery for the treatment of craniopharyngioma in 98 consecutive cases. J Neurosurg 103(6 Suppl):482–488
19. Kramer S, McKissock W, Concannon JP (1961) Craniopharyngiomas: treatment by combined surgery and radiotherapy. J Neurosurg 18:217–226
20. Kramer S, Southard M, Mansfield CM (1968) Radiotherapy in the management of craniopharnygioma: further experiences and late results. Am J Roentgenol Radium Ther Nucl Med 103:44–52
21. Matson DD, Crigler JF Jr (1969) Management of craniopharyngioma in childhood. J Neurosurg 30:377–390
22. Nakamizo A, Inamura T, Nishio S, Inoha S, Ishibashi H, Fukui M (2001) Neuroendoscopic treatment of cystic craniopharyngioma in the third ventricle. Minim Invasive Neurosurg 44:85–87
23. Nicolato A, Foroni R, Rosta L, Gerosa M, Bricolo A (2004) Multimodality stereotactic approach to the treatment of cystic craniopharyngiomas. Minim Invasive Neurosurg 47:32–40
24. Prabhu VC, Brown HG (2005) The pathogenesis of craniopharyngiomas. Childs Nerv Syst 21:622–627
25. Raimondi AJ (1993) Craniopharyngioma: complications and treatment failures weaken case of aggressive surgery. Crit Rev Neurosurg 3:7–24
26. Reda WA, Hay AA, Ganz JC (2002) A planned combined stereotactic approach for cystic intracranial tumors. Report of two cases. J Neurosurg 97(5 Suppl):610–612
27. Regine WF, Kramer S (1993) Pediatric craniopharyngioma: long-term results of combined treatment with surgery and radiation. Int J Radiat Oncol Biol Phys 24:611–617
28. Sainte-Rose C, Puget S, Wray A, Zerah M, Grill J, Brauner R, Boddaert N, Pierre-Kahn A (2005) Craniopharyngioma: the pendulum of surgical management. Childs Nerv Syst 21:691–695
29. Shi XE, Wu B, Fan T, Zhou ZQ, Zhang YL (2008) Craniopharyngioma: surgical experience of 309 cases in China. Clin Neurol Neurosurg 110:151–159
30. Sosa IJ, Krieger MD, McComb JG (2005) Craniopharyngiomas of childhood: the CHLA experience. Childs Nerv Syst 21:785–789
31. Úlfarsson E, Lindquist C, Roberts M, Rähn T, Lindquist M, Thorén M, Lippitz B (2002) Gamma knife radiosurgery for craniopharyngiomas: long term results in the first Swedish patients. J Neurosurg 97(Suppl 5):613–622
32. Vinchon M, Dhellemmes P (2008) Craniopharyngiomas in children: recurrence, reoperation and outcome. Childs Nerv Syst 24:211–217
33. Wang KC, Hong SH, Kim SK, Cho BK (2005) Origin of craniopharyngiomas: implication on the growth pattern. Childs Nerv Syst 21:628–634
34. Weiner HL, Wisoff JH, Rosenberg ME, Kupersmith MJ, Cohen H, Zagzag D, Shiminski-Maher T, Flamm ES, Epstein FJ, Miller DC (1994) Craniopharyngiomas: a clinicopathological analysis of factors predictive of recurrence and functional outcome. Neurosurgery 35:1001–1011
35. Yang I, Sughrue ME, Rutkowski MJ, Kaur R, Ivan ME, Aranda D, Barani IJ, Parsa AT (2010) Craniopharyngioma: a comparison of tumor control with various treatment strategies. Neurosurg Focus 28(4):E5
36. Yasargil MG, Curcic M, Kis M, Siegenthaler G, Teddy PJ, Roth P (1990) Total removal of craniopharyngiomas. Approaches and long-term results in 144 patients. J Neurosurg 73:3–11
37. Yomo S, Hayashi M, Chernov M, Tamura N, Izawa M, Okada Y, Hori T, Iseki H (2009) Stereotactic radiosurgery of residual or recurrent craniopharyngioma: new treatment concept using Leksell gamma knife model C with automatic positioning system. Stereotact Funct Neurosurg 87:360–367

Role of Radiosurgery in the Management of Intracranial Malignancies

Jeremy C. Ganz

Keywords Gamma Knife radiosurgery • Malignant intracranial tumor • Management • Stereotactic radiosurgery

Stereotactic radiosurgery (SRS) works by applying highly localized, focused radiation to a pathological target. It produces cure by damaging the target with the high dose and sparing adjacent tissues by a rapid dose falloff outside the target. The targets should not be large. It follows that a well-defined lesion with a clear-cut margin is the ideal target. This being so, apart from cerebral metastases, most malignancies would seem to be unsuitable for the method. They have unclear margins as a consequence of invading surrounding normal tissue. Also, they have been seen to be resistant to conventional radiotherapy. Moreover, many of them are larger than ideal for SRS.

Nonetheless, experience demonstrates that while being guided by theoretical principles, as outlined in the previous paragraph, we should perhaps not be slaves to them. For example, with glioblastomas it is well known that tumor cells extend well beyond the boundaries of the visible tumor. Yet recurrences almost invariably appear at the site of the original tumor. It is also known that a certain percentage of glioblastomas have a considerably longer survival than is usually expected, and there is at present no means to predict which tumor will behave in this way except by following up after treatment.

In the context of the tumors that are the subject of this discussion, the aim is (with one or two notable exceptions) palliation, not cure. However, adding a year or more of useful life following only a few days of treatment is not a negligible aim. Nonetheless, if SRS is to be applied for the treatment of such tumors, it must be done with strictness in the setting of indications. Moreover, in view of the complexity of the conditions, and with many patients having disease elements outside the cranium, it should not be undertaken by individual practitioners but by teams of experts covering—at the very least—the fields of neurosurgery, radiation and medical oncology, diagnostic neuroradiology, and in some cases other specialties for specific diseases, such as endocrinologists for pituitary adenomas.

The articles dedicated to a malignant topic in this volume of *Acta Neurochirurgica Supplement* illustrate the problems in a variety of ways. Takakura et al. [3] focus on a specific aspect of the treatment of brain metastases. They have developed a new dose-planning technique aimed at reducing the incidence of adverse radiation effects (AREs) following SRS. They demonstrate convincingly on a large number of patients that using multiple small collimator radiation shots has not demonstrated negative effects compared with the more conventional treatment of metastases with fewer but larger collimator shots. The tumor control rate is similar with these two methods. However, the incidence of complications is significantly lower. This is important. AREs following a palliative treatment in patients with an overall expected short survival have greater significance than those in patients with a long expected survival. The aim with using Gamma Knife surgery (GKS) for brain metastases is prolonged survival with a good quality of life. More than 10 % of AREs appeared in the group of patients who received a conventional dose plan and were demonstrated by the authors of this article. Using the multiple small collimator method resulted in this rate being reduced by nearly half. This is admirable, and there is every reason to consider applying this dose planning more widely.

It would be most helpful if the authors of this study considered providing us with more quantitative information about their method. The integral dose to the brain would be of interest. Even more interesting would be the 12 Gy volume of the brain, excluding tumors. With this information, other users could calculate more easily if they are to treat optimally. Another parameter of interest would be the gradient index. It is mentioned that the small collimator technique

J.C. Ganz
Department of Neurosurgery,
Haukeland University Hospital, Bergen, Norway

53 Market Street, Ulverston LA12 7LT, UK
e-mail: jcganz@gmail.com

M.F. Chernov et al. (eds.), *Gamma Knife Neurosurgery in the Management of Intracranial Disorders*,
Acta Neurochirurgica Supplement, Vol. 116, DOI 10.1007/978-3-7091-1376-9_10, © Springer-Verlag Wien 2013

produces a better gradient index, and the authors are aiming for a value of less than 3. It would again be helpful to know the actual values in the conventional and small collimator dose plans. It is hoped the authors will consider writing a supplementary paper to document this information.

Unlike the other two articles discussed in this short editorial, Dr. McCutcheon [1] presents not an original contribution but a valuable review of the status of treatment of a variety of intracranial malignant conditions with the Gamma Knife. The review is based on the extensive experience of one of the world's leading cancer treatment centers. The well-known difficulties of skull base surgery with involvement of vessels and nerves within the tumors are considered. The impossibilities of radical resection are noted. A further point that can easily be forgotten is the sad truth that chemotherapy of these various tumors has little or no part to play in their management. This makes radiation therapy of various kinds of great importance, given the limitations of surgery. However, perhaps the major value of this article is to provide a framework of what is possible. In almost all instances, management is palliative not therapeutic, yet this author provides evidence of the value of this palliation related to a variety of diagnoses.

Certain technical difficulties are reviewed with simple clarity. Invasive tumors often have highly complex shapes and so require complex treatment plans. Previous therapy may complicate the definition of targets because of postoperative scarring, local fibrosis, and other changes. Another problem arises because of the rarity of these tumors, so individual centers find it difficult to acquire broad experience. It is exactly this difficulty that Dr. McCutcheon's article helps to rectify. It covers a wide variety of topics, which the interested reader would do well to peruse. However, its major interest lies in pointing out diagnoses where good results can be obtained. Although not exactly stating it, the article provides support for the work of others who now think that GKS can be applied as a primary treatment for glomus tumors. For chondrosarcomas and the rare pituitary carcinoma, long-term survival is possible. Five-year survival for patients with a chordoma is encouraging. Thus, those of us faced with a malignant intracranial extracerebral malignancy would do well to familiarize ourselves with this article, which provides a most useful guide to sensible practice. It also demonstrates that although management remains largely palliative, it can be surprisingly worthwhile in a significant number of cases.

The possibilities of GKS for treating higher World Health Organization (WHO) grades of meningioma are illustrated in the study of Mori et al. [2]. Although there are too few patients with WHO grade III neoplasms to draw any clear conclusions, for the entire series (mostly atypical meningiomas) the tumor control rate was 74 % at 1 year, 52 % at 2 years, and 34 % at 3 years. This is in keeping with the findings of others, as noted in the discussion. Thus, the article demonstrates that although GKS does not cure these patients it produces useful extra survival. The study is a little less clear in the relations of the dose and volume to the results. Nonetheless, the article provides evidence that GKS for WHO grade II meningiomas has a useful role in prolonging a life of good quality. There has been until recently doubt about the appropriateness of GKS for these tumors, but this study provides a basis for an aggressive approach to the tumors, which is rather helpful.

The authors of all three articles [1–3] are to be congratulated on providing information that assists in the management of difficult conditions. Optimal treatment remains elusive, but work such as discussed herein is surely a useful step on the way to providing it.

Conflict of Interest The author works as a consultant for Elekta AB Company, which manufactures the Gamma Knife. He has received no financial support in the preparation of this Editorial and can state that there is no conflict of interest.

References

1. McCutcheon IE (2013) Stereotactic radiosurgery for malignant extracerebral intracranial tumors: patient selection, efficacy, and technical nuances. Acta Neurochir Suppl 116:71–83 (present volume)
2. Mori Y, Tsugawa T, Hashizume C, Kobayashi T, Shibamoto Y (2013) Gamma knife stereotactic radiosurgery for atypical and malignant meningiomas. Acta Neurochir Suppl 116:85–89 (present volume)
3. Takakura K, Hayashi M, Chernov MF, Tamura N, Izawa M, Okada Y, Tamura M, Muragaki Y, Iseki H (2013) Gamma knife treatment strategy for metastatic brain tumors. Acta Neurochir Suppl 116:63–69 (present volume)

Gamma Knife Treatment Strategy for Metastatic Brain Tumors

Kintomo Takakura, Motohiro Hayashi, Mikhail F. Chernov, Noriko Tamura, Masahiro Izawa, Yoshikazu Okada, Manabu Tamura, Yoshihiro Muragaki, and Hiroshi Iseki

Abstract From 1993 to 2011, a total of 3,095 patients with brain metastases underwent Gamma Knife radiosurgery (GKS) at Tokyo Women's Medical University. Follow-up information on 2,283 of these patients was available for retrospective analysis. The cases were separated into three groups according to the treatment period, the model of the Gamma Knife used, main goals of treatment, and technical nuances of radiosurgery. In the latest cohort of patients treated with the Leksell Gamma Knife model 4C with automatic positioning system, an optimized treatment strategy was applied. It was based on highly selective dose planning, with the use of multiple small isocenters located within the bulk of the mass, which was done for prevention of the excessive irradiation of the perilesional brain and avoidance of its posttreatment edema. In cases of large cystic tumors, selective coverage of the contrast-enhancing capsule with chain-like application of multiple small isocenters was done. Introduction of the new treatment strategy did not affect the 1-year tumor control rate, which was consistently >90 %. However, it did result in a statistically significant reduction of severe posttreatment peritumoral brain edema (from 15.5 % to 6.3 %; $P<0.0001$). In conclusion, recent technical and methodological achievements of GKS seemingly do not affect its high efficacy in cases of brain metastasis with regard to tumor control. However, it may result in a prominent reduction of treatment-associated morbidity, which is particularly important in patients with large and/or critically located neoplasm.

Keywords Automatic positioning system • Brain edema • Complication • Gamma Knife radiosurgery • Metastatic brain tumor • Treatment

K. Takakura (✉)
Institute of Advanced Biomedical Engineering and Science,
Tokyo Women's Medical University,
8-1 Kawada-cho, Shinjuku-ku, Tokyo 162-8666, Japan
e-mail: ktakakura@abmes.twmu.ac.jp

M. Hayashi, M.F. Chernov, M. Tamura, Y. Muragaki, and H. Iseki
Faculty of Advanced Techno-Surgery,
Institute of Advanced Biomedical Engineering and Science,
Tokyo Women's Medical University,
Tokyo, Japan

Department of Neurosurgery, Neurological Institute,
Tokyo Women's Medical University,
Tokyo, Japan

N. Tamura, M. Izawa, and Y. Okada
Department of Neurosurgery, Neurological Institute,
Tokyo Women's Medical University,
Tokyo, Japan

Introduction

Cancer is a leading cause of death in Japan. In the past, intracranial metastases were thought to reflect the terminal stage of the disseminated disease, so their management was considered useless. Recent clinical evidence has demonstrated, however, that many patients with metastatic brain tumors could survive long enough with a good quality of life after effective treatment. This is particularly true for stereotactic radiosurgery, which is currently one of the main standard therapeutic options in such cases. Particularly in Japan, Gamma Knife radiosurgery (GKS) is widely performed for management of brain metastases because its cost is fully covered by national health insurance.

Nevertheless, radiosurgical treatment is sometimes accompanied by undesirable morbidity [2, 12], particularly that related to radiation-induced brain edema (Fig. 1). The incidence and severity of this complication is directly related to the volume of the target and the radiation dose. The greater the size and the higher the dose, the more frequent and severe is posttreatment peritumoral edema. The use of modern equipment, such as the automatic positioning system (APS) (Elekta Instruments AB, Stockholm, Sweden), may reduce the risk of complications after GKS of brain tumors. During the last decade, we developed and introduced an optimized radiosurgical concept for management of brain metastases, which is focused on avoidance of the excessive irradiation of the perilesional brain. This treatment method, based on the

M.F. Chernov et al. (eds.), *Gamma Knife Neurosurgery in the Management of Intracranial Disorders*,
Acta Neurochirurgica Supplement, Vol. 116, DOI 10.1007/978-3-7091-1376-9_11, © Springer-Verlag Wien 2013

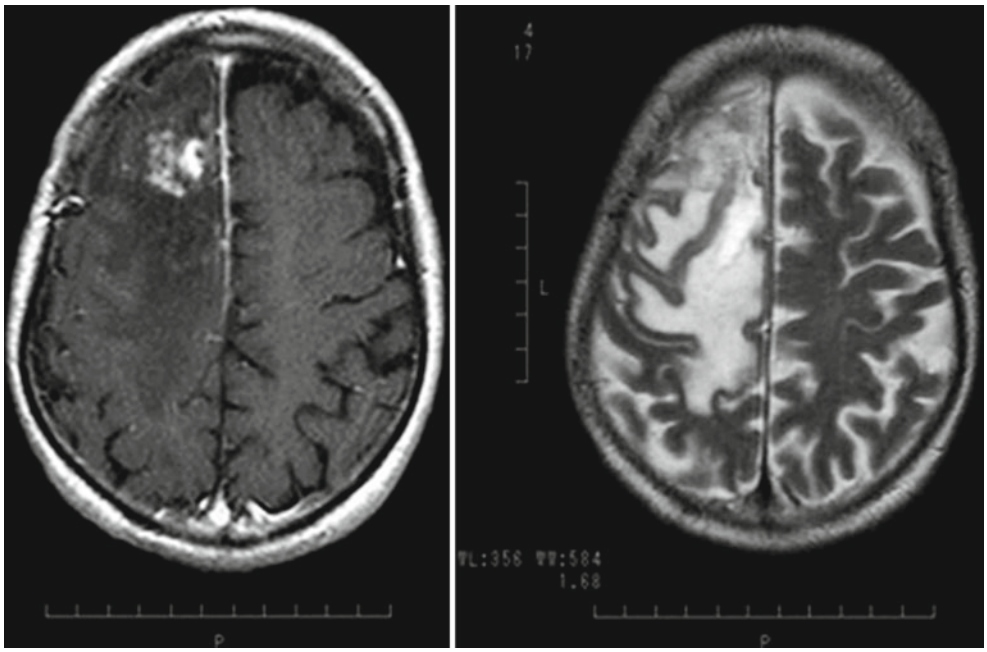

Fig. 1 Severe perilesional brain edema after Gamma Knife radiosurgery (GKS) of a brain metastasis demonstrated on gadolinium-enhanced T1-weighted (*left*) and T2-weighted (*right*) magnetic resonance imaging (MRI)

use of multiple small isocenters located within the bulk of the mass, was especially useful in cases of large, cystic, and/or deep-seated neoplasms, particularly located in or in close vicinity to the eloquent anatomical structures, such as the brain stem. The basic principles of this radiosurgical strategy are presented herein along with the main treatment results obtained in the large series of patients with intracranial metastases who underwent GKS at our clinic during the last 18 years.

Materials and Methods

From 1993 until 2011, a total of 5,833 patients underwent GKS in Tokyo Women's Medical University for management of various intracranial disorders, and 3,095 of them (53.1 %) had metastatic brain tumors. In 2,283 of the latter cases, more or less sufficient follow-up information was available for retrospective analysis of the treatment results obtained with different models of the Leksell Gamma Knife (Elekta Instruments AB) and various treatment concepts. The vast majority of tumors originated from the lung (63 %), followed by the breast (12 %), colon and rectum (8 %), kidney (4 %), and other organs (13 %). Patients with large neoplasms usually underwent initial partial tumor resection followed by GKS of the residual and/or distant lesions. Additional prophylactic whole-brain radiation therapy (WBRT) was not administered routinely.

Treatment Groups

The patients were separated into three groups according to the treatment period, model of the Gamma Knife used, main goals of treatment, and technical nuances of radiosurgery.

Group A

From 1993 to 2002, a total of 220 patients underwent radiosurgery using the Leksell Gamma Knife model B with manual setting of coordinates for each isocenter. The main goal of treatment was to control tumor growth as much as possible. Standard gadolinium-enhanced T1-weighted magnetic resonance imaging (MRI) with a slice thickness of 2.0 mm was applied to delineate the target. Typically, 8- and 14-mm collimators were utilized. The marginal dose usually corresponded to the 50 % isodose line and constituted 22–24 Gy.

Group B

From 2003 to 2004, a total of 542 patients underwent radiosurgery using the Leksell Gamma Knife model 4C-APS mainly with computer-controlled automatic setting of coordinates for the isocenters. The main goal of treatment was accuracy of the irradiation with regard to conformity and selectivity of dose planning. Standard gadolinium-enhanced T1- and T2-weighted MRI with a slice thickness of 2.0 mm

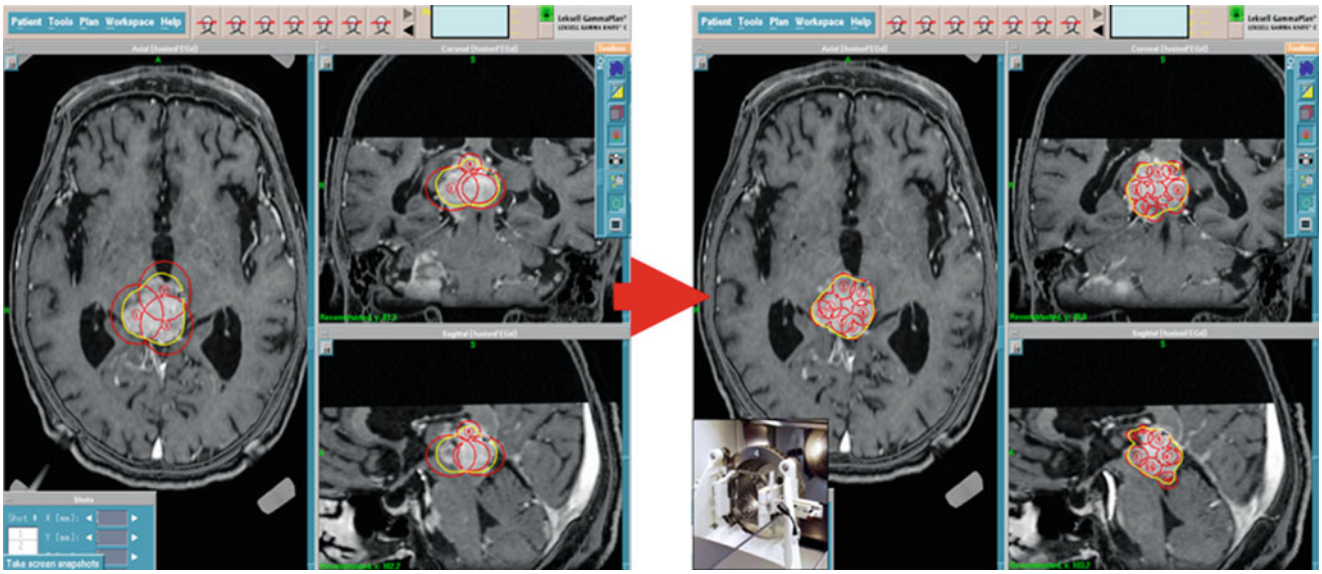

Fig. 2 Shift from traditional radiosurgery for a deep-seated metastatic brain tumor using a small number of large isocenters (*left*) to a new treatment strategy based on the advantages of the automatic positioning system (APS) with a large number of small isocenters selectively located within the bulk of the mass (*right*). The method focuses on avoidance of the excessive irradiation of the perilesional brain, thereby preventing posttreatment edema. Isocenters location (*red circles*) and 50 % isodose line covering the tumor margin (*yellow line*) are shown

was applied to delineate the target. Typically, a combination of 4-, 8, and 14-mm collimators was used. The marginal dose usually corresponded to the 50 % isodose line and constituted 20–22 Gy.

Group C

From 2005 to 2011, a total of 1,521 patients underwent radiosurgery using the Leksell Gamma Knife model 4C-APS mainly with computer-controlled automatic setting of coordinates for the isocenters. The main goal of GKS was defined as providing the best possible quality of life for the patients by maximally effective treatment while avoiding the risk of complications. To delineate the target, in addition to the standard gadolinium-enhanced T1- and T2-weighted MRI with a slice thickness of 2.0 mm, gadolinium-enhanced constructive interference in steady state (CISS) images with a slice thickness of 0.5 mm were applied. Typically, a combination of 4- and 8-mm collimators were utilized, and a 14-mm collimator was used very infrequently. The marginal dose usually corresponded to the 50 % isodose line and constituted 20–22 Gy.

The most recent 521 group C patients (mean age 62 years; range 20–92 years) were analyzed separately. This latest cohort was characterized by application of the original treatment concept based on the advantages of APS. To avoid excessive irradiation of the perilesional brain and prevent posttreatment edema, particularly in the presence of a large tumor, we used multiple small isocenters selectively located within the bulk of the mass (Fig. 2). In the case of huge cystic metastases—which, however, did not require immediate volume reduction—stereotactic aspiration of the cyst content was avoided, and GKS alone was performed with "donut-shaped" treatment planning [4] directed at selective coverage of the contrast-enhancing tumor capsule with chain-like application of the multiple small isocenters (Fig. 3). The mean follow-up after GKS in this latest cohort of patients constituted 264 days (range 5–1,380 days).

Analyzed Factors

The 1-year tumor control rate, local recurrence rate, incidence of severe posttreatment brain edema requiring specific management, and frequency of radiation-induced necrosis were evaluated and compared among the treatment groups. Statistical analysis was performed with the χ^2 test. The level of significance was determined at $P<0.05$.

Results

Reliable data on tumor control were not available for group A. Tumor control at 1 year was attained in 503 of 542 patients (92.8 %) in group B and in 487 of 521 cases (93.4 %) in our latest patient cohort. This difference did not reach statistical significance ($P=0.6672$).

Reliable data on the local recurrence rate were not available for group A. In group B it constituted 7.2 % (39/542

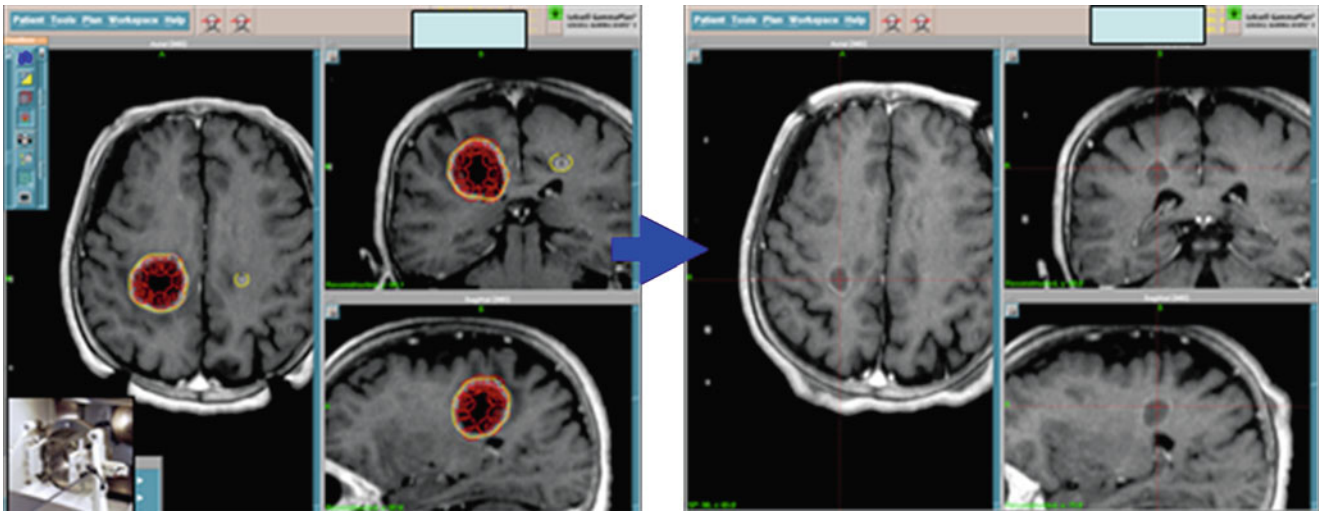

Fig. 3 "Donut-shaped" radiosurgical treatment for a large cystic metastatic brain tumor without stereotactic aspiration of the cyst content. Selective coverage of the contrast-enhancing tumor capsule by chain-like application of multiple small isocenters (*left*) resulted in significant volume reduction of the lesion (*right*). Note the absence of the perilesional edema after treatment (From Hayashi et al. [4])

cases). Altogether, 30 of these patients underwent a second GKS, but in 6 of them surgical resection of the residual lesion was required later. In our latest patient cohort, the local recurrence rate was 6.6 % (34/521 cases), whereas the mean and median time periods up to diagnosing treatment failure were, correspondingly, 277 and 183 days (Fig. 4). In all, 14 of these patients underwent surgical resection of the residual lesion later. The local recurrence rate did not differ significantly between the aforementioned treatment groups ($P=0.6672$), whereas the difference in number of patients requiring surgical resection of the neoplasm after initial GKS reached borderline significance (1.1 % vs. 2.7 %; $P=0.0574$).

Development of severe peritumoral brain edema after GKS of brain metastases was noted in 34 of 220 cases (15.5 %) in group A, 48 of 542 cases (8.9 %) in group B, and 33 of 521 cases (6.3 %) in our latest patient cohort (Fig. 5). The difference between treatment groups was statistically significant ($P<0.001$). The mean and median time periods up to diagnosing the complication in our latest patient cohort were 190 and 105 days, respectively (Fig. 6).

Reliable data on the incidence of radiation-induced necrosis were not available for group A. It had developed in 8 of 542 patients (1.5 %) in group B. Surgical resection of the lesion was required in two of them. The complication was seen in 10 of 521 patients (1.9 %) in our latest cohort. This difference did not reach statistical significance ($P=0.5755$).

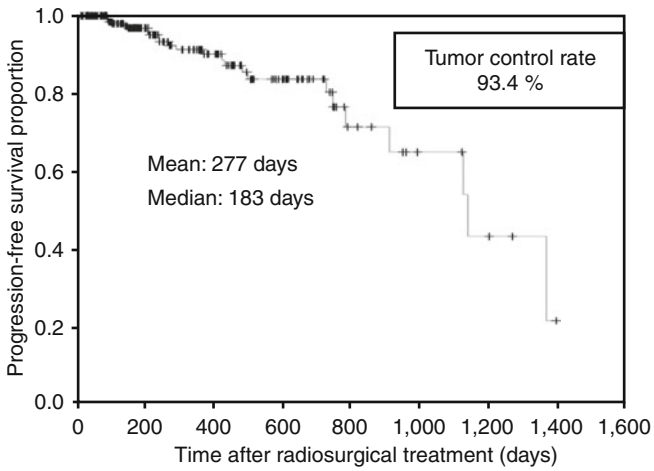

Fig. 4 Kaplan-Meier curve demonstrates local tumor control after GKS of brain metastases in our latest cohort of patients ($N=521$). Overall 1-year tumor control rate is shown, as are the mean and median time periods up to diagnosis of the local treatment failure in 34 cases

Discussion

Because life expectancy of patients with metastatic brain tumors is generally limited, the goal of their treatment should be defined as maximum prolongation of survival with a high quality of life. Such objectives can be attained by various modalities, including surgical resection, radiotherapy, chemotherapy, and immunotherapy [11], but minimally invasive therapeutic options are the most desirable. Therefore, stereotactic radiosurgery—which can provide highly effective, nearly noninvasive, relatively low cost, rather safe management of both single and multiple intracranial metastases—has been widely accepted among medical practitioners [8]. In Japan, patients with metastatic brain tumors comprise 56 % (53 % in the present series) of all patients undergoing GKS for various diseases. The corresponding proportion in other countries is approximately 35 %.

In cases of intracranial metastases radiosurgery provides a high rate of tumor control. In the present series of patients,

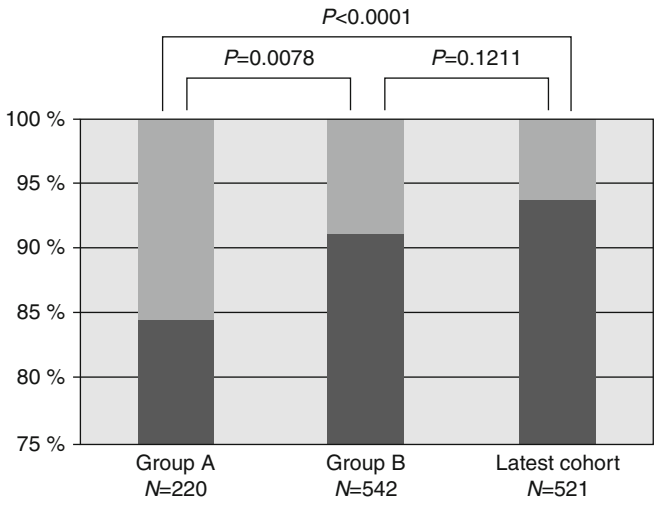

Fig. 5 Incidence of peritumoral brain edema after radiosurgery of brain metastases performed with different models of the Leksell Gamma Knife (Elekta Instruments AB) according to various treatment concepts. *N* number of case

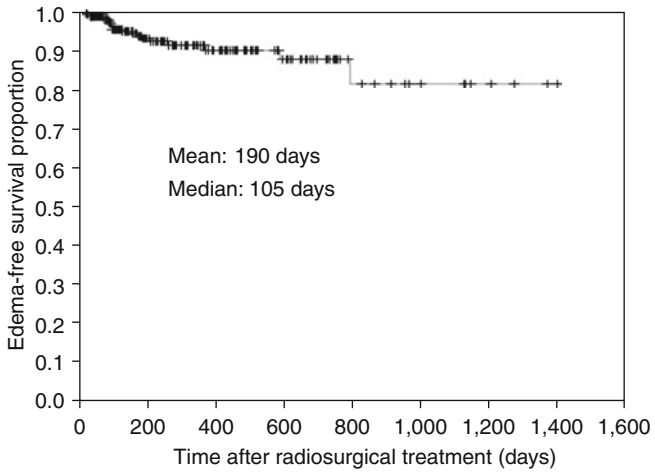

Fig. 6 Kaplan-Meier curve demonstrates development of severe peritumoral brain edema after GKS of brain metastases in our latest cohort of patients ($N=521$). Mean and median time periods up to diagnosis of the complication in 33 cases are shown

who were treated without routine administration of WBRT, the rate was >90 % at 1 year of follow-up. Nevertheless, some neoplasms demonstrate more or less prominent resistance to irradiation and progress thereafter [2]. Previously in such cases, we usually performed a second radiosurgery, whereas at present we more often proceed to open surgery, which was reflected in the increased number of patients who underwent lesion resection after initial GKS in our latest cohort.

Radiosurgery may be accompanied by various complications [12], among which the development of peritumoral brain edema is troublesome. Whereas mild-to-moderate edema can be successfully controlled with steroids, severe edema frequently presents a significant therapeutic challenge. This is especially true if the lesion is located in or in close proximity to important anatomical structures including the brain stem.

Among the main factors that lead to the development of brain edema after GKS, inadvertent irradiation of normal brain tissue adjacent to the target has special importance, particularly because of its possible avoidance by highly selective dose planning. To attain such a goal we currently use application of the multiple small isocenters located within the bulk of the mass. This technique seems especially useful for large tumors and usually permits us to keep the gradient index at <3, which is recommended for safe radiosurgical practice [3, 6]. Reducing the irradiation dose outside the target may preserve the function of the adjacent brain and prevent development of severe posttreatment perilesional brain edema. The incidence of such complication was reduced in our patients, from 15.5 % to 6.3 %, after introducing the described treatment strategy, whereas the tumor control rate was not affected. Of note: the relatively large number of isocenters does not create any obstacle for treatment because of the availability of APS, which significantly facilitates multi-isocenter GKS.

With some modification, a similar technique can be applied to management of large cystic metastases. In such cases, stereotactic aspiration of the cyst content before radiosurgery is usually recommended, although it is sometimes complicated by hemorrhage, infection, or tumor dissemination. Taking into consideration the limited life expectancy of patients with metastatic brain tumors, the risk of such morbidity is highly undesirable. Hence, stereotactic surgical intervention is avoided if strict indications are absent. In fact, during recent years we successfully treated 10 patients with large cystic neoplasms (which did not require immediate volume reduction) by GKS alone. The original "donut-shaped" treatment planning [4] was focused on selective coverage of the contrast-enhancing tumor capsule with chain-like application of multiple small isocenters leaving the central cystic part only minimally irradiated. Of the 10 lesions, 9 demonstrated significant shrinkage after GKS, and none of the patients developed posttreatment edema.

It should be emphasized that in the majority of cases metastatic brain tumors are multiple. Even in patients with a single neoplasm identifiable by CT or MRI, there is a high possibility of additional tiny lesions, the sizes of which are beyond the resolution of contemporary neuroimaging modalities. WBRT is frequently recommended to prevent further progression of such hidden neoplasms. However, this treatment, although relatively effective, can result in injury of normal brain tissue and may significantly reduce the quality of the patient's life, mainly owing to decline of higher cortical functions. There are several controversial reports on the results of studies evaluating the effectiveness of prophylactic WBRT after stereotactic radiosurgery [1, 5,

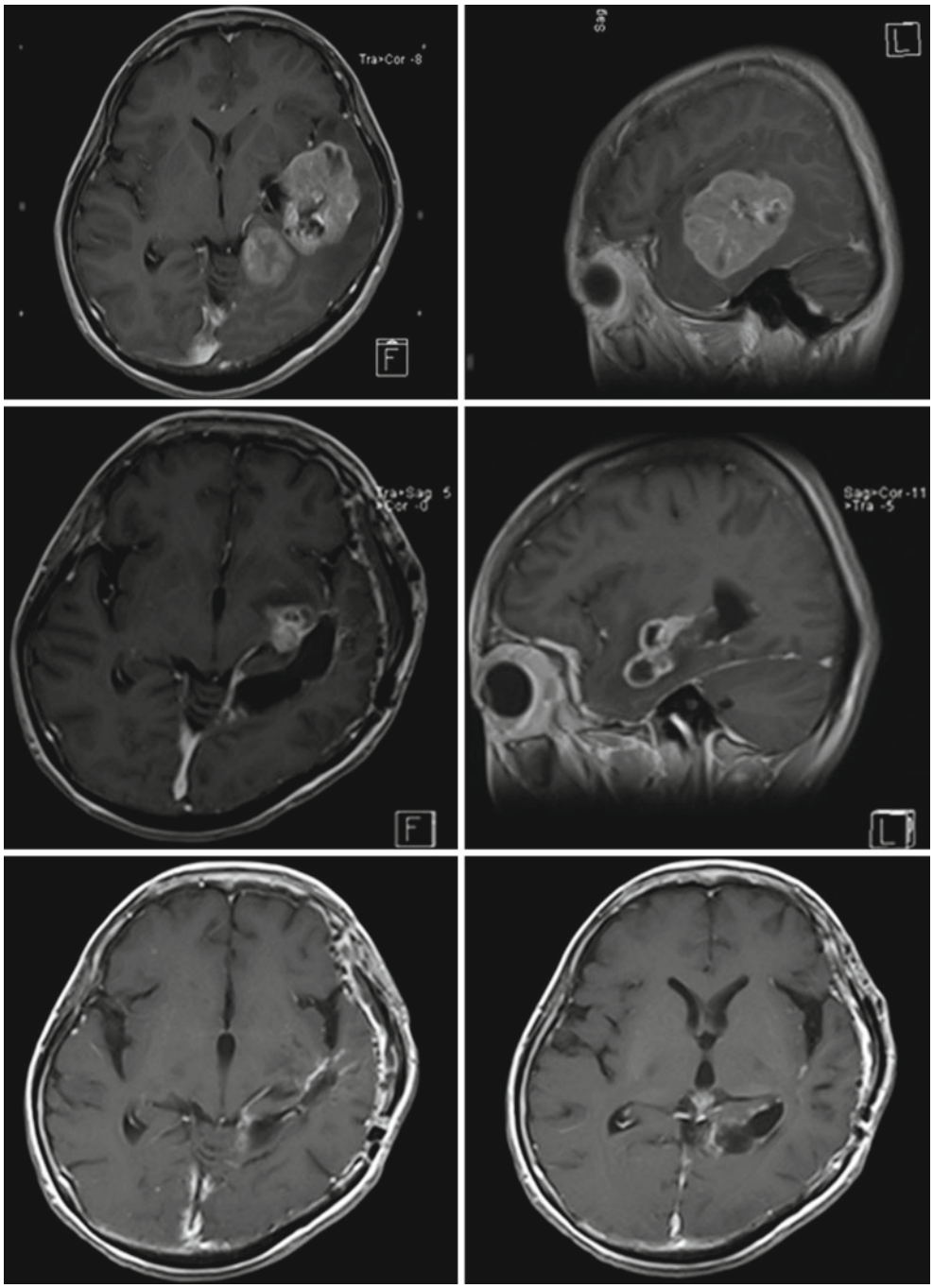

Fig. 7 Giant metastatic brain tumor at the time of diagnosis (*upper*), after partial surgical resection (*center*), and during follow-up after subsequent GKS of the residual neoplasm (*lower*). Complete tumor response to the combined treatment was attained

7–10]. In a randomized controlled trial, Aoyama et al. [1] revealed that there are no significant differences in overall survival or quality of life of patients treated with radiosurgery alone or with additional WBRT. Based on such results and taking into consideration that newly appearing brain metastases can be easily controlled with repeat GKS, we have practically abandoned administration of WBRT in our patients.

Despite the technical and methodological achievements of contemporary GKS, there are still limitations for its application in some patients, particularly related to the size of the tumor. Usually, brain metastases with a diameter of >3 cm are considered not suitable for radiosurgery. It is possible, however, that use of the described treatment strategy will permit application of GKS to relatively large lesions, which traditionally are considered not suitable for such treatment. However, in patients with giant neoplasms, combined treatment with initial surgical resection and subsequent GKS is still preferable and frequently result in long-term control of metastatic brain disease (Fig. 7).

Conclusions

Gamma Knife radiosurgery is highly effective in the management of single and multiple metastatic brain tumors. In our large series of patients treated without routine administration of WBRT, the tumor control rate at 1 year was >90 %. Moreover, an optimized treatment strategy based on the use of multiple small isocenters selectively located within the bulk of the mass avoids excessive irradiation of the adjacent brain and results in a significantly reduced incidence of severe posttreatment perilesional edema. It is especially important in the case of a large and/or a critically located tumor. For giant neoplasms, however, combined management with surgical resection and subsequent radiosurgery still represents the preferable option.

Conflict of Interest The authors declare that they have no conflict of interest.

References

1. Aoyama H, Shirato H, Tago M, Nakagawa K, Toyoda T, Hatano K, Kenjyo M, Oya N, Hirota S, Shioura H, Kunieda E, Inomata T, Hayakawa K, Katoh N, Kobashi G (2006) Stereotactic radiosurgery plus whole-brain radiation therapy vs stereotactic radiosurgery alone for treatment of brain metastases: a randomized controlled trial. JAMA 295:2483–2491
2. Chernov MF, Hayashi M, Izawa M, Usukura M, Yoshida S, Ono Y, Muragaki Y, Kubo O, Hori T, Takakura K (2006) Multivoxel proton MRS for differentiation of radiation-induced necrosis and tumor recurrence after Gamma Knife radiosurgery for brain metastases. Brain Tumor Pathol 23:19–27
3. Ganz JC (2011) Gamma Knife neurosurgery. Springer, Vienna, pp 101–102
4. Hayashi M, Chernov M, Tamura N, Tamura M, Izawa M, Muragaki Y, Iseki H, Okada Y (2011) "Donut's shape" radiosurgical treatment planning for large cystic metastatic brain tumors. Minim Invasive Neurosurg 54:286–289
5. Kondziolka K, Patel A, Lunsford LD, Kassam A, Flickinger JC (1999) Stereotactic radiosurgery plus whole brain radiotherapy versus radiotherapy alone for patients with multiple brain metastases. Int J Radiat Oncol Biol Phys 45:427–434
6. Paddick I, Lippitz B (2006) A simple dose gradient measurement tool to complement the conformity index. J Neurosurg 105(Suppl): 194–201
7. Serizawa T, Higuchi Y, Nagano O, Ono J, Matsuda S, Saeki N (2010) Gamma Knife® radiosurgery alone for one to four brain metastases: is prophylactic whole-brain radiation therapy really necessary? In: McDermott MW (ed) Radiosurgery, vol 7. Karger, Basel, pp 258–267
8. Serizawa T, Iuchi T, Ono J, Saeki N, Osato K, Odaki M, Ushikubo O, Hirai S, Sato M, Matsuda S (2000) Gamma knife treatment for multiple metastatic brain tumors compared with whole-brain radiation therapy. J Neurosurg 93(Suppl 3):32–36
9. Sneed PK, Lamborn KR, Forstner JM, McDermott MW, Chang S, Park E, Gutin PH, Phillips TL, Wara WM, Larson DA (1999) Radiosurgery for brain metastases: is whole brain radiotherapy necessary? Int J Radiat Oncol Biol Phys 43:549–558
10. Sneed PK, Suh JH, Goetsch SJ, Sanghavi SN, Chappell R, Buatti JM, Regine WF, Weltman E, King VJ, Breneman JC, Sperduto PW, Mehta MP (2002) A multi-institutional review of radiosurgery alone vs. radiosurgery with whole brain radiotherapy as the initial management of brain meastases. Int J Radiat Oncol Biol Phys 53:519–526
11. Takakura K, Sano K, Hojo S, Hirano A (1982) Metastatic tumors of the central nervous system. Igaku-Shoin, Tokyo, pp 195–279
12. Williams BJ, Suki D, Fox BD, Pelloski CE, Maldaun MV, Sawaya RE, Lang FF, Rao G (2009) Stereotactic radiosurgery for metastatic brain tumors: a comprehensive review of complications. J Neurosurg 111:439–448

Stereotactic Radiosurgery for Malignant Extracerebral Intracranial Tumors: Patient Selection, Efficacy, and Technical Nuances

Ian E. McCutcheon

Abstract Intracranial tumors extrinsic to the brain include a variety of histological types, including meningiomas and pituitary tumors, both of which are most commonly benign but can present with malignant biology and clinical behavior. In the same compartment arise a number of frankly malignant tumors, which include chordomas, metastases (to bone or dura), and sarcomas (e.g., chondrosarcoma). These malignant tumors derive from bone, dura, or vascular elements and pose significant therapeutic challenges. Because of the anatomical constraints imposed by the cranial base and by venous sinuses, and because of the relentless tendency to recur shown by malignant tumors of meningeal origin, surgery often achieves incomplete removal. Some tumors are not resectable without the use of complex approaches that endanger adjacent neurovascular structures. For these reasons, stereotactic radiosurgery (SRS) has an important role in primary treatment of malignant intracranial extracerebral tumors and, most commonly, in treating residual or recurrent disease after resection has established the diagnosis and decompressed the tumor's environs. Here we review the role and technique of SRS in a variety of these unusual lesions, including malignant meningioma, glomus tumor, pituitary carcinoma, skull base metastasis, chordoma, and chondrosarcoma. Understanding the specific nuances of each is helpful in allowing optimal planning of patient selection, dose level, and dose contours for best treatment results. Currently, SRS can be useful in achieving effective palliation of these malignant tumors but does not usually provide a cure. In the future, better results are anticipated because of new methods of metabolic imaging for delineating tumor extent and new radiosensitizers that enhance tumor kill within a safe range of doses at the tumor margin.

I.E. McCutcheon
Department of Neurosurgery,
The University of Texas M.D. Anderson Cancer Center,
1515 Holcombe Blvd., Houston, TX 77030, USA
e-mail: imccutch@mdanderson.org

Keywords Chordoma • Gamma Knife • Intracranial tumor • Malignant meningioma • Pituitary carcinoma • Stereotactic radiosurgery

Introduction

Although the majority of intracranial tumors arise from the cerebral parenchyma, a significant subset arise from the membranes overlying the brain (arachnoid and dura) or from the adjacent skull bone (calvarium or skull base). When tumors in those extracerebral layers are malignant by histology or clinical behavior, they pose significant therapeutic challenges. Complete resection can be difficult because of the involvement of important venous sinuses upon whose patency cerebral venous outflow depends. At the skull base, cranial nerves can be intimately adherent to the tumor surface, and for some tumors association with the internal carotid artery makes their resection risky. For these reasons, radiation therapy holds an important place in the therapeutic repertoire. Because of the convenience and efficacy of single-fraction radiotherapy delivered by stereotactic methods that allow precise and accurate targeting, stereotactic radiosurgery (SRS) has played an increasing role in the management of these malignant intracranial, yet extracerebral, tumors—for most of which no truly effective chemotherapy exists. Thus, SRS can be used as the primary treatment strategy when surgery is too risky or burdensome to the patient or as a secondary treatment after an incomplete resection leaves a remnant from which a new lesion can arise. Here, we review the role of SRS in treating malignant tumors in this narrow anatomical zone.

The layers involved by these tumors include the arachnoid, dura, and skull bone. Malignant tumors arising in the scalp are not generally treated with SRS but with radical excision followed when necessary by rotational or free flap reconstruction of the anatomical defect [19]. When large tumors of extracerebral origin distort and displace the adjacent brain or cranial nerves they provoke significant syndromes

M.F. Chernov et al. (eds.), *Gamma Knife Neurosurgery in the Management of Intracranial Disorders*,
Acta Neurochirurgica Supplement, Vol. 116, DOI 10.1007/978-3-7091-1376-9_12, © Springer-Verlag Wien 2013

Table 1 Malignant extracerebral tumors

Skull base		Convexity
Chordoma	Meningioma	Meningioma
Sarcomas	Glomus tumor	Hemangiopericytoma
Metastasis	Myeloma	Myeloma
Pituitary carcinoma	Chondrosarcoma	Sarcoma
		Metastases
Occasional other tumors (e.g., lymphoma, olfactory neuroblastoma)		

of neurological decline. Thus, radiosurgical strategies employing one of the systems used for this technique (e.g., Gamma Knife, LINAC, CyberKnife) can be important in retrieving or preserving good neurological function and extending both quality of life and survival.

Malignant tumors arising at the skull base differ from those found over the convexity (Table 1). Meningiomas occur in either location as dural sarcomas or metastases. However, other tumors (e.g., chordoma, pituitary adenoma) have more restricted patterns of distribution. As incomplete resection can lead to recurrence and to anaplastic transformation, SRS is often used as a postsurgical adjunct to suppress any remaining active tumor, either at the primary resection site or at secondary sites left untouched.

When planning SRS, important factors include location (i.e., distance of the tumor from the radiosensitive optic chiasm), size, shape, multiplicity, and histology. SRS can be used not only as the primary treatment for a tumor of known histology but also to sterilize the margins of a resection cavity, particularly when the risk of recurrence is high because of the tumor's invasive nature. Delayed recurrence at the operative site may also lead to radiosurgical treatment, as can metastasis to the dura or skull.

Specific Tumor Types

Glomus Tumor

The relevant subtype of glomus tumor whose treatment lies within the boundaries of SRS is the glomus jugulare, which is centered on the jugular foramen. It tends to erode bone at the base of the skull and is limited by the hyoid bone. Generally, it enhances after contrast administration as it is quite hypervascular. Its characteristic salt-and-pepper appearance signals its presence on magnetic resonance imaging (MRI). Glomus tumors originate in chemoreceptor cells along the jugular bulb. They generally occur as a single lesion, although 10 % present as multifocal lesions. One unusual variant is the glomus tympanicum, which originates in the cochlear promontory. It too may be treated with SRS rather than by surgical excision, which is associated with increased morbidity caused by manipulation or sacrifice of adherent lower cranial nerves. The clinical findings are typically hearing loss, pulsatile tinnitus, and arrhythmias and blood pressure fluctuations caused by the release of catecholamines intermittently into the tumor's venous drainage.

The hypervascularity adds challenge to any attempt to remove these tumors. They may require preoperative embolization, and intraoperative blood loss can be severe. Although originating in the jugular fossa, they can extend through the jugular foramen into the intracranial compartment and are known to go as high as the porus acousticus or even beyond. When they do extend in this fashion, lower cranial nerve function is at risk on the side ipsilateral to the tumor.

Good candidates for SRS include patients whose glomus tumor is associated with a classic appearance (and who thus present no diagnostic dilemma) and with incomplete cranial nerve palsy. Such patients risk cranial nerve injury at surgery, which almost guarantees some loss of function in cranial nerves IX, X, and XI. Also, blood loss can be high. Thus, in older patients the radiosurgical approach may be chosen as a less risky but still effective strategy.

Planning isodose contours for a glomus tumor can be somewhat tricky because the shape is never spherical but, rather, oblong with an irregular, almost knobby boundary (Fig. 1). Thus, with a Gamma Knife procedure it usually requires many shots and a significantly prolonged treatment time if the entire tumor is to be covered. However, complete coverage is not required if the goal of SRS is to control the tumor's pressure effect on adjacent brain. It is possible to treat only the portion of a glomus tumor that extends intracranially and leave the portion in the neck alone. This does not stop the possibility of hypertensive crisis from catecholamine release, but it does generally control that portion of the tumor responsible for neurological dysfunction.

The series of glomus tumors treated with SRS at the University of Virginia is not the largest such series, but it has been well analyzed recently and can serve as a good representation of what SRS can achieve with glomus tumors [3]. Of the 15 cases described, 3 required double-digit isocenters because of their large size or irregular shape. The dose at the margins was generally 13–16 Gy, with a maximum dose of 26–50 Gy. The general flaw of most SRS series is the lack of long-term follow-up. However, the Virginia study reported an average follow-up of 40 months. Tumor shrinkage occurred in 60 % of patients, with the remainder showing moderate growth, except for one tumor that almost doubled in size over the ensuing 5 years. Most of the tumors in this series were of small volume, with only two exceeding 12 cm^3. A meta-analysis just published by Guss et al. showed similar marginal doses but much higher rates of tumor control than are evident in the Virginia series [6]. In the meta-analysis, 15

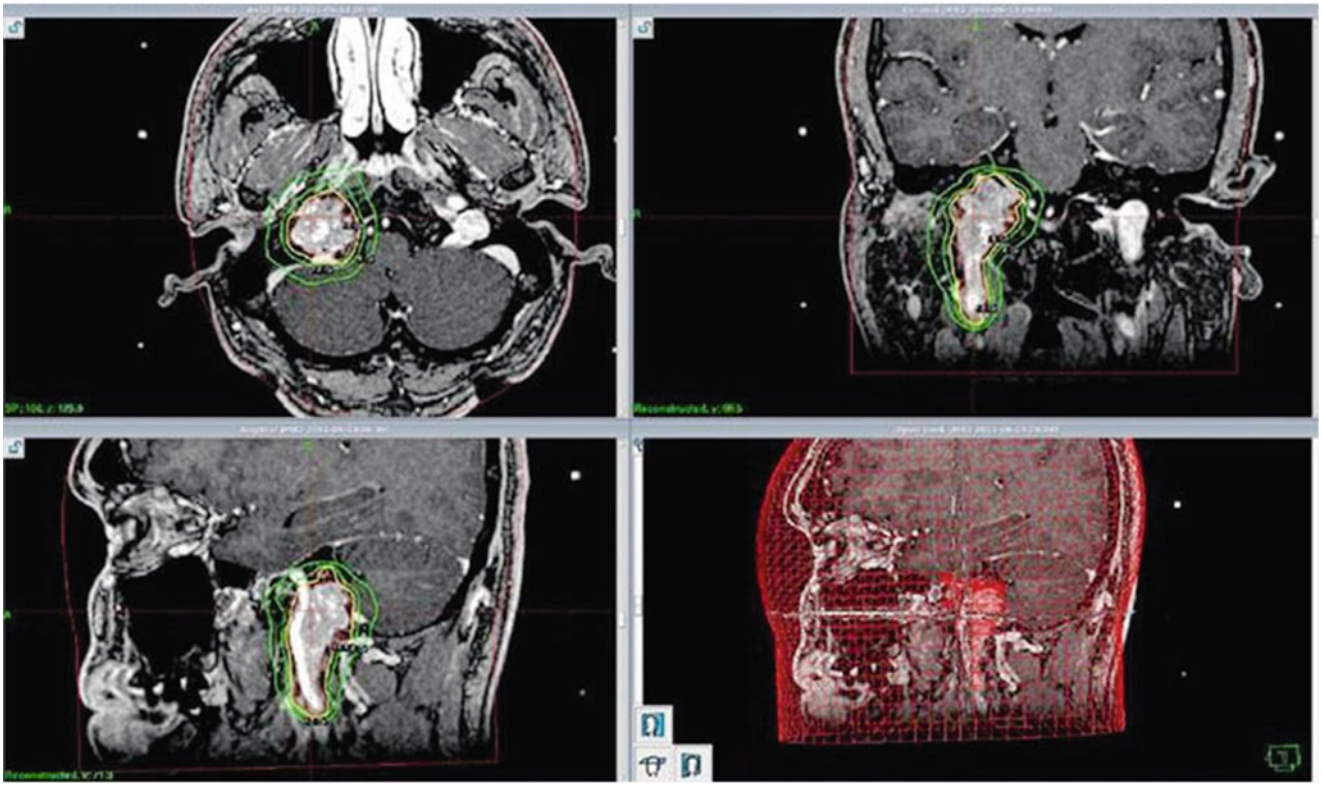

Fig. 1 Treatment plan for a patient with a glomus tumor (glomus jugulare). The tumor has the typical oblong shape. It lies along the jugular vein, with some intracranial extension through the jugular foramen, where it crowds the IX, X, and XI cranial nerves. The patient received 15 Gy to the 50 % isodose line with a total of 124 shots, requiring a treatment time of 357 min. The complexity of the plan and thus the treatment time could have been reduced by excluding the inferior portion of the tumor from treatment, but this strategy was not chosen as it would allow catecholamine hypersecretion to persist

of 19 studies showed glomus tumor control of 100 %, although somewhat more than half showed complete control of symptoms. Overall, the expected rate of tumor control was 90 %.

For glomus tumors, as for many other malignant tumors treated with SRS, patience is required as the effects are not immediate. Symptoms (when they are alleviated) take 6 months to abate, and tumor shrinkage takes a year or more. Of note: α- and β-blockade are both helpful in avoiding post-treatment hypertensive crisis—a statement as true for radiosurgery as it is for open resection. We generally decrease the blocking agents every 3 months after SRS to allow a smooth clinical transition as the drug is eliminated.

Malignant Meningioma

Malignant meningiomas (grade III) comprise 3 % of all meningiomas. They are defined by the World Health Organization (WHO) grading criteria: brain invasion, cellular atypia, and a high MIB-1 labeling index. About 40 % eventually metastasize, and there is a high risk of both local and regional recurrence. As chemotherapy options are limited and surgery is often unsuccessful in completely clearing these insidious tumors, SRS is used at some point in the treatment for most patients with this disease.

The range and efficacy of SRS for malignant meningioma are exemplified in the following representative case.

A 60-year-old woman presented with right hemiparesis and expressive dysphasia for the prior 3 months. In December 2008, she underwent resection of a dura-based tumor of the left frontal convexity. Pathology showed malignant meningioma with a high but unquantified MIB-1 labeling index. She completed external beam radiotherapy (59.4 Gy) in March 2009 but could not be weaned off steroids. She began having new seizures in August 2009. Although her scan at that time was relatively clear, she developed a significant recurrence inferior to the prior resection cavity in November 2009. This was resected by a second craniotomy at which time the tumor showed a MIB-1 labeling index of 47 %, which was high. The postoperative scan was clear of tumor, and she began hydroxyurea. A month later, a single new nodule appeared on the temporal convexity just inferior to the sylvian fissure. She underwent SRS for this single nodule, but scanning 2 weeks later revealed at least six new nodules

over the frontal convexity and the dura of the middle fossa. Gamma Knife SRS was undertaken, and five lesions were treated (instead of the original single lesion), each with 15 Gy to the 50 % isodose line. A total of 40 shots were required with a treatment time of 236 min. Two months later, the lesions on the upper convexity were controlled, but the lower lesions continued to grow. Repeat Gamma Knife SRS was undertaken with two areas targeted. A month later she showed six additional growing tumors on the dura, each of which was targeted with SRS yet again. She also started sunitinib. Again, the tumors in the middle fossa continued to grow but not those higher on the convexity. She began cytotoxic chemotherapy (ifosfamide, carboplatin, etoposide) and promptly developed subgaleal nodules of the tumor. She entered hospice care and died in November 2010 with a relentlessly progressive tumor over the entire left convexity. At no point in the course did she develop tumor over the right convexity or the right skull base, and there were no distant metastases.

This case offers several lessons regarding SRS for malignant meningioma. It can be useful for controlling focal intracranial metastases of this histology and may work for some lesions but not necessarily all. Large lesions are less likely to respond, and malignant meningioma may show itself as frankly resistant to SRS. However, judicious application of repeat SRS is feasible with careful planning to avoid interference with prior radiosurgical fields. It can provide palliation, although typically not cure, with these difficult tumors. In some cases, survival duration from the discovery of the original meningioma (which may start as a tumor of atypical or even benign grade) can exceed 5 years. MIB-1 labeling in these tumors can go as high as 50–70 %, and correlates well with the high risk of recurrence. Because there may be multiple prior operations, outlining these lesions for isodose contouring can be tricky and demands a full understanding of radiological interpretation to allow accurate delineation of the tumor from adjacent fibrosis or gliosis (Fig. 2).

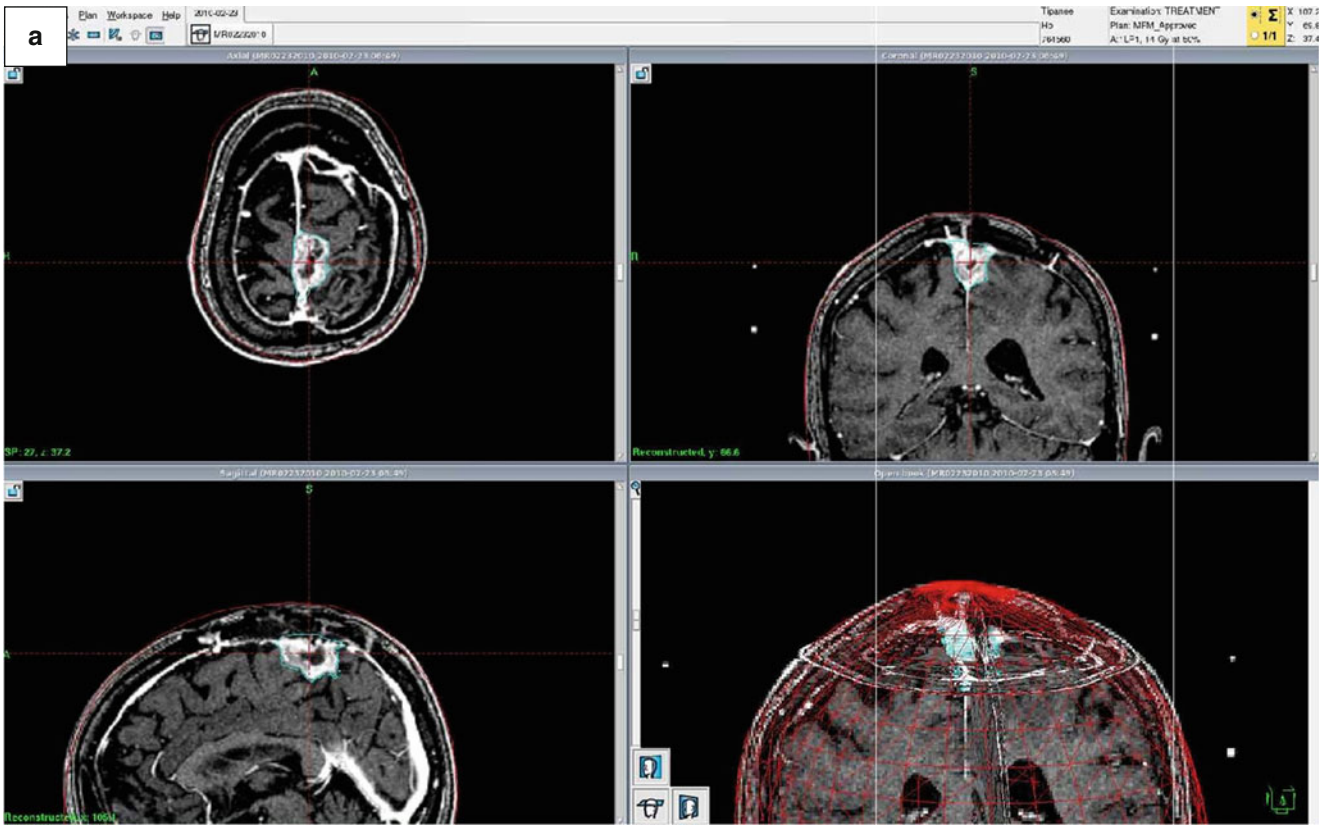

Fig. 2 A 59-year-old woman had a parafalcine meningioma that had been resected twice and also treated with limited-field radiotherapy using intensity modulated radiotherapy (IMRT) to 60 Gy. (**a**) Her second recurrence was treated with stereotactic radiosurgery (SRS) (14 Gy to the 50 % isodose line using 21 shots). (**b**) Isodose contours show apparently good coverage of the tumor, although it is difficult to tell how far along the falx the enhancement extends, and whether marginal enhancement represents tumor or fibrosis from previous treatment. (**c**) Edema worsened during the 4 months after the SRS, and the patient required further resection by redo craniotomy, at which time the sagittal sinus was resected en bloc with the tumor. Avastin was given for persistent edema and paraparesis, but leg function did not improve. (**d**) At 51 months after her original presentation, the tumor again recurred in the margins of the resection cavity. Reoperation is planned with radical en bloc removal and no expectation of restoration of function. She has never had systemic metastasis

Fig. 2 (continued)

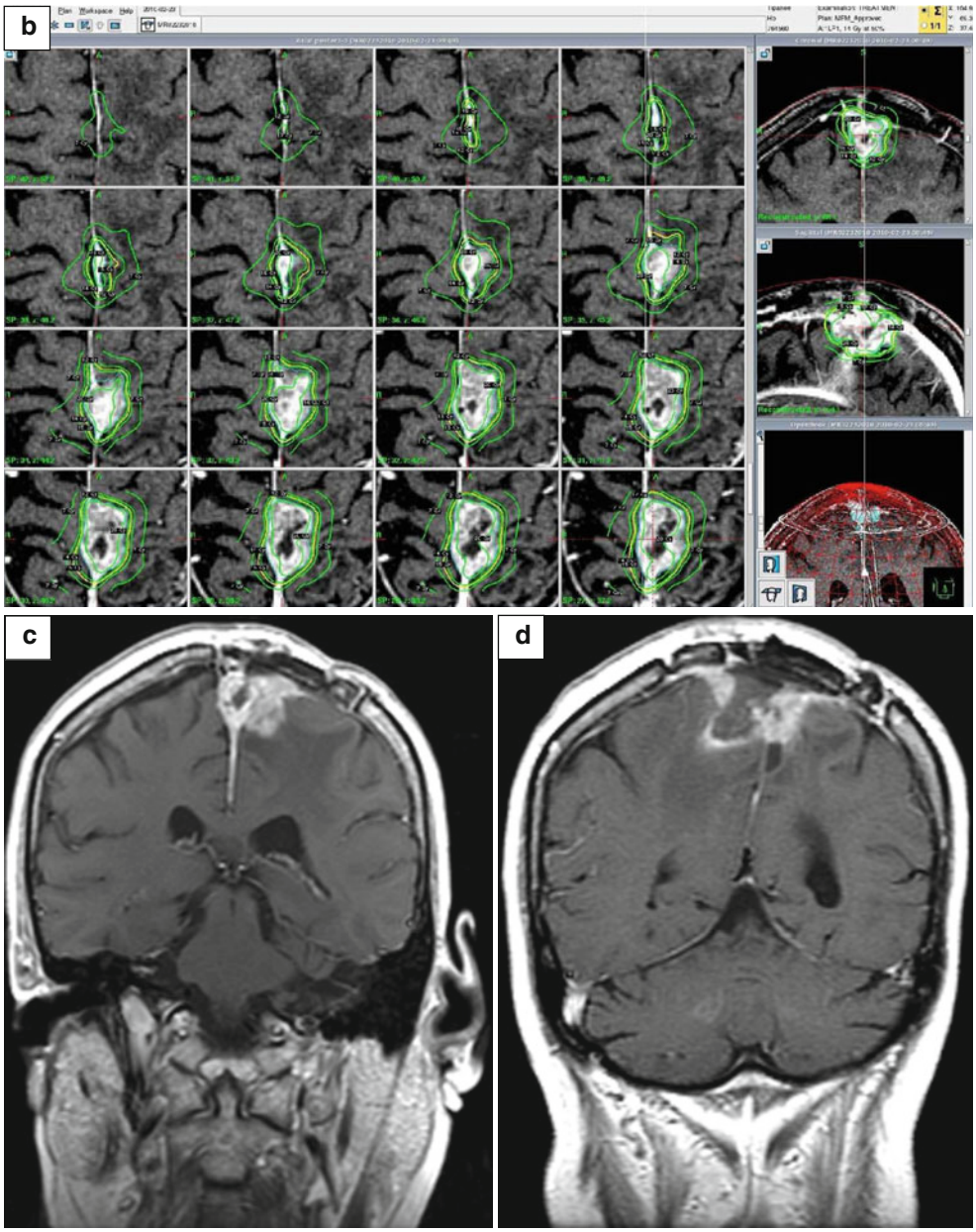

When caught early, even highly malignant meningiomas can be controlled by SRS, often for 6 months to 2 years. Salvage resection of a radical nature may be required when SRS fails to control the tumor. Unfortunately, the combination of multiple operations and multiple SRS sessions usually leads to the gradual onset of clinical decline. The onset of debility can be quite distressing to the patient and can significantly compromise quality of life.

No large series have been reported on the radiosurgical treatment of malignant meningioma. A well-described series from the University of California Los Angeles (UCLA) includes 20 tumors that were WHO grade II or III. Malignant progression occurred in one-third of these cases during the median follow-up period of 42 months. Progression-free survival rates at 3 years for grades II and III were 83 % and 0 % respectively. New tumors requiring additional treatment were common, 77 % of which occurred inside the original resection cavity. Sustained local control of grade II (atypical) meningiomas is thus feasible, whereas malignant meningiomas can usually be palliated but not cured [13].

The University of California San Francisco (UCSF) series reported in 2000 is one of the few studies to have focused purely on grade III meningiomas [16]. Patients were generally treated with radiosurgery for recurrent tumor after limited-field external beam radiotherapy. As is typical for meningiomas in general, there was a female predominance of 1.5:1.0, but males

were disproportionately represented in this (as in most series of aggressive meningioma) despite the female preponderance. Patients ($n=19$) were included who harbored 31 lesions, the majority at parafalcine sites, with 20 % at the skull base. The mean interval from radiotherapy to SRS was 5.4 years, with a mean follow-up of 2.3 years. The progression-free survival rates were 43 % at 3 years and 34 % at 5 years. Survival curves are shown in Fig. 3. Statistically significant factors that influenced time to progression were age and target volume. Location, prescription dose, conformity, and sex made no difference. Complications were seen anywhere from 3 to 30 months after Gamma Knife SRS. They were related to radiation necrosis or radiation-induced cerebritis and in three patients required reoperation. The relatively high incidence of radiation necrosis is not completely surprising given that all patients had undergone prior irradiation before the radiosurgery.

These control rates differ significantly from those seen with WHO grade II meningiomas. Choi et al. reported a series of such tumors treated by CyberKnife that shows actuarial rates of locoregional control of 90 % at 12 months and a similar percent at 24 months, after which the rate dropped to 47 % at 36 months [4]. Thus, grade II meningiomas that have undergone Gamma Knife SRS show a persistent degree of control over a long period of time but ultimately tend to relapse in a fashion similar to their malignant counterparts. In general, grade III meningiomas are included in more comprehensive series that include other grades, and thus teasing out the specifics for the rates of success for these tumors is not easy. All of these series share a main deficit: a lack of sufficient long-term follow-up. Ideally, the median follow-up would exceed 5 years for meaningful conclusions to be drawn from any series of meningiomas, benign or malignant.

Recurrence patterns for meningiomas after SRS are of some interest and are clinically relevant. The in-field rate of recurrence for benign (grade I) meningiomas is 25 % compared to 88 % for higher-grade meningiomas. This higher likelihood of recurrence in malignant tumors undoubtedly reflects the persistence of remnants of tumor after surgery, the infiltrative or adhesive quality of these tumors, and the frequent difficulty of distinguishing tumor margin from adjacent brain. Delineation of the tumor margin can also be difficult on imaging as most if not all malignant meningiomas undergoing SRS have had previous treatment by both surgery and radiotherapy, each of which can blur the radiographic boundaries just as they blur the intraoperative borders. Overall, recurrence-free survival for patients with grade I meningiomas at 5 years after SRS is 50 %, compared with 25 % at 5 years for those of higher grade. The median times to recurrence are 46 and 31 months, respectively. Thus, SRS is typically not a cure for malignant meningioma but does offer significant palliation for periods of 1–3 years in most cases [1].

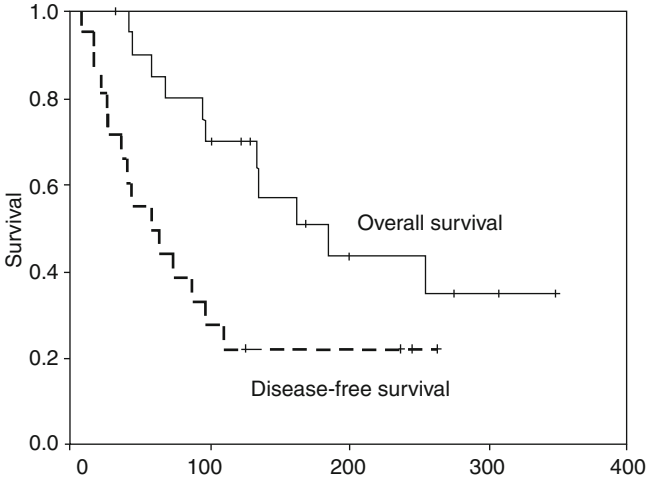

Fig. 3 Overall survival and freedom from tumor progression after the first SRS in a cohort of patients with malignant meningioma (WHO grade III). Note that 80 % of patients show tumor progression over time, and that long-term survival is achieved by only 35 % (*Source*: Ojemann et al. [16])

Malignant Pituitary Tumor

Pituitary tumors can be classified as (1) benign adenomas, (2) adenomas that are locally aggressive with parasellar invasion, or (3) carcinomas that are metastatic inside or outside the central nervous system. Locally aggressive adenomas and metastatic carcinomas may require radiosurgical treatment when resection is incomplete or not feasible. It is important to note that pituitary tumors can invade or even metastasize yet still have an indolent rate of growth. Thus, treatment is not automatic for all tumors. Charting the rate of growth of the aggressive or malignant pituitary tumor may help identify those tumors worthy of treatment versus those for which observation is the better strategy.

Unlike benign adenomas, the majority of malignant pituitary tumors are functional (>80 %) and thus are associated with syndromes of hormonal hypersecretion. The most common hormone excess in such tumors raises levels of prolactin or adrenocorticotropic hormone (ACTH). Thus, the relevant hormone level can often be used as a marker of tumor viability both before and after radiosurgical treatment.

When treating pituitary tumors with SRS, adjacent structures have varying degrees of radiosensitivity and must therefore be differentially preserved. The optics nerves, chiasm, and tracts require absolute protection and are best served by a dose limited to 8 Gy. For tumors that have reached the dorsum sellae, limiting the brain stem dose becomes important. By contrast, the cranial nerves in the cavernous sinuses on either side of the sella are more radioresistant than the optic nerve and can tolerate higher doses. Invasive tumors

usually have a highly complex shape and thus require many shots and complex treatment plans. The irregular tumor shapes and the need to preserve the optic apparatus from too much irradiation make planning difficult, as does the difficulty of anatomic interpretation in this area. It is easiest to delineate the tumor's extent on coronal MRI, although axial and sagittal images may also be needed.

Hormonal normalization with pituitary tumors requires higher doses than does control of tumor volume. For secretory tumors, the usual dose is 18–25 Gy, and for nonfunctional tumors it is 12–20 Gy. Also, the hormonal subtype of the adenoma affects the success rate of therapy and defines the criteria for tumor remission. For all adenomas, the success rate tends to be 50 % when rigorous criteria of hormonal normalization are applied to hypersecretory tumors treated with SRS. The time to remission tends to be longer for patients with acromegaly and is shortest for those with Cushing disease, who have an average delay to the onset of remission of 22 months [2]. Factors predictive of remission include initial hormone levels and for those with acromegaly the withdrawal of somatostatin agonist at the time of Gamma Knife SRS treatment. It has also been suggested that using a dopamine agonist at the time of SRS is a *negative* predictor of success [18].

Patients with pituitary carcinoma, the most aggressive pituitary tumor, usually follow complex and highly individualized treatment plans that unfold over a number of years. Although these tumors usually start out as adenomas with a low apparent risk of aggressive growth, they later transform into locally invasive and ultimately metastatic tumors that are difficult to eradicate completely. The degree of local invasion can be profound, and preservation of optic nerve function is difficult over time. Cavernous sinus involvement is common as is infiltration into the skull base, foramen ovale, infratemporal fossa, and tentorial dura extending back from the dorsum sellae (Fig. 4). Foci of metastasis can be indolent, but when strategically located they require treatment. Generally, we reserve focal therapy for tumors that are symptomatic or that are endangering neurological function. SRS can be a useful tool, particularly for intracranial pituitary carcinoma metastases and in some cases for sterilizing the primary tumor bed after resection. Surgery for malignant pituitary tumors almost invariably leaves behind some tumor because of the anatomical complexity of the substrate. As chemotherapeutic strategies have largely been ineffective, Gamma Knife SRS is often used for palliation in these unusual cases. Some enthusiasm in the recent literature for treating such patients with temozolomide is now giving way to a realization that many either never respond or ultimately fail after initial success [8, 20]. Thus, Gamma Knife and other forms of SRS used to control aggressive pituitary

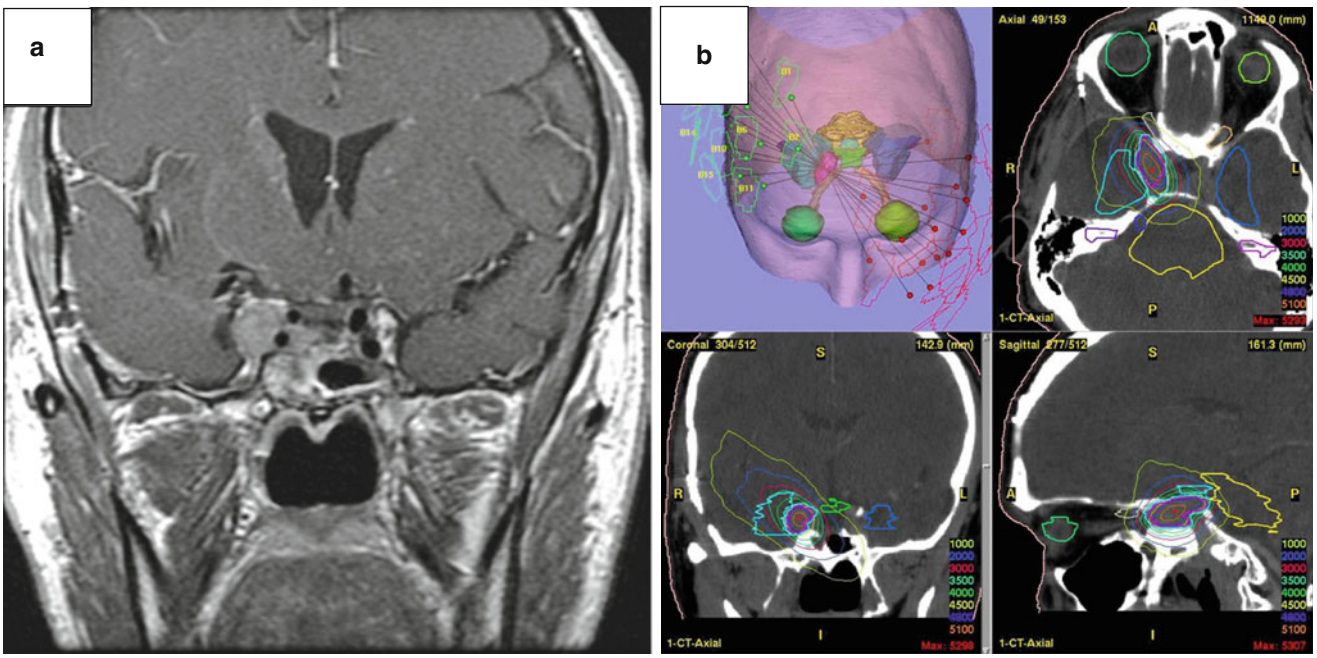

Fig. 4 A 44-year-old man had an aggressive pituitary adenoma that was resected twice and treated with SRS of the sella. (**a**) Tumor recurred in the right cavernous sinus and was subtotally removed by craniotomy. (**b**) Fractionated SRS by CyberKnife (45 Gy in 25 fractions with mini-multileaf collimator) was applied. (**c**) Good protection was afforded the optic apparatus, brain stem, cochlea, and eyes while maximizing the effective dose to the tumor. (**d**) Over the next 3 years, the tumor extended directly onto the petrous dura and metastasized to the dura of the middle and posterior fossae. (**e**) Leptomeningeal dissemination occurred, as did intramedullary metastasis. The patient is now in hospice

Fig. 4 (continued)

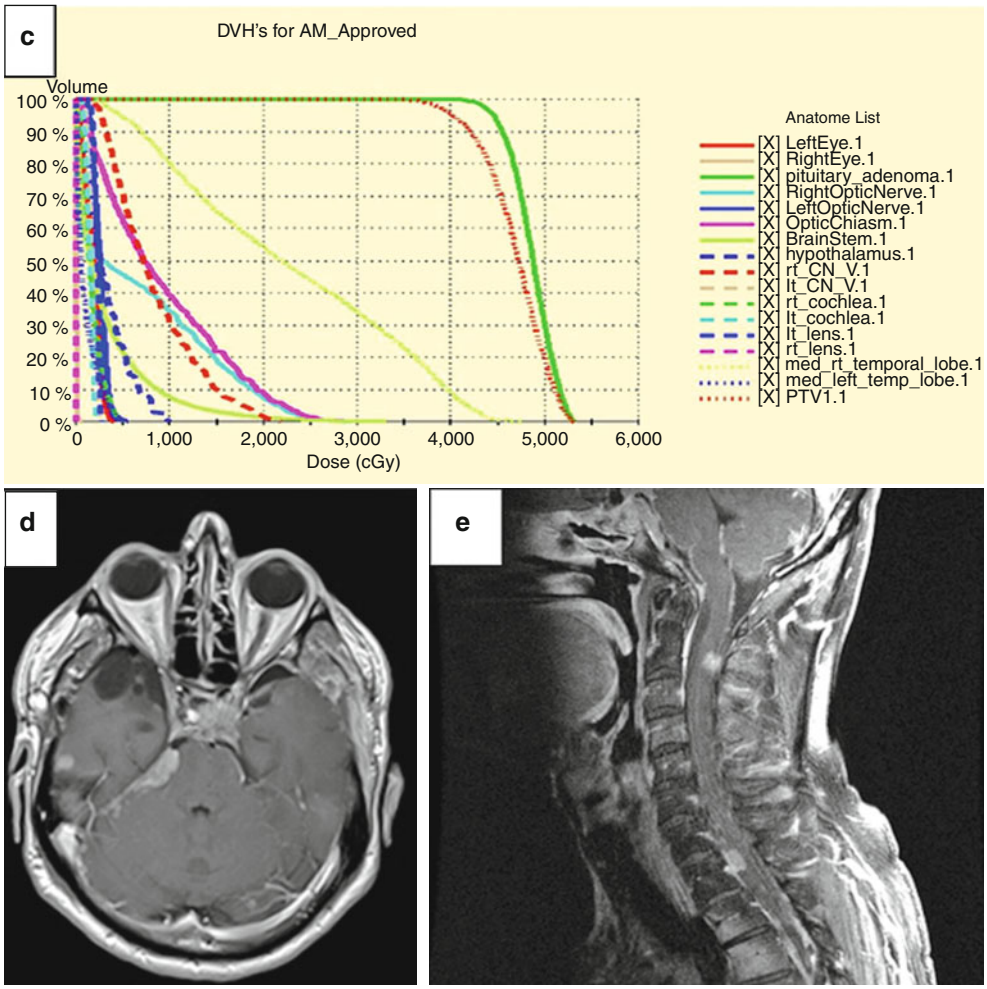

tumors remain a central part of the therapeutic armamentarium into the foreseeable future.

Points to note about pituitary tumors include the following.

1. SRS of a benign tumor does not prevent it from becoming frankly malignant. Although there is no proof that radiosurgical treatment of an adenoma contributes to later malignancy, we have seen several patients who developed pituitary carcinomas after initial treatment of a benign lesion with the Gamma Knife.
2. Treatment planning should include a targeted field that is as broad as possible. Although selectivity is the watchword with SRS, the pituitary region and adjacent structures should be liberally treated. The only truly protected areas are those sensitive neural structures (optic nerves, brain stem) that require exclusion from the field to prevent neurotoxicity.
3. Finally, a low MIB-1 index can be seen in a clinically aggressive pituitary tumor with significant invasive reach. Thus, the MIB-1 index should not be the driving factor in decisions on whether to give or withhold SRS in this tumor type.

In aggressive pituitary tumors, as in aggressive meningiomas, the contouring of targets on radiographic imaging can be difficult. Indeed, it may vary by operator, as Yamazaki et al. recently showed in a study on the variation of planning treatment volumes in such cases [22]. Thus, it is recommended that the planning process involve both the radiation oncologist and the neurosurgeon responsible for the patient. Input from a neuroradiologist may also be helpful. Consensus must generally be reached as the ability to formulate targets precisely in the new-generation radiosurgical systems exceeds the precision of delineating the tumor margins for these tumor types in the typical patient with multiple previous therapies resulting in local fibrosis and blurring of anatomical detail.

Metastases to the Skull Base

Metastases to the base of the skull are logical targets for SRS when they are symptomatic. As there is no barrier to

chemotherapeutic penetration of the tumor in such lesions, systemic chemotherapy given to patients with systemic metastases typically reaches such tumors and, when effective, controls them. Thus, the main subset of patients who become candidates for SRS with skull metastases are those with large, growing tumors that have broken through chemotherapy to endanger cranial nerve or brain stem function. Tumors in the skull convexity (i.e., the calvarium) are less likely to require SRS because they are treated with whole-brain irradiation, chemotherapy, or surgical excision given their relative accessibility. In patients who are treated with SRS for calvarial metastasis, the likelihood of local hair loss is high as the dose limit for depilation is only 3 Gy.

Skull base metastases are less amenable to resection as the surgical techniques are quite invasive and complex. Such surgery is undertaken in selected cases, but a Gamma Knife procedure is chosen in many in whom the tumor diameter is within the usual limit of 3 cm. Common histologies include cancers arising from the breast (40 %), lung (14 %), and prostate (12 %). Metastases from cancers of the colon, kidney, and thyroid are less often seen in the skull base but do occur occasionally [11]. The clinical syndromes triggered by skull base metastases include sellar and parasellar signs (double vision or loss of vision) in about 30 %, followed (in descending order) by syndromes of occipital condyle dysfunction, orbital involvement, gasserian ganglion involvement, and jugular foramen dysfunction. One-third of patients, however, have either no symptoms or symptoms that do not fit these categories. We have treated a number of patients with LINAC or Gamma Knife SRS for skull base metastases. They generally respond well to this treatment, and several patients have had long-term survival because of successful suppression of systemic disease. In such cases, recurrence is uncommon at the treated skull base sites.

One series from Pittsburgh specifically reported the results of Gamma Knife treatment of metastases to the pituitary gland from systemic cancers. This series included 18 patients with the typical pituitary metastatic profile in which lung carcinoma is most common followed by cancers arising in the breast and kidney [9]. Melanoma metastases to the pituitary gland are rare [14]. Only 3 of the 18 patients in the Pittsburgh series had had prior surgery, which does not follow our own practice in this regard. We usually attempt maximum resection to decompress the optic chiasm and then follow with stereotactic irradiation in either single or multiple fractions, as appropriate. These patients are usually also treated with chemotherapy for concomitant systemic disease. We have had good resolution of visual deficits after such resections [5]. After surgery, we use radiosurgical treatment to suppress residual disease, which is almost always present given that these tumors usually metastasize not only to the pituitary but also to the adjacent bone and dura as well as to the cavernous sinuses unilaterally or bilaterally (Fig. 5). In the Pittsburgh series, among the patients who underwent SRS, patients <60 years of age fared better than those who were older. They tended to be free of tumor progression for 10–12 months, after which they quickly began to exhibit further tumor growth. This pattern mirrors observations of our own patients with metastasis to the sella. Thus, SRS in this

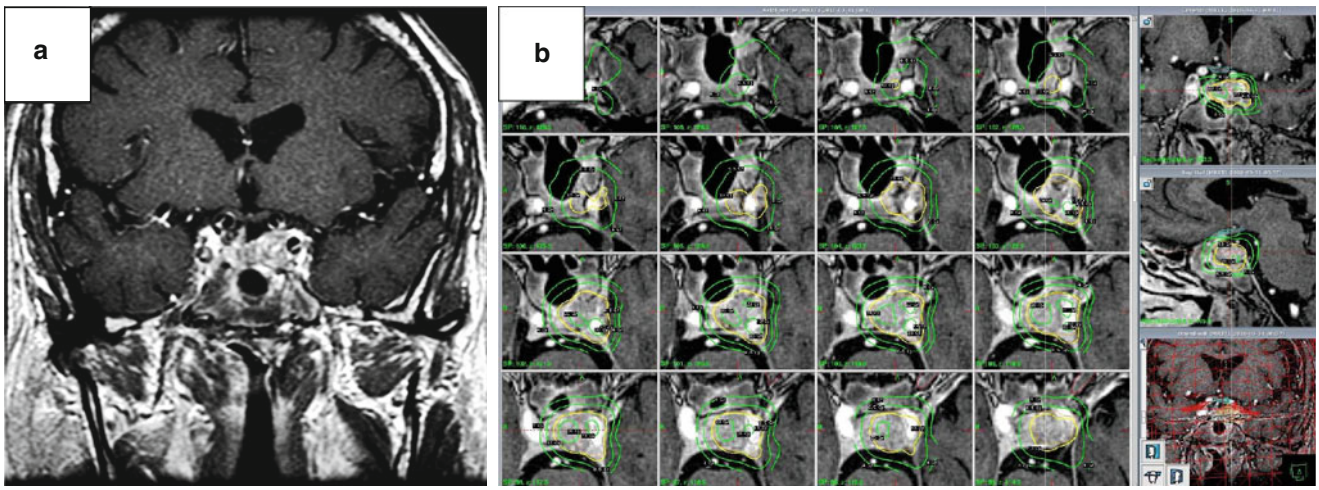

Fig. 5 Renal cell carcinoma metastatic to the sella. (**a**) After resection and immediately prior to Gamma Knife SRS. (**b**) The treatment plan used 13 shots to achieve a dose of 13.5 Gy to the 50 % isodose line. (**c**) Excellent sparing of the optic nerves and chiasm was achieved with the dose well below the safe cutoff of 8 Gy. Maximum doses to the chiasm and to the right and left optic nerves were 3.6, 3.1, and 4.4 Gy, respectively. The tumor recurred locally 11 months later, and the patient died of systemic metastasis 5 months after that, maintaining full vision in each eye until his death

Fig. 5 (continued)

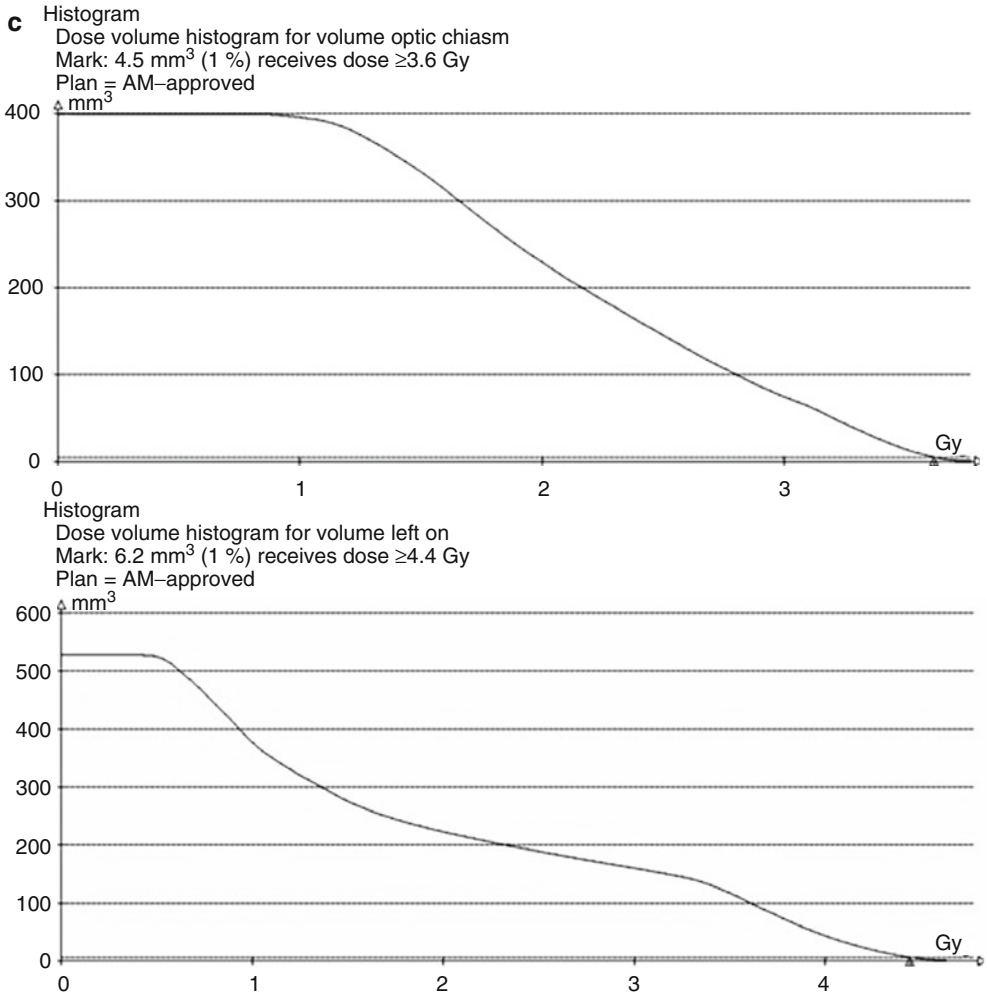

area, as in so many others involved by malignant extracerebral tumors, is palliative more often than it is curative.

Chordoma

Chordomas arise from notochordal rests in the clivus. They are expansile, lytic lesions typically occurring at the midline, but they can have lateral extension. They tend to be well-delineated tumors with a large soft tissue component that extrudes from the bone in some cases, typically causing brain stem compression but sometimes going anteriorly into the retropharyngeal space or the sphenoid bone. They enhance heterogeneously and are dark on T1-weighted images but bright on T2-weighted images. The differential diagnosis for them includes clival meningioma as well as chordoma and chondrosarcoma (Fig. 6).

Only 35 % of chordomas arise in the clivus. The remainder begin in the sacrum (50 %) or in vertebral bodies (15 %) and are slow-growing but locally aggressive tumors. They can metastasize, although it tends to occur only late in the course of the disease. Typically, they cause cranial nerve deficits when symptomatic. Ideally, they are treated with complete surgical excision. However, resection en bloc is extremely difficult in this region, and remnants are sometimes left behind as seeds for tumor regrowth. The role of SRS in chordoma tends to be for treatment of small, relatively asymptomatic lesions with the classic radiographic signature for chordoma or for controlling areas of recurrence after prior surgery.

Proton beam therapy has been proposed as the preferred form of radiotherapy for chordomas. In theory, it allows less scatter into the brain stem while allowing dose escalation to the tumor. Conventional photon radiation therapy does not give good local control of chordomas. In a series of patients treated with charged-particle therapy for chordomas of the cranial base, median doses were typically in the range of 65–75 CGE, which produced 10-year local control rates of 54–58 % [15]. None of the series, however, included only patients treated purely with proton beam therapy. Most patients were subjected to combined proton with photon therapy, and the exact contribution of the proton component is difficult to tease out. It appears that the

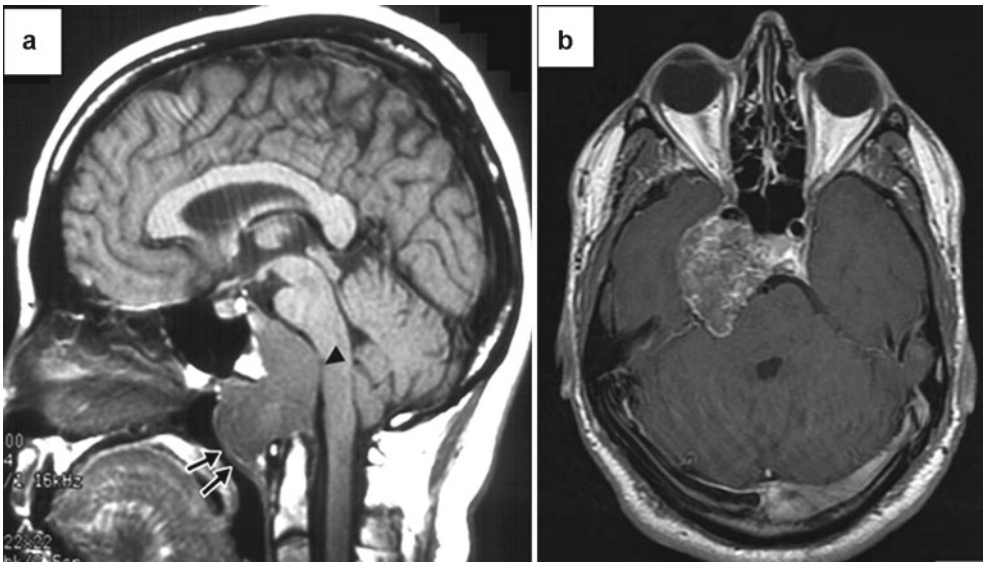

Fig. 6 (**a**) Clival chordoma shows extension posteriorly against brainstem and anteriorly into the retropharyngeal space. This homogeneous tumor enhances minimally. (**b**) In contrast, this chondrosarcoma has a heterogeneous appearance with patchy enhancement and small areas of calcification. It extends laterally from the sphenoclival region into the middle fossa, and it impinges to a lesser degree against the brain stem

best dosimetry comes from combining the two techniques [21]. In addition, no direct comparative study of proton beam therapy versus SRS has been performed, and the relative efficacy of the two treatment modalities remains unsettled.

The most comprehensive survey of SRS for chordomas comes from the North American Gamma Knife Consortium, which examined results in 71 patients from six centers. The overall control rate at 5 years was 66 %, which is comparable or even superior to that achieved by proton beam irradiation. The best results are seen if the tumor volume is small, the patient is young, there has been no prior radiotherapy, and fewer than three cranial nerve palsies are present (indicating a small tumor volume). A longer interval from the time of diagnosis also improves results. One-third of the patients in this series had undergone multiple craniotomies before SRS. Two-thirds had not had prior radiotherapy, so the Gamma Knife was often being used instead of (rather than in addition to) other radiotherapeutic modalities [10].

Two patients (3 %) had a complete response after SRS. The remainder were evenly divided among groups showing partial response, stable disease, or progressive disease. The best results are achieved when the margin dose is 15 Gy (Fig. 7). Although a few retreatments with the Gamma Knife were salvage treatment after failure of SRS, they were generally limited to resection. Complications after SRS were limited to new cranial nerve deficits or new loss of anterior pituitary hormone function. Nonetheless, symptomatic relief was occasionally seen for preexisting cranial nerve deficits, with the most likely to improve being abducens palsy, for which the improvement rate was 42 %.

Proton beam therapy is more widely used for chordoma despite the greater availability of the Gamma Knife (and other radiosurgical equipment) and the lower cost of SRS. Chordoma is a relatively rare disease, but we expect SRS to be applied to it more frequently in the future. The proof of superiority of one technique over the other still awaits a prospective randomized trial comparing SRS with proton beam radiotherapy in the chordoma population.

Chondrosarcoma

Tumors that extend from the posterior fossa and clivus into the middle fossa are likely to be chondrosarcomas, not chordomas. Only a minority of clival chordomas extend in this fashion, but most chondrosarcomas do so. Because chondrosarcomas are even less common than chordomas, compiling outcome data for them has been difficult. Chondrosarcomas present as an irregular destructive mass centered off the midline at the petrosphenoclival junction. In all, 70 % have calcification, and they tend to exhibit heterogeneous enhancement and low-T1/high-T2 signals. They originate from synchondroses or in some cases from a preexisting cartilaginous tumor. Their typical site of origin intracranially is from either the paranasal sinuses or the parasellar and retrosellar region (Fig. 6b).

The largest published series of chondrosarcomas treated by SRS was compiled at the University of Pittsburgh [12].

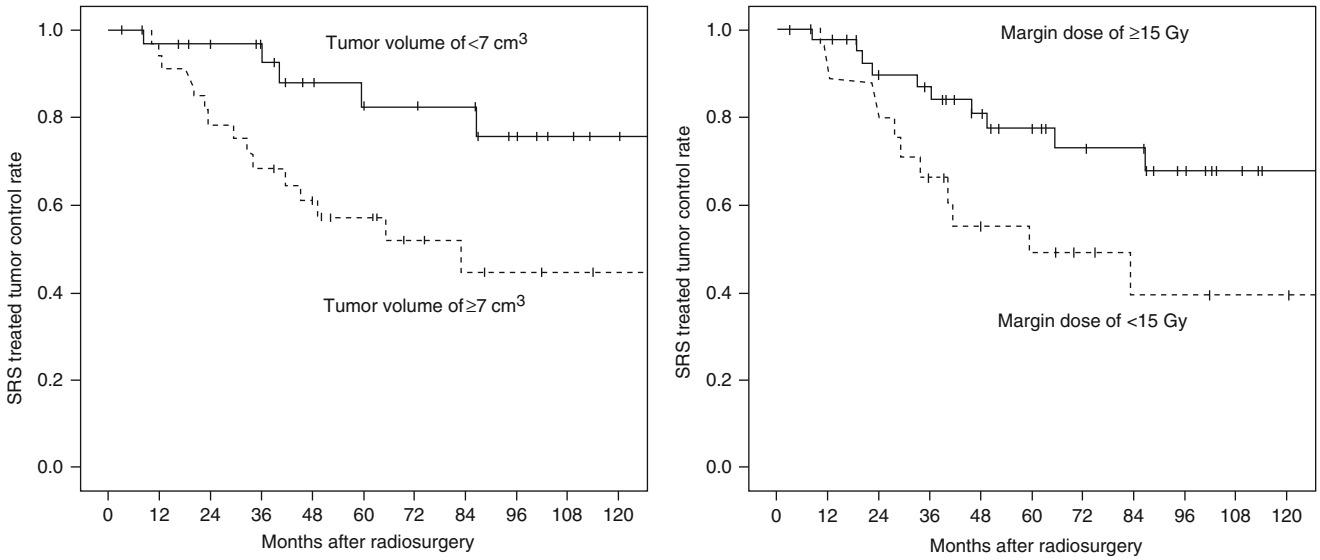

Fig. 7 Margin dose and tumor volume both affect tumor control in chordomas. When the dose can be kept at ≥15 Gy, control rates improve (*Source*: Kano et al. [10])

This series included 10 patients confirmed to have a chondrosarcoma by prior biopsy or resection. The mean follow-up was 76 months, making it an unusually well documented and assiduously tracked set of patients. No patient required additional surgery after Gamma Knife SRS, although one patient (who had tumor in a cavernous sinus at the outset) had a recurrence in the opposite cavernous sinus 12 years later and underwent repeat SRS for the second lesion. With a mean tumor volume of 9.8 cm^3, the tumors irradiated were quite small. The rate of local tumor control was 80 % at 5 years, an excellent result. Thus, chondrosarcomas do much better over time after SRS than do chordomas. This undoubtedly reflects not only a different radiobiology but different tumor biology in general.

Conclusion

Gamma Knife and other forms of SRS have a wide range of utility in treating malignant extracerebral tumors in the head. SRS is generally palliative, not curative, in these highly resistant tumors. Small case numbers make the nuances of treatment difficult to tease out, but certain principles can be noted for each of the tumor types. SRS is required more commonly for skull base tumors than for tumors of the convexity, with the exception of meningiomas, which are more likely to be malignant along the calvarium than at the skull base. Long-term survivals are seen in patients with glomus tumors, chondrosarcomas, and in some cases pituitary carcinomas. Targeting can be difficult because of peritumoral scarring and the anatomic disruption imposed by prior therapy. Further advances are likely to come from adding layers of metabolic or molecular imaging to the anatomical images now used. The only ways to improve results from SRS are to (1) enhance the completeness of coverage of the extent of the lesion and (2) make tumors more radiosensitive through pretreatment with radiosensitizing agents. Increasing targeting accuracy is the easier of the two ways to achieve better results as we can now image molecular signatures of neoplasia in tumor cells to a level not attainable previously. Thus, there is significant hope for an enhanced role for SRS not only for the malignant extracerebral tumors described here but for tumors of various grades in other intracranial compartments [7, 17].

Conflict of Interest The author declares that he has no conflict of interest.

References

1. Askoxylakis V, Zabel-du Bois A, Schlegel W, Debus J, Huber P, Milker-Zabel S (2010) Patterns of failure after stereotactic radiotherapy of intracranial meningioma. J Neurooncol 98:367–372
2. Castinetti F, Nagai M, Morange I, Dufour H, Caron P, Chanson P, Cortet-Rudelli C, Kuhn JM, Conte-Devolx B, Regis J, Brue T (2009) Long-term results of stereotactic radiosurgery in secretory pituitary adenomas. J Clin Endocrinol Metab 94:3400–3407
3. Chen PG, Nguyen JH, Payne SC, Sheehan JP, Hashisaki GT (2010) Treatment of glomus jugulare tumors with gamma knife radiosurgery. Laryngoscope 120:1856–1862
4. Choi CY, Soltys SG, Gibbs IC, Harsh GR, Jackson PS, Lieberson RE, Chang SD, Adler JR (2010) Cyberknife stereotactic radiosurgery for treatment of atypical (WHO grade II) cranial meningiomas. Neurosurgery 67:1180–1188
5. Feiz-Erfan I, Rao G, White WL, McCutcheon IE (2008) Efficacy of trans-septal trans-sphenoidal surgery in correcting visual

symptoms caused by hematogenous metastases to the sella and pituitary gland. Skull Base 18:77–84
6. Guss ZD, Batra S, Limb CJ, Sughrue ME, Redmond K, Rigamonti D, Parsa AT, Chang S, Kleinberg L, Lim M (2011) Radiosurgery of glomus jugulare tumors: a meta-analysis. Int J Radiat Oncol Biol Phys 81:e497–e502
7. Iqbal U, Trojahn U, Albaghadadi H, Zhang J, O'Connor-McCourt M, Stanimirovic D, Tomanek B, Sutherland G, Abulrob A (2010) Kinectic analysis of novel mono- and multivalent VHH-fragments and their application for molecular imaging of brain tumours. Br J Pharmacol 160:1016–1028
8. Jouanneau E, Wierinckx A, Ducray F, Favrel V, Borson-Chazot F, Honnorat J, Trouillas J, Raverot G (2012) New targeted therapies in pituitary carcinoma resistant to temozolomide. Pituitary 15:37–43
9. Kano H, Niranjan A, Kondziolka D, Flickinger JC, Lunsfoud LD (2009) Stereotactic radiosurgery for pituitary metastases. Surg Neurol 72:248–255
10. Kano H, Iqbal FO, Sheehan JP, Mathieu D, Seymour ZA, Niranjan A, Flickinger JC, Kondziolka D, Pollock BE, Rosseau G, Sneed PK, McDermott MW, Lunsfoud LD (2011) Stereotactic radiosurgery for chordoma: a report from the North American Gamma Knife Consortium. Neurosurgery 68:379–389
11. Laigle-Donadey F, Taillibert S, Martin-Duverneuil N, Hildrebrand J, Delattre JY (2005) Skull-base metastases. J Neurooncol 75:63–69
12. Martin JJ, Niranjan A, Kondziolka D, Flickinger JC, Lozanne KA, Lunsfoud LD (2007) Radiosurgery for chordomas and chondrosarcomas of the skull base. J Neurosurg 107:758–764
13. Mattozo CA, De Salles AA, Klement IA, Gorgulho A, McArthur D, Ford JM, Agazaryan N, Kelly DF, Selch MT (2007) Stereotactic radiation treatment for recurrent nonbenign meningiomas. J Neurosurg 106:846–854
14. McCutcheon IE, Waguespack SG, Fuller GN, Couldwell WT (2007) Metastatic melanoma to the pituitary gland. Can J Neurol Sci 34:322–327
15. Nguyen QN, Chang EL (2008) Emerging role of proton beam radiation therapy for chordoma and chondrosarcoma of the skull base. Curr Oncol Rep 10:338–343
16. Ojemann SG, Sneed PK, Larson DA, Gutin PH, Berger MS, Verhey L, Smith V, Petti P, Wara W, Park E, McDermott MW (2000) Radiosurgery for malignant meningioma: results in 22 patients. J Neurosurg 93(Suppl 3):62–67
17. Pal A, Glekas A, Doubrovin M, Balatoni J, Namavari M, Beresten T, Maxwell D, Soghomonyan S, Shavrin A, Ageyeva L, Finn R, Larson SM, Bornmann W, Gelovani JG (2006) Molecular imaging of EGFR kinase activity in tumors with 124l-labeled small molecular tracer and position emission tomography. Mol Imaging Biol 8:262–277
18. Pouratian N, Sheehan JP, Jagannathan J, Laws ERJ, Steiner L, Vance ML (2006) Gamma knife radiosurgery for medically and surgically refractory prolactinomas. Neurosurgery 59:255–266
19. Soma PF, Chibbaro S, Makiese O, Marsella M, Diemidio P, Fricia M, Passanisi M, Catania V, Sirago P, Ventura F (2008) Aggressive scalp carcinoma with intracranial extension: a multidisciplinary experience of 25 patients with long-term follow-up. J Clin Neurosci 15: 988–992
20. Syro LV, Ortiz LD, Scheithauer BW, Lloyd R, Lau Q, Gonzalez R, Uribe H, Cusimano M, Kovacs K, Horvath E (2011) Treatment of pituitary neoplasms with temozolomide: a review. Cancer 117:454–462
21. Torres MA, Chang EL, Mahajan A, Lege DG, Riley BA, Zhang X, Lii M, Kornguth DG, Pelloski CE, Woo SY (2009) Optimal treatment planning for skull base chordoma: photons, protons, or a combination of both? Int J Radiat Oncol Biol Phys 74: 1033–1039
22. Yamazaki H, Shiomi H, Tsubokura T, Kodani N, Nishimura T, Aibe N, Udono H, Nishikata M, Baba Y, Ogita M, Yamashita K, Kotsuma T (2011) Quantitative assessment of inter-observer variability in target volume delineation on stereotactic radiotherapy treatment for pituitary adenoma and meningioma near optic tract. Radiat Oncol 6:10

Gamma Knife Stereotactic Radiosurgery for Atypical and Malignant Meningiomas

Yoshimasa Mori, Takahiko Tsugawa, Chisa Hashizume, Tatsuya Kobayashi, and Yuta Shibamoto

Abstract *Background*: Non-benign meningioma has a known trend to recur repeatedly. The results of Gamma Knife stereotactic radiosurgery (GKS) for recurrent or residual atypical and malignant meningiomas are reported.

Methods: Thirty patients (13 men, 17 women) with World Health Organization (WHO) grade II (24 cases) or grade III (6 cases) intracranial meningiomas underwent GKS. Their age varied from 30 to 86 years (mean 64 years). Before GKS, the tumor was surgically resected in all patients, and 11 of them also underwent conventional external beam radiation therapy, LINAC-based stereotactic radiotherapy (SRT), or intensity-modulated radiation therapy.

Findings: Of the 30 patients, 23 were followed after the initial GKS for a median period of 28 months (range 2–135 months). Local tumor control after treatment was 74 % at 1 year, 52 % at 2 years, and 34 % at 3 years. A total of 15 patients underwent repeat GKS (one to nine times) because of local or distant intracranial tumor progression, seven were subjected to surgical re-resection of the neoplasm, and four had additional SRT. At the time of the last follow-up, 21 patients were alive, and 2 had died. One of the latter expired because of brain tumor progression at 91 months after the initial GKS, and the other patient died from lung cancer.

Conclusions: Although atypical and malignant meningiomas have a trend to recur repeatedly, aggressive tumor management with repeat GKS at the time of progression can provide long survival in these patients.

Y. Mori (✉) and Y. Shibamoto
Department of Radiology and Radiation Oncology,
Nagoya City University Graduate School of Medical Sciences,
1 Kawasumi, Mizuho-Cho, Mizuho,
Nagoya, Aichi 467-8601, Japan
e-mail: yoshim@med.nagoya-cu.ac.jp

T. Tsugawa, C. Hashizume, and T. Kobayashi
Nagoya Radiosurgery Center,
Nagoya Kyoritsu Hospital, Nagoya, Japan

Keywords Anaplastic meningioma • Atypical meningioma • Malignant meningioma • Meningioma • Radiosurgery • Recurrence • Re-growth

Introduction

Meninigomas arise from the dura mater covering the brain. The majority of these tumors are benign, slow-growing, and well-circumscribed. Histologically, 4–7 % of meningiomas are considered atypical, and 1–2 % are anaplastic [9]. Non-benign neoplasms tend to recur within a relatively short time even after radical surgical resection. The 5-year survival rate for these histologically aggressive tumors is 50–70 % [7, 13].

Many recent reports demonstrated that benign meningiomas can be well controlled with stereotactic radiosurgery (SRS) or stereotactic radiotherapy (SRT) if their size after the initial surgical resection is not too large [7]. In the present series, Gamma Knife radiosurgery (GKS) was applied as salvage treatment in cases of recurrent or residual atypical or malignant meningiomas if the localized lesion after initial surgical resection had suitable volume. The objective of this study was to evaluate the efficacy of such treatment for control of the tumor growth and prolongation of the patient's survival.

Materials and Methods

Patient Characteristics

Between May 2004 and April 2011, a total of 30 patients (13 men, 17 women) with an intracranial atypical (24 cases) or malignant (6 cases) meningioma were treated with GKS. Their age at the time of first radiosurgical procedure varied from 30 to 86 years (mean 64 years). There were 6 convexital, 13 parasagittal, 3 tentorial, and 8 skull base tumors. All of the patients underwent surgical resection of the neoplasm before GKS. Additionally, external beam radiation therapy

M.F. Chernov et al. (eds.), *Gamma Knife Neurosurgery in the Management of Intracranial Disorders*,
Acta Neurochirurgica Supplement, Vol. 116, DOI 10.1007/978-3-7091-1376-9_13, © Springer-Verlag Wien 2013

(EBRT) was done in eight cases, LINAC-based SRT in two, and intensity-modulated radiation therapy in one. Initial GKS was performed on 36 intracranial tumors (one to three per patient; median was one). Their volume varied from 0.4 to 35.3 cm^3 (median 8.6 cm^3).

GKS Procedure

The Leksell model G stereotactic coordinate frame (Elekta Instruments AB, Stockholm, Sweden) was fixed on the patient's head under local anesthesia supplemented by intramuscular and/or intravenous sedation. Stereotactic magnetic resonance imaging (MRI) was performed to define the tumor location and shape. Images were transferred via an ethernet connection to the Gamma Knife computer workstation (Leksell GammaPlan version 5.34 or, later, 10.1.1; Elekta Instruments AB), where treatment planning took place. Contrast-enhanced MRI was used for identifying irregular borders of the neoplasm. A neurosurgeon and a radiation oncologist identified the target and selected the dose. Choice of the prescription irradiation dose depended on the tumor volume and its spatial relation with adjacent anatomical structures, particularly the cranial nerves. The marginal irradiation dose varied from 11.0 to 20.15 Gy (mean 16.7 Gy). In all cases, stereotactic radiosurgery was performed using the Gamma Knife model C (Elekta Instruments AB) or, later, Perfexion (Elekta Instruments AB).

Follow-Up

The patients underwent regular follow-up at 2- to 6-month intervals. At each examination, the tumor response was evaluated by detailed comparison with the initial MRI scans. The response was categorized as complete (CR), defined as tumor disappearance; partial (PR), defined as >50 % reduction of the tumor volume; stable disease (SD); or tumor progression (PG), defined as >25 % increase in its volume or the appearance of new lesions. If development of the new tumors or progression of the treated neoplasm were revealed during follow-up, the patient typically was offered additional treatment with either repeat GKS or other modality.

Results

In all, 23 of the 30 patients (19 with atypical and 4 with anaplastic meningiomas) were followed after initial GKS for a median period of 28 months (range 2–135 months). A total of 15 patients underwent one to nine additional GKS procedures after the initial radiosurgery because of the development of new tumors or progression of the treated meningioma. Therefore, in total 68 GKS procedures were done in 30 patients (from 1 to 10 in each case). Additionally, during follow-up after initial radiosurgery, surgical re-resection of the tumor was performed in seven patients and SRT in four. No adverse effects—defined as deterioration of the patient's neurological status without tumor progression—were observed during the follow-up either after the initial or repeat GKS.

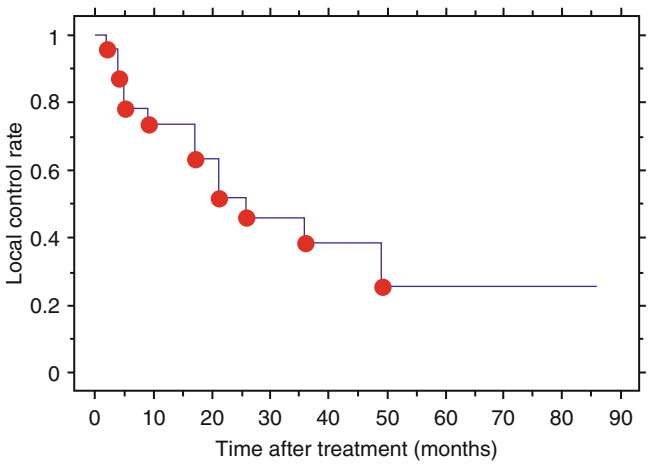

Fig. 1 Kaplan-Meier curve demonstrates the local tumor control rate after the first Gamma Knife radiosurgery of non-benign meningioma

Local Tumor Control

Local tumor control was evaluated in the 23 patients who were followed after first GKS. At the time of the initial treatment they had 26 tumors (mean volume 9.8 cm^3) that were irradiated with a mean marginal dose of 16.5 Gy (range 11.0–20.15 Gy). All of the patients were subjected to regular MRI examinations during the posttreatment follow-up.

The treated neoplasms were controlled (CR + PR + SD) in 10 patients until the last follow-up examination at 9–86 months after initial GKS. In the other 13 patients the treated tumors recurred within 2–49 months after treatment. Local tumor control after initial GKS for atypical and malignant meningiomas was 74 % at 1 year, 52 % at 2 years, and 34 % at 3 years (Fig. 1).

Patient Survival

Of the 23 followed patients, 21 remained alive, and 2 had died. One patient expired because of progression of the intracranial tumor 91 months after initial GKS. The second patient died from lung cancer 17 months after initial GKS.

Thus, cause-specific survival up to 91 months after initial GKS for atypical and malignant meningiomas in the series was 100 %.

Illustrative Case

A 67-year-old man underwent surgical resection of the parieto-occipital parasagittal tumor, which caused bone destruction and protruded under the skin. Histological investigation revealed an atypical meningioma. At 2 months after the operation the residual neoplasm, which had a volume of 18.6 cm^3, was treated with GKS with a marginal dose of 12.5 Gy (Fig. 2). Three years later, marginal progression of the anterosuperior part of the treated tumor was revealed. The enlarging lesion had a volume of 14.1 cm^3 and was selectively treated with a second GKS with a marginal dose of 14 Gy. However, 1.5 year later two newly developed tumors located at the occipital and parietal convexity in the vicinity of the craniotomy flap were disclosed during follow-up MRI investigation. The volumes of these lesions were 2.1 and 2.9 cm^3, respectively, and both underwent a third GKS with a marginal dose of 18 Gy. Six months later the marginal treatment failures in the two portions of the main parasagittal tumor were disclosed. The volumes of the progressing lesions were 23 and 4.5 cm^3, and they were selectively treated with a fourth GKS with marginal doses of 13 and 18 Gy, respectively. During the subsequent 10 months there was no evidence of further tumor progression. With the help of four GKS procedures, the growth of the lesion seems controlled at 6 years after the initial surgical resection, and the neurological condition of the patient remains stable.

Discussion

Compared to their benign (WHO grade I) counterparts, atypical (WHO grade II) and malignant (WHO grade III) meningiomas have higher local recurrence rates and lower patient survival. Previously, the typical initial management of such tumors included surgical removal followed by EBRT. Although this procedure should definitely be considered if gross total resection of the lesion is attained, it should be noted that residual or recurrent high-grade meningiomas are not particularly sensitive to conventional irradiation [2]. Therefore, early SRS in such cases was proposed [4, 5]. Because SRS and SRT can deliver higher irradiation doses to the tumor while sparing adjacent normal tissues, it can be expected that such treatment would be more effective for managing localized neoplasms of a suitable size. It is widely recognized that benign meningiomas, both residual and recurrent after initial surgical resection, can be effectively treated with SRS or SRT. In fact, 5-year local control rates of >90 % can be attained with both techniques [8, 11, 14]. However, only a few reports have mentioned treatment outcomes after such treatment in cases of WHO grade II and III meningiomas [4–6, 10–12, 14]. Moreover, some of the series included an overwhelming number of benign tumors, which does not permit detailed analysis of results [1, 3].

Previously published studies of GKS for atypical and malignant meningiomas are summarized in Table 1. Low local tumor control rates and poor long-term survival were usually recorded, especially for WHO grade III tumors. Stafford et al. [14] showed a striking difference in 5-year local control rates in atypical and anaplastic meningiomas (68 % vs. 0 %). In contrast, in the present series the 5-year local control rates for these two meningioma types did not differ (52 and 50 %, respectively, at 2 years after the initial GKS), although it should be noted that only 4 of our 23 patients that were followed after treatment had malignant tumors. The prescribed marginal radiation dose during GKS for non-benign meningiomas typically varied from 14 to 20 Gy, which is similar to doses for many other types of brain tumor. Of note: Kano et al. [6] reported the results of LINAC-based SRS for high-grade meningiomas and found significantly better outcomes for patients treated with a 20 Gy marginal irradiation dose than for those who received <20 Gy. Their 5-year progression-free survival rates were 63.1 % and 29.4 %, respectively. In the present series, dose selection depended on the tumor volume and location. For small tumors we usually used a marginal dose of 18–20 Gy; for neoplasms with a volume of ~10 cm^3, it was 16 Gy; and for larger lesions it was ~14 Gy. Seemingly, such dose selection permitted us to avoid adverse clinical effects, which were not observed during the follow-up in any patient either after the initial or repeated GKS.

It is evident that SRS fails to inhibit growth of high-grade meningiomas for a prolonged period of time. In the present series, the local tumor control rate after initial GKS was 74 % at 1 year, 52 % at 2 years, and 34 % at 3 years. The high risk of recurrence necessitates close clinical and neuroradiological follow-up. If detailed analysis of MRI scans reveals the appearance of new neoplasms or progression of the treated tumor, repeat GKS can be effective. As was clearly shown in our illustrative case, in patients with marginal treatment failure, further irradiation can be selectively applied only to the enlarging portion of the lesion. It may then lead to cessation of further growth for a prolonged period of time. Other treatment options (re-resection, SRT) should be considered as well. Such aggressive treatment strategy for non-benign meningiomas recurring after initial and repeat GKS permitted for us to obtain rather beneficial results. Although the presented series is not large and the follow-up period is

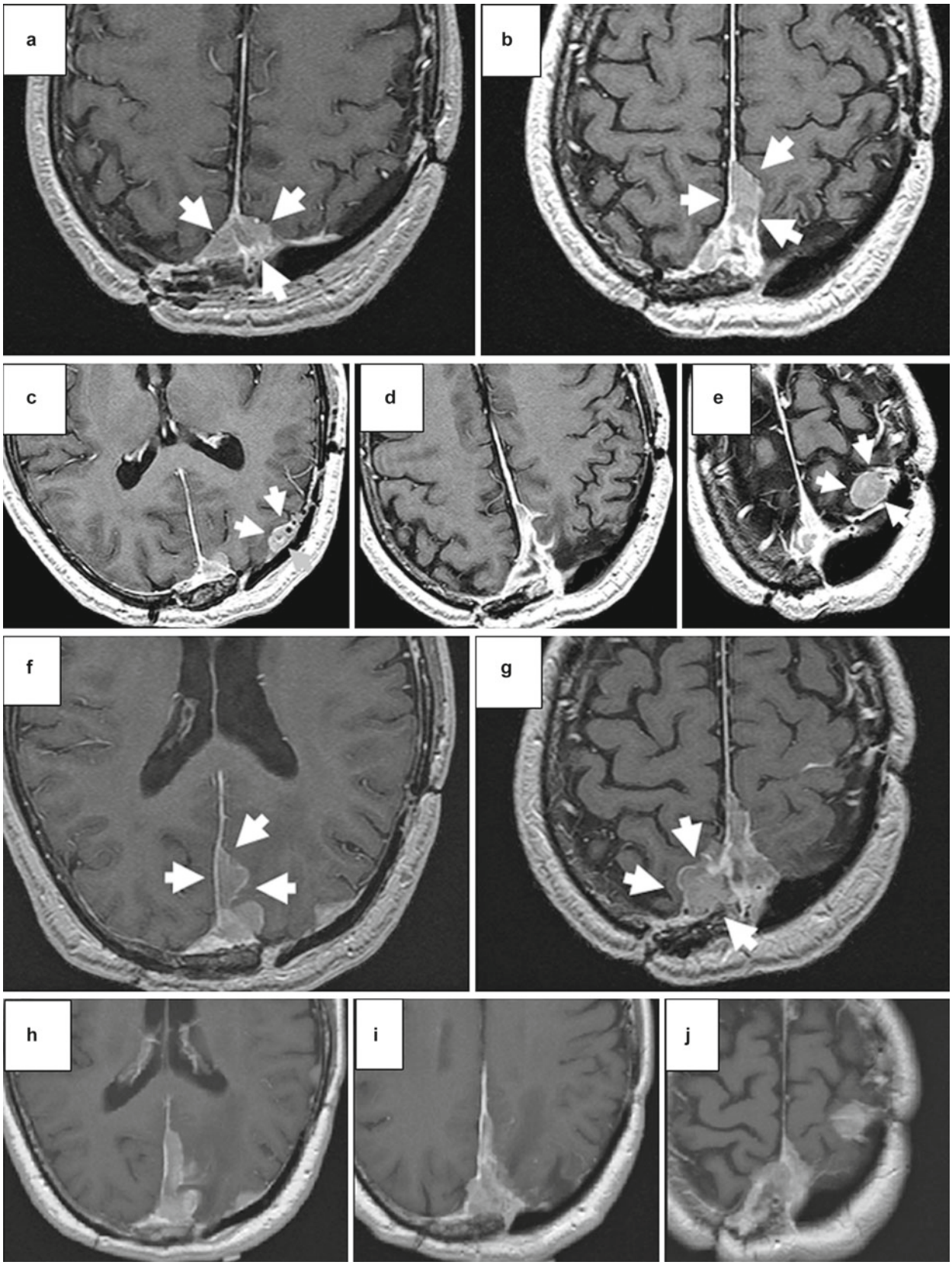

Fig. 2 Axial postcontrast magnetic resonance imaging (MRI) of an atypical meningioma in a 67-year-old man. (**a**) The first GKS was performed for residual tumor after the initial surgical resection (*arrows*). (**b**) The second GKS was performed 3 years later to treat regrowth of the anterosuperior portion of the tumor (*arrows*). (**c**–**e**) The third GKS was performed 1.5 years after the second GKS to address two newly developed distant tumors (*arrows*) in the occipital (**c**) and parietal (**e**) convexity adjacent to craniotomy flap. The main parasagittal lesion showed shrinkage (**d**). (**f**, **g**) The fourth GKS was performed 6 months after the third GKS to address two newly progressing portions of the tumor (*arrows*). (**h**–**j**) Ten months after the fourth GKS and 6 years after the initial surgical resection there is no evidence of further tumor progression

Table 1 Reported series of Gamma Knife stereotactic radiosurgery for non-benign meningiomas

Author, year of publication	Histological subtype	No. of patients (lesions)	Marginal dose (Gy)	Tumor control rate	Survival
Ojemann et al., 2000 [12]	Malignant	19[a] (23)	Mean 16; median 15.5	ND	PFS: 48 % at 2 years, 34 % at 5 years
Stafford et al., 2001 [14]	Atypical	13	Median 16; range 12–36[b]	68 % at 5 years	CSS: 76 % at 5 years
	Malignant	9		0 % at 5 years	CSS: 0 % at 5 years
Harris et al., 2003 [4]	Atypical	18	Mean 14.9	ND	PFS: 83 % at 5 years
	Malignant	12	Mean 15.7		PFS: 72 % at 5 years
Huffmann et al., 2005 [5]	Atypical	15 (21)	Range 14–18	93 % at 6 months	100 % within median follow-up of 35 months (range 21–67 months)
Present series	Atypical	19 (22)	Mean 16.5	74 % at 1 year	CSS: 100 % at 5 years
	Malignant	4 (4)		52 % at 2 years	
				34 % at 3 years	

ND no data, *PFS* progression-free survival, *CSS* cause-specific survival
[a]All patients had recurrent tumors after external beam radiation therapy
[b]Including benign meningiomas

limited, the 5-year cause-specific survival rate of 100 % among our patients seems impressive.

Conclusion

Based on results of the present study, it can be concluded that atypical and malignant meningiomas, both recurrent and residual after initial surgical resection, can be effectively treated with GKS if the volume of the neoplasm is not too large. Regular neuroradiological follow-up with timely identification of the development of new tumors or progression of the treated neoplasm followed by repeat management with GKS or other modalities (microsurgery, SRT) are important for prolongation of the patient's survival.

Conflict of Interest The authors declare that they have no conflict of interest.

References

1. Debus J, Wuendrich M, Pirzkall A, Hoess A, Schlegel W, Zuna I, Engenralt-Cabillic R, Wannenmacher M (2001) High efficacy of fractionated stereotactic radiotherapy of large base-of-skull meningiomas: long-term results. J Clin Oncol 19:3547–3553
2. Goldsmith BJ, Wara WM, Wilson CB, Larson DA (1994) Postoperative irradiation for subtotally resected meningiomas. A retrospective analysis of 140 patients treated from 1967 to 1990. J Neurosurg 80:195–201
3. Hakim R, Alexander E III, Loeffler JS, SHrieve DC, Wen P, Fallon MP, Stieg PE, Black PM (1998) Results of linear accelerator-based radiosurgery for intracranial meningiomas. Neurosurgery 42:446–453
4. Harris AE, Lee JYK, Omalu B, Flickinger JC, Kondziolka D, Lunsford LD (2003) The effect of radiosurgery during management of aggressive meningiomas. Surg Neurol 60:298–305
5. Huffmann BC, Reinacher PC, Gilsbach JM (2005) Gamma knife surgery for atypical meningiomas. J Neurosurg 102(Suppl): 283–286
6. Kano H, Takahashi JA, Katsuki T, Araki N, Oya N, Hiraoka M, Hashimoto N (2007) Stereotactic radiosurgery for atypical amd anaplastic meningiomas. J Neurooncol 84:41–47
7. Kondziolka D, Lunsford LD, Coffy RJ, Flickinger JC (1991) Gamma knife radiosurgery of meningiomas. Stereotact Funct Neurosurg 57:11–21
8. Kondziolka D, Levy EI, Niranjan A, Flickinger JC, Lunsford LD (1999) Long-term outcomes after meningioma radiosurgery: physician and patient perspective. J Neurosurg 91:44–50
9. Louis DN, Ohgaki H, Wiestler OD, Cavenee WK (2007) WHO classification of tumours of the Central Nervous System. IARC Press, Lyon, pp 164–172
10. Mattozo CA, De Salles AAF, Klement IA, Gorgulho A, McArthur D, Ford JM, Agazaryan N, Kelly DF, Selch MT (2007) Stereotactic radiation treatment for recurrent non-benign meningiomas. J Neurosurg 106:846–854
11. Milker-Zabel S, Zabel A, Schulz-Ertner D, Schlegel W, Wannenmacher M, Debus J (2005) Fractionated stereotactic radiotherapy in patients with benign or atypical intracranial meningioma: long-term experience and prognostic factors. Int J Radiat Oncol Biol Phys 61:809–816
12. Ojemann SG, Sneed PK, Larson DA, Gutin PH, Berger MS, Verhey L, Smith V, Petti P, Wara W, Park E, McDermott MW (2000) Radosurgery for malignant meningioma: results in 22 patients. J Neurosurg 93(Suppl 3):62–67
13. Palma L, Celli P, Franco C, Contore G (1997) Long-term prognosis for atypical and malignant meningiomas: a study of 71 surgical cases. J Neurosurg 86:793–800
14. Stafford SL, Pollock BE, Foote RL, Link MJ, Gorman DA, Schomberg PJ, Leavitt JA (2001) Meningioma radiosurgery: tumor control, outcomes, and complications among 190 consecutive patients. Neurosurgery 49:1029–1038

Management of Non-benign Meningiomas with Gamma Knife Radiosurgery

Manabu Tamura, Kenji Kubo, Ryuji Okita, Mitsuhiro Ogura, Naoyuki Nakao, Yuji Uematsu, Toru Itakura, Motohiro Hayashi, Yoshihiro Muragaki, and Hiroshi Iseki

Abstract *Objective*: Results of Gamma Knife radiosurgery (GKS) were retrospectively evaluated in 16 patients with histologically confirmed atypical and anaplastic intracranial meningiomas.

Materials and Methods: There were nine men and seven women (mean age 61.0 years). Atypical meningiomas were diagnosed in nine cases and anaplastic meningiomas in seven. In nine patients there was malignant transformation of a tumor that had initially proved to be benign. In total, 21 radiosurgical procedures were performed. The mean tumor volume at the time of GKS was 7.1 cm^3. The mean marginal and maximum irradiation doses were 18.8 and 37.0 Gy, respectively. The mean length of follow-up after treatment was 37.1 months.

Findings: Of 21 radiosurgical procedures, 6 (29 %) led to stabilization of tumor growth during the mean follow-up of 40.5 months. It was significantly associated with small lesion volume ($P=0.02$), and greater marginal ($P=0.04$) and maximum ($P=0.02$) irradiation doses. Seven patients underwent eight surgical resections of a progressing tumor during the mean period of 26.1 months after irradiation. Five patients (31 %) died because of tumor progression within the average time period of 16.8 months after GKS. Overall, at the time of the last follow-up just two patients (13 %) had no evidence of tumor regrowth, and only three patients (19 %) maintained good activities of daily living during 12, 59, and 69 months, respectively, after radiosurgery.

Conclusion: GKS has limited efficacy in cases of non-benign meningioma. Better tumor control rates can be attained for small neoplasms treated with greater marginal and maximum irradiation doses.

Keywords Activities of daily living • Atypical meningioma • Gamma Knife radiosurgery • Histopathological findings • Malignant meningioma • Radiation injury • Tumor control

Introduction

The development and wide application of contemporary neuroimaging modalities and their frequent use for screening brain diseases have resulted in increased number of patients with incidental intracranial tumors, particularly meningiomas. Various treatment options can be applied in such cases, including stereotactic radiosurgery by means of the Gamma Knife [7, 10], CyberKnife [2, 3], or dedicated linear accelerator [1]. Nevertheless, choice of the optimal management strategy for intracranial meningiomas is still a significant challenge, particularly because of the wide variation in their growth rates both before and after neurosurgical procedures, which are strongly related to the histopathological grade of the tumor.

Multiple reports demonstrated good tumor control and low risk of complications after Gamma Knife radiosurgery (GKS) applied either as primary treatment modality or after initial surgical resection of World Health Organization (WHO) histopathological grade I intracranial meningiomas [4, 5, 7, 9, 10, 13]. Therefore, incidentally found small meningioma-like neoplasms are frequently regarded as benign and undergo radiosurgery without preliminary radiological evaluation of the growth rate or histopathological confirmation of the diagnosis. Such cohorts should definitely include some proportions of atypical (WHO histopathological grade II)

M. Tamura (✉), M. Hayashi, Y. Muragaki, and H. Iseki
Faculty of Advanced Techno-Surgery,
Institute of Advanced Biomedical Engineering and Science,
TWIns, Tokyo Women's Medical University,
8-1 Kawada-cho, Shinjuku-ku, Tokyo 162-8666, Japan

Department of Neurosurgery, Neurological Institute,
Tokyo Women's Medical University,
Tokyo, Japan
e-mail: manabu97@abmes.twmu.ac.jp

K. Kubo
Gamma Knife Center, Koyo Hospital, Wakayama, Japan

R. Okita, M. Ogura, N. Nakao, Y. Uematsu, and T. Itakura
Department of Neurological Surgery, Wakayama Medical University,
Wakayama, Japan

M.F. Chernov et al. (eds.), *Gamma Knife Neurosurgery in the Management of Intracranial Disorders*,
Acta Neurochirurgica Supplement, Vol. 116, DOI 10.1007/978-3-7091-1376-9_14,

and anaplastic (WHO histopathological grade III) tumors. Moreover, stereotactic irradiation at the time of recurrence or regrowth of the typical meningioma after its initial surgical resection also does not guarantee a benign nature of the lesion owing to possible malignant transformation. On the other hand, the efficacy of GKS in cases of atypical and anaplastic meningiomas is much lower than for their benign counterparts [11, 12].

The objective of the present study was to evaluate results of GKS for histologically confirmed non-benign meningiomas. Particular emphasis is placed on factors associated with tumor growth control and patients' activities of daily living (ADL) after treatment.

Materials and Methods

A total of 96 consecutive patients with intracranial meningiomas underwent GKS in the Gamma Knife Center of the Koyo Hospital between 1995 and 2010. A histopathological diagnosis of atypical (WHO grade II) or anaplastic (WHO grade III) meningioma was established in 16 of the 96 patients before radiosurgery. These cases represented the clinical basis of the present retrospective analysis.

There were nine men and seven women. Their age at the time of GKS varied from 31 to 81 years (mean 61.0 years). All patients underwent at least one surgical resection of the intracranial tumor before radiosurgery. Atypical meningioma was diagnosed in nine cases, whereas the diagnosis was anaplastic meningioma in seven. In 7 of the 16 patients, a non-benign type of intracranial meningioma was revealed after the first surgical resection of the neoplasm, whereas in nine other patients there was malignant transformation of tumors that had initially been diagnosed as benign. The average interval between histopathological establishment of the diagnosis and GKS was 26.9 months (range 1–60 months) in the former group and 10.1 months (range 3–44 months) in the latter group.

In all, 13 patients underwent a single radiosurgical procedure, whereas 2 patients were treated twice and another patient was subjected to four GKS for spatially separate lesions. Therefore, a total of 21 radiosurgical procedures were performed in the investigated cohort.

Radiosurgery

All of the patients were admitted to the hospital the day before the scheduled radiosurgery and provided informed consent related to the procedure. On the day of treatment, a Leksell stereotactic frame type G (Elekta Instruments AB, Stockholm, Sweden) was fixed on the patient's head under local anesthesia accompanied by light sedation. Axial T2-weighted and volumetric T1-weighted images without and with gadolinium enhancement were obtained under stereotactic conditions using a 1.5 T clinical magnetic resonance imaging (MRI) scanner (Toshiba Medical Systems, Tokyo, Japan). All images were imported into the Leksell GammaPlan (Elekta Instruments AB), and the tumor volume was assessed. It varied from 0.4 to 28.5 cm^3 (mean 7.1 cm^3). The peripheral isodose varied from 50 % to 70 % (mean 51 %). The marginal irradiation dose varied from 6 to 23 Gy (mean 18.8 Gy), whereas the maximum dose ranged from 12 to 46 Gy (mean 37 Gy). The number of isocenters varied from 1 to 43 (mean 15).

Follow-Up

All patients were followed at least 1 year after GKS or until death. MRI and neurological assessments with determination of the Karnofsky Performance Scale (KPS) score [8] and evaluation of ADL were performed regularly every 3 months, which in our practice represents the standard interval for follow-up investigations after radiosurgery for malignant intracranial tumors. The mean length of the clinicoradiological follow-up period was 37.1 months (range 1–118 months).

Tumor control was evaluated after all 21 radiosurgical procedures, and its association with the following factors was assessed with univariate statistical analysis: histopathological diagnosis of meningioma (WHO grade II vs. grade III), tumor volume, applied peripheral isodose, marginal and maximum irradiation doses, and number of isocenters. The nonparametric Mann-Whitney two-sample *T*-test was used to evaluate continuous variables, and Fisher's exact probability test was used for categorical variables. The results were considered significant for P less than 0.05. The statistical analysis was performed with commercially available software.

The ADL measure was considered good if the KPS score was 80 and more; it was poor, if the KPS score was 70 or less.

Results

At the time of the last follow-up after GKS, just 2 of 16 patients (13 %) had no evidence of tumor recurrence. Seven patients underwent eight surgical resections because of progression of the lesion within the mean period of 26.1 months after irradiation. Histopathological investigation revealed in-field tumor recurrence in six cases treated with an average marginal dose of 15.5 Gy, out-of-field tumor recurrence in one case treated with a marginal dose of 20 Gy, and fibrous organization of the lesion after radiation-induced necrosis in one case after irradiation with a marginal dose of 23 Gy (Table 1).

Table 1 Summary of patients who underwent surgical resection of a lesion after GKS for non-benign meningioma

Case no.	Tumor location	WHO histopathological grade before GKS	Tumor volume at the time of GKS (cm^3)	Marginal/maximum irradiation doses (Gy)	Time interval between GKS and tumor resection (months)	Location of regrowing tumor	Histopathological diagnosis after lesion resection
1	Cerebellar convexity	II	2.0	18/36	8	In-field	Tumor recurrence (WHO grade II meningioma)
2	Temporal convexity	III	0.4	23/33	15	In-field	Fibrous organization of the neoplasm after radiation-induced necrosis
3	Temporal convexity	III	3.4	20/40	25	Out-of-field	Tumor recurrence (WHO grade III meningioma)
4a	Parietal convexity	III	1.6	18/36	12	In-field	Tumor recurrence (WHO grade III meningioma)
4b	Temporal convexity	III	7.1	18/36	18	In-field	Tumor recurrence (WHO grade III meningioma)
5	Tentorial	II	15.5	13/26	118	In-field	Tumor recurrence (WHO grade II meningioma)
6	Frontal convexity	II	10.6	20/40	7	In-field	Combined radiation injury and tumor recurrence (WHO grade II meningioma)
7	Temporal convexity	III	13.5	6/12	6	In-field	Tumor recurrence (WHO grade III meningioma)

Two neoplasms were resected in case 4
GKS Gamma Knife radiosurgery

Tumor Control After Radiosurgery

Of 21 radiosurgical procedures 6 (29 %) led to stabilization of the tumor volume during the mean follow-up of 40.5 months (good control group). In the other 15 cases, despite the treatment the neoplasms increased in size during the mean follow-up of 31.3 months (poor control group). Statistical analysis revealed significant association of good tumor control after GKS with small tumor volume ($P=0.02$) and higher marginal ($P=0.04$) and maximum ($P=0.02$) irradiation doses (Table 2). Of note: tumor control did not depend on the WHO histopathological grade ($P=0.42$) and was attained in 2 of 10 cases (20 %) of atypical meningioma within a mean follow-up of 29.0 months (median 23.5 months) and in 4 of 11 cases (36 %) of anaplastic meningioma within a mean follow-up of 46.3 months (median 39.0 months).

ADL After Radiosurgery

Three patients (19 %) maintained good ADL after GKS for non-benign meningiomas (Fig. 1) during 12, 59, and 69 months, respectively (average 46.7 months). One of patients had a WHO grade II meningioma and two others had WHO grade III meningioma. A total of six radiosurgical procedures were performed in this cohort. The mean volume of the neoplasms at the time of irradiation was 2.1 cm^3, and the marginal dose varied from 20 to 23 Gy. One anaplastic meningioma was surgically resected 15 months after GKS.

Eight patients (50 %) had poor ADL after GKS for non-benign meningiomas but were alive at the time of the last follow-up, which was an average of 49.3 months after treatment. Nine radiosurgical procedures were performed in this cohort. Seven patients had WHO grade II meningiomas, three of whom underwent surgical resection of their tumor at 7, 8, and 118 months, respectively, after radiosurgery. One patient had a WHO grade III meningioma, which was resected at 25 months after GKS.

Five patients (31 %) died because of tumor progression during an average follow-up of 16.8 months (range 1–42 months) after GKS. Six radiosurgical procedures were performed in this cohort. One of the patients had WHO grade II, and four others had WHO grade III meningioma. Two patients with anaplastic meningioma underwent three surgical resections of the lesions at 6, 12, and 18 months, respectively, after GKS.

Illustrative Cases

A 62-year-old woman (case 2 in Table 1 and Fig. 2) underwent GKS for residual anaplastic meningioma (WHO grade III), which was diagnosed after the first surgical resection. At

Table 2 Factors associated with tumor control after 21 GKS procedures for non-benign meningiomas

Analyzed factors	Tumor control		*P*
	Good (*N* = 6; mean follow-up 40.5 months)	Poor (*N* = 15; mean follow-up 31.3 months)	
WHO histopathological grade of meningioma (II/III)	2/4	8/7	0.42[a]
Tumor volume (cm^3)	Mean, 2.3; range, 0.4–5.0	Mean, 9.0; range, 0.4–28.5	0.02[b]
Peripheral isodose (%)	Mean, 50.0; range, 50–50	Mean, 51.3; range, 50–70	0.53[b]
Marginal irradiation dose (Gy)	Mean, 21.2; range, 15–23	Mean, 17.9; range, 6–23	0.04[b]
Maximum irradiation dose (Gy)	Mean, 42.3; range, 30–46	Mean, 34.9; range, 12–44	0.02[b]
No. of isocenters	Mean, 10.0; range, 3–28	Mean, 16.5; range, 1–43	0.17[b]

N number of cases
[a]According to Fisher's exact probability test
[b]According to the Mann-Whitney two-sample *T*-test

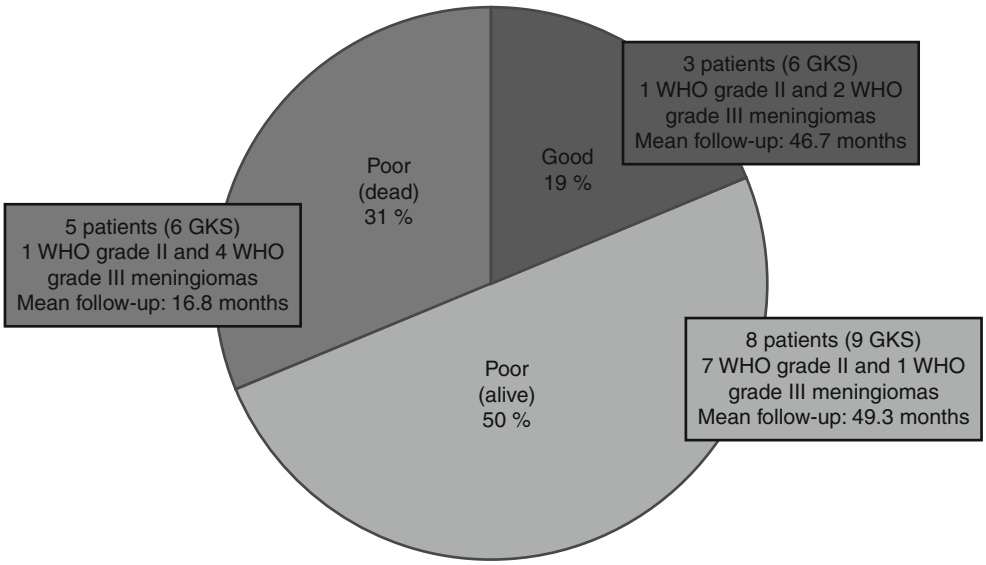

Fig. 1 Activities of daily living after Gamma Knife radiosurgery (GKS) for non-benign intracranial meningiomas. Good and poor correspond to KPS scores of 80 and more, and 70 or less, respectively

the time of radiosurgery the volume of the neoplasm was 0.4 cm^3. The marginal dose corresponding to the 70 % isodose line was 23 Gy. Tumor regrowth was diagnosed 15 months later and was surgically resected. Histopathological investigation of the irradiated neoplasm revealed only its fibrous organization after radiation-induced necrosis, and infiltrating neoplastic cells were seen outside the peripheral isodose line. During the 3 years after the second surgery there was no evidence of tumor recurrence. The patient maintained good ADL (KPS 100).

A 64-year-old man (case 6 in Table 1 and Fig. 2) was treated with GKS for residual atypical meningioma (WHO grade II), which at the time of the initial surgery proved to be benign but later underwent malignant transformation. At the time of radiosurgery, the volume of the neoplasm was 10.6 cm^3. The marginal dose corresponding to the 50 % isodose line was 20 Gy. The frontal convexity tumor did not change its size after GKS, but an associated parasagittal neoplasm, which was also irradiated, showed progression. Therefore, another surgical resection was performed at 7 months after GKS. Histopathological investigation of the irradiated lesion within the peripheral isodose line revealed combined radiation injury and recurrence of the WHO grade II meningioma. Subsequently, no recurrence of the frontal convexity tumor was disclosed, but the parasagittal neoplasm showed continuous progression, accompanied by gradual decline of the KPS up to 40.

Discussion

Results of GKS for non-benign meningiomas in the present series were definitely poor. Overall, just 29 % of radiosurgical procedures resulted in stabilization of tumor growth during more or less prolonged period of time. During the mean posttreatment follow-up of 37.1 months, 44 % of patients required surgical resection of the lesion, and 31 % of patients died owing to progression of the neoplasm despite irradiation. Just 13 % had no evidence of tumor regrowth, and only

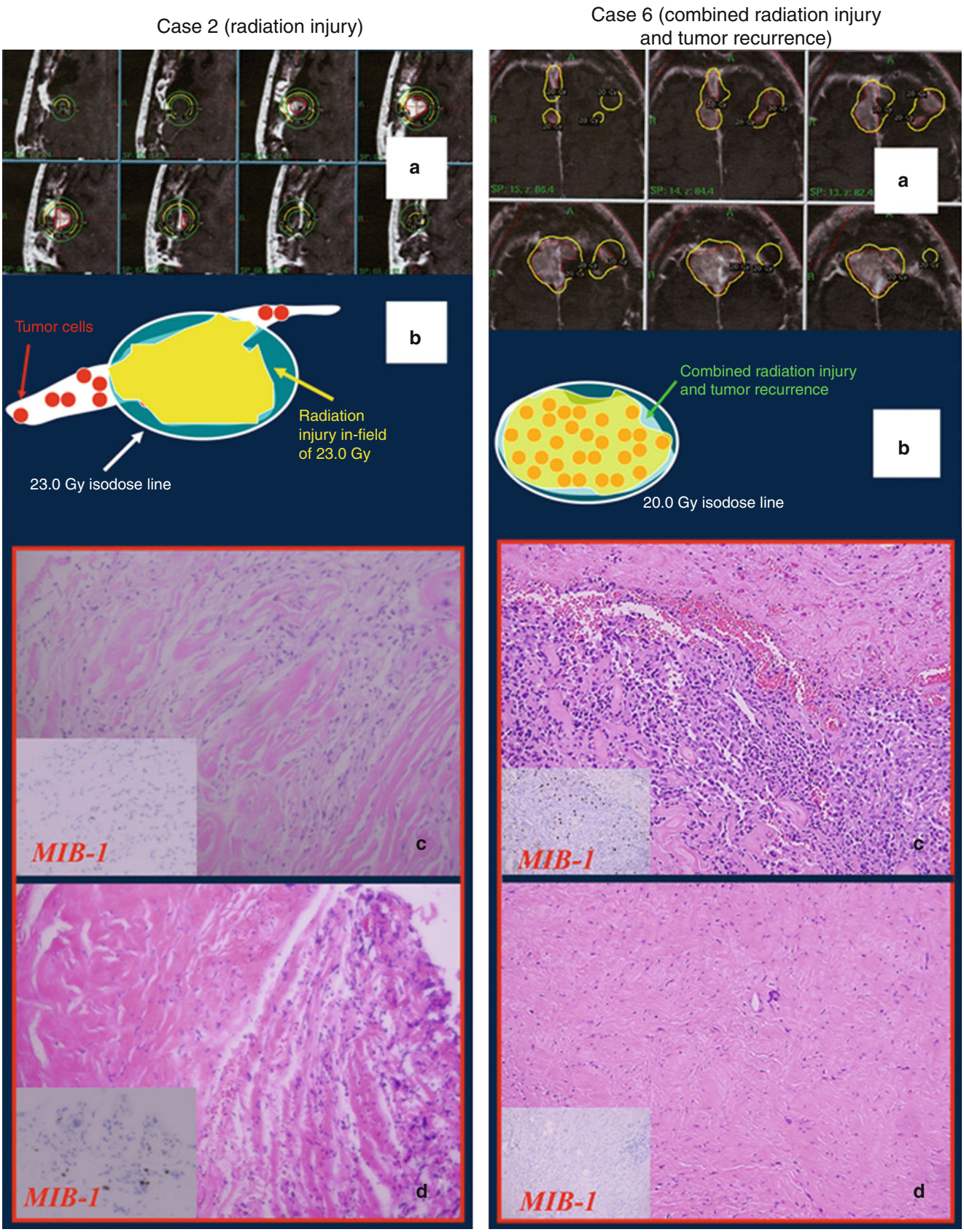

Fig. 2 Radiosurgical treatment planning (**a**), schematic explanation of the histopathological findings after subsequent lesion resection (**b**), and the microscopic view (H&E and MIB-1; ×200) of the pathological tissue obtained within (**c**) and outside (**d**) the irradiation field in cases of GKS for non-benign meningiomas. In case 2 (*left*), only fibrous organization after radiation-induced necrosis of the irradiated neoplasm was revealed; infiltrating neoplastic cells were seen outside the peripheral isodose line. In case 6 (*right*), combined radiation injury and recurrence of World Health Organization grade II meningioma was disclosed within the irradiation field. Microphotographs of MIB-1 immunostaining correspond to those stained with H&E

19 % maintained good ADL. The questions are whether it is possible to improve the efficacy of radiosurgery in such cases and, if so, how to do it.

In a large series of patients with intracranial meningiomas treated with GKS, Kondziolka et al. [10] found a 50 % control rate during a median follow-up of 24 months in 54 WHO grade II tumors and a 17 % control rate during a median follow-up of 15 months in 29 WHO grade III neoplasms. In our series, growth control rates was not associated with the histopathological grade of the tumor and constituted 20 % during a median follow-up of 23.5 months for the atypical meningiomas and 36 % during a median follow-up of 39.0 months for anaplastic meningiomas. On the other hand, both marginal and maximum irradiation doses showed statistically significant associations with tumor control after GKS. Our study suffers from the small number of analyzed cases and retrospective design, but it can be speculated that delivery of high irradiation doses during radiosurgery of non-benign meningiomas may be more important for growth control than the histopathological grade of the neoplasm.

Furthermore, advantages of the high irradiation doses were demonstrated in our series during histopathological analysis of the tissue samples obtained during surgical resection of lesions progressing after GKS. In all five cases treated with marginal doses of 6–18 Gy, pure in-field tumor regrowth was identified. In two cases treated with a marginal dose of 20 Gy either out-of-field tumor regrowth or radiation injury intermixed with viable tumor were demonstrated. Moreover, in the patient who received the highest marginal dose in the series (23 Gy), there was no viable neoplasm in the irradiated field. Thus, it seems that marginal doses of 12–14 Gy, which are currently used for GKS of benign meningiomas, may be insufficient for atypical and anaplastic meningiomas. In the latter cases we are currently applying marginal doses >18 Gy, which is comparable to intracranial metastases. The validity of such an approach should be proved in additional studies. Also, the possible risk of long-term complications associated with high irradiation doses, such as development of symptomatic perilesional edema [14] or cyst formation [6], should be borne in mind. Although achieving tumor control represents the primary goal of radiosurgery, improving the functional outcome, particularly reflected in ADL, may be also very important.

The irradiation dose is determined by the volume of the tumor. This factor was also significantly associated with tumor control in our patients, which corresponds to the data of Ojemann et al. [12], who analyzed the series of malignant meningiomas after fractionated radiotherapy combined with GKS and showed a trend for better growth control in neoplasms with a volume of <8 cm^3.

Application of multi-isocenter dose planning with delivery of the greater radiation energy per tumor volume [5] may increase efficacy and decrease the risk of complications after GKS, particularly for large lesions. On the other hand, less selective treatment with inclusion of some of the adjacent tissues in the isodose area may be preferable in cases of non-benign neoplasms because it potentially eliminates infiltrating neoplastic cells—which are frequently seen microscopically in the vicinity of the main mass—and thereby prevent out-of-field recurrence. Close radiological follow-up after radiosurgery of atypical and anaplastic meningiomas and application of the repeated treatment as soon as lesion progression is identified represents another option for improving tumor control [9]. Finally, several factors that were not analyzed in the present study (e.g., the MIB-1 index [11] or the patient's age [12]) may be associated with control of non-benign meningiomas after GKS and therefore may influence the choice of the parameters for radiosurgical treatment.

Conclusion

The present study demonstrated limited efficacy of GKS in cases of histologically confirmed non-benign meningiomas. Just 29 % of radiosurgical procedures led to tumor control and only 19 % of patients maintained good ADL with KPS scores of at least 80 during prolonged periods of time after treatment. Surgical resection, undertaken because of tumor progression despite irradiation, was required in 44 % of patients. Nevertheless, better tumor control rates were found in patients with small neoplasms that were treated with greater marginal and maximum irradiation doses. These findings should be taken into consideration during GKS of non-benign intracranial meningiomas.

Acknowledgment This study used a Grant-in-Aid for Scientific Research (B) No. 22300093 and was supported by the Global COE Program: The Multidisciplinary Education and Research Centre for the Establishment of Regenerative Medicine (MERCREM), Ministry of Education, Culture, Sports, Science, and Technology (MEXT) of Japan. Additional support was obtained from the Japan Society for the Promotion of Science (JSPS) through the "Funding Program for World-Leading Innovative R&D on Science and Technology (FIRST Program)" initiated by the Council for Science and Technology Policy (CSTP). The authors are grateful to Gautam A. Deshpande, M.D. for his assistance with editing the manuscript.

Conflict of Interest The authors declare that they have no conflict of interest.

References

1. Abdelaziz OS, Kandil A, El-Assaal S, Abdelaziz A, Rostom Y, Rashed Y (2011) Linear accelerator-based stereotactic radiosurgery of intracranial meningiomas: results of the first 5 years of clinical practice. Neurosurg Rev 34:87–99

2. Bria C, Wegner RE, Clump DA, Vargo JA, Mintz AH, Heron DE, Burton SA (2011) Fractionated stereotactic radiosurgery for the treatment of meningiomas. J Cancer Res Ther 7:52–57
3. Choi CY, Soltys SG, Gibbs IC, Harsh GR, Jackson PS, Lieberson RE, Chang SD, Adler JR (2010) Cyberknife stereotactic radiosurgery for treatment of atypical (WHO grade II) cranial meningiomas. Neurosurgery 67:1180–1188
4. Hasegawa T, Kida Y, Yoshimoto M, Iizuka H, Ishii D, Yoshida K (2011) Gamma Knife surgery for convexity, parasagittal, and falcine meningiomas. J Neurosurg 114:1392–1398
5. Hayashi M, Chernov M, Tamura N, Izawa M, Muragaki Y, Iseki H, Okada Y, Takakura K (2011) Gamma knife robotic microradiosurgery for benign skull base meningiomas: tumor shrinkage may depend on the amount of radiation energy delivered per lesion volume (unit energy). Stereotact Funct Neurosurg 89:6–16
6. Igaki H, Maruyama K, Tago M, Shin M, Murakami N, Koga T, Nakagawa K, Kawahara N, Ohtomo K (2008) Cyst formation after stereotactic radiosurgery for intracranial meningioma. Stereotact Funct Neurosurg 86:231–236
7. Jo KW, Kim CH, Kong DS, Seol HJ, Nam DH, Park K, Kim JH, Lee JI (2011) Treatment modalities and outcomes for asymptomatic meningiomas. Acta Neurochir (Wien) 153:62–67
8. Karnofsky DA, Burchenal JH (1949) The clinical evaluation of chemotherapeutic agents in cancer. In: MacLeod CM (ed) Evaluation of chemotherapeutic agents. Columbia University Press, New York, pp 191–205
9. Kobayashi T, Kida Y, Mori Y (2001) Long-term results of stereotactic gamma radiosurgery of meningiomas. Surg Neurol 55:325–331
10. Kondziolka D, Mathieu D, Lunsford LD, Martin JJ, Madhok R, Niranjan A, Flickinger JC (2008) Radiosurgery as definitive management of intracranial meningiomas. Neurosurgery 62:53–60
11. Nakaya K, Chernov M, Kasuya H, Izawa M, Hayashi M, Kato K, Kubo O, Muragaki Y, Iseki H, Hori T, Okada Y, Takakura K (2009) Risk factors for regrowth of intracranial meningiomas after gamma knife radiosurgery: importance of the histopathological grade and MIB-1 index. Minim Invasive Neurosurg 52:216–221
12. Ojemann SG, Sneed PK, Larson DA, Gutin PH, Berger MS, Verhey L, Smith V, Petti P, Wara W, Park E, McDermott MW (2000) Radiosurgery for malignant meningioma: results in 22 patients. J Neurosurg 93(Suppl 3):62–67
13. Sheehan JP, Williams BJ, Yen CP (2010) Stereotactic radiosurgery for WHO grade I meningiomas. J Neurooncol 99:407–416
14. Unger KR, Lominska CE, Chanyasulkit J, Randolph-Jackson P, White RL, Aulisi E, Jacobson J, Jean W, Gagnon GJ (2012) Risk factors for post-treatment edema in patients treated with stereotactic radiosurgery for meningiomas. Neurosurgery 70:639–645

Treatment of Cavernoma: An Evidence-Based Dilemma?

Bodo Lippitz

Keywords Brain cavernoma • Gamma Knife • Management • Radiosurgery • Surgery

Intracranial cavernoma is a serious condition, and treatment should be necessary. But how necessary? The treatment comes with side effects. How can they be predicted? The treatment for cavernoma is rarely acute and hence primarily preventive. How effective is the treatment? The treatment decision for cavernoma is based on consideration of all these factors—on an educated computation of various risk levels influenced by subjective assessments and objective calculations. With all data generally available, how can final conclusions differ completely?

Currently, there are three options for addressing a cavernoma: operative resection, radiosurgery, no active treatment. The discussion has a long history and is still controversial [16]. The present two publications by Bertalanffy and Gerganov [1] and Liscak et al. [7] are interesting because they reflect the opposite ends of a highly polarized spectrum of potential decisions. In times of increasing medical conformity, how can we explain opposing recommendations to our patients? Is evidence-based medicine based on evidence in general or only on evidence we chose as appropriate?

The effect of radiosurgery on cavernoma is still hypothetical as only sporadic postirradiation histological specimens exist and magnetic resonance imaging (MRI) follow-up is generally inconclusive as to ascertaining the treatment effect. MRI generally shows local reactions and possibly shrinkage but hardly disappearance of the cavernoma. Hence, the effect of the treatment can be expressed only as a reduced hemorrhage rate for large groups of patients, which then requires reliable data of the natural course. On an individual level, the treatment effect is highly theoretical.

B. Lippitz
Gamma Knife Centre, Bupa Cromwell Hospital,
London SW50TU, UK
e-mail: bodo.lippitz@cromwellhospital.com

Here is one aspect of the dilemma: In an earlier analysis, Robinson et al. [13] identified 66 patients with 76 cavernomas, with a symptomatic hemorrhage rate of 0.7 % per lesion-year. Another study reported an annual hemorrhage rate of 6.8 % per patient [14]. Thus, published estimated hemorrhage rates vary widely [13, 14, 17]. This large variation is important since treating a cavernoma means weighing a potential risk of later hemorrhage against an immediate treatment risk. The outcomes of various treatment options can be measured, but we need to know the natural history of the condition to ensure that we have achieved a benefit. That seems difficult for cavernomas.

Included in the earlier reports of radiosurgery for cavernoma were those of Kondziolka et al., who published two studies wherein they defined the natural history of cavernoma based on a prospective registry between 1987 and 1993 [6]. In patients without a prior bleed, the prospective annual rate of hemorrhage rate was 0.6 %, and patients with prior hemorrhage had an annual bleed rate of 4.5 %. The same group, in Pittsburgh, demonstrated elegantly that the proportion of patients with hemorrhage after radiosurgery was significantly reduced, although an 8.8 % annual hemorrhage rate was still found during the first 2 years after radiosurgery. Only during the 2- to 6-year interval after radiosurgery was the annual bleeding rate decreased to 1.1 % [5]. A later, updated series of 82 patients from the same group had an annual hemorrhage rate of 12.3 % per year for the first 2 years after radiosurgery followed by 0.76 % per year from years 2 to 12 [3]. Other groups reported similar results, with the annual rebleeding rate after Gamma Knife treatment being 10.3 % for the first 2 years and 3.3 % thereafter [9]. Hence, with a rebleeding rate of 10–12 % within 2 years after radiosurgery the efficacy of the treatment is determined based on the natural history.

A recent study of 113 patients with cavernomas of the brain stem, thalamus, and basal ganglia calculated both the risks for bleeding and rebleeding. In the group of patients with multiple bleedings before radiosurgery the first-ever bleed rate was 2.9 % per lesion per year. Thereafter, the annual

M.F. Chernov et al. (eds.), *Gamma Knife Neurosurgery in the Management of Intracranial Disorders*,
Acta Neurochirurgica Supplement, Vol. 116, DOI 10.1007/978-3-7091-1376-9_15, © Springer-Verlag Wien 2013

rebleeding rate was 30.5 % per lesion per year [12]. A similar rebleeding risk of 33.9 % was found by others [3]. New bleeds were associated with an increasing risk of new, more severe disabilities [12]. Obviously, the cavernoma with previous bleeds must be considered as a different entity.

Side effects after radiosurgery comprise a second important issue. The risk for side effects has been considerable in previous studies. In 1995, Kondziolka et al. reported that 26 % of patients sustained neurological worsening that correlated with imaging changes after radiosurgery [5]. In 2000, Liscak et al. reported that transient morbidity caused by collateral edema or rebleeding occurred in 28 % of brain stem cavernomas [8], which has to be considered a high risk for treatment-induced side effects. Hence, the radiosurgical treatment regimen has been modified during the last decade. Avoidance of the methemoglobin ring [15], definition of the treatment volume according to T2-weighted MRI-defined margins, and reduced radiosurgical doses [4] have contributed considerably to reducing the side effects after Gamma Knife treatment. In 2010, the group in Pittsburgh reported in a summarizing review of 103 patients that new neurological deficits due to adverse radiation effects following radiosurgery developed in 13.5 %, with most cases occurring early in their experience [10]. Also, a recent study that had applied modern treatment standards for radiosurgery of cavernomas in the brain stem and basal ganglia described transient neurological effects in fewer than 8.0 % and mild permanent defects in fewer than 7.3 % [12]. These lower incidences are a consequence of the modified radiosurgical regimen.

The alternative treatment is microsurgical resection of the cavernoma. Resection, when possible, prevents further bleedings with immediate effect. Surgery is definitive treatment and must be considered curative. Gross et al. [2] reviewed 46 published surgical series where 92 % of 745 brain stem cavernomas were documented as completely resected. Because of the frequently deep location of cavernomas and the resulting problematic surgical access, perioperative morbidity and even mortality is an important issue. According to this extensive review, the early postoperative, often transient morbidity rate ranged from 29 to 67 % in large surgical series, and the combined postoperative rebleeding and surgery-related mortality rate was 1.9 % [2]. In cases of incomplete resection, 58 % of the partially resected lesions rebled. A microsurgical series from the Karolinska Hospital showed a 69 % risk of perioperative transitory neurological deterioration with significant permanent morbidity in 8 % [11]. Hence for a validation of surgery, the percentage of untreated and inoperable cases, the immediate morbidity and mortality rates, and the risk of incomplete resection with the possibility of later hemorrhage have to be quantified.

In a position paper, Bertalanffy and Gerganov [1] cited an experience with 147 brain stem cavernomas with a favorable risk/benefit ratio—unfortunately without mentioning specific data or results. The authors argued that complete resection of the cavernoma is indicated if the lesion is symptomatic or hemorrhagic. On the other hand, in a subgroup of patients with symptomatic or hemorrhagic cavernomas that are considered inoperable, Bertalanffy and Gerganov recommended no treatment at all because in the senior author's experience the vast majority remain free of hemorrhage and symptoms [1]. Data were not provided. There is an issue of logic in this reasoning: It remains unclear why the authors started with recommending a surgical resection if they assume, against prevailing evidence, that the bleeding risk is negligible even in cases with previous hemorrhage.

As already pointed out, it is important to differentiate between the annual bleeding risk in randomly discovered cavernomas, bleeding risk per patient, bleeding risk per lesion before and after treatment, and the rebleeding risks for cavernomas that have bled before. As a concrete example from a recent article [12], there was a first-ever bleed rate of 2.9 % per lesion per year (39 bleeds in 1,341 patient-years), but there were 57 rebleedings in 187 patient-years, with a resulting risk for rebleeding of 30.5 % until treatment. Within 2 years after radiosurgery, there was a reduced rebleed risk of 15 %, which fell to 2.4 % per patient-year thereafter. These typical differentiated hemorhage rates appear to be less clear in the position paper by Bertalanffy and Gerganov [1].

Many cavernomas are considered inoperable because of their critical location in basal ganglia and brain stem. Hence, surgically accessible cavernomas comprise a specific selection, whereas many conventionally inoperable cases can potentially be treated with radiosurgery. Hence, the efficacy of microsurgery and radiosurgery can be compared only based on a precise definition of exclusion criteria and specific risks for complications and rebleeding for both therapeutic options. The position paper by Bertalanffy and Gerganov does not provide these data [1].

Liscak et al. [7] reported the results of a large series of 112 cavernoma that were treated relatively early, between 1992 and 2000, using the Gamma Knife. The risk of edema on follow-up MRI after radiosurgery was 27.3 %. It was associated with temporary morbidity in 14.6 % of cavernomas and permanent morbidity of 0.9 %. Rebleeding occurred in 10 % after radiosurgery and was associated with permanent morbidity in 5.4 %, among whom were two patients (1.8 %) with brain stem cavernoma who died. It is noteworthy that the risk of edema increased significantly with radiation doses >13 Gy, and cavernoma rebleeding occurred more frequently in patients whose dose to the cavernoma margin was <14 Gy. These results are important because they define a narrow window of efficacy. It is also important that the bleeding risk for patients with previous hemorrhage during the first 2 years after radiosurgery increased from 3.7 to 5.3 % and was then reduced to 0.2 % after 2 years. Unfortunately, the authors did not mention statistical significance.

Liscak et al. [7] calculated the risk of bleeding before treatment as the number of hemorrhages divided by the years at risk from the patient's birth. In contrast, others calculate the number of years at risk from the time of the first hemorrhage. The resulting risks differ considerably, which does not make comparisons easier.

Coming back to the confused patient who was given opposing evidence-based recommendations by two trustworthy specialists. It would be helpful if we could provide a synthesis: There is overwhelming evidence that there is a difference in bleeding risks for incidental cavernomas and for lesions that have bled before. The general attitude is to recommend treatment for the latter. The cornerstone of cavernoma treatment is evidence to support a quantifiable bleeding risk. We are left with a persisting gap between evidence and credibility.

The available radiosurgical data are generally interpreted as evidence for a reduced risk for rebleeding after initial hemorrhages, whereas it appears difficult to find arguments for treatment-induced significant improvement for incidental cavernomas. Because of the immediate curative effect of surgery, there is a strong argument that cavernomas should be resected when the perioperative risk level is low. However, the mentioned modern radiosurgical series defined a risk level for treatment-related side effects that has to serve as a standard even for surgical approaches. In fact, the perioperative risk should be as low as that in comparable radiosurgical series when the early rebleeding rate, latency, adverse radiation effects, and potential morbidity are considered. There is strong evidence that radiosurgery is an effective option for cavernomas in cases where a higher perioperative risk level is anticipated. In effect, for most deep-seated cavernomas it is difficult to offer a microsurgical alternative at a comparable level of perioperative risk. This generally comprises the majority of brain stem cavernomas.

The quality of a physician lies in the accuracy of predicting individual risks that take the patient's and the method's prerequisites into consideration. While Gamma Knife treatment is rather standardized, the individual experience of an operating neurosurgeon can clearly modify the risk assessment. However, both "radiosurgeon" and neurosurgeon must allow benchmarking by objective comparisons of their individual predictions with individual outcomes. Rather than recommending solitary treatment options, the published data should serve as a general standard that has to be matched if we are to provide state-of-the-art therapy.

The dilemma of our evidence-based credo is that there is evidence for most opposing views. The result is a decision often based on availability, credibility, and belief. This is the opposite of evidence. Is it a coincidence that the objective scientific literature rarely provides data for the superiority of treatments that are not provided in the publishing center? Credibility cannot be reduced to the factual background of medical data. Credibility reflects the ability to integrate all available information and personal prerequisites.

Conflict of Interest The author declares that he has no conflict of interest.

References

1. Bertalanffy H, Gerganov VM (2013) Microsurgical or radiosurgical management of intracranial cavernomas. Acta Neurochir Suppl 116:103–106 (present volume)
2. Gross BA, Batjer HH, Awad IA, Bendok BR (2009) Brainstem cavernous malformations. Neurosurgery 64:E805–E818
3. Hasegawa T, McInerney J, Kondziolka D, Lee JY, Flickinger JC, Lunsford LD (2002) Long-term results after stereotactic radiosurgery for patients with cavernous malformations. Neurosurgery 50:1190–1198
4. Ivanov P, Chernov M, Hayashi M, Nakaya K, Izawa M, Murata N, Kubo O, Ujiie H, Muragaki Y, Nakamura R, Iseki H, Hori T, Takakura K (2008) Low-dose gamma knife radiosurgery for cavernous sinus hemangioma: report of 3 cases and literature review. Minim Invasive Neurosurg 51:140–146
5. Kondziolka D, Lunsford LD, Flickinger JC, Kestle JR (1995) Reduction of hemorrhage risk after stereotactic radiosurgery for cavernous malformations. J Neurosurg 83:825–831
6. Kondziolka D, Lunsford LD, Kestle JR (1995) The natural history of cerebral cavernous malformations. J Neurosurg 83:820–824
7. Liscak R, Urgosik D, Simonova G, Vymazal J, Semnicka J (2013) Gamma knife radiosurgery of brain cavernomas. Acta Neurochir Suppl 116:107–111 (present volume)
8. Liscak R, Vladyka V, Simonova G, Vymazal J, Novotny J Jr (2000) Gamma knife radiosurgery of the brain stem cavernomas. Minim Invasive Neurosurg 43:201–207
9. Liu KD, Chung WY, Wu HM, Shiau CY, Wang LW, Guo WY, Pan DH (2005) Gamma knife surgery for cavernous hemangiomas: an analysis of 125 patients. J Neurosurg 102(Suppl):81–86
10. Lunsford LD, Khan AA, Niranjan A, Kano H, Flickinger JC, Kondziolka D (2010) Stereotactic radiosurgery for symptomatic solitary cerebral cavernous malformations considered high risk for resection. J Neurosurg 113:23–29
11. Mathiesen T, Edner G, Kihlstrom L (2003) Deep and brainstem cavernomas: a consecutive 8-year series. J Neurosurg 99:31–37
12. Nagy G, Razak A, Rowe JG, Hodgson TJ, Coley SC, Radatz MW, Patel UJ, Kemeny AA (2010) Stereotactic radiosurgery for deep-seated cavernous malformations: a move toward more active, early intervention. Clinical article. J Neurosurg 113:691–699
13. Robinson JR, Awad IA, Little JR (1991) Natural history of the cavernous angioma. J Neurosurg 75:709–714
14. Sandalcioglu IE, Wiedemayer H, Secer S, Asgari S, Stolke D (2002) Surgical removal of brain stem cavernous malformations: surgical indications, technical considerations, and results. J Neurol Neurosurg Psychiatry 72:351–355
15. St George EJ, Perks J, Plowman PN (2002) Stereotactic radiosurgery XIV: the role of the haemosiderin 'ring' in the development of adverse reactions following radiosurgery for intracranial cavernous malformations: a sustainable hypothesis. Br J Neurosurg 16:385–391
16. Steiner L, Karlsson B, Yen CP, Torner JC, Lindquist C, Schlesinger D (2010) Radiosurgery in cavernous malformations: anatomy of a controversy. J Neurosurg 113:16–22
17. Washington CW, McCoy KE, Zipfel GJ (2010) Update on the natural history of cavernous malformations and factors predicting aggressive clinical presentation. Neurosurg Focus 29(3):E7

Microsurgical or Radiosurgical Management of Intracranial Cavernomas

Helmut Bertalanffy and Venelin M. Gerganov

Abstract Cranial cavernous malformations (CCMs) constitute a heterogeneous group of lesions that tend to change dynamically over time with related periods of repeated exacerbation and alternating periods of remission. The decision on their management is based on estimating the inherent risk of further morbidity and the risk/benefit related to the particular treatment mode. Incidentally detected CCMs or lesions in asymptomatic patients presenting without major hemorrhage are best followed up. Complete resection of a CCM is the only healing option and is indicated for symptomatic or hemorrhagic lesions. In the large published series 83–92 % of the patients improved or remained unchanged after surgery, with only 8–11 % showing significant deterioration. For most patients, quality of life is improved. Analysis of the risk/benefit ratio for radiosurgery shows that it should not be regarded as an alternative option: It confers limited protection against bleeding and is related to a certain morbidity risk. In the subgroup of patients with symptomatic or hemorrhagic CCMs in locations that preclude surgical resection with acceptable risks, we recommend follow-up. The senior author is following a group of more than 80 such patients, and the vast majority remain free of hemorrhage and symptoms.

Keywords Brain stem • Cerebral cavernous malformation • Radiosurgery • Surgery

Introduction

Cerebral cavernous malformations (CCMs) consist of a cluster of thin-walled capillary-like channels, or "caverns," without intervening brain parenchyma. These channels are lined with a single layer of leaky endothelium that has impaired tight junctions and barrier function [6, 24]. As a consequence, red blood cells may leak into the surrounding parenchyma and cause a hemosiderin-laden rim circumferentially around the lesion, which is detectable on T2-weighted and T2-weighted echo-gradient magnetic resonance imaging (MRI) [23].

The CCMs occur sporadically or as a familial form. The familial form of the disease is inherited in an autosomal dominant pattern with incomplete penetrance and variable expression pattern. Up to 30 % of all cases are familial [30, 48]. The familial CCMs have different biological behaviors. They are more likely to bleed, grow, and form new lesions than sporadic CCMs. Three genes have been identified in association with familial CCM: *CCM1*, *CCM2*, *CCM3* [41]. All three protein products are expressed in vascular endothelium and play a crucial role in the organization of the cytoskeletal and interendothelial junction proteins [24, 35, 47]. The loss of function ultimately impairs endothelial cell–cell junctions and vasculogenesis [47, 48].

Cavernous malformations account for 8–15 % of all cerebral vascular lesions [6, 44]. Their incidence, based on MRI and autopsy studies, is approximately 0.5 %. The clinical prevalence, however, is much lower. Only approximately 25 % of the affected individuals become symptomatic [23, 44].

These CCMs constitute a heterogeneous group in regard to their biological characteristics, natural evolution, and clinical behavior. They are dynamic lesions that tend to change over time, with periods of repeated exacerbation of complaints and alternating periods of remission. Patients with CCMs may present with seizures, hemorrhage, focal neurological deficits, and/or nonspecific headaches [1, 32, 44]. The management of each patient with CCM is based on an estimation of the inherent risk of further morbidity and the risk/benefit related to the particular treatment mode. As a general principle, the treatment for CCMs should be individualized and tailored to the clinical presentation and history of the patient and the location, characteristics, and hemorrhagic activity of the lesion.

H. Bertalanffy and V.M. Gerganov (✉)
Department of Neurosurgery, International Neuroscience Institute, Rudolf Pichlmayrstr. 4, 30625 Hannover, Germany
e-mail: gerganov@ini-hannover.de

M.F. Chernov et al. (eds.), *Gamma Knife Neurosurgery in the Management of Intracranial Disorders*,
Acta Neurochirurgica Supplement, Vol. 116, DOI 10.1007/978-3-7091-1376-9_16, © Springer-Verlag Wien 2013

Conservative Management

Incidentally detected CCMs or lesions in asymptomatic patients who present without major hemorrhage are best followed with regular MRI and clinical examinations. This strategy is recommendable even in patients with mild symptoms, especially if the malformation is located deeply within functionally important areas of the brain [6].

Surgery

Complete resection of CCMs is the only healing option and is indicated in surgically accessible symptomatic or hemorrhagic supratentorial and infratentorial lesions. Its safety and efficacy in terms of preventing rebleeding has been well established in CCMs [6, 13, 14, 34, 40, 44]. Therefore, even young patients with such cavernomas not located in deep or eloquent areas and less severe symptoms are considered as surgical candidates in view of the cumulative risk of hemorrhage or neurological disability over time [6].

Other candidates for surgery are patients with cavernoma-related epilepsy that cannot be well controlled with medications. According to a recent multicenter study of 168 consecutive patients with a single supratentorial CCM and symptomatic epilepsy [5], 70 % of the patients were seizure-free during the first 3 postoperative years, and only rare seizures or a worthwhile improvement (Engel grades II–III) occurred in 25 % of patients. No mortality was observed, and only 7 % of the patients had mild postoperative neurological deficits. Similar surgical outcomes have been presented by other authors [3, 8, 12]. Although some reports suggest a beneficial effect of Gamma Knife radiosurgery on epilepsy [39], its efficacy is less than that following lesionectomy [42].

CCMs in Eloquent Brain Areas

Controversy exists about the best management of CCMs located in critical areas: highly eloquent cortical and subcortical structures, thalamus, basal ganglia, brain stem. Surgery is indicated if they cause progressive neurological deficits, evidence of hemorrhage, or uncontrolled seizures. Our experience with 147 brain stem CCMs, in agreement with others, has proven that even such CCMs can be treated microsurgically with a favorable risk/benefit ratio. The operative strategy must be tailored to the individual characteristics of each CCM, considering its location and relation to essential cortical/subcortical structures and fiber tracts, and the relation between the cavernoma and the pial or ependymal surface [6]. The optimal approach must provide straight-line access to the lesion with the least impact on the surrounding brain and allow manipulations around the lesion. To remove the CCM completely and avoid recurrence, a clear dissection plane to the surrounding parenchyma should be established. Modern technological advancements enhance the safety and efficacy of surgery. Intraoperative guidance with anatomical and functional navigation, including integrated fMRI and fiber tracking data, is essential for selecting the optimal approach, trajectory, and parenchymal entry zone. Electrophysiological monitoring and stimulation, especially for brain stem CCMs, are obligatory. Notably, the great individual anatomical variability (e.g., of the facial nerve response area) should be considered [7]. Following these principles allows successful management of the vast majority of patients and improvement of their quality of life, as assessed by the Patzold Rating and Karnofsky Performance Status Scale [10]. In large published series, the majority of patients (83–92 %) improved or remained unchanged after surgery, with only 8–11 % showing significant deterioration [6, 11, 13, 14, 29, 34, 40, 43].

Gamma Knife Radiosurgery

Gamma Knife radiosurgery has been promoted as an alternative treatment for selected CCMs [17, 21, 28, 31] or for all lesions, regardless of their location and surgical accessibility [20, 25, 27]. Based on our experience and on a profound study of the literature, we believe that the value of radiosurgery has not been proven. Analysis of its risk/benefit ratio shows that radiosurgery should not be regarded as an alternative to surgery [18, 37, 45]. The issue to discuss is whether radiosurgery offers some benefits when compared to the natural evolution of the disease in patients who are poor surgical candidates—and if so, at what price.

Radiosurgery causes partial obliteration or decreases the size of some cavernomas [18, 26, 45]. To what extent this effect decreases the risk of future hemorrhage is controversial. Clatterbuck et al. [9] performed a volumetric MRI study in 68 untreated patients and found that CCMs exhibit a range of dynamic behavior: 10–22 % of the lesions remained stable, 35–43 % increased in volume, and 35–55 % decreased. Furthermore, there is no evidence of direct correlation between the size of a cavernoma and the risk of hemorrhage. The postradiosurgical rates of hemorrhage are therefore the only method by which to assess treatment success.

The CCMs are not static lesions with a constant annual bleeding risk. Thus, the presumed protective effect of irradiation may reflect their biological development [15, 32]. Studies on the natural evolution of cavernomas have shown that there is a temporarily increased risk of hemorrhage, lasting approximately 2 years following the earlier bleeding

episode [4]. This temporary natural hemorrhage clustering is not always accounted for by authors describing the beneficial effect of radiosurgery.

A sound scientific evaluation of the outcome of radiosurgery and comparison with the natural evolution of the cavernoma is difficult because of some methodological flaws inherent in the studies, such as selection bias, variable definition of hemorrhage, variable methods to calculate the annual risk of new bleeding, and the heterogeneity of the patient population. The estimated annual incidence of hemorrhage of untreated CCMs in large studies ranges from 0.25 % to 5.0 % per patient and from 0.7 % to 2.5 % per lesion [6, 15, 22, 32, 38]. In the radiosurgical literature, however, the benefit of the procedure is assessed by comparing posttreatment versus pretreatment bleeding rates. Thus, the pretreatment risk of hemorrhage in these series is assumed to be as high as 17–36 % [2, 16, 19, 27, 28, 33, 46]. A subgroup of CCMs does have a higher bleeding tendency that is inferred from the clinical history and radiological features. Although radiosurgical series are not restricted to such patients, the high incidence of hemorrhage prior to treatment is the only indicator of their assumed more-aggressive behavior, a form of "circular reasoning," as Steiner pointed out [45]. The annual rebleeding rate after radiosurgery is 8–10 % for the first 2 years and 0.8–4.5 % thereafter [16, 27, 28, 33, 37, 42]—rates that well correspond to the bleeding incidence in studies on the natural evolution of CCMs. Altogether, 9–45 % of patients with brain stem CCMs rebleed after radiosurgery, with the total permanent morbidity rates from radiation injury and rebleeding ranging from 7 % to 40 % [13]. On the other hand, radiosurgery is associated with 13–59 % transient and 4–10 % permanent complication rates [18, 26, 28, 31, 36, 46]. The radiation-induced complication rate for CCMs has been evaluated to be five to seven times higher than that expected for arteriovenous malformations of the same size and location [18, 37].

Although the imaging characteristics of CCMs on MRI are nearly pathognomonic, in some cases they cannot be clearly differentiated from other lesions, such as hemorrhagic neoplasms or metastases, gliomas, or inflammatory lesions, which precludes primary radiosurgery [6].

There is a subgroup of patients who present with symptomatic or hemorrhagic CCM in a location that precludes surgical resection with acceptable risks. The fundamental question is how to define these patients. The outcome is obviously related to the experience of the surgeon and the proper utilization of technological advancements. It differs from person to person. We believe that if surgery is deemed too risky the best option is to follow the patient conservatively. The senior author is following a group of more than 80 nonsurgical patients who harbor deep-seated CCMs with regular MRI checks. The vast majority of these patients have remained free of hemorrhage and symptoms over a long period of time—some individuals up to more than two decades. None of these patients underwent stereotactic radiosurgery. The absence of any intervention does not affect the natural evolution of the disease but does avoid the morbidity associated with radiosurgery.

Conflict of Interest The authors declare that they have no conflict of interest.

References

1. Aiba T, Tanaka R, Koike T, Kameyama S, Takeda N, Komata T (1995) Natural history of intracranial cavernous malformations. J Neurosurg 83:56–59
2. Amin-Hanjani S, Ogilvy CS, Candia GJ, Lyons S, Chapman PH (1998) Stereotactic radiosurgery for cavernous malformations: Kjellberg's experience with proton beam therapy in 98 cases at the Harvard Cyclotron. Neurosurgery 42:1229–1238
3. Awad I, Jabbour P (2006) Cerebral cavernous malformations and epilepsy. Neurosurg Focus 21(1):E7
4. Barker FG 2nd, Amin-Hanjani S, Butler WE, Lyons S, Ojemann RG, Chapman PH, Ogilvy CS (2001) Temporal clustering of hemorrhages from untreated cavernous malformations of the central nervous system. Neurosurgery 49:15–25
5. Baumann CR, Acciarri N, Bertalanffy H, Devinsky O, Elger CE, Lo Russo G, Cossu M, Sure U, Singh A, Stefan H, Hammen T, Georgiadis D, Baumgartner RW, Andermann F, Siegel AM (2007) Seizure outcome after resection of supratentorial cavernous malformations: a study of 168 patients. Epilepsia 48:559–563
6. Bertalanffy H, Benes L, Miyazawa T, Alberti O, Siegel AM, Sure U (2002) Cerebral cavernomas in the adult. Review of the literature and analysis of 72 surgically treated patients. Neurosurg Rev 25:1–55
7. Bertalanffy H, Tissira N, Krayenbuhl N, Bozinov O, Sarnthein J (2011) Inter- and intrapatient variability of facial nerve response areas in the floor of the fourth ventricle. Neurosurgery 68(1 Suppl Operative):23–31
8. Cappabianca P, Alfieri A, Maiuri F, Mariniello G, Cirillo S, de Divitiis E (1997) Supratentorial cavernous malformations and epilepsy: seizure outcome after lesionectomy on a series of 35 patients. Clin Neurol Neurosurg 99:179–183
9. Clatterbuck RE, Moriarity JL, Elmaci I, Lee RR, Breiter SN, Rigamonti D (2000) Dynamic nature of cavernous malformations: a prospective magnetic resonance imaging study with volumetric analysis. J Neurosurg 93:981–986
10. Dukatz T, Sarnthein J, Sitter H, Bozinov O, Benes L, Sure U, Bertalanffy H (2011) Quality of life after brainstem cavernoma surgery in 71 patients. Neurosurgery 69:689–695
11. Ferroli P, Sinisi M, Franzini A, Giombini S, Solero CL, Broggi G (2005) Brainstem cavernomas: long-term results of microsurgical resection in 52 patients. Neurosurgery 56:1203–1214
12. Folkersma H, Mooij JJ (2001) Follow-up of 13 patients with surgical treatment of cerebral cavernous malformations: effect on epilepsy and patient disability. Clin Neurol Neurosurg 103:67–71
13. Gross BA, Batjer HH, Awad IA, Bendok BR (2009) Brainstem cavernous malformations. Neurosurgery 64:E805–E818
14. Gross BA, Batjer HH, Awad IA, Bendok BR (2009) Cavernous malformations of the basal ganglia and thalamus. Neurosurgery 65:7–19
15. Gross BA, Lin N, Du R, Day AL (2011) The natural history of intracranial cavernous malformations. Neurosurg Focus 30(6):E24

16. Hasegawa T, McInerney J, Kondziolka D, Lee JY, Flickinger JC, Lunsford LD (2002) Long-term results after stereotactic radiosurgery for patients with cavernous malformations. Neurosurgery 50:1190–1198
17. Huang YC, Tseng CK, Chang CN, Wei KC, Liao CC, Hsu PW (2006) LINAC radiosurgery for intracranial cavernous malformation: 10-year experience. Clin Neurol Neurosurg 108:750–756
18. Karlsson B, Kihlstrom L, Lindquist C, Ericson K, Steiner L (1998) Radiosurgery for cavernous malformations. J Neurosurg 88: 293–297
19. Kida Y (2009) Radiosurgery for cavernous malformations in basal ganglia, thalamus and brainstem. Prog Neurol Surg 22:31–37
20. Kim DG, Choe WJ, Paek SH, Chung HT, Kim IH, Han DH (2002) Radiosurgery of intracranial cavernous malformations. Acta Neurochir (Wien) 144:869–878
21. Kondziolka D, Flickinger JC, Lunsford LD (2007) Radiosurgery for cavernous malformations. Prog Neurol Surg 20:220–230
22. Kondziolka D, Lunsford LD, Kestle JR (1995) The natural history of cerebral cavernous malformations. J Neurosurg 83: 820–824
23. Krisht KM, Whitehead KJ, Niazi T, Couldwell WT (2010) The pathogenetic features of cerebral cavernous malformations: a comprehensive review with therapeutic implications. Neurosurg Focus 29(3):E2
24. Leblanc GG, Golanov E, Awad IA, Young WL (2009) Biology of vascular malformations of the brain. Stroke 40:E694–E702
25. Liscak R, Vladyka V, Simonova G, Vymazal J, Novotny J Jr (2000) Gamma knife radiosurgery of the brain stem cavernomas. Minim Invasive Neurosurg 43:201–207
26. Liscak R, Vladyka V, Simonova G, Vymazal J, Novotny J Jr (2005) Gamma knife surgery of brain cavernous hemangiomas. J Neurosurg 102(Suppl):207–213
27. Liu KD, Chung WY, Wu HM, Shiau CY, Wang LW, Guo WY, Pan DH (2005) Gamma knife surgery for cavernous hemangiomas: an analysis of 125 patients. J Neurosurg 102(Suppl):81–86
28. Lunsford LD, Khan AA, Niranjan A, Kano H, Flickinger JC, Kondziolka D (2010) Stereotactic radiosurgery for symptomatic solitary cerebral cavernous malformations considered high risk for resection. J Neurosurg 113:23–29
29. Mathiesen T, Edner G, Kihlstrom L (2003) Deep and brainstem cavernomas: a consecutive 8-year series. J Neurosurg 99:31–37
30. Mindea SA, Yang BP, Shenkar R, Bendok B, Batjer HH, Awad IA (2006) Cerebral cavernous malformations: clinical insights from genetic studies. Neurosurg Focus 21(1):E1
31. Monaco EA, Khan AA, Niranjan A, Kano H, Grandhi R, Kondziolka D, Flickinger JC, Lunsford LD (2010) Stereotactic radiosurgery for the treatment of symptomatic brainstem cavernous malformations. Neurosurg Focus 29(3):E11
32. Moriarity JL, Clatterbuck RE, Rigamonti D (1999) The natural history of cavernous malformations. Neurosurg Clin N Am 10:411–417
33. Nagy G, Razak A, Rowe JG, Hodgson TJ, Coley SC, Radatz MW, Patel UJ, Kemeny AA (2010) Stereotactic radiosurgery for deep-seated cavernous malformations: a move toward more active, early intervention. Clinical article. J Neurosurg 113:691–699
34. Ohue S, Fukushima T, Kumon Y, Ohnishi T, Friedman AH (2010) Surgical management of brainstem cavernomas: selection of approaches and microsurgical techniques. Neurosurg Rev 33:315–324
35. Petit N, Blecon A, Denier C, Tournier-Lasserve E (2006) Patterns of expression of the three cerebral cavernous malformation (CCM) genes during embryonic and postnatal brain development. Gene Expr Patterns 6:495–503
36. Pollock BE (2008) Radiosurgery for cavernous malformations: theory and practice. Clin Neurosurg 55:97–100
37. Pollock BE, Garces YI, Stafford SL, Foote RL, Schomberg PJ, Link MJ (2000) Stereotactic radiosurgery for cavernous malformations. J Neurosurg 93:987–991
38. Porter PJ, Willinsky RA, Harper W, Wallace MC (1997) Cerebral cavernous malformations: natural history and prognosis after clinical deterioration with or without hemorrhage. J Neurosurg 87: 190–197
39. Regis J, Bartolomei F, Kida Y, Kobayashi T, Vladyka V, Liscak R, Forster D, Kemeny A, Schrottner O, Pendl G (2000) Radiosurgery for epilepsy associated with cavernous malformation: retrospective study in 49 patients. Neurosurgery 47:1091–1097
40. Samii M, Eghbal R, Carvalho GA, Matthies C (2001) Surgical management of brainstem cavernomas. J Neurosurg 95:825–832
41. Shenkar R, Shi C, Check IJ, Lipton HL, Awad IA (2007) Concepts and hypotheses: inflammatory hypothesis in the pathogenesis of cerebral cavernous malformations. Neurosurgery 61:693–703
42. Shih YH, Pan DH (2005) Management of supratentorial cavernous malformations: craniotomy versus gammaknife radiosurgery. Clin Neurol Neurosurg 107:108–112
43. Sindou M, Yada J, Salord F (2000) Functional results after microsurgical resection of brain stem cavernous malformations (retrospective study of a 12 patient series and review of the recent literature). Acta Neurochir (Wien) 142:843–853
44. Smith ER, Scott RM (2010) Cavernous malformations. Neurosurg Clin N Am 21:483–490
45. Steiner L, Karlsson B, Yen CP, Torner JC, Lindquist C, Schlesinger D (2010) Radiosurgery in cavernous malformations: anatomy of a controversy. J Neurosurg 113:16–22
46. Steiner LS, Lindquist C, Stroila M, Prasad D, Steiner M (2005) Gamma knife surgery for cerebral vascular malformations, tumors and functional disorders. In: Schmidek HH, Roberts DW (eds) Schmidek and Sweet's operative neurosurgical techniques: indications, methods, and results, vol 1, 5th edn. WB Saunders, Philadelphia, pp 530–576
47. Sure U, Freman S, Bozinov O, Benes L, Siegel AM, Bertalanffy H (2005) Biological activity of adult cavernous malformations: a study of 56 patients. J Neurosurg 102:342–347
48. Yadla S, Jabbour PM, Shenkar R, Shi C, Campbell PG, Awad IA (2010) Cerebral cavernous malformations as a disease of vascular permeability: from bench to bedside with caution. Neurosurg Focus 29(3):E4

Gamma Knife Radiosurgery of Brain Cavernomas

Roman Liscak, Dusan Urgosik, Gabriela Simonova, Josef Vymazal, and Jitka Semnicka

Abstract *Purpose*: Radiosurgery of cavernomas should prevent rebleeding, growth of the lesion, and deterioration of clinical symptoms. However, there is no direct diagnostic tool to verify the endpoints of treatment. At present, the positive effects of radiosurgery are identified by clinical observation and analysis of imaging changes on magnetic resonance imaging during a sufficiently long follow-up period.

Methods: Between 1992 and 2000, a total of 112 patients with brain cavernomas were treated with Gamma Knife radiosurgery at our center. In all, 59 patients experienced bleeding before radiosurgery; the remainder did not. The median age of patients was 42 years, the median volume of the cavernomas was 0.9 cm^3, and the median applied marginal dose was 16 Gy.

Results: After a 2-year latent interval after treatment (median follow-up 84 months), the risk of bleeding in the group of patients with bleeding before radiosurgery had decreased from 3.7 % to 0.2 %. For the patients without bleeding before radiosurgery, the annual risk of bleeding was 0.8 %. The cavernoma size decreased in 53.0 % of cases and increased in 6.4 %. Epilepsy, if present before the treatment, was alleviated in 45 % of cases. The risks of temporary or permanent morbidity caused by radiosurgery were 14.6 % and 0.9 %, respectively.

Conclusion: Radiosurgery of cavernomas was associated with a low risk of permanent morbidity. The risk of rebleeding after the 2-year latent interval after radiosurgery had decreased. Treatment of cavernomas with no history of bleeding was halted at our center.

Keywords Bleeding • Cavernoma • Gamma Knife radiosurgery • Results

R. Liscak (✉), D. Urgosik, G. Simonova, J. Vymazal, and J. Semnicka
Hospital Na Homolce, Roentgenova 2, Prague 150 30, Czech Republic
e-mail: roman.liscak@homolka.cz

Introduction

The goal of Gamma Knife radiosurgery (GKS) of brain cavernomas is mainly to prevent the risk of rebleeding after the treatment. An arteriovenous malformation (AVM) visible on angiography is treated through proliferative and degenerative changes of tiny vessels inside the capillary nidus, leading to their obliteration [16]. Feeding arteries with larger diameters and sometimes even monstrous draining varicose veins are passively obliterated thereafter by formation of thrombus when blood flow is halted through the nidus. The cure can be verified by angiography, showing that the AVM has disappeared after its obliteration. Both these aspects are missed by treating cavernomas with radiosurgery. Cavernomas are often formed by larger lacunas with no capillary nidus, and there is no diagnostic tool to verify the successful endpoint of the treatment because cavernomas are angiographically occult. However, it is possible to hypothesize that focused irradiation hits the angiographically occult feeders around the cavernoma, depriving the lesion from its sustenance. Indeed, the regression and decrease of a cavernoma is frequently observed after radiosurgery, although the pathophysiological process behind these changes is not fully understood. These features make the cavernoma a controversial candidate for radiosurgery, because the difference in the clinical course after the treatment compared to the natural course of the disease can be evaluated only after a long follow-up.

Material and Methods

Between 1992 and 2000, a total of 112 patients with brain cavernoma were treated by the Leksell Gamma Knife in Prague, as published earlier [6]. The outcomes for this group of patients are upgraded herein after a significantly longer follow-up. The age of the patients ranged from 13 to 81 years (median 42 years). All locations were represented: brain

M.F. Chernov et al. (eds.), *Gamma Knife Neurosurgery in the Management of Intracranial Disorders*,
Acta Neurochirurgica Supplement, Vol. 116, DOI 10.1007/978-3-7091-1376-9_17, © Springer-Verlag Wien 2013

Table 1 Annual risk of bleeding in patients with brain cavernomas

Patient conditions	Before GKS (%)	≤2 years after GKS (%)	>2 years after GKS (%)
Whole group (*N*=112)	2.0	3.2	0.5
With bleeding before GKS (*N*=59)	3.7	5.3	0.2
Without bleeding before GKS (*N*=53)	0	1.0	0.8

GKS Gamma Knife radiosurgery, *N* number of patients

stem 33 patients, temporal 24, frontal 13, parietal 10, thalamus 9, basal ganglia 8, occipital 7.

The cavernoma was solitary in 99 patients and multifocal in 13 patients. In cases of multiple cavernomas, the lesion causing symptomatic bleeding was treated. Seven patients had undergone previous partial microsurgical resection of the cavernoma, whereas GKS was the primary treatment in 94 % of cases. The cavernomas evoked epilepsy in 44 patients. Neurological deficit (according to the anatomical localization) persisted before radiosurgery in 51 patients, and 30 patients complained of headaches.

There were 89 events reported as bleeding before radiosurgery in the case histories of 59 patients. In 23 of these patients the episodes were noted repeatedly (maximum of four bleedings per patient). The risk of bleeding before radiosurgery was calculated from the number of hemorrhages divided by the years at risk starting at the birth of the patient (Table 1). The volume of the cavernomas ranged from 0.06 to12.5 cm^3 (median 0.9 cm^3). The maximum dose ranged from 16 to 50 Gy (median 30 Gy). The marginal dose ranged from 9 to 36 Gy (median 16 Gy); it was applied to a median isodose of 50 %.

Results

Clinical follow-up was available for all patients, and radiological follow-up for 110 of them. Both ranged from 5 to 184 months (median 84 months). Rebleeding was observed in 11 patients at 5–168 months after radiosurgery (median 24 months). The annual risk of rebleeding was calculated from the number of events divided by the number of follow-up years (Table 1). Rebleeding was associated with morbidity (impaired neurological deficit) in seven patients (6.5 %). It was temporary in one patient and persistent in six. Two patients with brain stem cavernoma died.

Radiological follow-up (median duration 84 months) after GKS with at least one magnetic resonance imaging (MRI) session was performed in 110 patients. The size of the cavernoma decreased at 8–131 months after radiosurgery (median 26 months) in 58 patients (53 %) and increased at 8–168 after radiosurgery (median 86 months) in 7 patients (6.4 %). Collateral edema was detected in 30 patients (27.3 %) at 3–49 months after radiosurgery (median

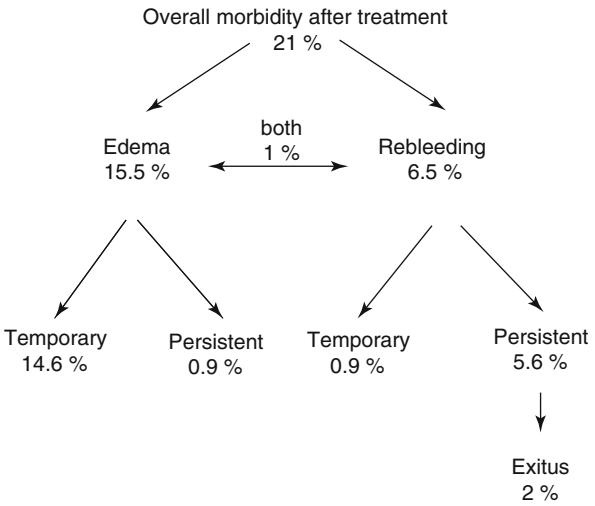

Fig. 1 Morbidity after Gamma Knife radiosurgery of brain cavernomas

11 months). In 17 of them (15.5 %), brain edema was symptomatic. Therapy with corticosteroids was administered to 16 of these patients for a period of 1–12 months (median 2.5 months). The edema resolved in 23 patients within 8–40 months after radiosurgery (median 18 months). Symptoms resolved in 16 patients within 8–37 months after radiosurgery (median 12 months), although one patient (0.9 %) experienced persistent morbidity caused by edema. Morbidity from the radiosurgery itself (symptomatic edema) and unaffected natural course of the disease (rebleeding) is shown in Fig. 1. Of note: One patient had symptomatic edema associated with rebleeding.

Twenty out of 44 patients (45%) with epileptic seizures before treatment demonstrated improvement within 1–30 months (median 6 months) after GKS. Two patients were affected by impairment due to seizures caused by collateral edema at 6 and 8 months, respectively, after radiosurgery. The problems had resolved by 12 months after treatment. Persistent morbidity from epilepsy impairment was not observed.

Six patients died during the follow-up. Two patients with brain stem cavernomas died at 6 and 51 months, respectively, after radiosurgery. Rebleeding probably caused both deaths, but no computed tomography, or autopsy results were available to prove it. The other two patients died from trauma and suicide. One patient died 14 years after radiosurgery for a gradually increasing brain stem cavernoma, but there was no

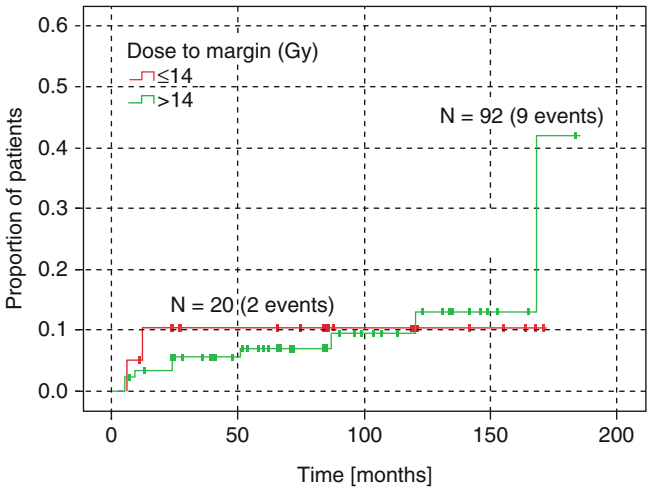

Fig. 2 Kaplan-Meier curve reflects the rebleeding risk after radiosurgery of brain cavernomas in the groups of patients with radiation doses to the margins of ≤14 Gy or >14 Gy. Censored observations are marked. *N* number of patients

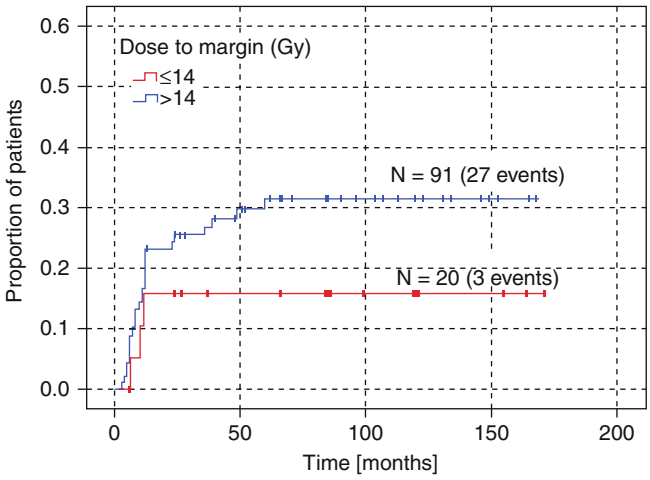

Fig. 3 Kaplan-Meier curve reflects the risk of edema occurrence after radiosurgery of brain cavernomas in the groups of patients with radiation doses to the margins of ≤14 Gy or >14 Gy. Censored observations are marked. *N* number of patients

ictal event classified as rebleeding. Another 61-year-old patient with temporal cavernoma died 5 years after radiosurgery for unknown reason.

A total of 11 patients underwent repeated treatment for their cavernoma. Nine of these patients had open microsurgery: one patient for collateral edema, two for rebleeding, three for cavernoma volume increase, and three for epilepsy (which was not cured by radiosurgery). Four patients with epilepsy and cavernoma located in the region of amygdalohippocampal complex underwent repeated radiosurgery. However, instead of selective irradiation of the cavernoma, the whole amygdalohippocampal complex was the target for retreatment. This treatment was effective in two patients, whereas two others underwent microsurgical resection at a later time.

Among the whole group of patients, new cavernomas were detected during the follow-up in two. In one patient multiple new small cavernomas were detected 14 years after radiosurgery, and in the other patient a new small cavernoma was detected 10 years after treatment. Both of these patients were treated conservatively. One patient with a medial temporal cavernoma with secondary epilepsy–which improvement was accompanied by regression of the lesion 8 years after radiosurgery–had a new bizarre diffuse bilateral dural AVM detected 10 years after GKS with several hemorrhages at different sites in the brain. Additionally, multiple organ angiomatosis (liver, kidney, lung, spleen) and carcinoma uteri were diagnosed. This patient underwent five endovascular embolizations of her new dural malformation, and 14 years after the initial radiosurgery she was in poor condition.

Univariate analysis was performed using Kaplan-Meier statistics with the log-rank test. Multivariate statistical analysis was performed with the Cox proportional hazards model. Statistical analysis showed that cavernoma rebleeding after GKS can be expected more frequently in middle-aged patients (30–45 years), in patients with a history of hemorrhage, and in patients in whom the dose to the cavernoma margin was <14 Gy (Fig. 2). Edema after Gamma Knife treatment occurred more frequently in patients who had undergone prior surgery, those with a large cavernoma volume, and those in whom the dose to the cavernoma margin was >13 Gy (Fig. 3). Therefore, we consider that marginal dose of 14 Gy is a reasonable compromise for radiosurgery of cavernomas and use it in our current practice.

Discussion

Controversies regarding radiosurgery of cavernomas arise from several aspects. First, knowledge of the natural course of the disease is not complete, and the definition of bleeding is ambiguous. Overt bleeding from a cavernoma (a blood clot inside or outside the hemosiderin ring of the lesion or evidence of hemorrhage after a lumbar puncture) is rarely diagnosed. Usually, any sudden onset of new symptoms or exacerbation of old symptoms is considered a hemorrhage despite the lack of any neuroimaging signs of overt bleeding. Second, growth of the cavernoma observed in some cases could simply be bleeding with no symptoms in functionally silent areas. Third, no diagnostic tool so far can indicate cure in patients, which has a significant impact on treatment results. Although GKS was repeated in 23 % of AVMs because their complete obliteration was not achieved within 3 years after the first treatment [7], such subgroup of

"functioning" lesions cannot be distinguished in patients with cavernomas. It seems logical to consider repeated radiosurgery of a cavernoma when the initial treatment failed. Unfortunately, treatment failure of cavernoma radiosurgery is diagnosed only after rebleeding occurs, which downgrades the results.

We have calculated the risk of bleeding before treatment as the number of hemorrhages divided by the years at risk beginning at the birth of the patient. Other authors prefer to calculate the number of years at risk from the time of the first hemorrhage [4, 9, 15], and the annual risk is consequently higher in such cases. The reasons given the latter calculation are mainly the absence or low incidence of hemorrhage from cavernomas in children and the de novo appearance of cavernomas in familial cases [4, 15]. We considered patients with cavernoma to be at risk of bleeding from their birth because the clinical manifestation of cavernomas does not differ from that of AVMs, which in both of our series (cavernoma and AVM) usually appeared at 30–45 years of age, although children are included in both series [6, 7]. The youngest patient with cavernoma treated at our center, in 2008, was a 4.5 year-old boy with the lesion in the right thalamus and first bleeding at the age of 31 months. De novo appearance of cavernoma is possible but rare. It was seen in our series in just two patients (<2 %) during the follow-up.

A tendency for decreased risk of rebleeding after the latent period of 2 years after radiosurgery was reported in several articles. Lunsford at al. [9] reported an annual risk of rebleeding of 1.06 % (mean follow-up of 5.65 years) after the 2-year latency period (the risk before the treatment was 32.5 % from the time of the first symptomatic hemorrhage). Experience of colleagues at Karolinska University does not support the treatment of cavernomas with GKS, because the results were considered too limited [3, 4, 10]. However, the tendency toward a decreased risk of rebleeding after a 4-year period following radiosurgery was noted. The risk of complications was higher than for AVMs. In addition, lower, rather than higher, doses for cavernoma were recommended [4]. Along with the 2-year latency period, the decrease in the risk of rebleeding was observed in the group of patients treated by Kjellberg [1]. Using a cyclotron, radiosurgery resulted in morbidity in 16 % of cases. Chang et al. [2] observed a decrease in the risk of rebleeding after the treatment of cavernomas 3 years after radiosurgery, which was associated with morbidity in 11 % of cases. Protection from rebleeding after GKS of cavernomas was also observed by Mitchell et al. [11]. Liu et al. [8] observed an annual rebleeding rate of 10.3 % after treatment for the first 2 years and 3.3 % thereafter (mean follow-up 5.4 years). Nagy et al. [12] evaluated 113 patients with brain cavernomas. They found that 41 patients with multiple bleedings had a first-ever bleed rate of 2.9 %/lesion/year, a rebleed rate of 30.5 %/lesion/year, and an annual risk of rebleeding of 2.4 % after the 2-year latency period. In that series, 77 patients with a single episode of bleeding in their history (annual risk 2.2 %) had annual risk of rebleeding of 1.3 % after the 2-year latency period, although adverse radiation effects were observed in 7.3 %. The authors concluded that radiosurgery reduces the rebleeding rate in patients with repeated pretreatment hemorrhage, but they noted that the benefit of treating cavernomas with a single bleeding episode was less clear.

Another important effect of cavernoma radiosurgery can be observed in patients with secondary epilepsy. In the present series, improvement of epilepsy was marked in 45 % of the affected patients. In a multicentric study, Régis et al. [14] observed even better results: 53 % of 49 patients were seizure-free after radiosurgery, and the number of seizures had decreased in another 20 % of patients. The same epilepsy improvement (53 %) was reported by Liu et al. [8].

One of the detectable effects after radiosurgery is regression of the cavernoma, which was observed in 53 % of our patients, usually within 2 years after treatment. Spontaneous regression of the cavernoma could be expected as absorption of the hematoma after previous bleeding. In the case of bleeding, radiosurgery in our patients was postponed for at least 3 months, but usually treatment was initiated 6 months after the bleeding episode. Therefore, we believe that a decrease in cavernoma volume after radiosurgery is a positive result of the treatment. Some authors have also observed a regression of the cavernoma after radiosurgery in as many as 57.3 % of cases [3, 5, 9], although others noted only small changes [2].

Cavernomas are thought to be at higher risk of complications after radiosurgery than AVMs [3, 4, 13]. In our experience, the risk of edema on follow-up MRI after radiosurgery of AVMs was 21.3 % [7], whereas for cavernomas it was 27.3 %. Edema was associated with temporary morbidity in 7.7 % of patients with AVMs and in 14.6 % of those with cavernomas. There was permanent morbidity in 2.7 % of AVM patients and in 0.9 % of cavernoma patients. We do not consider this morbidity as unacceptably high; complications from rebleeding constituted the main risk (Fig. 1). Eventually, the higher risk of temporary complications after radiosurgery of cavernomas compared to AVMs was caused by our tendency to apply high doses, similar to those used for AVMs. Nowadays, these doses seem inadequate as cavernoma doses >13 Gy significantly increase this risk of complications [6]. The median marginal dose in the study group of patients with cavernoma was 16 Gy, the same as in the series published by Lunsford et al. [9]. They observed a 13.5 % risk of morbidity, which is similar to the 14.6 % from our experience. Pollock et al. [13] observed complications in 59 % of cases, and the median marginal dose in their series was 18 Gy.

Analysis of our results changed our treatment strategy, and such high marginal doses are no longer used for cavernomas. Thus, the risk of radiosurgery is further decreased and does not stand out from the risks observed in patients with other pathologies that treated with radiosurgery. In a group of 125 patients with cavernoma and a mean marginal dose of 12.1 Gy, Liu et al. [8] observed symptomatic complications in only 3 cases. Marginal doses of 14–15 Gy in our current practice represents a compromise between the higher risk of edema with increasing marginal dose and the higher risk of rebleeding with the lower marginal dose.

Over the last 18 years, the indications for radiosurgery of cavernomas at our center have become stricter as they have evolved hand-in-hand with advances in microsurgery. Cavernomas are considered easily operable today, whereas two decades ago, in the absence of neuronavigation and stereotactic support, they frequently were not even identified during surgery. Therefore, the view of what was operable was different. Unlike AVMs, which usually are treated even when diagnosed incidentally, cavernomas in the same situation are treated conservatively. However, cavernomas with no history of bleeding do not display indolent behavior, which one might have expected. In the presented group, 53 of 112 patients had no bleeding before GKS. The reason to treat them, in fact, was mainly secondary epilepsy. Rebleeding after radiosurgery was observed in four of these patients (Table 1). However, based on the comparison of the protective effect, which is pronounced only in bleeding cavernomas, we have abandoned radiosurgery for cavernomas that had not bled before treatment.

Conclusion

A decreased risk of rebleeding after the 2-year latent interval was observed after radiosurgery of cavernomas in patients who bled before treatment. The risk of permanent complications after radiosurgery was <1 %, and temporary morbidity can be reduced by using lower marginal doses. Controversial issues—incomplete knowledge of the natural course of disease and the absence of diagnostic tools that can confirm elimination of the risk of rebleeding—led us gradually to reserve radiosurgery for a selected group of patients with repeated bleeding or progressive impairment because of a neurological deficit if the alternative treatment (microsurgical resection) poses an unacceptable risk. Up to now, the only proof of treatment failure after radiosurgery is rebleeding or an increase in the cavernoma after the 2-year latent interval following radiosurgery. Future studies should evaluate whether repeated radiosurgery in such cases might result in a further decrease in the risks that accrue during the natural course of the disease.

Conflict of Interest The authors declare that they have no conflict of interest.

References

1. Amin-Hanjani S, Ogilvy CS, Candia GJ, Lyons S, Chapman PH (1998) Stereotactic radiosurgery for cavernous malformations: Kjellberg's experience with proton beam therapy in 98 cases at the Harvard cyclotron. Neurosurgery 42:1229–1238
2. Chang SD, Levy RP, Adler JR, Martin DP, Krakovitz PR, Steinberg GK (1998) Stereotactic radiosurgery of angiographically occult vascular malformations: 14-years experience. Neurosurgery 43:213–221
3. Karlson B, Kihlstrom L, Lindquist C, Ericson K, Steiner L (1998) Radiosurgery for cavernous malformations. J Neurosurg 88: 293–297
4. Karlsson B, Soderman M (2009) Stereotactic radiosurgery for cavernomas. In: Lunsford LD, Sheehan JP (eds) Intracranial stereotactic radiosurgery. Theme, New York, pp 48–57
5. Kim DG, Choe WJ, Paek SH, Chung HT, Kim IH, Han DH (2002) Radiosurgery if intracranial cavernous malformations. Acta Neurochir (Wien) 144:869–878
6. Liščák R, Vladyka V, Šimonová G, Vymazal J, Novotný J Jr (2005) Gamma knife surgery of brain cavernous hemangiomas. J Neurosurg 102(Suppl):207–213
7. Liščák R, Vladyka V, Šimonová G, Urgošík D, Novotný J Jr, Janoušková L, Vymazal J (2007) Arteriovenous malformations after Leksell gamma knife radiosurgery: rate of obliteration and complications. Neurosurgery 60:1005–1016
8. Liu KD, Chung WY, Wu HM, Shiau CY, Wang LW, Guo WY, Pan DH (2005) Gamma knife surgery for cavernous hemangiomas: an analysis of 125 patients. J Neurosurg 102(Suppl):81–86
9. Lunsford LD, Khan AA, Niranjan A, Kano H, Flickinger JC, Kondziolka D (2010) Stereotactic radiosurgery for symptomatic solitary cerebral cavernous malformations considered high risk for resection. J Neurosurg 113:23–29
10. Mathiesen T, Edner G, Kihlstrom L (2003) Deep and brainstem cavernomas: a consecutive 8-years series. J Neurosurg 99:31–37
11. Mitchell P, Hodgson TJ, Seaman S, Kemeny AA, Forster DMC (2000) Stereotactic radiosurgery and the risk of haemorrhage from cavernous malformations. Br J Neurosurg 14:96–100
12. Nagy G, Razak A, Rowe JG, Hodgson TJ, Coley SC, Radatz MW, Patel UJ, Kemeny AA (2010) Stereotactic radiosurgery for deep-seated cavernous malformations: a move toward more active, early intervention. J Neurosurg 113:691–699
13. Pollock E, Garces YI, Stafford SL, Foote RL, Schomberg PJ, Link MJ (2000) Stereotacic radiosurgery for cavernous malformations. J Neurosurg 93:987–991
14. Régis J, Bartolomei F, Kida Y, Kobayashi T, Vladyka V, Liscàk R, Forster D, Kemeny A, Schröttner O, Pendl G (2000) Radiosurgery for epilepsy associated with cavernous malformation: retrospective study in 49 patients. Neurosurgery 47:1091–1097
15. Steiner L, Karlsson B, Yen CP, Torner JC, Lindquist C, Schlesinger D (2010) Radiosurgery in cavernous malformations: anatomy of a controversy. J Neurosurg 113:16–22
16. Szeifert GT, Timperley WR, Forster D, Kemeny A (2007) Histopathological changes in cerebral arteriovenous malformations following gamma knife radiosurgery. In: Szeifert GT, Kondziolka D, Levivier M, Lunsford LD (eds) Radiosurgery and Pathological Fundamentals. Prog Neurol Surg, vol 20. Karger, Basel, pp 212–219

Gamma Knife Radiosurgery for the Management of Intracranial Dural Arteriovenous Fistulas

David Hung-Chi Pan, Cheng-Chia Lee, Hsiu-Mei Wu, Wen-Yuh Chung, Huai-Che Yang, and Chung-Jung Lin

Abstract *Background:* This report presents our 15-year experience with Gamma Knife radiosurgery (GKS) for the treatment of 321 patients with dural arteriovenous fistulas (DAVFs) in different locations.

Methods: The most common locations of DAVFs were the cavernous sinus (206 cases) and transverse-sigmoid sinus (72 cases), which together accounted for 86.6 % of cases. In all, 54 patients had undergone embolization or surgery prior to radiosurgery, and the other patients underwent GKS as the primary treatment. During GKS, radiation was confined to the involved sinus wall, which was considered the true nidus of the DAVF. Target volume ranged from 0.8 to 52 cm^3. Marginal and maximum doses to the nidus ranged from 14 to 25 Gy and from 25 to 36 Gy, respectively.

Results: The mean follow-up time was 28 months (range 2–149 months). In 264 of 321 patients (82 %) available for follow-up study, 173 (66 %) showed complete obliteration of DAVFs with symptomatic resolution, 87 (33 %) had partial obliteration, 2 (0.8 %) had stationary status, 1 (0.4 %) had progression, and 1 (0.4 %) died from a new hemorrhagic episode. Complications were found in only two (0.8 %) patients, one with venous hemorrhage and one with focal brain edema after GKS.

Conclusions: GKS is a safe, effective treatment for DAVFs. It provides a minimally invasive therapeutic option for patients who harbor less-aggressive DAVFs but who suffer from intolerable clinical symptoms. For some aggressive DAVFs with extensive venous hypertension or hemorrhage, multimodal treatment with combined embolization or surgery is necessary.

Keywords Dural arteriovenous fistula • Gamma Knife radiosurgery • Outcome • Treatment

Introduction

Intracranial dural arteriovenous fistulas (DAVFs) are direct arteriovenous shunts between meningeal arteries and dural sinuses or leptomeningeal veins [2, 16]. The incidence of DAVFs has been estimated at 5–20 % of all intracranial vascular malformations [1, 21, 30]. DAVFs are thought to be acquired secondary to inflammation, thrombosis, or trauma of the dural sinus [7, 17, 22]. The exact etiology and underlying disease in many DAVFs, however, are difficult to trace, in which case they are considered idiopathic.

The estimated annual hemorrhagic rate of DAVFs is approximately 1.8 % [5, 13, 31]. The clinical presentation is dependent on their location and the pattern of the venous drainage. Patients with cavernous sinus DAVFs often have ocular manifestations, whereas patients with transverse-sigmoid sinus DAVFs frequently suffer from headache and pulse-synchronous tinnitus on the affected side. DAVFs with antegrade cortical venous drainage (CVD) have been regarded as clinically benign, whereas DAVFs with retrograde CVD are considered aggressive in behavior [12, 27, 33]. The pattern of the venous drainage is not necessarily static. Gradual alternation of the venous flow from antegrade to retrograde or delayed recruitment of arterial feeders (sump effect) has been observed in some DAVFs [1]. It is hypothesized to occur as a result of progressive sinus hypertension with redirection of the blood flow into cortical veins [9, 16]. The progressive venous hypertension and cortical venous reflux may eventually lead to cerebral hemorrhage or other aggressive neurological deficits [2].

D.H.-C. Pan (✉), C.-C. Lee, W.-Y. Chung, and H.-C. Yang
Department of Neurosurgery, Taipei Veterans General Hospital, No. 201 Shi-Pai Rd., Sec. 2, Taipei, Taiwan
e-mail: hcpan@vghtpe.gov.tw

School of Medicine, National Yang-Ming University, Taipei, Taiwan

H.-M. Wu and C.-J. Lin
Department of Radiology, Taipei Veterans General Hospital, Taipei, Taiwan

School of Medicine, National Yang-Ming University, Taipei, Taiwan

M.F. Chernov et al. (eds.), *Gamma Knife Neurosurgery in the Management of Intracranial Disorders*, Acta Neurochirurgica Supplement, Vol. 116, DOI 10.1007/978-3-7091-1376-9_18, © Springer-Verlag Wien 2013

Stereotactic radiosurgery has long been used for the treatment of intraparenchymal AVMs, and treatment of DAVFs would be a natural extension [6, 8, 14, 25, 30, 35]. While our experience of treating DAVFs using Gamma Knife radiosurgery (GKS) at the Taipei Veterans General Hospital has been reported before [15, 24, 34], we present here an update with an additional 83 patients and longer duration of follow-up.

Materials and Methods

Patients

Between 1993 and 2008, a total of 321 patients with intracranial DAVFs were treated using GKS at the Taipei Veterans General Hospital. In all, 141 patients (44 %) were male and 180 (56 %) were female. The age at the time of GKS ranged from 17 to 81 years (mean 57.8 years). Two potential inciting factors for DAVF formation could be traced: 31 patients (13.4 %) had a history of head trauma, and 14 patients (6 %) had a history of head and neck surgery prior to their DAVF diagnosis. Table 1 shows the anatomical location of the DAVFs in our patients. The most common locations are the cavernous sinus (CS, 206 cases) followed by the transverse-sigmoid sinus (TSS, 72 cases), which together account for 86.6 % of the cases. Because of the unique clinical characteristics of DAVFs involving the CS, we divided the DAVFs into two groups: the CS group and the noncavernous sinus (NCS) group. All NCS DAVFs are further classified based on their angiographic venous drainage pattern using the systems of Borden-Shucart and Cognard (Table 2) [3, 9]. Of the 115 NCS DAVFs, 63 were Borden type I (Cognard types I and IIa) with solely antegrade sinus drainage—and thus considered benign [12, 27, 28]. The remaining 52 cases were Borden type II or III (Cognard types IIb, III, IV, V), demonstrating retrograde cortical venous drainage and thus considered clinically "aggressive" [11, 33].

Table 1 Anatomical locations of DAVFs in 321 patients treated with Gamma Knife radiosurgery

Location	No. of cases	
Cavernous sinus	206	64.2 %
Transverse-sigmoid sinus	72	22.4 %
Petrosal sinus	9	2.8 %
Superior sagittal sinus	8	2.5 %
Anterior cranial fossa	6	2.0 %
Vein of Galen	2	0.6 %
Foramen magnum	1	0.3 %
Jugular foramen	2	0.6 %
Tentorium	9	2.8 %
Sphenoparietal	4	1.2 %
Clivus	2	0.6 %
Total	321	100 %

DAVFs dural arteriovenous fistulas
From Pan et al. [25]

Table 2 Angiographic classifications of 115 patients with noncavernous sinus DAVFs treated with Gamma Knife radiosurgery

Type	No. of patients	
A. Borden classification		
I	63	54.8 %
II	35	30.4 %
III	17	14.8 %
B. Cognard classification		
I	25	21.7 %
IIa	38	33.0 %
IIb	9	7.9 %
IIa + b	26	22.6 %
III	6	5.2 %
IV	8	7.0 %
V	3	2.6 %

From Pan et al. [25]

Treatment Modality

Before radiosurgery, some of the patients had attempted other therapeutic approaches for the treatment of their DAVFs. In all, 13 of the CS DAVFs and 28 of the NCS DAVFs had undergone prior endovascular embolization one to four times in an attempt to obliterate the lesion. The 13 patients who suffered from intracranial hemorrhage from NCS DAVFs had undergone craniotomy for hematoma evacuation and clipping of feeding vessels. GKS was performed as the secondary treatment in these 54 patients because of residual filling of the fistula seen angiographically. In three patients with CS DAVFs (1.5 % of CS DAVFs), spontaneous remission of symptoms or regression of the DAVFs was seen angiographically, and no further intervention was taken. The remaining patients underwent radiosurgery as the primary treatment. The indications for GKS are intolerable symptoms (ocular symptoms, headache, pulsatile tinnitus), focal neurological deficit, and the presence of a residual shunt following other therapeutic techniques.

Radiosurgical Method

A standard GKS procedure was performed using a Gamma Knife (Elekta Instruments AB, Stockholm, Sweden) either model B (from 1993 to 2006) or model 4C (after 2007).

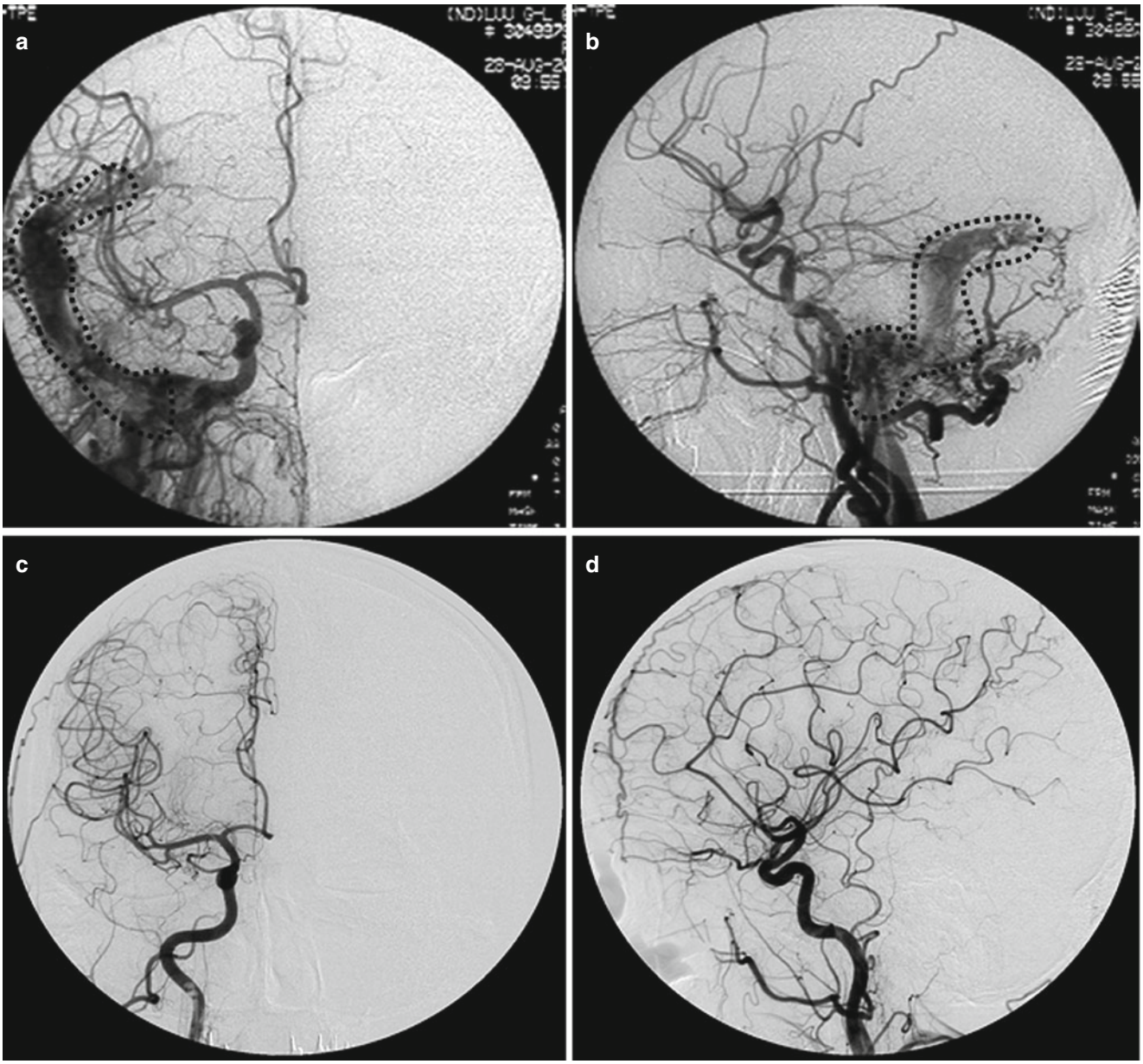

Fig. 1 A 60-year-old women with a Cognard type IIa + b dural arteriovenous fistula (DAVF) involving the right transverse-sigmoid sinus. The patient presented with symptoms of mental status change and epilepsy. Transarterial embolization for the DAVF was performed three times prior to Gamma Knife radiosurgery (GKS). Anteroposterior (AP) (**a**) and lateral (**b**) angiographic views of the right common carotid before GKS revealed persistent DAVF. During GKS treatment planning, the radiosurgical target was delineated along the involved dural sinus wall (*dotted lines* in **a** and **b**). The arterial feeders and drainage veins distal to the sinus were excluded from the radiation field. In this case, the treatment volume was 36.6 cm^3, marginal dose was 16.5 Gy, and maximum dose was 30.4 Gy. (**c**, **d**) Follow-up angiograms 26 months after GKS revealed complete obliteration of the DAVF. Clinical symptoms of the patient had also completely resolved

The target was localized by integrating imaging data from stereotactic noncontrast magnetic resonance imaging (MRI), thin-cut axial views time-of-flight (TOF) magnetic resonance angiography (MRA), and cerebral X-ray angiography. The goal of treatment was to occlude the fistulous shunts completely. It is crucial to delineate the treatment target such that all abnormal arteriovenous shunts on the sinus wall are enclosed in the treatment area [25]. The target volume was defined along the involved dural sinus wall where the true arteriovenous fistula occurs [1, 16, 22]. The remote arterial feeders and drainage veins distal to the sinus were excluded from the treatment target as they are not considered part of the nidus (Fig. 1). In our patients, the mean treatment volume for CS DAVFs was 4.7 cm^3 (range 0.2–28.4 cm^3), whereas NCS DAVF comprised a larger mean treatment volume of 16.9 cm^3 (range 0.8–52 cm^3).

Table 3 Treatment data of Gamma Knife radiosurgery for 206 patients with CS DAVFs and 115 patients with NCS DAVFs

Parameter	Cavernous sinus DAVF		Noncavernous sinus DAVF	
Radiation volume (cm^3)	0.2–28.0	(4.7)	0.8–52.0	(16.9)
Marginal dose (Gy)	14–25	(17.2)	15–21	(17.2)
Maximum dose (Gy)	18–38	(25.2)	21–36	(30)
Isodose level (%)	50–96	(68.5)	50–90	(57.5)
No. of isocenters	1–14	(3.3)	1–27	(13)

Numbers within parenthesis indicate mean values
CS cavernous sinus, *NCS* noncavernous sinus
From Pan et al. [25]

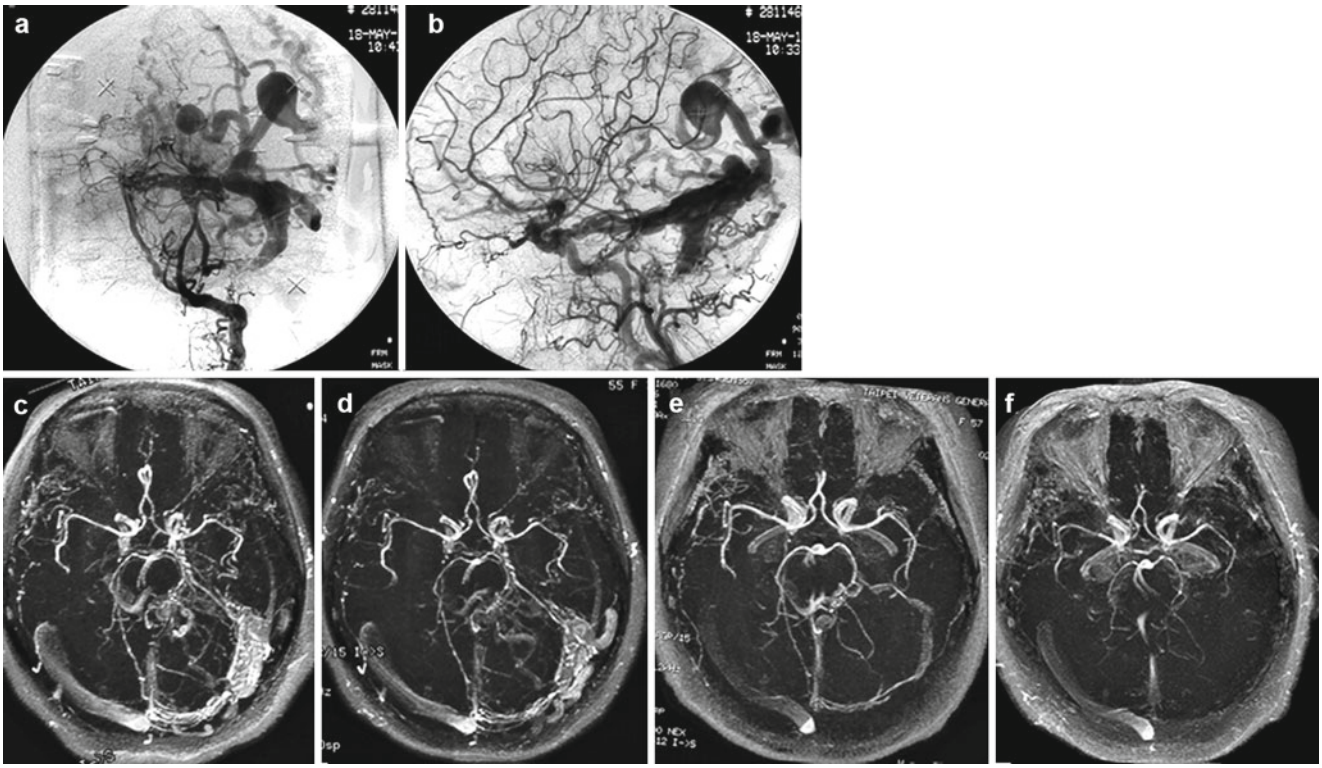

Fig. 2 A 55-year-old women with a Cognard type IIb DAVF involving the left transverse-sigmoid sinus. The patient presented after undergoing endovascular embolization of the DAVF. Before GKS, lateral view of the vertebral angiogram (**a**) and common carotid angiogram (**b**) revealed extensive retrograde cortical venous drainage with aneurysmal dilation of veins and occlusion of the left sigmoid sinus. (**c**) Time-of-flight magnetic resonance angiography (MRA) of the patient on the day of GKS treatment. In this case, the treatment volume was 20.9 cm^3, marginal dose was 17.5 Gy, and maximum dose was 31.8 Gy. After GKS, sequential MRA follow-up at 6 months (**d**) and 26 months (**e**) revealed gradual regression of the DAVF nidus. There was complete obliteration of the DAVF at 50 months (**f**)

The radiation dose profile is shown in Table 3. The prescribed margin dose for both CS and NCS DAVFs were similar, with a mean dose of 17.2 Gy, although the mean maximum dose differed: 25 Gy for CS DAVFs and 30 Gy for NCS DAVFs. For the treatment of CS DAVFs, we prefer to use a large (14 or 18 mm) collimator to cover the margin of the CS. The average number of isocenters was three. For the NCS DAVFs, a larger number isocenters (several large and many small shots) were used to cover the treatment volume, with a mean number of 13 isocenters (range 1–27). Care was taken to protect the adjacent critical structures, such as the optic nerve and brain stem, from receiving radiation of >8–9 Gy.

Follow-up Program

After GKS, a clinical neurological examination and radiographic imaging study (MRI with MRA) were performed at 6-month intervals. Cerebral X-ray angiography was performed 1–3 years after GKS if complete regression of the lesion had been shown on MRI (Fig. 2). For CS DAVFs, noninvasive color Doppler ultrasonography (CDU) examined through eyeballs was performed every 3 months to evaluate flow direction and velocity in the superior ophthalmic vein. Frequently, normalization of the CDU was associated with concomitant findings of complete obliteration of the DAVF on MRI and cerebral angiography [25].

Table 4 Clinical outcomes for 264 patients with DAVFs treated by Gamma Knife radiosurgery

Outcome	Cavernous sinus DAVF		Noncavernous sinus DAVF	
Complete improvement	109	(70 %)	64	(59 %)
Partial improvement	47	(30 %)	40	(37 %)
Stationary (no change)	–		2	(2 %)
Progression	–		1	(1 %)
Death	–		1	(1 %)
Total	156	(100 %)	108	(100 %)

From Pan et al. [25]

Patient outcomes after radiosurgery were grouped into four categories: (1) complete improvement, indicating complete resolution of symptoms with complete obliteration of DAVF on cerebral angiography and/or MRA; (2) partial improvement, indicating partial resolution of clinical symptoms with >50 % regression of DAVF on MRA; (3) stationary, indicating no change of the DAVF on follow-up MRA; (4) progression, indicating enlargement or aggressive change of the DAVF on MRA.

Results

Post-GKS follow-up studies were available for 156 (76 %) of the 206 patients with CS DAVFs and 108 (94 %) of the 115 patients with NCS DAVFs. The mean follow-up period was 20.8 months (range 2–149 months) for the CS group and 28 months (range 2–141 months) for the NCS group. Table 4 summarizes the clinical outcomes for the 264 DAVF patients with follow-up. For the CS DAVFs, 109 of the 156 patients (70 %) showed complete improvement, and 47 (30 %) had partial improvement with significant flow reduction. No lesion was stationary or progressed after radiosurgery. For the NCS DAVFs, 64 of the 109 (58 %) showed complete improvement, 40 (37 %) were partially improved, 2 (2 %) were stationary, and 1 (1 %) showed progression.

One patient died from a new intracerebral hemorrhage after treatment. He was a 70-year-old man with a Borden type III DAVF involving the tentorial region. Thus, the mortality rate of the entire series is 0.4 % (1/264 with follow-up available). Postradiosurgical hemorrhage due to uncontrollable venous hypertension was found in another patient with an extensive, aggressive DAVF (Borden type II) involving the transverse-sigmoid sinus. This patient recovered from the hemorrhage and improved after further combined treatment with endovascular embolization and repeated radiosurgery.

In this series, 98 % (260/264 patients) had a stable or improved clinical condition after radiosurgery. For the assessment of adverse reactions to radiation seen on MRI scans, there was only one patient who developed radiation-induced brain edema, which occurred 6 months after radiosurgery. The edema subsided gradually after steroid treatment.

To evaluate the response to GKS of DAVFs with different venous drainage patterns, we further analyzed treatment results of the 108 patients with NCS DAVFs based on the Borden classification. The results show that radiosurgery was effective in treating Borden type I lesions, with a 72 % complete obliteration rate; the remaining 28 % had partial improvement. A lower success rate was achieved for Borden type II and III lesions. Of the 48 Borden type II and III patients, complete obliteration was observed in 21 (44 %) patients, with another 48 % showing partial improvement, 4 % remaining stationary, and 2 % being progressive. There was one death, which was due to recurrent hemorrhage, as described above.

For some DAVFs with extensive involvement of dural sinuses and cortical veins, repeated radiosurgery might be necessary for complete obliteration of the DAVFs. In this series, 5 CS DAVFs and 14 NCS DAVFs required repeat radiosurgeries 1–3 years after the first treatment. The method and dose selection of the repeated radiosurgery were similar to those of the first treatment.

Discussion

Efficacy of DAVF Radiosurgery

The current series of 264 DAVF patients treated by GKS at the Taipei Veterans General Hospital over the last decade and a half shows a 66 % complete obliteration rate, with another 33 % of the patients demonstrating a reduction in DAVF size and alleviation of symptoms. These results are similar to those reported by other institutions. Shin et al. reported two patients with tentorial DAVFs treated with >20 Gy to the fistula, with complete obliteration in both patients at 27 and 29 months, respectively [29]. Söderman et al. reported 49 patients with 52 DAVFs, showing a 68 % obliteration rate and another 24 % with flow regression at 2 years [30]. O'Leary et al. achieved a 77 % complete obliteration rate with improvement in another 15 % of patients [23]. In the series of Brown et al., of the 50 patients with angiographic follow-up, 68 % demonstrated complete obliteration, with another 14 % showing near-total obliteration [4]. In Koebbe et al.'s series, all 18 patients had complete or near-complete resolution of their presenting

symptoms [20]. More recently, Yang et al. reported a series of 40 DAVF patients treated at the University of Pittsburgh. They found an 83 % obliteration rate for patients who had upfront GKS with embolization, and a 67 % obliteration rate in patients who underwent GKS alone [35]. At the University of Virginia, Cifarelli et al. reported a 65 % obliteration rate in a series of 55 patients [8]. Although some of the patients in these publications had been treated with embolization or surgery prior to radiosurgery, they were referred for GKS for further management of the residual DAVFs. From these studies, we can estimate an overall success rate of complete obliteration associated with radiosurgery of DAVFs at 65–83 %, with more patients gaining symptomatic relief from radiosurgical treatment. Complications directly related to the radiosurgical procedure are rare, as shown in our series.

Rationale for DAVF Radiosurgery

The treatment of a DAVF should be individualized, taking into consideration the clinical presentation of the patient, the anticipated natural history of the lesion based on location and angioarchitecture of the DAVF, and the benefit and inherent risk of the treatment modality. It is widely accepted that DAVFs presenting with hemorrhage, progressive neurological deficits, or increased intracranial pressure require prompt treatment by endovascular embolization, surgery, or a combination of these procedures to provide immediate relief of the venous congestion. However, when DAVFs involve dural sinuses with multiple complex feeders and CVD, surgical or endovascular treatment can be technically challenging. Multisession and/or combined treatment is often needed. The rate of complete obliteration of DAVFs achieved by endovascular procedures differs from center to center, ranging from 27.3 % to 81.0 % [18]. It has been well known that partially treated DAVFs may recruit new collaterals to the fistula or redirect the venous outflow [10].

For DAVFs with antegrade sinus drainage alone (Borden type I) and no progressive focal neurological deficits, intervention may not be necessary unless the patient's symptoms (e.g., headache, pulsatile tinnitus) are intolerable. When a treatment is indicated for Borden type I DAVF, its benefit should outweigh its risk. Evidence has shown that injury or increased pressure in the dural sinus can trigger the development of a DAVF or cause neurological deficits secondary to venous hypertension [16]. Therefore, sacrificing a functioning dural sinus in a Borden type I DAVF by transvenous intervention or surgery may not be justified. Furthermore, it is difficult to achieve complete obliteration of Borden type I DAVFs by transarterial embolization alone because of the frequently complex, tortuous course of the arterial supply [27]. Studies have shown that local ischemia caused by incomplete closure of DAVFs after endovascular and/or surgical intervention can increase expression of various vascular growth factors, which can recruit new collaterals, resulting in recanalizaton of the DAVFs [19, 32]. Thus, the use of endovascular intervention or surgery as a first-line treatment for Borden type I DAVFs with the intention of palliation rather than cure should be carefully considered, balancing the risks and benefits of the procedure. Our study and others have shown that DAVFs with benign venous drainage can be safely treated using radiosurgery, with a high angiographic complete obliteration rate and preservation of the functioning dural sinuses [15, 24, 31, 34].

Retrograde CVD has long been recognized as an angioarchitecture precursor of aggressive behavior of DAVFs. However, not all DAVFs with CVDs are symptomatic. In 2009, Zipfel et al. presented a modified classification system for DAVFs that factors in the patients' symptoms and outcome [36]. They divided Borden type II/III patients into two subgroups: those with symptomatic CVD who present with hemorrhage or aggressive neurological deficits and those with nonsymptomatic CVD who present with benign symptoms of tinnitus or ophthalmological phenomena with a less-aggressive clinical course. They suggested that, for patients with asymptomatic CVD the lower risk of immediate hemorrhage or neurological deficits impels a more judicious approach to therapeutic intervention. In many cases, endovascular or surgical intervention is still indicated, although the timing of treatment may be performed in an elective nature. For others, particularly patients who are elderly, medically frail, or those harboring complex DAVF—posing risks and technical difficulties with traditional treatments—radiosurgery is a reasonable alternative.

Our radiosurgical results support the above observation. Among our 48 patients with Borden type II/III NCS DAVFs, 21 (44 %) achieved complete obliteration and 23 (48 %) showed a >50 % reduction of the lesion size with symptomatic alleviation. These data indicate that radiosurgery is also suitable for certain DAVFs with CVD but without immediate risk of hemorrhage or focal neurological deficits.

Conclusions

Gamma Knife radiosurgery is a safe and effective alternative treatment for DAVFs. It provides a minimally invasive therapeutic modality for patients who harbor less-aggressive DAVFs but who suffer from intractable headache, pulsatile tinnitus, or ocular symptoms. For aggressive DAVFs with extensive CVD, hemorrhage, or severe venous hypertension, initial treatment with endovascular embolization or surgery is suggested. In such cases, GKS can serve as a secondary treatment for further management of the residual nidus. It is believed that using a multidisciplinary approach to DAVF management yields better results.

Conflict of Interest The authors declare that they have no conflict of interests.

References

1. Awad IA (1991) The diagnosis and management of intracranial dural arteriovenous malformations. Contemp Neurosurg 13:1–5
2. Awad IA, Little JR, Akarawi WP, Ahl J (1990) Intracranial dural arteriovenous malformations: factors predisposing to an aggressive neurological course. J Neurosurg 72:839–850
3. Borden JA, Wu JK, Shucart WA (1995) A proposed classification for spinal and cranial dural arteriovenous fistulous malformations and implications for treatment. J Neurosurg 82:166–179
4. Brown RD Jr, Flemming KD, Meyer FB, Cloft HJ, Pollock BE, Link ML (2005) Natural history, evaluation, and management of intracranial vascular malformations. Mayo Clin Proc 80:269–281
5. Brown RD Jr, Wiebers DO, Nichols DA (1994) Intracranial dural arteriovenous fistulae: angiographic predictors of intracranial hemorrhage and clinical outcome in nonsurgical patients. J Neurosurg 81:531–538
6. Chandler HC Jr, Friedman WA (1993) Successful radiosurgical treatment of a dural arteriovenous malformation: case report. Neurosurgery 33:139–142
7. Chaudhary MY, Sachdev VP, Cho SH, Weitzner I Jr, Puljic S, Huang YP (1982) Dural arteriovenous malformation of the major venous sinuses: an acquired lesion. AJNR Am J Neuroradiol 3:13–19
8. Cifarelli CP, Kaptain G, Yen CP, Schlesinger D, Sheehan JP (2010) Gamma knife radiosurgery for dural arteriovenous fistulas. Neurosurgery 67:1230–1235
9. Cognard C, Gobin YP, Pierot L, Bailly AL, Houdart E, Casasco A, Chiras J, Merland JJ (1995) Cerebral dural arteriovenous fistulas: clinical and angiographic correlation with a revised classification of venous drainage. Radiology 194:671–680
10. Cognard C, Houdart E, Casasco A, Gabrillargues J, Chiras J, Merland JJ (1997) Long-term changes in intracranial dural arteriovenous fistulae leading to worsening in the type of venous drainage. Neuroradiology 39:59–66
11. Davies MA, ter Brugge K, Willinsky R, Wallace MC (1997) The nature history and management of intracranial dural arteriovenous fistulae: part 2 aggressive lesions. Interv Neuroradiol 3:303–311
12. Davies MA, TerBrugge K, Willinsky R, Coyne T, Saleh J, Wallace MC (1996) The validity of classification for the clinical presentation of intracranial dural arteriovenous fistulas. J Neurosurg 85:830–837
13. Duffau H, Lopes M, Janosevic V, Sichez JP, Faillot T, Capelle L, Ismail M, Bitar A, Arthuis F, Fohanno D (1999) Early rebleeding from intracranial dural arteriovenous fistulas: report of 20 cases and review of the literature. J Neurosurg 90:78–84
14. Friedman JA, Pollock BE, Nichols DA, Gorman DA, Foote RL, Stafford SL (2001) Results of combined stereotactic radiosurgery and transarterial embolization for dural arteriovenous fistulas of the transverse and sigmoid sinuses. J Neurosurg 94:886–891
15. Guo WY, Pan DH, Wu HM, Chung WY, Shiau CY, Wang LW, Chiou HJ, Yen MY, Teng MM (1998) Radiosurgery as a treatment alternative for dural arteriovenous fistulas of the cavernous sinus. AJNR Am J Neuroradiol 19:1081–1087
16. Hamada Y, Goto K, Inoue T, Iwaki T, Matsuno H, Suzuki S, Matsushima T, Fukui M, Miyake E (1997) Histopathological aspects of dural arteriovenous fistulas in the transverse-sigmoid sinus region in nine patients. Neurosurgery 40:452–458
17. Houser OW, Campbell JK, Campbell RJ, Sundt TM Jr (1979) Arteriovenous malformation affecting the transverse dural venous sinus – an acquired lesion. Mayo Clin Proc 54:651–661
18. Kirsch M, Liebig T, Kuhne D, Henkes H (2009) Endovascular management of dural arteriovenous fistulas of the transverse and sigmoid sinus in 150 patients. Neuroradiology 51:477–483
19. Klisch J, Kubalek R, Scheufler KM, Zirrgiebel U, Drevs J, Schumacher M (2005) Plasma vascular endothelial growth factor and serum soluble angiopoietin receptor sTIE-2 in patients with dural arteriovenous fistulas: a pilot study. Neuroradiology 47:10–17
20. Koebbe CJ, Singhal D, Sheehan J, Flickinger JC, Horowitz M, Kondziolka D, Lunsford LD (2005) Radiosurgery for dural arteriovenous fistulas. Surg Neurol 64:392–399
21. Newton TH, Cronqvist S (1969) Involvement of dural arteries in intracranial arteriovenous malformations. Radiology 93:1071–1078
22. Nishijima M, Takaku A, Endo S, Kuwayama N, Koizumi F, Sato H, Owada K (1992) Etiological evaluation of dural arteriovenous malformations of the lateral and sigmoid sinuses based on histopathological examinations. J Neurosurg 76:600–606
23. O'Leary S, Hodgson TJ, Coley SC, Kemeny AA, Radatz MW (2002) Intracranial dural arteriovenous malformations: results of stereotactic radiosurgery in 17 patients. Clin Oncol (R Coll Radiol) 14:97–102
24. Pan DH, Chung WY, Guo WY, Wu HM, Liu KD, Shiau CY, Wang LW (2002) Stereotactic radiosurgery for the treatment of dural arteriovenous fistulas involving the transverse-sigmoid sinus. J Neurosurg 96:823–829
25. Pan DHC, Wu HM, Kuo YH, Chung WY, Lee CC, Guo WY (2013) Intracranial dural arteriovenous fistulas: natural history and rationale for treatment with stereotactic radiosurgery. In: Niranjan A, Kano H, Lunsford LD (eds) Gamma Knife Radiosurgery for Brain Vascular Malformations. Prog Neurol Surg, vol. 27. Karger, Basel, pp 176–194
26. Pollock BE, Nichols DA, Garrity JA, Gorman DA, Stafford SL (1999) Stereotactic radiosurgery and particulate embolization for cavernous sinus dural arteriovenous fistulae. Neurosurgery 45:459–467
27. Sarma D, ter Brugge K (2003) Management of intracranial dural arteriovenous shunts in adults. Eur J Radiol 46:206–220
28. Satomi J, van Dijk JM, Terbrugge KG, Willinsky RA, Wallace MC (2002) Benign cranial dural arteriovenous fistulas: outcome of conservative management based on the natural history of the lesion. J Neurosurg 97:767–770
29. Shin M, Kurita H, Tago M, Kirino T (2000) Stereotactic radiosurgery for tentorial dural arteriovenous fistulae draining into the vein of Galen: report of two cases. Neurosurgery 46:730–734
30. Soderman M, Edner G, Ericson K, Karlsson B, Rahn T, Ulfarsson E, Andersson T (2006) Gamma knife surgery for dural arteriovenous shunts: 25 years of experience. J Neurosurg 104:867–875
31. Soderman M, Pavic L, Edner G, Holmin S, Andersson T (2008) Natural history of dural arteriovenous shunts. Stroke 39:1735–1739
32. Tirakotai W, Bertalanffy H, Liu-Guan B, Farhoud A, Sure U (2005) Immunohistochemical study in dural arteriovenous fistulas and possible role of local hypoxia for the de novo formation of dural arteriovenous fistulas. Clin Neurol Neurosurg 107:455–460
33. van Dijk JM, terBrugge KG, Willinsky RA, Wallace MC (2002) Clinical course of cranial dural arteriovenous fistulas with long-term persistent cortical venous reflux. Stroke 33:1233–1236
34. Wu HM, Pan DH, Chung WY, Guo WY, Liu KD, Shiau CY, Wang LW, Chen SJ (2006) Gamma Knife surgery for the management of intracranial dural arteriovenous fistulas. J Neurosurg 105(Suppl):43–51
35. Yang HC, Kano H, Kondziolka D, Niranjan A, Flickinger JC, Horowitz MB, Lunsford LD (2010) Stereotactic radiosurgery with or without embolization for intracranial dural arteriovenous fistulas. Neurosurgery 67:1276–1284
36. Zipfel GJ, Shah MN, Refai D, Dacey RG Jr, Derdeyn CP (2009) Cranial dural arteriovenous fistulas: modification of angiographic classification scales based on new natural history data. Neurosurg Focus 26(5):E14

Radiosurgery as Neuromodulation Therapy!

Jean Régis

Abstract Radiosurgery is commonly considered to be effective through a destructive physical mechanism acting on neural tissue. However, the results of modern neurophysiological, radiological, and histological studies are providing a basis on which to question this assumption. There are now multiple pieces of evidence pointing to a nonlesional mechanism of the radiosurgical action. It appears that tissue destruction is absent or minimal and in almost all cases insufficient to explain the clinical effects produced. There is a real possibility that radiosurgery induces changes in the functioning of neural tissue by differential effects on various neuronal populations and remodeling the glial environment, leading to modulation of function while preserving basic processing. Hence, the majority of radiosurgical procedures induce the desired biological effect without histological destruction of tissue. These findings may result in a major paradigm shift in the treatment of functional brain disorders.

Keywords Apoptosis • Gamma Knife Radiosurgery • Glia • Plasticity • Subnecrotic dose

Introduction

Radiosurgery was clearly intended to be an instrument for use in functional neurosurgery. The first disorders treated were trigeminal neuralgia and Parkinson disease. Radiosurgery is commonly considered to exert its effects through a destructive physical mechanism that acts on neural tissue. Increasing evidence, however, suggests a more subtle mechanism of action especially relevant for functional neurosurgical indications.

J. Régis
Department of Stereotactic and Functional Neurosurgery, Aix Marseille University, Timone University Hospital, and INSERM U751, 264 rue Saint Pierre, Marseille 13385, Cedex 05, France

Faculty of Advanced Techno-Surgery, Institute of Advanced Biomedical Engineering and Science, Tokyo Women's Medical University, Tokyo, Japan
e-mail: jregis@ap-hm.fr

Radiosurgery, always considered a purely ablative treatment, today relies on a *nonlesional mechanism of action*. In the mind of its creator Lars Leksell, radiosurgery was clearly intended to mimic the lesional effects of a surgeon's knife, hence he gave the name "Gamma Knife" for the first such instrument. The high doses initially selected for thalamotomy [50], capsulotomy [7], and benign tumors [29, 56] were rapidly identified as being unnecessarily toxic. With functional neurosurgery, the strategy is to target a small volume of normal tissue (e.g., ventralis intermedius nucleus (VIM) thalamotomy, capsulotomy, trigeminal neuralgia) with a high dose (80–140 Gy maximum) or a large volume of tissue (e.g., 5–9 cm^3 for epilepsy) with a moderate dose (17–24 Gy at the marginal isodose).

The dose reduction policy for vestibular schwannomas resulted in a dramatic decrease in the incidence of facial palsy, from 27 % to <1 %, and an increase in hearing preservation to 80 % with no loss of tumor control [10, 39, 49]. With this new regimen of lower doses for benign tumors, the predominant mechanism of action was presumed to be *apoptosis* (cell death mediated by DNA breakage in the populations of cells that were entering mitosis) [2, 20, 23]. The goal of radiosurgery to treat arteriovenous malformations (AVMs) is to create thrombosis of the nidus to prevent further hemorrhage. This clinical effect is caused by a histological change marked by *endothelial proliferative thrombosis* [52, 59]. This is typically a biological effect specifically induced by radiosurgery without any frank destruction of vascular tissue but, rather, a proliferative response within the arterial wall of the vessels to radiation injury. Consequently, radiosurgery has been redefined as "a neurosurgical procedure where narrow ionizing beams, given in a single high dose fraction, are used either to destroy a predetermined target volume or to induce a desired biological effect in the target volume" [53]. Furthermore, the lower incidence of hemorrhage after AVM radiosurgery (compared to embolization) may have something to do with modulation of another specific biological effect—a *decrease in the angiogenic response to injury* with reduced expression of vascular endothelial growth factor [1].

M.F. Chernov et al. (eds.), *Gamma Knife Neurosurgery in the Management of Intracranial Disorders*, Acta Neurochirurgica Supplement, Vol. 116, DOI 10.1007/978-3-7091-1376-9_19, © Springer-Verlag Wien 2013

Hypothalamic hamartoma radiosurgery for *epilepsy control* is an even more convincing example of the functional, nonlesional effect [3, 34, 40, 47]. More than 50 % of our 79 patients who underwent radiosurgery (50 with >3 years of follow-up) are seizure-free, and a large portion of the others report a significant reduction in seizure frequency, and they welcomed the associated significantly improved quality of life [34, 47]. The vast majority of the patients show no radiographic changes on their follow-up magnetic resonance imaging (MRI) studies. Interestingly, the psychiatric [47] and neuropsychological symptoms are also improving dramatically or resolving completely in a large percentage of patients, even in those without complete seizure cessation. The clinical observation of profound therapeutic antiepileptic effect with no histological necrosis induced by radiosurgery is encouraging and speaks again to some neuromodulatory effect of radiosurgery [46].

Differential Biologic Effect

A differential biologic effect is induced by radiosurgery under certain conditions. When an AVM located in a highly functional area is associated with focal seizure disorder, the probability of curing this epilepsy after radiosurgery is roughly 85 % [9, 12, 16, 22, 51]. Interestingly, seizure cessation in these patients frequently occurs before the AVM occlusion or even despite failure of radiosurgery to occlude the nidus and in the absence of any neurological deficit specific to the function of the surrounding brain. Thus, the biological changes leading to cessation of epileptogenic activity in the brain adjacent to the AVM are independent of the occlusion of the AVM and are not dependent on radiographic or histological evidence of a destructive effect on tissue. Such destructive changes would have been expected to lead to a functional deficit, with or without AVM obliteration [16, 35, 36, 43, 45]. This common clinical experience with AVM demonstrates the capability of radiosurgery to eliminate epileptic activity from a previously epileptogenic cortex while preserving its underlying normal function. This kind of observation led us to hypothesize the existence of some kind of differential biological effect of radiosurgery on tissue: that low-dose radiosurgery applied to normal neuronal tissue, relying on subtle but specific biological changes, may affect some processes while sparing others, thereby producing the desired clinical effect [41]. In 1996, we published the first article to demonstrate the existence of such a differential effect manifested at the biochemical level [41]. In rats, targeting the striatum with radiosurgery was shown to lower the level of the enzyme choline acetyltransferase while not affecting the levels of glutamate decarboxylase. Conversely, the levels of the excitatory amino acids were reduced, and the nonexcitatory amino acids (particularly γ-aminobutyric acid) were stable [41]. However, clinically safe and efficient implementation of radiosurgery to effect some form of neuromodulation requires further basic science work to provide better understanding of the influence of dose, volume, target topography, and dose distribution homogeneity on the modulation of specific biological systems [35, 41].

Specific Glial Tissue Changes Induced by Radiosurgery

At the cellular level, it is well-known that noncycling cells (e.g., neurons) exposed to moderate amount of energy with radiosurgery are quite resistant, with a low level of cell loss. On the other hand, cycling cells (e..g., supporting glial and endothelial cells) can be severely injured by radiosurgery and are part of the radiation-induced biological cascade [57], with a significant rate of cell loss. Lunsford's group described a delayed astrogliosis reaction and cell loss in the field of radiosurgery of animal models [18]. Interestingly, such glial cell death has been reported to induce migration of progenitor cells from subependymal matrix germinal zones (Lars Kihlstrom, 1998, personal communication). These progenitors, arising within the radiosurgical target volume, are differentiated into mature glial cells with a phenotype clearly different from those of the destroyed glia [60]. In 2005, Nagayama et al. studied radiation-induced apoptosis of oligodendrocytes in the adult rat brain. They reported rapid apoptotic depletion of the oligodendrocytes (maximum after 8 h) and a significant decrease in cell density in the white matter 24 h after irradiation [28].

"Cockade" Model

The "cockade" model is an original concept that we proposed some years ago summarizing the regional effect of a radiosurgery dose on normal brain by artificially separating it into four concentric zones [35, 38]. When sufficient dose/volume parameters are used, a "necrotic core" central zone (histological necrosis) is surrounded by a "subnecrotic area" where cellular death is observed without coagulative necrosis. This subnecrotic area is typically the area where cellular differential effects of radiosurgery are observed, with considerable wash-out of glial cells and only a few noncycling cells (neurons) dying. Outside the "subnecrotic area" is the "neuromodulatory area," where more subtle changes are visible without a significant increase in cell deaths. Inflammatory compounds produced in the subnecrotic area are likely to account for a significant portion of the changes observed in

this area. No effect is observed outside this neuromodulatory area. Messengers, proteins, and small molecules are likely to play a major role in mediating the cellular changes seen in the tissues in and around the area of the radiosurgery. Changes observed in subnecrotic or neuromodulatory areas may be the sum of the area's direct and indirect local radiation effects and those induced from neighboring areas (subnecrotic area influencing the neuromodulatory area and necrotic core influencing the subnecrotic area). Thus, the relative extent of each zone is not only dependent on the dose delivered to each zone but also on the volume of treatment, the histological and biochemical nature of the targeted brain tissue, and finally the genetics of the patient.

White matter and capillaries are classically more sensitive to the effects of radiation. Diffusion-weighted imaging has shown signs of vasogenic edema in the subcortical white matter, with a decrease of fractional isotropy associated with dissociation of the neuronal fibers by extracellular water. Also, there are signs of cellular edema (ischemia) with no change of the fractional anisotropy maps associated with myelin sheath splitting and periaxonal space enlargement (Naoyuki Miyasaka, 2002, personal communication). MRI changes are sometimes misleading [24]. Typically, the extent of white matter abnormalities are related more to an increase in extracellular fluid than to the locally delivered dose affecting the role of secondary messengers. For example, in medial temporal lobe epilepsy (MTLE), the major white matter changes extend far from the target laterally, following association fiber tracts. The fiber tracts within the brain stem, however, which receive similar energy, are not modified on follow-up imaging studies. Obviously, these distant changes are caused by propagation of inflammatory small molecules through the white matter tracts and are not induced directly by ionizing radiation—not dissimilar to the diffuse white matter changes sometimes observed after treatment of small midline meningiomas. Not surprisingly, when these inflammatory mechanisms are considered, the time course of the observed biological effects in tissue can be explained.

Rahn et al. studied results of radiosurgery for brain metastases and demonstrated that the patients treated in the morning did substantially better than those treated in the afternoon [33], suggesting that some sort of cellular circadian rhythm affects the response of tumor and normal tissues to irradiation. The genetic profile of the individual is crucial. For thalamotomy, the treatment is standard in terms of the volume of the target, location, and dose. Although the tissue reaction to radiosurgery is reportedly focal in some series [17, 61], up to 10 % of the patients have a larger reaction, seen on MRI. These imaging changes may be associated with hemiparesis, usually transient. Kondziolka et al. demonstrated the radioprotective effect of the 21-aminosteroid U-74389G in an experimental study in rats [19, 21]. They reported that this drug reduces the cytokine expression normally seen after radiation injury and can be overexpressed in patients who exhibit a clinically obvious reaction to radiosurgery.

Changes of Specific Properties of Neurons as Response to Radiosurgery

VIM thalamotomy is classically performed using a maximum dose of 130–140 Gy, which induces a small area of necrosis after several months that is well seen on the 12-month follow-up MRI. This is one of the infrequent indications for radiosurgery, where the intended effect is to mimic the histologically destructive effect produced by thermocoagulation. However, in 2000, Ohye et al. proposed that the clinical effect on tremor was not only the result of the necrotic lesion [30]. Their main argument was that the size of the lesion induced by radiosurgery was too small to account for the clinical effect seen. (It is interesting to note that the limit of the lesion seen on MRI corresponds, in our experience, to the volume of the 90 Gy isodose line.) Some experimental observations [62] support this hypothesis, but more studies are still necessary to better understand the nature and respective role of nonlesional and lesional mechanisms in VIM radiosurgery. In 2008, Terao et al. reported that the somatotopic distribution of kinesthetic cells was modified by Gamma Knife surgery (GKS) of the VIM, raising the possibility that the specific properties of the neurons are changed in response to irradiation [55].

Selective vulnerability of certain neuronal subtypes has been suggested to contribute to our proposed "neuromodulative" effect by some experimental works. Jenrow et al. reported in epileptic rats (kindling model) that the selective reduction of densities in the dentate granular cell layer and medial CA3 pyramidal cell layer was prevented or reversed by irradiation at 25 Gy but not at 18 Gy [15]. This is consistent with the dose effect we have found in humans [42]. From a histological standpoint, Lee et al. reported on epileptic rats irradiated with 40 Gy to the medial temporal lobe. Their immunohistochemical findings suggested that at least one subtype of hippocampal interneurons are selectively vulnerable to GKS. The neuronal cells appeared to have undergone a phenotypic shift with respect to calbindin and GAD-67 expression (K. Lee, 2009, personal communication).

Central Nervous System Regenerative Process

The central nervous system (CNS) regenerative process fails because (among other reasons) extracellular inhibitory factors make it nonpermissive to growth [14]. Thus, a radical change in the phenotype of the glial environment may allow a functional readjustment phenomenon. Neurons may have a

more impressive capacity for adjusting than previously thought [31]. Our hypothesis is that under certain conditions radiosurgery, relying on nonnecrotizing dose parameters, induces an important turnover of the glial environment of neurons, allowing functional connections the opportunity to reset, reorganize, and overcome errors disturbing their functional capability [38]. If supported by further experimental evidence, this hypothesis may open new perspectives for radiosurgery as a neuromodulation therapy in functional neurosurgery.

MTLE Model

The MTLE model illustrates the clinical feasibility of a neuromodulatory radiosurgical approach. Until the 1990s, curative epilepsy surgery was limited to open microsurgery, with which abnormal epileptogenic tissue was physically removed. The first cases of temporal lobe epilepsy treated with GKS in Marseille in 1993 [37, 43] were encouraging, with short-term results demonstrating the safety and efficacy of this approach. Seizure control rates were similar to those of resective surgery, and these early results are now confirmed to be durable responses on medium [4, 44] and long-term [6] follow-up. The impressive MRI findings observed roughly 1 year after radiosurgery led us initially to speculate that a necrotic lesional effect was responsible for the clinical result [48]. However, medium-term disappearance of these MRI findings leaves the medial structures of the temporal lobe either similar to or only slightly more atrophic than that seen preoperatively. It suggests a more subtle neuromodulating effect of radiosurgery than initially thought and indicates that a more limited volume of the temporal lobe is involved compared to the effect of microsurgery [44]. Further studies correlating the efficacy of the quality of the coverage of each structure of the medial temporal lobe area on seizure outcome have demonstrated the importance of targeting the anterior parahippocampal cortex and especially the perirhinal and entorhinal cortex [11]. This is consistent with the Wieser and Yasargil series of microsurgical amygdalohippocampectomies [58]. The perirhinal and entorhinal cortex plays a major role in memory processing [5]. Overall, it is estimated that 40 % of the patients with MTLE operated on microsurgically on the dominant side have a significant postoperative short-term verbal memory deficit [8, 32, 54]. Our first prospective trial of GKS for MTLE found that in 65 % of those who underwent dominant temporal lobe treatment there was no evidence of any neuropsychological deficit [6, 44]. Our subsequent experience has confirmed this observation [6]. Today, we consider this memory-sparing benefit as the major advantage of radiosurgery over microneurosurgery in patients with dominant temporal lobe MTLE. Thus, the MTLE patients currently selected for GKS are those who might suffer more and longer if additional memory deficit is produced—that is, young patients with a high level of functioning who are socially adapted, working, concerned by the risk of microsurgery and the time off from work, and presenting with risk factors for verbal memory loss in case of resection (no atrophy, dominant side, few neuropsychological deficits before surgery) [13]. This group of patients is often highly functioning with a sufficient intelligence to allow them to understand the peculiarities and nuances of radiosurgery. In addition, they frequently do not have severe epilepsy, which affords them the luxury of waiting.

The San Diego group has observed neuropsychological worsening in some patients tested during the "acute phase" (when the acute MRI signs are still present) [27]. The group has not reported the long-term results of their neuropsychological testing after resolution of the acute MRI signs. We have seen the same verbal memory sparing in our long-term MTLE patients treated on the dominant side [6]. The observation was recently confirmed by a multicenter Phase I–II trial in the United States [4]. The mechanism of this functional preservation is still a matter of speculation. It may be that the dose regimen we use is simply not lesional. It also may be that the cell loss is selective, primarily affecting the glial environment. Perhaps we are inducing a certain degree of neuronal and astrocytic damage, but the process is so slow and delayed that the brain has sufficient time to reorganize functionally. Maesawa et al., in an elegant study, tested in a rat kainic acid model of epilepsy both the efficacy of radiosurgery and memory sparing [25, 26]. The control group (not treated) continued to seize, whereas the rats treated with 30 Gy (maximum dose) had a reduction in their seizure frequency. The group treated with 60 Gy (maximum) had cessation of seizure activity 5–11 weeks after GKS. The Morris water maze test was used for spatial memory testing and showed that spatial memory was highly abnormal in the control group, whereas the radiosurgically treated 30 Gy group had normal spatial memory [25, 26].

Conclusion

Functional radiosurgical procedures using the Gamma Knife have been proposed, technically performed, and evaluated based on the hypothesis that their mechanism of action was purely destructive. However, modern neurophysiological, radiological, and histological studies have led us to question this assumption. It seems that tissue destruction is either absent or minimal and in almost all cases insufficient to explain the clinical effects obtained. One possibility to explain these effects is that radiosurgery induces changes in

the functioning of neural tissue by inducing differential effects on different neuronal populations or by remodeling the glial environment, leading to modulation of function while preserving basic processing. Thus, the majority of radiosurgery procedures may induce the desired biological effect without requiring a histological destructive effect to meet the therapeutic goal. Thus, the concept of "lesional" radiosurgery may be incorrect, and a hidden world of neuromodulatory effects may remain to be discovered [38]. It may require a major paradigm shift in functional neurosurgery.

Conflict of Interest The Author is recipient of the research grant from Elekta Instruments AB and Meetings' sponsorships from Accuray, BrainLab, Elekta Instruments AB, and Varian, none of which is related to the present study.

References

1. Akakin A, Ozkan A, Akgun E, Koc DY, Konya D, Pamir MN, Kilic T (2010) Endovascular treatment increases but gamma knife radiosurgery decreases angiogenic activity of arteriovenous malformations: an in vivo experimental study using a rat cornea model. Neurosurgery 66:121–130
2. Anniko M, Arndt J, Noren G (1981) The human acoustic neurinoma in organ culture. II. Tissue changes after gamma irradiation. Acta Otolaryngol 91:223–235
3. Arita K, Kurisu K, Iida K, Hanaya R, Akimitsu T, Hibino S, Pant B, Hamasaki M, Shinagawa S (1998) Subsidence of seizure induced by stereotactic radiation in a patient with hypothalamic hamartoma. Case report. J Neurosurg 89:645–648
4. Barbaro NM, Quigg M, Broshek DK, Ward MM, Lamborn KR, Laxer KD, Larson DA, Dillon W, Verhey L, Garcia P, Steiner L, Heck C, Kondziolka D, Beach R, Olivero W, Witt TC, Salanova V, Goodman R (2009) A multicenter, prospective pilot study of gamma knife radiosurgery for mesial temporal lobe epilepsy: seizure response, adverse events, and verbal memory. Ann Neurol 65:167–175
5. Bartolomei F, Barbeau E, Gavaret M, Guye M, McGonigal A, Regis J, Chauvel P (2004) Cortical stimulation study of the role of rhinal cortex in deja vu and reminiscence of memories. Neurology 63:858–864
6. Bartolomei F, Hayashi M, Tamura M, Rey M, Fischer C, Chauvel P, Regis J (2008) Long-term efficacy of gamma knife radiosurgery in mesial temporal lobe epilepsy. Neurology 70:1658–1663
7. Cecconi JP, Lopes AC, Duran FL, Santos LC, Hoexter MQ, Gentil AF, Canteras MM, Castro CC, Noren G, Greenberg BD, Rauch SL, Busatto GF, Miguel EC (2008) Gamma ventral capsulotomy for treatment of resistant obsessive-compulsive disorder: a structural MRI pilot prospective study. Neurosci Lett 447:138–142
8. Clusmann H, Schramm J, Kral T, Helmstaedter C, Ostertun B, Fimmers R, Haun D, Elger CE (2002) Prognostic factors and outcome after different types of resection for temporal lobe epilepsy. J Neurosurg 97:1131–1141
9. Eisenschenk S, Gilmore RL, Friedman WA, Henchey RA (1998) The effect of LINAC stereotactic radiosurgery on epilepsy associated with arteriovenous malformations. Stereotact Funct Neurosurg 71:51–61
10. Flickinger JC, Kondziolka D, Lunsford LD (1996) Dose and diameter relationships for facial, trigeminal and acoustic neuropathies following acoustic neuroma radiosurgery. Radiother Oncol 41:215–219
11. Hayashi M, Bartolomei F, Rey M, Farnarier P, Chauvel P, Regis J (2002) MR changes after Gamma knife radiosurgery for mesial temporal lobe epilepsy: an evidence for the efficacy of subnecrotic doses. In: Kondziolka D (ed) Radiosurgery, vol 4. Karger, Basel, pp 192–202
12. Heikkinen ER, Konnov B, Melnikow L (1989) Relief of epilepsy by radiosurgery of cerebral arteriovenous malformations. Stereotact Funct Neurosurg 53:157–166
13. Helmstaedter C, Reuber M, Elger CC (2002) Interaction of cognitive aging and memory deficits related to epilepsy surgery. Ann Neurol 52:89–94
14. Jacobs WB, Fehlings MG (2003) The molecular basis of neural regeneration. Neurosurgery 53:943–950
15. Jenrow KA, Ratkewicz AE, Lemke NW, Kadiyala M, Zalinski DN, Burdette DE, Elisevich KV (2004) Effects of kindling and irradiation on neuronal density in the rat dentate gyrus. Neurosci Lett 371:45–50
16. Kida Y, Kobayashi T, Tanaka T, Mori Y, Hasegawa T, Kondoh T (2000) Seizure control after radiosurgery on cerebral arteriovenous malformations. J Clin Neurosci 7:6–9
17. Kondziolka D (2002) Gamma knife thalamotomy for disabling tremor. Arch Neurol 59:1660; author reply 1662–1664
18. Kondziolka D, Linskey L, Lunsford LD (1993) Animal models in radiosurgery. In: Alexander E III, Loeffler JS, Lunsford LD (eds) Stereotactic radiosurgery. McGraw Hill, New York, pp 51–64
19. Kondziolka D, Mori Y, Martinez A, McLaughlin M, Flickinger J, Lunsford L (1999) Beneficial effects of the radioprotectant 21-aminosteroid U-74389G in a radiosurgery rat malignant glioma model. Int J Radiat Oncol Biol Phys 44:179–184
20. Kondziolka D, Niranjan A, Lunsford LD, Flickinger JC (2007) Radiobiology of radiosurgery. Prog Neurol Surg 20:16–27
21. Kondziolka D, Somaza S, Martinez A, Jacobsohn J, Maitz A, Lunsford L, Flickinger J (1997) Radioprotective effects of the 21-aminosteroid U-74389G for stereotactic radiosurgery. Neurosurgery 41:203–208
22. Kurita H, Kawamoto S, Suzuki I, Sasaki T, Tago M, Terahara A, Kirino T (1998) Control of epilepsy associated with cerebral arteriovenous malformations after radiosurgery. J Neurol Neurosurg Psychiatry 65:648–655
23. Linskey ME, Martinez AJ, Kondziolka D, Flickinger JC, Maitz AH, Whiteside T, Lunsford LD (1993) The radiobiology of human acoustic schwannoma xenografts after stereotactic radiosurgery evaluated in the subrenal capsule of athymic mice. J Neurosurg 78:645–653
24. Lunsford L, Kondziolka D, Maitz A, Flickinger J (1998) Black holes, white dwarfs and supernovas: imaging after radiosurgery. Stereotact Funct Neurosurg 70(Suppl 1):2–10
25. Maesawa S, Kondziolka D, Balzer J, Fellows W, Dixon E, Lunsford LD (1999) The behavioral and electroencephalographic effects of stereotactic radiosurgery for the treatment of epilepsy evaluated in the rat kainic acid model. Stereotact Funct Neurosurg 73:115
26. Maesawa S, Kondziolka D, Dixon C, Balzer J, Fellows W, Lunsford L (2000) Subnecrotic stereotactic radiosurgery controlling epilepsy produced by kainic acid injection in rats. J Neurosurg 93:1033–1040
27. McDonald CR, Norman MA, Tecoma E, Alksne J, Iragui V (2004) Neuropsychological change following gamma knife surgery in patients with left temporal lobe epilepsy: a review of three cases. Epilepsy Behav 5:949–957
28. Nagayama K, Kurita H, Nakamura M, Kusuda J, Tonari A, Takayama M, Fujioka Y, Shiokawa Y (2005) Radiation-induced apoptosis of oligodendrocytes in the adult rat optic chiasm. Neurol Res 27:346–350
29. Noren G (2004) Gamma knife radiosurgery of acoustic neurinomas. A historic perspective. Neurochirurgie 50:253–256
30. Ohye C, Shibazaki T, Ishihara J, Zhang J (2000) Evaluation of gamma thalamotomy for parkinsonian and other tremors: survival

of neurons adjacent to the thalamic lesion after gamma thalamotomy. J Neurosurg 93(Suppl 3):120–127
31. Oltvai ZN, Barabasi AL (2002) Systems biology. Life's complexity pyramid. Science 298:763–764
32. Pilcher WH, Roberto DW, Flanigin HF, Crandall PH, Wieser HG, Ojemann GA, Peacock WJ (1993) Complications of epilepsy surgery. In: Engel J (ed) Surgical treatment of epilepsies. Raven Press, New York, pp 565–581
33. Rahn D, Dibyendu K, Schlesinger D, Steiner L, Sheehan J, O'Quigley J, Rich T (2011) Gamma Knife radiosurgery for brain metastasis of non small cell lung cancer: is there a difference in outcome between morning and afternoon treatment? Cancer 117:414–420
34. Regis J, Bartolomei F, de Toffol B, Genton P, Kobayashi T, Mori Y, Takakura K, Hori T, Inoue H, Schrottner O, Pendl G, Wolf A, Arita K, Chauvel P (2000) Gamma knife surgery for epilepsy related to hypothalamic hamartomas. Neurosurgery 47:1343–1352
35. Regis J, Bartolomei F, Hayashi M, Chauvel P (2002) Gamma Knife surgery, a neuromodulation therapy in epilepsy surgery! Acta Neurochir Suppl 84:37–47
36. Regis J, Bartolomei F, Hayashi M, Roberts D, Chauvel P, Peragut JC (2000) The role of gamma knife surgery in the treatment of severe epilepsies. Epileptic Disord 2:113–122
37. Régis J, Bartolomei F, Rey M, Genton P, Dravet C, Semah F, Gastaut J, Chauvel P, Peragut J (1999) Gamma knife surgery for mesial temporal lobe epilepsy. Epilepsia 40:1551–1556
38. Regis J, Carron R, Park M (2010) Is radiosurgery a neuromodulation therapy?: A 2009 Fabrikant award lecture. J Neurooncol 98:155–162
39. Regis J, Delsanti C, Roche PH, Thomassin JM, Pellet W (2004) Functional outcomes of radiosurgical treatment of vestibular schwannomas: 1000 successive cases and review of the literature. Neurochirurgie 50:301–311 (in French)
40. Regis J, Hayashi M, Eupierre LP, Villeneuve N, Bartolomei F, Brue T, Chauvel P (2004) Gamma knife surgery for epilepsy related to hypothalamic hamartomas. Acta Neurochir Suppl 91:33–50
41. Régis J, Kerkerian-Legoff L, Rey M, Viale M, Porcheron D, Nieoullon A, Peragut J-C (1996) First biochemical evidence of differential functional effects following gamma knife surgery. Stereotact Funct Neurosurg 66:29–38
42. Regis J, Levivier M, Hayashi M (2003) Radiosurgery for intractable epilepsy. Tech Neurosurg 9:191–203
43. Régis J, Peragut JC, Rey M, Samson Y, Levrier O, Porcheron D, Regis H, Sedan R (1994) First selective amygdalohippocampic radiosurgery for mesial temporal lobe epilepsy. Stereotact Funct Neurosurg 64:191–201
44. Regis J, Rey M, Bartolomei F, Vladyka V, Liscak R, Schrottner O, Pendl G (2004) Gamma knife surgery in mesial temporal lobe epilepsy: a prospective multicenter study. Epilepsia 45:504–515
45. Regis J, Roberts D (1999) Gamma Knife radiosurgery relative to microsurgery: epilepsy. Stereotact Funct Neurosurg 72(Suppl 1): 11–21
46. Regis J, Scavarda D, Tamura M, Nagayi M, Villeneuve N, Bartolomei F, Brue T, Dafonseca D, Chauvel P (2006) Epilepsy related to hypothalamic hamartomas: surgical management with special reference to gamma knife surgery. Childs Nerv Syst 22:881–895
47. Regis J, Scavarda D, Tamura M, Villeneuve N, Bartolomei F, Brue T, Morange I, Dafonseca D, Chauvel P (2007) Gamma knife surgery for epilepsy related to hypothalamic hamartomas. Semin Pediatr Neurol 14:73–79
48. Regis J, Semah F, Bryan R, Levrier O, Rey M, Samson Y, Peragut J (1999) Early and delayed MR and PET changes after selective temporomesial radiosurgery in mesial temporal lobe epilepsy. AJNR Am J Neuroradiol 20:213–216
49. Regis J, Tamura M, Delsanti C, Roche PH, Pellet W, Thomassin JM (2008) Hearing preservation in patients with unilateral vestibular schwannoma after gamma knife surgery. Prog Neurol Surg 21:142–151
50. Steiner L, Forster D, Leksell L (1980) Gammathalamotomy in intractable pain. Acta Neurochir (Wien) 52:173–184
51. Steiner L, Lindquist C, Adler J, Torner J, Alves W, Steiner M (1992) Clinical outcome of radiosurgery for cerebral arteriovenous malformations. J Neurosurg 77:1–8
52. Steiner L, Lindquist C, Adler JR, Torner JC, Alves W, Steiner M (1992) Outcome of radiosurgery for cerebral AVM. J Neurosurg 77:823
53. Steiner L, Lindquist C, Steiner M (1992) Radiosurgery. Adv Tech Stand Neurosurg 19:19–102
54. Stroup E, Langfitt J, Berg M, McDermott M, Pilcher W, Como P (2003) Predicting verbal memory decline following anterior temporal lobectomy (ATL). Neurology 60:1266–1273
55. Terao T, Yokochi F, Taniguchi M, Kawasaki T, Okiyama R, Hamada I, Nishikawa N, Izawa N, Shin M, Kumada S, Takahashi H (2008) Microelectrode findings and topographic reorganisation of kinaesthetic cells after gamma knife thalamotomy. Acta Neurochir (Wien) 150:823–827
56. Thoren M, Rahn T, Hall K, Backlund EO (1978) Treatment of pituitary dependent Cushing's syndrome with closed stereotactic radiosurgery by means of 60Co gamma radiation. Acta Endocrinol (Copenh) 88:7–17
57. Van Der Kogel AJ (1991) Central nervous system radiation injury in small animal models. In: Gutin PH, Leibel SA, Sheline G (eds) Radiation injury to the nervous system. Raven Press, New York, pp 91–112
58. Wieser HG, Siegel AM, Yasargil GM (1990) The Zurich amygdalohippocampectomy series: a short up-date. Acta Neurochir Suppl 50:122–127
59. Yamamoto M, Jimbo M, Lindquist C (1992) Radiation-induced edema after radiosurgery for pontine arteriovenous malformation. A case report and detection by magnetic resonance imaging. Surg Neurol 37:15–21
60. Yang T, Wu SL, Liang JC, Rao ZR, Ju G (2000) Time-dependent astroglial changes after gamma knife radiosurgery in the rat forebrain. Neurosurgery 47:407–416
61. Young RF, Jacques S, Mark R, Kopyov O, Copcutt B, Posewitz A, Li F (2000) Gamma knife thalamotomy for treatment of tremor: long-term results. J Neurosurg 93(Suppl 3):128–135
62. Zerris VA, Zheng Z, Noren G, Sungarian A, Friehs GM (2002) Radiation and regeneration: behavioral improvement and GDNF expression after Gamma Knife radiosurgery in the 6-OHDA rodent model of hemi-parkinsonism. Acta Neurochir Suppl 84:99–105

Long-Term Outcome of Gamma Knife Surgery Using a Retrogasserian Petrous Bone Target for Classic Trigeminal Neuralgia

Jung Kyo Lee, Deok Ryeong Kim, Yeon Hee Huh, Jin Kyung Kim, Won Chul Namgung, and Seok Ho Hong

Abstract *Background*: Gamma knife surgery (GKS) is the prevailing method for treatment of medically intractable trigeminal neuralgia (TN), although there are some technical differences among radiosurgical centers. We assessed the long-term outcomes of GKS using retrogasserian petrous bone targeting and evaluated factors associated with the clinical outcomes.

Methods: Between December 2003 and June 2009, a total of 91 GKS treatments were performed in 90 patients with classic TN. The surgical target was defined at the anterior portion of the trigeminal nerve, just above the retrogasserian petrous bone. A single 4-mm collimator was used to deliver a median 88.0 Gy (range 75–90 Gy) dose of radiation.

Findings: During follow-up, which ranged from 24 to 90 months, 89 patients (97.8 %) reported initial pain relief, 75 (82.4 %) experienced pain control, and 47 (51.6 %) achieved a pain-free state without medications at the last follow-up. Barrow Neurological Institute (BNI) scores of I–III at 2, 3, 4, 5, and 7 years were observed in 84 of 91, 68 of 77, 46 of 53, 33 of 36, 17 of 19, and 7 of 7 patients, respectively. Trigeminal nerve dysfunction was experienced by 34 patients, with 12 having BNI facial numbness scores of III–IV (13.2 %). In all, 14 patients (15.4 %) experienced pain recurrence at a mean 32 months (range 10–62 months) after treatment. The actuarial rates of pain control at 2, 4, and 6 years were 93 %, 88 %, and 79 %, respectively.

Conclusions: Gamma Knife radiosurgery is an efficient option for intractable TN. Our results can help medical practitioners to counsel their patients on the likelihood of achieving successful pain control.

Keywords Root entry zone • Gamma Knife radiosurgery • Retrogasserian ganglion • Trigeminal neuralgia

J.K. Lee (✉), D.R. Kim, Y.H. Huh, J.K. Kim, W.C. Namgung, and S.H. Hong
Department of Neurosurgery, Asan Medical Center, University of Ulsan, College of Medicine, 88, Olympic Ro 43-Gil, Songpa-Gu, Seoul 138-736, Korea
e-mail: jklee3745@gmail.com

Introduction

The International Association for the Study of Pain (IASP) has defined trigeminal neuralgia (TN) as sudden, usually unilateral, severe, brief, stabbing, recurrent episodes of pain in one or more branches of the trigeminal nerve [24]. Its overall incidence has been estimated to be approximately three to five cases per 100,000 people per year, increasing with age [10]. The mean age of disease presentation is 63 years [6]. Usually TN is initially managed with anticonvulsant medications. However, about 25 % of patients do not respond to such treatment, and others develop intolerance to it usually associated with the need for escalating doses, resulting in side effects such as imbalance, cognitive dysfunction, and hyponatremia [3]. Among the treatment options available for patients with medically refractory TN are microvascular decompression (MVD), percutaneous rhizotomy with glycerol, radiofrequency (RF) or balloon compression, and stereotactic radiosurgery, particularly with the use of Gamma Knife (GKS). Although indications for radiosurgery are still evolving, it is considered an option for patients with medical co-morbidities who are poor candidates for craniotomy or who refuse to undergo more invasive procedures [23, 30]. In addition, GKS is safe, accurate, and the least invasive technique, which requires a short hospital stay and provides favorable long-term results [9, 12, 17, 34, 35]. We therefore retrospectively evaluated the clinical outcomes obtained at our institution with GKS treatment of patients with classic TN.

Methods and Materials

Patient Population

We analyzed 91 GKS procedures in 90 patients with refractory TN who had been treated at the Gamma Knife Center of Asan Medical Center between December 2003 and June 2009 by a single neurosurgeon (J.K. Lee). All included patients presented

M.F. Chernov et al. (eds.), *Gamma Knife Neurosurgery in the Management of Intracranial Disorders*, Acta Neurochirurgica Supplement, Vol. 116, DOI 10.1007/978-3-7091-1376-9_20, © Springer-Verlag Wien 2013

Table 1 Characteristics of patients in the present series

Median age at surgery (years)	61.0 (range 34–85)
Median duration of symptoms (months)	69.4 (range 2–240)
Male:female	30:61
Side of surgery[a]	
Right	54 (59.3 %)
Left	37 (40.7 %)
Distribution of pain	
V1 only	0
V2 only	30 (33.0 %)
V3 only	24 (26.3 %)
V1 + V2	11 (12.1 %)
V2 + V3	21 (23.1 %)
V1 + V2 + V3	5 (5.5 %)
Previous surgical treatment	17 (18.7 %)
Alcohol injection	8
MVD	3
RF rhizotomy	2
Neurectomy	1
MVD + alcohol injection	2
Neurectomy + RF	1

[a]One patient underwent treatment on both sides, which were considered as separate cases
MVD microvascular decompression, *RF* radiofrequency

with a clinical profile consistent with the IASP diagnosis of TN. Treatments were administered to 30 men and 61 women, of a median age 61 years (range 34–85 years). All patients had failed or were intolerant of previous medical treatment (e.g., carbamazepine or oxcarbazepine). The median symptom duration was 69.4 months (range 2–240 months). Pain was located predominantly in the V2 distributions of the trigeminal nerve (33.0 %), followed by V3 (26.3 %), V2 + V3 (23.1 %), V1 + V2 (12.1 %), and all trigeminal distributions (5.5 %). The preoperative characteristics of our patients are summarized in Table 1. In all, 17 (18.7 %) had undergone invasive treatment prior to GKS, including 8 who were treated with one or more alcohol injections, 3 with MVD, 2 with RF rhizotomy, 1 with peripheral neurectomy, 2 with a combination of MVD and alcohol injection, and 1 with both peripheral neurectomy and RF rhizotomy. In the remaining 74 cases (81.3 %), radiosurgery was the first surgical procedure performed. The decision to proceed with GKS instead of an invasive procedure was almost universally driven by patient choice.

Radiosurgical Technique

Altogether, 4 patients underwent radiosurgery with a Leksell Gamma Knife model B (Elekta Instruments AB, Stockholm, Sweden) before March 2004, and the other 86 were treated after March 2004 with the model C Leksell Gamma Knife. The Leksell stereotactic frame (Elekta Instruments AB) was fixed on the patient's head under local infiltrative anesthesia and intravenous sedation. Magnetic resonance imaging (MRI) scans were obtained using a constructive interference in steady state (CISS) sequence. MRI and computed tomography (CT) images were fused to minimize magnetic distortion errors, with MPRAGE enhanced images used occasionally (Fig. 1). Leksell GammaPlan (Elekta Instruments AB) software was used for treatment planning, with the target being the anterior portion of the trigeminal nerve just above the retrogasserion petrous bone identified on MRI and CT fusion images. All patients were treated with one isocenter. A single 4-mm collimator was used to deliver a median maximum dose of 87.7 Gy (range 75–90 Gy). A plugging pattern was used to limit the dose to the brain stem in 72 cases, such that the surface of the brain stem of each patient was irradiated with no more than 12 Gy. In our Gamma Knife Center, radiosurgical treatment for TN is routinely performed on an outpatient basis.

Outcome Measures

Data were obtained by reviewing patients' medical records or conducting telephone interviews. Pain relief was measured using the Barrow Neurological Institute (BNI) pain scale (Table 2), with successful pain control defined as scores of I–III. Trigeminal nerve dysfunction was measured using the BNI facial numbness score (Table 3). Symptoms of dry eye or mastication weakness were not routinely assessed. All patients were regularly examined by the treating neurosurgeon and were questioned regarding the onset of pain relief, the intensity of pain, and any newly developed facial nerve dysfunction. Patients were advised to make nonscheduled outpatient visits in case of exacerbation of pain or any other clinical deterioration. Imaging evaluations were not routinely performed during follow-up.

Statistical Analysis

Descriptive statistics were computed using standard methods to calculate means or medians. Statistical evaluation was performed with commercially available statistical software (SPSS version 17.0). Student's *t*-tests were used to compare continuous variables, and analysis of nominal data was completed using two-tailed Fisher's exact tests. A P value <0.05 was considered significant. Kaplan-Meier curves were calculated to determine the percentage of patients who were free from pain recurrence after GKS.

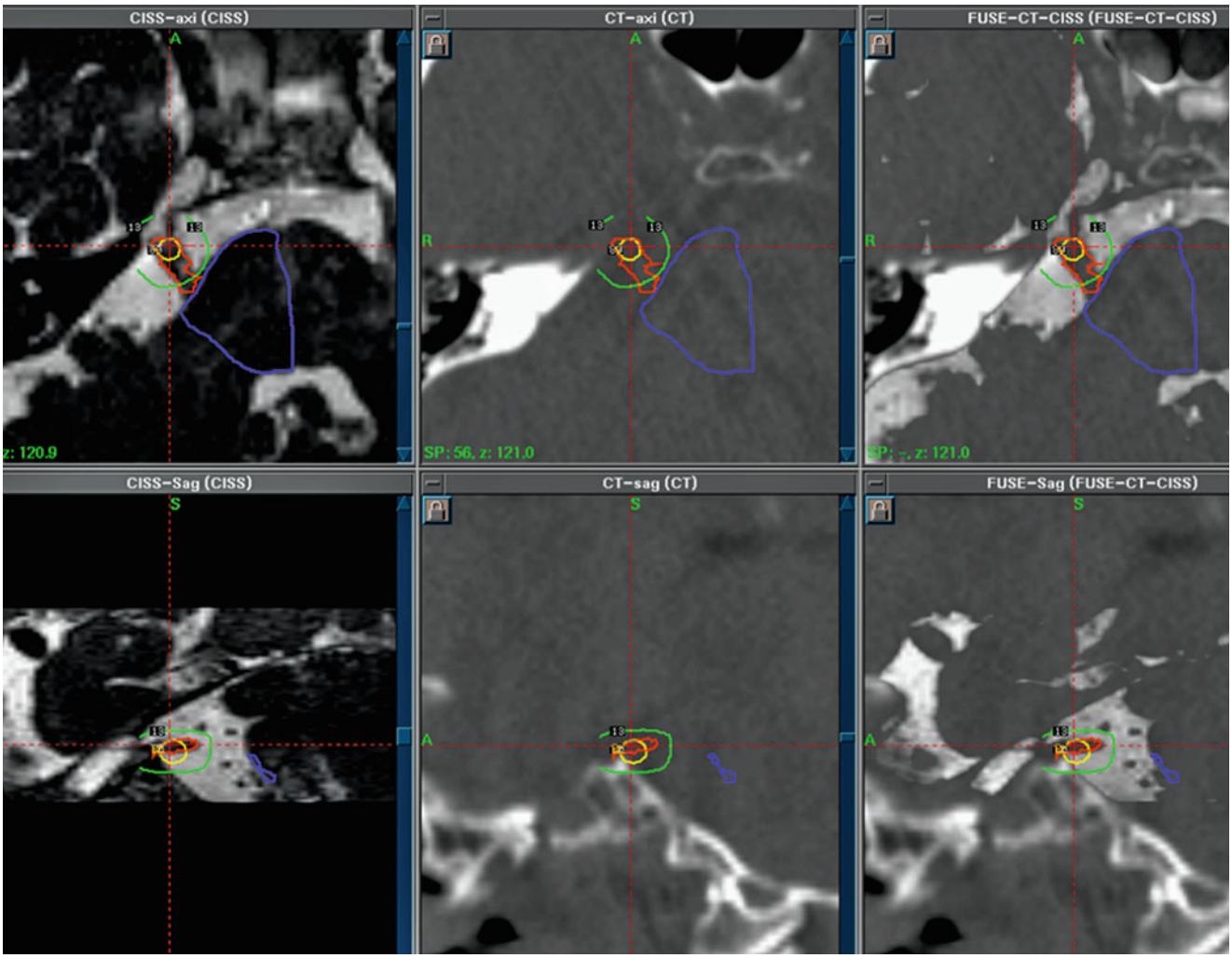

Fig. 1 Treatment planning shows the right trigerminal nerve targeted for Gamma Knife radiosurgery. The axial (*upper row*) and sagittal (*bottom row*) constructive interference in steady state magnetic resonance imaging (MRI) (*left*), bone window computed tomography (CT) (*center*), and fused MRI and CT (*right*) images are displayed. The *yellow* and *green lines* correspond to 80 and 13 % isodose lines, respectively. The *red line* delineates the trigeminal nerve, and the *blue line* depicts the adjacent half of the brain stem

Table 2 Barrow Neurological Institute Pain Intensity Scale

Score	Characteristics
I	No trigeminal pain, no medication
II	Occasional pain, not requiring medication
III	Some pain, adequately controlled with medication
IV	Some pain, not adequately controlled with medication
V	Severe pain/no pain relief

Table 3 Barrow Neurological Institute Facial Numbness Scale

Score	Characteristics
I	No facial numbness
II	Mild facial numbness, not bothersome
III	Facial numbness, somewhat bothersome
IV	Facial numbness, very bothersome

Results

Overall Pain Outcome

Patients were evaluated for up to 7 years after GKS, including 36 who were followed up for more than 5 years. Initially successful pain control (scores I–III) at some time point after GKS was observed following 89 of 91 procedures (97.8 %), with 47 (51.6 %) of patients being pain-free as determined by a BNI score of I and 75 (82.4 %) attaining pain control (scores of I–III). In contrast, 16 (17.6 %) were not adequately controlled with medication (score IV) at the time of the last follow-up. Successful pain control (scores I–III) at 2, 3, 4, 5, 6, and 7 years was achieved after 84 of 91 (92.3 %), 68 of 77 (88.3 %), 46 of 53 (86.8 %), 32 of 36 (88.9 %), 17 of 19

Table 4 Overall pain outcomes after GKS for trigeminal neuralgia

Follow-up duration and no. of cases	BNI pain intensity score and no. of cases	Pain control (BNI score I–III) (%)
2 years ($N=91$)	I ($N=50$)	92.3
	II ($N=12$)	
	III ($N=22$)	
	IV ($N=2$)	
	Recurrence ($N=5$)	
3 years ($N=77$)	I ($N=41$)	88.3
	II ($N=9$)	
	III ($N=18$)	
	IV ($N=1$)	
	Recurrence ($N=8$)	
4 years ($N=53$)	I ($N=26$)	86.8
	II ($N=6$)	
	III ($N=14$)	
	Recurrence ($N=7$)	
5 years ($N=36$)	I ($N=18$)	88.9
	II ($N=4$)	
	III ($N=10$)	
	Recurrence ($N=4$)	
6 years ($N=19$)	I ($N=9$)	89.5
	II ($N=2$)	
	III ($N=6$)	
	Recurrence ($N=2$)	
7 years ($N=7$)	I ($N=4$)	100
	III ($N=3$)	
	Recurrence ($N=0$)	

BNI Barrow Neurological Institute

(89.5 %), and 7 of 7 (100 %) procedures, respectively (Table 4). There were no significant differences in pain control rate between patients with and without previous surgery.

Trigeminal Nerve Dosimetry and Outcome

We divided patients into dosage groups, including 50 prescribed 90 Gy irradiation with or without plugging and 41 prescribed 75–88 Gy with or without plugging. With the use of GammaPlan we calculated the mean and integrated doses delivered to the target point. Successful pain control at the time of the last follow-up was achieved after 43 of 50 procedures (86.0 %) at 90 Gy, 12 of 15 (80.0 %) at 88 Gy, 17 of 22 (77.3 %) at 85 Gy, 2 of 3 (66.7 %) at 80 Gy, and 1 of 1 (100 %) at 75 Gy ($P>0.05$) (Table 5).

Table 5 Trigeminal nerve dosimetry and pain outcomes

Irradiation dose (Gy)	No. of patients	BNI pain intensity score					Pain control (%)
		I	II	III	IV	V	
90	50	27	5	11	7	0	86.0
88	15	8	2	2	3	0	80.0
85	22	10	2	5	5	0	77.3
80	3	2	0	0	1	0	66.7
75	1	0	0	1	0	0	100
Total	91	47	9	19	16	0	82.4

Distance from the Target to the Brain Stem and Outcome

We measured the distance from the emergence of the nerve at the brain stem to the surgical target. The most favorable

Table 6 Distance from the target to the brain stem and outcomes

Distance from the emergence of the trigeminal nerve at the brain stem to the GKS target (mm)	No. of cases	Mean irradiation dose	Pain control (%)	BNI facial numbness scores III + IV (%)
<6	10	86.3	8 (80.0)	1 (11.1)
6–7	22	87.2	18 (81.8)	2 (9.1)
7–8	25	88.6	20 (80.0)	4 (16.0)
8–9	21	88.2	18 (85.7)	4 (19.0)
9–10	4	87.8	3 (75.0)	1 (25.0)
10–11	3	90	3 (100)	1 (33.3)
11–12	3	90	2 (66.6)	2 (66.6)
12–13	3	89.6	3 (100)	1 (33.3)

GKS Gamma Knife surgery

Table 7 Trigeminal nerve dysfunction after GKS for trigeminal neuralgia

Analyzed variables	Patients without trigeminal nerve dysfunction	Patients with trigeminal nerve dysfunction	*P* value
Patient age at surgery (years)			
Median	60	70	0.010
Range	34–85	55–79	
Maximum irradiation dose (Gy)			
Median	88.1	87.8	0.740
Range	75–90	85–90	
Mean energy delivered to the nerve (mJ)			
Median	2.08	2.39	0.255
Range	0.6–4.4	1.1–3.7	
Cisternal volume of the trigeminal nerve (mm^3)			
Median	52.73	59.73	0.405
Range	9.1–131.9	16.5–101	
Distance from the emergence of the trigeminal nerve at the brain stem to the GKS target (mm)			
Median	7.53	8.52	0.052
Range	4.7–12.4	5.6–12.1	

outcome was observed at distances of 8–9 mm (85.7 % pain control rate), but there were no significant differences among groups ($P > 0.05$) (Table 6). Somewhat or very bothersome numbness (BNI facial numbness score III or IV) was mostly reported in patients with distances of >9 mm.

Trigeminal Nerve Dysfunction

Trigeminal nerve dysfunction was observed after 34 procedures (37.3 %), including 10 (11.0 %) with somewhat bothersome (BNI facial numbness score III) and 2 (2.2 %) with very bothersome (BNI facial numbness score IV) facial numbness. When we analyzed factors associated with trigeminal nerve dysfunction—patient age, maximum radiation dose, mean energy, cisternal volume of the trigeminal nerve, distance from the emergence of the nerve at the brain stem to the surgical target—we found that patient age at surgery ($p=0.010$) was the only factor related to facial nerve dysfunction (Table 7). When we analyzed the association between plugging and the development of trigeminal dysfunction, we found no association ($P > 0.05$).

Maintenance of Successful Pain Control

We also analyzed the duration of pain control after initial response in all patients using the Kaplan-Meier product limit method. Altogether, 14 recurrences were observed at

Table 8 Characteristics of patients with recurrence of pain

Patient no.	Sex	Date of GKS treatment	Age at the time of GKS (years)	Irradiation dose (Gy)	Initial BNI Pain Intensity Score	Duration of pain control until recurrence (months)	Additional treatment
1	F	2004-01-19	41	90	1	25	Medication
2	F	2004-09-17	56	80	1	62	Lost to follow-up
3	F	2005-09-21	71	90	3	13	Second GKS
4	M	2006-03-13	65	85	3	29	Second GKS
5	F	2006-06-12	59	85	1	58	Medication
6	F	2006-08-14	50	85	3	17	Second GKS
7	M	2006-09-29	66	85	3	56	Second GKS
8	M	2006-12-04	70	85	3	52	MVD
9	M	2006-12-04	65	88	3	28	MVD
10	F	2007-01-03	51	90	3	10	MVD
11	M	2007-04-23	68	90	3	30	Second GKS
12	F	2007-07-25	68	88	1	38	Medication
13	F	2008-04-25	72	90	3	18	Alcohol injection
14	F	2008-09-01	48	90	3	18	Second GKS

GKS Gamma Knife surgery, *MVD* microvascular decompression

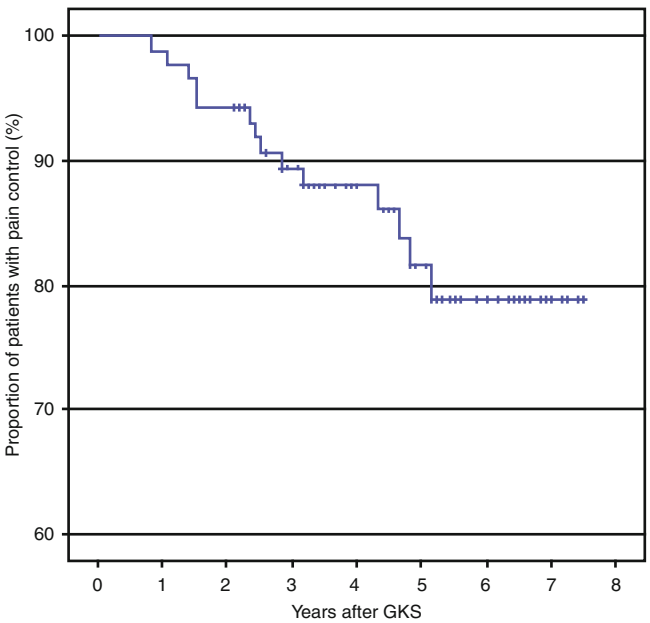

Fig. 2 Kaplan-Meier curve depicts the likelihood of maintaining successful pain control based on Barrow Neurological Institute (BNI) scores I–III after Gamma Knife radiosurgery (GKS) for trigeminal neuralgia. The actuarial rates of pain control at 2, 4, and 6 years were 93 %, 88 %, and 79 %, respectively

10–62 months after initial pain control. Six patients underwent a second GKS, three had MVD, one received an alcohol injection, and the remaining four continue to be managed pharmacologically with incomplete pain relief (Table 8). Results of an actuarial life-table analysis of clinical response are shown in Fig. 2. Successful pain control was achieved and maintained by 93.3 % of patients at 2 years, 88.4 % at 4 years, and 79.0 % at 6 years.

Discussion

Stereotactic irradiation of the trigeminal ganglion was first reported by Leksell [15] in 1951 as one of the earliest radiosurgical procedures. A focused dose of radiation was delivered concentrically to the trigeminal ganglion with an X-ray tube attached to a stereotactic arc-centered device, resulting in long-lasting pain relief [14]. Subsequently, the target of stereotactic radiosurgery was redirected to the proximal trigeminal nerve. This ablative procedure is the only minimally invasive technique that modifies the trigeminal pathway at the same site as modern microsurgery [8]. The first GKS treatment of classic TN in our medical center was performed in 1992, resulting in freedom from pain for 11 years.

Among the procedures used to treat patients with medically unresponsive TN there are various percutaneous techniques, MVD, and GKS. Gasserian ganglion percutaneous techniques, including RF thermocoagulation, balloon compression, and percutaneous glycerol rhizolysis, are all destructive. Postoperative pain relief with these procedures correlates with the degree of trigeminal injury. Therefore, almost half of these patients develop facial numbness, decreasing their quality of life [37]. These procedures are usually used on patients who are elderly, suffer from significant medical co-morbidities, or have recurrent facial pain after prior surgery [7, 28]. MVD is a nondestructive procedure in which the trigeminal nerve is decompressed, preserving its normal function; it has the lowest relative risk for recurrence and remains the gold standard of treatment [13]. It is, however, a major surgical procedure that entails craniotomy to reach the trigeminal nerve in the posterior fossa. Thus, its potential risks include postoperative morbidity and mortality including cerebrospinal fluid leakage,

aseptic meningitis, hearing loss, wound infection, stroke, and death [1]. Therefore, MVD is frequently recommended for young, healthy patients.

GKS is associated with a high rate of pain control, 68–97 % of patients having an excellent or good response, although efficacy results vary considerably among radiosurgical centers [2, 4, 5, 18–20, 25, 27, 30, 36]. Because patient preference has emerged as an important deciding factor, many patients choose GKS as the least invasive procedure for TN. In addition, GKS can be safely applied to patients who failed other methods. Initial pain relief after GKS has been observed in 94 % of patients, with 83 % having an excellent or good response at the last follow-up [20]. Similarly, we have shown here that 97.8 % of patients responded initially to treatment, with 82.4 % having successful pain control at the last follow-up (minimum 24 months) and GKS being equally effective in patients who failed other procedures.

Initially, GKS attempted to target the root entry zone (REZ) near its entry into the pons [16, 31, 32]. Selection of the proximal nerve and root entry zone as targets for low-dose irradiation was based on the observation of a critical region in which the central myelin (oligodendrocytes) is changed to peripheral myelin (Schwann cells) [11]. The target for the 50 % isodose line is the proximal nerve, with the dose to the pons being reduced. Because oligodendrocytes are more sensitive to irradiation than Schwann cells, a stronger radiobiological effect likely occurs at this portion of the proximal nerve. Also, the compact union of fibers from different divisions facilitates irradiation of the entire nerve with the smallest volume of energy. Since then, satisfactory results have been reported using this target with a dose of 80 Gy. Moreover, long-term results (up to 16 years) in 503 medically refractory patients with TN after MRI-guided GKS using a single 4-mm isocenter and a maximum dose of 80 Gy were presented [12]. Among these patients, 89 % achieved initial pain relief, with 80 %, 71 %, 46 %, and 30 % showing adequate control with medication (BNI scores of I–IIIb) after 1, 3, 5, and 10 years, respectively [12]. A total of 53 patients (10.5 %) developed new or increased subjective facial paresthesias or numbness and 1 (0.19 %) developed deafferentation pain [12].

Alternatively, targeting the retrogasserion zone of the trigeminal nerve, which is just posterior to the gasserian ganglion, is seemingly safer regarding brain stem injury. Of 100 patients with TN who were followed up for a minimum of 12 months after GKS with a median maximum dose of 85 Gy (range 70–90 Gy), 94 % experienced initial pain relief. At the last follow-up, only 69 % were pain-free without additional surgical treatment, and 57 % were free of medication for pain control [33, 35]. Of 130 patients with essential TN who were treated with the Leksell Gamma Knife model C and automatic positioning system (APS) and who followed for at least 24 months, 127 (98 %) experienced initial pain relief, and at the time of last follow-up 112 (86 %) were pain-free, including 86 (66 %) who remained both pain- and medication-free after the initial radiosurgery [9]. These outcomes may have been influenced by various technical nuances, suggesting that treatment should be performed using an updated device (the APS) and by physicians with sufficient expertise in the management of TN. One study found that posterior targeting (REZ) with 80 Gy resulted in better pain control and a lower complication rate [21]. Another study found that retrogasserian targeting resulted in better treatment success, with fewer bothersome complications [26].

Although we initially treated TN by targeting REZ using poor-quality MRI and a low radiation dose, unsatisfactory results we obtained resulted in a change to an retrogasserian target with improved MRI, a higher dose (maximum 90 Gy), and use of Gamma Knife model C with the APS system. Nowadays we consistently target the anterior portion of the trigeminal nerve just above the retrogasserian petrous bone using MRI and CT fusion images to minimize the risk of mislocalization due to distortion artifacts. The distance from the emergence of the nerve at the brain stem to the surgical target was related to the patient's cisternal volume. However, we could not find any statistically significant differences in outcomes related to that distance, although patients with distances of 8–9 mm had better outcomes. Other studies using the same target have found that distances of 5–8 mm [19] and 7.5–8.0 mm [35] are preferable. Nevertheless, the optimal target of GKS for TN remains to be determined.

Use of high maximum doses, up to 85–90 Gy, has been associated with improved pain control. For example, a comparison of two dose regimens (70 and 90 Gy) with a REZ target showed that higher doses correlated with better facial pain outcomes and significant trigeminal nerve dysfunction [29]. There is a tendency to prescribe a maximum of 80 Gy to a REZ target and a maximum of 90 Gy to the retrogasserian target, with doses adjusted to safe irradiation of the brain stem with or without plugging techniques. In our series, high doses were associated with a higher clinical control rate, but the correlation was not statistically significant. One young patient achieved excellent results with 75 Gy.

In contrast to other destructive percutaneous techniques, trigeminal nerve dysfunction was the only GKS-related morbidity and had an incidence ranged from 7 % to 49 %. The reason most patients do not have trigeminal nerve dysfunction after radiosurgery remains unclear. A significant association has been reported between radiation dose and the risk of trigeminal neuropathy, an association that may be related to the proximity of the brain stem [29, 30]. Dry eye syndrome was found to be significantly related to the irradiated brain stem volume with >12 Gy, suggesting that the affected volume should be kept to <28 mm^3 to avoid such a bothersome complication [22]. An analysis was conducted of three dosimetric strategies: <90 Gy and no selective beam channel

blocking (group 1); 90 Gy and no selective beam channel blocking (group 2); 90 Gy and selective beam channel blocking (group 3). The results indicated that the rates of good and excellent pain relief were 81 % and 66 %, respectively, for group 1; 85 % and 77 %, respectively, for group 2; and 90 % and 84 %, respectively, for group 3. The pain relief was related to the amount of energy received by the nerve root volume [20]. The prescribed dose and use of selective beam channel blocking were significantly associated with higher energy received by the retrogasserian trigeminal nerve root. Therefore, the radiobiological effect of GKS may be associated with the energy delivered to the nerve root volume rather than related to the maximum dose. High-dose irradiation of the proximal nerve root is potentially dangerous, with the anterior targeting method was found preferable for avoiding complications and for superior pain control [33]. Even with the distal targeting method, variable morbidity rates (10–44 %) and bothersome complications (0–12 %) were observed [9, 20]. In a study of 503 patients, the rate of trigeminal nerve dysfunction was 10.5 %, and one case of anesthesia dolorosa was reported [12]. It is unclear whether mild facial numbness, corresponding to BNI facial numbness score II, after GKS for TN should be considered a complication or a side effect corresponding to the pain response to treatment. We observed posttreatment trigeminal nerve dysfunction in 37 % of cases, including bothersome dysfunction in 13.2 %. Our statistical analysis showed that patient age at surgery was the only variable correlated with bothersome trigeminal nerve dysfunction. Other factors, including the irradiation dose, amount of delivered energy, intracisternal volume of the nerve root, and distance from the emergence of the trigeminal nerve at the brain stem to the GKS target, were not statistically significant.

Overall, our findings suggest that the long-term outcomes after GKS may be equivalent to those of MVD. Retrogasserian targeting of GKS may improve long-term results while reducing the complication rates.

Conclusion

Gamma Knife radiosurgery may be a reliable option for treating classic TN because it yields durable pain control in most patients and improves their quality of life with limited risk of complications. Our results can help medical practitioners to counsel their patients on the likelihood of achieving successful pain control. This analysis, however, is limited by its retrospective nature and small number of cases. Therefore, the presented findings should be validated in larger-scale, prospective studies.

Conflict of Interest The authors declare that they have no conflict of interest.

References

1. Barker FG, Jannetta PJ, Bissonette DJ, Larkins MV, Jho HD (1996) The long-term outcome of microvascular decompression for trigeminal neuralgia. N Engl J Med 334:1077–1083
2. Brisman R (2004) Gamma knife surgery with a dose of 75 to 76.8 Gray for trigeminal neuralgia. J Neurosurg 100:848–854
3. Fields HL (1996) Treatment of trigeminal neuralgia. N Engl J Med 334:1125–1126
4. Flickinger JC, Pollock BE, Kondziolka D, Phuong LK, Foote RL, Stafford SL, Lunsford LD (2001) Does increased nerve length within the treatment volume improve trigeminal neuralgia radiosurgery? A prospective double-blind, randomized study. Int J Radiat Oncol Biol Phys 51:449–454
5. Fountas KN, Lee GP, Smith JR (2006) Outcome of patients undergoing gamma knife stereotactic radiosurgery for medically refractory idiopathic trigeminal neuralgia: Medical College of Georgia's experience. Stereotact Funct Neurosurg 84:88–96
6. Greenberg M (1997) Handbook of neurosurgery, 4th edn. Greenberg Graphics, Lakeland, 964 p
7. Gronseth G, Cruccu G, Alksne J, Argoff C, Brainin M, Burchiel K, Nurmikko T, Zakrzewska JM (2008) Practice parameter: the diagnostic evaluation and treatment of trigeminal neuralgia (an evidence-based review): report of the Quality Standards Subcommittee of the American Academy of Neurology and the European Federation of Neurological Societies. Neurology 71:1183–1190
8. Guo S, Chao ST, Reuther AM, Barnett GH, Suh JH (2008) Review of the treatment of trigeminal neuralgia with gamma knife radiosurgery. Stereotact Funct Neurosurg 86:135–146
9. Hayashi M, Chernov M, Tamura N, Taira T, Izawa M, Yomo S, Nagai M, Chang CS, Ivanov P, Tamura M, Muragaki Y, Okada Y, Iseki H, Takakura K (2011) Stereotactic radiosurgery of essential trigeminal neuralgia using Leksell Gamma Knife model C with automatic positioning system: technical nuances and evaluation of outcome in 130 patients with at least 2 years follow-up after treatment. Neurosurg Rev 34:497–508
10. Kitt CA, Gruber K, Davis M, Woolf CJ, Levine JD (2000) Trigeminal neuralgia: opportunities for research and treatment. Pain 85:3–7
11. Kondziolka D, Lunsford LD, Flickinger JC, Young RF, Vermeulen S, Duma CM, Jacques DB, Rand RW, Regis J, Peragut JC, Manera L, Epstein MH, Lindquist C (1996) Stereotactic radiosurgery for trigeminal neuralgia: a multiinstitutional study using the gamma unit. J Neurosurg 84:940–945
12. Kondziolka D, Zorro O, Lobato-Polo J, Kano H, Flannery TJ, Flickinger JC, Lunsford LD (2010) Gamma Knife stereotactic radiosurgery for idiopathic trigeminal neuralgia. J Neurosurg 112:758–765
13. Koopman JS, de Vries LM, Dieleman JP, Huygen FJ, Stricker BH, Sturkenboom MC (2011) A nationwide study of three invasive treatments for trigeminal neuralgia. Pain 152:507–513
14. Leksell L (1968) Cerebral radiosurgery. I. Gammathalanotomy in two cases of intractable pain. Acta Chir Scand 134:585–595
15. Leksell L (1971) Sterotaxic radiosurgery in trigeminal neuralgia. Acta Chir Scand 137:311–314
16. Lindquist C, Kihlstrom L, Hellstrand E (1991) Functional neurosurgery – a future for the gamma knife? Stereotact Funct Neurosurg 57:72–81
17. Little AS, Shetter AG, Shetter ME, Bay C, Rogers CL (2008) Long-term pain response and quality of life in patients with typical trigeminal neuralgia treated with gamma knife stereotactic radiosurgery. Neurosurgery 63:915–924
18. Maesawa S, Salame C, Flickinger JC, Pirris S, Kondziolka D, Lunsford LD (2001) Clinical outcomes after stereotactic radiosurgery for idiopathic trigeminal neuralgia. J Neurosurg 94:14–20

19. Massager N, Lorenzoni J, Devriendt D, Desmedt F, Brotchi J, Levivier M (2004) Gamma knife surgery for idiopathic trigeminal neuralgia performed using a far-anterior cisternal target and a high dose of radiation. J Neurosurg 100:597–605
20. Massager N, Nissim O, Murata N, Devriendt D, Desmedt F, Vanderlinden B, Regis J, Levivier M (2006) Effect of beam channel plugging on the outcome of gamma knife radiosurgery for trigeminal neuralgia. Int J Radiat Oncol Biol Phys 65:1200–1205
21. Matsuda S, Serizawa T, Nagano O, Ono J (2008) Comparison of the results of 2 targeting methods in Gamma Knife surgery for trigeminal neuralgia. J Neurosurg 109(Suppl):185–189
22. Matsuda S, Serizawa T, Sato M, Ono J (2002) Gamma knife radiosurgery for trigeminal neuralgia: the dry-eye complication. J Neurosurg 97:525–528
23. McNatt SA, Yu C, Giannotta SL, Zee CS, Apuzzo ML, Petrovich Z (2005) Gamma knife radiosurgery for trigeminal neuralgia. Neurosurgery 56:1295–1303
24. Merskey H, Bogduk N (1994) Classification of chronic pain. Descriptions of chronic pain syndromes and definitions of pain terms. IASP Press, Seattle, pp 59–71
25. Nicol B, Regine WF, Courtney C, Meigooni A, Sanders M, Young B (2000) Gamma knife radiosurgery using 90 Gy for trigeminal neuralgia. J Neurosurg 93((Suppl) 3):152–154
26. Park SH, Hwang SK, Kang DH, Park J, Hwang JH, Sung JK (2010) The retrogasserian zone versus dorsal root entry zone: comparison of two targeting techniques of gamma knife radiosurgery for trigeminal neuralgia. Acta Neurochir (Wien) 152:1165–1170
27. Petit JH, Herman JM, Nagda S, DiBiase SJ, Chin LS (2003) Radiosurgical treatment of trigeminal neuralgia: evaluating quality of life and treatment outcomes. Int J Radiat Oncol Biol Phys 56: 1147–1153
28. Pollock BE, Ecker RD (2005) A prospective cost-effectiveness study of trigeminal neuralgia surgery. Clin J Pain 21:317–322
29. Pollock BE, Phuong LK, Foote RL, Stafford SL, Gorman DA (2001) High-dose trigeminal neuralgia radiosurgery associated with increased risk of trigeminal nerve dysfunction. Neurosurgery 49:58–64
30. Pollock BE, Phuong LK, Gorman DA, Foote RL, Stafford SL (2002) Stereotactic radiosurgery for idiopathic trigeminal neuralgia. J Neurosurg 97:347–353
31. Rand RW (1997) Leksell Gamma Knife treatment of tic douloureux. Neurosurg Clin N Am 8:75–78
32. Rand RW, Jacques DB, Melbye RW, Copcutt BG, Levenick MN, Fisher MR (1993) Leksell Gamma Knife treatment of tic douloureux. Stereotact Funct Neurosurg 61(Suppl 1):93–102
33. Regis J (2002) High-dose trigeminal neuralgia radiosurgery associated with increased risk of trigeminal nerve dysfunction. Neurosurgery 50:1401–1402; author reply 1402–1403
34. Regis J, Arkha Y, Yomo S, Murata N, Roussel P, Donnet A, Peragut JC (2009) Radiosurgery in trigeminal neuralgia: long-term results and influence of operative nuances. Neurochirurgie 55:213–222 (in French)
35. Regis J, Metellus P, Hayashi M, Roussel P, Donnet A, Bille-Turc F (2006) Prospective controlled trial of gamma knife surgery for essential trigeminal neuralgia. J Neurosurg 104:913–924
36. Young RF, Vermeulen SS, Grimm P, Blasko J, Posewitz A (1997) Gamma Knife radiosurgery for treatment of trigeminal neuralgia: idiopathic and tumor related. Neurology 48:608–614
37. Zakrzewska JM, Jassim S, Bulman JS (1999) A prospective, longitudinal study on patients with trigeminal neuralgia who underwent radiofrequency thermocoagulation of the Gasserian ganglion. Pain 79:51–58

Complications of Gamma Knife Neurosurgery and Their Appropriate Management

Jeremy C. Ganz

Abstract There are four main risks with Gamma Knife neurosurgery. Firstly, there are direct complications that would not have arisen if the patient had not undergone the specific treatment under consideration. For radiosurgery, the direct complications are radiation-induced damage to the tissues, which may be temporary or permanent. They may be expressed clinically or be clinically silent. In addition, there are complications that are specific to certain diseases and their locations, such as pituitary failure following treatment of pituitary adenomas and deafness, facial palsy, or trigeminal deficit following the treatment of vestibular schwannomas. Second, there are indirect or management-related complications arising from delayed control of the disease process, such as a re-bleed after treatment of a vascular lesion before its occlusion. Third, there is the risk of induction of neoplasia from irradiation of normal tissue or tumor. These are separate processes. An example of the first would be induction of a glioma after treatment of a vascular malformation. An example of the second would be induction of malignant change in a benign vestibular schwannoma. Finally, there is treatment failure, where tumors continue to grow after treatment or vascular malformations fail to occlude.

Keywords Adverse radiation effects • Radiation-induced neoplasia • Radiotoxicity

Introduction

The overriding principle regarding patient management is ascribed to Hippocrates, who wrote in his "Epidemics" (not as supposed in The Oath) "σκέειν, περὶ τὰ νουσήματα, δύο, ὠφελέειν, ἡ μὴ βλάπτειν" which is translated as: "As to diseases, make a habit of two things—to help, or at least to do no harm." This is often referred to as "Primum non nocere" (First do no harm) probably because we are more familiar with Latin than with Greek. Yet there is no reason to believe the authors of the "Hippocratic Corpus" knew any Latin. An alternative explanation has been that Galen was responsible for "Primum non nocere." However, although Galen may have lived and worked in Rome for many years, he was also Greek and wrote in Greek. Hence, this supposition is not based on clear evidence. Thus, the derivation and attribution of this crucial aphorism is muddled. The same can sometimes be true of the way we assess the risks of a management strategy.

The risk of complications must be weighed against the risk posed by the untreated disease. Although overly cautious treatment may reduce the incidence of treatment-related complications, it may provide inadequate protection from the disease process. Thus, the "harm" from the disease must be considered together with the "harm" from the treatment. To ignore the risks of inadequately treated disease to ensure avoidance of treatment-induced complications is to fail to think clearly.

There is another related difficulty that is not easy to quantify and control. It is the communication of the risks and dangers to the patient. These risks must be discussed with the patient or, where appropriate, the relatives so those affected by the treatment are in a position to make responsible choices. This is not an easy process because the patient perceives the situation from the individual's point of view, whereas the physician can only give advice based on statistical material. Thus, a degree of residual uncertainty is unavoidable. The patient's final choices are inevitably swayed by emotional factors, some of which are based on his/her personal feelings about his/her physician.

There are four main phenomena following a treatment that in different ways may be considered complications. First, there are direct complications that would not have arisen if the patient had not received the specific treatment under consideration. For radiosurgery, the direct complications are radiation-induced damage to normal tissues, which

J.C. Ganz
Department of Neurosurgery, Haukeland University Hospital, Bergen, Norway

53 Market Street, Ulverston, LA12 7LT, UK
e-mail: jcganz@gmail.com

M.F. Chernov et al. (eds.), *Gamma Knife Neurosurgery in the Management of Intracranial Disorders*,
Acta Neurochirurgica Supplement, Vol. 116, DOI 10.1007/978-3-7091-1376-9_21, © Springer-Verlag Wien 2013

may be temporary or permanent and may be expressed clinically or be clinically silent. In addition, temporary swelling of the pathological tissues of tumors sometimes occurs, which may be associated with marked edema in the surrounding brain. This process occurs most commonly in metastases and occasionally in meningiomas. This is a separate process from direct radiation damage to the brain or other intracranial structures. Second, there are management-related complications arising from inadequate control of the disease process. In the context of radiosurgery, the best known management complication is a re-bleed after treating a vascular lesion before that lesion is occluded. There is the risk of induction of neoplasia from irradiation of normal tissue or tumor. These are separate processes. An example of the first would be induction of a glioma after treatment of a vascular malformation. An example of the second would be induction of malignant change in a benign vestibular schwannoma. Finally, there is treatment failure, where tumors continue to grow after treatment or vascular malformations fail to occlude. Although it is necessary to mention this last factor for the sake of clarity, it falls outside the scope of the present article.

Radiotoxicity of Normal Brain

The commonest complication following any irradiation is damage to normal tissue because of exposure to excess radiation. Several treatment parameters are involved in this form of damage, including dose, dose volume, dose rate, and tissue radiosensitivity. They are considered one by one, except for radiosensitivity, which at the time of writing cannot be measured. The basic principle of managing radiotoxicity is that prevention is better than cure, and every attempt is made to limit the amount of radiation absorbed in healthy tissue. Because there is no low safe radiation dose threshold, this can never be completely achieved, but the normal tissue dose can still be kept as low as possible. The following parameters affect the dose to normal tissue.

Prescription Dose

The prescription dose is the dose to the target margin. It is selected on the basis of known effective therapeutic doses and the known risk of complications. For example, the high risk of morbidity and mortality from untreated arteriovenous malformations (AVMs) means that a dose of 16–25 Gy is commonly used and adjusted according to the volume of the lesion. This practice is associated with a risk of temporary clinical complications of about 10 % and of permanent complications of about 3 %. These risks are considered acceptable given the 30 % mortality associated with untreated AVMs over 30 years. The problem is that the complications occur early.

Although the prescription dose to the target is determined on the basis of information in the literature, the distribution of that dose must be optimized on the day of treatment. The dose should be limited as far as possible to the target with minimum spread to the tissues. How this is done is described later.

Dose Volume

It has long been appreciated that the volume of a target is an important determinant of the success of radiotherapy on that target. In general, larger targets do less well than smaller targets. On the other hand, it is known that for the same dose the larger the volume of tissue receiving the dose the greater is the chance of radiotoxicity complications from that dose. Dose volume may be defined, for convenience, as the volume within a given isodose. Its significance can be demonstrated as follows. Whereas 5 Gy to the whole human body is usually lethal, 5 Gy to a tumor volume is wholly inadequate. Indeed, fractionated doses of up to 50 Gy can be tolerated with gastrointestinal cancer while it is the gastrointestinal tract, which is one of the main victims of whole-body irradiation. Moreover, considerations of volume must be made within the bounds of a single species. Some insects and bacteria can survive radiation doses greatly in excess of those tolerated by mammals.

Within the brain, the volume of normal brain receiving a high dose of radiation is crucial to the development of adverse radiation effects. This is the factor that limits the volume of the target that can be safely treated by radiosurgery. However, the permissible volume that can be treated has been on the increase over the years with the use of repeated partial treatments on the one hand and the reduction of the prescription dose on the other. Although a target diameter of 2.5–3.0 cm remains a reasonable guideline, there are ways to treat larger lesions, provided the dose to sensitive adjacent tissues is kept within acceptable bounds.

How does an increasing target volume increase the risk of radiotoxicity? As the target volume increases, surrounding tissue is put at risk in two ways. This is made easier to understand if one considers the cells in a notional shell 1 mm thick immediately outside the target. If it is accepted that the cells in the tissue are mainly of the same size, the number of cells in, for example, a 1-mm shell at risk from the highest dose outside the target has to be larger with a larger target volume. However, there is a second factor that increases the number of cells at risk. With larger volumes, the gradient of the dose falling outside the target is less steep than with smaller volumes, irrespective of the radiosurgery treatment technology used. Thus, the dose at the outside of a 1-mm shell with a diameter of 3 cm is not placed 1 mm outside the target margin with a larger-volume target but farther away. This means that

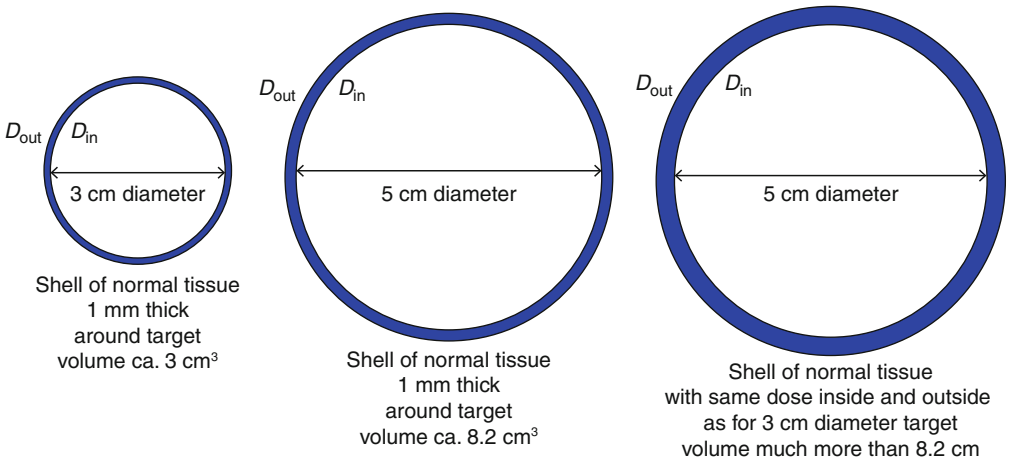

Fig. 1 Effect of the target volume on normal tissue at risk. A notional 1-mm shell of tissue around a target is drawn. The maximum dose is in the inside of the shell (D_{in}). On the outside of the shell is a significant, although lower, dose (D_{out}). Assuming that the cell size is the same in each of these shells, the number of cells at risk of radiation damage with a large target is substantially more than the number in a smaller target. However, because the dose is decreased with a bigger target, with all existing treatment methods it is not as steep as with a smaller target. This then increases the number of cells exposed to the dose between D_{out} and D_{in}. This mechanism underlies the increased risk of radiation damage in patients with a large lesion (target)

the shell between the two doses is wider for a larger target volume, which further increases the number of cells at risk for a toxic radiation dose. The principle is illustrated on Fig. 1.

Dose Rate

Dose rate is the dose per unit time. Between 1 Gy/min and 0.01 Gy/min there is a gradual falloff in the biological effectiveness of a given dose. Increasing or decreasing the dose rate beyond these limits has little extra effect. The mechanism behind the dose rate effect is attributed to the speed of repair processes in the affected cell. Radiation damage occurs in microseconds. Repair processes take several hours. With lower dose rates, there is a bigger chance for repair for a given dose. Dose rate calculations become important when the radiation source is an isotope, where the age of the isotope has reduced the dose rate to <1 Gy/min.

The half-life of ^{60}Co is 5.27 years. This means that with the passage of time the dose rate for the Gamma Knife is steadily decreasing. Put another way, the same treatment with the same dose takes longer and longer the older the machine becomes. There is some anecdotal evidence that reducing the dose rate reduces the biological effectiveness of Gamma Knife surgery (GKS), especially if the dose is <1 Gy/min. Doses as low as this are found at the lesion's edge even with a fairly new Gamma Knife, although their significance is not clear at this time. However, as the results of GKS are so good, it seems unlikely that a low dose rate within the target is of any great importance.

One advantage of the geometry of the Gamma Knife is that because a lower isodose is associated with a lower dose rate a measure of extra protection is provided for the normal tissue outside the target volume. This is because the maximum dose rate is set by the activity level of the gamma source. Thus, for a single shot, the dose rate at the 50 % isodose is half that at the dose center, and the dose rate farther out from the center decreases in proportion. This means that with a dose of 100 Gy at the center and a 3 Gy/min dose rate, the dose rate at the 50 % isodose is 1.5 Gy/min and at the 10 % isodose it is 0.3 Gy/min, which is a dose rate low enough to reduce the effectiveness of the dose, thereby producing a measure of extra protection in the surrounding tissue.

Measuring the effect of the dose rate in clinical series has not been possible until recently because Gamma Knife treatment involved periods of irradiation and periods of frame adjustment. Only since the introduction of the Gamma Knife Perfexion, which enables continuous treatment, has it been possible to calculate the dose rate. To date, there is no work to suggest that it is crucial for treatment. However, the dose rate does determine the time at which it is necessary to renew the radioactive cobalt. Although there is no hard evidence that the lower dose rate with the aging isotope affects the results, the falling dose rate leads to longer and longer treatment times, which eventually become impractical.

Other Dose Parameters

A variety of formalisms have been derived to facilitate an optimal dose distribution and to increase the consistency of treatment. The usual procedure is to determine the target volume and prescription dose. Then these formulas are used to optimize the distribution of the dose in each particular case [11].

Dose Conformity

This parameter reflects the match between the shape of the dose and the shape of the target. However, it does not contain a parameter for location, so its adequacy is dependent on the care and awareness of the users. Ian Paddick introduced a refinement that resulted in the dose being located in the right place if his formula is used.

The conventional formula for dose conformity is:

$$\text{PITV} = \frac{\text{PIV}}{\text{TV}}$$

where PIV is the volume of the prescription isodose, and TV is the target volume.

Paddick's modification is shown below.

$$\frac{\text{TV}_{\text{PIV}}{}^{2}}{\text{TV} \times \text{PIV}}$$

This contains the new parameter, $\text{TV}_{\text{PIV,}}$ which is the volume of the prescription dose within the target. This variable compels the dose to be in the right place.

Dose Selectivity

This parameter is a simple measure that compares the volume of the treatment isodose and the volume of the dose that is within the target. The formula is as follows.

$$\frac{\text{TV}_{\text{PIV}}}{\text{PIV}}$$

This formula also includes TV_{PIV}, which again means that the measurements are related to the radiation dose within the target.

Gradient Index

This measures the steepness of the dose fall. The formula is as follows.

$$\frac{\text{PIV}_{(x/2)\%}}{\text{PIV}_{x\%}}$$

where $x\%$ is the isodose that carries the prescription isodose, and $(x/2)\%$ is the isodose carrying half that dose. Thus, in a typical situation, x would be 50 % and $x/2$ would be 25 %.

The indices do *not* tell what dose to normal tissue is acceptable. They merely help keep that dose to a minimum. The following guidelines are a reasonable starting point.

Target cover	Presciption dose within the target (PIV) ≥ 95 %.
1/Conformity Index	This value should not exceed 1.05 and does not if the target cover is >95 %.
1/Selectivity	This should not exceed 1.25.
Gradient Index	This should be <3.

Radiation-Induced Swelling of Pathological Tissue

Radiation-induced swelling of pathological tissue is considered later with the complications related to individual diagnoses.

Avoiding Radiotoxicity

To avoid radiotoxicity, the dose should be as low as is consistent with therapeutic success. Targets should be of a volume consistent with minimizing damage to normal tissue. Dose planning should be optimized using available formulas to ensure correct placement and distribution of the therapeutic radiation dose. Other means of limiting radiation damage are discussed under the sections on individual diseases.

Induction of Malignancy

Induction of malignancy is the other potential non-specific direct complication that would not arise if the treatment had not been given. There is no clear agreement about the incidence. The first difficulty is recording that a malignancy has occurred in a patient who has undergone GKS. There is no certainty that every patient will come to the attention of the treating doctor, particularly if the malignancy develops a long time after the GKS. In principle, the induction of a new tumor by GKS although not impossible is improbable. The Gamma Knife supplies a high dose to a low-volume target. With the rapid dose fall outside the target, the adjacent low-dose volume is low. Neoplasia induction is typically found following low-dose delivery to high volumes of tissue. The large volume and relatively low dose increase the chance that an oncogenic mutation may take place. With high doses the chance of such a mutation are substantially reduced as the radiation is more likely to induce cell death at higher doses. The low volume of the radiation dose outside a target reduces the number of cells at risk for an oncogenic mutation.

Induction of a New Tumor

The difficulty of establishing a causal relation between radiation exposure and the subsequent development of a malignancy can be shown by examining those exposed to a higher radiation dose as a result of their occupation. Because oncogenesis is always multifactorial, it does not lend itself to simple definitions of cause and effect. Any study of a relationship between an agent and the development of a neoplasm is an exercise in the assessment of probabilities. This can be illustrated by considering some natural assumptions about the risks from exposure to occupational radiation. There is no convincing evidence to date that the risk of developing cancer is increased by working in a nuclear power plant, by being an astronaut, or even working as a diagnostic radiologist [5, 16, 36]. The authors of one study published the rather absurd finding that in the U.S. Air Force, in an age-adjusted study, military rank carried a greater risk of developing a brain tumor than did exposure to ionizing radiation [16]. Brain tumors seem to be highly unlikely to develop after exposure to environmental radiation, even in high doses. Authors of publications concerning the survivors of the two nuclear explosions at Hiroshima and Nagasaki have reported an increased incidence only of meningiomas in long-term survivors [31, 35], but there has been no report of any other brain tumor despite many reports of oncogenesis affecting other tissues. To codify the problem of the causal relation between radiotherapy and the subsequent development of a tumor, guidelines were drawn up many years ago by Cahan et al. [6] and have come to be known as the Cahan rules. For a postirradiation tumor to be considered a consequence of that treatment:

1. It must occur within the original radiation field.
2. It must not be present prior to irradiation.
3. There must be a histological difference between the primary and the induced tumor.
4. There must be no known genetic predisposition for secondary malignancy.

It should be borne in mind that Cahan's rules are guidelines, not natural laws.

In 2002, the author outlined three cases from the literature that could have been the result of radiation induction following Gamma Knife treatment [10]. If all three were accepted as true cases of neoplastic induction, it would have amounted to a total prevalence of 3/200,000 GKS-treated patients. More cases have been reported subsequently, but the incidence remains uncertain. Moreover, there is broad agreement that this phenomenon is rare and is not a reason to change current practice. Among these later reports, Loeffler reported two more cases associated with acromegaly [24], but the patients were treated with a particle accelerator, not a Gamma Knife. In one case a parasellar meningioma was observed. In the other, a tumor was observed in the internal auditory canal. The Sheffield group showed that with a cohort of approximately 5000 patients with 30,000 patient-years of follow-up and with more than 1200 patients having a follow-up period longer than 10 years the incidence of astrocytomas was below the national average in the United Kingdom [30]. It should be noted that the quoted risk figures in the literature vary widely from this author's low risk figures [10] to risk assessments from others that are much higher [26, 33]. None of the figures should be taken as other than an informed guess. The point is that some patients should be informed that there is a tiny risk for developing a secondary malignancy. However, the occurrence is so rare and the statistics in consequence so unreliable, that it remains a matter of judgment as to which patient would be best served by imparting information about these risks.

Transformation of a Benign Tumor

Transformation of a benign tumor is a different and also rare phenomenon and in practice is limited to vestibular schwannomas [1, 7, 17, 27, 34]. Spontaneous malignant change of a known benign vestibular schwannoma has been recorded only twice in the literature [7]. Of the cases where such transformation occurred after radiosurgery, not all were simple benign schwannomas. There is one case of neurofibromatosis type 2 (NF2) being treated without biopsy that subsequently became malignant after treatment [3]. This is clearly a situation where the risk of malignancy is increased even without treatment. Cahan's rules do not apply to malignant transformation of a vestibular schwannoma because it concerns change in a preexisting tumor so rule 3 is not applicable. Indeed, in the case of NF2, rule 4 is not applicable either. The possibility of this malignant transformation is not something that can be avoided. However, it does impose a duty to keep meticulous records to improve the documentation of therapeutic activity. However, at the end of the day, the extreme rarity of postradiosurgery malignant transformation of a vestibular schwannoma is such that there would seem to be no need to change current practice.

Ethnicity and Induction of Malignant Transformation

One curiosity may be mentioned. A comprehensive database of more than 6700 articles on radiosurgery maintained by this author was searched with the terms "malignant transformation," "malignant change," "carcinogen," and "transformation." There were numerous articles on this topic from the

United States, the United Kingdom, Canada, France, Japan, and Korea. An article from the United States was a review, not a report [27]. Another reports on meningiomas, which are a somewhat different problem as they are the one intracranial tumor known to be induced by radiation [33]. The US article mentioned above concerns a particle accelerator, not a Gamma Knife, and again one of the tumors was a meningioma [24]. A fourth US article reported a glioma induced after treatment of an AVM using a LINAC [4]. One US case was not included here as the technique used was fractionated stereotactic radiotherapy [25]. One UK article reported malignant transformation of an NF2 vestibular schwannoma [3]. Another analyzed the incidence of new malignancy in a large population of patients who had undergone GKS and found it slightly lower than in the general population [30]. The third examined malignant transformation of vestibular schwannomas in the light of a single case and a review of the literature [7]. An article from France reviewed the literature and reported one glioma and one malignant change in a vestibular schwannoma [26]. A Canadian article reported induction of a glioma after treatment of a vestibular schwannoma using fractionated stereotactic radiotherapy to the internal acoustic meatus following recurrence of a radically operated tumor [32]. The other article from Canada reviewed almost all reported cases and reported a convincing new case with a temporal lobe glioblastoma after treatment of a vestibular schwannoma [2]. There were reports of ten cases related to malignant transformation or malignancy induction from Japan [1, 17–20, 22, 34, 38–40]. There was a single case from Korea [41]. From experience with germinomas, it is well known that neoplasia patterns in some Asian populations differ from those in Occidental populations. Only Kubo et al. cast doubt on the relation between radiosurgery and malignant induction [22]. The other eight articles reported new cases [1, 17–20, 34, 38–40] for a total of 11 cases in Japan and Korea combined. Is it possible that Japanese and/or Korean people are more susceptible to radiation-induced malignant complications than Occidentals? In view of the distribution of articles on this topic it seems not unreasonable to look further into ethnicity in relation to risk in this context.

Region/Diagnosis Specific Complications

The principle of prevention is better than cure guides therapeutic practice. Where possible, attempts have been made to derive helpful mathematical formalisms. These could in principle guide the physician as to the appropriate dose for a given patient. However, none has achieved universal acceptance, and all of them have problems of one sort or another.

Arteriovenous Malformations [13]

The commonest tissue to be affected with these lesions is cerebral tissue. In view of the high doses required to achieve an adequate occlusion rate, many attempts have been made to calculate risk. Most calculate the degree of risk at the time of treatment and attempt to edit the dose plan to minimize this risk. Today, perhaps the most useful of these methods is the volume of normal tissue receiving 12 Gy. To some extent, if adjusted for different locations, this can be helpful. Every effort is made to minimize the 12 Gy volume, particularly if the brain stem is involved in the radiation field. The maximum acceptable volume of this parameter remains unknown. Thus, the surgeon must still make an assessment of risk versus benefit based on experience rather than calculation. The 12 Gy volume is just another way of assisting the process, but it is not definitive.

Nonetheless, while realizing the limits of the 12 Gy volume, there is in fact another assessment that can be made prior to treatment and that is not dependent on treatment parameters. It arose when it was found that the conventional method of assessing risks from surgical intervention—the Spetzler-Martin Classification—was not useful for GKS.

Spetzler-Martin Grade [37]

Parameter	Points
Size of lesion	
Small (< 3 cm)	1
Medium (3–6 cm)	2
Large (> 6 cm)	3
Location	
Noneloquent site	0
Eloquent site	1
Pattern of venous drainage	
Superficial only	0
Any deep	1

The Spetzler-Martin grade equals the sum of the points (maximum is grade 5). The application of this system to radiosurgery is not completely straightforward for the following reasons. First, grade I (small) ranges from 0 to 3 cm in diameter. That basically encompasses the entire range of volumes treated with GKS and all within one subsection. The other factor that does not work so well for radiosurgery is the eloquent site. It is designed so the motor cortex, basal ganglia, and brain stem all have the same value. The experience of radiosurgery indicates that treatment of superficial lesions is much less likely to produce a radiation-induced complication than treatment of deeper lesions. This is presumably related to the dispersal of function in a superficial location.

Therefore, a new system was devised for assessing patients due to udergo GKS.

AVM score [29] = (0.1)(AVM volume in cm^3) + 0.02(patient age in years) + 0.5(location)

Locations were scored as follows: deep, 1; other, 0.

The approximate AVM volume is derived from the following formula [28].

AVM volume prior to treatment = $(\pi/6) \times$ width $\times$ length $\times$ height.

The scoring system has been found useful. Scores of ≤1.5 for deep-seated AVMs had a noticeably better outcome than those with higher scores [28, 29]. Moreover, this simple score can be derived before the patient is taken in for treatment.

The scores correlated well with excellent outcomes and deterioration of the modified Rankin score [28, 29], a sensitive scoring system for clinical neurological function as shown below.

Modified Rankin Score	
0	No symptoms
1	No significant disability despite symptoms; able to carry out all usual duties and activities
2	Slight disability; unable to carry out all previous activities but able to look after own affairs without assistance
3	Moderate disability; requires some help but able to walk without assistance
4	Moderately severe disability; unable to walk without assistance and unable to attend to own bodily needs without assistance
5	Severe disability; bedridden, incontinent, and requires constant nursing care and attention
6	Dead

These various methods enable the Gamma Knife user to optimize the dose plan, but final decisions on patient selection and the dose to be used, with the current state of knowledge, is still determined from the clinical context, the AVM volume, and location and the experience of the surgeon.

Finally, there is the risk of complications associated with inadequately treated disease, including morbidity and death from a re-bleed. This is not something that can be treated as it occurs suddenly and unexpectedly. Although wholly undesirable, the risk of this complication is only around 2.5 %, which is again much lower than the risks associated with the untreated disease [23].

Tumors of the Pituitary Region [12]

Tumors of the pituitary region include most often pituitary adenomas, meningiomas, and craniopharyngiomas. The visual pathways are at risk for all these diagnoses. There has been much discussion about the optimal dose to these pathways. Recently there has been cogent evidence indicating that 10 Gy should be easily tolerated [14]. However, this statement is subject to certain stringent conditions. The 10 Gy referred to is the maximum dose within the volume of the anterior visual pathways as measured in the Leksell GammaPlan. The evidence suggests that measured in this way the dose is safe [12]. However, in certain circumstances it may be higher. There is no need to have a distance between the target and visual pathways. It is simply necessary to shape the dose plan away from the visual fibers and accept that a small portion of the target will receive a suboptimal dose. In addition, a slightly excessive dose is permitted provided the volume receiving >10 Gy does not exceed 9 mm^3.

It can be difficult to visualize the visual pathways in individual patients, particularly those with operated craniopharyngiomas. Every attempt must be made to achieve optimal images. In the case of pituitary adenomas, there can be real difficulty determining the outline of the tumor. It can be advantageous to have T1-weighted magnetic resonance imaging (MRI) scans with and without contrast in the axial and coronal planes, especially if the patient has previously been operated on. The unenhanced images are often surprisingly informative as to tumor detail.

With pituitary adenomas, there is the additional problem of pituitary failure. This evenuality has been analyzed carefully in recent years. The problem is that whereas the pituitary adenoma as a tumor is fairly easy to control with a moderate dose, endocrinopathies require a much higher dose, which inevitably affects the normal residual anterior lobe tissue. Hypopituitarism is not uncommon, with its reported incidence varying from 10 % to 50 % depending on pretreatment function, tumor dose, and tumor volume [10]. Although unwanted, these conditions are treatable. It may be a necessary price to pay for normalizing hypersecretion of a particular hormone.

Vestibular Schwannomas

The commonest complications of GKS for vestibular schwannomas are facial palsy, trigeminal deficit, and hearing loss. In the early days, prior the introduction of MRI and the GammaPlan dose planning system, the complication rate was quite high. Also, the prescription dose was higher back then. Today most users aim at a dose of 12–14 Gy. Moreover, nowadays it is unusual to find a facial palsy rate reported that is more than 1 %, and nearly all of the palsies are temporary. Trigeminal deficits are now reported in 0–12 % of cases, without satisfactory explanations for the differences among centers. The problem of hearing loss has greatly diminished. If one considers useful hearing, classified as Gardner-Robertson classes I and II, the preservation rate was reported

recently to be 50–75 %. This improvement is partly related to more accurate dose planning with GammaPlan and MRI. The introduction of CISS MRI with gadolinium provides improved definition of the nerves in the subarachnoid space with small tumors. Another contributing factor is dose planning aimed at excluding the cochlea. Today, the recommended dose to the cochlea should not exceed 4 Gy. However, the ability to achieve this aim and at the same provide adequate radiation cover of the tumor is dependent on the lateral extent of schwannoma in the internal auditory meatus.

Cerebral Metastases

With cerebral metastases, the commonest practical problem is interpreting increased tumor volume after treatment. Is it due to growth or radionecrosis? A recent article made answering this question much easier by comparing T2-weighted images with T1-weighted images with contrast. If the extent and clarity of the lesion is similar in both image series, the greatest chance is that it is a recurrent or uncontrolled tumor. If the lesions do not match and the margins are less clearly defined, it is most likely radionecrosis [21]. There are other methods for achieving the same aim, but none seems to be more reliable and certainly none is as simple in practice. Other problems relating to metastases are the usual radiotoxicity described above. In general, to avoid this complication, the total tumor volume of all the tumors should not exceed 20 cm^3 and the tumor margin dose should not exceed 20 Gy. These tumors are life-threatening, so lower doses should be avoided if possible. It must be understood that not all patients are suitable for GKS. However, at the time of writing, the problem is rather the other way around in that many patients who could be treated with GKS are for various reasons not referred.

Meningiomas

In a small number of cases, meningiomas exhibit clinically significant swelling after radiosurgery. This phenomenon was observed in an unusual patient who was treated for a posterior midline meningioma that lay just under the skin near the torcula as at surgery the bone flap had been removed and never replaced. For a few weeks, the tumor swelled up and was hot and hard before regressing again. This phenomenon may explain the higher morbidity in nonbasal meningiomas where tumor swelling can compress cerebral veins [8]. In addition, tumor swelling visible on MRI has been observed in a few tumors. It can produce dramatic symptoms of elevated intracranial pressure and local compression, but it usually responds well to dexamethasone [9].

Trigeminal Neuralgia

Trigeminal neuralgia is a satisfactory indication for GKS. There have been only a few reports of bothersome posttreatment neurological deficits, which have included hypesthesia and hypalgesia of the face. Dry eye has been reported but can be avoided with suitable dosimetry. The greatest strength of the treatment is its low morbidity rate—not least the virtual absence of anesthesia dolorosa. Its greatest weakness is the delay between treatment and results as well as a recurrence rate that is quite high. The treatment may be repeated and seems to be an excellent interventional treatment, even a possible first choice. However, this condition has multiple treatment options, and there is naturally a debate as to the optimal choice.

Epilepsy

In keeping with other surgical techniques, GKS seems best suited for mesial temporal lobe epilepsy. It may also have a role to play in the treatment of epilepsy associated with hypothalamic hamartomas. However, there are complications associated with it, which makes it more appropriate for research centers than as a suitable method for general use. Two cases of life-threatening radionecrosis have been reported [15]. Also, many patients have required dexamethasone for brain swelling about a year after treatment.

It has been reasonably suggested that this treatment paradigm should be adapted. The aim would be to reduce the total volume of anatomically normal cerebral tissue receiving 20–25 Gy or more. In no other condition is so much anatomically normal brain tissue irradiated with such a high dose. This volume could in principle be reduced if the treatment were preceded with careful stereotactic electroencephalographic recordings to identify the focus more precisely. The treatment could also for the time being be restricted to patients in whom surgery had not controlled the seizures because then much of the excess dose would be placed in a resection cavity and would not damage normal brain.

Conclusions to Minimize Complications and their Effects

1. Before Treatment
   (a) Management of radiosurgery-related complications in the first instance is a matter of prevention.
   (b) The physician knows the indications, doses, and associated risks compared with the risks of the untreated disease.

(c) Thus, it is important to treat the right lesion in the right patient at the right time.
(d) Ensure that the patient receives adequate information.

2. On the Treatment Day
   (a) Correct frame application and optimal images increase the chances of accurate dose placement and reduce the chances of treatment failure.
3. Use the dose planning parameters described above to optimize dose distribution.
   (a) Avoid unnecessary overdosing, which would increase the chances of radiotoxicity. Also, avoid underdosing, which would increase the chances of treatment failure.
4. Most complications are not treatable.
   (a) They just have to be observed and the patient supported.
   (b) In severe cases, dexamethasone may be tried for radiotoxic edema, although it seems to work better with tumors than with AVMs.
   (c) Hyperbaric oxygen has been tried for radiotoxic damage after AVM treatment, but the results have not encouraged its general use.
5. After Treatment
   (a) Follow the patients carefully and regularly and note their clinical development. Manage symptoms as they occur insofar as it is possible.

Conflict of Interest The author works as a consultant for Elekta AB Company, which manufactures the Gamma Knife. He has received no financial support in the preparation of this article and can state that there is no conflict of interest.

References

1. Akamatsu Y, Murakami K, Watanabe M, Jokura H, Tominaga T (2010) Malignant peripheral nerve sheath tumor arising from benign vestibular schwannoma treated by gamma knife radiosurgery after two previous surgeries: a case report with surgical and pathological observations. World Neurosurg 73: 751–754
2. Balasubramaniam A, Shannon P, Hodaie M, Laperriere N, Michaels H, Guha A (2007) Glioblastoma multiforme after stereotactic radiotherapy for acoustic neuroma: case report and review of the literature. Neuro Oncol 9:447–453
3. Bari ME, Forster DMC, Kemeny AA, Walton L, Hardy D, Anderson JR (2002) Malignancy in a vestibular schwannoma. Report of a case with central neurofibromatosis, treated by both stereotactic radiosurgery and surgical excision, with a review of the literature. Br J Neurosurg 16:284–289
4. Berman EL, Eade TN, Brown D, Weaver M, Glass J, Zorman G, Feigenberg SJ (2007) Radiation-induced tumor after stereotactic radiosurgery for an arteriovenous malformation: case report. Neurosurgery 61:E1099
5. Berrington A, Darby SC, Weiss HA, Doll R (2001) 100 years of observation on British radiologists: mortality from cancer and other causes 1897–1997. Br J Radiol 74:507–519
6. Cahan WG, Woodard HQ, Higinbotham NL, Stewart FW, Coley BL (1998) Sarcoma arising in irradiated bone: report of eleven cases. 1948. Cancer 82:8–34
7. Demetriades AK, Saunders N, Rose P, Fisher C, Rowe J, Tranter R, Hardwidge C (2010) Malignant transformation of acoustic neuroma/vestibular schwannoma 10 years after gamma knife stereotactic radiosurgery. Skull Base 20:381–387
8. El Shehaby A, Ganz JC, Reda WA, Hafez A (2005) Mechanisms of edema after gamma knife surgery for meningiomas.Report of two cases. Neurosurg 102(Suppl):1–3
9. El Shehaby A, Ganz JC, Reda WA, Hafez A (2005) Temporary symptomatic swelling of meningiomas following gamma knife surgery. Report of two cases. J Neurosurg 102(Suppl): 293–296
10. Ganz JC (2002) Gamma knife radiosurgery and its possible relationship to malignancy: a review. J Neurosurg 97(suppl 5): 644–652
11. Ganz JC (2011) Gamma Knife neurosurgery. Springer, Wien, pp 99–102
12. Ganz JC (2011) Gamma Knife neurosurgery. Springer, Wien, p 222
13. Ganz JC (2011) Gamma Knife neurosurgery. Springer, Wien, pp 263–271
14. Ganz JC, El Shehaby A, Reda W, Abdelkarim K (2010) Protection of the anterior visual pathways during gamma knife treatment of meningiomas. Br J Neurosurg 24:233–243
15. Ganz JC, Reda WA (2011) Radionecrosis following gamma knife treatment for mesial temporal lobe epilepsy. Br J Neurosurg 25:649–651
16. Grayson JK (1996) Radiation exposure, socioeconomic status, and brain tumor risk in the US Air Force: a nested case–control study. Am J Epidemiol 143:480–486
17. Hanabusa K, Morikawa A, Murata T, Taki W (2001) Acoustic neuroma with malignant transformation. J Neurosurg 95:518–521
18. Hasegawa T, Kida Y, Kobayashi T, Yoshimoto M, Mori Y, Yoshida J (2005) Long-term outcomes in patients with vestibular schwannomas treated using gamma knife surgery: 10-year follow up. J Neurosurg 102:10–16
19. Iwai Y, Yamanaka K, Ikeda H (2008) Gamma Knife radiosurgery for skull base meningioma: long-term results of low-dose treatment. J Neurosurg 109:804–810
20. Kaido T, Hoshida T, Uranishi R, Akita N, Kotani A, Nishi N, Sakaki T (2001) Radiosurgery-induced brain tumor. Case report. J Neurosurg 95:710–713
21. Kano H, Kondziolka D, Lobato-Polo J, Zorro O, Flickinger JC, Lunsford LD (2010) T_1/T_2 matching to differentiate tumor growth from radiation effects after stereotactic radiosurgery. Neurosurgery 66:486–491
22. Kubo O, Chernov M, Izawa M, Hayashi M, Muragaki Y, Maruyama T, Hori T, Takakura K (2005) Malignant progression of benign brain tumors after gamma knife radiosurgery: is it really caused by irradiation? Minim Invasive Neurosurg 48:334–339
23. Liscak R, Vladyka V, Simonova G, Urgosik D, Novotny J Jr, Janouskova L, Vymazal J (2007) Arteriovenous malformations after Leksell gamma knife radiosurgery: rate of obliteration and complications. Neurosurgery 60:1005–1014
24. Loeffler JS, Niemierko A, Chapman PH (2003) Second tumors after radiosurgery: tip of the iceberg or a bump in the road? Neurosurgery 52:1436–1440
25. McIver JI, Pollock BE (2004) Radiation-induced tumor after stereotactic radiosurgery and whole brain radiotherapy: case report and literature review. J Neurooncol 66:301–305
26. Muracciole X, Regis J (2008) Radiosurgery and carcinogenesis risk. Prog Neurol Surg 21:207–213
27. Niranjan A, Kondziolka D, Lunsford LD (2009) Neoplastic transformation after radiosurgery or radiotherapy: risk and realities. Otolaryngol Clin North Am 42:717–729

28. Pollock BE, Flickinger JC (2002) A proposed radiosurgery-based grading system for arteriovenous malformations. J Neurosurg 96:79–85
29. Pollock BE, Flickinger JC (2008) Modification of the radiosurgery-based arteriovenous malformation grading system. Neurosurgery 63:239–243
30. Rowe J, Grainger A, Walton L, Silcocks P, Radatz M, Kemeny A (2007) Risk of malignancy after gamma knife stereotactic radiosurgery. Neurosurgery 60:60–65
31. Sadamori N, Shibata S, Mine M, Miyazaki H, Miyake H, Kurihara M, Tomonaga M, Sekine I, Okumura Y (1996) Incidence of intracranial meningiomas in Nagasaki atomic-bomb survivors. Int J Cancer 67:318–322
32. Shamisa A, Bance M, Nag S, Tator C, Wong S, Noren G, Guha A (2001) Glioblastoma multiforme occurring in a patient treated with gamma knife surgery. J Neurosurg 94:816–821
33. Sheehan J, Yen CP, Steiner L (2006) Gamma knife surgery-induced meningioma. Report of two cases and review of the literature. J Neurosurg 105:325–329
34. Shin M, Ueki K, Kurita H, Kirino T (2002) Malignant transformation of a vestibular schwannoma after gamma knife radiosurgery. Lancet 360:309–310
35. Shintani T, Hayakawa N, Hoshi M, Sumida M, Kurisu K, Oki S, Kodama Y, Kajikawa H, Inai K, Kamada N (1999) High incidence of meningioma among Hiroshima atomic bomb survivors. J Radiat Res (Tokyo) 40:49–57
36. Smith PG, Doll R (1981) Mortality from cancer and all causes among British radiologists. Br J Radiol 54:187–194
37. Spetzler RF, Martin NA (1986) A proposed grading system for arteriovenous malformations. J Neurosurg 65:476–483
38. Tamura K, Aoyagi M, Wakimoto H, Tamaki M, Yamamoto K, Yamamoto M, Ohno K (2006) Malignant transformation eight years after removal of a benign epidermoid cyst: a case report. J Neurooncol 79:67–72
39. Tsuboi Y, Hayashi N, Kurimoto M, Nagai S, Sasahara M, Endo S (2007) Malignant transformation of clival chordoma after gamma knife surgery – case report. Neurol Med Chir (Tokyo) 47:479–482
40. Uozumi Y, Kawano T, Kawaguchi T, Kaneko Y, Ooasa T, Ogasawara S, Yoshida H, Yoshida T (2003) Malignant transformation of meningeal melanocytoma: a case report. Brain Tumor Pathol 20:21–25
41. Yu JS, Yong WH, Wilson D, Black KL (2000) Glioblastoma induction after radiosurgery for meningioma. Lancet 356: 1576–1577

How to Control Propofol Infusion in Pediatric Patients Undergoing Gamma Knife Radiosurgery

Kotoe Kamata, Motohiro Hayashi, Yoshihiro Muragaki, Hiroshi Iseki, Yoshikazu Okada, and Makoto Ozaki

Abstract *Introduction*: Although Gamma Knife radiosurgery (GKS) is commonly performed under local anesthesia, general anesthesia is sometimes required. The authors previously reported a remote-controlled patient management system consisting of propofol-based general anesthesia with a target-controlled infusion (TCI) that we designed for pediatric GKS. However, a commercially available propofol TCI system has age and weight limitations (<16 years and <30 kg). We examined a manually controlled regimen of propofol appropriate for pediatric GKS.

Methods: A pharmacokinetic model of the TIVA Trainer© with Paedfusor's parameter was used. A manually controlled infusion scheme to achieve a sufficient level of propofol for pediatric GKS was examined in five models ranging from 10 to 30 kg.

Results: Following a loading dose of 3.0 mg/kg, the combination of continuous infusion of 14, 12, 10, and 8 mg/kg/h resulted in a target concentration of 3.0–4.0 μg/ml, the required level for pediatric GKS.

Conclusion: Propofol titration is a key issue in GKS. Manual infusion is less accurate than TCI, but the combination of a small bolus and continuous infusion might be a substitute. Considering the characteristics of propofol pharmacokinetics in children, co-administration of opioids is recommended.

Keywords Gamma Knife radiosurgery • General anesthesia • Pediatric anesthesia • Propofol infusion

Introduction

Because of the increase in availability and indications for Gamma Knife radiosurgery (GKS), the number of patients who require general anesthetic management has been increasing. Pediatric patients, those who suffer from claustrophobia, or those whose pathological lesion seems to lead easily to a respiratory disorder after irradiation should be managed under general anesthesia [1, 2]. In a previous report, we demonstrated a remote-controlled patient management system consisting of propofol-based general anesthesia for pediatric GKS [6]. An automated computer-driven target-controlled infusion (TCI) system developed by our group was used for propofol administration. Because we can directly control propofol concentrations as the target values for its administration, TCI has been recognized as much superior to manual infusion [7, 9, 11]. However, the currently available propofol TCI (Diprifusor®; AstraZeneca, London, UK) has both age and weight limitations; patients who are <16 years old or who weight <30 kg cannot be managed by TCI. The purpose of this study was to examine a manually controlled regimen of propofol infusion that can be used for pediatric GKS.

Materials and Methods

Calculation of Propofol Effect-Site Concentration

A pharmacokinetic model of the TIVA Trainer© (http://www.eurosiva.org) version 8 (calculation interval of 30 s) with Paedfusor's parameter was used for computer simulation [9]. The propofol effect-site concentration (ESC) required for GKS was determined based on our initial experience with four pediatric patients aged 3–10 years. Morphometric characteristics and operative data are shown in Table 1.

K. Kamata (✉) and M. Ozaki
Department of Anesthesiology, Tokyo Women's Medical University, 8-1 Kawada-cho, Shinjuku-ku, Tokyo 162-8666, Japan
e-mail: macaroon@nifty.com

M. Hayashi, Y. Muragaki, and H. Iseki
Department of Neurosurgery, Neurological Institute, Tokyo Women's Medical University, Tokyo, Japan

Faculty of Advanced Techno-Surgery, Institute of Advanced Biomedical Engineering and Science, Tokyo Women's Medical University, Tokyo, Japan

Y. Okada
Department of Neurosurgery, Neurological Institute, Tokyo Women's Medical University, Tokyo, Japan

M.F. Chernov et al. (eds.), *Gamma Knife Neurosurgery in the Management of Intracranial Disorders*, Acta Neurochirurgica Supplement, Vol. 116, DOI 10.1007/978-3-7091-1376-9_22, © Springer-Verlag Wien 2013

Table 1 Characteristics of our initial patients

	Case 1 (10 y/o, M, 27 kg) Craniopharyngioma		Case 2 (3 y/o, F, 10 kg) Medulloblastoma		Case 3 (4 y/o, M, 20 kg) AVM		Case 4 (6 y/o, F, 16 kg) Craniopharyngioma	
Parameter	Time (min)	Propofol (μg/ml)[e]	Time (min)	Propofol (μg/ml)[e]	Time (min)	Propofol (μg/ml)[e]	Time (min)	Propofol (μg/ml)[e]
CT and MRI scan[a]	132	3.0–4.0	169	4.0	134	4.0–5.0	114	3.6–4.4
Angiography[b]	NR	–	NR	–	100	3.0–4.0	NR	–
GKS[c]	310	3.5–4.0	180	3.5–4.0	295	3.0–4.0	75	3.8–4.0
Emergence[d]	17	1.95	15	2.29	7	2.37	27	1.87

AVM arteriovenous malformation, *GKS* Gamma Knife radiosurgery, *CT* computed tomography, *MRI* magnetic resonance imaging, *y/o* years old, *M* male, *F* female, *NR* not required

[a]Interval from anesthetic induction to discharge from CT or MRI unit

[b]Interval from entry to and discharge from angiography room

[c]Interval from entry to and discharge from Gamma Knife unit

[d]Interval from termination of propofol infusion to appearance of clinical signs of emergence

[e]Effect-site concentration of propofol

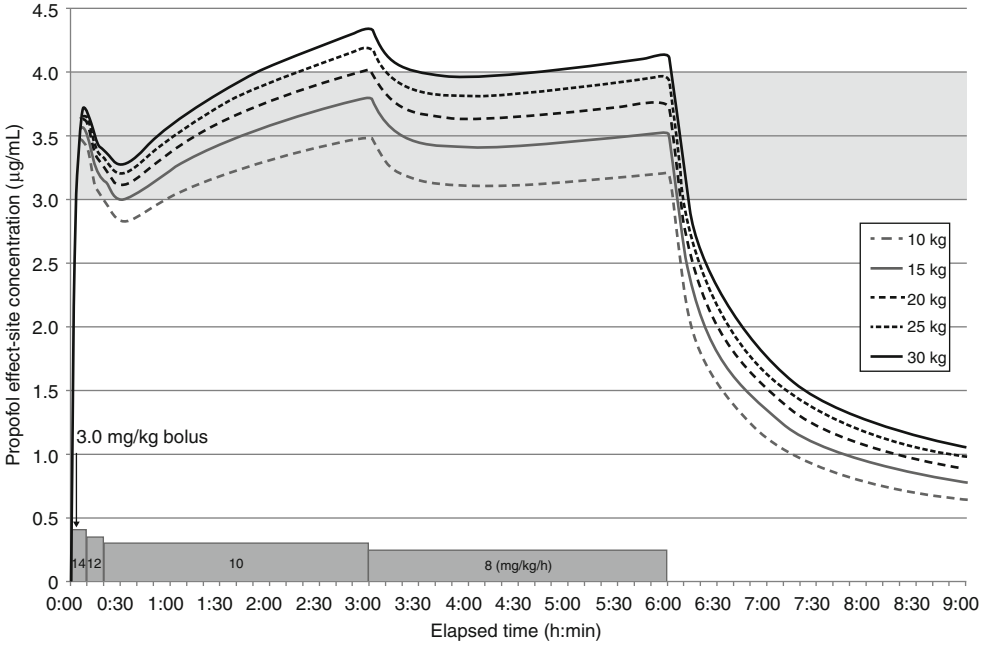

Fig. 1 Predicted time–concentration profiles of different models. The propofol effect-site concentration of five models was simulated based on the pharmacokinetic data sets of Paedfusor. Patient models ranged from 10 to 30 kg body weight, and the target propofol concentration was 3.0–4.0 μg/ml. *Inset* shows the bolus and infusion rate for propofol administration

Computer Simulation of Propofol Infusion for Pediatric GKS

Five weight models, ranging from 10 to 30 kg, were assumed for computer simulation. A manually controlled infusion scheme in combination with a loading dose of 3.0 mg/kg followed by continuous infusion was examined. The propofol ESC obtained as described above was the target value. Propofol infusion was assumed to be discontinued 6 h after it was started.

Results

A propofol ESC of 3.0–5.0 μg/ml was required in pediatric patients undergoing GKS. All patients regained consciousness when their propofol level reached 1.87–2.37 μg/ml.

A bolus of 3.0 mg/kg followed by infusion of 14 mg/kg/h (0–10 min), 12 mg/kg/h (10–20 min), 10 mg/kg/h (20–180 min), and 8 mg/kg/h resulted in a target concentration of 3.0–4.0 μg/ml in patients weighing 10–30 kg. The predicted time–concentration curve is shown in Fig. 1.

Discussion

Propofol pharmacokinetics in the pediatric population is characterized by a larger distribution volume and longer context-sensitive half-time (CSHT) than in adults. Reed et al. showed that propofol concentrations required for sedation of critically ill pediatric patients are similar to those of adults, except that children require much higher per-kilogram infusion rates [10]. Therefore, a manually controlled infusion scheme for continuous administration of propofol in adults is not transferable to pediatric cases [11]. Manual infusion regimens for pediatric patients have also been reported [9]. However, the scheme is probably unsuitable for pediatric GKS because the target propofol concentration is highly dependent on both noxious stimuli and an opioid [8].

To examine a practical manual infusion regimen of propofol dedicated to pediatric GKS, the characteristics of GKS itself must be taken into account. GKS is a minimally invasive procedure that is commonly performed under local anesthesia. The most, and probably the only, painful event that might occur is when a stereotactic frame is attached to the patient's head. Prior to irradiation therapy, multimodal imaging studies with multiple transfers of the patient are required. Because of the longer time required for a single treatment, the medical staff should stay away from the patients to avoid unnecessary exposure to radiation. With these points in mind, we concluded that a practical regimen of propofol manual infusion for pediatric GKS would require simple algorithms for attaining a stable propofol concentration.

Considering the sequence of treatment, we assumed that the propofol concentration should rapidly increase and be maintained while frame fixation is being performed. Consequently, we chose a relatively large initial bolus dose for induction. Although this bolus dose is comparable to standard induction doses in pediatric patients [9], both hypotension and bradycardia could occur during anesthetic induction. Precautions against hemodynamic alteration—e.g., atropine administration, careful measurement and control of hemodynamic parameters—are essential.

Propofol infusion should be used as part of balanced anesthesia, particularly in combination with opioids. Because of its longer CSHT in pediatric patients, recovery from propofol anesthesia is slower than in adults even though propofol is recognized as a rapid-onset and rapid-offset anesthetic [5]. As Drover et al. suggested, opioids generally lead to decreased propofol requirement [4]. It has also been suggested that a combination of propofol and postoperative pain prevention potentially reduces the incidence of emergence agitation, which is a typical problem in pediatric anesthesia [3].

In conclusion, propofol titration seems to be a key issue for pediatric patients undergoing GKS. Propofol ESC is not predictable during manual infusion, but it can be managed by using the combination of a small dose of a bolus and then continuous infusion. The simulation in this study was based on a limited number of patients. Further pharmacokinetic analysis should be performed with a larger patient group.

Conflict of Interest The authors report no conflict of interest concerning the materials or methods used in this article.

References

1. Chung SM (2001) Safety issues in magnetic resonance imaging. J Neuroophthalmol 22:35–39
2. Clifford W, Sharpe H, Khu KJ, Cusimano M, Knifed E, Bernstein M (2009) Gamma Knife patients' experience: lessons learned from a qualitative study. J Neurooncol 92:387–392
3. Dahmani S, Stany I, Brasher C, Lejeune C, Bruneau B, Wood C, Nivoche Y, Constant I, Murat I (2010) Pharmacological prevention of sevoflurane- and desflurane-related emergence agitation in children: a meta-analysis of published studies. Br J Anaesth 104: 216–223
4. Drover DR, Litalien C, Wellis V, Shafer SL, Hammer GB (2004) Determination of the pharmacodynamic interaction of propofol and remifentanil during esophagogastroduodenoscopy in children. Anesthesiology 100:1382–1386
5. Glaisyer HR, Sury MR (2005) Recovery after anesthesia for short pediatric oncology procedures: propofol and remifentanil compared with propofol, nitrous oxide, and sevoflurane. Anesth Analg 100:959–963
6. Kamata K, Hayashi M, Nagata O, Muragaki Y, Iseki H, Okada Y, Ozaki M (2011) Initial experience with the use of remote control monitoring and general anesthesia during radiosurgery for pediatric patients. Pediatr Neurosurg 47:158–166
7. Kataria BK, Ved SA, Nicodemus HF, Hoy GR, Lea D, Dubois MY, Mandema JW, Shafer SL (1994) The pharmacokinetics of propofol in children using three different data analysis approaches. Anesthesiology 80:104–122
8. Kazama T, Ikeda K, Morita K (1997) Reduction by fentanyl of the Cp50 values of propofol and hemodynamic responses to various noxious stimuli. Anesthesiology 87:213–227
9. MacFarlan CS, Anderson BJ, Short TG (1999) The use of propofol infusions in paediatric anaesthesia: a practical guide. Paediatr Anaesth 9:209–216
10. Reed MD, Yamashita TS, Marx CM, Myers CM, Blumer JL (1996) A pharmacokinetically based propofol dosing strategy for sedation of the critically ill, mechanically ventilated pediatric patient. Crit Care Med 24:1473–1481
11. Roberts FL, Dixon J, Lewis GT, Tackley RM, Prys-Roberts C (1988) Induction and maintenance of propofol anaesthesia. A manual infusion scheme. Anaesthesia 43:14–17

Blood DNA Radiosensitivity May Be Predictive for Efficacy of Experimental Glioma Irradiation: An Animal Study

Sergey D. Ivanov, Alexander L. Semenov, Elena G. Kovan'ko, and Vladimir A. Yamshanov

Abstract *Objective*: An animal study was conducted to evaluate the association between blood DNA radiosensitivity, assessed by determining the original S-index, and the response of experimental gliomas to irradiation. Possible modifications of the latter after administration of iron-containing water (ICW) were also explored.

Methods: The study was performed on Wistar rats with subcutaneously implanted experimental glioma-35. The tumors were locally X-irradiated with a single 15 Gy dose. ICW (60–63 mg·Fe^{2+}/l) was administered in the drinking water for 3 days before treatment. The animals underwent blood sampling for analysis of the DNA concentration and leukocyte count. DNA index was estimated 3 days before irradiation and 24 h thereafter. The S-index was evaluated within 4 h before irradiation.

Results: The mean initial S-index in the blood samples of glioma-bearing rats was 0.73 ± 0.05. Addition of ICW in vitro resulted in a significantly increased S-index in half of the samples. In general, the irradiated rats, which had been given pretreatment ICW and demonstrated an in vitro increase of the S-index to >1.0, showed the most marked inhibition of tumor progression and the smallest tumor volume 25 days after irradiation. They also exhibited the lowest rate of lesion growth and the longest survival.

Conclusion: Determination of the biochemical S-index and evaluation of its changes in vitro caused by ICW may be predictive of the response of experimental glioma to irradiation. Because in vivo administration of ICW was associated with a somewhat better tumor response to treatment, it may be considered as a potential radiosensitizer.

Keywords Blood DNA radiosensitivity • Experimental glioma • Experimental radiotherapy • S-index • Tumor response

Introduction

Fractionated radiation therapy (FRT) constitutes one of the main management options for malignant gliomas, although frequently its effectiveness is limited because of the well-known radioresistance of these neoplasms. Escalating the radiation dose, particularly with the use of a radiosurgical boost, and/or administration of effective radiosensitizers can be utilized to overcome such a problem. These strategies are sometimes accompanied by undesirable side effects, however, so preferably they are applied selectively after individual assessment of the tumor's radiosensitivity.

Our group demonstrated previously that disease-free survival after FRT in patients with breast and bladder cancer may be predicted before initiation of treatment by testing in vitro the radiosensitivity of the blood DNA with determining the original S-index [2]. Further investigation revealed that in the case of glioma the S-index is rather low, usually not exceeding 1.0 (mean 0.61 ± 0.05), which may reflect relative radioresistance of these tumors. We conducted the present animal study to evaluate the association between the S-index and the response of experimental gliomas to irradiation. We also looked at its possible modification after administration of iron-containing water (ICW).

Material and Methods

The study was performed on adult Wistar rats with subcutaneously implanted experimental glioma-35, originally induced by administration of ethylnitrosourea [9]. The tumor was implanted in 27 animals by subcutaneous injection of a

S.D. Ivanov (✉), A.L. Semenov, E.G. Kovan'ko,
and V.A. Yamshanov
Biotesting Laboratory,
Russian Research Center for Radiology and Surgical Technologies,
Leningradskaya Str. 70, Pesochny,
Saint Petersburg 197758, Russia
e-mail: sergey.d.ivanov@mail.ru

M.F. Chernov et al. (eds.), *Gamma Knife Neurosurgery in the Management of Intracranial Disorders*,
Acta Neurochirurgica Supplement, Vol. 116, DOI 10.1007/978-3-7091-1376-9_23, © Springer-Verlag Wien 2013

0.5 ml suspension of neoplastic cells (12×10^9 cell/l) in the leg. The control group included seven rats that did not undergo implantation of the neoplasm.

All experiments were conducted in accordance with the standards of humane animal care and local institutional regulations.

Blood Sampling and Analysis

Blood (0.4 ml) was collected from the rat tail vein. The samples were diluted 1:1 with physiological saline and separated into two parts: One served as the nontreated control, and the other was subjected to irradiation with a dose of 4 Gy (dose rate 4.0 Gy/min) using the linear accelerator Philips SL 75–5. ICW (60–63 mg·Fe^{2+}/l) was added (20 % of the total volume) to the irradiated samples 30 min before treatment. Irradiation was followed by incubation at 37 °C for 3 h. The total duration of the biochemical analysis was 4 h. Of note: If chromosomal aberrations were to have been evaluated, >48 h would have been necessary for lymphocyte cultivation [4, 6].

Fluorescence-based measurements of the DNA concentration (μg/ml) and leukocyte count (cells/ml) in the control and irradiated blood samples were performed (in the latter both before and after ICW addition). Also, the DNA index and S-index (designated the S_{Fe}-index if assessed after in vitro ICW addition) were estimated according to a previously described method [5] and the following formulas:

$$\text{DNA-index (control)} = \text{DNA concentration (control)} / \text{Leukocyte count (control)}$$

$$\text{DNA-index (irradiated)} = \text{DNA concentration (irradiated)} / \text{Leukocyte count (irradiated)}$$

$$\text{S-index} = \text{DNA-index (control)} / \text{DNA-index (irradiated)}$$

In all cases, the analysis was performed 3 days before tumor irradiation and 24 h thereafter. The S-index was evaluated within 4 h before treatment in 14 glioma-bearing animals that had been scheduled for treatment after 3 days of ICW administration as drinking water available ad libitum (groups 3 and 4).

Irradiation and Follow-Up

Of the 27 glioma-bearing rats carrying developed tumor nodules, 20 underwent local irradiation of the tumor with a single 15 Gy dose using an X-ray unit (RUM-17; Mosrentgen, Russia) under the following conditions: dose rate 0.8 Gy/min, $I = 13$ mA, $U = 200$ kV, filtered through 0.5 mm Cu and 1.0 mm Al. The volume of the neoplasm was calculated before irradiation and at regular intervals thereafter according to the following formula: $V\ (cm^3) = (4\pi/3) \times A \times B^2/8$ where A and B reflect the width and height of the lesion, respectively. The period of tumor growth up to a volume of 2.6 cm^3, which approximates the size of the whole volume of the adult Wistar rat brain (2.4–2.8 cm^3), and the survival of the animals after irradiation were recorded.

Statistical Analysis

Student's t-test and the Mann–Whitney U-test were used for statistical analysis. The level of significance was determined at $P < 0.05$.

Results

S-Index

The mean initial S-index in the blood samples of 14 glioma-bearing rats scheduled for irradiation after 3 days of ICW administration was 0.73 ± 0.05. Addition of ICW during in vitro analysis of blood samples had different effects on the S-index values. In half of the cases there was a statistically nonsignificant decrease (mean S_{Fe}-index 0.47 ± 0.06), whereas the other half exhibited a statistically significant ($P < 0.01$) increase to >1.0 (mean S_{Fe}-index 1.52 ± 0.13). The mean initial S-index in the latter group was slightly higher (0.83 ± 0.08 vs. 0.63 ± 0.04), although the difference did not reach statistical significance.

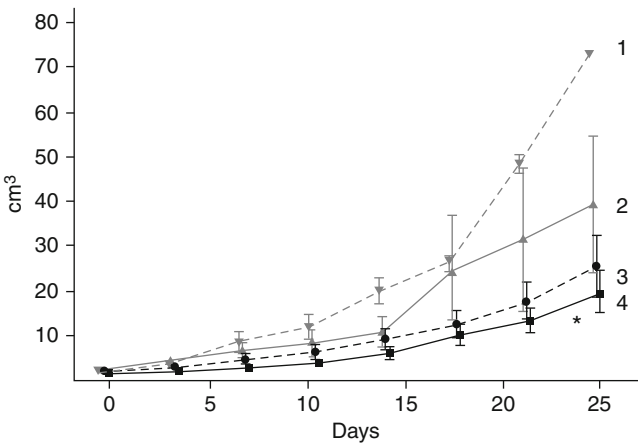

Fig. 1 Volume of the subcutaneous tumors (cm^3) in different groups of glioma-bearing rats. *Asterisk* indicates the presence of statistically significant differences ($P < 0.05$) of the lesion volume at 25 days after treatment between nonirradiated animals (group 1) and irradiated animals after pretreatment administration of ICW (groups 3 and 4)

Table 1 Hematological parameters, speed of tumor growth, and survival in different groups of experimental animals

Experimental animals	Changes at 24 h after irradiation relative to pretreatment values (%)		Mean tumor growth period up to the volume of 2.6 cm^3 (days)	Mean survival of animals (days)
	Leukocyte count	DNA index		
Control group ($N=7$)	100.0 ± 9.7^{a}	$100 \pm 9.1^{c,d}$	–	–
Group 1: nonirradiated animals ($N=7$)	110.0 ± 9.3^{b}	133.6 ± 11.5^{c}	5.3 ± 1.3^{e}	$19.9 \pm 2.6^{g,h}$
Group 2: irradiated animals ($N=6$)	$69.7 \pm 6.0^{a,b}$	125.5 ± 16.5	5.6 ± 0.4^{f}	33.0 ± 5.4
Group 3: irradiated animals with pretreatment administration of ICW; in vitro S_{Fe}-index <1.0 ($N=7$)	93.2 ± 15.5	104.9 ± 14.3	9.2 ± 1.6	37.3 ± 3.0^{g}
Group 4: irradiated animals with pretreatment administration of ICW; in vitro S_{Fe}-index >1.0 ($N=7$)	74.4 ± 10.9	166.6 ± 18.3^{d}	$13.9 \pm 2.4^{e,f}$	42.7 ± 5.2^{h}

Groups 1–4 glioma-bearing rats, *N* number of animals, *ICW* iron-containing water
[a–h]Statistically significant differences between the marked groups ($P<0.01$)

Irradiation and Follow-Up

The subcutaneously implanted gliomas gradually progressed in both the nonirradiated rats (group 1) and the irradiated animals (groups 2–4), although treatment definitely inhibited tumor growth to various degrees (Fig. 1). The investigated hematological parameters, rate of tumor growth, and survival of the experimental animals are shown in Table 1.

DNA Index

Compared to the control group, there was a statistically significant (P <0.01) increase in the DNA index 24 h after treatment in the nonirradiated glioma-bearing rats (group 1). Similar changes were marked in irradiated animals treated with ICW before irradiation, who had an in vitro S_{Fe}-index of >1.0 (group 4).

Effect of ICW Administration

The animals subjected to pretreatment administration of ICW (groups 3 and 4) had smaller tumor volumes at 25 days after irradiation (P <0.05) and longer survival (P <0.01) than the nonirradiated animals (group 1). Additionally, they did not demonstrate statistically significant changes in the leukocyte count in blood samples 24 h after irradiation compared to nonirradiated animals (group 1) and the control group. In contrast, the leukocyte count was statistically significantly decreased (P <0.01) in irradiated rats that did not receive ICW before treatment (group 2).

In Vitro Determination of S_{Fe}-Index and Tumor Progression

In general, irradiated animals that were administered ICW before treatment and had an in vitro S_{Fe}-index >1.0 (group 4) showed the most significant inhibition of the tumor progression and the smallest tumor volume 25 days after irradiation. They also had the lowest rate of the lesion growth up to a volume of 2.6 cm^3, and the longest survival. However, none of these parameters had differences that reached statistical significance when compared to irradiated animals that had been given ICW before treatment and demonstrated an in vitro S_{Fe}-index of <1.0 (group 3).

Discussion

There is increasing interest in possible predictive markers of cancer response to various alternative treatment options. In contrast to general clinical prognostic factors, which mainly reflect the condition of the patient and the biology of the neoplasm, such markers can provide information on the expected effectiveness of the given therapy in the particular case. They can be helpful for selecting the optimal candidates, particularly for FRT and stereotactic radiosurgery, limiting potentially toxic management to those who can definitely benefit from its application. On the other hand, if the radioresistance of the neoplasm could be anticipated with some accuracy, the treatment strategy could be modified with dose escalation or administration of a radiosensitizer or use an alternative modality.

Predictive factors for tumor response to irradiation are usually sought in the pathological tissue itself or within the circulating plasma and/or blood cells using various genetic, cytogenetic, immunological, and other methods [1, 7, 8]. Recently we were able to demonstrate in both clinical and experimental studies that the effects of FRT can be anticipated by determining the biochemical S-index [2, 3, 5]. The latter showed a strong direct correlation with the prominence of unstable chromosomal aberrations [4, 6]. Indeed, its determination is fast and easy, and it does not require prolonged lymphocyte cultivation. Therefore, application of the S-index is rather convenient in clinical practice for rapid characterization of DNA radiosensitivity in a sample of human blood leukocytes.

The results of the present study demonstrated that evaluation of S-index and its changes after addition of ICW in vitro can be predictive of the response of an experimental glioma to irradiation. Tumor-bearing rats that underwent the described treatment and that had an S_{Fe}-index of >1.0 before irradiation demonstrated significant inhibition of lesion progression and had the longest survival. These animals showed the most prominently elevated DNA index 24 h after irradiation, which probably reflected early genotoxic effects. The differences in the investigated parameters generally did not reach statistical significance, which might be explained by the small number of samples in the experimental groups. However, we can still speculate that the cutoff level of 1.0 for the S_{Fe}-index may differentiate radiosensitive and radioresistant experimental gliomas.

Moreover, administration of ICW in vivo before irradiation was associated with a somewhat better tumor response to treatment. These results correspond well to those of our previous investigations, which demonstrated that iron ions might increase the efficacy of FRT [3]. Therefore, ICW can be considered a potential radiosensitizer that may improve treatment results in patients with malignant gliomas.

The search for biomarkers to predict differential effects of radiation on human cancers has just begun. Few dedicated clinical trials of sufficient size have been performed to date, and the obtained results are frequently confounding and inconsistent. Although our study demonstrated that some biochemical parameters, such as the S-index, are potentially useful for predicting tumor response and hematotoxic reactions after irradiation, the data should be considered preliminary. Our final goal is identification of effective biomarkers that can be used during decision-making before initiating irradiation in patients with malignant brain tumors. The search requires more extensive laboratory and clinical investigations. The realization of this goal is necessary before we can introduce individualized radiation treatment into clinical practice.

Conclusion

Testing blood DNA radiosensitivity by determining the pretreatment biochemical S-index and evaluation of its changes after treatment with ICW in vitro may be predictive of the response of experimental gliomas to irradiation. If our results are confirmed in further studies, it may open a perspective for optimized selection of candidates for irradiation, provide an objective choice of treatment's parameters, and give a precise estimation of the results. Moreover, because administration of ICW in vivo is associated with a somewhat better tumor response to irradiation, we believe it can be considered a potential radiosensitizer. Additional laboratory and clinical investigations are necessary for identification of biochemical predictive markers for FRT and stereotactic radiosurgery in patients with brain tumors.

Conflict of Interest The authors declare that they have no conflict of interest.

References

1. Cheng C, Omura-Minamisawa M, Kang Y, Hara T, Koike I, Inoue T (2009) Quantification of circulating cell-free DNA in the plasma of cancer patients during radiation therapy. Cancer Sci 100: 303–309
2. Ivanov SD (2008) Prognosis for therapeutic effectiveness of radiotherapy in the combined treatment of cancer. Vopr Onkol 54: 483–489 (in Russian)
3. Ivanov SD, Semenov AL, Kovan'ko EG, Yamshanov VA, Zabezhinskii MA (2010) Effect of additional administration of iron ions on the efficacy of radiotherapy of glioma-bearing animals. Vopr Onkol 56:692–699 (in Russian)
4. Ivanov SD, Sobutskiy MP, Monakhov AS, Kovan'ko EG (2008) Express-evaluation of genotoxic effects for radio-mercury exposures with low doses. Toxicol Vestn N1:21–25 (in Russian)
5. Ivanov SD, Yamshanov VA, Maslyukova EA (2008) Method for determination of testimony to carry out organ-preservation treatment of patients with bladder cancer. Patent No. 2319963 (Russian Federation)
6. Ivanov SD, Yamshanov VA, Kovan'ko EG, Vorobtsova IE, Poroshina TE, Bershtein LM (2006) Comparative study of postradiation genotoxic changes in mammalian cells by biochemical and cytogenetic methods. Bull Exp Biol Med 142:679–682
7. Monakhov AS, Semiglazov VF, Vagner RI, Guliaev AV, Anisimov VV, Barchuk AS (2008) Cytogenetic check-up and treatment of cancer patients. Vopr Onkol 54:565–572 (in Russian)
8. Paul S, Barker CA, Turner HC, McLane A, Wolden SL, Amundson SA (2011) Prediction of in vivo radiation dose status in radiotherapy patients using ex vivo and in vivo gene expression signatures. Radiat Res 175:257–265
9. Romodanov AP, Zhmareva EN, Butsenko OI (1983) Experimental study of the antitumor activity of nitrosomethylurea, adriablastine and ftorafuron model gliomas with different growth rates. Zh Vopr Neirokhir Im NN Burdenko N4:11–19 (in Russian)

Importance of Neuroimaging Accuracy in Radiosurgery

Julio C. Antico

Keywords Gamma Knife radiosurgery • Neuroimaging • Stereotactic radiosurgery • Treatment planning

Introduction

In 1951, Lars Leksell described a novel way to treat brain disorders without craniotomy but with application of multiple narrow ionizing beams delivered during a single session. He then coined the term "radiosurgery" [7]. Twenty years later he wrote in his autobiography: "I have in my hands a new type of brain surgery, an operative system, a more sophisticated and less risky surgical procedure based on progressively improving imaging of the brain and on mechanical accuracy and modern physics, a necessary addition to classical bloody surgery." Ladislau Steiner noted: "Additionally to novelty, his idea featured other ingredients characteristic of creativity: the ability to be fruitful, the ability to select the required tool for the idea work, and the ability to stimulate the minds of others to work with excellence." It should be specifically emphasized that the radiosurgical method was created and successfully introduced into clinical practice before development of the modern neuroimaging techniques, such as computed tomography (CT), magnetic resonance imaging (MRI), and digital angiography.

Precise determination of the target's location, volume, and interrelations with the surrounding structures is of paramount importance for successful use of stereotactic radiosurgery, particularly Gamma Knife radiosurgery (GKS). Therefore, from the past until now, this method has critically relied on radiological techniques because application of the single-session relatively high-dose irradiation has no other spatial control other than the available medical images. It demands the highest requirements for imaging accuracy to provide optimal treatment precision with minimal, if any, damage to healthy brain tissue and a low risk of undue side effects. Understanding the basic principles of neuroimaging modalities, their advantages and limitations, is mandatory for effective and safe radiosurgery. Additionally, knowledge of the typical changes in the lesion after irradiation and their relation to clinical outcome is important during follow-up examinations.

J.C. Antico
Department of Functional and Stereotactic Neurosurgery and Leksell Gamma Knife Radiosurgery, FLENI, Montañeses 2325 (1428), Buenos Aires, Argentina
e-mail: jantico@fleni.org.ar

Neuroimaging Modalities for Gamma Knife Radiosurgery

Current versions of the Leksell GammaPlan (Elekta Instruments AB, Stockholm, Sweden) permit installation, stereotactic co-registration, and fusion of the various images obtained not only with such standard methods as CT, MRI and digital cerebral angiography but also with functional MRI (fMRI), diffusion tensor imaging (DTI), magnetic resonance angiography (MRA), positron emission tomography (PET), and other radiological techniques [3–5, 12]. Variability of the contemporary imaging modalities and their possible application for GKS and for subsequent follow-up examinations opens new perspectives but also creates definite challenges for radiosurgical practitioners. High-level expertise in visualized anatomical, functional, and metabolic data is important for their correct interpretation. It is specifically discussed by Ono et al. [8], who highlighted their experience with optimal visualization of multiple brain metastases for GKS. It should be emphasized that various radiological methods significantly complement each other in providing important medical information. Therefore, in general, precise target delineation, selection of the optimal treatment strategy, and accurate dosimetry planning during radiosurgery can be most effectively attained by applying the multimodal neuroimaging approach based on various combinations of the available images within the three-dimensional (3D) workspace of the Leksell GammaPlan.

M.F. Chernov et al. (eds.), *Gamma Knife Neurosurgery in the Management of Intracranial Disorders*,
Acta Neurochirurgica Supplement, Vol. 116, DOI 10.1007/978-3-7091-1376-9_24, © Springer-Verlag Wien 2013

CT

Introduction of CT during the 1970s represented a tremendous step forward for clinical practice in general and for GKS in particular [1]. The method provides sufficient anatomical resolution and permits calculation of electron density maps. It is still widely applied for radiosurgical treatment planning. It provides precise stereotactic localization of the lesion, although detailed delineation of the soft tissue targets derived from CT alone may be suboptimal, particularly compared to what MRI offers.

MRI

At present, MRI represents the standard modality for radiosurgery because it provides excellent resolution and allows perfect 3D localization of soft tissue targets. Various aspects of its usefulness to GKS are emphasized in the articles included in this volume of *Acta Neurochirurgica Supplement* [6, 8, 11, 17]. It should be noted, however, that because of the complexity of the nuclear interactions involved in the magnetic resonance phenomenon this imaging modality has multiple sources of potential errors. These errors may result in distortion artifacts and affect image quality and accuracy. Therefore, the use of MRI alone for radiosurgical treatment planning must be undertaken with caution. At the same time, although the resolution of CT is lower, it is more resistant to localization errors. The automated algorithm of the Leksell GammaPlan permits easy co-registration of MRI and CT. In fact, such fused images may provide information superior to that obtained with each of the aforementioned modalities if used separately. Moreover, CT has superb potential for visualization of bone structures, which can be used for 3D evaluation and correction of MRI distortion artifacts. Therefore, routine acquisition of CT scans and use of fused images are reasonable even if the radiosurgical target seems well identified on MRI.

The constructive interference in steady state (CISS) sequence plays an important role in evaluating anatomical structures within the cerebral ventricles and subarachnoid cisterns. It can be particularly useful for lesions producing a signal that is relatively isointense to cerebrospinal fluid on T1- and T2-weighted images. Hayashi et al. [6] advocated use of 3D CISS for skull base lesions, as it seems to be effective when assessing the cerebellopontine cistern, internal auditory canal and, after fusion with "bone window" CT, the inner ear structures. The described technique permits clear visualization of the facial and vestibulocochlear nerves, which is important during GKS of vestibular schwannomas. It has been demonstrated that CISS is superior to 3D turbo-spin echo (3D-TSE) for cranial nerve visualization [15], and that for such a purpose images are most effectively acquired in the axial plane [2, 13, 14, 16].

Technological advances in fMRI and DTI may further refine dosimetry planning during GKS, particularly for lesions located in or in close vicinity to critical brain structures [3]. In such cases, functional information on the eloquent cortex or functionally important white matter tracts may result in avoidance of excessive irradiation and may potentially reduce the risk of posttreatment complications. Tamura et al. [11] demonstrated an effective technique for installation of DTI in the Leksell GammaPlan and its fusion with T1- and T2-weighted MRI scans for identifying the corticospinal tract and optic radiation. Initial dose planning is possible using structural data, being subsequently adjusted with regard to available functional information. Such advanced MRI techniques are effectively attained at high-field MRI, which potential application in radiosurgery is discussed by Zamecnik and Essig [17]. However, although 3 T devices provide superior image quality and resolution compared to 1.0 T or 1.5 T scanners, they are susceptible to magnetic field inhomogeneities and related distortions, which may result in decreased image accuracy, limiting their use for radiosurgical treatment planning.

Other MRI techniques, such as perfusion-weighted, diffusion-weighted, and spectroscopic imaging, can be effectively applied in GKS as well [4]. This scientific field is growing rapidly, with constant development of new sequences that provide better image quality, greater accuracy and resolution, and higher speed of investigation. Therefore, it can be expected that advanced neuroimaging modalities, particularly those based on the use of high-field MRI scanners, will constantly refresh routine radiosurgical practice.

Digital Cerebral Angiography

For decades, conventional cerebral angiography has been used for GKS of arteriovenous malformations (AVMs). However, it offers only two-dimensional visualization of the nidus, whereas loss of detailed spatial information may result in inaccurate target delineation [9]. On the other hand, although CT and MRI provide perfect anatomical resolution and 3D visualization of the lesion and surrounding structures, they provide only limited data on vessel architecture and do not permit precise discrimination between feeding arteries, draining veins, and the nidus itself. This deficiency decreases their usefulness as single neuroimaging modalities during radiosurgery of AVMs [10]. Hence, for optimal dosimetry in such cases and precise delivery of radiation to the 3D nidus, the combined use of cerebral angiography, CT, and MRI seems appropriate.

MRA

Magnetic resonance angiography (MRA) is based on the effects of moving spins on a magnetic resonance signal, and the intensity of each pixel depends on the velocity of the detected spins. Selective detection of the moving spins is not dependent on pulsatile flow. Therefore not only arteries but venous structures as well can be effectively visualized without use of contrast agents. Integration of MRA into dosimetry planning during GKS for AVMs is technically feasible and has been effectively applied [12]. Moreover, noninvasive evaluation of blood flow provided by this imaging modality is also useful during posttreatment follow-up.

PET

Integration of the metabolic data in radiosurgical treatment planning may optimize target selection in cases of infiltrating lesions with ill-defined borders, particularly recurrent neoplasms. Positron emission tomography (PET) provides useful information, and current versions of the Leksell GammaPlan permit its automatic co-registration with structural MRI. It facilitates application of GKS, especially in patients with intraaxial brain tumors, and it can potentially lead to improved clinical results. However, additional challenges with dosimetry may appear as the structural and metabolic images of the location of the optimal target do not necessarily correspond to each other. Moreover, spatial accuracy of such fused images requires clarification. On the other hand, metabolic and functional data obtained with PET can effectively differentiate tumor recurrence from radiation-induced effects during follow-up after radiosurgery.

Conclusion

There is no doubt that advances in neuroimaging can help refine all aspects of radiosurgical treatment planning, improve its efficacy, and provide greater accuracy of follow-up examinations. Nevertheless, indications for clinical application of many radiological techniques remain poorly defined and require further clarification. The main challenge for radiosurgeons and radiation oncologists is related to understanding the advantages and limitations of the various available modalities. Ultimately, prospective studies correlating imaging findings and clinical outcomes are needed so we can establish precise guidelines for optimal patient care.

Conflict of Interest The author declares that he has no conflict of interest.

References

1. Battista JJ, Rider WD, Van Dyk J (1980) Computed tomography for radiotherapy planning. Int J Radiat Oncol Biol Phys 6:99–107
2. Becker M, Kohler R, Vargas MI, Viallon M, Delavelle J (2008) Pathology of trigeminal nerve. Neuroimaging Clin N Am 18:283–307
3. Cernica G, de Boer SF, Diaz A, Fenstermaker RA, Podgorsak MB (2005) Dosimetric accuracy of a staged readiosurgery treatment. Phys Med Biol 50:1991–2002
4. Chan AA, Lau A, Pirzkall A, Chang SM, Verhey LJ, Larson D, McDermott MW, Dillon WP, Nelson SJ (2004) Proton magnetic resonance spectroscopy imaging in the evaluation of patients undergoing gamma knife surgery for grade IV glioma. J Neurosurg 101:467–475
5. Dong RH, Gao ZU, Hu ZQ, Xu WM, Pan L (1996) Preliminary application of Gamma Knife in the treatment of nasopharyngeal carcinoma. Stereotact Funct Neurosurg 66(Supp1 1):201–207
6. Hayashi M, Chernov MF, Tamura N, Yomo S, Tamura M, Horiba A, Izawa M, Muragaki Y, Iseki H, Okada Y, Ivanov P, Regis J, Takakura K (2013) Usefulness of the advanced neuroimaging protocol based on plain and gadolinium-enhanced Constructive Interference in Steady State images for Gamma Knife radiosurgery and planning microsurgical procedures for skull base tumors. Acta Neurochir Suppl 116:167–178 (present volume)
7. Leksell L (1951) The stereotaxic method and radiosurgery of the brain. Acta Chir Scand 102:316–319
8. Ono Y, Abe K, Hayashi M, Chernov MF, Okada Y, Sakai S, Takakura K (2013) Optimal visualization of multiple brain metastases for Gamma Knife radiosurgery. Acta Neurochir Suppl 116:159–166 (present volume)
9. Perks J, St George EJ, Doughty D, Plowman PN (2001) Is distortion correction necessary for digital subtraction angiography in the gamma knife treatment of intracranial arteriovenous malformations? Stereotact Funct Neurosurg 76:94–105
10. St George EJ, Butler P, Plowman PN (2002) Can magnetic resonance imaging alone accurately define the arteriovenous nidus for gamma knife radiosurgery? J Neurosurg 97(5 Suppl):464–470
11. Tamura M, Konishi Y, Tamura N, Hayashi M, Nakao N, Uematsu Y, Itakura T, Rejis J, Mangin JF, Muragaki Y, Iseki H (2013) Usefulness of Leksell GammaPlan for preoperative planning of brain tumor resection: Delineation of the cranial nerves and fusion of the neuroimaging data, including diffusion tensor imaging. Acta Neurochir Suppl 116:179–185 (present volume)
12. Taschner CA, Le Thuc V, Reyns N, Gieseke J, Gauvrit JY, Pruvo JP, Leclerc X (2007) Gamma knife surgery for arteriovenous malformations in the brain: integration of time-resolved contrast-enhanced magnetic resonance angiography into dosimetry planning. Technical note. J Neurosurg 107:854–859
13. Tash RR, Sze G, Leslie DR (1989) Trigeminal neuralgia: MR imaging features. Radiology 172:767–770
14. Thomas B, Krishnamoorthy T, Arvinda HR, Kesavadas C (2008) 3D-CISS MRI in a purely intracanalicular cochlear schwannoma. J Neuroradiol 35:305–307
15. Yang D, Korogi Y, Ushio Y, Takahashi M (2000) Increased conspicuity of intraventricular lesions revealed by three-dimensional Constructive Interference in Steady State sequences. AJNR Am J Neuroradiol 21:1070–1072
16. Yousry I, Moriggl B, Schmid UD, Naidich TP, Yousry TA (2005) Trigeminal ganglion and its divisions: detailed anatomic MR imaging with contrast-enhanced 3D Constructive Interference in the Steady State sequences. AJNR Am J Neuroradiol 26:1128–1135
17. Zamecnik P, Essig M (2013) Perspectives of 3 T magnetic resonance imaging in radiosurgical treatment planning. Acta Neurochir Suppl 116:187–191 (present volume)

Optimal Visualization of Multiple Brain Metastases for Gamma Knife Radiosurgery

Yuko Ono, Kayoko Abe, Motohiro Hayashi, Mikhail F. Chernov, Yoshikazu Okada, Shuji Sakai, and Kintomo Takakura

Abstract *Background*: Optimal management of metastatic brain disease requires precise detection and detailed characterization of all intracranial lesions.

Methods: We analyzed an experience with 3200 brain MRI investigations performed at 1.5 T and 3.0 T for identification and/or evaluation of intracranial metastases. Usually axial T1- and T2-weighted images and contrast-enhanced T1-weighted images in axial and coronal and/or sagittal projections were obtained. Fluid-attenuated inversion recovery and diffusion-weighted imaging were sometimes used as well. Routinely, 0.2 mmol/kg of gadoteridol (ProHance®) was administered intravenously, but the dose was reduced to 0.1 mmol/kg in elderly patients or in patients with mild renal dysfunction.

Findings: Magnetic resonance imaging (MRI) provided excellent information on tumor location; interrelations with functionally important intracranial structures; type of growth; vascularity; recent, old or multiple hemorrhages within or in the vicinity of the mass; presence of peritumoral edema; necrotic changes; subarachnoid dissemination; meningeal carcinomatosis. However, without administration of gadoteridol or without contrast enhancement, small metastatic tumors could not be reliably distinguished from brain lacunes. Some metastases (malignant melanoma, thyroid cancer, endocrine carcinoma, small cell lung carcinoma) may demonstrate specific neuroimaging features. Non-metastatic multiple brain lesions caused by vascular, inflammatory, demyelinative or lymphoproliferative diseases require a thorough differential diagnosis with metastatic brain tumors based not only on neuroimaging but on additional analysis of various clinical data.

Conclusion: Contemporary MRI techniques provide excellent options for detection, detailed characterization, and differential diagnosis of metastatic brain tumors, which is extremely important when choosing the optimal treatment strategy, particularly with Gamma Knife radiosurgery.

Keywords Brain metastases • Diagnosis • Differential diagnosis • MRI • Multiple brain lesions

Introduction

Recent achievements in cancer management have resulted in definitely improved local disease control, but there has been an increased incidence of metastatic brain tumors. Although prognosis in such cases is generally poor, it is widely accepted that early, precise diagnosis may facilitate effective treatment. Particularly, Gamma Knife radiosurgery may result in meaningful prolongation of patient survival and significantly improved quality of life. The optimal management of metastatic brain disease—surgery, irradiation, chemotherapy, or their combination—requires precise detection of all intracranial lesions. Here we present our magnetic resonance imaging (MRI)-based diagnostic approach to intracranial metastases directed at their optimal visualization, detailed characterization, and effective differential diagnosis with non-metastatic multiple brain lesions.

Y. Ono (✉), K. Abe, and S. Sakai
Department of Diagnostic Imaging and Nuclear Medicine,
Tokyo Women's Medical University,
8-1 Kawada-cho, Shinjuku-ku, Tokyo 162-8666, Japan
e-mail: yono@nij.twmu.ac.jp

M. Hayashi, M.F. Chernov, and K. Takakura
Faculty of Advanced Techno-Surgery,
Institute of Advanced Biomedical Engineering and Science,
Tokyo Women's Medical University, Tokyo, Japan

Department of Neurosurgery, Neurological Institute,
Tokyo Women's Medical University, Tokyo, Japan

Y. Okada
Department of Neurosurgery, Neurological Institute,
Tokyo Women's Medical University, Tokyo, Japan

M.F. Chernov et al. (eds.), *Gamma Knife Neurosurgery in the Management of Intracranial Disorders*,
Acta Neurochirurgica Supplement, Vol. 116, DOI 10.1007/978-3-7091-1376-9_25, © Springer-Verlag Wien 2013

Table 1 Main parameters of MRI investigations performed for identification and/or evaluation of brain metastases

No. of MRI scanner	Magnetic field strength (T)	TR/TE of T1-weighted images (ms)	TR/TE of T2-weighted images (ms)	TR/TE of postgadolinium T1-weighted images (ms)	Flip angle	TR/TE/TI of FLAIR (ms)
1	3	2,650/40 TI: 110	3,500/90	576/10	90°	10,000/120/2,700
				3D-SE: 16/5.5	18°	
2	1.5	415/15	3,200/100	415/15	90°	9,600/120/2,400
				3D-GR: 25/6.8	20°	
3	1.5	430/15	3,500/10	430/15	T1: 70°	10,000/120/2,700
					T2: 90°	
				3D-GR: 17/5.5	20°	
4	1.5	401/11	3,282/100	401/11	T1: 70°	6,000/100/2,000
					T2: 90°	
5	1.5	400–500/12	3,500–4,000/90	400–500/12	T1: 80°	9,000/102/2,500
					T2: 90°	

MRI magnetic resonance imaging, *TR* repetition time, *TE* echo time, *TI* inversion time, *FLAIR* fluid attenuation inversion recovery, *3D-SE* three-dimensional spin echo, *3D-GR* three-dimensional gradient echo

Materials and Methods

We reviewed 3200 brain MRI investigations performed for identification or evaluation of intracranial metastases in patients seen in the Department of Diagnostic Imaging and Nuclear Medicine of the Tokyo Women's Medical University from September 2009 to August 2011. The vast majority of metastatic brain tumors originated from the lung (56 %), breast (12 %), and gastrointestinal tract (11 %). Among other locations of the primary disease, the most common were the kidney, liver, ovary, uterus, prostate, head and neck, thyroid, and endocrine organs.

Five MRI scanners were utilized: one with a magnetic field strength of 3 T and four with a strength of 1.5 T. The main parameters of the sequences used are presented in Table 1. The investigation included axial T1- and T2-weighted images with 7 mm slice thickness and contrast-enhanced T1-weighted images with 5 mm slice thickness in axial and coronal and/or sagittal projections. For radiosurgical management of intracranial metastases, three-dimensional (3D) gradient echo sequences at 1.5 T are usually used in our practice. In the same time for routine examination of these patients we prefer spin-echo sequences (or 3D spin-echo sequences at 3 T) because they provide excellent information needed for lesion characterization [3, 7–9]. If gadolinium-enhanced T1-weighted images were obtained with 3D gradient echo sequence at 1.5 T or 3D spin echo sequence at 3 T, they were reconstructed with 2 mm slice thickness. A b-factor of 1000 s/mm^2 was used for diffusion-weighted imaging (DWI).

Routinely, for MRI examination of patients with metastatic brain disease a double dose (0.2 mmol/kg) of the gadolinium-based contrast medium gadoteridol (ProHance®; Eisai, Tokyo, Japan) was administered intravenously. It was reduced to 0.1 mmol/kg in patients >80 years of age or who had mild renal dysfunction defined as a serum creatinine level of 1.2–1.8 mg/dl and/or an estimated glomerular filtration rate (GFR) of 60–120 ml/min. For patients with significant renal dysfunction (serum creatinine >1.8 mg/dl and/or estimated GFR <60 ml/min) or allergy to the contrast medium, the examination was limited to plain T1- and T2-weighted imaging with additional fluid attenuation inversion recovery (FLAIR) images and DWI.

Results

In the absence of a history of intralesional bleeding, the majority of metastatic brain tumors typically showed a hypointense signal on T1-wighted images and slightly hypointense or isointense signals on T2-weighted images. In contrast, hemorrhagic tumors were characterized by a hyperintense signal on precontrast T1-weighted images and a hypointense signal on T2-weighted images. They were also typically associated with various degrees of perilesional edema (Fig. 1).

Approximately 60 % of our patients suspected to have metastatic brain disease were examined with the use of double-dose gadoteridol. Contrast administration typically led to identification of various types of tumor enhancement (punctate, solid, single or multiple ring, mixed) and clear separation of the neoplasm from the area of perilesional edema (Fig. 2). Without the use of gadoteridol or in cases of absent contrast enhancement, small metastatic tumors of any origin could not be reliably distinguished from brain

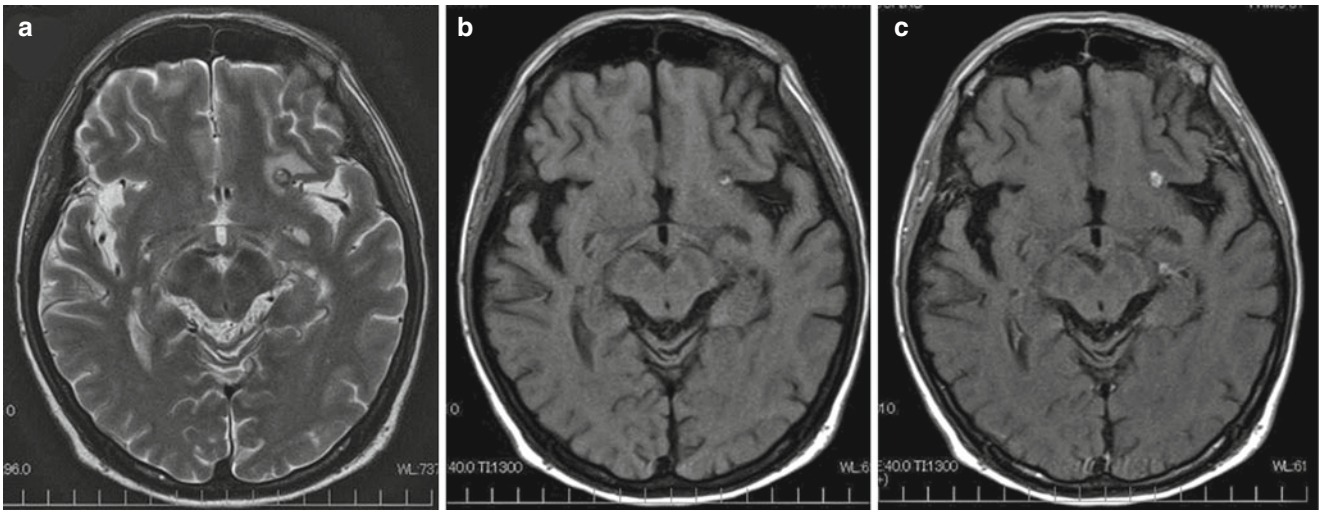

Fig. 1 Brain metastasis of lung adenocarcinoma with previous small intralesional hemorrhage, which appears as a low intensity signal on T2-weighted (**a**) and high intensity signal on precontrast T1-weighted (**b**) images. There is marked contrast enhancement (**c**) and mild perilesional edema

lacunes even with the use of FLAIR and/or DWI. Moreover, whereas single-dose gadoteridol was sufficient for contrast enhancement of large tumors, its use at both 1.5 T and 3.0 T was sometimes associated with difficulty distinguishing tiny brain lesions from normal vascular structures. Small tumors were better characterized with the use of a higher contrast dose, which facilitated their differentiation from normal arteries and veins. Meningeal or subarachnoid tumor dissemination also was better demonstrated after double-dose contrast administration (Fig. 3). However, administration of the higher-dose gadoteridol caused strong enhancement of the dural sinuses, which in some cases caused pulsation artifacts.

Specific MRI Features of Some Tissue Types

In contrast to other lesions, brain metastases of malignant melanoma typically demonstrated high intensity on T1-weighted MRI (Fig. 4). Tumors originated from the thyroid carcinoma usually had mixed isointense to hyperintense signals on T2-weighted images in the absence of the previous hemorrhagic episode and frequently showed strong contrast enhancement of the stroma and capsule (Fig. 5). Metastases of endocrine carcinomas were characterized by low signal intensity on T1- and T2-weighted images and only slight contrast enhancement. Finally, early-stage tiny metastases of small cell lung carcinoma typically were not accompanied by peritumoral edema and could be identified only by the presence of contrast enhancement.

Discussion

Patients with known cancer routinely undergo brain MRI to detect or rule out metastatic brain disease. If intracranial tumors are disclosed, it is important to characterize them precisely with regard to location; interrelations with functionally important intracranial structures; type of growth; vascularity; recent, old, or multiple hemorrhages within or in the vicinity to the mass; presence of peritumoral edema; necrotic changes; subarachnoid dissemination; and/or meningeal carcinomatosis [11]. Each of these factors is important for choice of the optimal treatment strategy and prediction of the prognosis.

The MRI appearance of brain metastases is strongly associated with their histopathological features: vascularity, cellularity, necrosis, previous hemorrhage [5, 11]. On T2-weighted images the solid areas of tumors usually have a slightly hypointense or isointense signal, although the signal may be different if the neoplasm originated from thyroid carcinoma or there was a previous episode of intralesional or perilesional bleeding. There are various types of contrast enhancement. Large metastases are typically accompanied by prominent peritumoral edema, whereas it is usually mild or even absent with small lesions. Particularly, early-stage metastases of small cell lung carcinoma are known to have only punctate or faint ring enhancement and are not accompanied by perifocal edema [10, 13]. This appearance fully corresponds to our own experience and can create significant diagnostic problems. In general, without administration of contrast medium it is nearly impossible to detect small parenchymal or meningeal metastasis even with FLAIR or DWI and/or the use of a 3 T MR scanner.

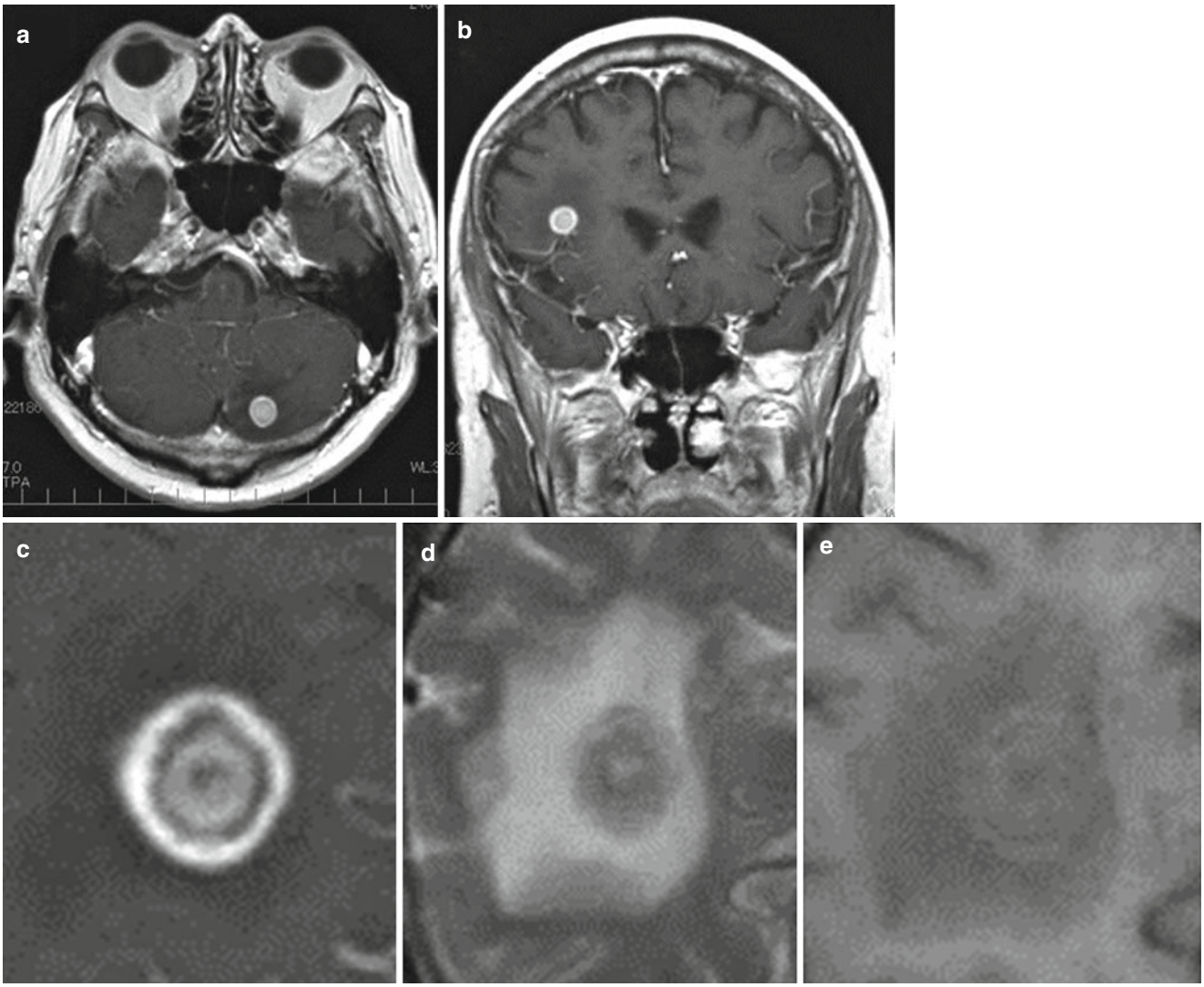

Fig. 2 Prominent contrast enhancement of brain metastases of small cell lung carcinoma in the left cerebellar hemisphere (**a**) and frontal lobe (**b**), with a multiple-layered ring pattern (**c**, *with magnification*). The solid part of the tumor has slightly low intensity, whereas its deeper necrotic part has high intensity on T2-weighted (**d**, *with magnification*) and low intensity on T1-weighted (**e**, *with magnification*) images

It is well known that double-dose contrast medium is preferable because, compared to the single dose, it increases detection of small metastatic brain tumors [13, 14]. However, the amount of administered contrast medium should be reduced in patients with renal failure. In fact, we prefer to perform MRI investigations without the use of any contrast medium in patients with significantly deteriorated renal function or who have an allergy to gadoteridol. Certainly such approach may reduce the diagnostic efficacy, but it avoids complications and/or side effects. Also, high-dose contrast enhancement may result in pulsation artifacts, particularly in patients with well-developed lateral sinuses investigated at 3 T. Sometimes it significantly complicates the evaluation of metastases in the posterior cranial fossa and requires multiple planes of reconstruction.

Some metastatic brain tumors carry specific neuroimaging features that reflect their tissue type. Neoplasms originating from kidney and liver cancers have abundant vasculature and a well-known propensity for intratumoral or peritumoral bleeding. Acute hemorrhages are better demonstrated on computed tomography (CT) than on MRI, although with time an area of hyperintense or hypointense signal can be identified on T2-weighted images that reflect, respectively, the presence of methemoglobin or hemosiderin. Metastases of thyroid cancer, present as localized hypervascular lesions, are mainly located in subcortical brain tissue. They rarely bleed, progress slowly, have an easily identifiable capsule, and are frequently associated with bone metastases in the skull, which sometimes resemble meningioma or hemangiopericytoma. Metastatic melanotic melanomas usually have

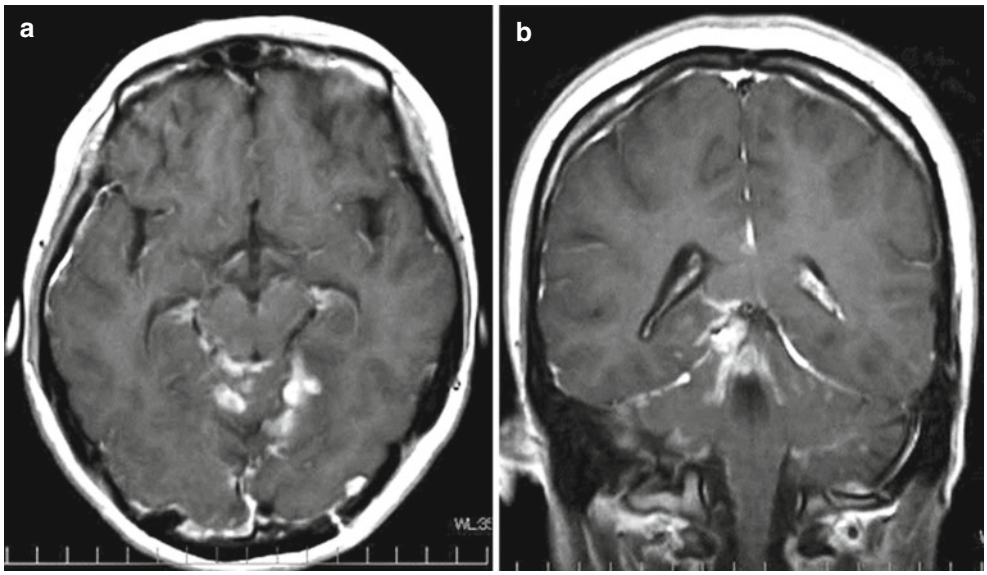

Fig. 3 Disseminated metastases of breast carcinoma. Note the multiple prominently enhanced tumors in the subarachnoid space (**a**) and contrast enhancement around the fourth ventricle (**b**)

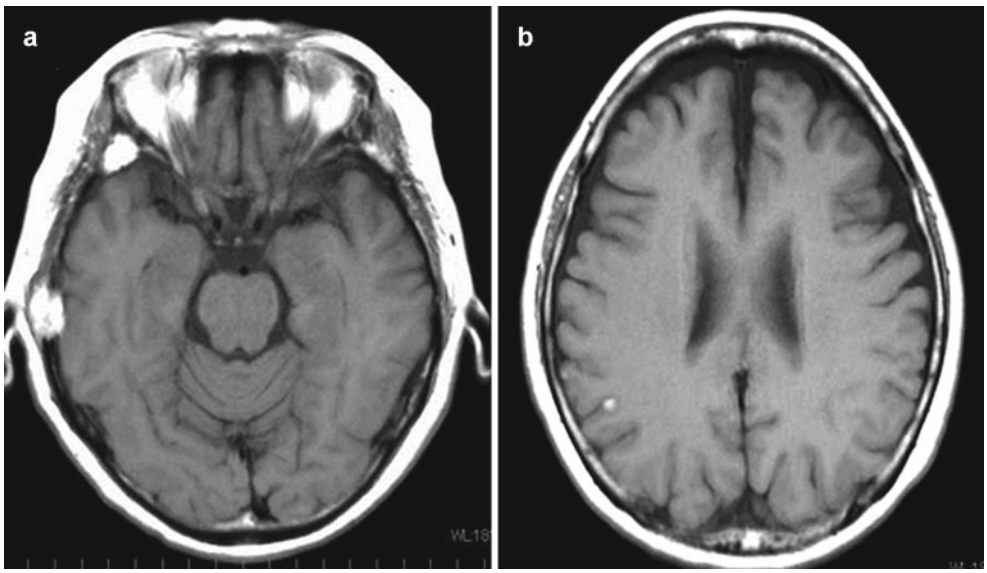

Fig. 4 Intracranial metastases of melanoma. Both bone (**a**) and parenchymal (**b**) lesions have high signal intensity on precontrast T1-weighted images, reflecting the presence of melanin

high intensity on T1-weighted images because of the presence of the paramagnetic substance melanin. Hence, the presence of intratumoral bleeding should be excluded in such cases with FLAIR images or CT. According to our experience, the rather rare intracranial metastases of endocrine carcinomas are characterized by low signal intensity on both T1- and T2-weighted images and display only slight contrast enhancement. Double-ring or triple-ring enhancement with intermittent high-intensity and low-intensity layers is typical for metastases of small cell lung carcinoma, which may correspond to rapid tumor growth with coexistent areas of well-developed vasculature and necroses (however this hypothesis requires histopathological confirmation). Meningeal carcinomatosis and leptomeningeal dissemination are more typical for gastrointestinal, ovarian, and breast carcinomas, which metastases initially affect the mediastinal or retroperitoneal lymph nodes, with subsequent invasion of the spinal nerves, and later perineural spread directly into the subarachnoid space [4, 6]. Recognizing these specific features may be helpful when searching for the primary tumor in cases of intracranial metastases of unknown origin.

It is important to note that not all multiple brain lesions are metastases, even in patients with known malignancy. The differential diagnosis includes multicentric glioma, particularly glioblastoma, lymphoma, leukemia, posttransplant lymphoproliferative disorder (Fig. 6), Behçet's disease, multiple sclerosis (Fig. 7), toxoplasmosis (Fig. 8), multiple abscesses, sarcoidosis, and other infectious and parasitic diseases

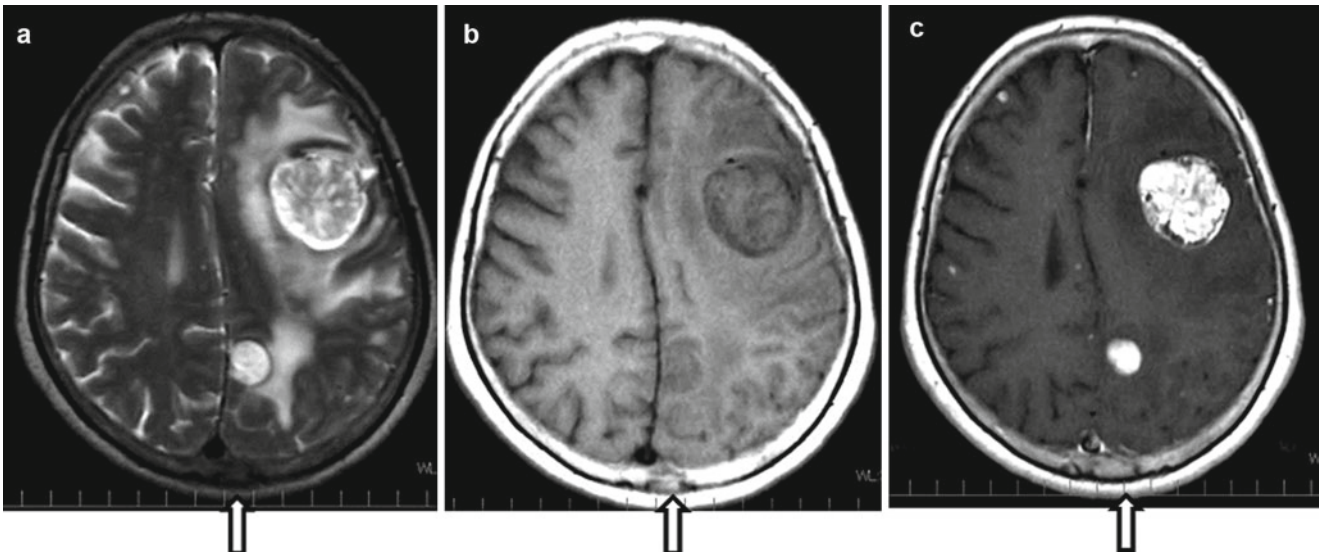

Fig. 5 Multiple parenchymal and bone (*arrow*) metastases of thyroid carcinoma. Hypervascular tumors have heterogeneous signal intensity on T2-weighted (**a**) and T1-weighted (**b**) images. Note the prominent heterogeneous contrast enhancement (**c**). The capsule of the parenchymal tumors is clearly seen

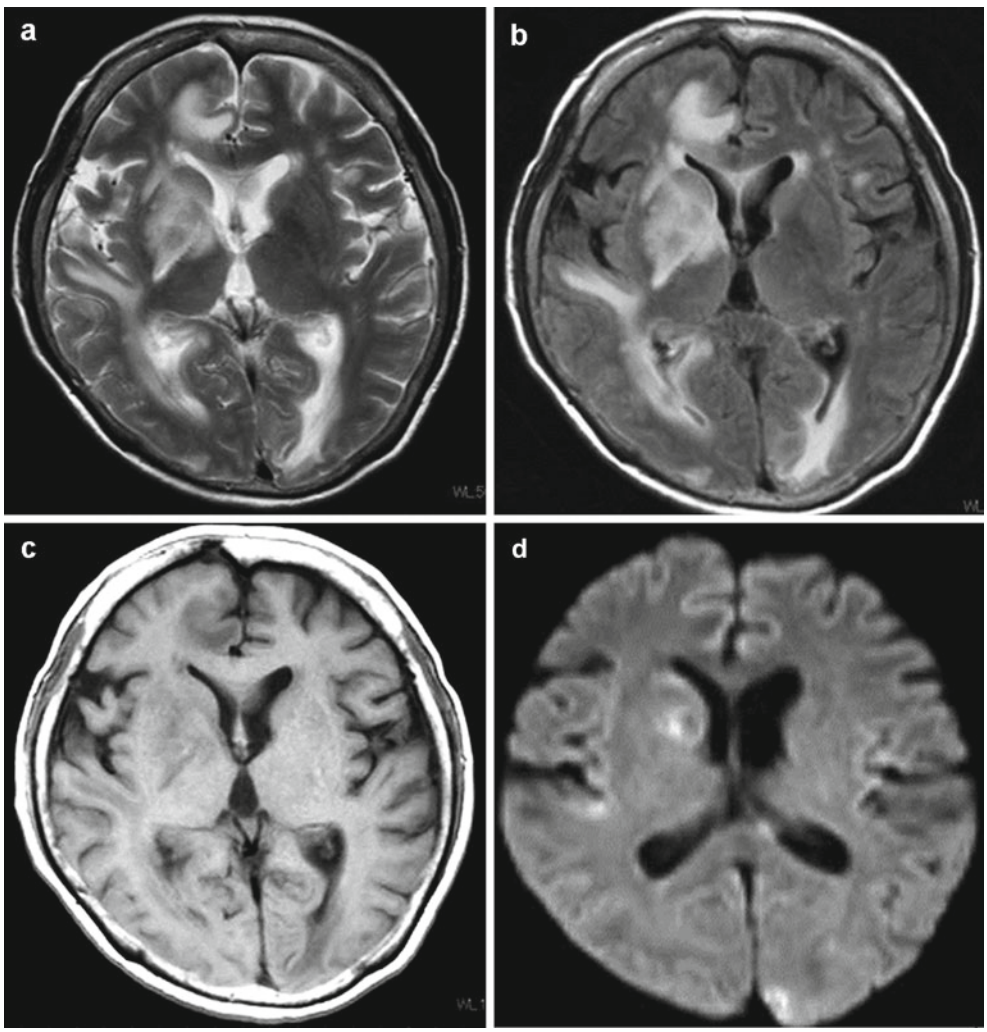

Fig. 6 Posttransplant lymphoproliferative disorder after renal transplantation. Note the multiple, mainly periventricular lesions with prominent perifocal edema and heterogeneous signal intensity on T2-weighted (**a**) and fluid-attenuated inversion recovery (FLAIR) (**b**) images. Almost isointense signal intensity is seen on T1-weighted images (**c**). There is a high intensity signal on diffusion-weighted imaging (**d**)

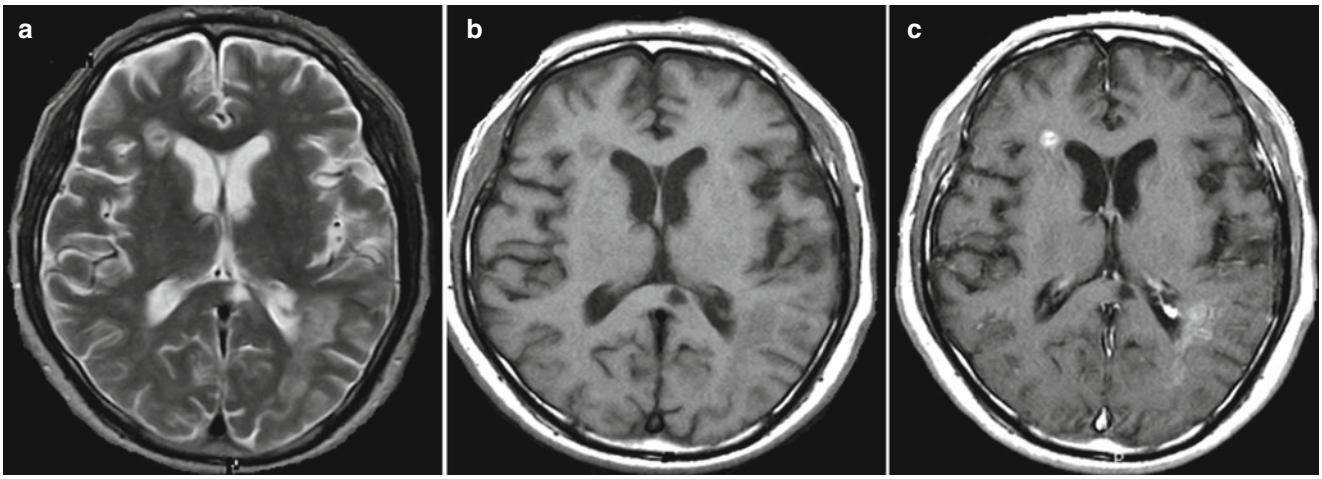

Fig. 7 Multiple sclerosis in an active stage. Several small lesions located in the vicinity of the lateral ventricles present with low signal intensity on T2-weighted (**a**) and isointensity on T1-weighted (**b**) images, perifocal edema, and prominent contrast enhancement (**c**)

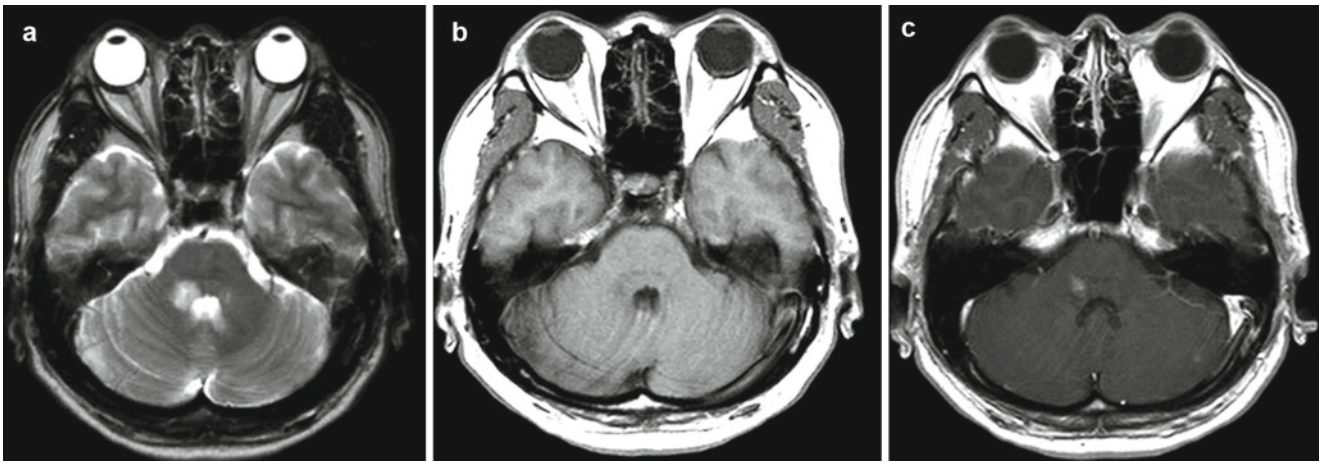

Fig. 8 *Toxoplasma* meningitis. Note the small localized lesion in the pons with inhomogeneously high intensity signal on T2-weighted (**a**) and a hypointense signal on T1-weighted (**b**) images. There is also a patchy contrast enhancement (**c**)

[1, 2, 11, 12]. Certainly, the differential diagnosis in such cases should be based not only on neuroimaging findings but also on a thorough clinical examination, including evaluation of the history and course of the disease, investigation of tumor markers, and sometimes even on brain biopsy results.

Conclusion

Contemporary MRI techniques provide excellent options for detection, detailed characterization, and the differential diagnosis of metastatic brain tumors. These factors are extremely important when choosing the optimal treatment strategy, particularly with Gamma Knife radiosurgery. Intravenous administration of double-dose gadolinium-based contrast medium gadoteridol increases the diagnostic efficacy, especially for small lesions. Specific MRI features of some metastases provide clues for identification of the primary cancer location if it has remained undetected. The possibility of non-metastatic multiple brain lesions in patients with known cancer should be always taken into consideration and requires a thorough differential diagnosis, based not only on neuroimaging, but on additional analysis of the various clinical data.

Conflict of Interest The authors declare that they have no conflict of interest.

References

1. Abe K, Ono Y, Suzuki M, Akagawa H, Omoto K, Sannomiy A, Kohno M, Hayano T, Tanabe K, Teraoka S, Uchiyama S, Okada Y, Sakai S (2010) MRI findings of the post-transplant lymphoproliferative disorder of the Central Nervous System. In: Program and abstracts of the second Japanese-Russian neurosurgical symposium, 9–11 May 2010, Fujiyoshida, Japan, p 17
2. Camacho DL, Smith JK, Castillo M (2003) Differentiation of toxoplasmosis and lymphoma in AIDS patients by using apparent diffusion coefficients. AJNR Am J Neuroradiol 24:633–637
3. Chappell PM, Pelc NJ, Foo TK, Glover GH, Haros SP, Enzmann DR (1994) Comparison of lesion enhancement on spin-echo and gradient-echo images. AJNR Am J Neuroradiol 15:37–44
4. Fidler IJ, Yano S, Zhang RD, Fujimaki T, Bucana CD (2002) The seed and soil hypothesis: vascularization and brain metastases. Lancet Oncol 3:53–57
5. Hayashida Y, Hirai T, Morishita S, Kitajima M, Murakami R, Korogi Y, Makino K, Nakamura H, Ikushima I, Yamura M, Kochi M, Kuratsu JI, Yamashita Y (2006) Diffusion-weighted imaging of metastatic brain tumors: comparison with histologic type and tumor cellularity. AJNR Am J Neuroradiol 27:1419–1425
6. Herman DL, Courville CB (1965) Pathogenesis of meningeal carcinomatosis: report of a case secondary to carcinoma of cecum via perineural extension – with a review of 146 cases. Bull Los Angeles Neurol Soc 30:107–117
7. Lu H, Nagae-Poetscher LM, Golay X, Lin D, Pomper M, van Zijl PC (2005) Routine clinical brain MRI sequences for use at 3.0 Tesla. J Magn Reson Imaging 22:13–22
8. Kato Y, Higano S, Tamura H, Mugikura S, Umetsu A, Murata T, Takahashi S (2009) Usefulness of contrast-enhanced T_1-weighted sampling perfection with application-optimized contrasts by using different flip angle evolutions in detection of small brain metastasis at 3 T MR Imaging: comparison with magnetization-prepared rapid acquisition of gradient echo imaging. AJNR Am J Neuroradiol 30:923–929
9. Mugler JP 3rd, Bao S, Mulkern RV, Guttmann CR, Robertson RL, Jolesz FA, Brookeman JR (2000) Optimized single-slab three-dimensional spin-echo MR imaging of the brain. Radiology 216:891–899
10. Nomoto Y, Miyamoto T, Yamaguchi Y (1994) Brain metastasis of small cell lung carcinoma: comparison of Gd-DTPA enhanced magnetic resonance imaging and enhanced computerized tomography. Jpn J Clin Oncol 24:258–262
11. Schaefer PW, Budzik RF Jr, Gonzalez RG (1996) Imaging of cerebral metastases. Neurosurg Clin N Am 7:393–423
12. Smith AB, Smirniotopoulos JG, Rushing EJ (2008) From the archives of the AFIP: central nervous system infections associated with human immunodeficiency virus infection – radiologic-pathologic correlation. Radiographics 28:2033–2058
13. Suzuki K, Yamamoto M, Hasegawa Y, Ando M, Shima K, Sako C, Ito G, Shimokata K (2004) Magnetic resonance imaging and computed tomography in the diagnoses of brain metastases of lung cancer. Lung Cancer 46:357–360
14. Tatsuno S, Hata Y, Tada S (1996) Double-dose Gd-DTPA: detectability of intraparenchymal brain metastasis. Nihon Igaku Hoshasen Gakkai Zasshi 56:855–859 (in Japanese)

Usefulness of the Advanced Neuroimaging Protocol Based on Plain and Gadolinium-Enhanced Constructive Interference in Steady State Images for Gamma Knife Radiosurgery and Planning Microsurgical Procedures for Skull Base Tumors

Motohiro Hayashi, Mikhail F. Chernov, Noriko Tamura, Shoji Yomo, Manabu Tamura, Ayako Horiba, Masahiro Izawa, Yoshihiro Muragaki, Hiroshi Iseki, Yoshikazu Okada, Pavel Ivanov, Jean Régis, and Kintomo Takakura

Abstract *Background*: Gamma Knife radiosurgery (GKS) is currently performed with 0.1 mm preciseness, which can be designated microradiosurgery. It requires advanced methods for visualizing the target, which can be effectively attained by a neuroimaging protocol based on plain and gadolinium-enhanced constructive interference in steady state (CISS) images.

Methods: Since 2003, the following thin-sliced images are routinely obtained before GKS of skull base lesions in our practice: axial CISS, gadolinium-enhanced axial CISS, gadolinium-enhanced axial modified time-of-flight (TOF), and axial computed tomography (CT). Fusion of "bone window" CT and magnetic resonance imaging (MRI), and detailed three-dimensional (3D) delineation of the anatomical structures are performed with the Leksell GammaPlan (Elekta Instruments AB). Recently, a similar technique has been also applied to evaluate neuroanatomy before open microsurgical procedures.

Results: Plain CISS images permit clear visualization of the cranial nerves in the subarachnoid space. Gadolinium-enhanced CISS images make the tumor "lucid" but do not affect the signal intensity of the cranial nerves, so they can be clearly delineated in the vicinity to the lesion. Gadolinium-enhanced TOF images are useful for 3D evaluation of the interrelations between the neoplasm and adjacent vessels. Fusion of "bone window" CT and MRI scans permits simultaneous assessment of both soft tissue and bone structures and allows 3D estimation and correction of MRI distortion artifacts.

Conclusion: Detailed understanding of the neuroanatomy based on application of the advanced neuroimaging protocol permits performance of highly conformal and selective radiosurgical treatment. It also allows precise planning of the microsurgical procedures for skull base tumors.

Keywords CISS • Gadolinium-enhanced CISS • Gamma Knife radiosurgery • Leksell GammaPlan • Microsurgery • Skull base tumor

M. Hayashi (✉)
Department of Neurosurgery, Neurological Institute,
Tokyo Women's Medical University,
8-1 Kawada-cho, Shinjuku-ku, Tokyo 162-8666, Japan

Faculty of Advanced Techno-Surgery,
Institute of Advanced Biomedical Engineering and Science,
Tokyo Women's Medical University, Tokyo, Japan

Saitama Gamma Knife Center, Sanai Hospital,
Saitama, Japan
e-mail: gkrmoto@aol.com

M.F. Chernov, Y. Muragaki, H. Iseki, and K. Takakura
Department of Neurosurgery, Neurological Institute,
Tokyo Women's Medical University, Tokyo, Japan

Faculty of Advanced Techno-Surgery,
Institute of Advanced Biomedical Engineering and Science,
Tokyo Women's Medical University, Tokyo, Japan

N. Tamura, A. Horiba, M. Izawa, and Y. Okada
Department of Neurosurgery, Neurological Institute,
Tokyo Women's Medical University, Tokyo, Japan

S. Yomo
Saitama Gamma Knife Center, Sanai Hospital, Saitama, Japan

M. Tamura
Faculty of Advanced Techno-Surgery,
Institute of Advanced Biomedical Engineering and Science,
Tokyo Women's Medical University, Tokyo, Japan

P. Ivanov
Radiosurgical Center, International Institute of the Biological Systems,
Saint Petersburg, Russia

J. Régis
Department of Functional and Stereotactic Neurosurgery,
Timone University Hospital, Marseille, France

Faculty of Advanced Techno-Surgery,
Institute of Advanced Biomedical Engineering and Science,
Tokyo Women's Medical University, Tokyo, Japan

Introduction

The beginning of achievements in contemporary neurosurgical techniques occurred around five decades ago with introduction of the operating microscope into clinical practice. It

M.F. Chernov et al. (eds.), *Gamma Knife Neurosurgery in the Management of Intracranial Disorders*,
Acta Neurochirurgica Supplement, Vol. 116, DOI 10.1007/978-3-7091-1376-9_26, © Springer-Verlag Wien 2013

initiated a shift from traditional surgical principles to microsurgery, making it possible to effectively manage intracranial lesions while sparing adjacent functionally important anatomical structures. New treatment goals and requirements stimulated extensive studies of relevant microanatomy and neurophysiology, which were further enhanced by the introduction of advanced neuroimaging modalities, such as computed tomography (CT) and magnetic resonance imaging (MRI). Today, the latter represents the main investigative tool for patients with brain disorders. It allows detailed evaluation of the structural, functional, and metabolic characteristics of intracranial lesions and permits the neurosurgeon to make reasonable choices regarding the optimal treatment strategy in individual cases directed at the best possible outcome with minimal risk of complications.

Development of Gamma Knife radiosurgery (GKS) followed a similar pathway. It was created during the 1950s and was introduced into wide clinical practice at the end of the 1960s. Further advances in GKS were stimulated by the progress being made with neuroimaging methods. Simultaneous to establishment of radiosurgical treatment standards, the technique gradually became widely accepted for managing a variety of brain disorders. Recent technological achievements and the introduction of computer-aided robotized devices, such as the automatic positioning system (APS) and PerfeXion (Elekta Instruments AB, Stockholm, Sweden), which allow treatment with 0.1 mm precision, have initiated a shift from traditional radiosurgery to microradiosurgery. The latter definitely requires advanced methods for visualizing the target and detailed evaluation of the relevant neuroanatomy. Microradiosurgery also requires new concepts regarding treatment planning, with the goal of performing effective stereotactic irradiation of the lesion while sparing the normal functioning of adjacent structures.

Traditional GKS is mainly based on gadolinium-enhanced T1-weighted MRI, which is a useful sequence that provides excellent information on tumor location and its interrelations with major anatomical structures. However, the images do not permit detailed evaluation of the tiny cranial nerves and vessels. Moreover, contrast enhancement on T1-weighted images is not selective because of the partial volume effect. Thus, nuances of the target neuroanatomy cannot be seen, thereby precluding, for example, evaluation of the interrelations between the lesion and adjacent cranial nerves (Fig. 1) or delineation of the separate structures in the internal acoustic canal (IAC) and in the cavernous sinus. Such pitfalls create a significant obstacle to application of conformal and selective radiosurgical treatment planning. This, in turn, may result in inadvertent irradiation of functionally important anatomical structures with possible development of post-treatment complications. Therefore, new methods directed at reliable evaluation of the microanatomy within the target are definitely required.

Development of an advanced neuroimaging protocol for radiosurgical treatment planning was initiated by our group at Tokyo Women's Medical University in 2001 and was fully established by the beginning of 2003 [8]. Since then, it has been in constant use for skull base lesions. It corresponds in part to our concept of robotic microradiosurgery [4–9, 16] using the Leksell Gamma Knife model 4C with APS (Elekta Instruments AB). We have recently been applying a similar technique to detailed evaluation of neuroanatomy in cases planned for the combined management with subtotal surgical resection and subsequent radiosurgery (e.g., for skull base meningiomas) or even for pure microsurgical management (e.g., paraclinoid aneurysms [10]). The details and advantages of the neuroimaging protocol, based on plain and gadolinium-enhanced constructive interference in steady state (CISS) images, and the results of its application to skull base tumors are presented herein.

Materials and Methods

Our current practice is to obtain the following MRI sequences under stereotactic conditions before GKS of skull base lesions: (1) axial three-dimensional (3D) heavily T2-weighted (CISS) with a slice thickness of 0.5 mm; (2) gadolinium-enhanced axial CISS with a slice thickness of 0.5 mm; (3) gadolinium-enhanced axial modified time-of-flight (TOF) with a slice thickness of 1.0 mm. Additionally, plain, "bone window," and contrast-enhanced axial CT scans with the slice thickness of 1.0 mm are undertaken in each case.

All MRI scans are obtained using a 1.5 T clinical scanner (ExcellArt; Toshiba Medical Systems, Tokyo, Japan). In total, 300–500 slices are acquired for each sequence. The acquisition parameters for CISS images are as follows: repetition time (TR) 9.04 ms, echo time (TE) 4.52 ms, average 2, flip angle 70°, slice oversampling at 10 %, phase oversampling at 0 %, 80 slices per slab. Acquisition time is 6.47 min. Routinely, for MRI examinations of skull base lesions, a single dose (0.1 mmol/kg) of the gadolinium-based contrast medium gadoteridol (ProHance®; Eisai, Tokyo, Japan) is administered intravenously.

All neuroimaging data are exported to Leksell GammaPlan (Elekta Instruments AB), where "bone window" CT and MRI scans are fused and radiosurgical treatment planning is undertaken by referring to a simultaneous onscreen display of all obtained images in the original 3D workspace. Since recently we have also started to use pretreatment simulation of GKS with newly available software in the Leksell GammaPlan ("Image merge" and "Preplan"). A similar technique is frequently applied for detailed evaluation of the neuroanatomy in cases planned for subtotal surgical resection and subsequent radiosurgery or even for pure microsurgical management [10].

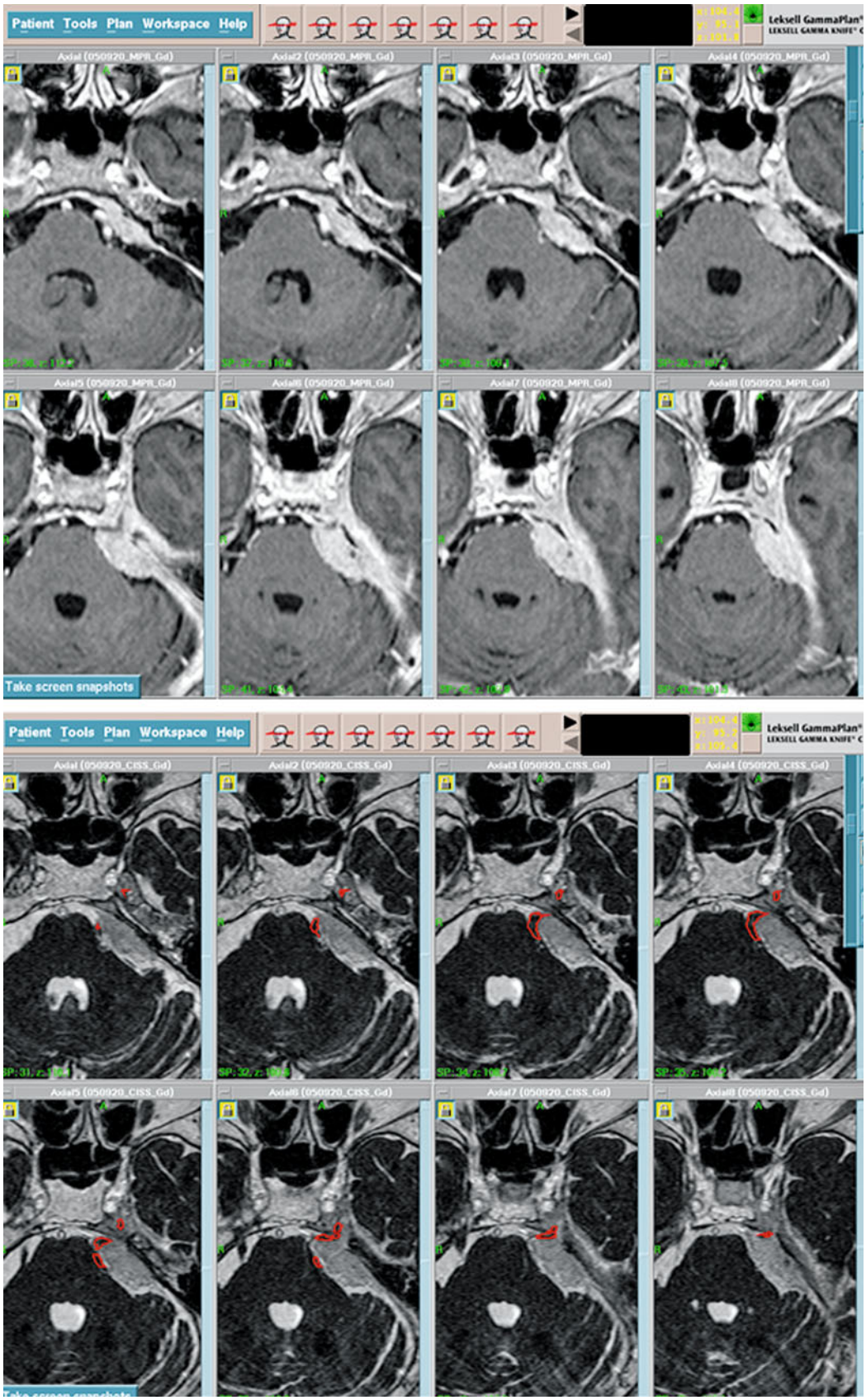

Fig. 1 Left-sided petrous apex meningioma. Gadolinium-enhanced T1-weighted magnetic resonance imaging (MRI) (*upper*) does not permit reliable evaluation of the interrelations between the tumor and the adjacent trigeminal nerve. In contrast, gadolinium-enhanced constructive interference in steady state (CISS images) (*lower*) provide a more detailed view, allowing delineation of the nerve (*red*)

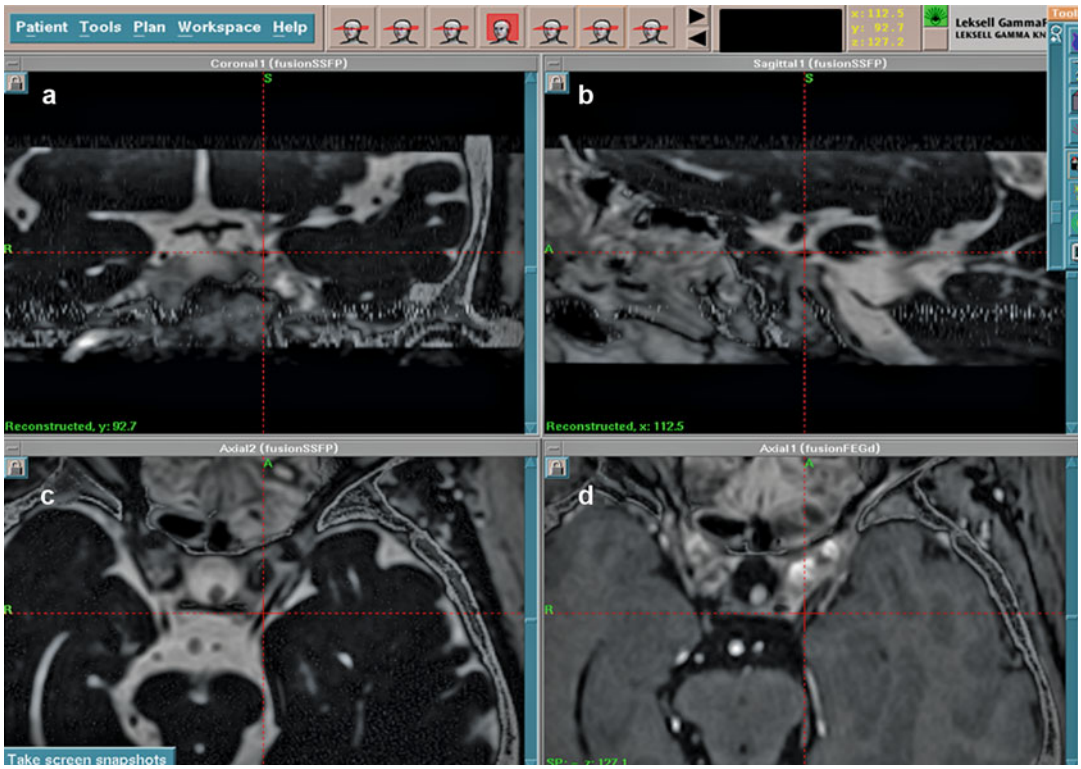

Fig. 2 Coronal (**a**), sagittal (**b**), and axial (**c**) CISS and time-of-flight (TOF) (**d**) images fused with "bone window" computed tomography (CT) permit detailed evaluation of the sellar anatomy and clearly demonstrate both cisternal and intracavernous segments of the oculomotor nerve (From Hayashi et al. [5])

Of note: gadolinium-enhanced T1- and T2-weighted images, which were widely used in our practice previously, have been practically abandoned for radiosurgery treatment planning.

Results

Compared to traditional radiological techniques, our current neuroimaging protocol for GKS has important advantages. First, thin-sliced plain CISS images permit clear visualization of the cranial nerves located intradurally (Meckel's cave, lateral wall of the cavernous sinus) or within the subarachnoid cisterns (Fig. 2). Moreover, separate components of some cranial nerves (e.g., trigeminal, vestibulocochlear) can be differentiated from each other even with 1.5 T MRI scanners. Second, gadolinium-enhanced CISS images make the tumor "lucid" but do not affect the signal intensity of the adjacent cranial nerves. Therefore, they can be clearly delineated (for example, in the vicinity of a vestibular schwannoma in IAC) (Fig. 3). Third, gadolinium-enhanced TOF, which is an original sequence for magnetic resonance angiography (MRA), provides information comparable to that attained with T1-weighted imaging but has an advantage of 3D grasping of the structures. Therefore, evaluation is easier, particularly for understanding the interrelations between the neoplasm and adjacent vessels. Finally, fusion of "bone window" CT and MRI permits simultaneous evaluation of soft-tissue and bone structures. This is particularly useful after previous skull base surgery and in cases of sellar tumors or lesions affecting the petrous bone (Fig. 4). This technique also allows 3D evaluation of the possible distortion artifacts on MRI and permits their correction, which may be important for GKS in the vicinity of eloquent brain areas.

Detailed understanding of neuroanatomy through application of the advanced neuroimaging protocol has permitted us to perform highly conformal and selective radiosurgical treatment of skull base tumors while sparing adjacent structures from excessive irradiation. It has also allowed detailed planning of the microsurgical procedures with regard to selecting the optimal approach and access to the lesion, choosing the strategy for managing the cranial nerves and functionally important vessels, and predetermining the limits of a safe resection.

Illustrative Cases

Case 1

A 33-year-old woman presented with a complaint of intermittent weakness of the facial muscles on the left side. MRI disclosed a tumor in the middle cranial fossa that extended

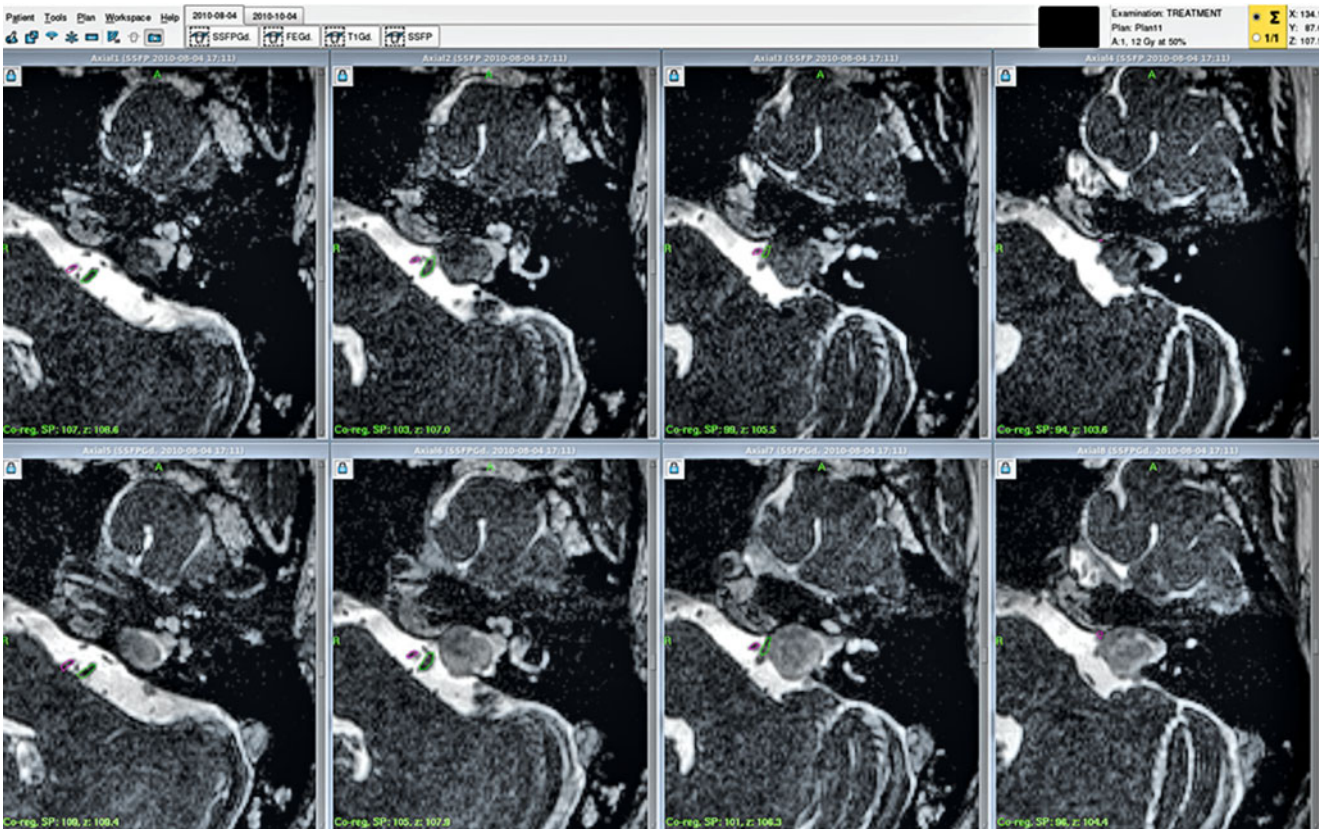

Fig. 3 Left-sided vestibular schwannoma. Delineation of the facial (*pink*) and vestibulocochlear (*green*) nerves using plain (*upper row*) and gadolinium-enhanced (*lower row*) CISS images

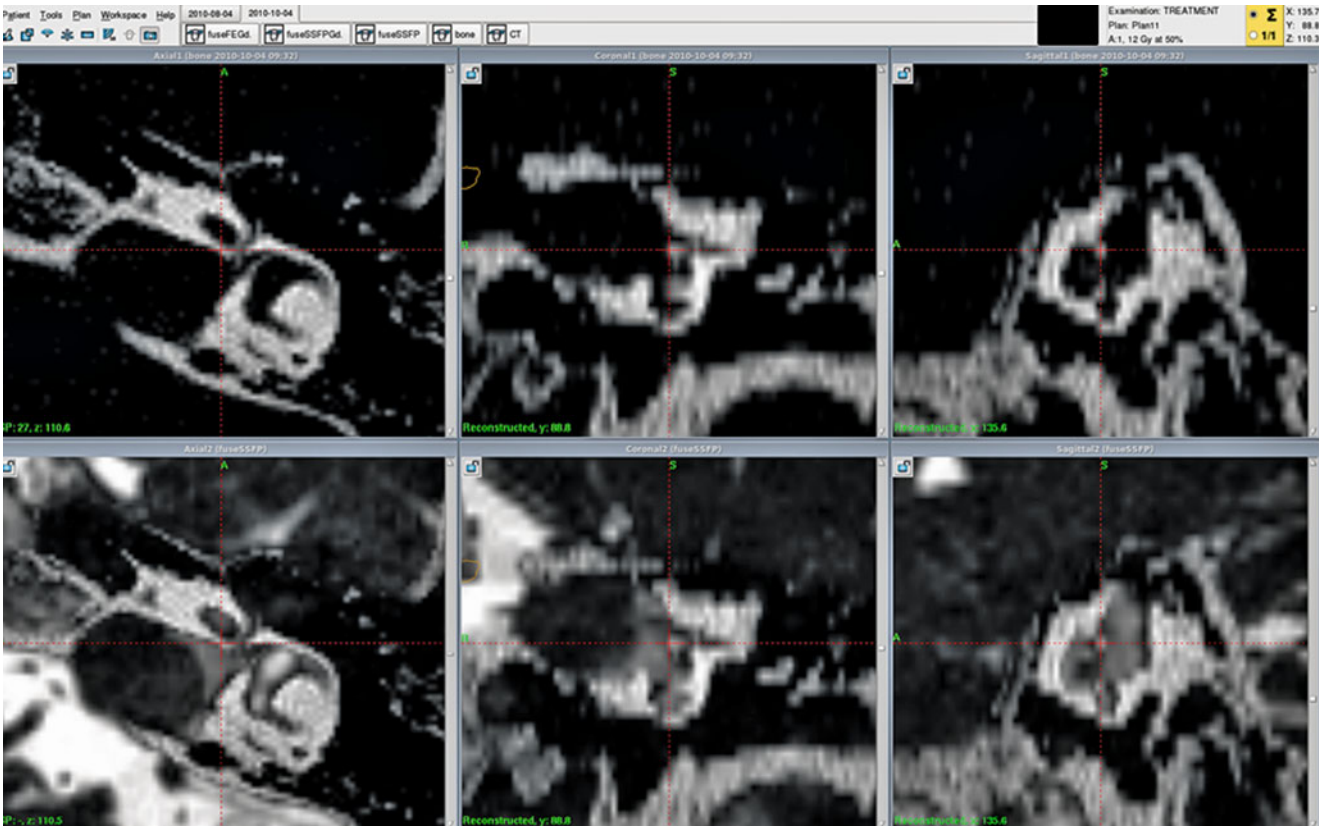

Fig. 4 Left-sided vestibular schwannoma of Koos stage II. Identification of the intrameatal horizontal bar on "bone window" CT (*upper row*) and on its fusion with plain CISS images (*lower row*)

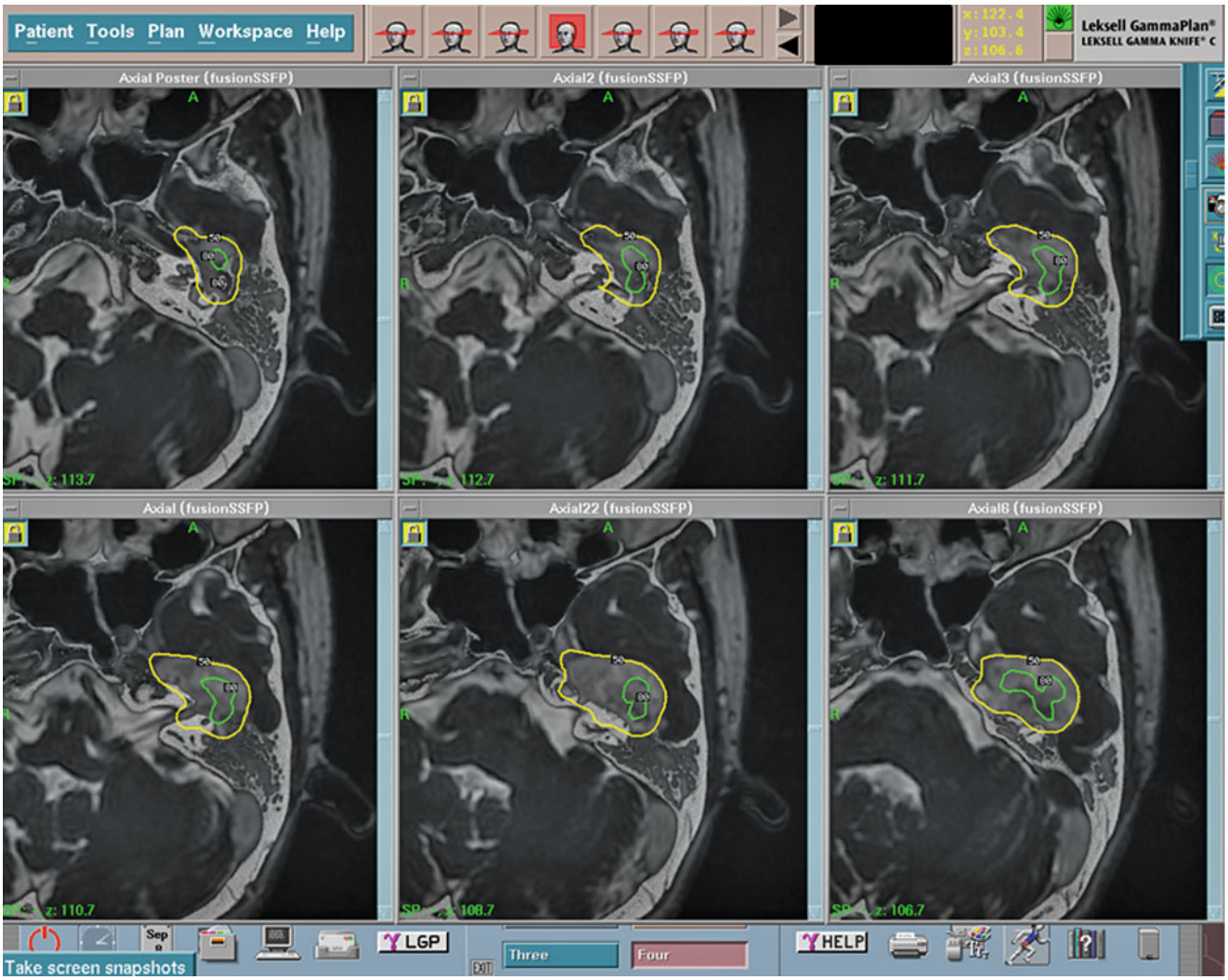

Fig. 5 Radiosurgical treatment plan for a large left-sided facial nerve schwannoma originating from the geniculate ganglion with extension into the middle cranial fossa. Fused axial thin-sliced gadolinium-enhanced CISS and "bone window" CT images provided detailed visualization of the neoplasm and adjacent anatomical structures, which permitted conformal and highly selective dose planning. *Yellow* and *green lines* correspond to 50 and 80 % isodose lines, respectively

into the IAC via the facial notch and seemingly originated from the geniculate ganglion. The largest diameter of the lesion, which was thought to be a facial nerve schwannoma, was 25 mm. Taking into consideration the young age and long life expectancy of the patient, microsurgical resection of the neoplasm was planned at first, but the patient preferred GKS because of the better chance of preserving facial nerve function. Radiosurgical treatment planning was based on fused axial thin-sliced gadolinium-enhanced CISS and "bone window" CT images (Fig. 5). The facial and vestibulocochlear nerves were perfectly visualized as were the cochlea and semicircular canals. The border between the floor of the middle cranial fossa and temporal lobe was clearly seen. A highly conformal and selective treatment plan was created with a margin dose of 12 Gy applied to the 50 % isodose line and wide intralesional 80 % isodose area for greater probability of tumor shrinkage. Adjacent anatomical structures, particularly the cranial nerves and cochlea, which were precisely identified on the fused gadolinium-enhanced CISS and "bone window" CT images, were effectively spared from excessive irradiation.

Case 2

A 54-year-old man had an incidentally discovered left-sided petroclival tumor, most likely meningioma. Gadolinium-enhanced T1-weighted images (Fig. 6, *upper*) showed the location of the neoplasm, mild compression of the pons, and extension of the lesion into the cavernous sinus.

However, adjacent cranial nerves could not be clearly seen. Gadolinium-enhanced CISS images demonstrated that the cavernous sinus was, in fact, free of tumor, which seemingly originated from the dura propria of the medial part of Meckel's cave and extended both anteriorly into it and posteriorly into the prepontine cistern. The trigeminal nerve was shifted laterally, whereas the oculomotor and abducent nerves were not affected, although they were located in close vicinity to the lesion. Such detailed visualization permitted us to create a conformal and highly selective radiosurgical treatment plan. The margin dose of 12 Gy was applied to the 50 % isodose line, sparing all adjacent cranial nerves from the excessive irradiation (Fig. 6, *lower*).

Case 3

A 55-year-old man presented with left-sided facial numbness. MRI disclosed a large multicystic tumor located in the left cerebellopontine cistern. Based on clinical and radiological findings, a vestibular schwannoma was strongly suspected. However, detailed evaluation of the neuroanatomy based on gadolinium-enhanced CISS images installed in the Leksell GammaPlan and delineation of the adjacent III, V, VI, VII, and VIII cranial nerves changed the diagnosis to trigeminal schwannoma, particularly because the ipsilateral V nerve could not be followed in the vicinity to the tumor (Fig. 7). Preoperative considerations were confirmed at the time of microsurgical resection of the neoplasm.

Case 4

A 48-year-old woman presented with mild swallowing problems. MRI demonstrated a large left-sided petrous tumor, most likely a meningioma, compressing the pons and adjacent cerebellar hemisphere (Fig. 8, *upper*). To obtain the optimal functional outcome, we planned combined treatment with subtotal resection followed by GKS of the residual lesion. The main goal of the first stage was to verify the histopathological diagnosis and to perform maximum possible reduction of the mass volume without injuring the adjacent and engulfed cranial nerves. Preoperative evaluation of neuroanatomy based on gadolinium-enhanced CISS images installed in the Leksell GammaPlan revealed that the tumor originated from the dura mater between the internal acoustic meatus and jugular foramen and slightly extended into the latter. The trigeminal, facial, and vestibulocochlear nerves were shifted superiorly by the mass, whereas the lower cranial nerves were shifted inferiorly (Fig. 8, *center*). Intraoperative microsurgical findings confirmed the preoperative considerations (Fig. 8, *lower*).

Case 5

A 73-year-old man presented with progressive left oculomotor nerve palsy. MRI demonstrated a huge sphenopetroclival tumor with extension into both cavernous sinuses. It was most likely a meningioma (Fig. 9). Combined treatment with subtotal resection followed by GKS of the residual lesion was planned. Preoperative evaluation of neuroanatomy based on gadolinium-enhanced CISS images installed in the Leksell GammaPlan revealed that the tumor originated from the dura mater of the superolateral part of the lateral wall of the left cavernous sinus and widely extended inferiorly into the cavernous sinus itself, laterally into the middle cranial fossa, and posteriorly into the prepontine and cerebellopontine cisterns. The left oculomotor nerve was shifted laterally. Intraoperative microsurgical findings confirmed the preoperative considerations.

Discussion

Modern equipment provides an opportunity to perform GKS with 0.1 mm precision, which initiated the shift from traditional radiosurgery to microradiosurgery. The main goals of the latter are similar to operative microneurosurgery: effective management of the lesion while sparing all functionally important anatomical structures for the best possible outcome with minimal risk of posttreatment complications. Realization of such objectives requires new radiological methods for detailed visualization and evaluation of the target area. These goals can be particularly attained with application of the described neuroimaging protocol based on plain and gadolinium-enhanced CISS images.

Application of the CISS-Based Neuroimaging Protocol for GKS

It is well known that the CISS sequence is highly effective for visualizing anatomical structures located in cerebrospinal fluid (CSF)-filled spaces, such as cerebral ventricles and subarachnoid cisterns [2, 8, 11, 12, 17–21]. We have already reported the usefulness and clinical advantages of its application to radiosurgical treatment planning [4–8, 16]. Installation of thin-sliced CISS images in the Leksell GammaPlan provides clear 3D visualization of the anatomical structures even with the use of 1.5 T clinical MRI scanners. For example, the cavernous sinus filled with blood appears "lucid," which permits clear delineation of the cranial nerves in its lateral wall [5, 15], as shown on Fig. 2. Visualizing anatomical structures in close vicinity to the tumor, particularly if it is large or confined to a

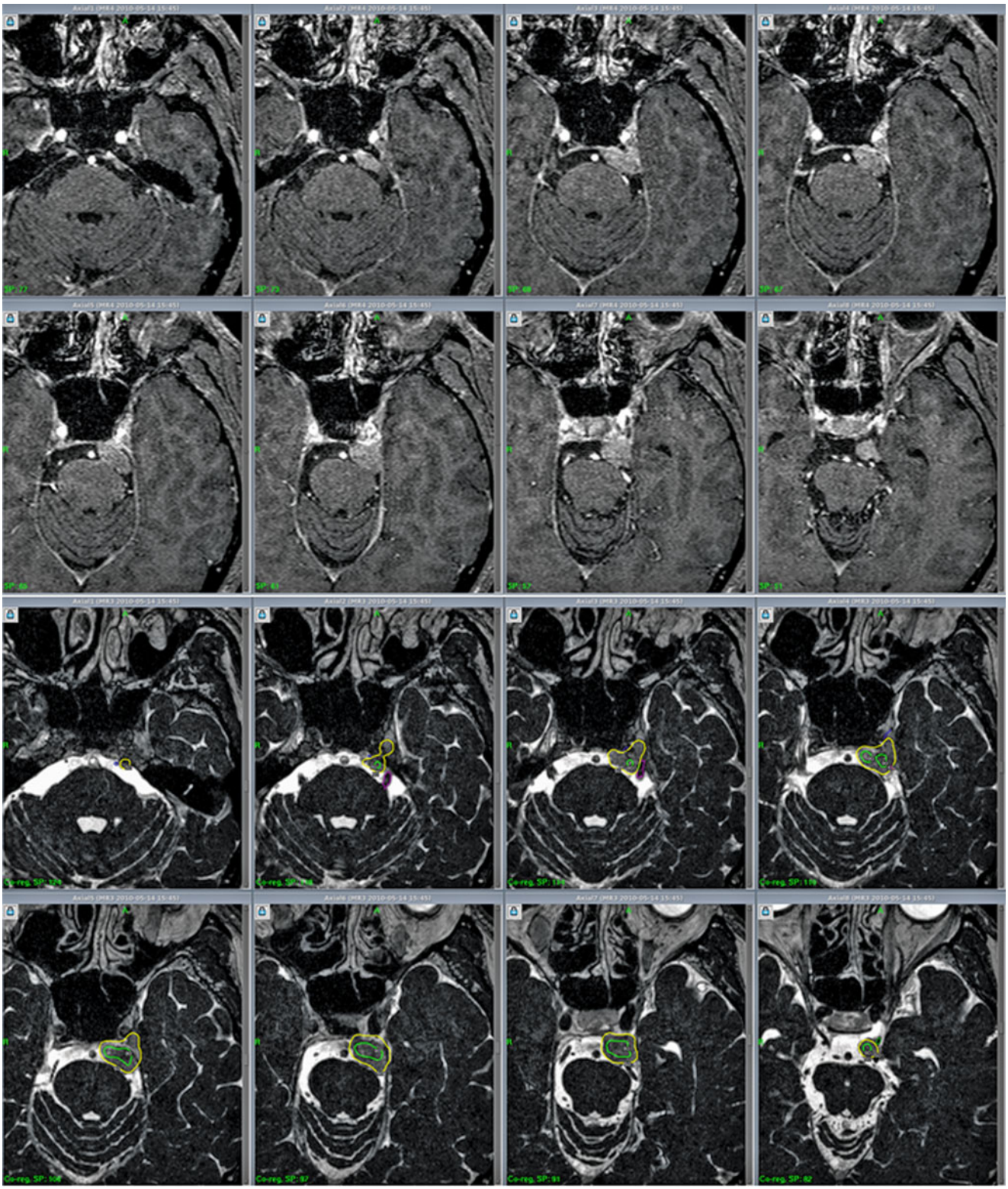

Fig. 6 Incidentally disclosed left-sided petroclival meningioma. Gadolinium-enhanced T1-weighted images (*upper*) clearly demonstrated tumor location but did not permit detailed evaluation of the related neuroanatomy. In contrast, gadolinium-enhanced CISS images showed the origin of the neoplasm from the medial part of Meckel's cave, absence of an intracavernous extension, lateral shift of the trigeminal nerve, and adjacent III and VI cranial nerves, which allowed application of conformal and highly selective radiosurgical treatment (*lower*). *Yellow* and *green lines* correspond to 50 and 80 % isodose lines, respectively

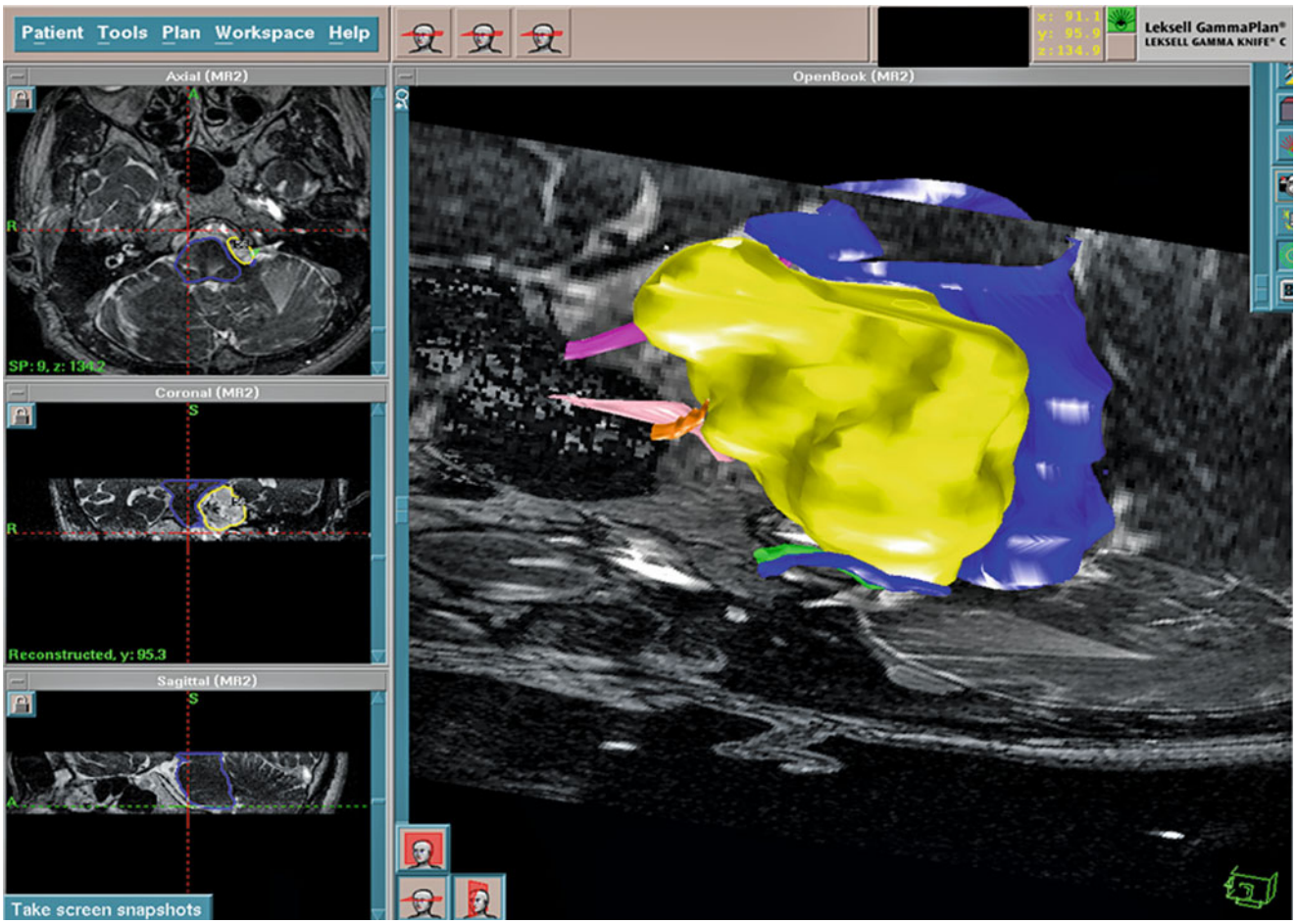

Fig. 7 Three-dimensional preoperative evaluation of a large left-sided trigeminal schwannoma using gadolinium-enhanced CISS images installed in the Leksell GammaPlan. The neoplasm originated from the trigeminal nerve and shifted the adjacent III, VI, VII, and VIII cranial nerves. Tumor (*yellow*), brain stem (*blue*), and left oculomotor (*rose*), abducent (*pink*), trigeminal (*orange*), facial (*green*), and vestibulocochlear (*blue*) nerves are delineated

limited anatomical space (e.g., IAC), is sometimes difficult. The problem can be effectively resolved by using gadolinium-enhanced CISS images. Administration of contrast medium results in moderate prolongation of the signal from the tumor and approximates it to that of CSF, but it does not affect significantly the signal intensity from the adjacent cranial nerves, thereby permitting their visualization and delineation.

At present, in many centers GKS is based solely on MRI findings. In contrast, we routinely use thin-sliced CT as well. The recognizable advantage of CT over MRI is clear visualization of the osseous structures, which in our opinion is particularly important during radiosurgery of skull base tumors. It is evident that in such cases the bone anatomy within or in the vicinity to the target is complex, particularly if the lesion had undergone previous resection. Also, cranial nerves and vessels located on the cranial base or traversing through it, and specific intraosseous anatomical structures (e.g., the cochlea) require clear visualization to avoid excessive irradiation during radiosurgery. Fused "bone window" CT and thin-sliced CISS images permit simultaneous visualization of soft tissues and bones. The usefulness of this technique for evaluating the lateral extension of the intracanalicular part of vestibular schwannomas and estimating the distance between the tumor and fundus was reported previously [12] and can be seen on Fig. 4. Additionally, the technique permits 3D evaluation and possible correction of MRI distortion artifacts [4].

Finally, application of the described neuroimaging protocol and "bone window" CT and MRI fusion frequently allows us to determine the origin of the mass lesion. Identification of such an area on the dura mater in cases of meningioma may lead to its inclusion in the high-dose irradiation field with possible effect on the abundant feeding vessels of the neoplasm [4]. Also, identification of a tumor's origin allows us to presume the process of its steady enlargement during growth and predict the direction in which the adjacent cranial nerves have shifted, which may permit the surgeon to avoid subjecting them to excessive radiation during treatment.

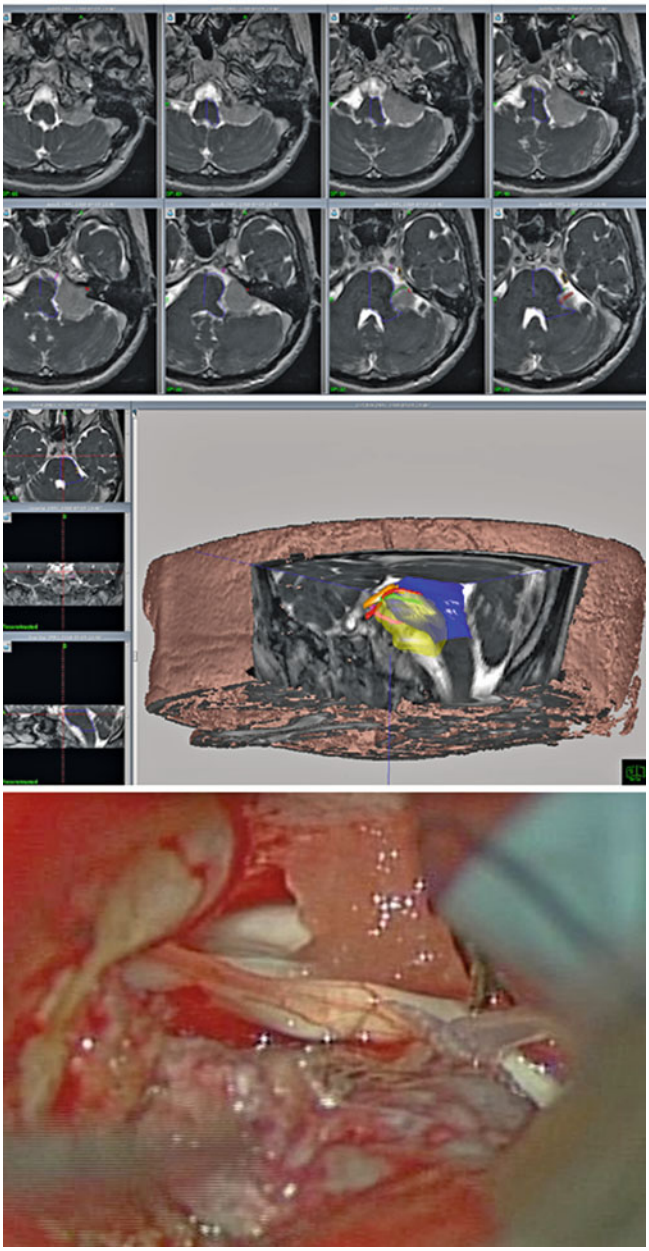

Fig. 8 Left-sided petrous meningioma. This middle-aged patient had a large tumor that originated from the dura mater between the internal acoustic meatus and jugular foramen (*upper*). The plan was to treat the tumor with initial subtotal surgical resection and subsequent GKS for residual neoplasm. Therefore, a detailed preoperative three-dimensional (3D) evaluation of the relevant neuroanatomy based on gadolinium-enhanced CISS images installed in the Leksell GammaPlan was undertaken (*center*). The intraoperative microsurgical findings (*lower*) confirmed the preoperative assumptions

Other Applications of the CISS-Based Neuroimaging Protocol

Although the proposed neuroimaging protocol was initially developed by us for planning radiosurgical treatment with the Gamma Knife, it is now being used with other objectives in mind.

Many intracranial disorders are being effectively treated by microsurgery and radiosurgery. The choice between these two options is usually based on the subjective criteria of the individual doctor, mainly based on his or her personal clinical experience. To make this decision-making process more objective, we are performing a simulation of the radiosurgical treatment in the Leksell GammaPlan based on use of the described neuroimaging protocol. It allows us to decide in advance whether GKS can be effectively applied in a particular case and to predict its results and risk of complications. This technique is particularly useful for tumors located in close proximity to functionally important intracranial structures (e.g., optic pathways). In our experience, simulation of radiosurgery can be effectively applied even in outpatient clinics. For such a purpose, we use two computers with installed Leksell GammaPlans interconnected via the Intranet. One is located in the Gamma Knife Unit, where the treatment planning is undertaken by an experienced neurosurgeon with subspecialization in radiosurgery. The other is in the outpatient clinic, where the data can be shown to a patient and his or her family and explained in detail.

In many patients, particularly those with large skull base meningiomas, the optimal functional outcome can be obtained with combined management, including initial subtotal tumor resection and subsequent stereotactic irradiation of the residual neoplasm. In such cases, detailed 3D evaluation of the intracranial lesion and adjacent structures in the Leksell GammaPlan facilitates planning of the microsurgical procedure. Particularly, it permits an objective preoperative determination regarding which part of the lesion can be safely resected and which one should be left in place for subsequent radiosurgery.

The same technique can also be used for planning pure microsurgical procedures. We have found it useful in patients with C2–C3 aneurysms [10]. In such cases, evaluation of gadolinium-enhanced CISS images in the Leksell GammaPlan may facilitate identification of the distal and proximal dural rings, which has a significant impact on the treatment strategy but is difficult to assess reliably with routine clinical methods [1, 3, 13, 14]. Similarly, the interrelations between cranial nerves and adjacent vessels can be evaluated before microvascular decompression procedures. It should be emphasized that patients usually experience greater satisfaction if they see a 3D view of the intracranial lesion and nearby anatomical structures on the computer display during the information session. It facilitates obtaining the patient's informed consent to proceed with treatment.

Conclusions

The proposed neuroimaging protocol based on plain and gadolinium-enhanced CISS images is useful for radiosurgical treatment planning in cases of skull base tumors. Clear delineation

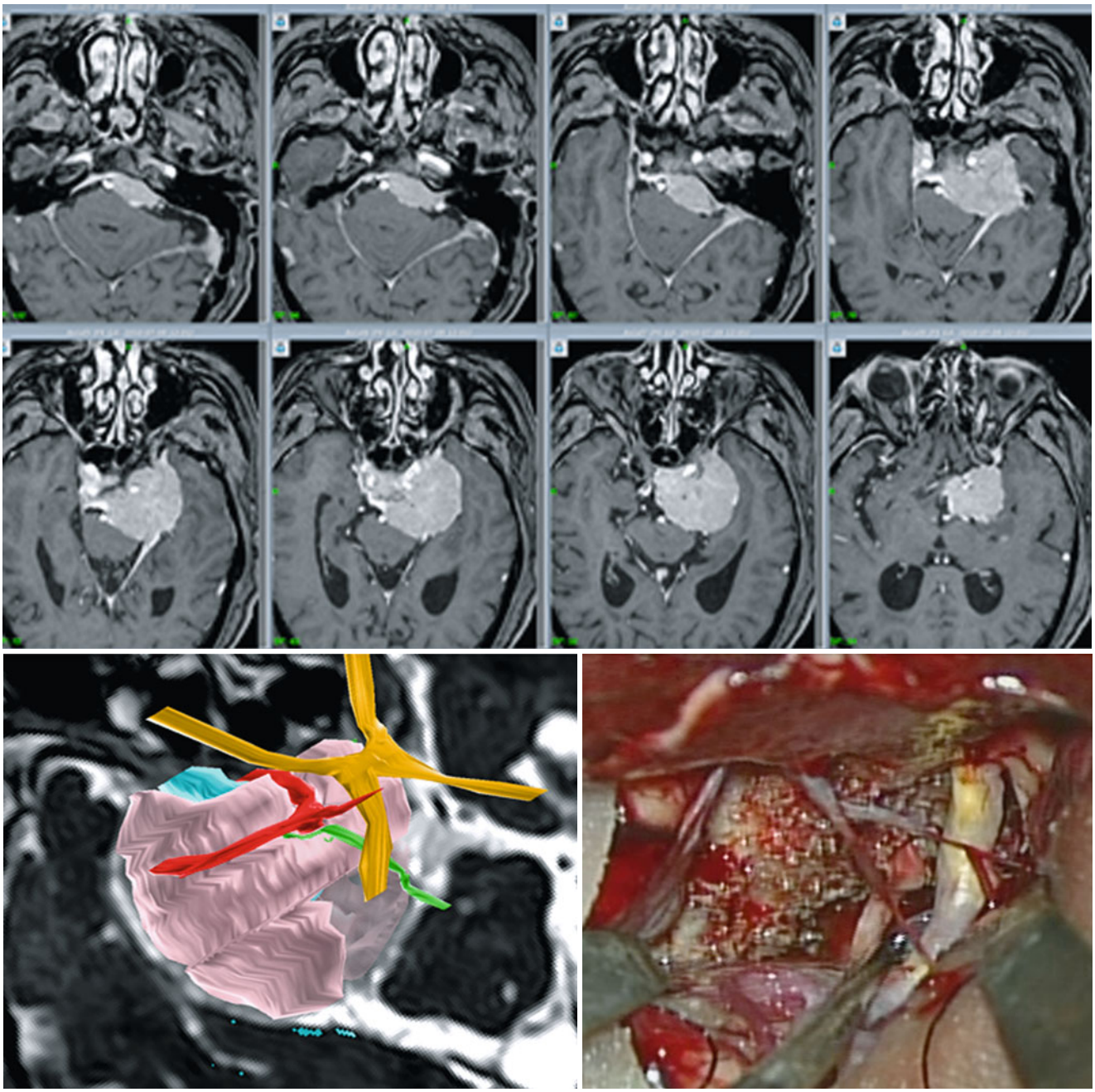

Fig. 9 Left-sided sphenopetroclival meningioma with involvement of both cavernous sinuses. The giant tumor originated from the dura mater of the superolateral part of the lateral wall of the left cavernous sinus and extended widely into the cavernous sinus itself and the middle and posterior cranial fossae (*upper*). Combined management was planned, with initial subtotal surgical resection and subsequent GKS. Therefore, detailed preoperative 3D evaluation of the relevant neuroanatomy based on gadolinium-enhanced CISS images installed in the Leksell GammaPlan was undertaken preoperatively (*lower left*). It revealed a lateral shift of the left oculomotor nerve, which was confirmed by the intraoperative microsurgical findings (*lower right*). A 3D view shows the delineated tumor (*pink*), optic pathways (*orange*), the left internal carotid artery and its bifurcation (*red*), and the left oculomotor nerve (*green*)

of the anatomical structures adjacent to the neoplasm, or engulfed by it, permits application of highly conformal and selective stereotactic irradiation, which can result in a better treatment outcome, particularly with regard to preservation and restoration of cranial nerve functions. A similar technique has been used effectively for preoperative planning of open microsurgical procedures with the Leksell GammaPlan.

Conflict of Interest The authors declare that they have no conflict of interest.

References

1. Beretta F (2004) The paraclinoid aneurysms and the distal dural ring: a new classification. J Neurosurg Sci 48:161–175
2. Erbay SH, Bhadelia RA, Riesenburger R, Gupta P, O'Callaghan M, Yun E, Oljeski S (2006) Association between neurovascular contact on MRI and response to gamma knife radiosurgery in trigeminal neuralgia. Neuroradiology 48:26–30
3. Gonzalez LF, Walker MT, Zabramski JM, Partovi S, Wallace RC, Spetzler RF (2003) Distinction between paraclinoid and cavernous sinus aneurysms with computed tomographic angiography. Neurosurgery 52:1131–1139
4. Hayashi M, Chernov M, Tamura N, Izawa M, Muragaki Y, Iseki H, Okada Y, Takakura K (2011) Gamma Knife robotic microradiosurgery for benign skull base meningiomas: tumor shrinkage may depend on the amount of radiation energy delivered per lesion volume (unit energy). Stereotact Funct Neurosurg 89:6–16
5. Hayashi M, Chernov M, Tamura N, Nagai M, Yomo S, Ochiai T, Amano K, Izawa M, Hori T, Muragaki Y, Iseki H, Okada Y, Takakura K (2010) Gamma Knife robotic microradiosurgery of pituitary adenomas invading the cavernous sinus: treatment concept and results in 89 cases. J Neurooncol 98:185–194
6. Hayashi M, Chernov M, Tamura N, Yomo S, Ochiai T, Nagai M, Tamura M, Izawa M, Muragaki Y, Iseki H, Okada Y, Takakura K (2010) Gamma Knife surgery for abducent nerve schwannoma: report of 4 cases. J Neurosurg 113(Suppl):136–143
7. Hayashi M, Ochiai T, Nakaya K, Chernov M, Tamura N, Maruyama T, Yomo S, Izawa M, Hori T, Takakura K, Regis J (2006) Current treatment strategy for vestibular schwannoma: image-guided robotic microradiosurgery. J Neurosurg 105(Suppl):5–11
8. Hayashi M, Ochiai T, Nakaya K, Chernov M, Tamura N, Yomo S, Izawa M, Hori T, Takakura K, Regis J (2006) Image-guided microradiosurgery for skull base tumors: advantages of using gadolinium-enhanced constructive interference in steady-state imaging. J Neurosurg 105(Suppl):12–17
9. Ivanov P, Chernov M, Hayashi M, Nakaya K, Izawa M, Murata N, Kubo O, Ujiie H, Muragaki Y, Nakamura R, Iseki H, Hori T, Takakura K (2008) Low-dose gamma knife radiosurgery for cavernous sinus hemangioma: report of 3 cases and literature review. Minim Invasive Neurosurg 51:140–146
10. Kawashima A, Okada Y, Hayashi M, Kawamata T, Hori T (2009) Application of contrast-enhanced constructive interference in steady state magnetic resonance imaging to Leksell GammaPlan for localizing C2–C3 aneurysms: technical note. Neurosurgery 65:1188–1190
11. Nakagawa A, Kusaka Y, Jokura H, Shirane R, Tominaga T (2004) Usefulness of constructive interference in steady state (CISS) imaging for the diagnosis and treatment of a large extradural spinal arachnoid cyst. Minim Invasive Neurosurg 47:369–372
12. Regis J, David P, Wikler D, Porcheron D, Levrier O (2004) Stereotactic mapping for radiosurgical treatment of vestibular schwannomas. Neurochirurgie 50:270–281 (in French)
13. Thines L, Delmaire C, Le Gars D, Pruvo JP, Lejeune JP, Lehmann P, Francke JP (2006) MRI location of the distal dural ring plane: anatomoradiological study and application to paraclinoid carotid artery aneurysms. Eur Radiol 16:479–488
14. Wiesmann M, Yousry I, Seelos KC, Yousry TA (2001) Identification and anatomic description of the anterior choroidal artery by use of 3D-TOF source and 3D-CISS MR imaging. AJNR Am J Neuroradiol 22:305–310
15. Yagi A, Sato N, Taketomi A, Nakajima T, Morita H, Koyama Y, Aoki J, Endo K (2005) Normal cranial nerves in the cavernous sinuses: contrast-enhanced three-dimensional constructive interference in the steady state MR imaging. AJNR Am J Neuroradiol 26:946–950
16. Yomo S, Hayashi M, Chernov M, Tamura N, Izawa M, Okada Y, Hori T, Iseki H (2009) Stereotactic radiosurgery of residual and recurrent craniopharyngioma: new treatment concept using Leksell Gamma Knife model C with automatic positioning system. Stereotact Funct Neurosurg 87:360–367
17. Yousry I, Camelio S, Wiesmann M, Schmid UD, Moriggl B, Bruckmann H, Yousry TA (1999) Detailed magnetic resonance imaging anatomy of the cisternal segment of the abducent nerve: Dorello's canal and neurovascular relationships and landmarks. J Neurosurg 91:276–283
18. Yousry I, Moriggl B, Holtmannspoetter M, Schmid UD, Naidich TP, Yousry TA (2004) Detailed anatomy of the motor and sensory roots of the trigeminal nerve and their neurovascular relationships: a magnetic resonance imaging study. J Neurosurg 101:427–434
19. Yousry I, Moriggl B, Schmid UD, Naidich TP, Yousry TA (2005) Trigeminal ganglion and its divisions: detailed anatomic MR imaging with contrast-enhanced 3D constructive interference in the steady state sequences. AJNR Am J Neuroradiol 26:1128–1135
20. Yousry I, Moriggl B, Schmid UD, Wiesmann M, Fesl G, Bruckmann H, Naidich TP, Yousry TA (2002) Detailed anatomy of the intracranial segment of the hypoglossal nerve: neurovascular relationships and landmarks on magnetic resonance imaging sequences. J Neurosurg 96:1113–1122
21. Zerris VA, Noren GC, Shucart WA, Rogg J, Friehs GM (2005) Targeting the cranial nerve: microradiosurgery for trigeminal neuralgia with CISS and 3D-flash MR imaging sequences. J Neurosurg 102(Suppl):107–110

Usefulness of Leksell GammaPlan for Preoperative Planning of Brain Tumor Resection: Delineation of the Cranial Nerves and Fusion of the Neuroimaging Data, Including Diffusion Tensor Imaging

Manabu Tamura, Yoshiyuki Konishi, Noriko Tamura, Motohiro Hayashi, Naoyuki Nakao, Yuji Uematsu, Toru Itakura, Jean Régis, Jean François Mangin, Yoshihiro Muragaki, and Hiroshi Iseki

Abstract Leksell GammaPlan (LGP) software was initially designed for Gamma Knife radiosurgery, but it can be successfully applied to planning of the open neurosurgical procedures as well. We present our initial experience of delineating the cranial nerves in the vicinity of skull base tumors, combined visualization of the implanted subdural electrodes and cortical anatomy to facilitate brain mapping, and fusion of structural magnetic resonance imaging and diffusion tensor imaging performed with the use of LGP before removal of intracranial neoplasms. Such preoperative information facilitated choosing the optimal approach and general surgical strategy, and corresponded well to the intraoperative findings. Therefore, LGP may be helpful for planning open neurosurgical procedures in cases of both extraaxial and intraaxial intracranial tumors.

M. Tamura (✉), Y. Konishi, M. Hayashi, Y. Muragaki, and H. Iseki
Faculty of Advanced Techno-Surgery,
Institute of Advanced Biomedical Engineering and Science,
TWIns, Tokyo Women's Medical University,
8-1 Kawada-cho, Shinjuku-ku, Tokyo 162-8666, Japan
e-mail: manabu97@abmes.twmu.ac.jp

N. Tamura
Department of Neurosurgery, Neurological Institute,
Tokyo Women's Medical University, Tokyo, Japan

N. Nakao, Y. Uematsu, and T. Itakura
Department of Neurological Surgery,
Wakayama Medical University, Wakayama, Japan

J. Régis
Department of Functional and Stereotactic Neurosurgery,
Timone University Hospital, Marseille, France

Faculty of Advanced Techno-Surgery,
Institute of Advanced Biomedical Engineering and Science,
Tokyo Women's Medical University, Tokyo, Japan

J.F. Mangin
The Computer Assisted Neuroimaging Laboratory,
NeuroSpin, Biomedical Imaging Institute, CEA,
Gif sur Yvette, France

Keywords Brain tumor surgery • Diffusion tensor imaging • Gamma Knife radiosurgery • Image co-registration • Leksell GammaPlan

Introduction

Clear understanding of the neuroanatomy of the target area is a prerequisite for realization of safe and effective neurosurgical procedures, particularly those directed at removal of intracranial tumors. Contemporary neuroimaging, mainly T1- and T2-weighted magnetic resonance imaging (MRI), provides detailed visualization of the intracranial structures and allows the surgeon to perform reasonable selection of the surgical approach, access to the lesion, and a general intraoperative strategy. Valuable additional information can be obtained with other modalities, such as functional MRI, magnetic resonance spectroscopy, diffusion-weighted imaging (DWI), and diffusion tensor imaging (DTI) [8, 14, 15, 18, 22, 23]. Nevertheless, interpretation of the minute neuroanatomical details in the vicinity of the lesion and integrated evaluation of the various data is difficult without dedicated software for image analysis.

The Leksell GammaPlan (LGP) (Elekta Instruments AB, Stockholm, Sweden) is a computer-aided program designed for treatment planning and dosimetry during Gamma Knife radiosurgery (GKS). It provides an opportunity to make highly accurate and precise co-registration and fusion of the various images obtained with various modalities, such as MRI, computed tomography (CT), positron emission tomography, magnetoencephalography, within the same workspace; their magnification; reconstruction in axial, coronal, and sagittal planes; and three-dimensional (3D) visualization. Moreover, the anatomical structures delineated on the different images can be combined on a composite view and evaluated from different angles and directions. These advantages can be used not only for radiosurgery but for planning open neurosurgical procedures as well [4, 5, 16]. Herein, we present the initial experience with delineation of the cranial

M.F. Chernov et al. (eds.), *Gamma Knife Neurosurgery in the Management of Intracranial Disorders*,
Acta Neurochirurgica Supplement, Vol. 116, DOI 10.1007/978-3-7091-1376-9_27, © Springer-Verlag Wien 2013

nerves in the vicinity of skull base tumors, combined visualization of the implanted subdural electrodes and cortical anatomy for facilitation of brain mapping, and fusion of structural MRI and DTI in a case of a parenchymal brain lesion performed with LGP before surgery for intracranial neoplasms.

Materials and Methods

Several functions available in the latest versions of the LGP software were utilized for analysis of the various MRI scans before neurosurgical procedures. The cranial nerves and other anatomical structures were delineated for 3D evaluation of their interrelations with the lesion using "Regions and Volumes." The automatic fusion algorithm of "Co-registration" was applied for simultaneous visualization of the various images obtained with different scanners and/or neuroimaging modalities, whereas the manual setting was used if correction and/or modification of the fusion technique seemed necessary. Simulation of the radiosurgical procedures was performed with "Pre-plan."

Cranial nerves were delineated in the vicinity of a skull base meningioma (6 cases), vestibular schwannoma (1 case), and pituitary adenoma (1 case). The delineations were performed using 3D reconstructed plain and gadolinium-enhanced constructive interference in steady state (CISS) images (slice thickness 1.0 mm, TE 5.9 ms, TR 9.04 ms, flip angle 70°) obtained with a 1.5 T MRI scanner (Siemens MagnetomPlus; Siemens, New York, NY, USA) and installed in the LGP.

Subdural electrodes were delineated in a patient with a left parietal glioma manifesting as seizures. Location of the neoplasm in the eloquent cortex necessitated precise brain mapping before tumor removal. In this case, 3D co-registration of volumetric MRI and thin-sliced "bone window" CT scans were obtained with the use of LGP before and after implantation of the grid electrodes, respectively. Additional matching of the cortical sulci and gyri was done with BrainVISA software based on T1-weighted MRI scans [9, 10, 20].

A fractional anisotropy (FA) map and fiber tracking images ("fiber map") were installed in the LGP in a case of a right parieto-occipital glioma for preoperative visualization of the anatomical interrelations of the neoplasm with the corticospinal tract (CST) and area of optic radiation. High signal-to-noise ratio and low-distortion DTI with 32 directions of the diffusion sensitizing gradient and nearly isotropic voxel size was acquired with a 3 T MRI scanner (Philips MRI Equipment, Eindhoven, The Netherlands). Its installation into LGP and 3D fusion with volumetric MRI was attained as a two-step procedure. First, DTI was analyzed using dedicated software (Stealth DTV; Medtronic, Grand Rapids, MI, USA). A FA map was then created by tracking the CST and optic radiation with location of the regions of interest (ROI) in the lower brain stem and the lateral geniculate nucleus, respectively. Second, the FA map and "fiber map" in 3D volumetric DICOM format were exported into the LGP independently from each other, and they underwent co-registration with T1- and T2-weighted MRI using an automatic setting for the FA map and a manual setting for the "fiber map." Subsequently, both the CST and optic radiation were delineated, and the lesion itself was visualized by simulation of the radiosurgical procedure based on the location of the hyperintense area on T2-weighted MRI scans.

Results

Delineation of Cranial Nerves

Plain and gadolinium-enhanced CISS images used to delineate the anatomical structures adjacent to extraaxial tumors in the LGP generally provided complementary information, but postcontrast MRI permitted somewhat better visualization of the cranial nerves (Fig. 1). Overall, their delineation was successful in seven of eight cases (Table 1). In one case the hypoglossal nerve was not identified, and subsequent surgery revealed its full engulfment by the neoplasm. In another case, according to preoperative delineation the hypoglossal nerve was located within the bulk of the petrosal meningioma. However, during surgery it was identified on the ventral side of the lesion. In six other cases, preoperative data accurately predicted the position of the cranial nerve(s) adjacent to the tumor, as was verified intraoperatively.

Delineation of Subdural Electrodes

Use of LGP for co-registration of MRI performed before implantation of subdural grid and "bone window" CT obtained thereafter permitted accurate delineation of each electrode and precise identification of their location relatively to the brain surface in axial, coronal, and sagittal planes (Fig. 2). In this case, simultaneous 3D visualization of the cortical anatomy, the lesion, and implanted subdural electrodes significantly facilitated interpretation of the neurophysiological data obtained during cortical mapping, and planning the tumor resection.

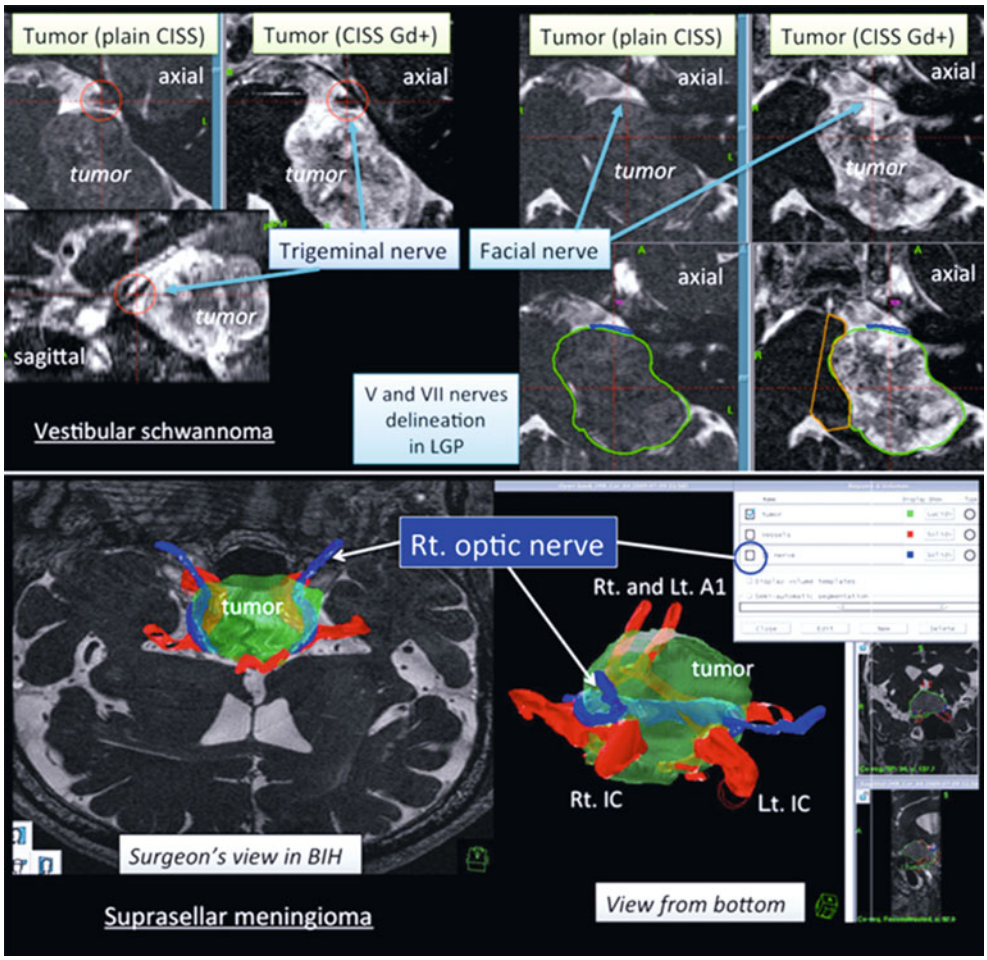

Fig. 1 Use of Leksell Gamma Plan (LGP) for constructive interference in steady state (CISS)-based preoperative delineation of the cranial nerves and cerebral arteries adjacent to a tumor in patients with vestibular schwannoma (*upper*) and suprasellar meningioma (*lower*). *BIH* bilateral interhemispheric approach

Table 1 Correspondence of constructive interference in steady state (CISS)-based preoperative delineation of the cranial nerves using Leksell GammaPlan to intraoperative findings

Case no.	Type of pathology	Delineated cranial nerve	Results of CISS-based preoperative delineation	Intraoperative confirmation
1[a]	Vestibular schwannoma	V, VII	Accomplished	Confirmed
2	Suprasellar meningioma	II	Accomplished	Confirmed
3	Petrosal meningioma	XII	Not delineated	Nerve was fully engulfed in the tumor
4	Pituitary adenoma	II	Accomplished	Confirmed
5	Petrosal meningioma	XII	Accomplished (nerve was located within the tumor)	Nerve was identified ventral to the tumor
6	Petrosal meningioma	VII	Accomplished	Confirmed
7	Petrosal meningioma	IX, X	Accomplished	Confirmed
8[a]	Suprasellar meningioma	II	Accomplished	Confirmed

[a]Results of delineation of the cranial nerves in these cases are presented in Fig. 1

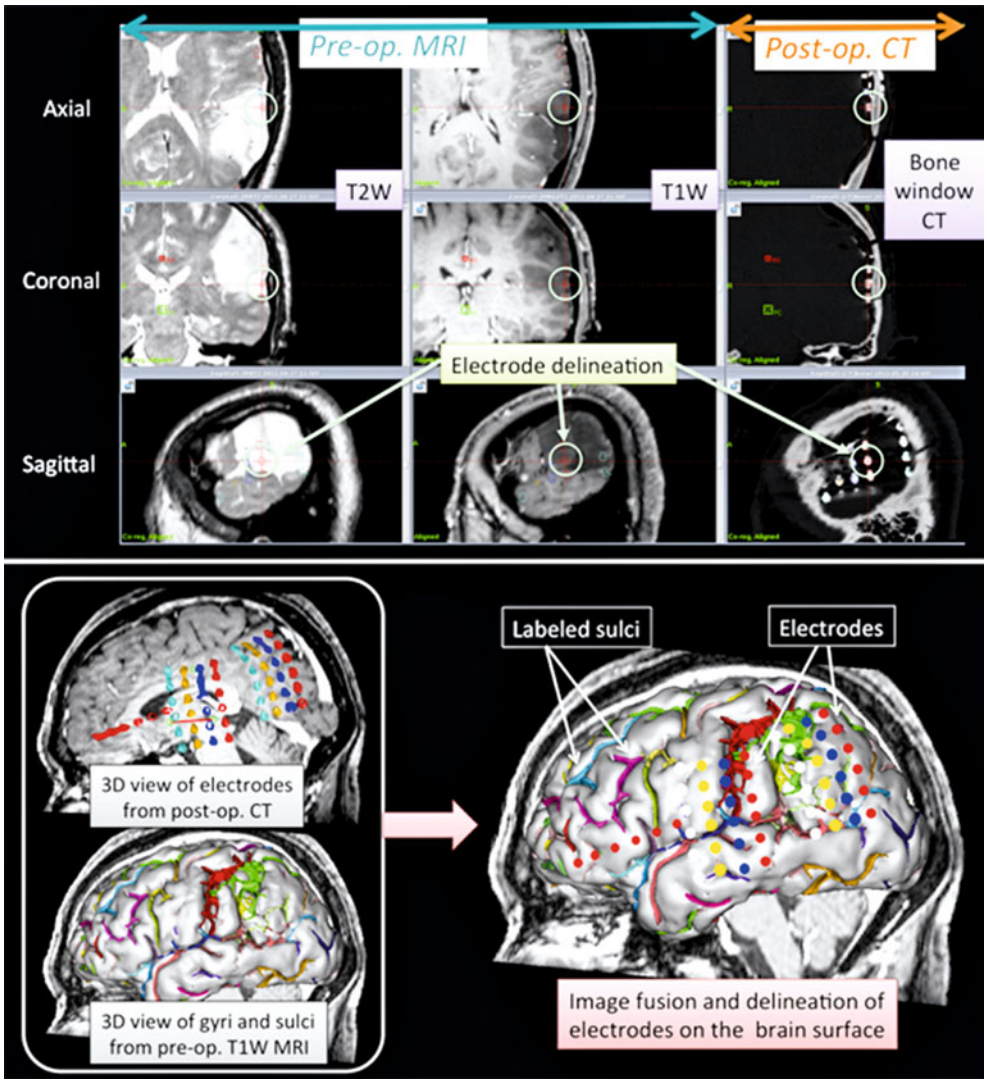

Fig. 2 Use of LGP for delineation of subdural electrodes and their matching with the cortical anatomy in a patient with a left parietal glioma. Note the three-dimensional (3D) co-registration of volumetric magnetic resonance imaging (MRI) obtained before grid implantation (*Pre-op. MRI*) and "bone window" CT obtained thereafter (*Post-op. CT*). Sulci and gyri were labeled using BrainVISA software

Installation of DTI into LGP

Simultaneous 3D visualization of the tumor, CST, and optic radiation (Fig. 3) facilitated planning resection of the parieto-occipital glioma, which focused on avoiding postoperative deterioration of motor and visual functions.

Discussion

Various functions of the LGP allow safe and effective treatment planning for GKS. For example, precise delineation of functionally important anatomical structures leads to avoidance of exposing them to excessive radiation. Fusion of "bone window" CT and MRI provides an opportunity to estimate and correct distortion artifacts. Also, evaluation of the target area on co-registered images facilitates the differential diagnosis for various neoplasms with the same location (e.g., meningioma versus schwannoma) and precise identification of the tumor origin from the specific dural area or cranial nerve [3, 4]. Moreover, 3D visualization of the various structures adjacent to the lesion and their evaluation from different angles and directions allows the surgeon to simulate the surgical field, which can be helpful for planning open neurosurgical procedures. It can result in greater effectiveness, lower morbidity, and better outcome. In fact, we recently started using the LGP to evaluate complex regional neuroanatomy before removing skull base tumors and clipping cerebral aneurysms [4, 5, 16].

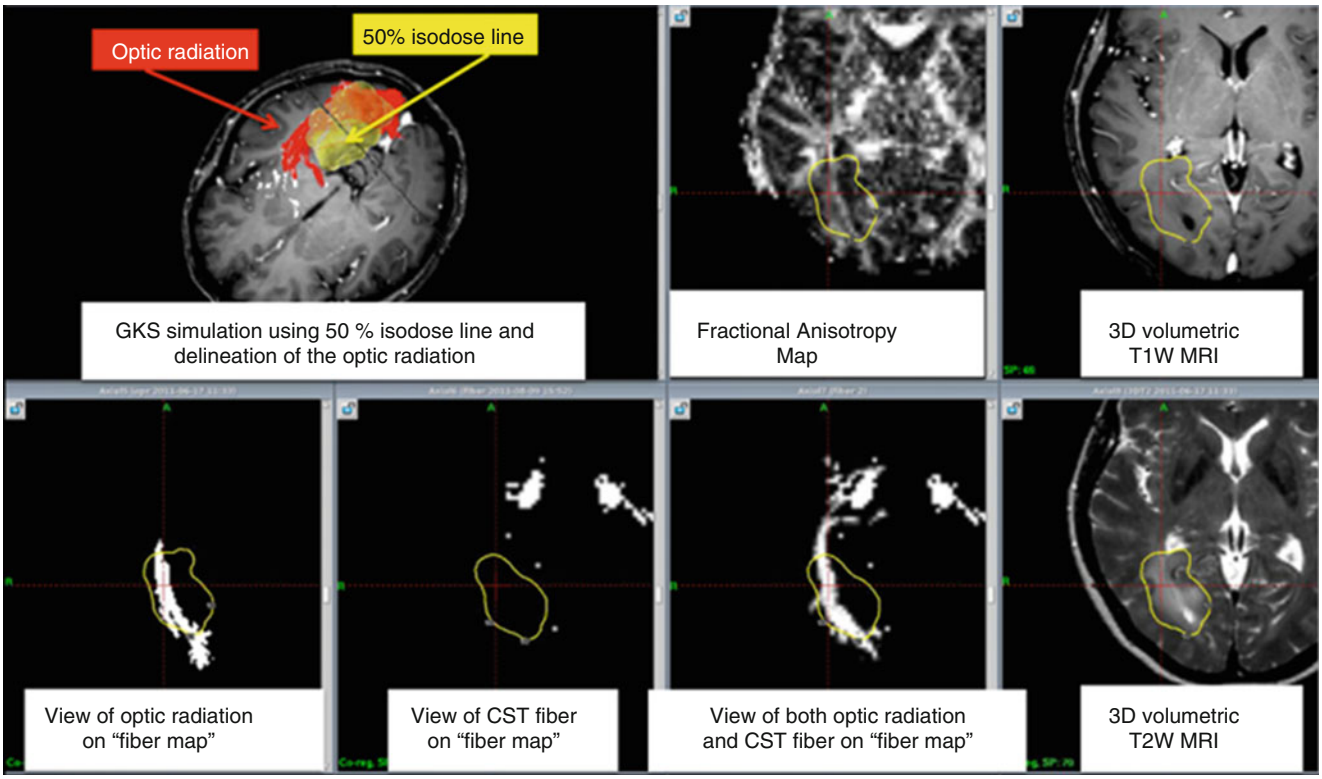

Fig. 3 Installation of the fractional anisotropy map and fiber tracking images ("fiber map") into LGP and their 3D co-registration with T1- and T2-weighted MRI scans in a patient with a right parieto-occipital glioma. The 3D interrelations between delineated optic radiation and the lesion, visualized by simulating the radiosurgical treatment, are clearly seen. *GKS* Gamma Knife surgery, *CST* corticospinal tract

The present study demonstrated that CISS-based preoperative delineation of the cranial nerves closely reflects their interrelations with the neoplasm. In six of eight cases (75 %), full correspondence of the presumed and actual nerve position was confirmed during surgery. Nevertheless, accuracy of cranial nerve delineation may depend on its size and degree of shift by the tumor. In two cases of a large petrosal meningioma, the hypoglossal nerve was mislocalized preoperatively. There were no such errors when relatively thicker cranial nerves (optic, trigeminal, facial) were evaluated.

A similar LGP-based technique was used to delineate subdural electrodes and evaluate their positions relative to the cerebral cortex in a patient with a left parietal glioma that required precise brain mapping before surgical resection. At present, computer-aided tools, particularly BrainVISA software [9, 10, 20], permit precise determination of the individual sulcal and gyral anatomy based on MRI findings. MRI, however, does not permit clear visualization of the implanted grid electrodes because of significant artifacts, so their position should be evaluated with telemetric radiographic imaging [20] or CT. Therefore, it was decided to perform co-registration of MRI acquired before implantation of the grid electrodes and thin-sliced "bone window" CT obtained afterward. Although it was successful in the presented case, a possible limitation of the technique should be mentioned. The problem is that the cortical anatomy is not always the same on the images obtained before and after grid implantation because the brain may have undergone some degree of shift after craniotomy [17]. Hence, the proposed method requires further validation and at present should be considered a useful adjunct, but not a substitute, for intraoperative brain mapping with direct electrical stimulation of the cortex [1, 18].

The same technical principles can be applied for delineating brain anatomy in cases of parenchymal brain tumors, although it may require use of additional MRI-based modalities. Particularly, DTI provides extremely valuable information on the position of white matter tracts through creation of FA maps and neural fiber tracking based on the single tensor deterministic method or the probabilistic Monte Carlo random walk method [2, 8, 13, 15, 19, 21]. In the case presented here, both FA map and fiber tracking images were successfully incorporated into the LGP and fused with T1- and T2-weighted MRI for preoperative evaluation of the interrelations between the parieto-occipital glioma and the CST and optic radiation. The technical feasibility of installing DTI into the LGP, particularly in cases of arteriovenous malformations, has been demonstrated in several reports [6, 7, 11, 12]. It definitely offers new possibilities

for further improving the efficacy and safety of stereotactic radiosurgery and may be helpful for estimating distortion artifacts on DTI. Nevertheless, additional studies should evaluate the accuracy of co-registration of FA maps and volumetric MRI, determine the optimal ROI for fiber tracking, and define the most appropriate tracking algorithm.

Conclusion

LGP may be helpful during planning neurosurgical procedures for both extraaxial and intraaxial intracranial tumors. Delineation of the various anatomical structures, their integrated 3D visualization, and possible evaluation from different angles and directions can facilitate the choice of the optimal surgical strategy. Our preliminary data confirmed good correspondence of such preoperative information to subsequent intraoperative findings, but it requires further validation in additional studies.

Acknowledgment This study used funds from Grant-in-Aid for Scientific Research (B) No. 22300093 and was supported by the Global COE Program, namely The Multidisciplinary Education and Research Centre for the Establishment of Regenerative Medicine (MERCREM) from the Ministry of Education, Culture, Sports, Science, and Technology (MEXT) of Japan. Additional support was obtained from the Japan Society for the Promotion of Science (JSPS) through the "Funding Program for World-Leading Innovative R&D on Science and Technology (FIRST Program)" initiated by the Council for Science and Technology Policy (CSTP). The authors thank Gautam A. Deshpande, MD for his assistance with editing this manuscript.

Conflict of Interest The authors declare that they have no conflict of interest.

References

1. Giussani C, Roux FE, Ojemann J, Sganzerla EP, Pirillo D, Papagno C (2010) Is preoperative functional magnetic resonance imaging reliable for language areas mapping in brain tumor surgery? Review of language functional magnetic resonance imaging and direct cortical stimulation correlation studies. Neurosurgery 66:113–120
2. Guevara P, Poupon C, Riviere D, Cointepas Y, Descoteaux M, Thirion B, Mangin JF (2011) Robust clustering of massive tractography datasets. Neuroimage 54:1975–1993
3. Hayashi M, Chernov M, Tamura N, Nagai M, Yomo S, Ochiai T, Amano K, Izawa M, Hori T, Muragaki Y, Iseki H, Okada Y, Takakura K (2010) Gamma Knife robotic microradiosurgery of pituitary adenomas invading the cavernous sinus: treatment concept and results in 89 cases. J Neurooncol 98:185–194
4. Hayashi M, Chernov MF, Tamura N, Yomo S, Tamura M, Horiba A, Izawa M, Muragaki Y, Iseki H, Okada Y, Ivanov P, Regis J, Takakura K (2013) Usefulness of the advanced neuroimaging protocol based on plain and gadolinium-enhanced Constructive Interference in Steady State images for Gamma Knife radiosurgery and planning microsurgical procedures for skull base tumors. Acta Neurochir Suppl 116:167–178 (present volume)
5. Kawashima A, Okada Y, Hayashi M, Kawamata T, Hori T (2009) Application of contrast-enhanced constructive interference in steady state magnetic resonance imaging to Leksell GammaPlan for localizing C2-C3 aneurysms: technical note. Neurosurgery 65:1188–1190
6. Koga T, Maruyama K, Kamada K, Ota T, Shin M, Itoh D, Kunii N, Ino K, Terahara A, Aoki S, Masutani Y, Saito N (2012) Outcomes of diffusion tensor tractography-integrated stereotactic radiosurgery. Int J Radiat Oncol Biol Phys 82:799–802
7. Koga T, Shin M, Maruyama K, Kamada K, Ota T, Itoh D, Kunii N, Ino K, Aoki S, Masutani Y, Igaki H, Onoe T, Saito N (2012) Integration of corticospinal tractography reduces motor complications after radiosurgery. Int J Radiat Oncol Biol Phys 83: 129–133
8. Leclercq D, Duffau H, Delmaire C, Capelle L, Gatignol P, Ducros M, Chiras J, Lehericy S (2010) Comparison of diffusion tensor imaging tractography of language tracts and intraoperative subcortical stimulations. J Neurosurg 112:503–511
9. Mangin JF, Riviere D, Cachia A, Duchesnay E, Cointepas Y, Papadopoulos-Orfanos D, Collins DL, Evans AC, Regis J (2004) Object-based morphometry of the cerebral cortex. IEEE Trans Med Imaging 23:968–982
10. Mangin JF, Riviere D, Cachia A, Duchesnay E, Cointepas Y, Papadopoulos-Orfanos D, Scifo P, Ochiai T, Brunelle F, Regis J (2004) A framework to study the cortical folding patterns. Neuroimage 23(Suppl 1):S129–S138
11. Maruyama K, Kamada K, Ota T, Koga T, Itoh D, Ino K, Aoki S, Tago M, Masutani Y, Shin M, Saito N (2008) Tolerance of pyramidal tract to gamma knife radiosurgery based on diffusion-tensor tractography. Int J Radiat Oncol Biol Phys 70:1330–1335
12. Maruyama K, Koga T, Kamada K, Ota T, Itoh D, Ino K, Igaki H, Aoki S, Masutani Y, Shin M, Saito N (2009) Arcuate fasciculus tractography integrated into Gamma Knife surgery. J Neurosurg 111:520–526
13. Mori S, Crain BJ, Chacko VP, van Zijl PC (1999) Three-dimensional tracking of axonal projections in the brain by magnetic resonance imaging. Ann Neurol 45:265–269
14. Muragaki Y, Iseki H, Maruyama T, Tanaka M, Shinohara C, Suzuki T, Yoshimitsu K, Ikuta S, Hayashi M, Chernov M, Hori T, Okada Y, Takakura K (2011) Information-guided surgical management of gliomas using low-field-strength intraoperative MRI. Acta Neurochir Suppl 109:67–72
15. Nimsky C, Ganslandt O, Hastreiter P, Wang R, Benner T, Sorensen AG, Fahlbusch R (2005) Preoperative and intraoperative diffusion tensor imaging-based fiber tracking in glioma surgery. Neurosurgery 56:130–138
16. Obara T, Hayashi M, Ino H, Ochiai T, Suzuki M, Suzuki T, Watayou T (2009) Surgical management of skull base meningiomas: a treatment strategy using multi-modality. CI Kenkyu 31:73–81 (in Japanese)
17. Ozawa N, Muragaki Y, Nakamura R, Hori T, Iseki H (2009) Shift of pyramidal tract during resection of the intraaxial brain tumors estimated by intraoperative diffusion-weighted imaging. Neurol Med Chir (Tokyo) 49:51–56
18. Ozawa N, Muragaki Y, Nakamura R, Iseki H (2009) Identification of the pyramidal tract by neuronavigation based on intraoperative

diffusion-weighted imaging combined with subcortical stimulation. Stereotact Funct Neurosurg 87:18–24
19. Parker GJ, Haroon HA, Wheeler-Kingshott CA (2003) A framework for a streamline-based probabilistic index of connectivity (PICo) using a structural interpretation of MRI diffusion measurements. J Magn Reson Imaging 18:242–254
20. Regis J, Tamura M, Park MC, McGonigal A, Riviere D, Coulon O, Bartolomei F, Girard N, Figarella-Branger D, Chauvel P, Mangin JF (2011) Subclinical abnormal gyration pattern, a potential anatomical marker of epileptogenic zone in patients with MRI-negative frontal lobe epilepsy. Neurosurgery 69:80–94
21. Reisert M, Mader I, Anastasopoulos C, Weigel M, Schnell S, Kiselev V (2011) Global fiber reconstruction becomes practical. Neuroimage 54:955–962
22. Sakai KL (2005) Language acquisition and brain development. Science 310:815–819
23. Tamura M, Nishibayashi H, Kakishita K, Ogura M, Uematsu Y, Mangin J-F, Regis J, Itakura T (2010) Preoperative MRI-based delineation of the central sulcus and its usefulness for the intraoperative navigation of the epidural electrodes implantation for the motor cortex stimulation. Funct Neurosurg 49:201–207 (in Japanese)

Perspectives of 3 T Magnetic Resonance Imaging in Radiosurgical Treatment Planning

Patrik Zamecnik and Marco Essig

Abstract The introduction of 3 T magnetic resonance imaging (MRI) scanners for neuro-oncological diagnostics showed a general improvement of image quality, especially in terms of the detection and differentiation of intracranial tumors. Among the advantages of 3 T scanners compared to 1.5 T scanners are the possibility of higher spatial image resolution or shorter investigation times and the availability of functional imaging in sufficient quality. Consequently, the use of 3 T MRI for radiosurgery planning is highly desired. Functional MRI techniques (perfusion-weighted imaging, dynamic contrast-enhanced MRI, MR spectroscopy, diffusion-weighted imaging, and diffusion tensor imaging) available at 3 T scanners provide not only better detection and differentiation but also significantly better delineation of intracranial tumors, which is a crucial feature for successful radiosurgical treatment planning. The use of multimodal morphological and functional MRI methods allows identification of the biologically most active parts of the tumors with consecutive changes in therapy planning. On the other hand, there are increased geometric distortions on MRI scans obtained at 3 T compared to 1.5 T, which makes their use limited for now. However, the newest studies show an acceptable degree of geometric distortion on the 3 T planning images using special imaging protocols, while additional investigations on this issue are needed to find the optimal technical solution.

Keywords 3 T MRI • Functional MRI • Radiosurgery • Therapy planning

P. Zamecnik (✉)
Department of Radiology,
Radboud University Nijmegen Medical Centre,
Heidelberg 6500, Nijmegen, The Netherlands
e-mail: p.zamecnik@rad.umcn.nl

M. Essig
Department of Neuroradiology, Universitätsklinikum Erlangen,
Erlangen, Germany

Introduction

Radiosurgery has undergone rapid development during the last few years. This noninvasive procedure allows precise delivery of high-dose radiation to small intracranial targets while minimizing the dose to surrounding normal structures [20]. For radiosurgical treatment planning, an imaging modality is needed that provides high-quality information on the target lesion and the organs at risk with good geometric accuracy. At the moment, the standard diagnostic procedure for diagnostics and radiosurgery planning is contrast-enhanced morphological magnetic resonance imaging (MRI). This diagnostic method delivers sufficient imaging quality of intracranial lesions and normal tissue and can also be used for treatment planning. Because of the good availability and geometric accuracy, clinical 1.5 T MRI scanners are used as standard hardware for therapy planning imaging.

During the last few years 3 T MRI scanners were introduced into clinical practice and improved especially neuroimaging approaches. The next logical step is to use 3 T MRI systems for therapy planning imaging. This would have several advantages: An available 3 T MRI scanner could be used for diagnostics and therapy planning imaging without the need for additional diagnostic hardware. It is a known fact that 3 T MRI systems offer a higher signal-to-noise ratio (SNR)—up to twice that of the 1.5 T scanners depending on the sequence used. Consequently, MRI examinations of the same quality could be performed in less time at 3 T than at 1.5 T. Also, during the same examination time, higher spatial resolution of morphological images can be obtained at 3 T that at 1.5 T. In general, higher image quality improves the detection rate of suspicious intracranial lesions and provides better delineation for therapy planning [20]. Moreover, the advantage of using 3 T MRI systems for treatment planning is not only higher spatial image resolution. A variety of functional MRI techniques that improve detection and delineation of the suspect intracranial lesions are available in sufficient quality only with 3 T scanners. Particularly, only

M.F. Chernov et al. (eds.), *Gamma Knife Neurosurgery in the Management of Intracranial Disorders*,
Acta Neurochirurgica Supplement, Vol. 116, DOI 10.1007/978-3-7091-1376-9_28, © Springer-Verlag Wien 2013

by using and combining functional MR imaging methods can the biologically most aggressive parts of the tumors be visualized and the information fed into the radiation therapy planning process. On the other hand, there are increased geometric distortions of MRI images obtained at 3 T compared to 1.5 T, which limits their use for radiosurgical treatment planning. The aim of this review is to highlight the functional imaging techniques available at 3 T that can be used for detection, delineation, and consequently treatment planning. It includes also a discussion of the possible solutions for the above-mentioned image distortion problems in terms of perspective technical developments.

Advanced Functional MRI Neuroimaging at 3 T in Radiosurgical Treatment Planning

The standard MRI imaging protocol used for radiotherapy planning of brain tumors consists of conventional spin-echo (SE) or turbo spin-echo (TSE) T1- and T2-weighted sequences, postcontrast T1-weighted SE or TSE, and T1-weighted sequences with magnetization transfer contrast. The use of contrast media is mandatory for such protocols, preferably high relaxivity agents, which demonstrated benefits in imaging at 3 T [1, 13]. Advanced brain tumor functional imaging, which can be used for detection, delineation, and "noninvasive grading" of the target tumor lesions, uses techniques such as contrast-enhanced perfusion-weighted imaging (PWI), dynamic contrast-enhanced MRI (DCE-MRI), MR spectroscopy (MRS), diffusion-weighted imaging (DWI), and diffusion tensor imaging (DTI). Normally, the functional MRI techniques are incorporated into the multimodal imaging protocols in combination with morphological sequences [8]. The multimodal MRI provides hemodynamic, metabolic, and quantitative cellular information corresponding to the biological properties and behavior of the tumor [17]. Consequently, the extent and the most biologically aggressive parts of the target lesions can be identified, and the target volume can be modified to arrive at the best possible treatment.

Contrast-Enhanced Perfusion-Weighted Imaging

Perfusion-weighted imaging is already an established tool for the detection, differential diagnosis, and treatment monitoring of brain tumors. For neuro-oncological purposes, PWI is mostly performed using first-pass dynamic susceptibility-weighted contrast-enhanced (DSC)-MRI echo-planar imaging [4]. Although this approach is available on 1.5 T scanners as well, the technique profits by the 3 T magnetic field strength in terms of better signal quality [15]. In previous studies, DSC-MRI showed benefits in pretherapeutic diagnosis and differentiation of gliomas, lymphomas, and metastases and in the differentiation of tumorous lesions from infections and demyelinating diseases [5]. In neuro-oncological studies, DSC-MRI gave a superior diagnostic performance in predicting glioma grade and treatment response and in differentiating glioblastomas from other tumors when compared to DCE-MRI and MRS. For example, because of significantly higher tumor perfusion in glioblastomas compared with brain lymphomas, this method showed sensitivity, specificity, positive (PPV), and negative (NPV) prediction values of 100 %, 50 %, 90 %, and 100 %, respectively [19]. Whereas the regional cerebral blood volume (rCBV) or flow (rCBF) values did not allow a clear discrimination between metastases and high-grade gliomas directly, the peritumoral nonenhancing, T2-weighted hyperintense regions showed significantly elevated CBV by glioblastomas on the contrary to metastases. These regions represent a glioma-specific kind of perifocal tumorous infiltration or lower grade tumor parts, which are invisible on conventional contrast-enhanced MRI. This fact should be considered when defining the treatment volume in terms of consecutive inclusion, if possible, of these areas into the therapeutic volume. Especially for radiosurgical treatment planning, glioma heterogeneity with high-grade and low-grade components is a challenge: The extent of low-grade components and the identification of high-grade areas are of an utmost importance. In this case, the PWI based on DSC-MRI technique can improve the delineation of all tumor components, which has a direct influence on the therapy planning. This approach can be easily included in the routine treatment planning MRI protocols as part of multimodal imaging because it significantly improves the definition of the target area.

Dynamic Contrast-Enhanced MRI

The next functional MRI technique using a contrast medium is DCE-MRI. Technically, DCE-MRI is the acquisition of serial images before, during, and after administration of extracellular MRI contrast medium. The resulting signal intensity measurements of the tumor area reflect a combination of tumor perfusion, vessel permeability, and diffusion of contrast medium into the extravascular-extracellular space [2, 16]. DCE-MRI clearly profits with 3 T scanners in terms of higher spatial and temporal resolution of the sequences used. DCE-MRI has been found to correlate with some prognostic factors such as tumor grade, microvessel density, and vascular endothelial growth factor expression and with

recurrence and survival outcomes [3]. This information is not only important for general patient management, but high-quality DCE images allow identification of "hot spots" within the tissue that correspond to areas of high biological activity in the tumor. Studies have shown changes on DCE-MRI in follow-up studies during therapeutic intervention that correlated with the general outcome, suggesting a possible role for DCE-MRI as a predictive marker [6]. The most distinctive feature of DCE-MRI is assessment of the wash-in and wash-out contrast behavior in tumors corresponding to microvascular tissue properties. This dynamic information reflects the microcirculatory heterogeneity of the tumor and suggests its angiogenic properties. This information can be used for improved treatment planning by identifying the biologically aggressive parts of the malignant lesion, which need to be treated with a higher dose or require adjuvant therapy.

MR Spectroscopy

Proton magnetic resonance spectroscopy imaging is a functional MRI method that shows the metabolic properties of the tissue. Spectroscopic characterization of brain tissue relies on ratios between the main proton spectrum metabolites—*N*-acetylaspartate (NAA), a marker for normal neuronal tissue; choline-containing compounds (Cho), a marker of membrane turnover; creatine/phosphocreatine (Cr)—and on the presence of lipids and lactate [7, 8, 12]. Malignant cerebral lesions typically show loss of NAA, indicating the loss of normal neuronal structures, and increased choline compounds in the spectrum, representing a higher concentration of cell membrane components because of increased cell destruction and proliferation processes. The presence of lipids or lactate represents heavy hypoxia with consecutive necrosis, which can be interpreted as a consequence of rapid tumor growth. Because of the weak spectroscopy signal, this method benefits from the higher magnetic field with consecutive better quality of the spectral curves. In a previous study, MRS showed higher sensitivity and a higher PPV than conventional MRI when assessing the glioma grade [7]. Most recurrences of high-grade gliomas after irradiation or combined therapy continue to be local. This trend indicates that the therapeutic volume of radiation did not cover all of the tumor, primarily a consequence of insufficient visualization of all tumor parts during the planning process. MRS is able to detect metabolic abnormalities beyond the tumor volume seen on conventional MRI, assess early response to treatment, and delineate the regions at high risk for failure in high-grade gliomas, which can be used for therapy planning [17]. However, MRS also has limitations. Because of the low spatial resolution of MRS and tumor heterogeneity, pathologic MRS findings in terms of decreased NAA peaks may indicate variable histological findings, such as inflammatory macrophage infiltration, radiation necrosis, and gliosis. Therefore, MRS, similar to PWI or DCE-MRI, is dependent on comparison with other functional and morphological sequences used in multimodal MRI protocols for treatment planning.

Diffusion-Weighted and Diffusion Tensor Imaging

Diffusion-weighted imaging is a common MRI approach used in neuroimaging for diagnosis of ischemic changes in terms of cerebral infarction. It is also helpful in the differential diagnosis of infections in the central nervous system. Similar to other functional MRI techniques, DWI and DTI can be used for the primary diagnosis and for follow-up of patients with cerebral tumors and hence for therapy planning as a part of multimodal MRI using high-field scanners [14]. Fast-growing neoplasms have less free diffusion than normal brain tissue, and DWI shows consistent signal elevation. Areas with highly constricted free diffusion correspond to fast-growing tumor parts or fibrotic/connective tissue, however, the possibility of their differentiation is limited with DWI. Therefore, similar to other aforementioned functional MRI techniques, DWI must be used in combination with other morphological and functional sequences to be suitable for delineation of the tumor infiltration and for treatment planning/therapeutic volume definition.

DTI shows diffusion anisotropy effects. It can be used to analyze the diffusion properties of the tissue and provide additional details on its structure. The most common application of DTI at present is fiber tracking in the brain, which has proved to be a valuable diagnostic tool in determination of the neoplastic infiltration of cerebral structures [9, 14]. This information is important for radiosurgical therapy planning when the tumor is located in the vicinity of critical structures, such as neuronal tracts in the central nervous system.

Geometric Distortion on 3 T MRI and Its Correction

The degree of geometric accuracy of MRI scans used for radiosurgery planning is a crucial factor because of the higher geometric inaccuracy of MRI compared to CT. Distortions on MRI scans are caused by several factors: magnetic field inhomogeneities, gradient magnetic field nonlinearity, patient-related effects including chemical shift and susceptibility artifacts [18, 20]. The problem is that by increasing the magnetic field from 1.5 T to 3 T the susceptibility artifacts

and chemical shift effects increase as well. Additionally, the magnetic and gradient field inhomogeneities are greater at higher magnetic fields. These factors lead to greater geometric distortions at 3 T than at 1.5 T. In the first publications on this subject, the greater distortions were generally considered unacceptable for therapy planning in radiosurgery [10]. Although later studies still showed higher distortion at 3 T than at 1.5 T images, the results were evaluated as acceptable for such planning [11]. The majority of investigations concerning the geometric integrity of 3 T MRI for radiosurgical treatment planning were performed using phantoms [10, 18]. Thus, the issue is still controversial, without a clear consensus. A new study was proposed recently in which a special geometrically accurate imaging protocol for treatment planning was developed. This approach tested both patients and phantoms to develop a standardized distortion evaluation technique. The technique produced acceptable data on spatial validity for using 3 T MRI for targeting (under the imaging conditions investigated) [20]. The use of 3 T scanners for therapy planning seems possible, but the small number of studies concerning this subject makes consensus difficult.

Conclusion

The 3 T MRI scanners in neuroradiology have generally improved image quality, in particular of neuro-oncological examinations in terms of detection and differentiation of the intracranial tumors. The most important advantage of 3 T scanners compared to 1.5 T scanners is the better SNR, which allows higher spatial image resolution and shorter scanning times. A variety of functional diagnostic imaging approaches are available in sufficient quality but only at high-field MRI. Consequently, the use of 3 T MRI for radiosurgical treatment planning is highly desired. The functional MRI techniques (contrast-enhanced PWI, DCE-MRI, MRS, DWI, DTI) available for 3 T scanners provide not only better detection and differentiation but also delineation of cerebral tumors, which is a crucial feature for successful radiosurgical treatment planning. In general, all of the functional methods described above are suitable for radiosurgical planning as a part of multimodal 3 T MRI protocols, showing better definition of the therapeutic target volume compared to that seen with standard morphological MRI. The combination of morphological and functional MRI methods allows identification of the biologically most active parts of the tumors. This information can be used in the following radiotherapy planning process. On the other hand, the MRI scans obtained at 3 T have more geometric distortions than those acquired at 1.5 T. The newest studies, however, show an acceptable degree of geometric distortion in the 3 T planning images using special MRI protocols. Additional studies on this issue are needed to reach a consensus on the best technical solution.

Conflict of Interest The authors declare that they have no conflict of interest.

References

1. Biswas J, Nelson CB, Runge VM, Wintersperger BJ, Baumann SS, Jackson CB, Patel T (2005) Brain tumor enhancement in magnetic resonance imaging: comparison of signal-to-noise ratio (SNR) and contrast-to-noise ratio (CNR) at 1.5 versus 3 Tesla. Invest Radiol 40:792–797
2. Brix G, Semmler W, Port R, Schad LR, Layer G, Lorenz WJ (1991) Pharmacokinetic parameters in CNS Gd-DTPA enhanced MR imaging. J Comput Assist Tomogr 15:621–628
3. de Lussanet QG, Langereis S, Beets-Tan RG, van Genderen MH, Griffioen AW, van Engelshoven JM, Backes WH (2005) Dynamic contrast-enhanced MR imaging kinetic parameters and molecular weight of dendritic contrast agents in tumor angiogenesis in mice. Radiology 235:65–72
4. Fayed N, Dávila J, Medrano J, Olmos S (2008) Malignancy assessment of brain tumours with magnetic resonance spectroscopy and dynamic susceptibility contrast MRI. Eur J Radiol 67:427–433
5. Hartmann M, Heiland S, Harting I, Tronnier VM, Sommer C, Ludwig R, Sartor K (2003) Distinguishing of primary cerebral lymphoma from high-grade glioma with perfusion-weighted magnetic resonance imaging. Neurosci Lett 338:119–122
6. Lacerda S, Law M (2009) Magnetic resonance perfusion and permeability imaging in brain tumors. Neuroimaging Clin N Am 19:527–557
7. Law M (2004) MR spectroscopy of brain tumors. Top Magn Reson Imaging 15:291–313
8. Law M, Yang S, Wang H, Babb JS, Johnson G, Cha S, Knopp EA, Zagzag D (2003) Glioma grading: sensitivity, specificity, and predictive values of perfusion MR imaging and proton MR spectroscopic imaging compared with conventional MR imaging. AJNR Am J Neuroradiol 24:1989–1998
9. Lu S, Ahn D, Johnson G, Law M, Zagzag D, Grossman RI (2004) Diffusion-tensor MR imaging of intracranial neoplasia and associated peritumoral edema: introduction of the tumor infiltration index. Radiology 232:221–228
10. Mack A, Wolff R, Scheib S, Rieker M, Weltz D, Mack G, Kreiner HJ, Pilatus U, Zanella FE, Böttcher HD, Seifert V (2005) Analyzing 3 Tesla magnetic resonance imaging units for implementation in radiosurgery. J Neurosurg 102(Suppl):158–164
11. MacFadden D, Zhang B, Brock KK, Hodaie M, Laperriere N, Schwartz M, Tsao M, Stainsby J, Lockwood G, Mikulis D, Ménard C (2010) Clinical evaluation of stereotactic target localization using 3 T MRI for radiosurgery planning. Int J Radiat Oncol Biol Phys 76:1472–1479
12. Meyerand ME, Pipes JM, Mamourian A, Tosteson TD, Dunn JF (1999) Classification of biopsy-confirmed brain tumors using single-voxel MR spectroscopy. AJNR Am J Neuroradiol 20:117–123
13. Runge VM, Biswas J, Wintersperger BJ, Baumann SS, Jackson CB, Herborn CU, Patel T (2006) The efficacy of gadobenate dimeglumine (Gd-BOPTA) at 3 Tesla in brain magnetic resonance imaging: comparison to 1.5 Tesla and a standard gadolinium chelate using a rat brain tumor model. Invest Radiol 41:224–248
14. Stieltjes B, Schluter M, Didinger B, Weber MA, Hahn HK, Parzer P, Rexilius J, Konrad-Verse O, Peitgen HO, Essig M (2006) Diffusion tensor imaging in primary brain tumors: reproducible quantitative

analysis of corpus callosum infiltration and contralateral involvement using a probabilistic mixture model. Neuroimage 31:531–542
15. Thilmann O, Larsson EM, Björkman-Burtscher IM, Ståhlberg F, Wirestam R (2005) Comparison of contrast agents with high molarity and with weak protein binding in cerebral perfusion imaging at 3 T. J Magn Reson Imaging 22:597–604
16. Tofts PS, Kermode AG (1991) Measurement of the blood–brain barrier permeability and leakage space using dynamic MR imaging. 1. Fundamental concepts. Magn Reson Med 17:357–367
17. Tsien CI, Cao Y, Lawrence TS (2009) Functional and metabolic magnetic resonance imaging and positron emission tomography for tumor volume definition in high-grade gliomas. Semin Radiat Oncol 19:155–162
18. Watanabe Y, Chung L, Gerbi B (2006) Geometrical accuracy of a 3 Tesla magnetic resonance imaging unit in Gamma Knife surgery. J Neurosurg 105(Suppl):190–193
19. Weber MA, Zoubaa S, Schlieter M, Jüttler E, Huttner HB, Geletneky K, Ittrich C, Lichy MP, Kroll A, Debus J, Giesel FL, Hartmann M, Essig M (2006) Diagnostic performance of spectroscopic and perfusion MRI for distinction of brain tumors. Neurology 66:1899–1906
20. Zhang B, MacFadden D, Damyanovich AZ, Rieker M, Stainsby J, Bernstein M, Jaffray DA, Mikulis D, Ménard C (2010) Development of a geometrically accurate imaging protocol at 3 Tesla MRI for stereotactic radiosurgery treatment planning. Phys Med Biol 55:6601–6615

Differentiation of Tumor Progression and Radiation-Induced Effects After Intracranial Radiosurgery

Mikhail F. Chernov, Yuko Ono, Kayoko Abe, Masao Usukura, Motohiro Hayashi, Masahiro Izawa, Sergey V. Diment, Pavel I. Ivanov, Yoshihiro Muragaki, Hiroshi Iseki, Tomokatsu Hori, Yoshikazu Okada, and Kintomo Takakura

Abstract A number of intracranial tumors demonstrate some degree of enlargement after stereotactic radiosurgery (SRS). It necessitates differentiation of their regrowth and various treatment-induced effects. Introduction of low-dose standards for SRS of benign neoplasms significantly decreased the risk of the radiation-induced necrosis after management of schwannomas and meningiomas. Although in such cases a transient increase of the mass volume within several months after irradiation is rather common, it usually followed by spontaneous shrinkage. Nevertheless, distinguishing tumor recurrence from radiation injury is often required in cases of malignant parenchymal brain neoplasms, such as metastases and gliomas. The diagnosis is frequently complicated by histopathological heterogeneity of the lesion with coexistent viable tumor and treatment-related changes. Several neuroimaging modalities, namely structural magnetic resonance imaging (MRI), diffusion-weighted imaging, diffusion tensor imaging, perfusion computed tomography (CT) and MRI, single-voxel and multivoxel proton magnetic resonance spectroscopy as well as single photon emission CT and positron emission tomography with various radioisotope tracers, may provide valuable diagnostic information. Each of these methods has advantages and limitations that may influence its usefulness and accuracy. Therefore, use of a multimodal radiological approach seems reasonable. Addition of functional and metabolic neuroimaging to regular structural MRI investigations during follow-up after SRS of parenchymal brain neoplasms may permit detailed evaluation of the treatment effects and early prediction of the response. If tissue sampling of irradiated intracranial lesions is required, it is preferably performed with the use of metabolic guidance. In conclusion, differentiation of tumor progression and radiation-induced effects after intracranial SRS is challenging. It should be based on a complex evaluation of the multiple clinical, radiosurgical, and radiological factors.

Keywords Differential diagnosis • Functional neuroimaging • Gamma Knife radiosurgery • Metabolic neuroimaging • Radiation-induced necrosis • Stereotactic radiosurgery • Tumor progression

M.F. Chernov (✉), M. Hayashi, Y. Muragaki, H. Iseki, and K. Takakura
Faculty of Advanced Techno-Surgery, Institute of Advanced Biomedical Engineering and Science, Tokyo Women's Medical University, 8-1 Kawada-cho, Shinjuku-ku, Tokyo 162-8666, Japan

Department of Neurosurgery, Neurological Institute, Tokyo Women's Medical University, Tokyo, Japan
e-mail: m_chernov@abmes.twmu.ac.jp

Y. Ono, K. Abe, and M. Usukura
Department of Diagnostic Imaging and Nuclear Medicine, Tokyo Women's Medical University, Tokyo, Japan

M. Izawa, T. Hori, and Y. Okada
Department of Neurosurgery, Tokyo Women's Medical University, Tokyo, Japan

S.V. Diment and P.I. Ivanov
Radiosurgical Center, International Institute of the Biological Systems, Saint Petersburg, Russia

Introduction

Stereotactic radiosurgery (SRS), particularly Gamma Knife radiosurgery (GKS) is a widely approved management option for a variety of benign and malignant intracranial neoplasms, vascular lesions, and functional brain disorders. For brain tumors, the treatment usually results in stabilization of growth, and some degree of mass volume reduction is frequently seen. Nevertheless, a number of lesions demonstrate progression after irradiation, necessitating differentiation of tumor regrowth from treatment-induced effects. Some amount of increase in the mass volume after SRS is observed in 1–10 % of pituitary adenomas and benign meningiomas [19, 61, 86], 14–70 % of vestibular schwannomas [15, 24, 62, 65],

M.F. Chernov et al. (eds.), *Gamma Knife Neurosurgery in the Management of Intracranial Disorders*, Acta Neurochirurgica Supplement, Vol. 116, DOI 10.1007/978-3-7091-1376-9_29, © Springer-Verlag Wien 2013

16–60 % of intracranial metastases [10, 18, 23, 63, 71], and 73–84 % of malignant gliomas [71]. It may reflect failure of the SRS and true progression of the neoplasm or even malignant transformation of an initially benign tumor. In the same time, regrowth may be mimicked by delayed growth arrest, temporary enlargement of the mass after low-dose radiosurgery, or radiation-induced necrosis. In some cases, formation of the new radiosurgery-induced neoplasm within the target area is suspected. It is clear that an exact diagnosis in such cases is mandatory for timely initiation of the appropriate treatment and precise determination of prognosis [30, 34].

Progressing Lesions After Radiosurgery of Intracranial Tumors

Treatment-induced changes after SRS evolve over time, and tumor progression may be initiated in varying intervals after seemingly durable initial growth control. It emphasizes the importance of close, prolonged radiological follow-up after radiosurgery, which usually comprises regular investigations with structural magnetic resonance imaging (MRI) or computed tomography (CT). These methods permit dynamic evaluation of the lesion volume, structure, contrast enhancement, degree of peritumoral edema, and mass effect. While evaluation of these parameters is useful, sometimes it cannot reliably distinguish various radiosurgery-induced pathophysiological reactions within the target. Usually decreased peritumoral brain edema and appearance of central lucency on postcontrast MRI of the lesion are considered positive prognostic factors as they indicate growth arrest and further shrinkage of both benign and malignant neoplasms [39, 54, 64]. There may also be a temporary increase in contrast enhancement of the mass with blurring or an irregular margin [39, 71], but the prognostic significance of such findings remains unknown.

In fact, even volumetric changes, which are used to assess tumor response to irradiation, are not always sufficiently predictive for a prognosis [71]. For example, up to 60 % of intracranial metastases that demonstrated varying degrees of volume reduction soon after radiosurgery enlarged thereafter [23]. However, in 20–64 % of cases it is not caused by tumor regrowth due to treatment failure but by radiation-induced effects [23, 30, 32, 71], and even histopathological investigation after surgical resection of these lesions could not reveal viable neoplastic tissue. According to Huang et al. [30], a 65 % increase in the volume of a metastatic brain tumor after irradiation represents the best threshold for identifying recurrence. However, it has only 80 % specificity, which fell to 50 % for lesions irradiated with a biological effective dose (BED) of >200 Gy (approximately 19 Gy of marginal dose delivered at a single session) [30]. In the series of Essig et al. [17], volumetric changes in intracranial metastases at 6 weeks after SRS had just 64 % positive prediction value (PPV) and 43 % negative prediction value (NPV) for overall response to treatment.

Regrowth of the Intracranial Tumors due to Treatment Failure

Failure of radiosurgery to control the intracranial tumor may be caused by suboptimal targeting, insufficient treatment dose, and/or resistance of the neoplasm to irradiation, particularly due to prominent malignant growth potential. Inability to identify clearly the borders of the mass on conventional neuroimaging is considered one of the main reasons for SRS failure in such different tumors as adrenocorticotropic hormone-secreting pituitary adenomas and gliomas. Intentionally decreasing the radiation dose delivered to the target because of its large volume or critical location may be the main reason of regrowth of schwannomas and meningiomas after sterotactic irradiation [86]. Radiosurgery has limited effectiveness for malignant extracerebral intracranial tumors, especially if applied as salvage treatment at the time of evident tumor progression. Some brain metastases (e.g., those originating from sarcomas, colon and renal carcinomas, and malignant melanoma) are relatively resistant to SRS and may require greater radiation doses [38].

Malignant Transformation of Benign Intracranial Tumors

Malignant transformation of benign brain tumors after GKS is uncommon. In fact, it can be easily mistaken with spontaneous dedifferentiation, particularly if irradiation is performed at the time of regrowth or recurrence after initial lesion resection [48, 58]. Moreover, in some of such cases reexamination of the tissue specimen obtained at the time of surgery may reveal missed features of anaplasia [48]. It should be borne in mind that rare malignant subtypes of schwannomas and meningiomas can be radiologically indistinguishable from their typical benign counterparts. Thus, their progression, despite SRS, is easily confused with malignant transformation. Kubo et al. [48] analyzed 11 such cases after SRS or radiotherapy of vestibular schwannomas and found that in 7 of them irradiation was applied as a primary treatment modality without detailed examination of the neoplastic tissue, and 5 patients had neurofibromatosis type 2, which has known association with a high risk of malignancy. It should be

noted that in rare cases accelerated growth of benign tumors was observed during various time periods after SRS, but tissue investigation after subsequent resection usually confirmed preservation of the benign histopathological pattern [14].

Delayed Growth Arrest and Temporary Enlargement of Benign Brain Tumors

Stabilization of growth with or without subsequent shrinkage is the most typical outcome after low-dose SRS for benign intracranial tumors. However, other patterns of volumetric response to irradiation are not uncommon. Temporary enlargement of the irradiated neoplasm has become a recognizable clinical phenomenon, which is rather typical for slow-responding masses [64]. It usually does not reflect true tumor progression and only infrequently requires additional treatment.

Several months after radiosurgery 14–70 % of vestibular schwannomas demonstrate an increase in their volume [15, 24, 62, 65], which constitutes in median 75 %, although it may reach 200 % [15, 65]. Regarding linear measurements, the tumors may increase >5 mm in one axis [15, 65]. Hasegawa et al. [24] noted that such changes were more common in women with large, particularly cystic neoplasms. Temporary lesion enlargement may be more frequent after irradiation with higher doses as it was noted in 70 % of patients treated before introduction of low-dose SRS for benign intracranial tumors [62]. The phenomenon may be more profound in nonvestibular, particularly trigeminal, schwannomas [55]. Increased mass volume is usually accompanied by loss of central contrast enhancement on T1-weighted MRI, also known as the "black hole" [54]. The pathophysiological mechanism remains the subject of debate, but delayed growth arrest, radiation-induced necrosis, and/or apoptosis with inflammation and swelling are considered the main causes. Histopathological investigation may reveal parenchymal necrosis, thickening of the vascular walls as a result of endothelial and pericytic proliferation, perivascular infiltration of macrophages and small lymphoid cells, thrombus formation, and foci of minute hemorrhages [24, 26, 48]. Appearance of new symptoms, particularly hemifacial spasm, was noted in 20 % of patients, but they are usually self-limiting or resolve with steroid therapy [65].

The most important fact, which is clearly recognized at present, is that more than half of vestibular schwannomas exhibiting enlargement after SRS demonstrate shrinkage later on, whereas many others have growth stabilization without further progression. The appearance of central lucency on contrast-enhanced images is usually followed by reenhancement, and considered a favorable factor for further volume regression [24, 54, 64]. In such cases, residual inactive lesions with prominent fibrotic changes usually appear as small contrast-enhanced masses within the target area, resembling a "white dwarf" [54]. Only in 2–7 % of patients undergoing GKS for a vestibular schwannoma, serial neuroimaging demonstrates continuous tumor progression, cystic degeneration, or enlargement of preexisting cysts, which necessitates additional treatment with surgery or repeat radiosurgery [24, 65].

Similar volumetric changes are sometimes observed after low-dose radiosurgery of other benign tumors [19, 61, 62, 64]. In the series of Feigl et al. [19], around 3 % of World Health Organization (WHO) grade I meningiomas demonstrated an initial volume increase after GKS followed by shrinkage or growth stabilization. Pamir et al. [61] noted some enlargement of pituitary adenomas 3–9 months after GKS, although their size subsequently decreased in all cases. This phenomenon was also noted after SRS of a low-grade glioma [64].

Radiation-Induced Necrosis

Radiation-induced necrosis is a well-known phenomenon, mimicking brain tumor progression after irradiation. It corresponds to early-delayed or late injury and usually develops several months to several years after treatment, while clinical manifestation was occasionally reported even 13 years after SRS [7]. The incidence of symptomatic radiation-induced necrosis after intracranial radiosurgery varies in most series from 2 % to 14 %. Its risk is directly associated with greater radiation doses, radiation energy delivered to the target, prescription isodose volumes, 10 Gy and 12 Gy irradiation volumes; larger number of isocenters; tumor dose inhomogeneity; lower selectivity of the treatment plan; previous administration of SRS or radiotherapy; longer duration of follow-up [3, 5, 13, 20, 21, 32, 42, 47, 63, 64]. Radiation injury is rarely observed after low-dose treatment of benign neoplasms. The type of pathology is important: In the series of Chin et al. [13], the incidence of the complication after GKS was 17 % for gliomas but 6 % for other tumors. The development of radiation injury is a complex process, and it is difficult to predict its probability based on the limited number of clinical and radiosurgical parameters. It may be predisposed in some way by individual radiosensitivity [13, 21, 63] and specific medical conditions (e.g., diabetes), be more pronounced in well-oxygenated tissues [42], and be confounded by adjuvant and concurrent chemotherapy [5, 34].

The underlying pathophysiological mechanisms include initial direct cellular damage and microvascular injury with progressive thickening of the large vessel walls caused by hyalinization leading to thrombosis, infarction, and necrosis. Correspondingly, the most common histopathological findings in such cases are fibrinoid necrosis of the vascular

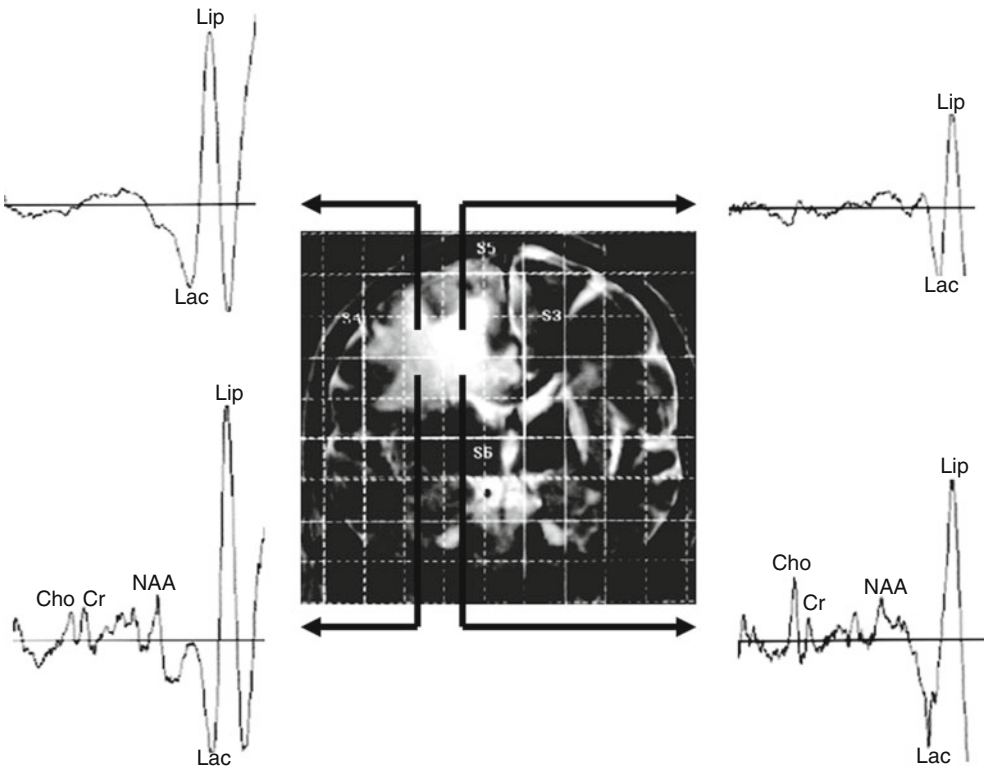

Fig. 1 Multivoxel proton magnetic resonance spectroscopy (^{1}H-MRS) in a case of radiation-induced necrosis of the peritumoral brain after Gamma Knife radiosurgery (GKS) of a metastatic brain tumor. Note the presence of a necrosis pattern in spectroscopic voxels containing brain tissue adjacent to the target. *NAA N*-acetylaspartate, *Cho* choline-containing compounds, *Cr* creatine, *Lac* lactate, *Lip* mobile lipids (*Source*: Chernov et al. [12])

walls with degradation of their basement membranes, endothelial damage with proliferation of endothelial cells and fibroblasts, vessel dilatation, telangiectasia, and perivascular infiltration of lymphocytes, plasma cells, and macrophages [7, 26, 34]. There is widespread permeation of the tissue by fibrin caused by increased permeability of the vessels [42]. Also, irradiation alters fibrinolytic enzyme activity and initiates the immune response, which may cause autoimmune vasculitis [34]. Other changes include minute hemorrhages, calcifications, fibrosis, and cyst formation [5, 26]. Microvascular proliferation in necrotic foci or in their vicinity is seen in some cases [26]. In the perilesional brain loss of oligodendrocytes, which are extremely sensitive to irradiation, leads to demyelination, whereas increased vascular permeability results in vasogenic brain edema; astrocytosis and shrunken neurons associated with local brain atrophy are seen subsequently [39, 70].

Unlike the tissue necrosis caused by wide-field radiotherapy, after SRS the radiation injury is usually localized and well restricted. In general, it is important to differentiate radiation-induced tumor necrosis and radiation-induced necrosis of the peritumoral brain [12]. Both conditions present as diffuse signal hyperintensity on T2-weighted images that exceed the target area. They are sometimes characterized as "supernovas" [54], and usually accompanied by perilesional contrast enhancement due to blood–brain barrier (BBB) disruption [62, 64]. Nevertheless, with radiation-induced tumor necrosis, the changes in the adjacent brain parenchyma are mainly caused by diffusion of metabolically active substances (i.e., cytokines) from the damaged neoplasm. Therefore, this condition is frequently reversible, although it may require surgical resection of the mass [64]. Hence, radiation-induced tumor necrosis may be considered a more or less acceptable side effect after radiosurgery of malignant lesions [13]. In contrast, radiation injury to the peritumoral brain caused by excessive radiation is an avoidable complication as it is usually due to suboptimal targeting with low selectivity (Fig. 1).

Table 1 Histopathological classification of radiation treatment effects on tumors (modified from Ohoshi and Shimosato)

Grade	Histopathological characteristics
0	No radiation effect
I	Cellular damage without destruction of tumor clusters
II	Cellular damage with destruction of tumor clusters
III	Nonviable tumor cells
IV	No tumor cells (including coagulation necrosis)

Source: Kamada et al. [38]

The main diagnostic and treatment challenges posed by intracranial lesion progression after radiosurgery and radiotherapy are related to their common histopathological heterogeneity, the nearby coexistence of a viable tumor, and radiation-induced changes (Table 1), which may be particularly evident at the periphery of the target [38]. Such findings were identified in 35–74 % of brain metastases and nearly

100 % of high-grade gliomas that underwent surgical resection after initial SRS [16, 32, 40, 41, 71]. They are also observed in some extracerebral intracranial neoplasms [48].

Presenting symptoms and clinical behavior of radiation-induced necrosis vary significantly. Incidental, self-limiting, steroid-controlled, progressive, and recurrent forms are well recognized [3, 7, 44, 47]. Space-occupying lesions resistant to medical therapy may require surgical resection [20, 40, 64]. Milder forms are mainly related to edema resulting from BBB disruption and demyelination. Hence, their radiological definition as "radiation-induced enhancement" (not "necrosis") might be more correct, at least at the early stages of development [42, 66]. Extensive radiation-induced necrosis and cyst formation may be observed after radiosurgical management of nonneoplastic pathology, such as an arteriovenous malformation (AVM) and cavernomas, which sometimes requires differentiation from new tumor formation [7, 20].

New Tumor Formation

There is no evidence that SRS increases the risk of malignancy, and formation of new radiosurgery-associated tumors is exceptionally rare [53, 72]. The roughly estimated risk is <0.001 % [58]. In 2009, Niranjan et al. [58] identified nine reported cases that met standard Cahan's criteria for radiation-induced neoplasms: four glioblastomas, one anaplastic astrocytoma, three meningiomas, and one vestibular schwannoma. The complication manifested within 5–16 years after SRS for benign brain tumors (four cases), malignant melanoma metastases (one case), and AVM (four cases).

Differentiation of the Tumor Regrowth and Radiation-Induced Effects After Radiosurgery

Various clinical and radiosurgery-related characteristics (e.g., histopathological type of the lesion, its volume, previously applied SRS or radiotherapy, radiation dose and its distribution, dynamics of symptoms, time elapsed until identification of progression) should be certainly taken into consideration during differentiating tumor regrowth from radiation-induced effects. However, such parameters are quite similar in both clinical entities and their assessment alone rarely establishes a clear diagnosis [30, 81]. Barajas et al. [2] reported that intraaxial metastatic tumors that later recurred had a trend to have larger volume and lower prescribed doses at the time of irradiation, although the differences were not statistically significant. Kano et al. [41] found that a shorter interval between GKS of brain metastasis and subsequent resection necessitated by lesion progression was associated with a greater incidence of finding viable neoplasm in the histopathological specimen. In concordance, Kihlstrom and Karlsson [42] noted that a tumor recurrence after radiosurgery is more likely during the first posttreatment year, whereas radiation injury is usually delayed. However, these temporal interrelations were not confirmed by others [2, 12, 27, 33, 56]. Our series of patients with intracranial metastases progressing after GKS included 11 cases of pure tumor recurrence or regrowth, 10 cases of pure radiation-induced tumor necrosis, and 11 cases of mixed lesions. None of the clinical and radiosurgical parameters (including location and initial volume of the intracranial neoplasm, previous irradiation by means of SRS or fractionated radiotherapy, maximum and marginal irradiation doses, initial volumetric tumor response after radiosurgery, time to deterioration) differed significantly between the groups [12]. Therefore, it is evident that various neuroimaging modalities must play the main diagnostic role in such cases.

Historical Methods (Angiography and Scintigraphy)

Attempts were made in the past to use cerebral angiography to differentiate tumor recurrence from radiation-induced necrosis, but the results were generally nonspecific [4, 5]. Currently, its use in such cases has been practically abandoned, although it represents the gold standard for evaluating AVMs after radiosurgery. Similarly, scintigraphy and tomoscintigraphy with such tracers as sodium pertechnetate, DTPA technetium, and iodoamphetamine (IMP) were widely performed before introduction of the contemporary neuroimaging modalities, but frequent false-positive and false-negative results were noted [5].

Structural CT and MRI

At the time of lesion progression after radiosurgery, CT has limited opportunities for differentiating tumor regrowth from radiation-induced necrosis because both conditions typically appears similarly as a contrast-enhancing low-density mass within the target area surrounded by brain edema and frequently associated with a mass effect [4, 5, 42, 45]. According to our experience, neither the lesion volume nor extent of the perilesional edema differs significantly in cases of pure tumor recurrence, pure radiation-induced necroses, and mixed pathology after GKS of intracranial metastases, whereas a midline shift at the time of clinical deterioration was relatively more common in cases of radiation injury [12].

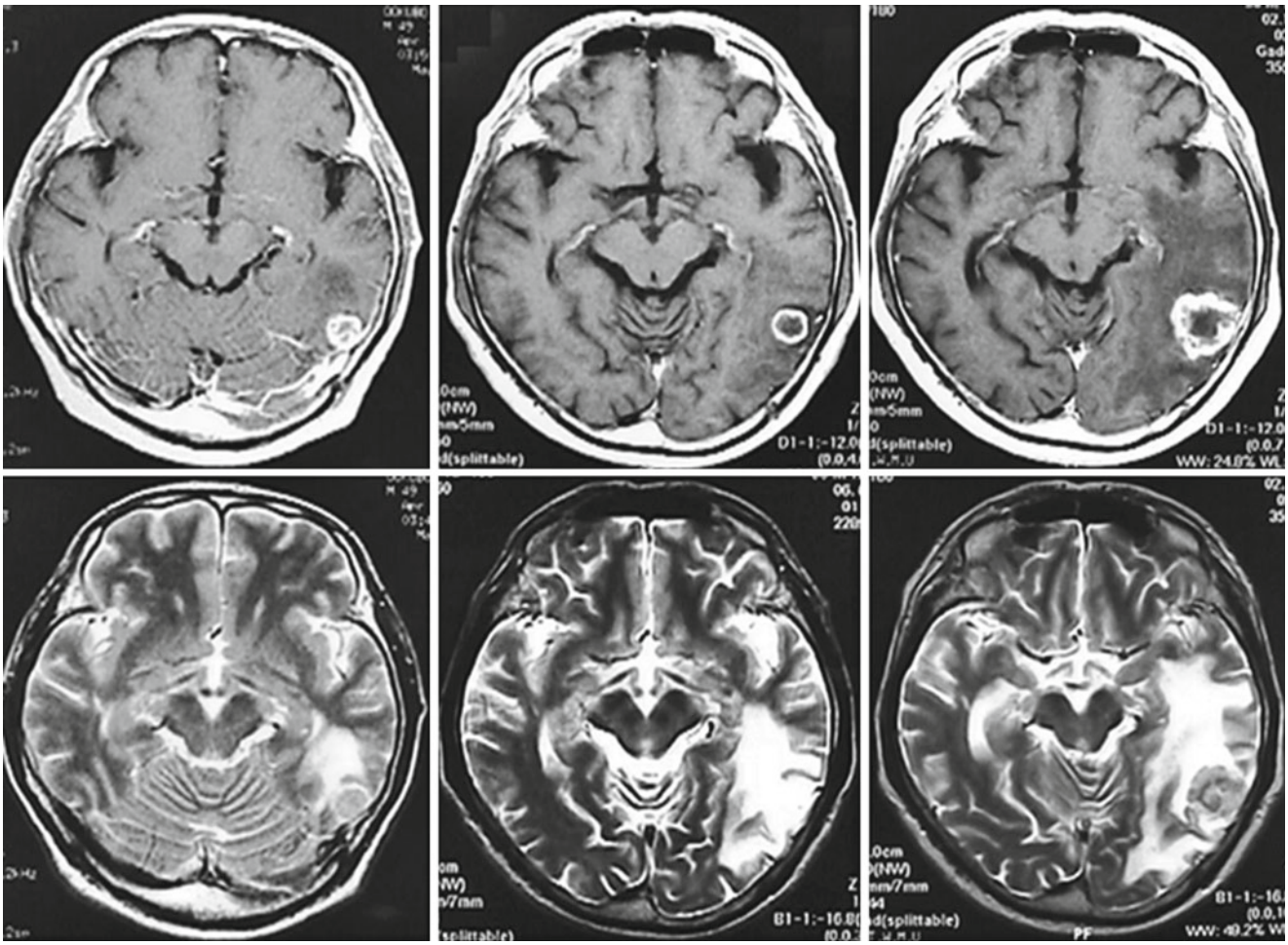

Fig. 2 Dynamics of the structural changes in a metastatic adenocarcinoma of the lung after GKS. At 1 month after treatment the size of the lesion had not changed significantly, although there was the appearance of a central lucency without any corresponding hypointense areas on T2-weighted images. At 10 months after treatment, there was a significantly increased heterogeneously enhanced lesion that well corresponded to the hypointense area on T2-weighted magnetic resonance imaging (MRI) on the background of a hyperintense signal caused by brain edema. Histopathological investigation after subsequent resection revealed mixed pathology with coexistent viable tumor and radiation-induced necrosis

On the other hand, structural MRI may provide some useful diagnostic information. Particularly helpful for identifying tumor regrowth is an evaluation of the correspondence of the target-related hypointense area on the background of the hyperintense signal on T2-weighted MRI to the contrast-enhanced lesion on T1-weighted MRI. It is defined as the lesion quotient or a T1/T2 match/mismatch [16, 40, 41]. The greater the correspondence of their cross-sectional areas to each other, the higher is the probability that a progressing tumor is present (Fig. 2). Dequesada et al. [16] reported that in all seven patients with histopathologically confirmed pure neoplastic pathology, this ratio was ≥0.6, and use of its cutoff level at 0.3 predicted the presence of a viable neoplasm in 26 of 27 cases. The reported sensitivity and specificity of a T1/T2 match for identifying recurrent brain metastases after GKS are 94 % and 77 %, respectively [40]. On the other hand, an indistinct hypointense lesion on T2-weighted MRI that failed to correlate with the T1-weighted contrast-enhanced volume was significantly associated with detection of pure necrotic changes in the tissue specimens. However, viable neoplastic elements were identified in 33 % of contrast-enhanced masses that did not have any corresponding hypointense area on T2-weighted images [40, 41].

Other features associated to some degree with progression of metastatic brain tumors after irradiation can be also identified on MRI: arteriovenous shunting, gyriform distribution of the hyperintense area corresponding to lesion and perilesional edema on T2-weighted images, cyst formation, and marginal or solid contrast enhancement [16]. On the other hand, some specific forms of contrast enhancement (Fig. 3), defined as “cut green pepper” (multiple irregular rings of enhancement), “Swiss cheese/soap bubble”

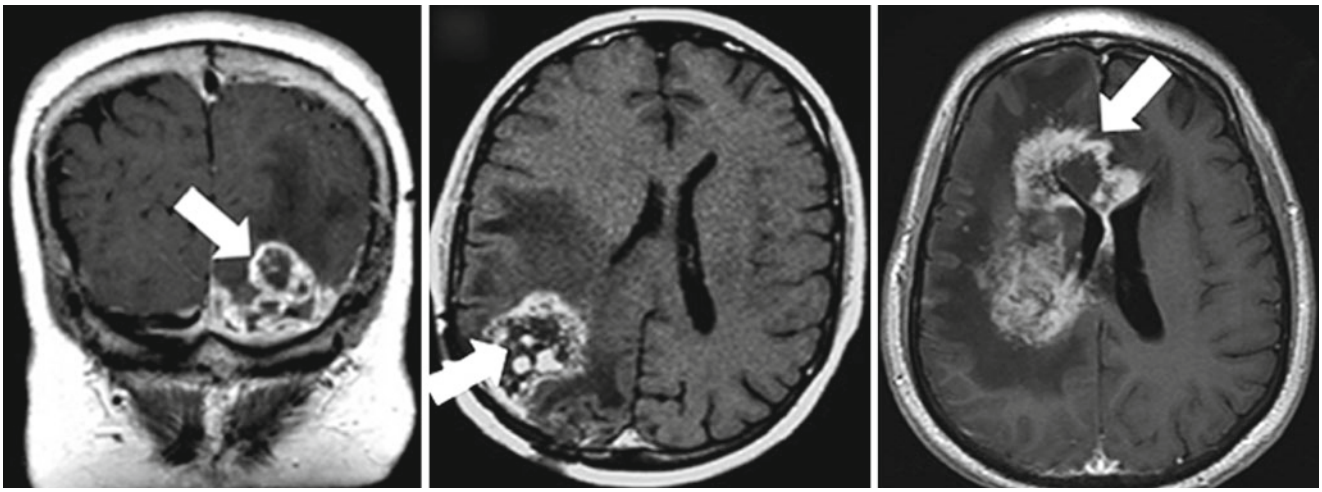

Fig. 3 Specific forms of contrast enhancement (*arrows*) typical for radiation-induced necrosis: "cut green pepper" (*left*), "soap bubble" (*center*), and "spreading wavefront" (*right*) (*Sources*: Dequesada et al. [16], Rogers et al. [70], and Jain et al. [34])

(multiple small or moderate-sized areas of enhancement intermixed with foci of necrosis), and "spreading wavefront" (blurred margin of enhancement) are considered more typical, although not highly specific, of radiation-induced necrosis [16, 34, 57, 70]. Overall, structural MRI is somewhat helpful in cases of parenchymal brain lesions progressing after irradiation, but the information provided usually is not enough for a precise diagnosis. There is general agreement that additional functional and metabolic radiological investigations are mandatory [22, 25, 34, 39, 59, 60, 66].

Diffusion-Weighted Imaging and ADC Mapping

Diffusion-weighted imaging (DWI) reveals microscopic Brownian motion in tissue water, and the apparent diffusion coefficient (ADC) quantitatively describes the effective mean diffusivity, which is determined by the tissue cellularity, viscosity of the medium, and spacing of the diffusion barriers. Highly cellular brain tumors usually appear on DWI as hyperintense lesions and have a low ADC. Treatment-related calcifications, gliosis, or fibrosis in the mass may influence the intensity of the signal. Of note: the ADC of brain tumors is relatively insensitive to steroid therapy, which facilitates use of DWI during posttreatment follow-up [84].

In contrast, a hypointense signal on DWI and high ADC are considered typical of radiation-induced necrosis [1, 22, 23, 31, 39], which may, however, exhibit a variety of signal patterns [66]. Particularly, necrosis with a viscous mucinous component may appear on DWI as a hyperintense lesion and have low ADC values, similar to brain abscesses [66]. A low ADC can also be caused by an inflammatory cellular composition at the early stages of radiation injury and by the presence of hemorrhages. Probably for these reasons direct comparison of ADC led to controversial results because higher values for both radiation injury [1] and tumor recurrence [75] were reported. In mixed lesions evaluation of the spatial heterogeneity of ADC by means of "diffusion mapping" may allow to define presence of tumor recurrence adjacent to necrotic areas [1, 22, 31].

Diffusion Tensor Imaging

The basic principles of diffusion tensor imaging (DTI) are similar to those of DWI except that DTI evaluates the directionality and magnitude of water diffusion characterized by fractional anisotropy (FA). FA was found to be slightly higher, whereas the FA ratio (FA values normalized by region-of-interest [ROI] in the contralateral white matter) was significantly higher in normal-appearing white matter adjacent to the perilesional edema in patients with treatment-related injury after radiochemotherapy of intracranial gliomas compared to patients with recurrent neoplasms [75]. Additionally, eigenvalues and the principal eigenvalue ratio were significantly higher in contrast-enhancing lesions in a group of patients with recurrence [75]. Thus, DTI may be somewhat helpful in differenting radiation-induced necrosis from regrowth of a brain neoplasm after SRS, at least for infiltrative gliomas, which justifies further research in this area [84].

Perfusion CT and MRI

At present, the hemodynamics of intracranial neoplasms can be evaluated in vivo with perfusion CT and MRI using first-pass dynamic susceptibility-weighted contrast-enhanced perfusion imaging or arterial spin labeling. Various

parameters determined by these techniques, including cerebral blood flow (CBF), cerebral blood volume (CBV), mean transit time (MTT), relative peak height (PH), percentage of signal-intensity recovery (PSR), contrast transfer coefficient (K^{trans}), allow detailed characterization of the lesion's microvascularity and the permeability of its vessels. They can be applied effectively to differentiate tumor progression from radiation-induced changes.

Increased neoangiogenesis and vascular density are characteristic features of most neoplasms, especially those that are malignant. Typically, CBV is greater in recurrent high-grade brain masses than in white matter and lower or equal to that in gray matter [27]. Its maximum values correspond to intralesional areas of increased mitotic activity [66]. Because effective irradiation alters the blood supply of the tumor, low CBV and CBF and increased MTT are usually seen in radiation-induced necrosis [2, 22, 34, 35, 66]. However, sometimes the contrast-enhanced component of the necrotic lesion has greater perfusion than is seen in white matter, probably owing to the relatively increased density of capillaries in the areas of inflammation, or to extension of the vascular lumen caused by telangiectasia and dilatation of the blood vessels [2, 33, 34, 66]. Of interest, several studies from various centers [27, 30, 56] determined similar optimal thresholds of the relative CBV (normalized to white matter) for identifying recurrent intracranial metastasis after irradiation: Its value of ≥2.0 proved to have 70–96 % diagnostic accuracy (Fig. 4). However, for gliomas the cutoff level may be lower: Jain et al. [35] used perfusion CT to investigate the optimal threshold of the relative CBV for identifying a progressing tumor, and determined that it was 1.65 providing 83 % sensitivity and 100 % specificity.

The perfusion abnormalities in tumors are related not only to the large number of neoplastic vessels but also to their abnormal characteristics, such as increased permeability, which may be detected in recurrent neoplasms and used for their diagnosis [2, 33, 34]. In the multivariate analysis performed by Jain et al. [33], the permeability surface area product and the relative CBV showed independent significant association with differentiating between the groups of regrowing tumors (mainly gliomas) and treatment-induced necrosis. Of note: Vascular leakiness in patients with a radiation injury is also increased because of the damaged endothelium and hypoxia-related up-regulation of vascular endothelial growth factor (VEGF), but its magnitude is less than that of viable high-grade neoplasms [33].

Perfusion CT provides robust data and better options for quantitative analysis because of the linear relation between the contrast agent's concentration and tissue attenuation. However, radiation exposure and use of relatively large volumes of iodinated contrast medium limit its utility for assessing brain tumors [33–35, 56]. On the other hand, perfusion MRI provides better anatomical resolution but is susceptible to multiple technical and methodological errors, and its results may be significantly affected by some pathophysiological characteristics of the investigated tissue [2, 34]. Artificially increased hemodynamic parameters are obtained if the examination is performed in the vicinity of major vascular structures [66]. Also, the presence of hemorrhage, melanin depositions, cysts, or significant extravasation of contrast medium in the investigated area may produce susceptibility artifacts and lead to erroneously decreased CBV values in the viable neoplasm [2]. Inaccurate estimation of CBF and CBV may be caused by BBB alteration as interstitial edema may compress the small vessels [33–35, 83]. In addition, the tumor vasculature is sometimes significantly compromised by rapid growth with necrotic changes [34, 35]. Low spatial resolution of the method may challenge a precise diagnosis in the presence of mixed lesions with a coexistent viable neoplasm and radiation injury, although creation of "perfusion maps" may resolve this problem [34, 35, 66]. Finally, the results of perfusion studies are significantly affected by administration of steroids or antiangiogenic therapy (e.g., bevacizumab), which is currently used for management of both recurrent parenchymal brain tumors and radiation-induced necrosis [34, 84].

Proton Magnetic Resonance Spectroscopy

Proton magnetic resonance spectroscopy (^{1}H-MRS) allows noninvasive biochemical characterization of human tissue located within the predefined voxel. The method is intrinsically multiparameter and permits simultaneous evaluation of the variety of metabolites, which in the human brain usually includes *N*-acetylaspartate (NAA), choline-containing compounds (Cho), creatine (Cr), lactate (Lac), and mobile lipids (Lip). These metabolites are associated with rather specific histopathological and pathophysiological properties of the investigated tissue (Table 2). In the clinical setting, the content of metabolites is frequently expressed semiquantitatively, as various ratios.

^{1}H-MRS showed high effectiveness for differentiating a recurrent tumor from radiation-induced necrosis. In such cases, use of a multivoxel investigation (also known as spectroscopic or chemical shift imaging) is particularly important because it provides the optimal spatial resolution required for distinguishing the coexistent viable neoplasm from treatment-induced changes [11, 49, 66]. Our study showed 100 % diagnostic accuracy of this method in cases of intracranial metastases enlarging after GKS [11]. The tumor is usually characterized by an elevated Cho peak, decreased NAA and Cr peaks, and frequent appearance of Lac and Lip peaks [10, 25, 49, 51, 84]. The two latter metabolites

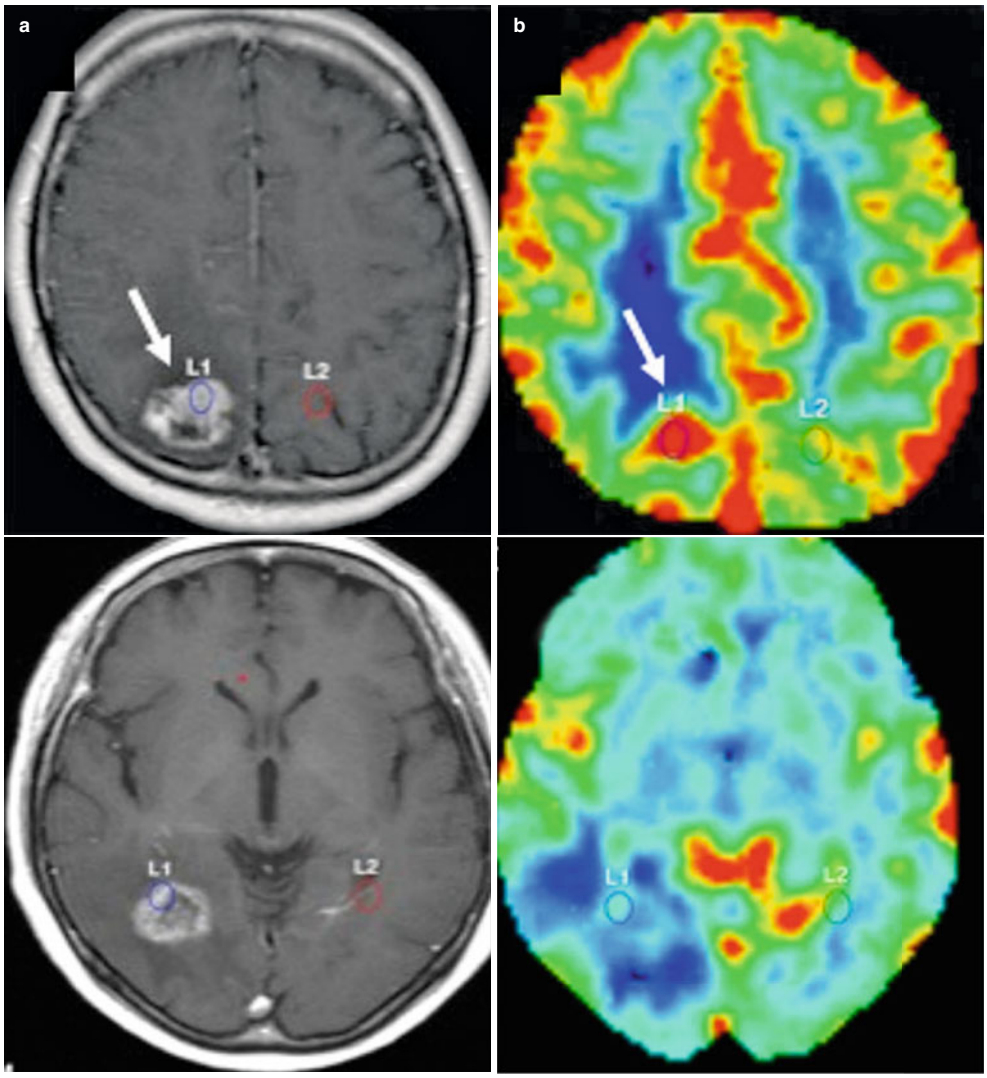

Fig. 4 Contrast-enhanced T1-weighted (**a**) and perfusion-weighted (**b**) MRI in cases of tumor recurrence (*upper*) and radiation-induced necrosis (*lower*) after radiosurgery of metastatic brain tumors. Note the clear difference in the cerebral blood volume of lesions (*Source*: Mitsuya et al. [56])

predominate on the spectrum of necrotic lesions, although in some of such cases no reliable peaks can be identified at all. However, in cases of early radiation-induced injury, Cho may be elevated because of inflammation, demyelination, and gliosis, and the spectroscopic pattern may resemble that of a tumor [49, 66, 84].

The list of proposed thresholds of different metabolic ratios for identifying a recurrent tumor is endless. It includes Cho/Cr >2.5 [43, 44, 51], Cho/Lip + Lac >0.3 [44], and Cho/nCho >1.2 [30] after SRS of brain metastases; and Cho/NAA >1.8 [75], Cho/Cr >1.8 [75], Cho/nCr >1.79 [68], and Lip + Lac/Cho <0.75 [68] after radiochemotherapy of intracranial gliomas. In our experience, the combination of NAA/Cho ratio <1 and Lip/Cho ratio <3 in at least one lesion-containing voxel of multivoxel ^{1}H-MRS showed high diagnostic accuracy for identification of regrowing brain metastases after GKS, and corresponded well to the histopathology in a surgically treated cases [11, 12]. It should be kept in mind that evaluated metabolite ratios have variability of, at least, 10–15 %, whereas technical differences of processing and postprocessing during spectroscopic examinations significantly complicate comparison of results obtained on different MRI scanners. Hence, additional pattern analysis of the ^{1}H-MR spectra can be helpful (Fig. 5).

In the series of patients with gliomas, Rock et al. [68, 69] found that spectroscopic imaging allows reliable differentiation between pure tumor and pure radiation-induced necrosis, but the distinction is less definitive for mixed lesions. Possible false-negative results of ^{1}H-MRS in the determination of recurrent neoplasms may be caused by the relatively large size of the spectroscopic voxel (usually ≥1 cm^{3}), incomplete coverage of the lesion, and/or the inability to differentiate between radiation-induced and tumor-induced necrosis. Some tumors, such as intracranial metastases of colorectal carcinoma, may have extremely high Lip content, which may complicate their differential diagnosis. Finally, the presence of hemorrhage in the investigated volume of tissue and location of the mass in the vicinity of cerebral

Table 2 Role of specific ^{1}H-MRS-detected metabolites in brain tissue characterization

Main ^{1}H-MRS-detected metabolites in human brain	Histopathological and pathophysiological correlates
N-Acetylaspartate (NAA)	Extremely sensitive axonal and neuronal marker that reflects their density, viability, and functional activity. Nonspecific decrease accompanies nearly all brain dysfunctions.
Choline-containing compounds (Cho)	Associated with both synthesis and degradation of cell membranes. Elevated in areas with increased proliferative activity, high cellularity, inflammation, and early necrosis. Decrease is associated with cell loss.
Creatine (Cr)	Reflects energetic properties of the investigated tissue. Usually, but not always, decreased in brain tumors. Frequently used as internal standard for evaluating the other metabolites' content.
Lactate (Lac)	Usually not detected in normal brain. Appears in areas of increased glycolysis, anaerobic metabolism, ischemia, or impaired mechanisms of lactate utilization.
Mobile lipids (Lip)	Usually not detected in normal brain. Appears in areas with high rate of cell membrane turnover, tissue breakdown, and necrosis.

^{1}*H-MRS* proton-magnetic resonance spectroscopy

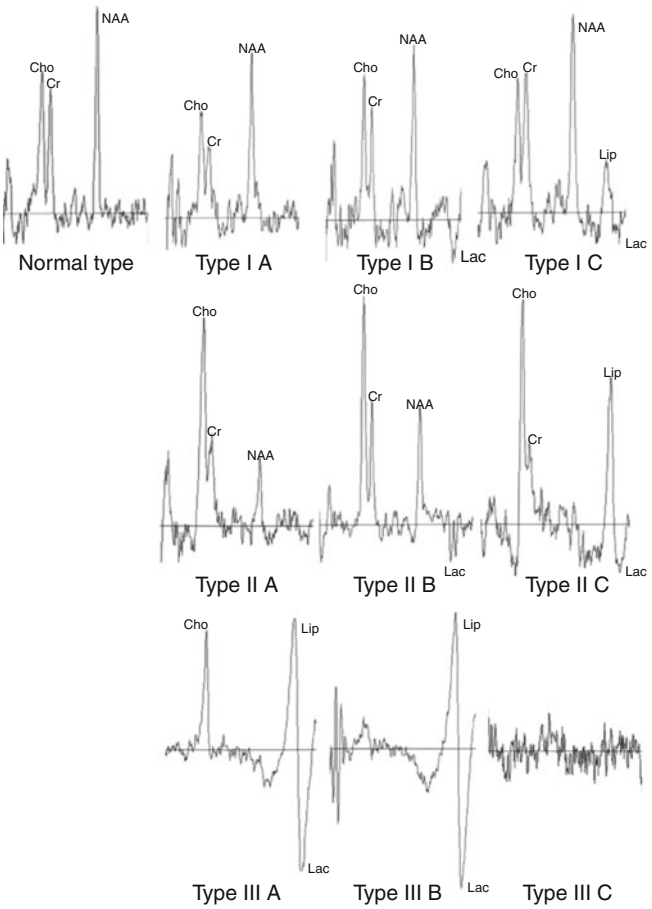

Fig. 5 Classification of the pathological ^{1}H-MR spectra based on determination of the main metabolites, namely *N*-acetylaspartate (*NAA*), choline-containing compounds (*Cho*), lactate (*Lac*), and mobile lipids (*Lip*). Types IC and IIC are further subdivided in cases with mild and moderate elevation of Lip. Types IIIB and IIIC are typical for necrotic lesions (*Source*: Chernov et al. [10])

ventricles or bone structures may create significant technical obstacles to spectroscopic investigation.

Single Photon Emission Computed Tomography

Single photon emission computed tomography (SPECT) is based on detection of tracers labeled with gamma-emitting isotopes by rotating scintillation detectors (gamma cameras). To evaluate progressing brain tumors after radiosurgery, several investigators have used thallium-201 chloride (^{201}Tl), the uptake of which is related to CBF, BBB alterations, and variability of Na/K-ATPase pump expression. Using ^{201}Tl SPECT, Serizawa et al. [74] prospectively evaluated 72 brain metastases that were enlarging after GKS. Tumor recurrence was diagnosed if the Tl index (ratio of the radioisotope activity in the tumor relative to that of normal brain tissue) was >5, whereas radiation injury was considered present if it was <3. If the Tl index was between 3 and 5, the investigation was repeated in 1 month (which was required for 57 % of the lesions). Using their criteria the authors found 90 % diagnostic accuracy for differentiating tumor recurrence from radiation injury. In another study, using a cutoff level for Tl index of 2.5, Kimura et al. [43] established the correct diagnosis in 74 % of patients with brain metastases that demonstrated enlargement after SRS.

Others, however, claimed that ^{201}Tl SPECT is a sensitive but relatively nonspecific modality for identifying progressing tumors after irradiation, and that its spatial resolution is too low (8–10 mm). False-positive and false-negative results were reported [20, 40, 71, 74, 79]. Nonneoplastic lesions with BBB disruption (radiation-induced necrosis, inflammation, infarct) as well as hematomas and abscesses may display increased ^{201}Tl uptake. The risk of diagnostic error is particularly high for small tumors and masses located infratentorially or in the vicinity of brain structures with high physiological tracer uptake (e.g., orbit, choroid plexus, hypophyseal region). False-negative results may be caused by administration of steroids [74]. In the series of Tsuyuguchi et al. [79] 81 % of brain metastases enlarging after SRS showed accumulation of ^{201}Tl, but no significant

difference was noted between the recurrence and necrosis groups. A review of studies on the use of ^{201}Tl SPECT for evaluating recurrent supratentorial gliomas after radiotherapy revealed that the sensitivity and specificity of the method vary widely: 43–100 % and 25–100 %, respectively [80]. Use of double isotope investigations (e.g., ^{201}Tl and ^{99m}Tc-HMPAO) or delayed scanning may result in greater diagnostic effectiveness of SPECT [77, 79].

Positron Emission Tomography

Among the diagnostic modalities used to differentiate tumor progression from radiation-induced necrosis, positron emission tomography (PET) has probably obtained the widest acceptance. Hypermetabolic tumor cells actively accumulate radioisotope tracer, whereas hypometabolic necrosis does not, which theoretically leads to a straightforward diagnosis (Fig. 6). Indeed, initial studies with the use of ^{18}F-fluorodeoxyglucose (FDG)-PET showed high efficacy for identifying recurrent brain tumors after irradiation [5, 6, 42, 50, 81, 85]. The reported sensitivity and specificity of the method for identifying recurrent brain metastases after SRS were 65–82 % and 80–97 %, respectively [6, 81]. The diagnostic accuracy was further improved by co-registration of the metabolic data with structural MRI and/or a computerized brain atlas [6, 81]. However, erroneous results of FDG-PET regarding identification of progressing neoplasms are not uncommon [40, 71]. Small tumors, reduced metabolic rate or predominantly anaerobic metabolism, and low resolution may cause false-negative results, whereas high radioisotope uptake in the normal cortex and basal ganglia, areas of inflammation, or epileptic foci may lead to false-positive findings [11, 25, 50]. Additionally, glucose metabolism is affected by steroid therapy [25]. Greater efficacy of FDG-PET in identifying recurrent brain tumors seemingly can be attained with initial glucose loading, delayed imaging, and dual phase investigations [29, 73], but the clinical usefulness of such techniques require further evaluation.

In contrast to FDG, the background uptake of radioisotopes based on aminoacids (e.g., L-methyl-^{11}C-methionine [MET]) in normal brain tissue is low (beside the pons), which may provide optimal visualization of the neoplasm. MET-PET showed high effectiveness in differentiating recurrent intracranial metastases and gliomas from radiation-induced necrosis after SRS or radiotherapy [76, 79]. Using a tumor/normal tissue ratio cutoff value of 1.42 Tsuyuguchi et al. [79] found 78 % sensitivity and 100 % specificity for identification of progressing metastases after SRS. The mechanisms of MET accumulation in the tumor are not clear but may be related to increased protein synthesis by proliferating cells, active transport of amino acid across the cell membrane, BBB disruption, and high vascular density. Its uptake rates correlate with immunopositivity to MIB-1 and PCNA [25]. Nevertheless, increased accumulation of MET is seen occasionally in intracerebral hematomas, areas of inflammation, reactive gliosis, and radiation-induced necrosis [76, 79].

There is continuing search for new tracers for PET, which can provide highly specific and sensitive identification of recurrent intracranial tumors. This list includes, but is not limited to, radioisotopes based on fluoroethyltyrosine (FET), fluorothymidine (FLT), fluoro-L-dihydroxyphenylalanine (FDOPA), and acetate [8, 25, 28, 52, 67]. However, they are generally not available for routine clinical practice, so their diagnostic usefulness in progressing lesions after SRS has not been clarified.

Comparative Evaluation of the Various Diagnostic Modalities

It is evident that functional and metabolic neuroimaging is helpful for diagnosing brain tumor recurrence after irradiation and for differentiating it from treatment-induced effects. It remains unclear, however, which modality provides superior diagnostic accuracy. Despite some comparative studies on this matter, reliable information remains scarce.

Several investigations demonstrated lower diagnostic performance of FDG-PET compared to multivoxel ^{1}H-MRS and MET-PET in cases of brain metastases progressing after SRS [11, 79]; compared to ^{201}Tl-SPECT, MET-, FLT-, and FDOPA-PET in cases of recurrent gliomas, particularly low-grade tumors [8, 28, 76]; and compared to acetate-PET for evaluating the response of meningiomas to GKS [52]. On the other hand MET-PET seems more efficient than ^{201}Tl-SPECT for identifying brain metastases that are progressing after SRS [79], and it provides results comparable to those achieved with FET-PET in recurrent gliomas [67]. In cases of brain metastases progressing after irradiation, the diagnostic accuracy of perfusion MRI is better than that of multivoxel ^{1}H-MRS [30], which in turn is slightly more effective than ^{201}Tl-SPECT [43]. Finally, multivoxel ^{1}H-MRS is somewhat more accurate than DWI with ADC measurements for identifying recurrent gliomas [69].

It should be kept in mind that various radiological modalities provide complementary information on irradiated intracranial masses, which justifies use of a multimodal diagnostic approach [30, 33, 49, 50, 59, 60, 69]. Spatial and temporal discordances are common with multiparametric imaging. Therefore, only by combining data derived from several techniques can we arrive at a unique multifaceted characterization of the lesion [59]. In 2006, our group proposed an

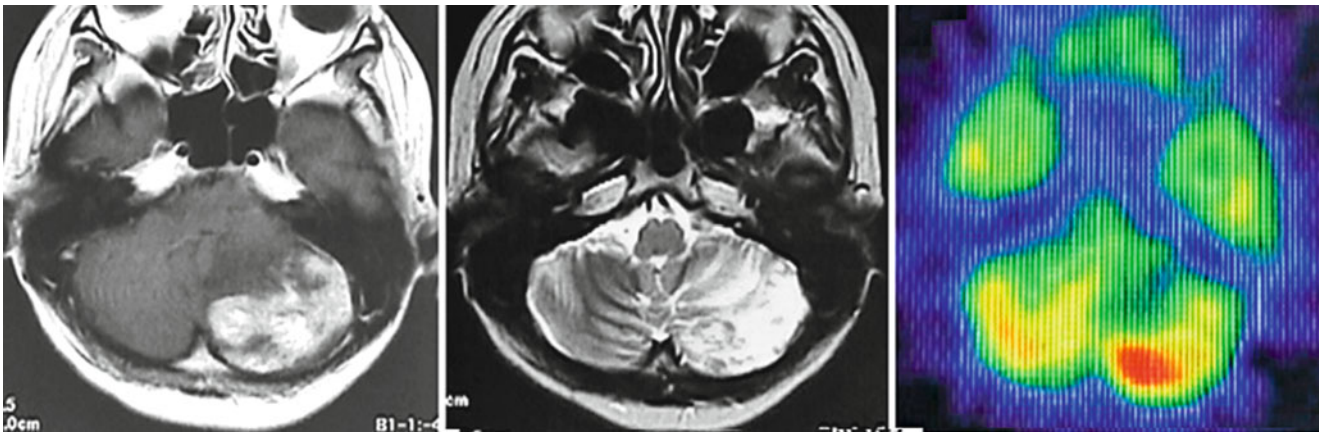

Fig. 6 T1-weighted (*left*) and T2-weighted (*center*) MRI and ^{18}F-fluorodeoxyglucose–positron emission tomography (FDG-PET) (*right*) of a metastatic adenocarcinoma in the left cerebellar hemisphere progressing after GKS (*Source*: Chernov et al. [11])

algorithm for differentiating tumor recurrence from treatment-induced effects after GKS of metastatic brain tumors. The algorithm was based on multivoxel ^{1}H-MRS and PET [12]. Its updated version is presented on Fig. 7, but the efficacy of this diagnostic strategy still requires detailed clinical evaluation.

Role of Serial Functional and Metabolic Imaging After Radiosurgery

Application of serial functional and metabolic evaluations during follow-up provides detailed information on the radiosurgery-induced pathophysiological reactions within the target [59]. DWI, PWI, and ^{1}H-MRS, seem particularly attractive because they can be applied with relative ease at the time of a routine MRI investigation. It was shown that successful radiosurgery results in a gradually increasing ADC [23, 31, 78] and decreased relative CBF [82, 83] and CBV [17] in patients with a metastatic brain tumor. Longitudinal spectroscopic changes in such cases are complex as the initial decrease in Cho, Lac, and Lip peak intensities reflect apoptotic cell loss and inhibition of tumor metabolism. An increase of these metabolites is characteristic of early necrotic changes, whereas further development of radiation-induced necrosis is associated with a decrease in Cho and further elevation of Lac and Lip or, in the late stage, even disappearance of all metabolite peaks [9, 43, 44, 46, 49, 51, 66, 82, 85]. An increase in the neuronal marker NAA usually accompanies tumor shrinkage but sometimes is evident even before initiation of volumetric changes [9]. It is possible that similar dynamics, although of lesser magnitude, of DWI-, PWI-, and ^{1}H-MRS-related parameters can also be observed after SRS of benign extracerebral tumors [46, 78].

Such changes may precede tumor shrinkage or even be detected at the time of mass enlargement. Hence, there is a promising potential to evaluate the effect of treatment long before a measurable response is detected [17, 23, 31, 43, 78, 83]. On the other hand, opposite dynamics usually accompany recurrence or regrowth of the neoplasm. Theoretically, serial functional and metabolic imaging can predict progression of the tumor before there is definite increase in its volume [9, 23, 31, 43, 78]. In the series of Goldman et al. [23], all of the brain metastases for which shrinkage after GKS was not accompanied by a significant increase in the ADC invariably recurred. Increased relative CBF and CBV at 6 weeks after SRS of brain metastases compared to the pretreatment level accurately predicted subsequent tumor progression [17, 83]. Our serial ^{1}H-MRS investigations of intracranial metastases after radiosurgery [9] revealed several subtle neurochemical alterations preceding definite regrowth of the neoplasm (Fig. 8). Nevertheless, the clinical applicability of this diagnostic approach and its possible usefulness for correcting therapy before evidence of volumetric change in the tumor requires additional validation.

Multiple metabolic assessments by means of SPECT or PET are difficult because of the need of special equipment, necessity of injecting radioactive isotopes, and cost of investigation. Nevertheless, Serizawa et al. [74] performed serial ^{201}Tl-SPECT of 41 brain metastases that had enlarged after radiosurgery. They found that tumor recurrence was typically associated with a steadily increasing Tl index, whereas in cases of radiation injury it had a fluctuating course. Based on their experience, the authors defined three metabolic responses after GKS: (1) good—with a prominent decrease in the Tl index within 1 month after SRS and continuous reduction thereafter; (2) early recurrence—with a prominent decrease in the Tl index within 1 month after SRS and steady increase thereafter; (3) poor—with a moderate decrease in the Tl index within

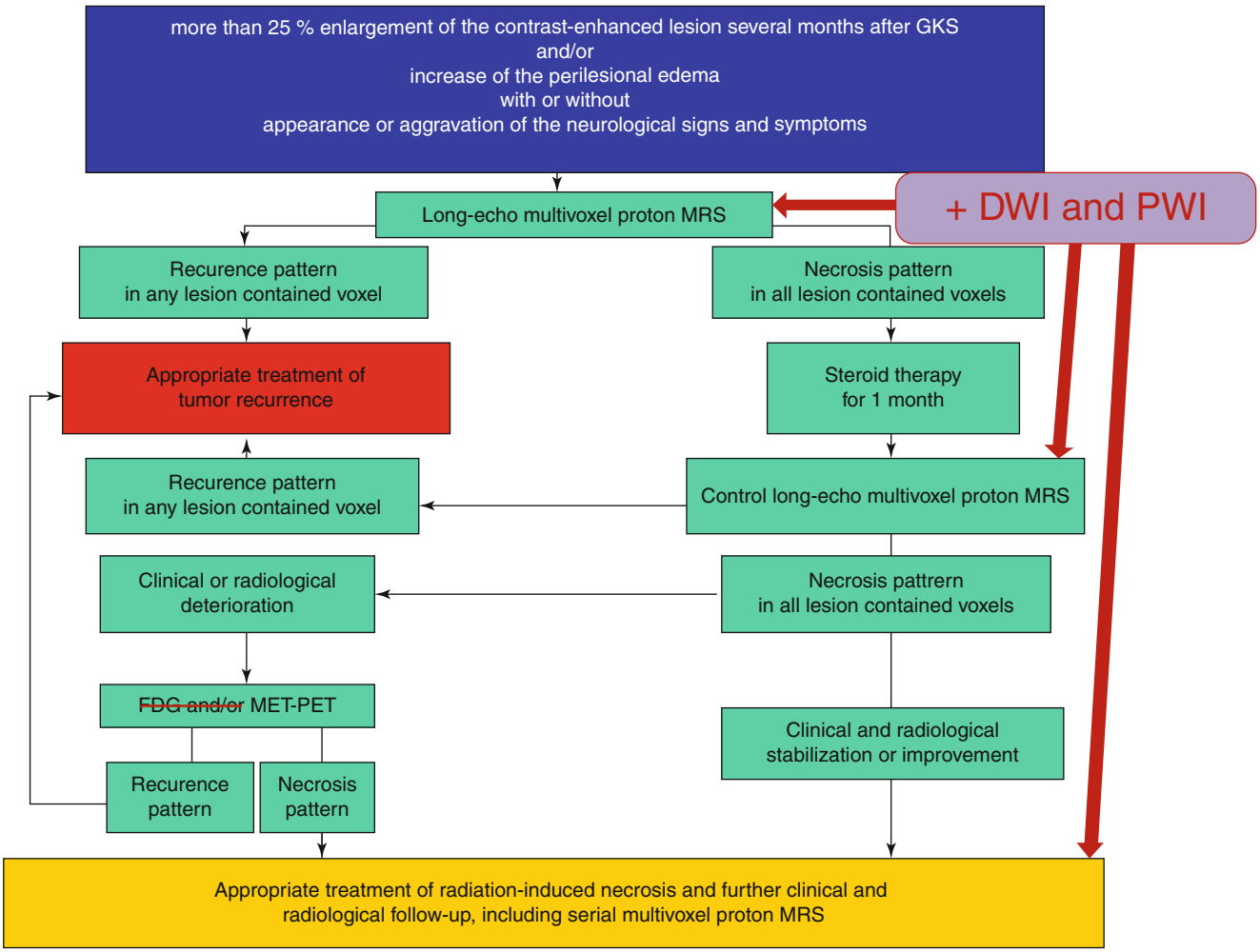

Fig. 7 Diagnostic algorithm for differentiating tumor recurrence from radiation-induced necrosis after irradiation of metastatic brain tumors (modified from Chernov et al. [12]). Compared to the previous version, diffusion-weighted (DWI) and perfusion-weighted (PWI) imaging are added to multivoxel ^{1}H-MRS, whereas FDG-PET is eliminated. *GKS* Gamma Knife radiosurgery

1 month after SRS and its fluctuation thereafter [74]. Tomura et al. [77] revealed that a decrease in the Tl index within the first week after stereotactic irradiation of various intracranial tumors is highly predictive of a subsequent volumetric response. Yoshino et al. [85] performed serial fluoroboronophenylalanine (FBPA)-PET and FDG-PET in a few patients after GKS on brain metastases and found a steady decrease of radioisotope uptake somewhat preceding and accompanying tumor shrinkage. Enlargement of the lesion caused by radiation-induced necrosis was not accompanied by metabolic changes. The similar findings on serial FDG-PET were noted previously after radiosurgery of intracranial meningiomas [62]. However, recently Liu et al. [52] compared acetate-PET and FDG-PET before and after GKS of these tumors. The former tracer showed reduced uptake after irradiation and predicted a volumetric response, but FDG accumulation was nonspecifically increased after irradiation in some cases, which was probably caused by temporary BBB alteration.

In general, it is clear that addition of functional and metabolic investigations to structural MRI during regular follow-up after intracranial radiosurgery allows detailed evaluation of the time-evolving treatment effects and assessment of their dynamics. However, the clinical significance of the obtained information should be defined in further studies.

Tissue Sampling of Lesions Progressing After Radiosurgery

Tissue investigation still represents the gold standard for precise characterization of brain lesions progressing after irradiation. However, the histopathological diagnosis can be challenging, especially if performed on small biopsy

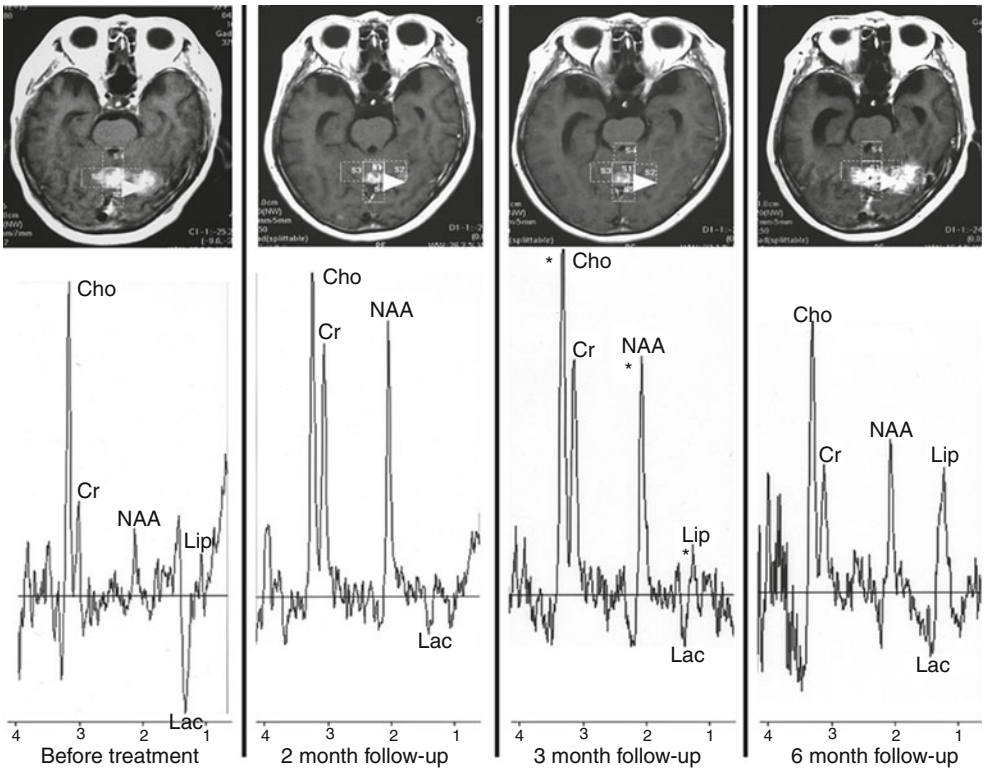

Fig. 8 ^{1}H-MRS-detected metabolic changes in an intracranial metastasis of breast cancer that initially showed prominent volume reduction but recurred at 6 months after GKS. Note the presence of a mild increase in choline-containing compounds (*Cho*) and mobile lipids (*Lip*) and a decrease in *N*-acetylaspartate (*NAA*) at the 3-month follow-up before an increase in tumor volume (*asterisks*). At the time of volumetric lesion progression, there was some decrease in *Cho* accompanied by an evident decrease in *NAA* and creatine (*Cr*) and an increase in *Lip*. *Lac* lactate (*Source*: Chernov et al. [9])

specimens. Various radiation-induced changes may be intermixed with the neoplastic elements, or they may predominate in different parts of the mass. Identification of tumor cells on the background of necrosis may raise a question on their viability and proliferative potential. False-positive results of MIB-1 immunostaining in quiescent tumors after SRS have been reported [37]. As improved tissue sampling can significantly facilitate a histopathological diagnosis, functional or metabolic guidance with PWI, ^{1}H-MRS, or MET-PET and/or neurochemical navigation with 5-aminolevulinic acid seem quite reasonable in such cases during stereotactic biopsy or open microsurgical resection.

Limitations of the Available Studies

The majority of available studies evaluating the various neuroimaging modalities for identification and characterization of brain tumor progression after irradiation suffer from significant methodological shortcomings. Thus, we must be extremely careful when interpreting their results. The main pitfalls typically include a retrospective design and a relatively small number of cases, which does not allow reliable determination of the specific cutoff levels and thresholds of the various diagnostic parameters. In many cases, the final decision on the nature of pathology is based not on the histopathological examination but on reliance on some neuroimaging modality defined as the gold standard or on a stable clinical course, the durations of which varied from one series to another. If tissue sampling was performed, the tissue was frequently obtained by stereotactic biopsy. Hence, the obtained specimen might not be representative of the whole lesion. Such inconsistencies result in significant variability of the reported diagnostic efficacy of the methods. Moreover, the absence of standard methodologies for functional and metabolic investigations and the differences in the equipment, methods of data evaluation (qualitative, semiquantitative, quantitative) and investigated parameters (mean, maximum, and various normalized values using subjectively defined ROIs) do not permit straightforward comparison of the results obtained in separate centers. These shortcomings create significant challenges for directly introducing the reported techniques into clinical practice without preliminary testing and validation.

Future Perspectives

Introduction of the multimodal diagnostic approach requires development of optimized radiological protocols for differentiating tumor progression from radiation-induced changes after SRS. The growing availability of multidetector CT and high magnetic field MRI scanners, the development of new

MRI sequences, and the search for more effective contrast media and radioisotope tracers will significantly extend diagnostic options. Further advances of the fusion techniques and hybrid imaging (e.g., PET-CT, PET-MRI) will improve effective lesion characterization, particularly when using methods with limited spatial resolution. Frequent coexistence of the viable neoplastic elements and postirradiation changes should encourage studies directed at evaluating their relative representation within the same lesion based on quantitative assessment of the heterogeneity of the radiological findings relevant to the histopathology and clinical course. Possible usefulness of serial functional and metabolic neuroimaging starting before SRS and continuing during the subsequent follow-up for early prediction of response to treatment and timely identification of tumor progression should be tested prospectively with strict predetermined diagnostic criteria and outcome measures. These investigations will require development of advanced software workspaces for integrated cross-correlated computer-aided analysis of the multiple data undergoing spatial and temporal changes [59]. Wide introduction of the results of such studies into routine clinical practice cannot be attained without technical standardization of the advanced neuroimaging modalities (e.g., perfusion MRI, ^{1}H-MRS). Finally, development of molecular imaging techniques, particularly those based on amide proton transfer MRI [36], may result in very effective noninvasive characterization of brain lesions after irradiation. Their practical application in the future seems promising.

Conclusion

Differentiation of tumor progression from radiation-induced effects after intracranial radiosurgery is challenging. It includes complex evaluation of various clinical, radiosurgical, and radiological factors. Evaluating volumetric changes by structural contrast-enhanced MRI seems sufficient after low-dose SRS of benign intracranial tumors. In such cases possible delayed growth arrest and transitory enlargement of the lesion should be always borne in mind, because usually they do not require additional treatment. Multimodal neuroimaging with application of the various functional and metabolic techniques is preferable in diagnostically difficult cases. Addition of DWI, perfusion studies, and ^{1}H-MRS to regular structural MRI investigations during follow-up after SRS of parenchymal brain tumors allows detailed longitudinal assessment of the treatment effects and, along with MET PET, provides valuable diagnostic information about progressing lesions. Finally, it should be kept in mind that differentiating tumor recurrence from radiation-induced effects after SRS does not indicate whether to apply surgical treatment or reserve it. In fact, resection of the lesion may be required for either condition. If indicated, it should be performed under metabolic guidance.

Conflict of Interest The authors declare that they have no conflict of interest. The research activities of Dr. Mikhail Chernov during 2010–2012 were supported by the Japan Society for the Promotion of Science (JSPS; ID No. P 10128).

References

1. Asao C, Korogi Y, Kitajima M, Hirai T, Baba Y, Makino K, Kochi M, Morishita S, Yamashita Y (2005) Diffusion-weighted imaging of radiation-induced brain injury for differentiation from tumor recurrence. AJNR Am J Neuroradiol 26:1455–1460
2. Barajas RF, Chang JS, Sneed PK, Segal MR, McDermott MW, Cha S (2009) Distinguishing recurrent intra-axial metastatic tumor from radiation necrosis following Gamma Knife radiosurgery using dynamic susceptibility-weighted contrast-enhanced perfusion MR imaging. AJNR Am J Neuroradiol 30:367–372
3. Blonigen BJ, Steinmetz RD, Levin L, Lamba MA, Warnick RE, Breneman JC (2010) Irradiated volume as a predictor of brain radionecrosis after linear accelerator stereotactic radiosurgery. Int J Radiat Oncol Biol Phys 77:996–1001
4. Brismar J, Roberson GH, Davis KR (1976) Radiation necrosis of the brain. Neuroradiological considerations with computed tomography. Neuroradiology 12:109–113
5. Castel JC, Caille JM (1989) Imaging of irradiated brain tumours: value of magnetic resonance imaging. J Neuroradiol 16:81–132
6. Chao ST, Suh JH, Raja S, Lee SY, Barnett G (2001) The sensitivity and specificity of FDG PET in distinguishing recurrent brain tumor from radionecrosis in patients treated with stereotactic radiosurgery. Int J Cancer 96:191–197
7. Chen HI, Burnett MG, Huse JT, Lustig RA, Bagley LJ, Zager EL (2006) Recurrent late cerebral necrosis with aggressive characteristics after radiosurgical treatment of an arteriovenous malformation. J Neurosurg 105:455–460
8. Chen W, Silverman DH, Delaloye S, Czernin J, Kamdar N, Pope W, Satyamurthy N, Schiepers C, Cloughesy T (2006) 18F-FDOPA PET imaging of brain tumors: comparison study with 18F-FDG PET and evaluation of diagnostic accuracy. J Nucl Med 47:904–911
9. Chernov MF, Hayashi M, Izawa M, Nakaya K, Tamura N, Ono Y, Abe K, Usukura M, Yoshida S, Nakamura R, Suzuki T, Muragaki Y, Iseki H, Kubo O, Hori T, Takakura K (2009) Dynamics of metabolic changes in intracranial metastases and distant normal-appearing brain tissue after stereotactic radiosurgery: a serial proton magnetic resonance spectroscopy study. Neuroradiol J 22:58–71
10. Chernov M, Hayashi M, Izawa M, Nakaya K, Ono Y, Usukura M, Yoshida S, Kato K, Muragaki Y, Nakamura R, Iseki H, Hori T, Takakura K (2007) Metabolic characteristics of intracranial metastases, detected by single-voxel proton magnetic resonance spectroscopy, are seemingly not predictive for tumor response to gamma knife radiosurgery. Minim Invasive Neurosurg 50:233–238
11. Chernov MF, Hayashi M, Izawa M, Ochiai T, Usukura M, Abe K, Ono Y, Muragaki Y, Kubo O, Hori T, Takakura K (2005) Differentiation of the radiation-induced necrosis and tumor recurrence after Gamma Knife radiosurgery for brain metastases: importance of multi-voxel proton MRS. Minim Invasive Neurosurg 48:228–234

12. Chernov MF, Hayashi M, Izawa M, Usukura M, Yoshida S, Ono Y, Muragaki Y, Kubo O, Hori T, Takakura K (2006) Multivoxel proton MRS for differentiation of radiation-induced necrosis and tumor recurrence after Gamma Knife radiosurgery for brain metastases. Brain Tumor Pathol 23:19–27
13. Chin LS, Ma L, DiBiase S (2001) Radiation necrosis following Gamma Knife surgery: a case-controlled comparison of treatment parameters and long-term clinical follow-up. J Neurosurg 94:899–904
14. Couldwell WT, Cole CD, Al-Mefty O (2007) Patterns of skull base meningioma progression after failed radiosurgery. J Neurosurg 106:30–35
15. Delsanti C, Roche PH, Thomassin JM, Regis J (2008) Morphological changes of vestibular schwannomas after radiosurgical treatment: pitfalls and diagnosis of failure. In: Regis J, Roche PH (eds) Modern Management of Acoustic Neuroma. Prog Neurol Surg, vol. 21. Karger, Basel, pp 93–97
16. Dequesada IM, Quisling RG, Yachnis A, Friedman WA (2008) Can standard magnetic resonance imaging reliably distinguish recurrent tumor from radiation necrosis after radiosurgery for brain metastases? A radiographic-pathological study. Neurosurgery 63:898–904
17. Essig M, Waschkies M, Wenz F, Debus J, Hentrich HR, Knopp MV (2003) Assessment of brain metastases with dynamic susceptibility-weighted contrast-enhanced MR imaging: initial results. Radiology 228:193–199
18. Feigl GC, Horstmann GA (2006) Volumetric follow up of brain metastases: a useful method to evaluate treatment outcome and predict survival after Gamma Knife surgery? J Neurosurg 105(Suppl):91–98
19. Feigl GC, Samii M, Horstman GA (2007) Volumetric follow-up of meningiomas: a quantitative method to evaluate treatment outcome of gamma knife radiosurgery. Neurosurgery 61:281–287
20. Foroughi M, Kemeny AA, Lehecka M, Wons J, Kajdi L, Hatfield R, Marks S (2010) Operative intervention for delayed symptomatic radionecrotic masses developing following stereotactic radiosurgery for cerebral arteriovenous malformations – case analysis and literature review. Acta Neurochir (Wien) 152:803–815
21. Ganz JC, Reda WA, Abdelkarim K (2009) Adverse radiation effects after Gamma Knife surgery in relation to dose and volume. Acta Neurochir (Wien) 151:9–19
22. Gao X, Zhang XN, Zhang YT, Yu CS, Xu DS (2011) Magnetic resonance imaging in assessment of treatment response of Gamma Knife for brain tumors. Chin Med J (Engl) 124:1906–1910
23. Goldman M, Boxerman JL, Rogg JM, Noren G (2006) Utility of apparent diffusion coefficient in predicting the outcome of gamma knife-treated brain metastases prior to changes in tumor volume: a preliminary study. J Neurosurg 105(Suppl):175–182
24. Hasegawa T, Kida Y, Yoshimoto M, Koike J, Goto K (2006) Evaluation of tumor expansion after stereotactic radiosurgery in patients harboring vestibular schwannomas. Neurosurgery 58: 1119–1128
25. Herholz K, Coope D, Jackson A (2007) Metabolic and molecular imaging in neuro-oncology. Lancet Neurol 6:711–724
26. Hirato M, Hirato J, Zama A, Inoue H, Ohye C, Shibazaki T, Andou Y (1996) Radiobiological effects of gamma knife radiosurgery on brain tumors studied in autopsy and surgical specimens. Stereotact Funct Neurosurg 66(Suppl 1):4–16
27. Hoefnagels FWA, Lagerwaard FJ, Sanchez E, Haasbeek CJA, Knol DL, Slotman BJ, Vandertop WP (2009) Radiological progression of cerebral metastases after radiosurgery: assessment of perfusion MRI for differentiating between necrosis and recurrence. J Neurol 256:878–887
28. Hong IK, Kim JH, Ra YS, Kwon DH, Oh SJ, Kim JS (2011) Diagnostic usefulness of 3′-deoxy-3′-[18F] fluorothymidine positron emission tomography in recurrent brain tumor. J Comput Assist Tomogr 35:679–684
29. Horky LL, Hsiao EM, Weiss SE, Drappatz J, Gerbaudo VH (2011) Dual phase FDG-PET imaging of brain metastases provides superior assessment of recurrence versus post-treatment necrosis. J Neurooncol 103:137–146
30. Huang J, Wang AM, Shetty A, Maitz AH, Yan D, Doyle D, Richey K, Park S, Pieper DR, Chen PY, Grills IS (2011) Differentiation between intra-axial metastatic tumor progression and radiation injury following fractionated radiation therapy or stereotactic radiosurgery using MR spectroscopy, perfusion MR imaging or volume progression modeling. Magn Reson Imaging 29: 993–1001
31. Huang CF, Chou HH, Tu HT, Yang MS, Lee JK, Lin LY (2008) Diffusion magnetic resonance imaging as an evaluation of the response of brain metastases treated by stereotactic radiosurgery. Surg Neurol 69:62–68
32. Jagannathan J, Bourne TD, Schlesinger D, Yen CP, Shaffrey ME, Laws ER Jr, Sheehan JP (2010) Clinical and pathological characteristics of brain metastases resected after failed radiosurgery. Neurosurgery 66:208–217
33. Jain R, Narang J, Schultz L, Scarpace L, Saksena S, Brown S, Rock JP, Rosenblum M, Gutierrez J, Mikkelsen T (2011) Permeability estimates in histopathology-proved treatment-induced necrosis using perfusion CT: can these add to other perfusion parameters in differentiating from recurrent/progressive tumors? AJNR Am J Neuroradiol 32:658–663
34. Jain R, Narang J, Sundgren PM, Hearshen D, Saksena S, Rock JP, Gutierrez J, Mikkelsen T (2010) Treatment induced necrosis versus recurrent/progressing brain tumor: going beyond the boundaries of conventional morphologic imaging. J Neurooncol 100:17–29
35. Jain R, Scarpace L, Ellika S, Schultz LR, Rock JP, Rosenblum ML, Patel SC, Lee TY, Mikkelsen T (2007) First-pass perfusion computed tomography: initial experience in differentiating recurrent brain tumors from radiation effects and radiation necrosis. Neurosurgery 61:778–787
36. Jandial R, Duenas VJ, Chen BT (2011) Molecular imaging based on differential protein content in differentiating glioma from radiation necrosis. Neurosurgery 68(6):N16–N17
37. Jennelle R, Gladson C, Palmer C, Guthrie B, Markert J (1999) Paradoxical labeling of radiosurgically treated quiescent tumors with Ki 67, a marker of cellular proliferation. Stereotact Funct Neurosurg 72(Suppl 1):45–52
38. Kamada K, Mastuo T, Tani M, Izumo T, Suzuki Y, Okimoto T, Hayashi N, Hyashi K, Shibata S (2001) Effects of stereotactic radiosurgery on metastatic brain tumors of various histopahtologies. Neuropathology 21:307–314
39. Kang TW, Kim ST, Byun HS, Jeon P, Kim K, Kim H, Lee J II (2009) Morphological and functional MRI, MRS, perfusion and diffusion changes after radiosurgery of brain metastasis. Eur J Radiol 72:370–380
40. Kano H, Kondziolka D, Lobato-Polo J, Zorro O, Flickinger JC, Lunsford LD (2010) Differentiating radiation effect from tumor progression after stereotactic radiosurgery: T1/T2 matching. Clin Neurosurg 57:160–165
41. Kano H, Kondziolka D, Lobato-Polo J, Zorro O, Flickinger JC, Lunsford LD (2010) T1/T2 matching to differentiate tumor growth from radiation effects after stereotactic radiosurgery. Neurosurgery 66:486–492
42. Kihlstrom L, Karlsson B (1999) Imaging changes after radiosurgery for vascular malformations, functional targets and tumors. Neurosurg Clin N Am 10:167–180
43. Kimura T, Sako K, Tanaka K, Gotoh T, Yoshida H, Aburano T, Tanaka T, Arai H, Nakada T (2004) Evaluation of the response of metastatic brain tumors to stereotactic radiosurgery by proton magnetic resonance spectroscopy, ^{201}TlCl single-photon emission computerized tomography, and gadolinium-enhanced magnetic resonance imaging. J Neurosurg 100:835–841

44. Kimura T, Sako K, Tohyama Y, Aizawa S, Yoshida H, Aburano T, Tanaka K, Tanaka T (2003) Diagnosis and treatment of progressive space-occupying radiation necrosis following stereotactic radiosurgery for brain metastases: value of proton magnetic resonance spectroscopy. Acta Neurochir (Wien) 145:557–564
45. Kingsley DP, Kendall BE (1981) CT of the adverse effects of therapeutic radiation of the Central Nervous System. AJNR Am J Neuroradiol 2:453–460
46. Kizu O, Naruse S, Furuya S, Morishita H, Ide M, Maeda T, Ueda S (1998) Application of proton chemical shift imaging in monitoring of gamma knife radiosurgery on brain tumors. Magn Reson Imaging 16:197–204
47. Korytko T, Radivoyevitch T, Colussi V, Wessels BW, Pillai K, Maciunas RJ, Einstein DB (2006) 12 Gy gamma knife radiosurgical volume is a predictor for radiation necrosis in non-AVM intracranial tumors. Int J Radiat Oncol Biol Phys 64:419–424
48. Kubo O, Chernov M, Izawa M, Hayashi M, Muragaki Y, Maruyama T, Hori T, Takakura K (2005) Malignant progression of benign brain tumors after gamma knife radiosurgery: is it really caused by irradiation? Minim Invasive Neurosurg 48:334–339
49. Kwock L, Smith JK, Castillo M, Ewend MG, Cush S, Hensing T, Varia M, Morris D, Bouldin TW (2002) Clinical applications of proton MR spectroscopy in oncology. Technol Cancer Res Treat 1:17–28
50. Langleben DD, Segall GM (2000) PET in differentiation of recurrent brain tumor from radiation injury. J Nucl Med 41:1861–1867
51. Lee PL, Gonzalez RG (2000) Magnetic resonance spectroscopy of brain tumors. Curr Opin Oncol 12:199–204
52. Liu RS, Chang CP, Guo WY, Pan DHC, Ho DMT, Chang CW, Yang BH, Wu LC, Yeh SH (2010) 1-^{11}C-Acetate versus ^{18}F-FDG PET in detection of meningioma and monitoring the effect of gamma-knife radiosurgery. J Nucl Med 51:883–891
53. Loeffler JS, Niemierko A, Chapman PH (2003) Second tumors after radiosurgery: tip of the iceberg or a bump in the road? Neurosurgery 52:1436–1442
54. Lunsford LD, Kondziolka D, Maitz A, Flickinger JC (1998) Black holes, white dwarfs and supernovas: imaging after radiosurgery. Stereotact Funct Neurosurg 70(Suppl 1):2–10
55. Lunsford LD, Niranjan A, Martin J, Sirin S, Kassam A, Kondziolka D, Flickinger JC (2007) Radiosurgery for miscellaneous skull base tumors. In: Szeifert GT, Kondziolka D, Levivier M, Lunsford LD (eds) Radiosurgery and Pathological Fundamentals. Prog Neurol Surg, vol. 20. Karger, Basel, pp 192–205
56. Mitsuya K, Nakasu Y, Horiguchi S, Harada H, Nishimura T, Bando E, Okawa H, Furukawa Y, Hirai T, Endo M (2010) Perfusion weighted magnetic resonance imaging to distinguish the recurrence of metastatic brain tumors from radiation necrosis after stereotactic radiosurgery. J Neurooncol 99:81–88
57. Mullins ME, Barest GD, Schaefer PW, Hochberg FH, Gonzalez RG, Lev MH (2005) Radiation necrosis versus glioma recurrence: conventional MR imaging clues to diagnosis. AJNR Am J Neuroradiol 26:1967–1972
58. Niranjan A, Kondziolka D, Lunsford LD (2009) Neoplastic transformation after radiosurgery or radiotherapy: risk and realties. Otolaryngol Clin North Am 42:717–729
59. Padhani AR, Miles KA (2010) Multiparametric imaging of tumor response to therapy. Radiology 256:348–364
60. Palumbo B (2008) Brain tumour recurrence: brain single-photon emission computerized tomography, PET and proton magnetic resonance spectroscopy. Nucl Med Commun 29:730–735
61. Pamir MN, Kilic T, Belirgen M, Abacioglu U, Karabekiroglu N (2007) Pituitary adenomas treated with gamma knife radiosurgery: volumetric analysis of 100 cases with minimum 3 year follow-up. Neurosurgery 61:270–280
62. Pan DHC, Guo WY, Chung WY, Shiau CY, Liu RS, Lee LS (1995) Early effects of gamma knife surgery on malignant and benign intracranial tumors. Stereotact Funct Neurosurg 64(Suppl 1):19–31
63. Patel TR, McHugh BJ, Bi WL, Minja FJ, Knisely JPS, Chiang VL (2011) A comprehensive review of MR imaging changes following radiosurgery to 500 brain metastases. AJNR Am J Neuroradiol 32:1885–1892
64. Plowman PN (1999) Stereotactic radiosurgery VIII. The classification of postirradiation reactions. Br J Neurosurg 13: 256–264
65. Pollock BE (2006) Management of vestibular schwannomas that enlarge after stereotactic radiosurgery: treatment recommendations based on a 15 year experience. Neurosurgery 58:241–248
66. Pruzincova L, Steno J, Srbecky M, Kalina P, Rychly B, Boljesikova E, Chorvath M, Novotny M, Procka V, Makaiova I, Belan V (2009) MR imaging of late radiation therapy- and chemotherapy-induced injury: a pictorial essay. Eur Radiol 19:2716–2727
67. Rachinger W, Goetz C, Popperl G, Gildehaus FJ, Kreth FW, Holtmannspotter M, Herms J, Koch W, Tatsch K, Tonn JC (2005) Positron emission tomography with *O*-(2-[^{18}F]fluoroethyl)-L-Tyrosine versus magnetic resonance imaging in the diagnosis of recurrent gliomas. Neurosurgery 57:505–511
68. Rock JP, Hearshen D, Scarpace L, Croteau D, Gutierrez J, Fisher JL, Rosenblum ML, Mikkelsen T (2002) Correlations between magnetic resonance spectroscopy and image-guided histopathology, with special attention to radiation necrosis. Neurosurgery 51:912–920
69. Rock JP, Scarpace L, Hearshen D, Gutierrez J, Fisher JL, Rosenblum ML, Mikkelsen T (2004) Associations among magnetic resonance spectroscopy, apparent diffusion coefficients, and image-guided histopathology with special attention to radiation necrosis. Neurosurgery 54:1111–1119
70. Rogers LR, Gutierrez J, Scarpace L, Schultz L, Ryu S, Lord B, Movsas B, Nonsowetz J, Jain R (2011) Morphologic magnetic resonance imaging features of therapy-induced cerebral necrosis. J Neurooncol 101:25–32
71. Ross DA, Sandler HM, Balter JM, Hayman JA, Archer PG, Auer DL (2002) Imaging changes after stereotactic radiosurgery of primary and secondary malignant brain tumors. J Neurooncol 56:175–181
72. Rowe J, Grainger A, Walton L, Silcocks P, Radatz M, Kemeny A (2007) Risk of malignancy after gamma knife stereotactic radiosurgery. Neurosurgery 60:60–66
73. Seo YS, Chung TW, Kim IY, Bom HS, Min JJ (2008) Enhanced detectability of recurrent brain tumor using glucose-loading F-18 FDG PET. Clin Nucl Med 33:32–33
74. Serizawa T, Saeki N, Higuchi Y, Ono J, Matsuda S, Sato M, Yanagisawa M, Iuchi T, Nagano O, Yamaura A (2005) Diagnostic value of thallium-201 chloride single-photon emission computerized tomography in differentiating tumor recurrence from radiation injury after Gamma Knife surgery for metastatic brain tumors. J Neurosurg 102(Suppl):266–271
75. Sundgren PC, Fan X, Weybright P, Welsh RC, Carlos RC, Petrou M, McKeever PE, Chenevert TL (2006) Differentiation of recurrent brain tumor versus radiation injury using diffusion tensor imaging in patients with new contrast-enhancing lesions. Magn Reson Imaging 24:1131–1142
76. Terakawa Y, Tsuyuguchi N, Iwai Y, Yamanaka K, Higashiyama S, Takami T, Ohata K (2008) Diagnostic accuracy of ^{11}C-Methionine PET for differentiation of recurrent brain tumors from radiation necrosis after radiotherapy. J Nucl Med 49: 694–699
77. Tomura N, Izumi J, Anbai A, Takahashi S, Sakuma I, Omachi K, Kidani H, Sasaki K, Watarai J, Suzuki A, Mizoi K (2005) Thallium-201 SPECT in the evaluation of early effects on brain tumors treated with stereotactic irradiation. Clin Nucl Med 30:83–86
78. Tomura N, Narita K, Izumi JI, Suzuki A, Anbai A, Otani T, Sakuma I, Takahashi S, Mizoi K, Watarai J (2006) Diffusion

changes in a tumor and peritumoral tissue after stereotactic irradiation for brain tumors: possible prediction of treatment response. J Comput Assist Tomogr 30:496–500
79. Tsuyuguchi N, Sunada I, Iwai Y, Yamanaka K, Tanaka K, Takami T, Otsuka Y, Sakamoto S, Ohata K, Goto T, Hara M (2003) Methionine positron emission tomography of recurrent metastatic brain tumor and radiation necrosis after stereotactic radiosurgery: is a differential diagnosis possible? J Neurosurg 98:1056–1064
80. Vos MJ, Tony BN, Hoekstra OS, Postma TJ, Heimans JJ, Hooft L (2007) Systematic review of the diagnostic accuracy of 201Tl single photon emission computed tomography in the detection of recurrent glioma. Nucl Med Commun 28:431–439
81. Wang SX, Boethius J, Ericson K (2006) FDG-PET on irradiated brain tumor: ten years' summary. Acta Radiol 47:85–90
82. Weber MA, Lichy MP, Thilmann C, Gunther M, Bachert P, Maudsley AA, Delorme S, Schad LR, Debus J, Schlemmer HP (2003) Monitoring of irradiated brain metastases using MR perfusion imaging and 1H MR spectroscopy. Radiologe 43:388–395 (in German)
83. Weber MA, Thilmann C, Lichy MP, Gunther M, Delorme S, Zuna I, Bongers A, Schad LR, Debus J, Kauczor HU, Essig M, Schlemmer HP (2004) Assessment of irradiated brain metastases by means of arterial spin-labeling and dynamic susceptibility-weighted contrast-enhanced perfusion MRI: initial results. Invest Radiol 39:277–287
84. Young GS (2007) Advanced MRI of adult brain tumors. Neurol Clin 25:947–973
85. Yoshino E, Ohmori Y, Imahori Y, Higuchi T, Furuya S, Naruse S, Mori T, Suzuki K, Yamaki T, Ueda S, Tsuzuki T, Takai S (1996) Irradaition effects on the metabolism of metastatic brain tumors: analysis by positron emission tomography and ^{1}H-magnetic resonance spectroscopy. Stereotact Funct Neurosurg 66(Suppl 1): 240–259
86. Zada G, Pagnini PG, Yu C, Erickson KT, Hirschbein J, Zelman V, Apuzzo MLJ (2010) Long-term outcomes and patterns of tumor progression after gamma knife radiosurgery for benign meningiomas. Neurosurgery 67:322–329

Author Index

M.F. Chernov et al. (eds.), *Gamma Knife Neurosurgery in the Management of Intracranial Disorders*,
Acta Neurochirurgica Supplement, Vol. 116, DOI 10.1007/978-3-7091-1376-9, © Springer-Verlag Wien 2013

Subject Index